

SUPERSONIC AND SUBSONIC AIRPLANE DESIGN

Gerald Corning

*Aeronautical Engineering Department
University of Maryland
College Park, Maryland*

SUPERSONIC AND SUBSONIC AIRPLANE DESIGN

by

Gerald Corning

Professor

Aeronautical Engineering Department

University of Maryland

College Park, Maryland

Box No. 14

College Park, Maryland

Copyright 1953
Gerald Corning
Fourth Printing

2nd Edition
1st Printing

Lithoprinted in U.S.A.
EDWARDS BROTHERS, INC.
ANN ARBOR, MICHIGAN

PREFACE

Preface to 2nd Edition "Supersonic and Subsonic Airplane Design".

Since the original text was written, many changes have taken place in the field of manned aircraft. The major ones that affect the contents of this text are:

1. jet transports are no longer merely a matter of conjecture, but are already on the major airlines cruising at about 500 knots.
2. our entire airforce is practically composed of all supersonic aircraft, with the few subsonic bombers soon to be displaced by the faster supersonic ones.
3. the aircraft companies already have large staffs working on supersonic transports which they hope to introduce into airline schedules by 1970.

The added importance of supersonic vehicles, and the much larger amount of unclassified material available in supersonic aerodynamics, has made it both desirable and possible to present some pertinent design material in the text.

Because of the development in the subsonic jet transport field, the data available on the Boeing 707, the Douglas DC-8 and the Convair 600 have been added to the existing material.

After much deliberation it was decided to present the supersonic data in new chapters instead of alongside the subsonic in the same chapters. Therefore there are Chapters II "Aerodynamic Design - Subsonic", III "Aerodynamic Design - Supersonic", IV "Airplane Layout - Subsonic and V "Airplane Layout - Supersonic"; and Aerodynamic Heating". In addition to Chapters IX and X on "Subsonic Stability and Control" there is XI "Supersonic Effects on Stability and Control". Having each type of airplane separated will increase the usefulness of the text to the student working on one particular airplane, and to the engineer using it as a reference. Having the Chapter III "Supersonic Aerodynamic Design" follow the same order of topics as presented in Chapter II "Subsonic Aerodynamic Design" should make it convenient for the instructor to either present each design separately, or both concurrently.

There are two other important changes in the book:

1. The chapter on "Airloads has been changed completely from the previously used series of static conditions as specified in the old C.A.M. 04, to the more rational dynamic conditions now used. Only a simplified brief approach has been presented to introduce the student to the subject of airloads.
2. A small additional section has been added to "Stability and Control" to introduce the undergraduate student to the vital subject of dynamic stability in airplane design. It is felt that it is more important than the static concept and the subject of stability and control should not be presented without the inclusion of the dynamics.

In addition to the above major changes and additions, many minor topics have been modified. Of these probably the most prominent is the change from the use of statute miles to nautical miles. These have been finally incorporated in the text since the use of the nautical mile has now been adopted completely by the military and commercial airplane industry and it is advisable to indoctrinate the students that they think in terms of these parameters.

Additional explanations and minor topics have been presented in the subsonic part of the text with the intent of rendering the material more complete and the presentation more thorough.

Again I wish to acknowledge the assistance of all the aircraft and engine manufacturers in providing me with the data on their products for presentation here. I am further indebted to the N.A.S.A. and other research organizations for the material from their many publications. I especially want to thank Mrs. Edna Brothers for her prodigious effort in the typing of the text.

PREFACE

Many books have been written in the fundamental fields of airplane design, aerodynamics, airplane performance, stability and control, and structures. Little has been presented on an actual method of arriving at an airplane design from a definite set of specifications. It is felt that this text fills this gap, and at the same time presents the latest information in the field, along with its related theory. The derivations of formulas, and the background of the material presented is also included.

Part I, "Aerodynamic Design" presents the method, and the material, for designing and laying out an airplane to a set of specifications. Chapter VI includes design data on propellers; performance and characteristics of reciprocating, turbo-prop and turbo-jet engines; and significant data on military, private and transport airplanes. Chapters II, III, and IV actually show the method of airplane design applied to a high speed jet transport.

Part II, "Stability and Control," presents a brief theoretical discussion of the subject as applied to airplane design. Although this theoretical analysis is not reliable enough for final design, (experimental data must also be obtained) it does indicate the important criteria. It is for this reason that such a theoretical presentation is essential to sound airplane design. For a more complete study, a text on Stability and Control¹ is suggested.

Part III, "Structural Design," indicates the method of determining the air loads and ground loads on the airplane, and how they are applied to the design of the airplane components. For a commercial transport, these loads must meet the requirements of the Civil Air Regulations. For this reason the bulletins, Civil Air Regulations 04 and Civil Air Manual 04, are suggested as auxiliary texts. Chapter IX discusses the important and significant features of these publications and at the same time has kept the duplication of material to a minimum. Chapter X presents the application of the loads to the airplane and special structural problems as related to airplane design.

The data used in the text is the most up-to-date available, consistent with security regulations, and parts of it, therefore, are subject to change. However the method, sequence of operations and the theories involved will not become obsolete and

1. "Airplane Performance, Stability and Control," Perkins and Hage.

may be applied to any design at any time.

The jet transport has been selected as the vehicle for presenting the design method for the following reasons. It involves a large number of parameters, it lends itself to a concise and logical analysis, and the direct operating cost is a convenient criteria for determining the optimum airplane.

The book has been prepared for the engineer in industry and for use in the classroom.

This material may be presented in class in two ways. The method of airplane design as applied to a jet transport can be offered in the lecture periods, while the students apply this method to other types of aircraft in their calculation periods. Or, each student or group of students can design jet transports to different specifications and then plot up their results as shown in Chapter V. The author has used the text, or the material comprising the text, in a senior course in "Airplane Design," for four years.

A comprehensive list of symbols and definitions is presented. It is felt that such a list is essential and time-saving for intelligent use of any engineering text, particularly to those who might use it as a reference.

I wish to acknowledge the assistance of all the aircraft, engine and propeller manufacturers in providing me with the data of their products for presentation in the text. I am indebted to the National Advisory Committee on Aeronautics for the material from their many publications. I want to thank Mrs. Edna Brothers for her help in the preparation of the text, and Dr. S. F. Shen for his advice on some technical problems.

TABLE OF CONTENTS

Preface	iii
Symbols	xv

Part I Aerodynamic Design

Chapter I. Introduction		
1-1	General - Importance of Judgment in Design	1:1
1-2	Procedures in Industry - Military	1:4
1-3	Procedures in Industry - Commercial	1:7
1-4	Presentation of Material	1:7
Chapter II. Subsonic Aerodynamic Design		
2-1	Design Method	2:1
2-2	Wing Thickness and Sweepback	2:2
	Thickness Ratio	2:4
	Sweepback	2:4
	Coefficient of Lift	2:5
	Aspect Ratio	2:6
	Effect of M_{CRD}	2:8
	Determination of Thickness Ratio and Sweepback	2:8
2-3	Wing Loading	2:12
	Refinement to Landing Distance Calculation	2:20
	Verification of Assumed Cruise C_L	2:22
2-4	Thrust Loading	2:23
	One Engine Inoperative	2:26
2-5	Weight Estimation	2:27
	Structural Weight	2:28
	Power Plant Weight	2:30
	Fuel Weight	2:33
	Payload	2:33
	Fixed Equipment	2:34
	Total Take-off Weight	2:34
2-6	Total Drag	2:35
	Parasite Drag	2:36
	Compressibility Drag	2:37
2-7	Range	2:37
	General	2:37
	Altitude	2:45
	Cruise at 35,000 ft.	2:46
	Climb	2:48

viii SUPERSONIC AND SUBSONIC AIRPLANE DESIGN

2-8	Fuel Storage	2:58
2-9	Climb Requirements	2:63
2-10	Optimum Airplane	2:66
	Selection of Criteria	2:66
	Direct Operating Cost	2:67
2-11	Optimum Altitude	2:72
Chapter III. Aerodynamic Design - Supersonic		
3-1	Design Method - General	3:1
3-2	Choice of Taper Ratio and Aspect Ratio	3:2
	Introduction	3:2
	Source of Data	3:3
	Method	3:4
3-3	Wing Loading	3:13
3-4	Thrust Loading	3:14
3-5	Weight Estimation	3:15
3-6	Total Drag - Theory	3:17
	Skin Friction Drag	3:17
	Wave Drag	3:17
	Drag due Normal Force	3:22
	Base Drag	3:23
	Total Drag	3:27
	Interference Effects	3:28
	Area Rules - General	3:28
	Transonic Area Rule	3:29
	Supersonic Area Rule	3:31
	Method of Reducing Interference Effect and Drag	3:32
	Total Drag - Calculation	3:34
	Skin Friction Drag	3:34
	Wave Drag	3:35
	Drag due Normal Force	3:36
	Total Drag	3:41
3-7	Range	3:41
	Cruise	3:41
	Climb	3:43
3-8	Fuel Storage	3:44
3-9	Climb Requirements	3:44
3-10	Optimum Airplane	3:44
3-11	Optimum Altitude	3:46

Chapter IV. Airplane Layout - Subsonic

4-1	Layout	4:1
4-2	Wing	4:1
	Plan form	4:1
	Mean Aerodynamic Chord	4:4
	Mean Aerodynamic Center	4:5
	Location of Spars	4:6
	Ailerons and Flaps	4:6
	Incidence	4:7
	Dihedral	4:11
	Airfoil Selection	4:13
4-3	Landing Gear	4:15
	Bicycle Type Gear	4:16
	Choice of Type	4:18
	Landing Gear Layout	4:19
	Main wheels	4:19
	Outrigger wheels	4:21
4-4	Vertical Location of Wing on Fuselage	4:23
	General	4:23
	Nacelle Arrangement	4:24
	Comparison of High Wing and Low Wing Designs	4:26
4-5	Fuselage	4:27
4-6	Nacelles	4:36
4-7	Tail Surfaces	4:38
4-8	Center of Gravity	4:41
	Center of Gravity Movement	4:43
	General	4:45

Chapter V. Airplane Layout - Supersonic, and
Aerodynamic Heating

5-1	Layout	5:1
	General - Conventional or Canard	5:1
5-2	Wing	5:3
	Plan Form	5:3
	Incidence	5:4
	Dihedral	5:4
	Airfoil Selection	5:5
5-3	Landing Gear	5:7
5-4	Vertical Location of Wing on Fuselage	5:8
5-5	Fuselage	5:9
5-6	Nacelles and Number of Engines	5:10
5-7	Control Surfaces	5:10
5-8	Center of Gravity	5:12

x **SUPERSONIC AND SUBSONIC AIRPLANE DESIGN**

5-9	Aerodynamic Heating - General	5:12
5-10	Nature of Problem	5:13
	Reduction in Allowable Stresses	5:13
	Thermal Stresses	5:14
	Reduction in E	5:15
	Change in Aerodynamic Properties	5:15
	Creep	5:16
	Effect of High Temperature on Passengers, Crew and Fuel	5:17
5-11	Methods of Alleviation of the Aerodynamic Heating Problems	5:18
	Major Portion of Outside Surfaces	5:19
	Leading Edge of Wing	5:20
	Nose of Fuselage	5:20
	Thermal Stresses	5:20
	Reduction in Rigidity	5:22
	Creep	5:22
	Effect of High Temperature on Passengers and Crew	5:22
Chapter VI. Special Problems		
6-1	Introduction	6:1
6-2	Navaer Method of Performance Calculation	6:1
	Thrust Required - Subsonic	6:2
	Thrust Required - Supersonic	6:3
	Engine Characteristics	6:3
	Method	6:4
6-3	Calculations of "f"	6:4
6-4	Take-off Distance	6:6
6-5	Cruise at Constant Altitude	6:9
Chapter VII. Discussion and Results		
7-1	General	7:1
7-2	Effect of Speed	7:2
	Take-off Weight	7:2
	Optimum Aspect Ratio	7:3
	Direct Operating Costs	7:4
7-3	Effect of Field Length	7:4
	Take-off Weight	7:4
	Aspect Ratio	7:5
	Direct Operating Costs	7:5
7-4	Effect of Payload	7:5
7-5	Effect of Range	7:6
7-6	Effect of Altitude	7:8
7-7	Theory of Max. W/S and W/T	7:9

TABLE OF CONTENTS

xi

7-8	Effect of Ground Deceleration	7:10
7-9	Take-off Distance	7:11
7-10	Equivalent Parasite Drag Area, "f"	7:11
7-11	Engine Choice	7:11
7-12	Airplane Efficiency Factor "e"	7:12
	Non-Elliptical Spanwise Air Distribution	7:12
	Trim Drag	7:13
	Drag due to Variation in Angle of Attack	7:13
	Determination of "e"	7:14
	Variation of "e" with A.R.	7:14
7-13	Supersonic Airplanes	7:15
	Effect of Gross Wt. on Range	7:15
	Effect of Cruise M on Gross Wt. and D.O.C.	7:15
Chapter VIII. Application of Methods to Other Types of Aircraft		
8-1	Introduction	8:1
8-2	General	8:1
8-3	Propellers	8:1
	Maximum Efficiencies	8:1
	Efficiencies of Individual Propellers	8:2
	Propeller Weights	8:5
	Definition of Propeller Efficiency	8:5
	Determination of Propeller Efficiencies	8:6
8-4	Reciprocating and Turbo Prop Transports	8:9
8-5	Bombers	8:20
8-6	Fighter or Interceptor	8:29
8-7	Private Planes	8:30
8-8	Executive Planes	8:38
8-9	Missiles	8:38

Part II

Chapter IX. Stability and Control

9-1	Introduction	9:1
	Controlability	9:1
	Stability	9:1
	Definition of Stability and Equilibrium	9:2
	General	9:3
9-2	Longitudinal Dynamic Stability	9:4
	Longitudinal Equations of Motion	9:4
	The Differential Equations	9:5
	Solutions to the Simultaneous Differential Equations (stick-fixed)	9:8
	Significance of λ	9:10

	Significance of Coefficients of Quartic	9:11
	Stick-Free Longitudinal Stability	9:13
	Stability Derivatives	9:14
	Outline of Stability Analysis	9:14
9-3	Motions of the Airplane	9:15
9-4	Significance of the Usual Motions	9:16
9-5	Variation of Parameters - Stability Diagrams . .	9:18
	Longitudinal, Stick Fixed - Phugoid Mode . . .	9:18
	Lateral - Stick Fixed, Spiral Mode and Pure Divergence	9:19
9-5a	Effects of Flexibility	9:20
9-6	Static Stability - Introduction	9:21
9-7	Method	9:22
9-8	Longitudinal Stability	9:22
9-9	Stick Fixed Longitudinal Stability	9:24
	Wing Effect	9:26
	Tail Effect	9:27
	A.R. Effect on Slope of Lift Curve	9:28
	Sweepback Effect on Slope of Lift Curve	9:29
	M Effect on Slope of Lift Curve	9:32
	Evaluation of $d\epsilon/d\alpha$	9:33
	Fuselage and Nacelles	9:35
	Stick Fixed Neutral Point	9:36
	Power Effects - General	9:37
	Direct Thrust	9:37
	Normal Forces at Duct Inlet	9:38
	Jet Induced Downwash at Horizontal Tail	9:39
	Net Effect of Thrust	9:39
9-10	Controlability in Landing	9:40
	Ground Effects	9:44
9-11	Design Parameters	9:45
9-12	Longitudinal Stability - Stick Free	9:46
	General	9:46
	Neutral Point	9:48
9-13	Effect of Thrust on Center of Gravity Limits . . .	9:49
	Forward Center of Gravity	9:50
	Aft Center of Gravity	9:51
9-14	Optimum Position of Center of Gravity	9:52
9-15	Canard Type Airplane	9:53

Chapter X. Directional and Lateral Stability and Control,
and Maneuvering Flight

10-1	Introduction	10:1
10-2	Directional Stability and Control	10:1
10-3	Lateral Stability and Control	10:4
	General	10:4
	Dihedral Effect	10:6
	Aileron Control	10:7
	Aileron Reversal Speed - Spoilers	10:9
10-4	Maneuvering Flight	10:10

Chapter XI. Supersonic Effects on Stability and Control

11-1	Introduction	11:1
11-2	Longitudinal Stability and Control	11:1
	Static	11:1
	Dynamic	11:2
11-3	Lateral Stability and Control	11:5
	Directional	11:5
	Aileron Control	11:6
	Lateral Dynamic Stability	11:8
	Spiral Divergence	11:8
	Dutch Roll	11:9
	Rolling Instability	11:11
	Physical Aspects of Cross-Coupling	11:11
	Analysis	11:13

Part III Loads

Chapter XII. Loads

12-1	Introduction	12:1
12-2	General	12:1
12-3	Load Factors	12:2
	General	12:2
	Maneuver	12:3
	Gust - Straight Wing	12:4
	Gust - Sweptback Wing	12:8
12-4	Airloads - Wing and Tail General	12:10
	Gust Loads - Wing and Tail	12:10
	Maneuver Loads - Wing and Tail	12:10
12-5	Airloads - Horizontal Tail, Maneuver	12:11
12-6	Maneuvering Balanced Condition	12:13
	General	12:13
	Damping Tail Load	12:13
	Tail Load due Moment	12:17
	Total Load due α	12:18

	Equilibrium Equations	12:18
	Determination of Tail Loads	12:19
12-7	Maneuvering Pitching Conditions	12:21
	General	12:21
	Derivation of Equations	12:22
	Determination of α	12:25
	Evaluation of Tail Loads	12:26
	Effects of Flexibility	12:31
	Effect of Canard Design	12:32
12-8	Spanwise Load Distribution	12:33
	Flexible Sweptback Wing	12:35
12-9	Critical Conditions	12:36
	Symmetrical Flight	12:36
	Unsymmetrical Flight	12:37
	Reduced Loads	12:39
	Reduced Weight	12:39
12-10	Effect of High Lift Devices	12:42
12-11	Vertical Tail Loads	12:43
12-12	Engine Loads	12:46
12-13	Pressurized Cabin Loads	12:47
12-14	Control Systems Loads	12:47
12-15	Ailerons, Flaps, Tabs and Fins	12:49
12-16	Ground Load Specifications	12:49
12-17	Ground Load Determination	12:54
	Static Conditions	12:54
	Dynamic Conditions	12:55

SYMBOLS

This list, divided into two groups, English and Greek, is presented to aid in understanding the text. In the cases where a symbol is used only once in the text and explained there, it is not included in this list.

English Symbols

a	acceleration slope of lift curve, $dC_L/d\alpha$	C_{h_0}	hinge moment coefficient at $\alpha = 0$
a_t	slope of lift curve of tail	C_m	pitching moment coefficient
a_w	slope of lift curve of wing	$C_{m_{c.g.}}$	pitching moment coefficient about the center of gravity
a.c.	aerodynamic center	C_n	yawing moment coefficient
A.R.	aspect ratio = b^2/S	C_p	power coefficient
A.F.	activity factor	C_{p_x}	effective power coefficient
A-T	airplane minus tail	C_l	rolling moment coefficient
b	wing span - tip to tip	C_y	yawing moment coefficient
c	specific fuel consumption, chord speed of sound	C_D	total drag coefficient - 3 di- mensional body
c_c	chord at center line	C_{D_i}	induced drag coefficient = $\frac{C_L^2}{\pi A Re}$
c_t	chord at tip	C_{D_p}	parasite drag coefficient = f/S
c_d	total drag coefficient - 2 di- mensional body	$C_{D_{comp}}$	drag coefficient due to com- pressibility of medium
c_l	lift coefficient - 2 dimen- sional body	C_L	lift coefficient - 3 dimensional body
c_{l_a}	section lift coefficient de- pendent on α	$C_{L_{max}}$	maximum lift coefficient
c_{l_b}	section lift coefficient de- pendent on airfoil section	$C_{L_{sw}}$	lift coefficient of swept surface
c.g.	center of gravity	$C_{L_{unsw}}$	lift coefficient of unswept surface
C_f	equivalent parasite drag coefficient	$C_{L_{T.O.}}$	lift coefficient at take-off
C_h	hinge moment coefficient	C_{HT}	horizontal tail volume coefficient
C_{h_α}	floating tendency of surface		
C_{h_δ}	restoring tendency of surface		

xvi SUPERSONIC AND SUBSONIC AIRPLANE DESIGN

C_N	side force coefficient normal force coefficient	l_{VT}	distance from wing a.c. to vertical tail a.c.
C_{VT}	vertical tail volume coefficient	L/D	lift drag ratio; also equal to C_L/C_D
C.A.A.	Civil Air Authority	m	mass
C.A.B.	Civil Air Board	M	Mach Number = $\frac{\text{speed}}{\text{speed of sound}}$ $= \frac{V}{c}$
C.A.M.	Civil Air Manual	M_{crit}	critical M = Free stream M at which local velocity over body first reaches $M = 1$
C.A.R.	Civil Air Regulation	M_{CRD}	Mach critical drag = free stream M at which $C_{D_{comp}}$ reaches .0020
D	drag, lbs., diameter	M_{CRD_0}	M_{CRD} at $C_L = 0$ and no as- pect ratio effect
$\frac{d}{d(t/\tau)}$	$\frac{d}{d(t/\tau)}$	M_{CRL}	Mach critical lift = free stream M at which C_L reaches a peak
D.O.C.	direct operating cost	M_{HS}	High speed M
e	airplane efficiency factor	M_{50}	M equivalent to 50 m.p.h.
f	equivalent parasite drag area = wetted area times C_f	MAC	Mean aerodynamic chord
F	force = Ma	n	load factor
F_s	stick force	Δn	load factor increment = a/g change in n
g	acceleration of gravity = 32.2 ft/sec^2	N	rotational speed in revolutions per minute
HM	hinge moment	N_c	number of crew
i	angle of incidence - the angle that the chord line of the surface makes with the center line of the fuselage	N_e	number of engines
i_t	angle of incidence of tail	N_p	number of passengers
i_w	angle of incidence of wing	N_0	stick fixed neutral point - c.g. location at which dC_m/dC_L = 0 with stick fixed
j	correction factor to slope of lift curve, dependent on M	N'_0	stick free neutral point - c.g. location at which dC_m/dC_L = 0 with stick free
JT-1 en- gine	jet engine used in the jet transport airplane	P	load, lbs, payload tons
J-1 engine	jet engine upon which all the JT-1 engines are based	R	range, statute miles
K	correction factor: used throughout text with and without subscripts. Ex- plained wherever presented	R/C	rate of climb
L	lift, lbs.	s	shear flow - pounds/inch
l	length		
l_{HT}, l_t	distance from wing a.c. to horizontal tail a.c.		

S	area shear, lbs.	V_{NE}	never exceed velocity
S_w	wing area	V_{50}	velocity over the 50 foot obstacle
S_{HT}	horizontal tail area	V_{TD}	velocity at touch down
S_{VT}	vertical tail area	V_D	dive velocity or max. velocity to be demonstrated
S_e	elevator area	V_{SO}	stalling velocity; velocity at C_{Lmax}
S_f	flap area	V_{S1}	stalling velocity in m.p.h. with flaps in position for particular flight condition being considered
S_G	distance on ground; ground run	$V_{L/Dmax}$	velocity at maximum lift drag ratio
S_{50}	distance required to descend from 50 foot obstacle	W_0	initial weight
S_F	field length required for landing	W_1	final weight
SHP	shaft horse power	W_a	weight of airframe
t	thickness	W_e	weight empty
t/c	thickness ratio = thickness/ chord	W_{eng}	weight of engine
t/c _{str}	streamwise t/c; t/c along the line of the free stream velocity	W_f	weight of fuel
T	thrust torsion absolute temperature	W_{fe}	weight of fixed equipment
T_e	thrust per engine	W_{pp}	weight of power plant
T_a	thrust available	W_{str}	weight of structure
T_r	thrust required	W/S	wing loading = weight/wing area. The W/S of an airplane refers to the take-off W/S unless otherwise specified.
T.R.	taper ratio = $\frac{c_t}{c_c}$	$(W/S)_{land}$	wing loading at landing weight
T.H.P.	thrust horse power	$(W/S)_{TO}$	wing loading at take-off weight
u	velocity component in x direction	W/T	thrust loading = weight/ thrust. Unless otherwise specified refers to take-off weight and sea level, static, standard day take-off thrust
U	gust velocity in feet per second	$X_{c.g.}$	distance between the c.g. and the leading edge of the MAC, divided by the MAC
V_C	cruise velocity	$X_{a.c.}$	distance between the a.c. and the leading edge of the MAC, divided by the MAC
V_f	velocity with flap extended		
V_g	glide velocity		
$V_{H.S.}$	high speed velocity		

X	adjustment factor for power y coefficient, C_p , dependent on AF	spanwise distance from centerline of wing
	Y	yawing moment



Greek Symbols

α	angle of attack
α_0	angle of attack - 2 dimensional body
β	angle of side slip
δ	pressure ratio = $\frac{\text{pressure at altitude}}{\text{pressure at sea level on standard day}}$
γ	angle between horizontal and flight path
δ_e	elevator deflection; up is negative
δ_r	rudder deflection
Δ	change; i.e. ΔM_{CR_D} is change in M_{CR_D}
ϵ	angle of downwash
ζ	factor correcting slope of lift curve
η	propeller efficiency
η_t	tail efficiency factor
θ	temperature ratio = $\frac{\text{abs. temp. at altitude}}{\text{abs. temp. at sea level on standard day}}$ angle of climb angle of pitch; angle between horizontal and reference line
$\sqrt{\theta}$	$\frac{\text{speed of sound at altitude}}{\text{speed of sound at sea level on standard day}}$
Λ	angle of sweepback
$\Lambda_{\frac{1}{4}c}$	angle of sweepback along the quarter chord
μ	coefficient of friction = .020 for rubber rolling on concrete
μ_g	airplane mass ratio
ν	kinematic viscosity - see fig. 2:26
ρ	density
σ	density ratio = $\frac{\text{density at altitude}}{\text{density at sea level on standard day}}$ axial stress
τ	$m/\rho SV$
ϕ	angle of bank correction factor for C_{D_1} dependent on T.R.

PART I
AERODYNAMIC DESIGN

Chapter I

INTRODUCTION

1-1 General: Importance of Judgement in Design

Airplane design is the application of the fundamentals of aerodynamics, structures, power plant, stability and control, based upon a certain degree of judgement and experience of the individual designer. All designers have practically the same sources of information and therefore essentially the same basic data. However, airplanes designed to the same specifications may, and do, vary radically, depending upon the individual designer. Evidently this variation in design must be a result in the difference in judgement and experience of the designer.

This difference in design, which is a result of judgement and experience, shows up in two areas. One is the area where there is little known or established data at the time the design is being initiated. Very often it is not possible for the design to wait for the establishment of this data. In this field the designer must use the best available material, and judgement which borders on intuition. The second area where judgement must be used is where a change in one criteria will cause variations in two or more characteristics which are of such different character that an exact solution to determine the optimum design is not possible.

A very simple example is in the choice of passenger seating arrangement in a commercial transport. Unquestionably it is desirable to design the airplane so that the passengers will be comfortable, although the exact degree of comfort desirable is not established. Practically every factor that tends to make the passenger more comfortable such as more space per passenger, more luxurious seats, etc., results in an increase in either airplane weight or drag or both, any of which is undesirable. It evidently is impossible to determine a formula which would relate the variation in weight or drag to passenger comfort. Therefore, the choice of seat arrangement depends upon the judgement of the designer. He must decide how much he is willing to sacrifice in passenger comfort to increase the efficiency of the airplane.

At this point an example of a mathematical solution must be presented so that a false impression is not obtained that all designs are based on judgement. The choice of aspect ratio is a

comparatively good example.

The main disadvantage to increasing aspect ratio is the resulting increase in weight. The greatest advantage is the resulting decrease in induced drag. At first these characteristics of weight and drag appear completely dissimilar. However, for the same specifications, airplanes may be designed with different wing aspect ratios, and the only significant difference will be in their final take-off weight. For some types of planes take-off weight is a good criteria for choosing the optimum, the smaller the weight, the better. For a commercial transport, a change in the direct operating cost, a better criteria for choice of the optimum, may be determined with change in aspect ratio. In this case a direct operating cost is calculated for each aspect ratio, and the aspect ratio that results in the minimum direct operating cost is evidently the best. This is an example of a mathematical solution that does not depend upon the judgement of the designer.

In the design of the jet transport as presented in this text, wherever possible an analytical method of solution such as indicated with the aspect ratio, is presented. As will be seen in the text, most of the design is accomplished by an analytical approach, although a considerable portion of it is dependent upon the judgement of the designer. Before a decision can be made there are the definite advantages and disadvantages of each characteristic that must be considered. In these cases the advantages and disadvantages will be presented, and a choice of criteria made for the design of this particular airplane. It must be emphasized that this choice is based upon the judgement of this designer for this particular airplane. The same advantages and disadvantages might result in a different choice by the same designer for a different set of specifications. Again the seating arrangement presents a simple example.

For a commercial transport that requires one half-hour flight, the passenger seats might be placed 36 inches apart. This is considered quite close and does not allow the passenger to stretch his legs a great deal. For a flight of one half-hour the passenger probably would not mind this inconvenience, and the resulting decreased weight and drag could result in either larger profit for the airline, or a lower fare for the passenger, or both. However, for a commercial transport that was flying non-stop from New York to London and might require an eight hour flight, a 36-inch seat spacing would probably result in such discomfort that it would be intolerable, indicating a seat spacing of possibly 40 to 44 inches. The advantages and disadvantages involved in

this choice are quite evident and simple to determine. However, this is not typical, as the problems in airplane design are usually much more complex.

In the cases where the judgement of the designer must be relied upon, not only will the advantages and disadvantages be presented, but wherever possible some reference to some established work will be made. However, it is the nature of the subject of airplane design, especially in an up-to-date design as exemplified by a commercial jet transport, that often such references are not available. Therefore, in many instances it is necessary to present all the advantages and disadvantages and then merely to state, that, considering these advantages and disadvantages, it has been found that a certain value of this criteria is close to the optimum for this particular airplane for the specifications presented. It does not imply that the value is the optimum for any other type of airplane. It only implies that it is felt that it is the best solution for this particular airplane at this particular time.

The judgement of the designer has been shown to play a vital role in the evolution of an airplane; it is in fact the characteristic that differentiates an outstanding engineer from the average one. Where does good judgement come from and how is it developed? Unquestionably this is a characteristic that is developed through many years and by various devices. However, an engineer's judgement can be developed and improved continually by approaching each problem in the following manner:

1. study the available material pertinent to the subject.
 2. a. make a decision based upon this material without being unduly influenced by the status quo; that is, seriously question whether previous solutions to a similar problem were correct when made; and more important, that even if correct then, whether it is correct now under a changed environment and with the new knowledge since unearthed.
- and b. using your own ideas and capabilities do what you feel is correct without fear of criticism from the promoters of the status quo.

Decisions like these must be made in your daily life in regard to your home, your family, and your politics, as well as in school and at work. If you practice making thoughtful decisions based upon the material available, and reasoning, not on emotion or conventionality, and do it from day to day in all your fields of endeavor, you will unquestionably improve your judgement and

increase your percentage of correct decisions.

Often one of the difficult decisions to make is when to stop collecting material and make a final decision. There are always pressures of time and efficiency that affect how much material can be gathered before the decision must be made. Here again reason, and the sound use of previous experience, will aid in arriving at better decisions, and improve your judgement.

1-2 Procedures in Industry - Military

Although the detailed procedures of preliminary design vary for the different types of airplanes and between different companies, the over-all methods are essentially the same. For a military airplane, the specifications may be set by the procurement division of the Air Force and sent to the aircraft companies to compete for the contract. These specifications might include any combination of the following: speeds, range, payload, field length, rate of climb, maximum weight, altitude and type of engines. The management of each company then decides whether or not it is interested in entering the competition to attain a contract. Its decision depends upon many factors: the experience of the company in that particular branch of airplane design and manufacture; the availability of their engineering personnel to make the study required; the availability of factory space and manpower to manufacture the planes if a contract is obtained; the possibilities of mass production of the plane, that is, if there will be a continuing demand for that type of airplane; and lastly, if the required investment in time to make a proposal is warranted by the chances of obtaining the contract. If it is decided that a proposal is to be made in this competition, the specifications are then sent to the preliminary design group for study.

The design engineer must then make a preliminary design of the most efficient airplane to meet these requirements, and exceed them if possible. It is required that a general arrangement of the airplane be made indicating all significant data. Figure 1:1 shows a typical general arrangement, or three view, drawing.

With this drawing the performance of the airplane must be presented. Besides the characteristics of speed, range, etc. that might be specified in the requirements, data on center of gravity, stability and control and other significant items must be submitted. In preparing for the design to be submitted in competition with the designs of other companies, the designer gathers all the up-to-date data available on specific engines available,

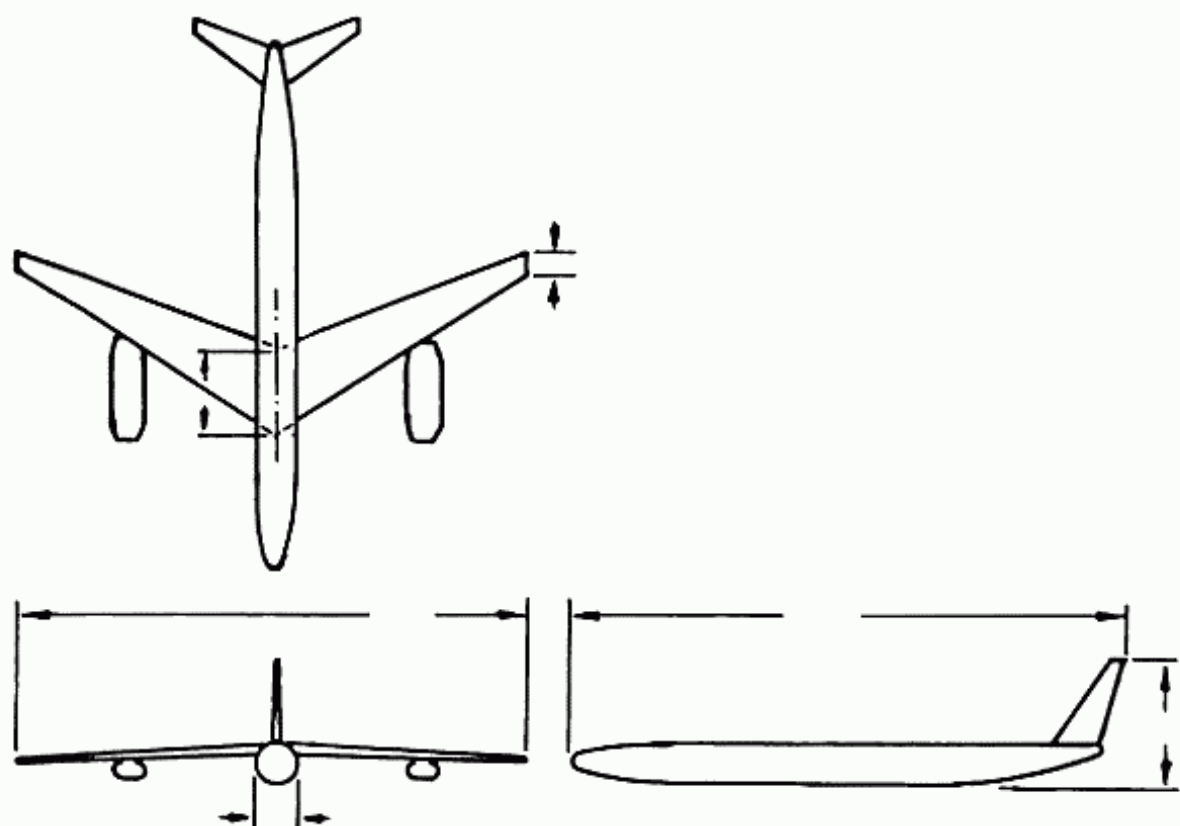


Fig. 1:1.

on aerodynamics, and on structures. This data takes the form of specifications of engine manufacturers, NACA reports, company studies and the designer's own personal experience. The engine characteristics are usually only preliminary design data, as the airplane will not fly from two to four years from the time of the proposal study and the most advanced engine design is desired.

It is desirable to have the airplane as efficient as possible, and therefore to arrive at the specific characteristics by as scientific a method as is available. Different values of wing aspect ratio, sweepback and thickness ratio combination, wing area and engine type and size may be tried and the optimum values of each obtained. Other factors as to type of landing gear, vertical position of wing on fuselage and number of engines may be studied. For many of these factors the final choice must rely upon the judgement of the designer based upon the results of these studies.

The design of the airplane is accomplished by a series of trials and errors in the design of many items. This is necessary because of the complex interrelation between the different parts of the airplane. A most significant example is the determination

of the airplane take-off weight. The weight cannot be calculated until the airplane is designed and drawn up. Yet the airplane cannot be designed and drawn up until the take-off weight is known. The only procedure available is to estimate a take-off weight based upon judgement, design an airplane based on this weight, and then have the weight checked for this design. This preliminary weight check is usually done by the preliminary weights department. They do a rough stress analysis to determine the weights of the wing and fuselage. They depend upon the manufacturer's estimates for engine weight and upon charts and calculations for estimating the weights of other items. If this weight does not check the original estimate, the design must be changed until the weight used in the design is equal to the preliminary weight group's calculated weight.

This method of trial and error, or it could probably be called investigation or study, presents itself throughout the entire airplane design. The weight of fuel necessary to accomplish the desired range must be estimated and the range calculated. If the range is not correct the weight of fuel must be changed to reach the desired range. This change in fuel weight changes the take-off weight and the entire design again. Many of these items are presented in greater detail in Chapter II, and actual methods obtained. Although much of this procedure is trial and error, there is some background and data from which the first intelligent estimate can be made. The closer to correct the first estimate, the less work is involved in obtaining the correct solution.

In some companies, after the preliminary design group with the aid of the preliminary weights group has decided on a complete design, the performance and weights are checked by the aerodynamic and structures groups. When all agree to the final presentation, a proposal is submitted to the Air Force. It is from these proposals that the Air Force decides which company or companies shall receive an experimental contract. Besides the actual proposal, which is checked by the Air Force, the reputation for reliability in design and manufacture of the individual company is carefully weighed in subletting contracts.

It must be realized that after the company receives a contract, the work just begins. The preliminary design might require anywhere from 1,000 to 10,000 man-hours depending upon the type and size of airplane, while the man-hours required for a complete design from which the airplane is built reaches tremendous figures. The Boeing B-52 jet bomber required 2,000,000 man-hours.

1-3 Procedures in Industry - Commercial

The procedure for designing a commercial airplane is quite similar to that of designing a military airplane, with one major difference. In the military, the procuring agency sets the requirements, and only on occasion might they modify them a little under the industry's pressure. However, in the commercial field the manufacturer himself sets the requirements so that he can sell as many of that type of airplane as possible. The advice and comments of the airlines are sought but the final decision rests with the company.

This one difference in design requires much more effort of the design department. An extensive scientific study of different designs and a survey of the airlines' opinions, practices and costs must be made to determine which airplane should be built. After the specifications of speed, range, number of passengers and field length are agreed upon, these are the most important requirements, there is still another factor that distinguishes the design of commercial airplanes from the military airplanes. This is the choice of criteria that should be used in determining the best airplane.

In the military, if two airplanes are designed to meet the specified requirements, the choice of the better airplane might depend on many items; the maximum weight, the maximum size, ease of manufacture, the possibility of increasing the speed and range with time, the cost of manufacture and its use of fuel. In the commercial field it can be boiled down to one factor, profit for the operating airline. This can be represented by the direct operating costs, which will be discussed in greater detail later in the text. This direct operating cost is a convenient and significant criteria for choosing the optimum airplane.

1-4 Presentation of Material

As explained in the preface, the jet transport has been chosen as the best type of airplane to be used as an example in presenting airplane design.

The important specifications for a commercial transport are:

- 1) Number of passengers and weight of cargo.
- 2) Range
- 3) Field length
- 4) Cruising speed and altitude

If less than the above criteria is specified, a lengthier study is required since another variable would be introduced. The main portion of Part I presents the method of designing a jet trans-

portion of Part I presents the method of designing a jet transport assuming the above four requirements are specified. Chapter VI presents comprehensive data that can be used to design reciprocating or turbo-prop engine transports and military aircraft, as well as small private planes.

For design purpose, many charts and formulas have been derived to facilitate the calculations. Those that are based upon true mathematical derivations are presented in the text. However many are based either upon empirical data or a combination of empirical and theoretical data. These charts and formulas are therefore often dependent upon the characteristics of the airplane or component used in obtaining the empirical data.

Before an analytical study is made to determine the characteristics of the airplane that are necessary to meet the specifications, some general decisions can be made even before the exact specifications are known. These items are among those that finally depend upon the judgement of the designer. A general layout of the fuselage, the number of engines and nacelles, the wing airfoil series and the landing gear type fall in this category. A detailed discussion of each of these items will be presented in a more appropriate section of the text, Chapter III, and V, relating to layout of supersonic and subsonic aircraft.

Chapter II

SUBSONIC AERODYNAMIC DESIGN

2-1 Design Method

In the design of the airplane, it would be convenient and simple if an exact solution could be reached with the first estimate. However, due to the interrelation of different components of the airplane to each other and to the airplane as a unit, this is impossible. The data and method presented permit the engineer to design the optimum airplane with the minimum amount of calculations. Since the design is dictated by the specifications, it follows a pattern of characteristics dependent on these specifications. So that an overall picture of the design method may be obtained, a very brief outline of the method to be used is now presented. The following table shows the order in which the design characteristics are determined and the principal factors upon which these characteristics are dependent.

Design Characteristic	Dependent Factors
1) Wing Sweepback and Thickness Ratio	Speed
2) Wing Loading (W/S)	Landing field t/c , Λ
3) Thrust Loading (W/T)	Take-off field W/S , t/c , Λ
4) Take-off Weight	W/S , W/T , number of passengers, fuel weight
5) Drag	Number of passengers, S , T , W , speed
6) Range	Fuel weight, cruise speed and altitude, take-off weight, S , T
7) Direct operating cost	Take-off weight, S , T , number of passengers, range, cruise speed, weight of fuel
8) Optimum airplane	Direct operating cost, aspect ratio, combination of sweepback and thickness ratio

(1) Since wing sweepback and thickness ratio are the most important factors affecting compressibility drag, they are

2:2 SUPERSONIC AND SUBSONIC AIRPLANE DESIGN

chosen in combination and are dependent on the cruising speed required.

- (2) W/S , the take-off weight divided by wing area is the most important design characteristic used in determining landing field length. With the required field length known and certain factors, such as maximum lift co-efficient, ground deceleration and fuel weight, either estimated or established, W/S can be determined.
- (3) The take-off field length is dependent on W/T , the take-off weight divided by sea level, static thrust of the airplane, as well as W/S and maximum C_L . W/T can then be determined since the take-off length requirement is known.
- (4) The take-off weight can be determined from a relationship of W/T , W/S , number of passengers, fuel weight, number of crew, aspect ratio, sweepback, and thickness ratio.
- (5) The drag of the airplane is dependent on the wing area, thrust, number of passengers, cruising speed, cruising altitude, sweepback and thickness ratio.
- (6) The range can then be determined based upon the fuel weight assumed, and the thrust based on take-off requirements. If the thrust is not enough to attain the cruise speed required, W/T must be reduced. Also if the assumed weight of fuel does not yield the range required, the fuel weight must be revised.
- (7) For the airplane finally determined, the direct operating cost is calculated. This cost, usually in cents/ton mile, is dependent on take-off weight, wing area, airplane thrust, number of passengers, range, cruise speed and weight of fuel.
- (8) The optimum airplane is obtained by varying aspect ratio and sweepback-thickness ratio combinations to determine the airplane with the lowest direct operating cost.

2-2 Wing Thickness Ratio and Sweepback

The first choice that can be made is the combination of wing sweepback and thickness ratio. These characteristics are chosen in combination because together they determine the effect that compressibility of the air will have on the aerodynamic characteristics of the wing.

Although air is a compressible fluid, the design of slow speed airplanes, 250 knots or less is usually based upon the assumption that it is incompressible. This leads to a negligible error and is therefore completely justified. However in the design of jet transports, with cruising speeds of 350 knots and above, the effect of the compressibility of the air cannot be neglected. In

this study, the Mach number, which is equal to speed divided by the speed of sound, is an important characteristic.

Due to the shape of the airfoil, the local velocity of the air around the airfoil is greater than the free stream velocity. The Mach number of the free stream at which the local velocity on any point on the airfoil reaches the speed of sound is called the critical Mach number. The effect of compressibility on the forces on the wing at this critical Mach number is still small but increases significantly as the free stream Mach number increases beyond this point. Figure 2:1 shows the variation of the coefficient of drag, C_D , with Mach number for a typical wing at a constant C_L .

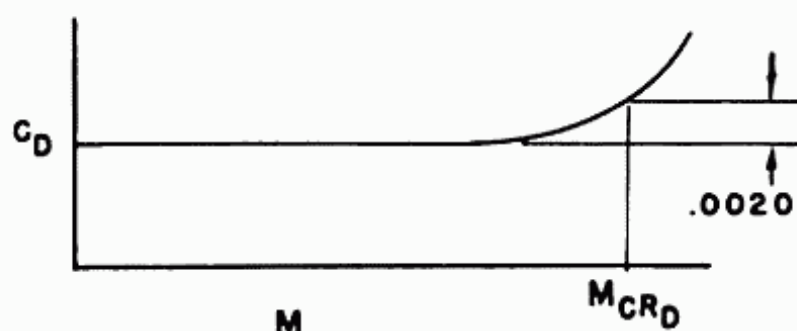


Fig. 2:1. C_D vs. M for typical wing. Ref.: RML7C24 "Effects of Combinations of A.R. and Sweepback at High Subsonic Mach Numbers" A.A. Adler, 1947.

It will be noted that C_D is shown to be constant until it begins to increase due to compressibility effects. Actually, C_D is not constant as shown, but decreases slightly due to the increase in Reynolds Number caused by the increase in velocity. (This effect will be discussed in greater detail in section 2:6).

For the following analysis it has been found convenient to define some point on this drag rise portion of the curve for reference purposes, and is referred to as the Mach critical drag, M_{CRD} . This M_{CRD} is the Mach number at which the C_D increases by $.002$ above the low speed C_D . Other criteria, such as the slope of the C_D versus M curve, or the increase in C_D as a percentage of the total C_D , present certain advantages but are not quite so easy to apply. The NACA has used the term drag divergence Mach number, M_{DD} , which is the M at which $dC_D/dM = 0.10$.

Fig. 2:2 shows the variation in C_L with M at a constant angle of attack for a typical airfoil. The M at which C_L reaches a maximum and then decreases is defined as the Mach critical lift, M_{CR_L} . This point cannot be calculated theoretically but has

been obtained from experiment. For some airfoils C_L decreases rather sharply beyond the Mach critical lift.

If an airplane is flown at a M greater than the Mach critical lift, care must be taken that an undesirable maneuver, the compressibility dive, does not occur. It is evident that this is no longer a serious problem as all supersonic airplanes pass beyond this point.

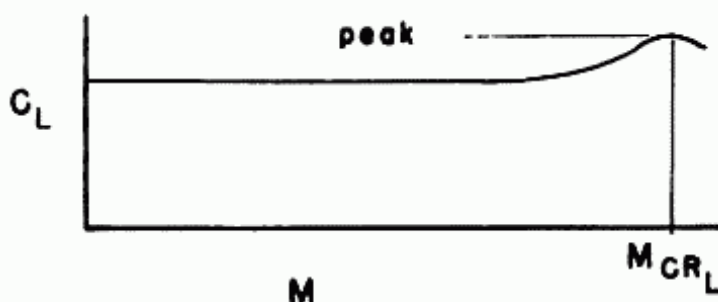


Fig. 2:2. C_L vs. M for typical wing. Ref.: T.N. 1739, "Comparison with Experiment of Several Methods of Predicting the Lift of Wings in Subsonic Compressible Flow" H. E. Murray, 1948.

Four characteristics that affect the critical Mach number are airfoil thickness ratio, wing sweepback, coefficient of lift and aspect ratio. Airfoil series, that is, the shape of the airfoil, also influences the critical Mach number.

Thickness Ratio

For the same free stream velocity, the local velocities around the airfoil increase as the thickness ratio increases. Therefore the critical Mach number of a thick wing is lower than for a thin wing.

Sweepback

The pressures on a wing of infinite aspect ratio and no taper is a function of the velocity perpendicular to the leading edge and is not affected by the flow parallel to it.

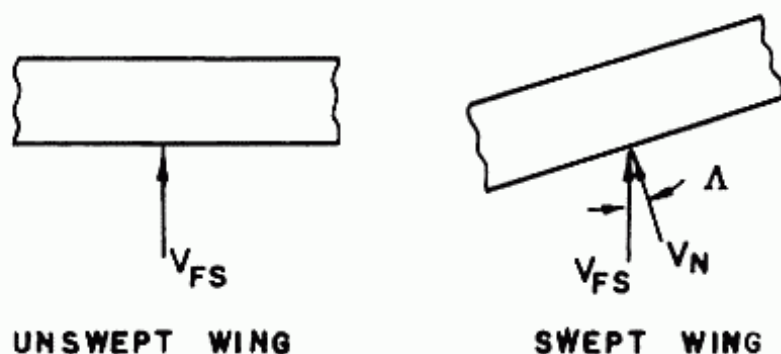


Fig. 2:4. Significant velocities over untapered wings.

From Figure 2:4 it can be seen that for a swept wing

$$V_{\text{normal}} = V_{\text{free stream}} \times \cos \Lambda \quad (2:1)$$

Therefore an untapered wing with its leading edge swept Λ^0 will have the same aerodynamic forces acting on it at a free stream velocity equal to $V_1/\cos V$, as an unswept wing with a free stream velocity equal to V_1 . For a tapered wing of finite aspect ratio, the full effect of $1/\cos V$ is not realized because of center line and tip effects. For a tapered wing, the leading edge sweepback is not the correct criteria for determining the forces on a wing. For practical purposes of design it has been found that if the quarter chord sweepback is used, satisfactory results are obtained. Figure 2:5 shows the significant velocities on a tapered wing. Since the velocity responsible for the forces on a swept-back wing is lower than on an unswept wing, the critical Mach number of the swept wing will be higher than for the unswept.

The data presented above for a sweptback wing is also true for a swept forward wing.

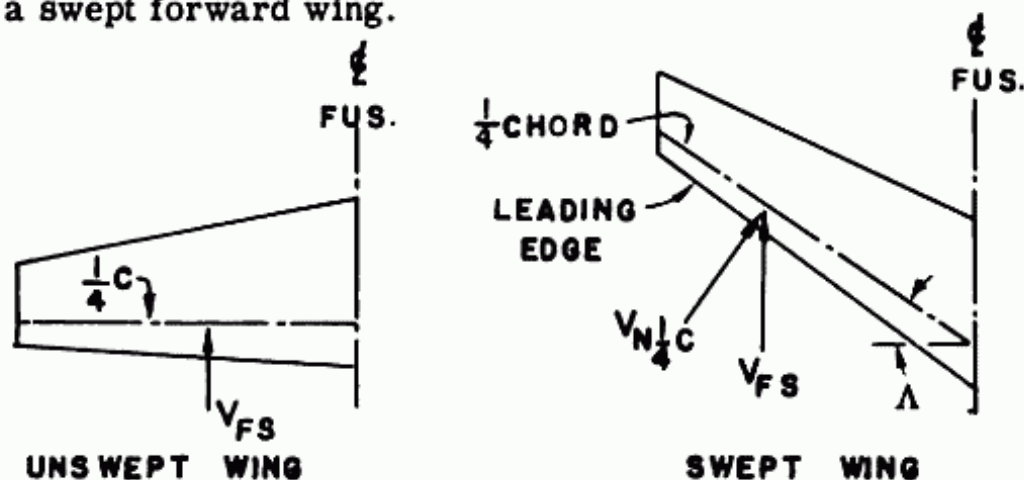


Fig. 2:5. Significant velocities over tapered wings.

Coefficient of Lift

The variation in critical Mach number with C_L must be determined. Figure 2:6 presents the chordwise pressure distribution on the upper surface of a typical airfoil for two coefficients of lift.

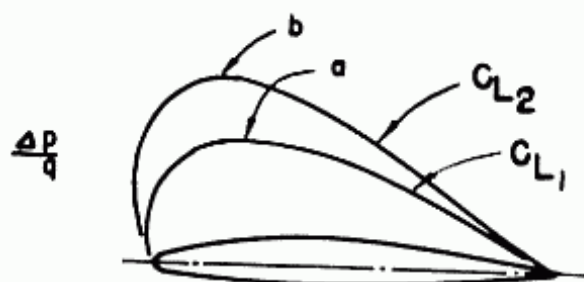


Fig. 2:6. Chordwise pressure distribution of a typical airfoil at two values of C_L .

Point a is the point of minimum pressure for C_{L_1} and b is the point of minimum pressure for C_{L_2} , where C_{L_2} is greater than C_{L_1} . Since a lower pressure corresponds to a higher velocity, the local velocity at point b is higher than at point a. Therefore the critical Mach number of the airfoil at C_{L_2} is lower than the critical Mach number at C_{L_1} .

Figure 2:7 shows the variation in Mach critical drag with lift coefficient for a typical wing. Although the values for this curve do vary somewhat depending upon the airfoil section and sweep-back, this curve is reliable for airfoils now in use and for sweep-backs of approximately 35° . It should be noted that ΔM_{CRD} due C_L varies from 0 to $-.10$. This is true since there is no effect on M_{CRD} at $C_L = 0$ and M_{CRD} decreases with increase in C_L .

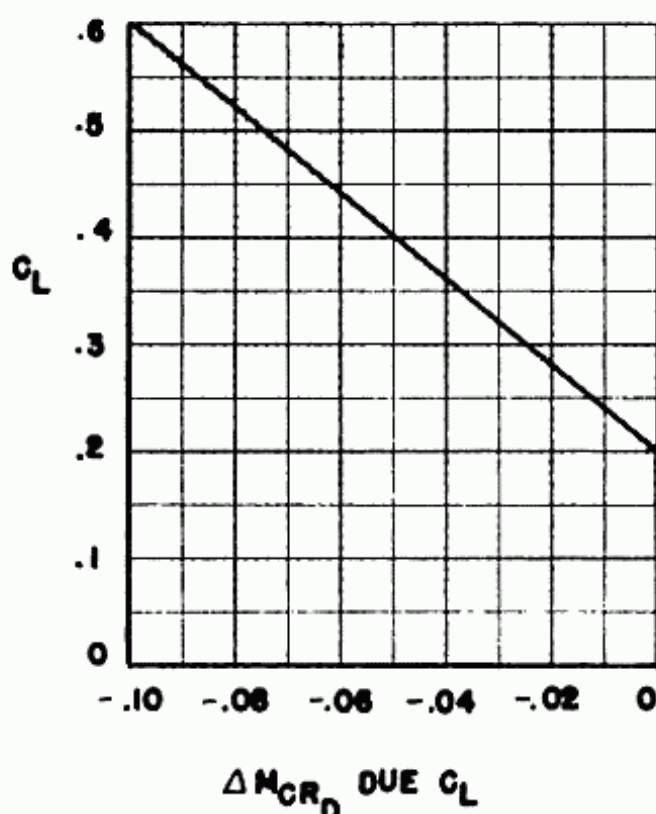


Fig. 2:7. Variation in M_{CRD} due to C_L . For references see explanation of Figure 2:9.

Aspect Ratio

At the wing tip of a finite wing there is an airflow from the high pressure side to the low pressure side. If the M_{crit} has been reached at some inboard point of the wing, that is, a certain

low pressure is present, the flow around the tip increases this pressure thereby increasing the value of the M_{crit} in this section. As the aspect ratio decreases, the portion of the wing affected is a greater percentage of the total and therefore the M_{CRD} for the entire wing is increased.

Figure 2:8 shows the trends obtained from a series of wind tunnel tests. Whereas ΔM_{CRD} due C_L as shown in Figure 2:7 is negative, ΔM_{CRD} due aspect ratio is positive. This is true since there is no effect on M_{CRD} at aspect ratio above 8.5 and M_{CRD} increases with decrease in aspect ratio.

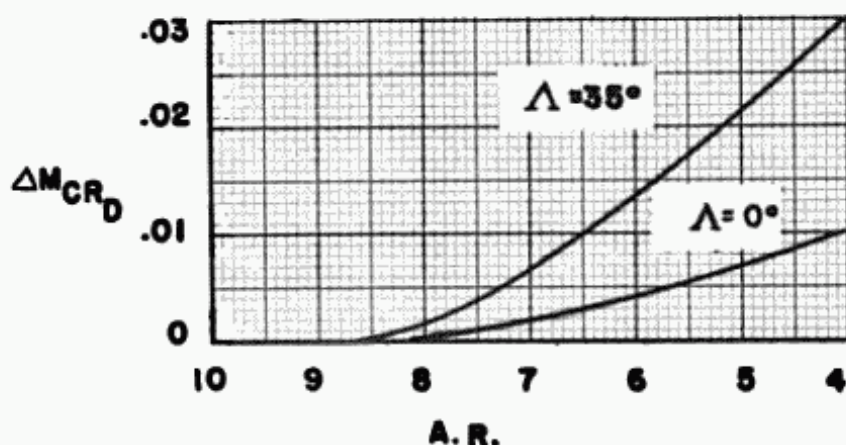


Fig. 2:8. Variation in M_{CRD} due to aspect ratio. For references, see explanation of Figure 2:9.

It should be noted that at aspect ratios above approximately 8.5 the effect of aspect ratio on M_{CRD} is negligible.

The effect of A.R. on M_{CRD} is also observed to be a function of sweepback. The change in M_{CRD} increases with larger sweepbacks up to approximately 35° . The use of sweepbacks greater than 35° with moderate aspect ratios is inadvisable in the design of jet transports in the speed ranges being considered because of added aero-elastic problems. Airloads cause the wing structure to deflect. On a swept wing these deflections can cause significant changes in the airloads. This interrelation between airloads and deflections is called aero-elasticity.

Effect on M_{CR_D}

A summary of the effect of the four factors, thickness ratio, sweepback, lift coefficient and aspect ratio is presented.

- 1) A decrease in thickness ratio causes an increase in M_{CR_D} .
- 2) An increase in sweepback causes an increase in M_{CR_D} .
- 3) $M_{CR_{D_0}}$ is the M_{CR_D} at $C_L = 0$ and no aspect ratio effect. As C_L increases from 0 to .2 there is no significant effect on M_{CR_D} . As C_L increases above .2 M_{CR_D} decreases.
- 4) There is no aspect ratio effect on M_{CR_D} for values of aspect ratio approximately 8.5 and above. As the aspect ratio decreases below 8.5, M_{CR_D} increases.

Determination of Thickness Ratio and Sweepback

The Civil Air Regulations state that " V_D should be sufficiently greater than V_C to provide for safe recovery from inadvertent upsets occurring at V_C . In the absence of a rational investigation the minimum value of V_D shall not be less than 1.25 V_C or $V_C + 61$ (knots), whichever is the greater in the altitude range between sea level and an altitude selected by the applicant. At higher altitudes it shall be acceptable to limit V_D to a Mach number selected by the applicant." This has been interpreted to mean that V_D , which must be demonstrated in flight, must be chosen so that it can be safely operated. As mentioned previously M_{CR_L} plays no part in this selection since for the airfoils used the drop-off in C_L beyond M_{CR_L} is very smooth and does not introduce any serious problems. The problems that may be encountered at V_D are those associated with stability, control, flutter and buffeting. And of course the airplane must be structurally sound at this speed.

The thickness ratio and sweepback combination must therefore be chosen so that it is economically efficient in cruise, and that it allows the airplane to be demonstrated safely at the chosen V_D . If V_D is chosen to be 50 knots greater than V_C for structural soundness and safety for demonstration purposes, and t/c and Λ are chosen so that compressibility $C_D = .0010$ at cruise it appears that an efficient airplane will result. This combination of V_C and V_D can, and will vary for different designers and different type airplanes. The one selected appears safe and economical for large commercial transports cruising at about 500 knots.

It should be noted that V_{NO} and V_C are assumed to be equal, and V_{NE} , the speed that should never purposely be exceeded, is assumed to equal $1.02 V_{NO}$. It has been established that the t/c and Λ should be of such a value so that $\Delta C_D = .0010$. Fig. 2:23 shows the variation in ΔC_D with ΔM , where $\Delta M = M_{CR_D}$ at $C_{L_{cruise}} - M_{cruise}$. Since $\Delta C_D = .001$, $\Delta M = .04$ from Fig. 2:23, that is, M_{CR_D} at cruising condition must equal $M_{cruise} + .04$. Therefore

$$M_{CR_D} = M_{cruise} + .04.$$

From this relationship the thickness ratio and sweepback can be determined.

Fig. 2:9 presents the variation of $M_{CR_{D_0}}$ with equivalent thickness ratio and quarter chord sweepback. $M_{CR_{D_0}}$ is the M_{CR_D} at $C_L = 0$, with no aspect ratio effect.

The data for Figures 2:7, 2:8 and 2:9, that is the effects of lift coefficient, aspect ratio, sweepback and thickness ratio on M_{CR_D} was obtained from many sources. The results of miscellaneous wind tunnel tests are available from numerous NACA reports. This data has been obtained for wings with various values of aspect ratio, sweepback, thickness ratio, taper ratio and lift coefficient. It must be realized that each of these tests were run for some specialized study and were not co-ordinated with each other in any manner. It therefore required an extensive study to isolate the effects of the significant parameters from each other. The following NACA reports were used in the study:

- | | |
|-----------|------------------------------------------------------------------------------------------------------------------------------------------------------------------------------------|
| T.M. 1102 | “High Speed Measurements on a Sweptback Wing” by B. Gothert, 1947. |
| T.R. 877 | “Summary Report on the High Speed Characteristics of 6 Model Wings having NACA 65 ₁ - Series Section” by Wm. T. Hamilton and W. H. Nelson, 1947. |
| RML7C24 | “Effects of Combinations of A. R. and Sweepback at High Subsonic Mach Numbers” by A. A. Adler, 1947. |
| RMA50K2Ba | “Effects of Increasing the Leading Edge Radius and Adding Forward Camber on the Aerodynamic Characteristics of a Wing with 35° Sweepback” by F. A. De Mele and F. B. Sutton, 1951. |

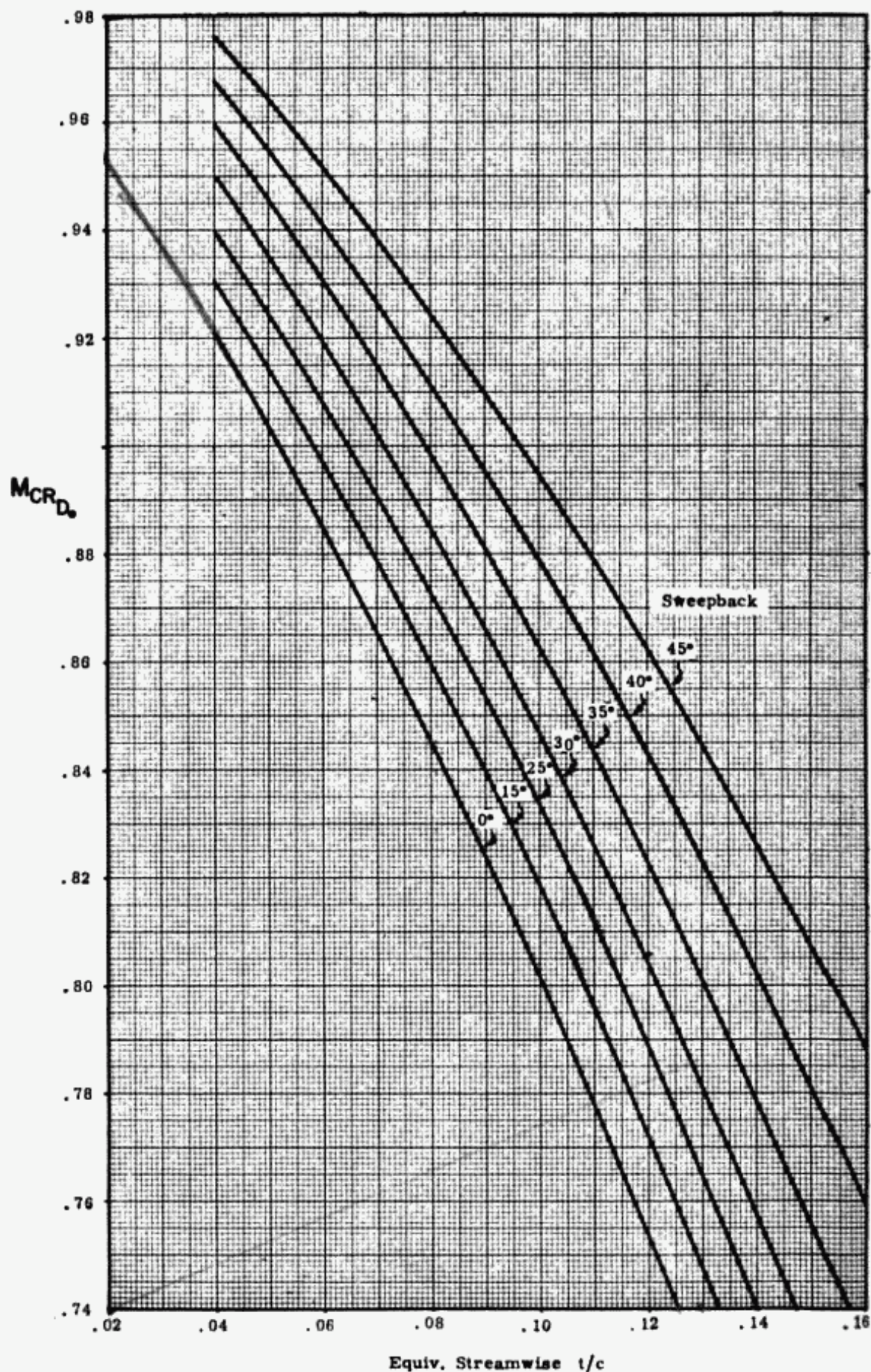


Fig. 2:9. Sweepback and thickness ratio as determined by $M_{CR_{D_0}}$.

- RMA50H23 "Wind Tunnel Investigation of Effects of a Jet Engine Nacelle on the Aerodynamic Characteristics of a 37.25° Sweptback Wing at High Subsonic Speeds" by F. Boltz and D. A. Buell, 1950.
- RML6K18a "Effects of 45° Sweepback on the High-speed Characteristics of a Wing Having a Modified NACA 16-012 Airfoil Section" by Luke L. Liccini, 1947.
- TN 3172 "Effects of Leading-Edge Radius and Maximum Thickness Chord Ratio on the Variation with Mach Number of the Aerodynamic Characteristics of Several Thin NACA Airfoil Sections" by Robert Berggren and Donald J. Graham, 1954.

It has been found that by varying the thickness ratio of the airfoil along the span of a sweptback wing, a more efficient wing results.

If the wing were rigid, due to sweepback the coefficient of lift would reach a peak value at some outboard section. At this point the critical M would first be reached, and the thickness ratio of the inboard sections could be increased until the M_{CRD} is the same for all sections of the span. However flexibility of the usual 35° sweptback wing throws the peak value of C_L inboard tending to cancel out the sweepback effect.

Nevertheless the t/c of a sweptback wing can be increased at the side of fuselage without increasing the M_{CRD} over the value of the two dimensional wing for two reasons:

- 1) the essentially free stream velocity along the body allows the increased velocity along the wing to be dispersed and therefore results in a higher local M_{CR} , and
- 2) a lower flow velocity in the forward section of the wing at side of fuselage due to the inherent outward flow near the leading edge of the wing due to sweepback results in a higher M_{CR} .

A 35° wing with airfoils of approximately .14 thickness ratio at the root, .10 at .45 of the semi-span and .08 at the tip has the same drag critical Mach number as a wing with an airfoil of .10 thickness ratio throughout. The .10 thickness ratio is the equivalent streamwise thickness ratio, as used in Figure 2:9. It will be noted that the wing with the larger root thickness ratio, where the bending moments are maximum, will be lighter. It is also more efficient for storing fuel. From the following equations

$M_{CR_{D_0}}$ can be determined for wings of aspect ratio = 8.5 or greater.

$$M_{CR_{D_0}} + M_{CR_D \text{ due } C_L} = M_{\text{cruise}} + .04 \quad (2:4)$$

where $\Delta M_{CR_D \text{ due } C_L}$ is negative as shown in Figure 2:7.

Therefore

$$M_{CR_{D_0}} = M_{\text{cruise}} + .04 - \Delta M_{CR_D \text{ due } C_L} \quad (2:5)$$

At this state of the design, the C_L of the airplane in cruise is not known. It is therefore necessary to use an estimated C_L which can be immediately checked in section 2:3, Wing Loading. With this assumed C_L , $\Delta M_{CR_D \text{ due } C_L}$ can be determined from Figure 2:7, and $M_{CR_{D_0}}$ calculated since M_{cruise} is specified in the airplane performance requirements. Knowing $M_{CR_{D_0}}$ the thickness ratio and sweepback can be chosen from Figure 2:9.

For aspect ratios smaller than 8.5 the thickness ratio and sweepback must be determined by trial and error. This is due to the fact that $\Delta M_{CR_D \text{ due } \text{aspect ratio}}$ is dependent on sweepback, and the sweepback is one of the variables. In the actual design this manipulation is avoided by first determining an optimum combination of thickness ratio and sweepback for aspect ratio equal ten, where there is no aspect ratio effect. This sweepback is then used in determining the optimum aspect ratio. This optimum airplane will be discussed more fully later in the text.

The effect of aspect ratios below 8.5 should be accounted for in determining the M_{CR_D} at $C_L = 0$. Then equation 2:5 becomes

$$M_{CR_{D_0}} = M_{\text{cruise}} + .04 - M_{CR_D \text{ due } C_L} - M_{CR_D \text{ due } A.R.} \quad (2:6)$$

where

$$M_{CR_{D_0}} = M_{CR_D \text{ at } C_L = 0} \quad \text{and} \quad A.R. \text{ effect} = 0$$

It should be noted that in choosing the t/c and Λ as indicated, taper ratio was assumed to have negligible effect since Λ was taken at the quarter chord, and the effect of A.R. was small.

2-3 Wing Loading

The landing wing loading, W/S , the landing weight divided by the wing area, can be determined by considering the field length requirements, specifically the landing distance.

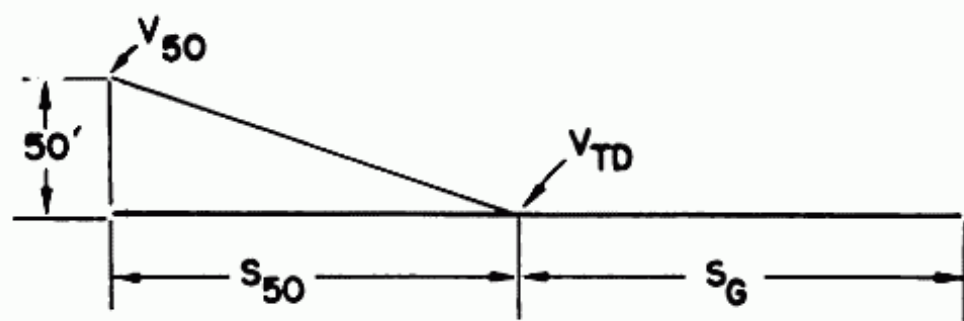


Fig. 2:10. Flight path in landing.

The landing distance specified by the Civil Air Regulations is the horizontal distance required to clear a 50 foot obstacle and then come to a complete stop. The distance can be divided into two parts, the descent from the 50 foot altitude to touchdown, and the deceleration distance to a complete stop. See Figure 2:10. Civil Air Regulations 4b* requires that at the 50 foot altitude a steady gliding approach be maintained at a true indicated airspeed equal $1.30 V_{SO}$, and at touchdown the speed shall equal $1.15 V_{SO}$. V_{SO} is the speed of the airplane at maximum C_L at the airplane weight being considered. These factors, 1.30 and 1.15, are used as safety factors to prevent a stall if, for any reason, the angle of attack of the airplane is increased.

Another factor of safety is employed by the Civil Air Regulations to account for variations from the optimum conditions and for variations in pilot technique. This specification is that the landing distance calculated be multiplied by 1/.6 to obtain the standard landing field required.

The descent distance is calculated by using the relationship that the change in kinetic energy + potential energy = retarding force x distance, that is

$$\frac{W(V_{50}^2 - V_{TD}^2)}{2g} + 50 W = F S_{50} \quad (2:7)$$

where W = landing weight in pounds

V_{50} = velocity at 50 foot altitude in ft/sec.

V_{TD} = velocity at touchdown in ft/sec.

S_{50} = horizontal distance required to descend 50 ft.

*Special Regulations SR 422

2:14 SUPERSONIC AND SUBSONIC AIRPLANE DESIGN

Therefore

$$S_{50} = \frac{W}{F} \left[\frac{V_{50}^2 - V_{TD}^2}{2g} + 50 \right] \quad (2:8)$$

Assuming that ϕ , the angle of descent is small enough to assume $\cos \phi = 1$, then the weight is equal to the lift. Since F , the retarding force is equal to the drag of the airplane, $W/F = L/D$. Using the relations $V_{50} = 1.30 V_{SO}$ and $V_{TD} = 1.15 V_{SO}$,

$$S_{50} = L/D (.0162 V_{SO}^2 + 50) \quad (2:9)$$

The deceleration distance on the ground may be calculated from

$$S_g = \frac{V_{TD}^2}{-2a} \quad (2:10)$$

$$= \frac{1.88 V_{SO}^2}{-a} \quad (2:11)$$

where $-a$ is the average deceleration in ft/sec.²
 V_{SO} is in knots

From the relations that

$$V_{SO}^2 = \frac{296 W/S}{\sigma C_{L_{max}}}; \quad \sigma \text{ is the density ratio} \quad (2:12)$$

$$S_F = \text{the landing field} = S_{50} + S_g \quad (2:13)$$

and using the factor of 1/.6, then

$$S_F = \frac{L}{D} \left(\frac{8.0 W/S}{\sigma C_{L_{max}}} + 83.3 \right) + \frac{925 W/S}{-a \sigma C_{L_{max}}} \quad (2:14)$$

To calculate W/S as a function of S_F the following characteristics must be evaluated: deceleration, maximum C_L and L/D .

The deceleration, $-a$, for a conventional design is primarily a function of the brakes and wheel sizes. For a conventional brake design, an average deceleration of 6 ft/sec² can be obtained for a jet airplane. A propeller driven airplane can increase this value to approximately 10 ft/sec² with the use of reversible pitch propellers. A jet airplane can increase the deceleration to about 8 ft/sec² with the use of a landing chute, and reverse thrust mechanisms on jet engines can also increase the average decelerations. Fig. 2:10a shows the variation in thrust that may be obtained with a particular type of reverser.

The maximum lift coefficient is a function of the airfoil section, the thickness ratio, the wing sweepback, the type of flap

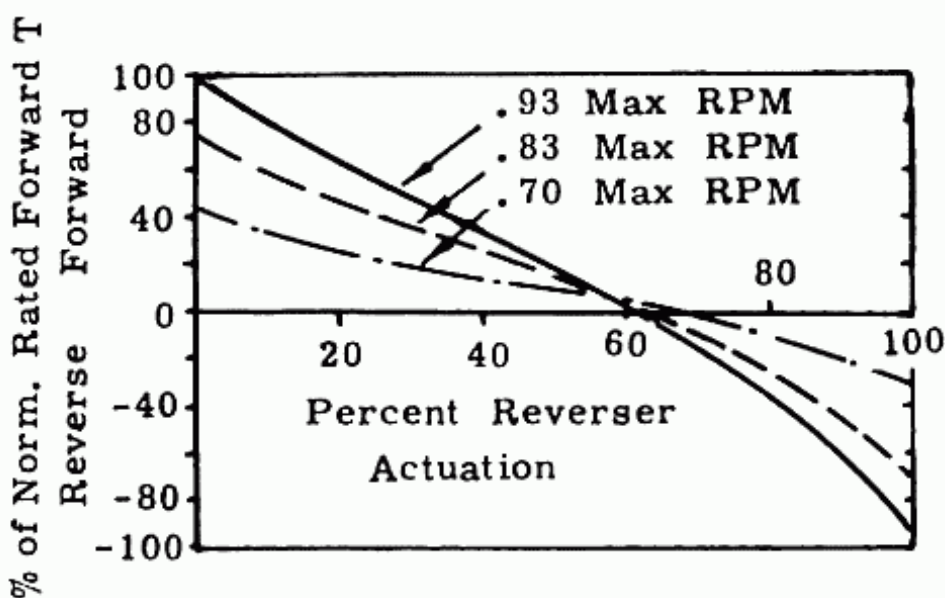


Fig. 2:10a. Effect of thrust reverser.

used and the amount of flap. The only criteria not known are those dealing with the flap. There are many varied types of flaps available for use, each with its advantages and disadvantages. A more detailed study of flaps is made in sections 4:2 and 10:3. However, at this time, the fowler flap has been chosen as the most suitable for this type of airplane.

Figures 2:11a and b show the variation of maximum C_L with sweepback, thickness ratio and flap area/wing area. The data for Figure 2:11 a has been obtained from wind tunnel tests of an airfoil with moderate camber. Although the flap chord/wing chord ratio is an important factor in the flap effectiveness, the flap area/wing area ratio is a satisfactory criterion for determining the effect of flap on maximum C_L for partial span flaps of approximately 60% span. Actually for an approximately constant span flap, the area ratio determines the chord ratio. Therefore for flaps of conventional proportions, from 20 to 35% of the chord, the flap area/wing area ratio is a simply applied and reliable criterion. Although the flap area/wing area is not known for this particular design, examination of a number of transports of this size shows that .16 is a good representative figure. See chart 2:1. Maximum C_L is then obtained by adding the values obtained from Figures 2:11 a and 2:11 b.

The values in Fig. 2:11 a, b are for a wing at a value of R.N. that a high subsonic jet transport would attain in landing. However, it should be noted that $C_{L_{max}}$ is a function of R.N. Fig.

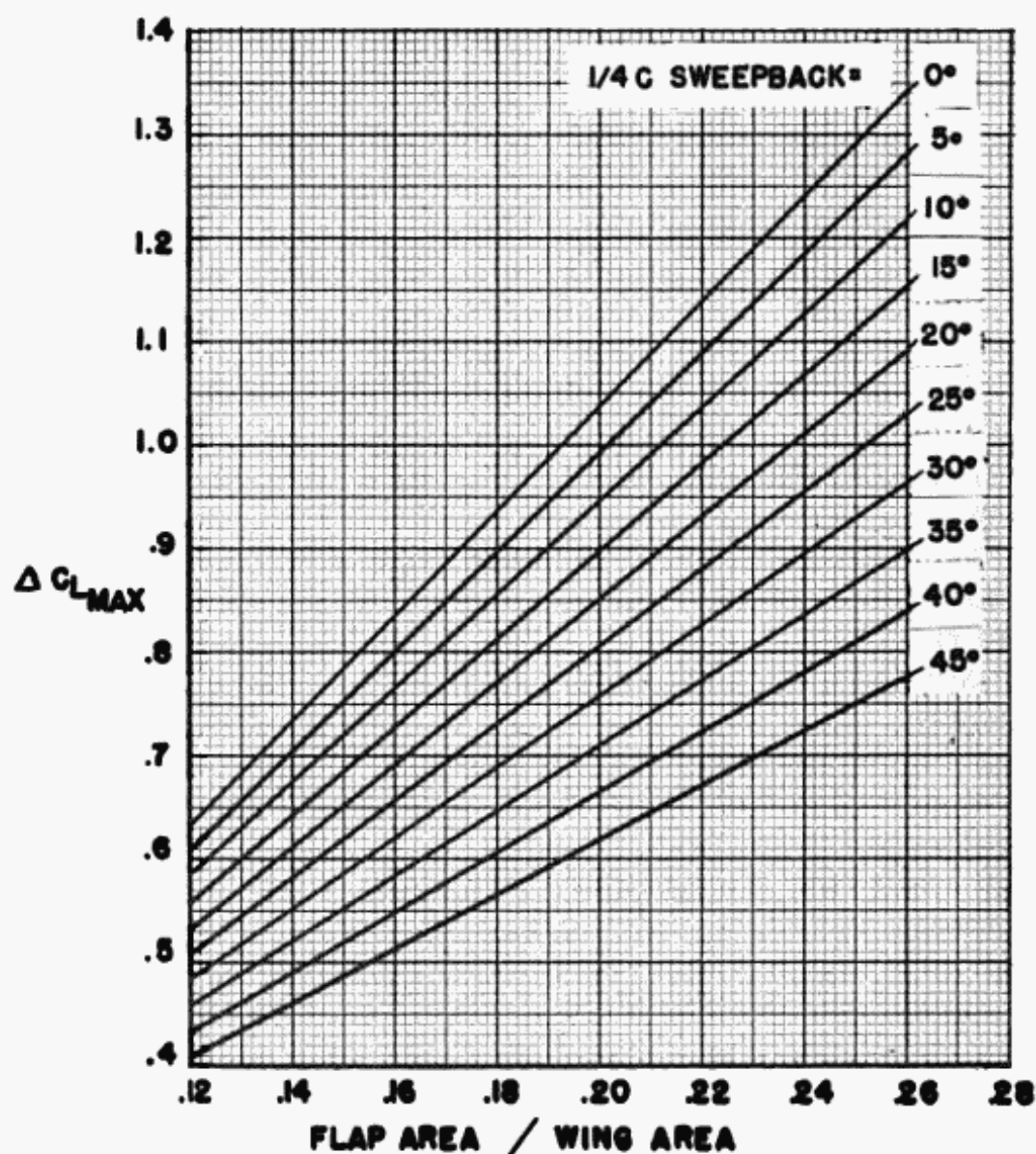
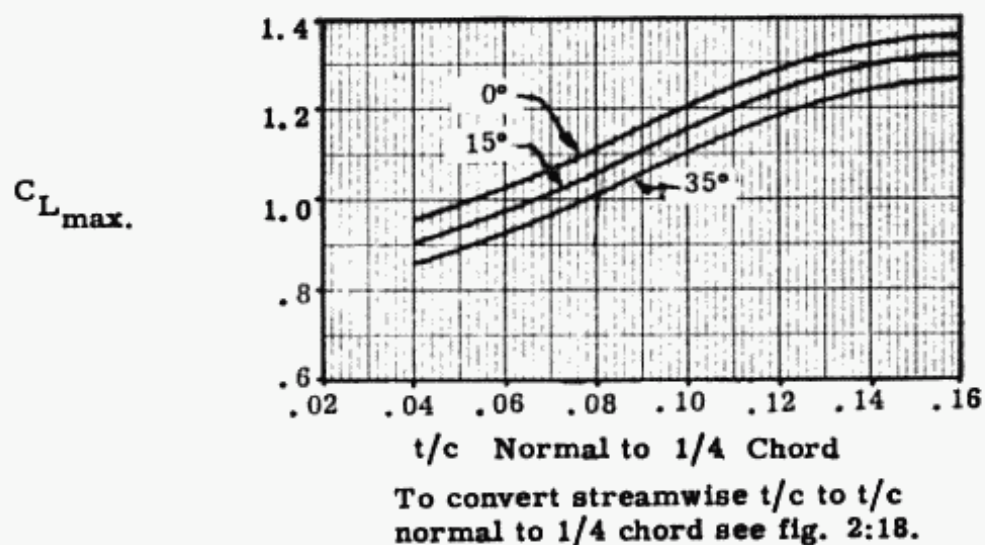


Fig. 2:11 a, 2:11 b. $C_{L_{max}}$ vs. a function of t/c , sweepback and flap area. (Obtained from Boeing Wind Tunnel tests, for Fowler flap.)

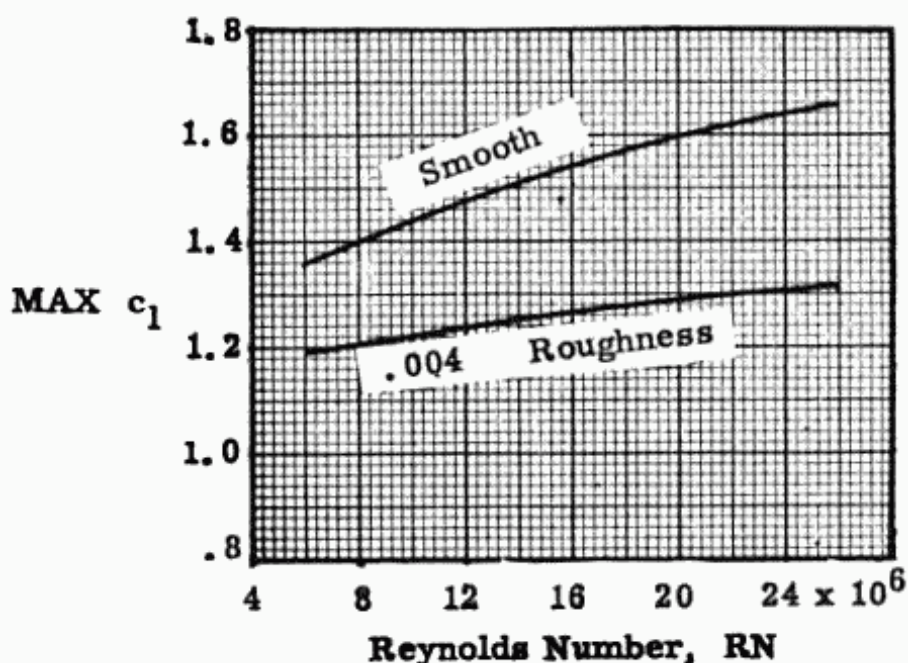
Fig. 2:11 c. Effect of R.N. on max. c_l .

Chart 2-1

Aircraft	Wing Area (sq. ft.)	Flap Area (sq. ft.)	Flap Area Wing Area
Propeller Driven			
Constellation L1049C	1650	302	.183
Convair 240	817	139	.170
Convair 340	920	182	.198
Douglas DC 4	1457	210	.144
Douglas DC 6	1463	229	.157
Martin 404	864	150	.174
Boeing Stratocruiser	1720	357	.208
Jet Powered			
Avro Jet Liner	1157	102	.088
DeHaviland Comet I	2015	446	.220
Boeing 707-320	3892	428	.148
Boeing 707-120	2433	337	.139
Douglas DC-8	2758	454	.164

2:11 c shows the variation in max C_L with R.N. for an extremely thick airfoil.

$$RN = \frac{V\ell}{\nu} \quad \text{where} \quad \begin{array}{l} V = \text{speed in ft/sec.} \\ \ell = \text{length in ft.} \\ \nu = \text{kinematic viscosity in ft}^2/\text{sec.;} \end{array}$$

for variation of value of ν with altitude see fig. 2:26.

The lift/drag ratio, L/D , can be represented as C_L/C_D and C_L is known.

$$C_D = C_{D_i} + C_{D_P} = \frac{C_L^2}{\pi A Re} + C_{D_P} \quad (2:15)$$

Section 2:6 presents a detailed explanation of the C_{D_P} term. The airplane efficiency factor, e , is discussed in detail in section 7:13.

Although C_L is known, both C_{D_i} and C_{D_P} are difficult to determine. This is due to the fact that besides the flaps and gears being down, ground effects must be considered. Figures 2:34, 35, and 36 show the variation of C_{D_P} with flaps deflected and with landing gear down; and the ground effects on C_{D_i} . In addition the speed during descent is varying from $1.30 V_{SO}$ to $1.15 V_{SO}$, thereby changing D and L/D . Any calculation at this stage of the design, to determine L/D for landing must involve many assumptions, resulting in only an approximate answer. Therefore it is felt that L/D equal to 9, which was obtained from a study of a large series of jet transports, is the best available value for this parameter.

Figure 2:12 shows the Civil Air Regulations landing field plotted against W/S landing, which is equation 2:14 in graph form. Various values of $\sigma C_{L_{max}}$ and deceleration have been shown. To calculate the take-off W/S from the landing W/S obtained from Figure 2:12, the landing weight must be determined and an estimate of fuel weight made.

The landing weight, which is a weight which will never be exceeded in a landing, is designated by the designer, as there are no set requirements. To make certain that the weight chosen could never be exceeded in landing, the landing weight would be assumed to equal the take-off weight. However, a more efficient airplane could be designed if the landing weight was assumed to be less than the take-off weight. Since the landing wing loading is determined by the landing field length requirement, it is the take-off wing loading that is affected by the relation of landing weight to take-off weight. If the landing weight is assumed to equal some value less than take-off weight then the take-off wing loading will be greater than the landing wing loading. Since the theory of this design is that the airplane with the highest wing loading and the highest thrust loading is the most efficient, it is

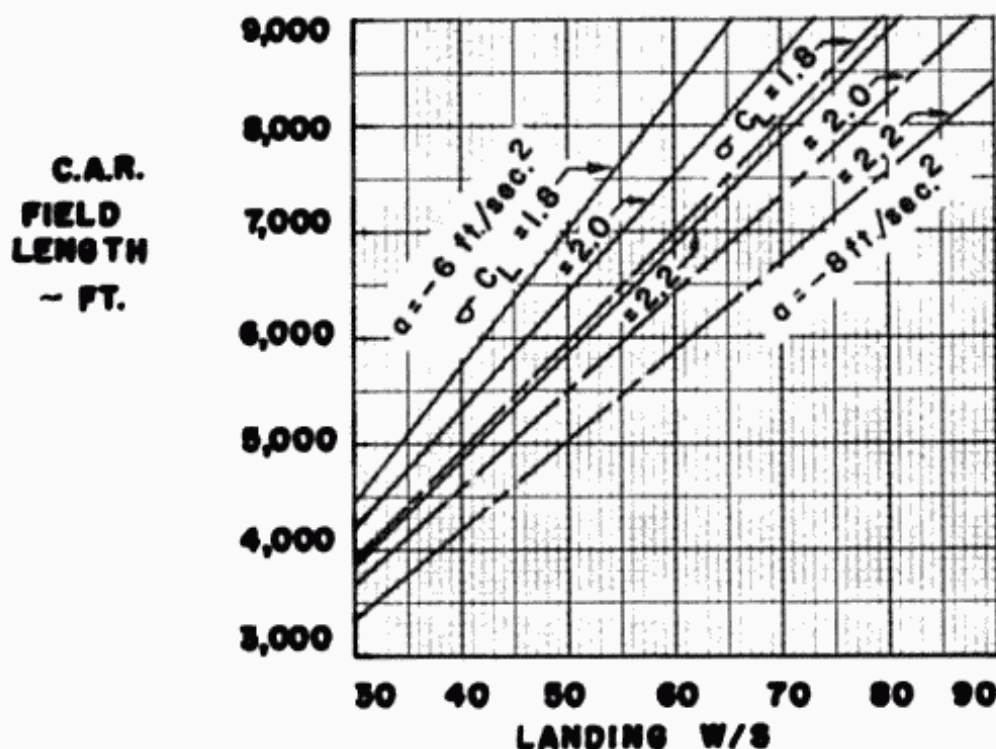


Fig. 2:12. Landing wing loading as a function of landing field.

desirable to assume a landing weight that is lower than the take-off weight.

It is therefore necessary to compromise between airplane efficiency and the reliability in being able to land at the chosen landing weight. First the landing weight should be chosen so that it will not be exceeded after a normal flight of the airplane. Secondly, a fuel dumping system should be provided so that the pilot can dump the fuel rapidly in case of emergency and thereby not exceed the landing weight.

Chart 2-2 presents a list of the relationship of take-off gross weights, design landing weights, and design fuel weights, for the modern transport aircraft.

The value of the fuel weight used to determine design landing weight varies from 25 to 83% of the design fuel weight. A reasonable compromise is to assume that the landing weight equals the take-off weight minus one-half the total fuel, at full payload.

Then

$$\left(\frac{W}{S}\right)_{TO} = \left(\frac{W}{S}\right)_{Land} \times \frac{1}{1 - .5 \left(\frac{Wt. \text{ of fuel}}{TO \text{ Weight}}\right)} \quad (2:16)$$

Since the weight of fuel is not known, an estimate must be made. Later when the weight of fuel is calculated accurately,

Chart 2-2

Aircraft	Des Gr Wt	Des Land Wt	Des Fuel Wt	% Design Fuel Assumed used for Des Land Wt
Propeller Driven				
Constellation L1049C	130,000	105,000	30,000	83
Convair 240	40,500	38,600	6,000	32
Douglas DC4	73,000	63,500	21,000	45
Douglas DC6	97,700	80,000	25,500	67
Martin 404	45,000	43,000	8,000	25
Boeing Strato-cruiser	145,800	121,700	46,600	52
Jet Powered				
Avro Jet Liner	65,000	55,000	18,500	54
DeHaviland				
Comet I	105,000	75,000	41,800	72
Comet 4A	152,500	113,000	68,000	58
Convair 600	238,200	180,000	98,000	60
Douglas DC-8-1910	287,500	190,500	122,700	79
Boeing 707-320	295,000	195,000	138,000	72
Boeing 707-120	246,000	175,000	101,000	70

$(W/S)_{TO}$ may be corrected. Fig. 2:13 shows an estimate of the variation of W_f/W_{TO} as a function of all out range. There is no significant change due to varying speeds from 350 to 500 knots.

It will be noted that the W/S calculated is the maximum W/S that will meet a specified landing distance. If a lower W/S is used it will meet the specified landing distance but will result in a less efficient airplane.

Refinement to Landing Distance Calculation

A refinement to the method of determining landing distance is significant if other than a conventional airplane configuration is used. From equation 2:14 it is seen that landing distance is a function of wing loading, W/S . This parameter is really not weight divided by wing area but wing lift divided by wing area. The Civil Aeronautics Authority accepts the assumption made in the derivation of the field length formula that lift equals weight. However for an airplane with the horizontal tail aft of the wing,

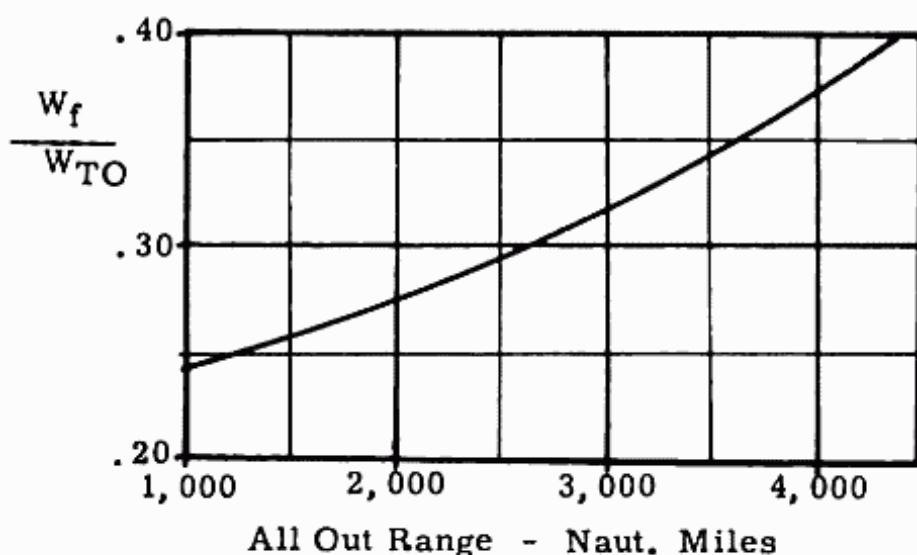


Fig. 2:13. Estimation of weight and fuel.

a large download on the tail actually is required to attain the angle of attack required for landing lift coefficient. For airplanes now in transport use, the ratio of horizontal tail load to landing weight ranges from .050 to .090 at touchdown, and to .120 during landing approach flight. Since for equilibrium vertical forces must equal zero, wing lift equals airplane weight plus tail load, not just airplane weight. The CAR field length, which is the calculated field length divided by .6, accounts for this approximation as well as variations in pilot technique and the difference between actual landing conditions and those assumed.

For a Canard type airplane (horizontal tail surface in front of wing) the canard surface requires an upload for control in landing. The lift on the wing is then equal to the landing weight minus the canard surface load. Therefore, for the same landing weight divided by wing area, the canard type airplane would have a landing field length considerably smaller than the conventional airplane. Or, for the same required field length, the wing loading on the canard airplane can be increased, with a resulting increase in efficiency. For airplanes with short field length requirements, the increase in efficiency can be appreciable.

It should be noted that equation 2:12 states

$$V_{so} = \sqrt{\frac{296 W/S}{\sigma C_{L_{max}}}}$$

This formula is based upon the assumption that the lift on the wing = W ; actually instead of W in equation 2:12, the lift on the wing should be used. Introducing the term load factor, design-

nated by n , where

$$n = \frac{L}{W}, \quad \text{or} \quad L = nW$$

then
$$V_{SO} = \sqrt{\frac{296 nW/S}{\sigma C_{L_{\max}}}}$$

or
$$V_{SO} = \sqrt{\frac{296 W/S}{\sigma C_{L_{\max}}/n}}$$

For an airplane that is sinking, as it is in landing, n is less than 1.0, and the effective $\max C_L$ can be used as the $\max C_L$ at $n = 1.0$, divided by n . If there was no lift on the wing that is $n = 0$, the airplane would descent vertically and V_{SO} would of course be zero. Therefore to obtain V_{SO} accurately the lift on the wing must be calculated and this involves the sinking speed, or n , as well as the load on the tail.

Verification of Assumed Cruise C_L

From the foregoing data the take-off wing loading can be determined. It is now possible to check the accuracy of the C_L assumed to determine the M_{CRD} , and therefore the wing thickness ratio and sweepback, also.

From the basic formula

$$L = 1/2\rho SV^2 C_L \quad (2:18)$$

Changing V from feet/sec to knots, and substituting W , the weight, for L , the lift, for level flight

$$C_L = \frac{296 W/S}{\sigma V^2} \quad (2:19)$$

where σ is the density ratio, $\frac{\rho \text{ alt}}{\rho \text{ sea level}}$

$$M = \frac{V}{662\sqrt{\theta}} \quad (2:20)$$

where 662 is equal to the speed of sound at sea level in knots; θ is the absolute temperature ratio,

$$\frac{T \text{ alt}}{T \text{ s.l.}}$$

$$C_L = \frac{296 W/S}{\sigma (662)^2 \theta M^2}; \quad \delta = (\sigma) (\theta) \quad (2:21)$$

$$\text{Therefore} \quad C_L = \frac{W/\delta S}{1481 M^2} \quad (2:22)$$

Assuming that the cruise condition starts at 35,000 feet and the airplane flies at constant $W/\delta S$, C_L can be determined. Another small correction must be estimated at this time. The W/S in equation 2:22 is the wing loading at 35,000 feet while the W/S from equation 2:16 is for take-off. From a series of calculations made on jet airplanes climbing to 35,000 and with an all-out range of 1,750 n. m., the fuel used in climb resulted in a reduction of approximately 3.5 per cent. This is only an estimate and will be checked later in the climb calculations.

If the C_L calculated is equal to the C_L assumed in determining ΔM_{CRD} due C_L , then the thickness ratio and sweepback are correct. If the calculated C_L does not equal the assumed C_L , other values of C_L must be assumed until the calculated C_L does equal the assumed C_L . The sweepback and thickness ratio will then be satisfactory.

2-4 Thrust Loading

The thrust requirement of an airplane may be critical for any one of a number of conditions. The thrust must be high enough to cruise at the desired speed at the desired altitude, to meet the required rates of climb, and to meet the take-off distance requirements. The critical conditions for certain type airplanes are self-evident; a pursuit plane, high speed conditions; an interceptor, rate of climb. For a four engine high speed jet transport it can be either of the three conditions, take-off, cruise speed, or a rate of climb condition.

The thrust loading, W/T , will first be calculated to meet the take-off requirements, and later checked to determine if other criteria are met.

Figure 2:14 shows the variation of take-off distance with factor K , where

$$K = W/S \times W/T \times 1/C_{L_{TO}} \times 1/\sigma \quad (2:23)$$

The derivation that follows shows the assumptions and limitations of this curve.

From the basic considerations

$$S = 1/2 at^2 \quad \text{and} \quad t = v/a$$

$$S_G = \frac{V_{TO}^2 (2.84)}{2a} \quad (2:24)$$

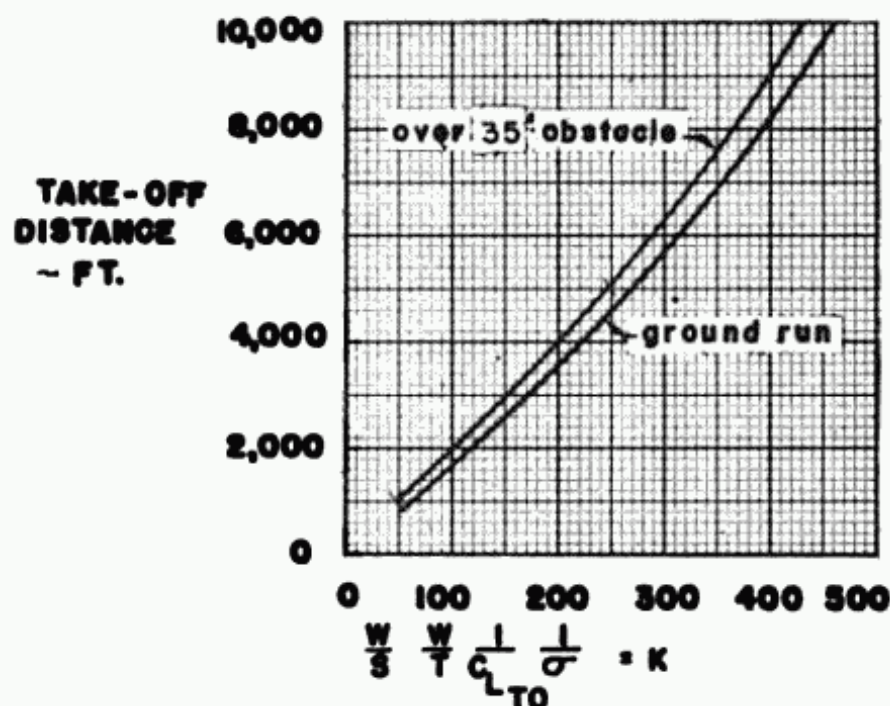


Fig. 2:14. Take-off chart: thrust loading as determined by field length.

where V_{TO} is in knots; S_G is the ground run

$$\text{From } F = ma \quad (2:25)$$

$$a = \frac{F}{M} = \frac{T - D}{W/g} \quad (2:26)$$

$$\text{From } W = L = 1/2\rho SV^2 C_{L_{TO}} \quad (2:27)$$

$$V_{TO}^2 = \frac{296 W/S}{C_{L_{TO}} \sigma} \quad (2:28)$$

substituting equations 2:26 and 2:28 into 2:24

$$S_G = \frac{296(2.84) W/S}{C_{L_{TO}} \sigma} \times \frac{W/g}{(2)(T - D)} \quad (2:29)$$

$$= 420 W/S \frac{1}{C_{L_{TO}} \sigma} \frac{W}{g} \frac{1}{T - D} \quad (2:30)$$

by the aid of simple algebra

$$S_G = \left(\frac{W}{S}\right) \left(\frac{W}{T}\right) \left(\frac{1}{C_{L_{TO}}}\right) \left(\frac{1}{\sigma}\right) \left(\frac{420}{g}\right) + S_G \frac{D}{T} \quad (2:31)$$

The preceding formula shows the ground run is a function of $(1/C_{L_{TO}})(W/S)(W/T)(1/\sigma)$. It is also dependent on D/T at take-off. Using empirical data derived from many jet airplanes, values of D/T at take-off were calculated and the ground run and take-off distance over a 35 foot obstacle were determined as a function of $(W/S)(W/T)(1/C_{L_{TO}})(1/\sigma)$, and plotted in Figure 2:14. SR422 for turbine airplanes, section 4T117 specified that the take-off distance should be calculated assuming a 35 foot obstacle.

$C_{L_{TO}}$ is used as equal to $.75 C_{L_{max}}$. If the take-off was accomplished at maximum C_L and the airplane encountered a gust that increased the angle of attack, an undesirable stall condition would be encountered. It is therefore necessary that the flaps be in the desired position and the angle of attack such that $C_L = .75$ maximum C_L at that flap position. The airplane must be so designed so that $.75$ maximum C_L can be obtained during the ground run. Since a bicycle type gear airplane must take off with all main gears on the ground, the angle of attack required for $.75$ maximum C_L must be attained by either a fairly large angle of incidence of the wing, a front gear that is longer than the rear gear or a combination of both. For most designs using only the required angle of incidence is most efficient and desirable.

From Figure 2:14, knowing the specified field length, W/S , $C_{L_{TO}}$ and σ , the W/T required for take-off can be obtained.

The W/T obtained is based upon sea level, standard day take-off thrust. It should be noted that the airplane should have enough thrust to meet the take-off requirements on a day hotter than standard. The hot day usually used is at 100° F when σ is $.926$, called Army hot day. To assure that there is enough thrust available for this hot day condition, not only should $\sigma = .926$ be used, but the fact that the thrust of a jet engine is appreciably reduced at high temperatures must be accounted for. Since the thrust of jet engines is reduced by approximately ten per cent due to this increase in temperature, the W/T obtained from Figure 2:14, using $\sigma = .926$, should be reduced by ten per cent. In addition, the possibility of an engine failure during any part of the take-off over a 35 foot obstacle must be accounted for.

Figure 2:15 shows a diagram of the path of the airplane taking off over a 35 foot obstacle.

a is the starting point

b is the point wheels leave ground
c is the point of the 35 foot obstacle

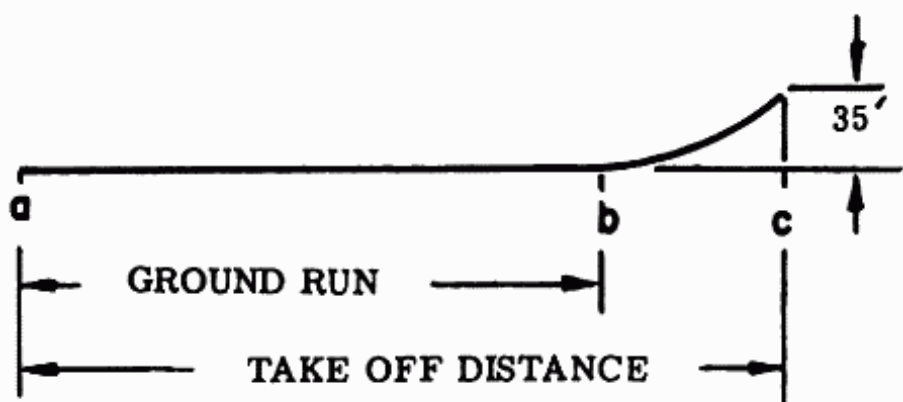


Fig. 2:15. Take-off Path.

One Engine Inoperative

If the engine failed at point b, the pilot has two alternatives: either to jam on the brakes and stop as fast as possible, called refused take-off, or climb over the 35 foot obstacle on the operating engines, called climb-out. For a 4 engine jet transport, the climb-out distance is far less than the refused take-off distance for an engine failing at point b. As the engine failure occurs further from b and closer to a, the climb-out distance increases and refused take-off decreases, as shown in Figure 2:16.

At some point, d, the climb-out will equal the refused take-off and this will be the critical distance. If the engine fails before point d, the pilot can stop by applying his brakes in less than the critical distance. If the engine fails after point d, the pilot should continue and climb over the 35 foot obstacle. For each point along the take-off there is a corresponding airplane speed, and the airplane can be placarded by this criteria of speed.

From a study of a series of four engine transports, it has been found that the critical distance for the one engine inoperative condition is equal to the take-off distance with all engines operating, divided by .83. Therefore to obtain the W/T required to meet the one engine out condition, K should be obtained from Figure 2:14, using .83 x the specified field length.

Since there have been some general assumptions made for all airplanes, this method of relating thrust loading to take-off field results is only a good approximation, within 10%. When the airplane is completely designed, an accurate calculation of take-off field can be made. See section 6:4.

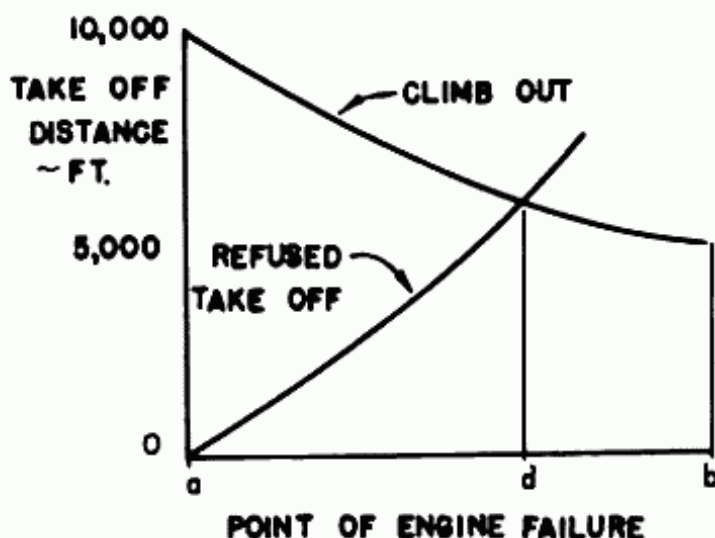


Fig. 2:16. One Engine Out Effect on Take-off Distance.

2-5 Weight Estimation

General

The preliminary weight estimation is one of the most difficult problems facing the designer. The procedure in an aeronautical company is usually as follows:

After having calculated the wing loading required by landing, and the thrust loading required for the critical condition, the designer makes the first estimate of the design weight based upon his previous experience. Using this estimate he finishes the design of the airplane and makes a general arrangement and an inboard profile drawing. These drawings with the first weight estimate are given to the preliminary design weights department. Using charts based upon their previous experience and doing a very rough stress analysis, a new weight estimate is made. The designer must now redesign the airplane with the latest weight estimate. If wing loading and thrust loading remain the same, then wing area and thrust must change, thereby changing weight and drag again. After a series of calculations between designer and weights department, a preliminary design weight is established.

For the purposes of this study, the weights are divided into five parts.

- 1) Structural
- 2) Power Plant
- 3) Fuel

- 4) Payload
- 5) Fixed Equipment

Structural Weight

This weight item is probably the one that depends upon the most variables. The structure consists of the wing, the fuselage, the landing gear, the engine nacelles and the empennage. The weight of each of these items is influenced by many factors. To indicate the complexity of the problem of predicting wing weight, reference is made to "Aircraft Wing Weight Estimation" by J. F. Carayette in a British publication, Aircraft Engineering, Jan. 1950. In this article, six existing methods were used to calculate the weight of wings that were actually built and weighed. About twenty-five civil monoplanes, varying in weight from 600 to 300,000 pounds were investigated. The calculated and the true weights were compared and the per cent error determined. Two of the methods had one parameter, two had ten, one had three and the last had seven. It is interesting to note that for these formulas and the wings studied, an increase in the number of parameters did not reduce the per cent error. In fact, the two methods with the single parameters, had the lowest average errors, 12.1 and 12.2%; one method with ten parameters was right behind with 12.4% error but the other ten parameter method had a 24% error. The other two methods were in between.

It is not intended to prove that the more parameters the less accurate the results. The article does devise a simple method based on two parameters which reduced the average error to 7.5% for the same twenty five wings. However the purpose of this discussion is only to show the difficulties involved in trying to predict wing weight accurately, not to mention the rest of the structure, fuselage, empennage, landing gear and nacelles.

For similar airplanes, such as jet transports based on the same assumptions, it is somewhat less difficult to arrive at an acceptable estimate. The take-off weight is an important factor in the structural weight since it determines the airloads on the wing and tail surfaces, as well as influencing the landing weight in landing gear design. The take-off weight also affects the drag of the airplane on which the engine size is dependent.

The wing area, thickness ratio, sweepback and aspect ratio are variables which affect the wing weight. The weight of the tail surfaces is a function of the wing weight.

Using the weight data from a study of current jet transports, the structural weight was determined as a function of the variables discussed above.

Weight of structure

$$= \left(.16 W_{TO} + \frac{9.8}{(100/W)^{.63}} \frac{W_{TO}}{W/S} \right) (K_{t/c}) (K_{A.R.}) (K_{\lambda}) \quad (2:32)$$

where

W_{TO} = Take-off weight

S = Wing area in square feet

$K_{t/c}$ = Correction factor for thickness ratio, Figure 2:20

$K_{A.R.}$ = Correction factor for aspect ratio, Figure 2:19

K_{λ} = Correction factor for taper ratio, Figure 2:19a

This structural weight is based upon the assumptions previously made as to type of fuselage, wing, engines and landing gear. It is also based upon a streamwise thickness ratio of .10, an aerodynamic aspect ratio = 8.7 and a quarter chord sweepback = 35° . However, the weight of the wing is dependent on the structural aspect ratio and the thickness ratio perpendicular to the quarter chord, not on the aerodynamic aspect ratio and streamwise thickness ratio. Figure 2:17 shows a typical sweptback wing.

The shear forces travel spanwise along the elastic axis of the wing. Therefore the wing bends along this axis and the bending moments are dependent upon the length of the elastic axis and not upon the aerodynamic span, b . Although the elastic axis is usually closer to .35 times the chord, for convenience the quarter chord is used in estimating the wing weight. "The

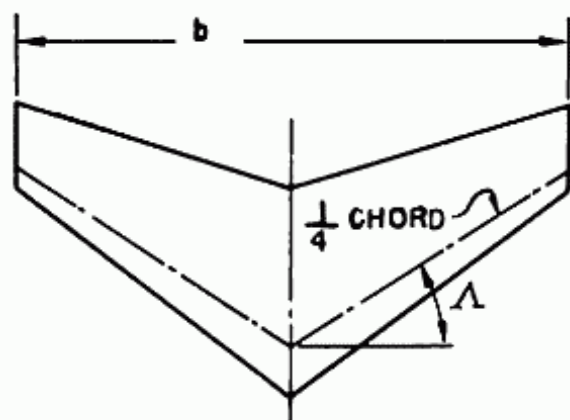


Fig. 2:17. Typical Sweptback Wing.

Deflection of Swept Cantilever Surfaces" by H. C. Martin and H. J. Gursahaney presented in the Journal of the Aeronautical Sciences, December 1951, indicates that for a sweptback wing the elastic axis is even further aft than that of a straight wing of the same cross-section. Therefore the structural aspect ratio equals $\frac{b^2}{S \cos^2 \Lambda}$ while the aerodynamic aspect ratio, usually referred to as merely the aspect ratio, equals $\frac{b^2}{S}$. Since the bending moment is assumed to vary along the quarter chord, the section perpendicular to this line is significant in determining the wing weight. Therefore the thickness ratio perpendicular to the quarter chord and not the streamwise thickness ratio influences the weight. For a wing of zero sweepback, the structural aspect ratio and the thickness ratio perpendicular to the quarter chord are equal respectively to the aerodynamic aspect ratio and the streamwise thickness ratio.

Figure 2:18 shows the thickness ratio perpendicular to the quarter chord divided by the streamwise thickness ratio as a function of quarter chord sweepback. Knowing t/c streamwise and sweepback, the t/c perpendicular to the quarter chord can be determined.

Figures 2:19 and 2:20 show the variation in structural weight with variation in thickness ratio and structural aspect ratio as functions $K_{t/c}$ and $K_{A.R.}$

These figures have been obtained from the calculations of a series of airplanes and give satisfactory results for the design considered. The wing sweepback affects the weight of the fuselage as well as the weight of the wing. Figure 2:21 shows the plan view of two identical airplanes, except for wing sweepback, with the aerodynamic centers at the same location. The fuselage bending moments due to tail load are also presented.

From the bending moment diagram it can be seen that the airplane with the greater sweepback has the highest maximum fuselage bending moment. Since the design bending moments forward of the front spar are always less than those at the rear spar, the fuselage of the airplane with the greater sweepback will be heavier.

Power Plant Weight

It is impossible to determine theoretically the variation in weight with T.O. thrust that may be expected for future manufacture. There are so many variables in design of an engine,

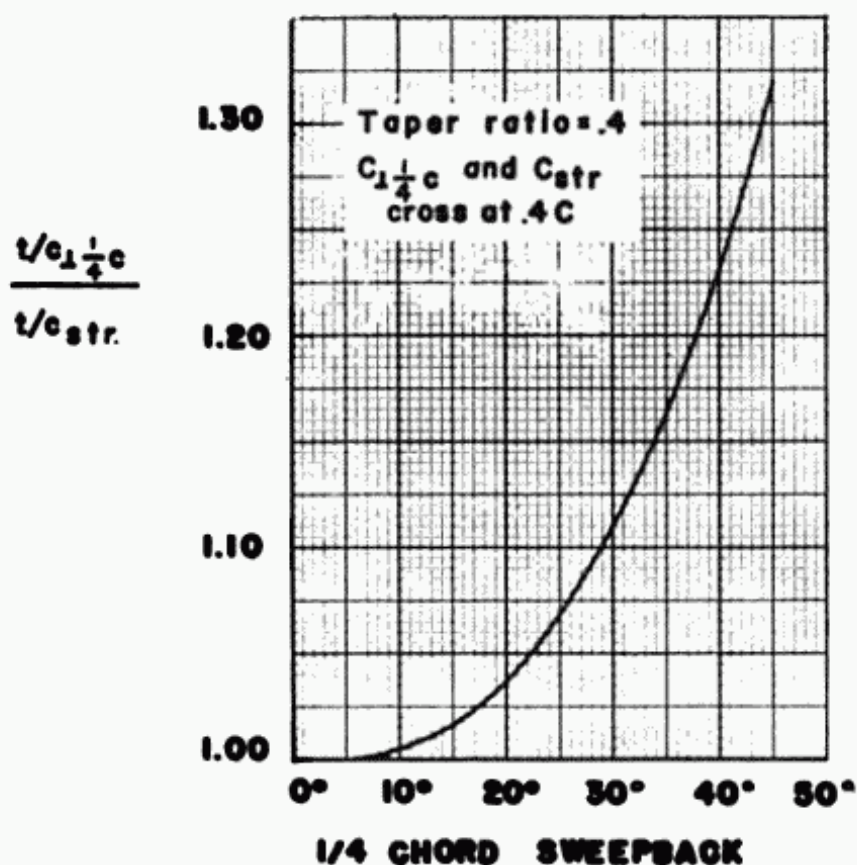


Fig. 2:18. Relation of Thickness Ratio Perpendicular to 1/4 chord to Streamwise Thickness Ratio.

just as in a complete airplane, that the weight depends upon the engine manufacturer and the men responsible.

The most direct method available is a completely empirical one, and is based upon the present information of the weights of available jet engines. These weights were plotted against the sea level, static, take-off thrust for each of the engines, and a curve drawn through the representative points. The formula of the curve resulted in the following variation:

$$W_{\text{engine}} = (1.95)(10^{-3})T_e^{1.55} \quad (2:33)$$

The total weight of the power plant is then equal to the engine weight times the number of engines.

$$W_{\text{pp}} = 1.95 N_e (10^{-3}) T_e^{1.55} \quad (2:34)$$

where

W_{pp} = total weight of power plant

T_e = sea level, static take-off thrust per engine

N_e = number of engines

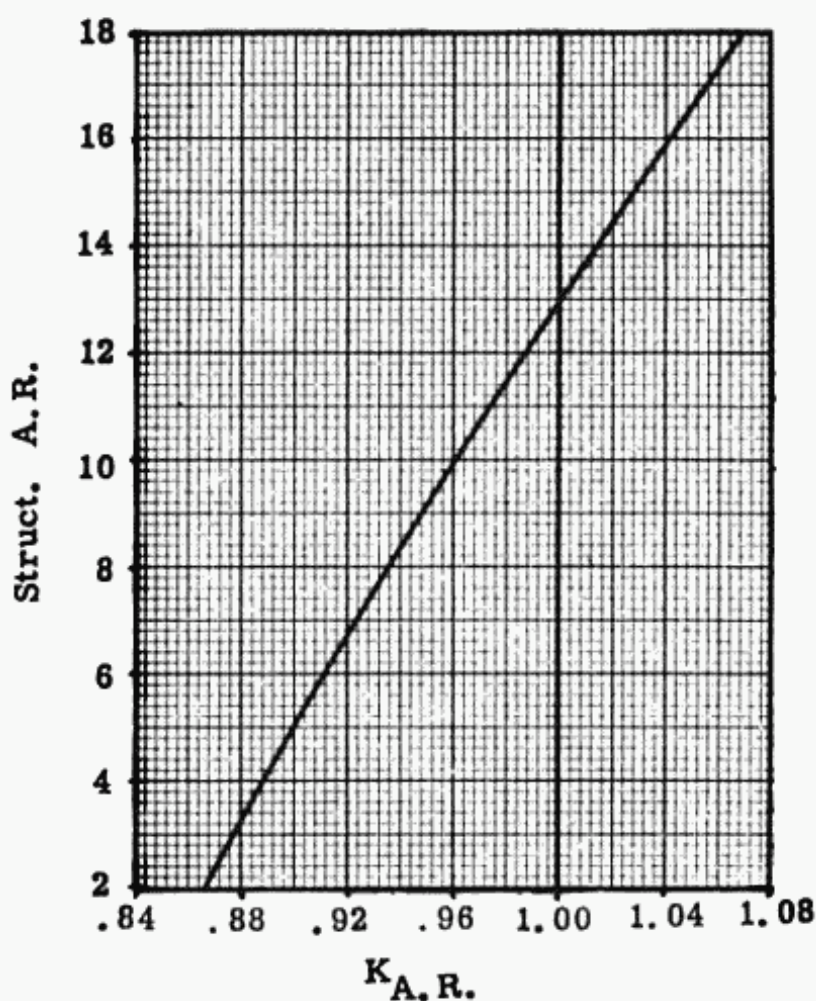


Fig. 2:19. Weight correction factor for A.R.

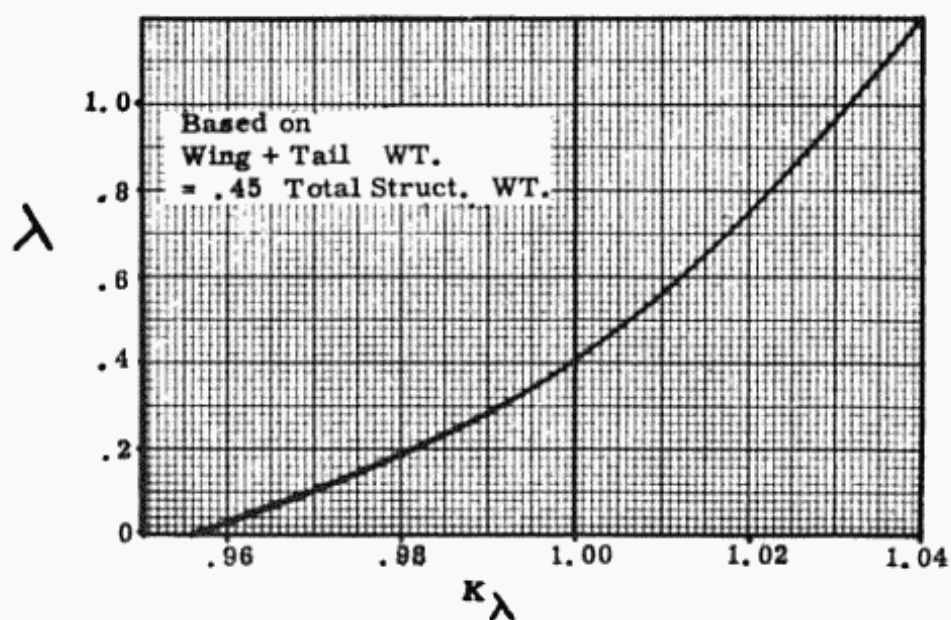


Fig. 2:19 a. Weight correction factor vs. taper ratio.

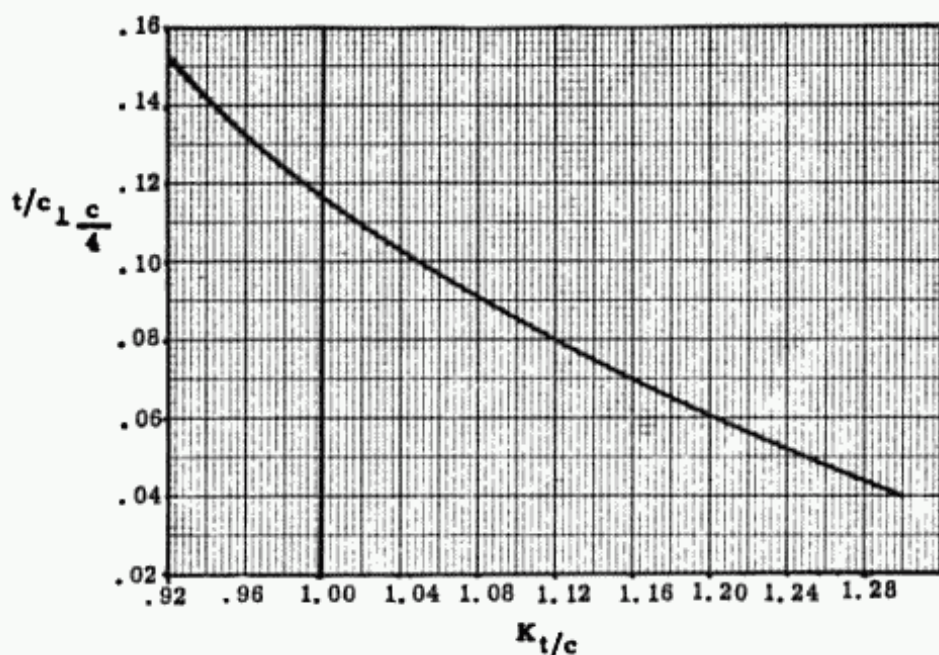


Fig. 2:20. Weight correction factor vs. t/c .

This formula is valid for engines at S.L., static, standard day, thrust from 2,000 to 15,000 pounds. It includes the weight of accessories; and of noise suppressers and thrust reversers for the larger engines.

Fuel

The weight of fuel as a function of take-off weight may be estimated from Figure 2:13. This curve is based on range. The actual weight of fuel is dependent on other variables. Later in the analysis the correct weight of fuel will be determined and the final take-off weight modified.

Since the fuel system weight is a function of the fuel weight, it is presented as a part of the fuel weight. With the acceptance of integral tanks in transport airplanes again, the fuel system weight is quite low. Based upon existing jet airplane designs, a good estimate is that the fuel tank weight is equal to 1.75% of the maximum fuel capacity. Therefore the fuel weight, with its fuel system is

$$W_f = 1.0175 \left(\frac{W_f}{W_{TO}} \right) W_{TO}$$

Payload

The payload is the weight which the airline is being paid to carry. This consists of the passenger weight, his baggage and the cargo. The cargo weight is specified as 40 pounds per passenger. The airlines estimate the average passenger weighs 160 pounds and is allowed to carry 40 pounds of baggage.

Therefore

$$W_{\text{payload}} = 240 N_P \quad (2:35)$$

where N_P = number of passengers

Fixed Equipment

This item consists of the crew and all the weight directly responsible to the crew, the furnishings and services for the passengers and many miscellaneous items such as hydraulic and electrical systems, instruments, surface controls, electronics, emergency equipment and anti-icing.

The crew weight, seats, food and baggage have been set at 230 pounds per member. The passenger items which include seats, food, baggage racks, lavatories, buffet equipment, water and air-conditioning adds up to approximately 160 pounds per passenger. The miscellaneous items are subject to considerable variation. However for this preliminary design purpose an estimate of .045 times take-off weight has been used. Even a comparatively large percentage error in this item will result in a small error in the take-off weight.

Therefore

$$W_{\text{f.e.}} = 160 N_P + 230 N_C + .045 W_{\text{TO}} \quad (2:36)$$

where

$W_{\text{f.e.}}$ = weight of fixed equipment

N_P = number of passengers

N_C = number of crew

$230 N_C$ allows for 3 flight crew members and one stewardess. For each additional flight member add 260 pounds and for each additional stewardess 170 pounds.

W_{TO} = take-off weight

Total Take-off Weight

The total take-off weight is equal to the sum of the structural, power plant, fuel, payload and fixed equipment weights.

$$W_{\text{TO}} = W_{\text{str}} + W_{\text{pp}} + W_f + W_{\text{payload}} + W_{\text{f.e.}} \quad (2:37)$$

$$W_{\text{TO}} = (K_t/c)(K_{AR})(K_\lambda) \left(.16 W_{\text{TO}} + \frac{9.8}{(100/W/S)^{.68}} \frac{W_{\text{TO}}}{W/S} \right) \quad (2:38)$$

$$+ 1.95(10^{-3})N_e T_e^{1.55} + W_{\text{fuel} + \text{system}} + 400 N_p \\ + W_{\text{crew}} + .045 W_{\text{TO}}$$

If all the variables can be stated as a function of W_{TO} the equation can be solved for the one unknown.

$$S = \frac{W_{\text{TO}}}{W/S} \quad (2:39)$$

$$N_e T_e = \frac{W_{\text{TO}}}{W/T} \quad (2:40)$$

$$T_e = \frac{W_{\text{TO}}}{W/T} \times \frac{1}{N_e}$$

$$T_e^{.75} = \left(\frac{W_{\text{TO}}}{W/T} \times \frac{1}{N_e} \right)^{.75} \quad (2:41)$$

$$W_f = W_{\text{TO}} \left(\frac{W_f}{W_{\text{TO}}} \right) \quad (2:42)$$

Since W/S , W/T and W_f/W_{TO} are known, S , T and W_f can be determined as a function of W_{TO} , as shown in the above equations. One equation can now be written with W_{TO} as the only unknown. Since this unknown appears with two different exponents, 1.55 and 1.0, the simplest way of solution is by trial and error. That is, various values of W_{TO} are tried until the equation is satisfied.

Chapter VIII, in the sections under transports and military aircraft, presents a series of charts and graphs from which weight estimates can be made from a more general approach. Although these charts may also be used for jet transport estimates, it is felt that the method just presented results in a more accurate weight.

2-6 Total Drag

Before the range of the airplane can be calculated the drag of the airplane must be known. Since there exist a few conflicting representations of drag notation in the field, C_D , the coefficient of drag will be defined in this text as:

$$C_D = C_{D_p} + C_{D_i} + C_{D_{\text{comp}}} \quad (2:43)$$

where

C_{D_i} = induced drag coefficient

$C_{D_{\text{comp}}}$ = change in C_D due compressibility effects = ΔC_D

C_{D_p} = parasite drag coefficient

Parasite Drag

$$C_{DP} \text{ the parasite drag coefficient} = \frac{f}{S}$$

where f , the equivalent parasite drag area = the summation of the wetted areas times their corresponding coefficient C_f .

The friction coefficient, C_f , may be determined from the theoretical curves as shown in figs. 2:21a and b which shows C_f vs. R.N. for various values of M , and for both turbulent and laminar boundary layer.

For the size and speed of the transports considered, the values of C_f should equal approximately .0030 for wing, .0024 for fuselage, .0060 for nacelles and .0025 for empennage. The total f is then increased by 5% for interference and miscellaneous excrescences.

Since the tail surface areas are a function of the wing area, the nacelle area a function of the engine thrust, and the fuselage area a function of the number of passengers, f can be written as a function of these variables.

From a study of jet transports and jet engines the following formula for f was evolved:

$$f = 1.10 + .128 N_p + .0070 S + .0021 N_e (T_e)^{.7} \quad (2:44)$$

where

N_p is the number of passengers

N_e is the number of engines

T_e is the static, sea level, take-off thrust per engine, and

1.10 represents the area of the nose and tail of the fuselage.

Since 1.10 is the value of f for a portion of the fuselage and C_f for the fuselage equals .0024, this 1.10 factor is equivalent to a wetted area of almost 500 square feet.

After the airplane is completely designed and drawn up, this value of f can be checked. Chapter VI presents this calculation as a simple special problem. A study of a large series of jet designs shows that values obtained from Equation 2:44 results in an error of only about 3%.

Induced Drag

The induced drag is the drag component of the normal force due to ϵ , the downwash angle.

$$C_{D_i} = \frac{C_L^2}{\pi A e}$$

and as previously developed

$$C_L = \frac{W/\delta S}{1481 M^2}$$

The term "e", the airplane efficiency factor, is discussed more fully in section 7:13, but is usually assumed to equal .8 for preliminary design purposes.

Compressibility Drag

The compressibility drag was discussed in section 2:2, "Wing Thickness Ratio and Sweepback." The value of $\Delta C_{D_{comp}}$ can be obtained from fig. 2:23 which presents

$$C_{D_{comp}} \text{ vs } (M_{CR_D} - M_{cruise})$$

Total Drag

$$C_{D_{total}} = C_{D_P} + C_{D_i} + C_{D_{comp}}$$

2-7 Range

General

There are various methods of calculating the range of an airplane. One of the classic methods is by the use of Breguet's formula.

$$R = 750 (L/D) (\eta/c) \log_{10} \frac{W_0}{W_1} \quad (2:45)$$

where

R = range in nautical miles

η = propeller efficiency

c = specific fuel consumption; lbs. fuel/BHP hr

W_0 = initial weight

W_1 = final weight

This formula, as can be seen from the propeller efficiency term, was originally developed for propeller engines, actually reciprocating engines. However, the term η/c can be converted so that the formula can be used for jet engines.

$$\frac{\eta}{c} = \frac{\text{THP/SHP}}{\text{lbs.fuel/SHP hr}} = \frac{\text{THP}}{\text{lbs.fuel/hr}} = \frac{\text{TV}/326}{\text{lbs.fuel/hr}} \quad (2:46)$$

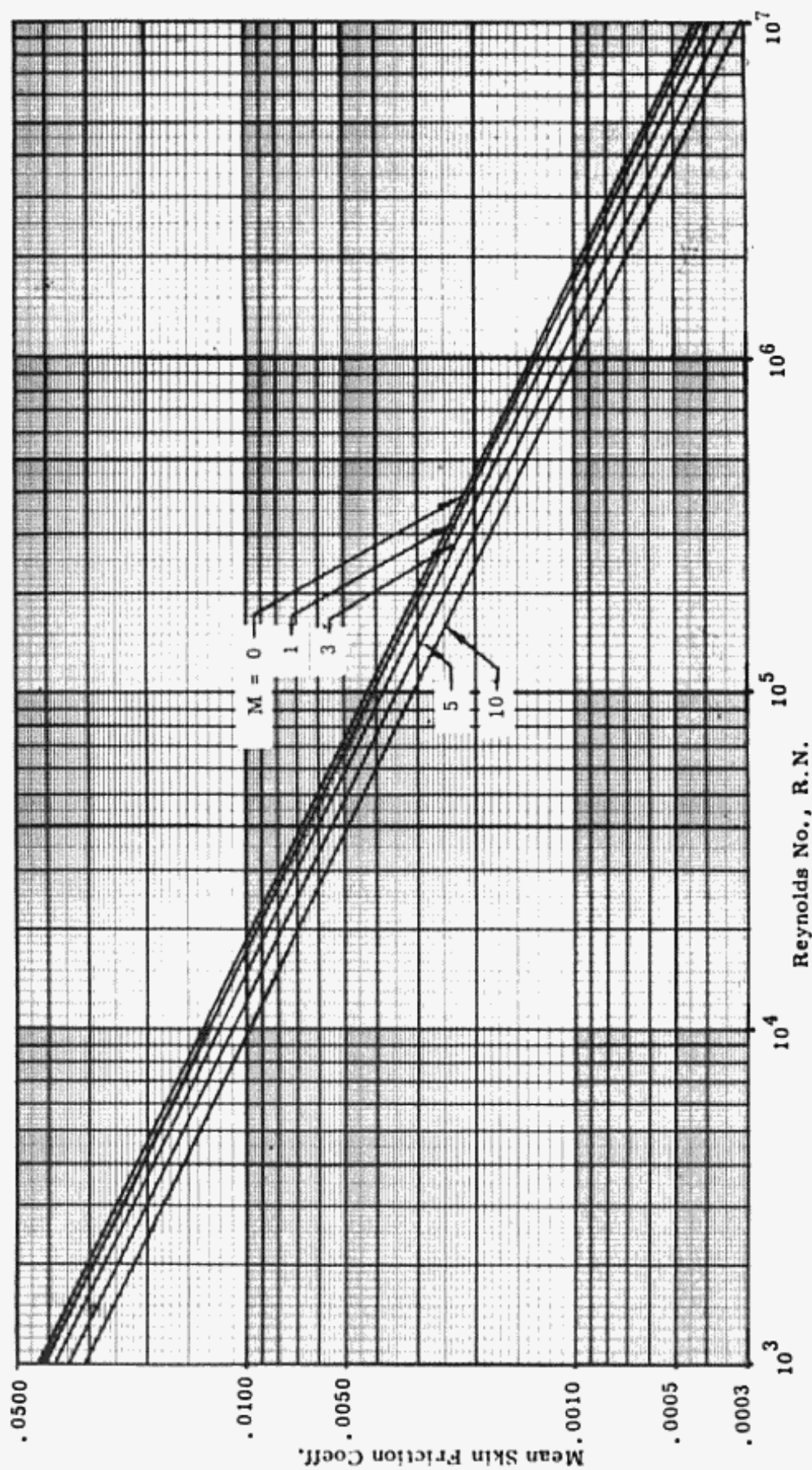
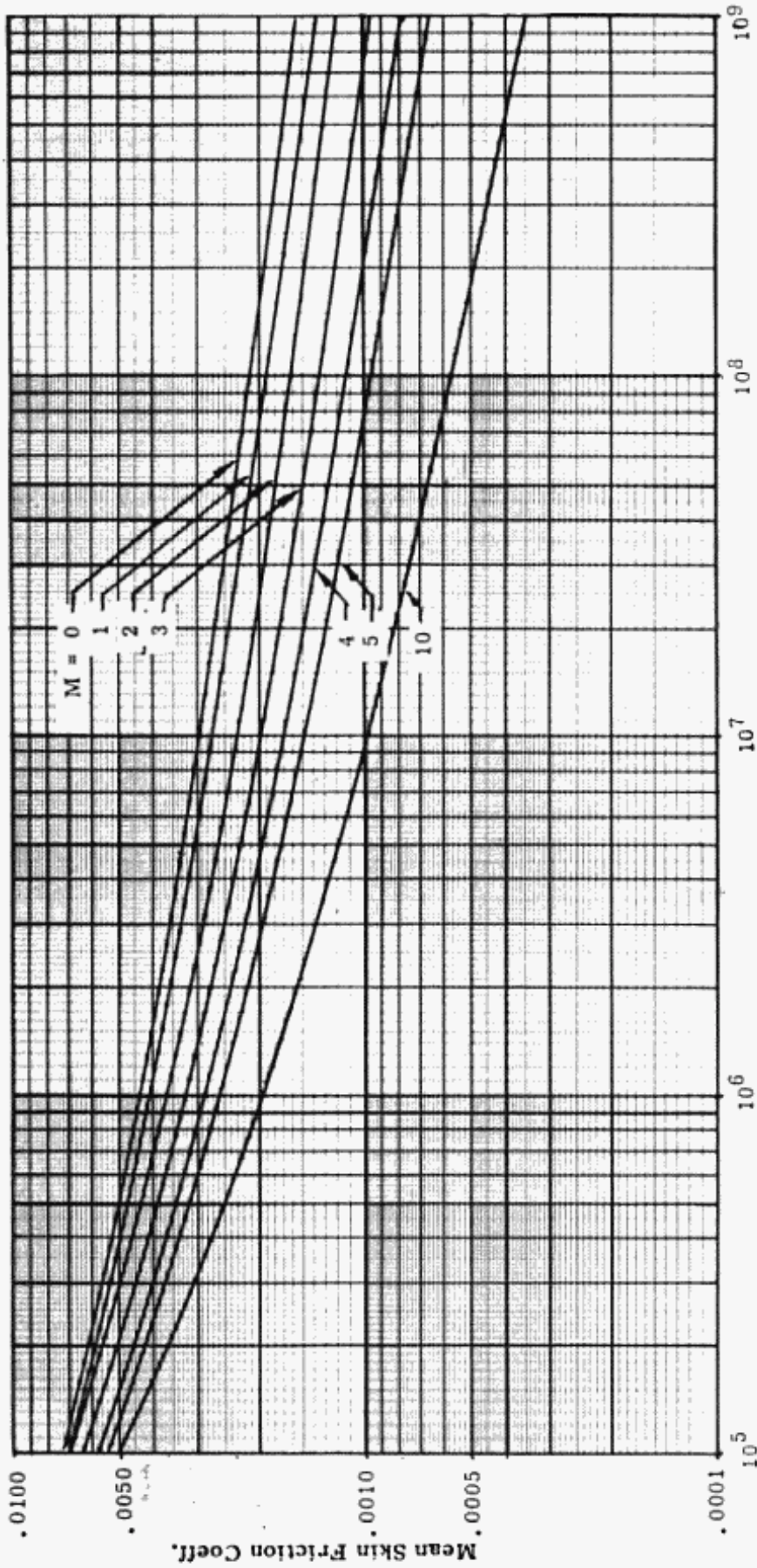


Fig. 2:21 a. Skin friction coef. vs. R.N. - laminar boundary layer.



Reynolds No., R.N.

Fig. 2:21 b. Skin friction coef. vs. R.N. - Turbulent boundary layer.

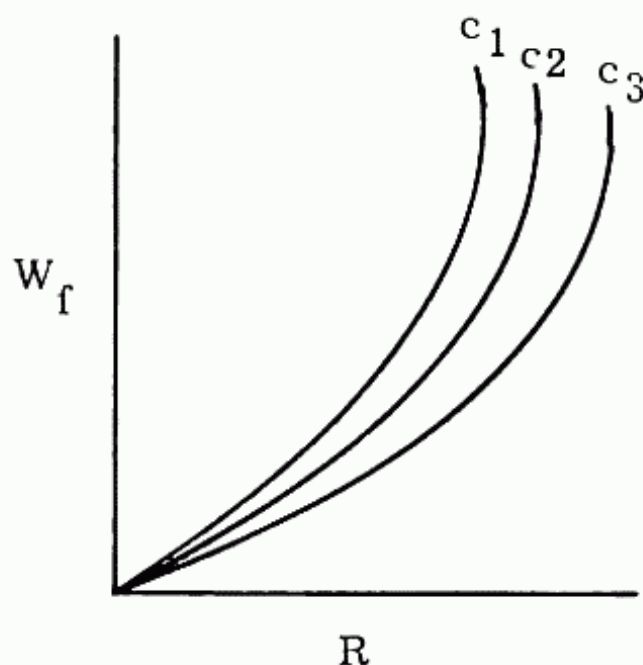


Fig. 2:21 c. Effect of increasing W_f on Range.

$$= \frac{V/326}{\text{lbs.fuel/T-hr}}$$

Substituting this value of η/c in Equation 2:45

$$R = 2.3 (L/D) (V/c) \log_{10} \frac{W_0}{W_1} \quad (2:47)$$

where

R = nautical miles

V = velocity in knots

c = specific fuel consumption; lbs.fuel/lb.T-hr

This form shows that range is a direct function of lift/drag ratio and is inversely proportional to the specific fuel consumption, as does Equation 2:45. However it also shows that, all these factors being constant, the range increases with speed.

Breguet's formula is useful in that it shows directly the factors that influence the range, L/D , V , c and $\log W_0/W_1$, and points up their relative importance. It should be noted that the final weight, or weight empty is probably the most significant figure. If $W_0/W_1 = 1.5$, $\log_{10} W_0/W_1 = 0.177$. Reducing W_1 by 25% increases W_0/W_1 to 2.0. The $\log_{10} 2.0$ is equal to .302, an increase of 70%. Therefore for these particular relations a de-

crease of 25% in weight empty results in an increase of 70% in range.

Breguet's formula can be used to show how maximum range is limited for a constant value of $(L/D)(V/c)$, even if W_f is increased.

$$W_0 = W_1 + W_{\text{fuel}}$$

$$\frac{W_0}{W_1} = \frac{W_1 + W_{\text{fuel}}}{W_1} = 1 + \frac{W_f}{W_1} \quad (2:48)$$

Substituting in equ. 2:47

$$R = 2.0 \frac{L}{D} \frac{V}{c} \log \left(1 + \frac{W_f}{W_1} \right) \quad (2:49)$$

The obvious method of attempting to increase R , assuming that V is kept constant and L/D and c are already at their optimum values, is to increase W_f . It is equally obvious that an increase in W_f causes an increase in W_1 if all performance characteristics, except range, are kept constant. Whether R increases or not depends upon the possibility of increasing W_f/W_1 assuming L/D and c remain constant.

At $W_f/W_1 = 1/10$, W_1 can increase by 9 pounds for every pound of W_f added and W_f/W_1 will still increase.

However at $W_f/W_1 = 1$, an increase in W_1 greater than 1 lb. for 1 pound of W_f added, will decrease the range. It is evident that as W_f/W_1 increases it becomes more and more difficult to increase W_f/W_1 by increasing W_f . In fact a point must be reached where an increase in W_f will decrease W_f/W_1 . This is the point of maximum range. Fig. 2:21 c shows the variation in range with W_f for particular airplanes with different values of c , assuming $V(L/D)$ is constant.

For jet powered aircraft a more direct and simpler method for calculating range is presented. If the miles of range per pound of fuel for the entire flight were constant the range could be calculated from

$$R = (\text{mi/lb.}) W_f \quad (2:50)$$

where W_f = the weight of fuel used

If mi/lb. varied during the flight then the range could be calculated by integration. It will be shown that for a constant $W \delta S$, mi δ /lb. remains constant. The factor, mi δ /lb., is a function of engine characteristics as well as the airframe. Engine characteristics are usually presented in either of a few forms. Some

2:42 SUPERSONIC AND SUBSONIC AIRPLANE DESIGN

manufacturers use a separate graph for the characteristics at each altitude at intervals of either 5,000 or 10,000 feet. Others present data in graphs introducing air pressure ratios and temperature ratios to account for various altitudes. In any case all the data is presented and any characteristic may be obtained. Figure 2:22 shows some of the characteristics of a typical jet engine, which will hereafter be referred to as the J-1 engine. The sea level, static, standard day take-off thrust equals 4,000 lbs.

These relationships are true only for 35,000 feet and above. With this engine chart it is now possible to obtain the $mi\delta/lb.$ if the T/δ and the velocity are known. A simple method is presented to determine T/δ for any cruise Mach number and any value of cruise $W/\delta S.$

$$1. C_D = C_{Dp} + C_{Di} + \Delta C_{Dcomp} \quad (2:51)$$

$$2. L/D = C_L/C_D \quad (2:52)$$

$$\frac{D}{W} = \frac{1}{L/D}$$

$$3. D/\delta = \frac{(W/\delta S)S}{L/D} \quad (2:53)$$

$$4. \text{ For constant speed, } T = D \quad (2:54)$$

$$\text{Therefore } T/\delta = D/\delta \quad (2:55)$$

$$T/\delta/\text{eng.} = D/\delta/\text{number of engines} \quad (2:56)$$

$$5. \text{ n.m. } \delta/lb. \text{ fuel from Figure 2:22}$$

In using the characteristics of the J-1 engine (Figure 2:22) for the jet transport engine, some explanation is required. The engines on the transport will be similar to the J-1 engine; that is, c , the specific fuel consumption will be the same, and the thrust under any condition will be directly proportional to the sea level, military, static, standard day thrusts of the engines.

Since Figure 2:22 does not present c but $mi\delta/lb.$ fuel, a relationship between these parameters must be set up.

$$c = \frac{\text{lbs.fuel}}{\text{lb.T-hr}} \quad (2:57)$$

By dimensional analysis it can be seen that

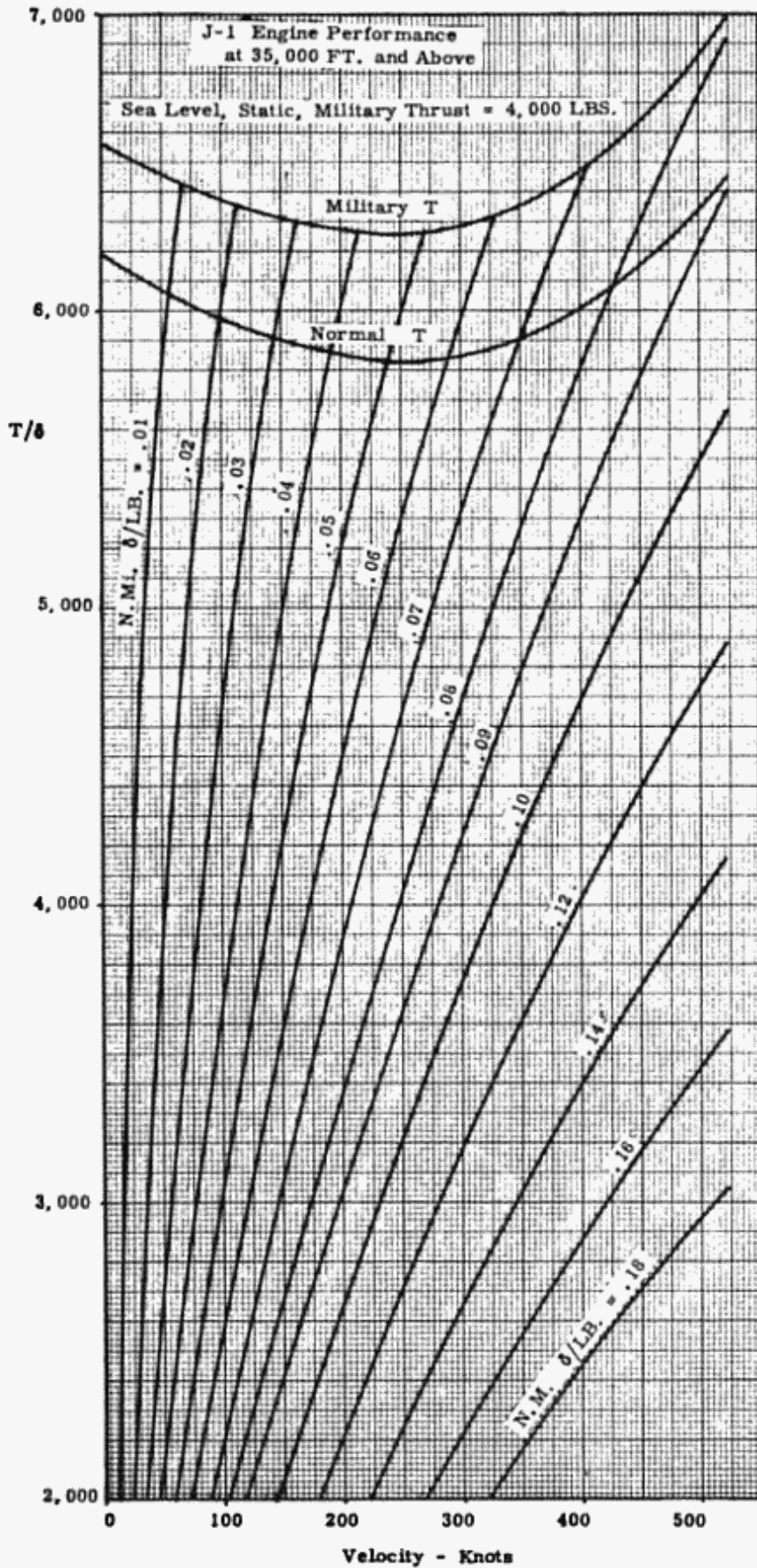


Fig. 2:22. Engine Performance at 35,000' and above for a Typical Jet Engine at 4,000 lbs. sea level, standard day, military thrust.

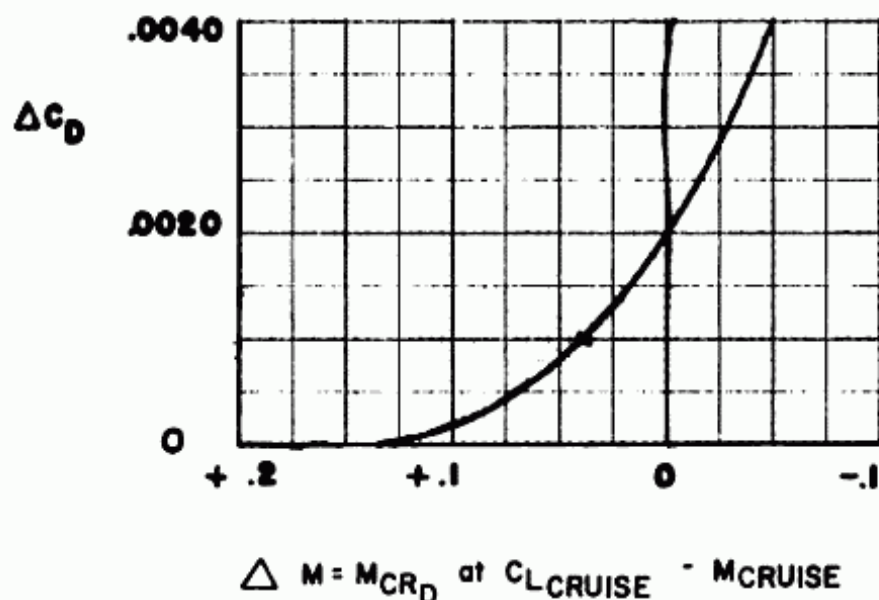


Fig. 2:23. Compressibility Drag Coefficient vs. ΔM . Ref.: RML7C24 "Effects of Combinations of A.R. and Sweepback at High Subsonic Mach Numbers" A.A. Adler, 1947.

$$mi\delta/lb. = \frac{\delta V}{T_c} \quad (2:58)$$

From Equation 2:58 it can be seen that for engines with the same c , operating at the same δ and V , $mi\delta/lb.$ is inversely proportional to thrust.

Therefore to obtain $mi\delta/lb.$ for any engine similar to the J-1 engine by use of Figure 2:22, the following steps must be followed.

- 1) Determine the military, sea level, static, standard day thrust for the transport engine from the take-off weight and W/T required for take-off.
- 2) Determine T/δ /engine from Equation 2:56.
- 3) Determine $K_e = \frac{\text{mil.,s.l.,st.,stand.day thrust of J-1} = 4,000}{\text{mil.,s.l.,st.,stand.day thrust from (1)}}$
- 4) Multiply (2) by (3) for T/δ corrected
- 5) Pick $mi\delta/lb.$ from Figure 2:22 for T/δ corr. and V_{cruise}
- 6) Multiply $mi\delta/lb.$ by K_e

Since $W/\delta S$ and S are constant, δ will vary directly as weight. Therefore for every weight from the beginning of cruise to end of cruise there will be a different δ . However δ varies directly as weight and therefore

$$\text{Range} = \left[(n.m./lb.)_0 + (n.m./lb.)_1 \right] \frac{W_f}{2} \quad (2:59)$$

where $(n.m./lb.)_0$ = initial n.m./lb.

$(n.m./lb.)_1$ = final n.m./lb.

W_f = weight of fuel used

From Figure 2:13 an estimate of the weight of fuel as a function of the take-off weight can be made. Since the take-off weight is known, the estimated weight of fuel and therefore the weight of the airplane at the end of cruise can be determined. To calculate the weight of airplane at the beginning of cruise, the fuel used in climb must be obtained.

Altitude

The choice of altitude at which a jet transport should cruise is a subject with many complex variables. As will be shown later, there is an optimum cruise altitude for each jet airplane. That is, an altitude which will result in the greatest range. However, there are other factors aside from airplane performance that influence the altitude at which a jet transport should cruise.

As altitude is increased, the atmospheric density and pressure decrease. Since humans cannot survive, or at least be comfortable, for a long period of time in atmospheric conditions higher than 8,000 feet, airplane cabins are usually pressurized to conditions equivalent to this altitude. It has been established by study that most humans could not survive atmospheric conditions equivalent to a certain altitude, in the vicinity of 40,000 feet, for more than a very short interval of time. Therefore, if an aircraft were flying at a higher altitude, approximately 50,000 feet, many problems would present themselves. First, in case of a failure of a window or a door and the resulting loss of high density, high pressure air from the cabin, can provisions be made so that the passengers and crew would survive? Would additional oxygen supply be sufficient? Will there be time to descend to a safe altitude? Or is it possible to design the openings that there would be as little chance of their failing as of a wing breaking off? The answers to these questions are beyond the scope of this text.

However there are some engineering aspects of the subject that should be studied. If the airplane is designed to cruise first at some altitude that is considered safe, 35,000 to 40,000 feet, and secondly at the optimum altitude, then a comparison of these airplanes can be used to decide as to the desirability of high altitude flight.

Cruise at 35,000 ft.

The flight during which the airplane climbs to 35,000 feet and then cruises will be considered first. As the airplane cruises its weight decreases due to the fuel being used. If the airplane is so designed to be efficient at the end of climb at 35,000 feet, the reduction in drag with reduction in weight during cruise can be used in two ways.

At 35,000 and at the corresponding weight, the C_L can be calculated.

$$C_L = \frac{W/\delta S}{1481 M^2} \quad (2:60)$$

As has been specified, the wing sweepback and thickness ratio have been chosen so the $\Delta C_{D_{comp}} = .0010$. If W decreases while at constant altitude, C_L decreases and the $\Delta C_{D_{comp}}$ decreases below the value of .0010, if C_L was originally above 0.20. Since it was assumed that it is most efficient to fly where $\Delta C_{D_{comp}} = .0010$, either of two alternatives exists. One is to increase M_{cruise} , and stay at 35,000 feet, until $\Delta C_{D_{comp}} = .0010$; the other is to keep speed constant and decrease δ with decrease in weight. That is, increase altitude, so that C_L is constant, thereby keeping $\Delta C_{D_{comp}} = .0010$.

It is not obvious, but calculations do verify, that the method of keeping $W/\delta S$ constant is more efficient than increasing speed, if the $W/\delta S$ at 35,000 feet is not already above the optimum. The optimum altitude or $W/\delta S$, will be discussed in Section 2:11.

In the calculation of $mi \delta/lb$, it is possible that the T/δ required to reach the cruise $W/\delta S$, is greater than the normal T/δ available, based upon W/T required for take-off. If this is so, it is necessary to increase thrust. This is accomplished by reducing W/T . A lower W/T will result in a lower take-off distance and therefore will certainly meet take-off requirements.

The problem is to evaluate W/T to result in the best airplane. It must be such so that at cruise $W/\delta S$, T/δ available is equal to or greater than T/δ required. The determination of the optimum $(T/\delta)_{avail}$, necessitates the investigation of the engine characteristics.

Using the engine data presented in Figure 2:22 and a variation of Equation 2:58, that is $c = \frac{V}{(n.m. \delta/lb.)(T/\delta)}$, the specific fuel

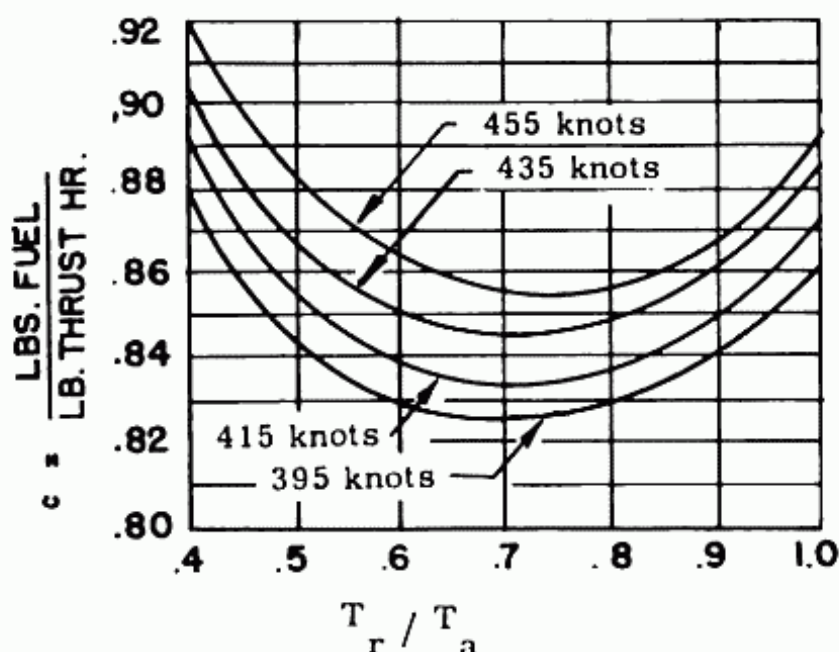


Fig. 2:24. Specific fuel consumption, lbs. fuel/lb thrust-hr vs. T_r/T_a . For same engine as Figure 2:22. Note: This data is for altitudes 35,000' and above.

consumption, may be calculated. Figure 2:24 presents a curve of c versus T_r/T_a for various speeds, where T_r is thrust required and T_a is thrust available.

There will be one T_r/T_a that will result in a minimum c . For the engine under discussion it is approximately 70% for 395 knots to approximately 75% for 455 knots. It is evident that if the airplane cruised at this value of T_r/T_a for minimum c , the engine would be used at its most efficient point. However consider the case where a smaller engine is used, so that the airplane cruised at T_r/T_a equals .90. For this airplane, although the specific fuel consumption would be higher, the drag and weight of airplane would be lower. This is true since the engine weighs less and the nacelle is smaller and therefore presents less drag. It is now obvious that the T_r/T_a that results in the lowest specific fuel consumption is not necessarily the one that is most efficient for the airplane.

The most efficient point of cruise is dependent upon the exact engine used and the specific airplane design. However, if T_r equals .85 to .95 T_a , the airplane will be very close to the most efficient one. For a more exact result, different designs must be worked out to completion.

Therefore, to obtain the optimum airplane, the thrust loading must meet two requirements. First, it must be low enough so that there is sufficient normal thrust so that it can cruise at the chosen $W/\delta S$ and speed. Secondly, at this cruise $W/\delta S$ and speed, the thrust required should be approximately .85 to .95 of the thrust available. This thrust loading must not be higher than that required for take-off. It must be noted that if the thrust loading required for cruising $W/\delta S$ is different than that required for take-off, a new weight calculation is required.

At this point some general philosophy of the design must be decided upon. Since thrust loading and weight are known, the sea level, static thrust required can be calculated. If just one particular design is to be studied there is no alternative but to pick an engine nearest to that required, and fit the airplane design to that engine. However if a study is being made to compare airplanes with various requirements, another method seems advisable. This method is to use the thrust as calculated and assign to each engine the same significant characteristics. These characteristics would be obtained from some typical engine as shown in Figure 2:22. If this method is used, the difference in direct operating cost of one airplane as compared to another is due to the difference in specifications only, not due to the difference in engine characteristics.

Climb

General

With the preceding data, it is now possible to choose the thrust loading so that the airplane can cruise at the desired $W/\delta S$. To complete the range calculations, the climb characteristics of the airplane must be determined; specifically the amount of fuel used in climb and the horizontal distance covered.

Since it is most efficient for range purposes to climb to altitude as quickly as possible, the take-off thrust of the engine is used. This is possible if the climb does not require more than thirty minutes, as the continuous use of take-off ratings for gas turbine engines is usually only allowed for that period. The airplane cabin pressure is equivalent to sea level conditions on the ground and is then reduced to conditions equivalent to 8,000 feet at the start of cruise. If the time to climb were thirty minutes, the cabin pressure would be depressurized at the rate of 267 feet equivalent pressure per minute. The Civil Air Regulations recommends a depressurization rate that should not be exceeded for passenger comfort. If this specification is exceeded by using take-off thrust, it would be desirable to have a lower

rate of climb. This can be accomplished most efficiently by reducing thrust.

Another method of reducing depressurization rate is to reduce the equivalent pressure in the cabin from 8,000 to 6,000 feet. If the equivalent altitude in the cabin is reduced, then not only is the depressurization rate reduced but passenger comfort increased. However this increased cabin pressure does result in a fuselage that is heavier.

The most direct way of obtaining the climb characteristics is fundamentally simple.

Usual Angles of Climb. Unaccelerated Flight

In level flight at constant speed, the thrust of the engines is equal to the drag of the airplane. If the thrust is increased, this added thrust can be used to either accelerate, climb or both accelerate and climb simultaneously. Figure 2:25 a shows the airplane forces in level unaccelerated flight. Figure 2:25 b shows the airplane in climbing unaccelerated flight.

In level unaccelerated flight, lift is equal to weight and thrust is equal to drag. If it is desired to use all the added thrust to climb while maintaining the same speed, the attitude of the airplane is changed by deflecting the elevators up. To reach equilibrium the airplane is rotated until

$$T = D + W \sin \theta \quad (2:61)$$

where θ = angle of climb

It should also be noted that the lift of the airplane must equal only $W \cos \theta$. This is accomplished by flying at a slightly smaller angle of attack which would decrease C_L and therefore the induced drag. However for the usual angles of climb, even up to 15° to 20° the effect is usually negligible.

Figure 2:25 c shows the relationship between the velocity, the rate of climb and the angle of climb.

$$\sin \theta = \frac{R/C}{V} \quad (2:62)$$

From Equations 2:61 and 2:62

$$T = D + W \frac{R/C}{V} \quad (2:63)$$

$$R/C = \frac{(T - D)V}{W} \quad (2:64)$$

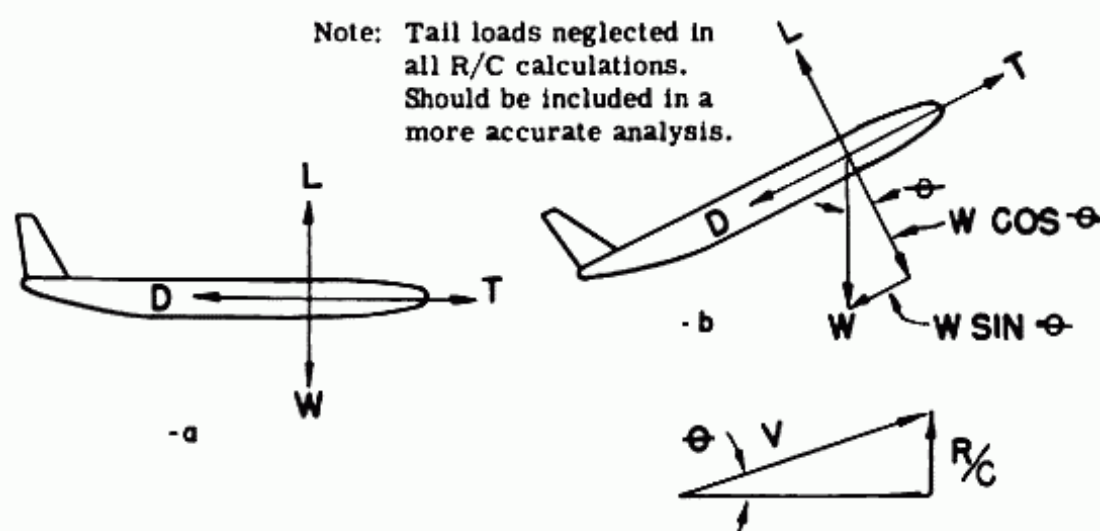


Fig. 2:25.a, Fig. 2:25 b, Fig. 2:25 c. Airplane forces in level and climbing flight.

R/C is usually expressed in feet per minute and V in knots.

Therefore

$$R/C = \frac{101 (T - D) V}{W} \quad (2:65)$$

where R/C = ft/min.

V = knots

This is the usual form of rate of climb formula and assumes that the angle of climb is small enough so that lift is assumed equal to the weight, or $\cos \theta$ equals 1.0.

High Angles of Climb. Unaccelerated Flight

For high angles of climb, it is necessary to account for the fact that the induced drag is reduced since the lift must equal only weight times cosine θ , as seen in Figure 2:25 b.

Therefore, since

$$C_{D_i} = \frac{C_L^2}{\pi A Re} \quad \text{and} \quad L = W \cos \theta \quad (2:66)$$

$$D_{i(1)} = D_{i(0)} \cos^2 \theta$$

where $D_{i(1)}$ = induced drag in high angle of climb

$D_{i(o)}$ = induced drag in level flight

θ = angle of climb

Therefore

$$R/C = \frac{101(T - [D - D_{i_o}(1 - \cos^2 \theta)])V}{W} \quad (2:67)$$

where

D = total drag of airplane in level flight

D_{i_o} = induced drag of airplane in level flight

It can be seen that this is the general form, and if $\cos \theta$ is equal to 1.0 the formula is the same as Equation 2:65.

Climb with Line of Thrust Not in Line with Line of Flight

The previous discussion of rate of climb assumes that the thrust is in line with the line of flight. Although this is rarely true, the error involved in this assumption is usually negligible. However for certain conditions of flight, its effect might be significant and should be accounted for.

The rate of climb formula must be derived from the following equilibrium Equation. (See Figure 2:25 d.)

$$T \cos \phi = D + W \sin \theta$$

$$L = W \cos \theta + T \sin \phi$$

It should be noted in some conditions the thrust might be so directed that

$$L = W \cos \theta - T \sin \phi$$

Acceleration

For subsonic airplanes the effect of acceleration in the rate of climb is usually negligible. However in fast climbing airplanes or rockets it is important, and a few notes will be added here. Since a force is required to produce acceleration,

$$F = ma \quad (2:68)$$

then, if an airplane is accelerated, not as much force is left for climbing. The following formula has been developed to account for variation in rate of climb due to acceleration. It can be used if the velocities are known at two altitudes, and it is desired to climb and accelerate from the lower altitude and lower speed to the higher altitude and higher speed.

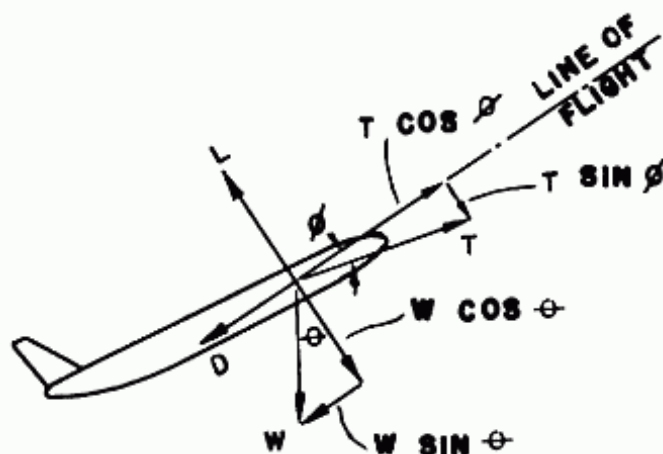


Fig. 2:25 d. Forces on an airplane in climb with thrust at an angle with line of flight.

$$R/C \text{ with acc.} = \left(\frac{1}{1 + K} \right) R/C_{\text{no acc.}} \quad (2:69)$$

where

$$K = \frac{(\Delta V) (V_{\text{ave}})}{(\Delta \text{alt.}) g}$$

ΔV = difference in velocities in ft/sec.

V_{ave} = average velocity in ft/sec.

Δalt = difference in altitude in feet

g = acceleration of gravity = 32.2 ft/sec²

$R/C_{\text{no acc.}}$ = average of the rates of climb at the low altitude and the low speed, and the high altitude at the high speed, assuming no acceleration.

Method

Assuming that the angle of climb is small and acceleration is negligible, then

$$R/C = \frac{(T_a - T_r)101V}{W} \quad (2:70)$$

Assume various velocities of climb, determine the thrust required, and the thrust available and calculate the rate of climb. Since $(T_a - T_r)$ and W vary with altitude the rate of climb should either be integrated over the entire climb or broken down into small increments and summed up, for accurate results. How-

ever this degree of accuracy is not warranted for preliminary design.

Since the fuel used in climb is a small per cent of the total weight, W , results of sufficient accuracy will be attained if the average total weight is used. A large percentage error in the estimate of the fuel used in climb will result in a negligible error in the average weight and therefore the rate of climb. From empirical data, it has been found that if an average altitude equal to 20/35 of the altitude at top of climb is used in the calculation of thrust required and thrust available, reasonably accurate results are obtained. Therefore for preliminary design purposes, Equation 2:70 may be used to determine the rate of climb if the average weight is used for W , T_a and T_{req} are determined at 20/35 of the altitude at top of climb and a constant V is assumed.

From a study of climb of jet transports it has been found that a speed of climb equal to approximately $1.3 V_{L/D_{max}}$ is close to the speed of maximum rate of climb, where

$$V_{L/D_{max}} = \frac{12.90}{\sqrt{f_e}} \sqrt{\frac{W}{\sigma b}} \quad (2:71)$$

This formula can be derived by differentiating C_D/C_L with respect to C_L , equating the result to zero for maximum L/D , and then determining the V that satisfies the condition.

The total thrust required at any speed, is equal to the induced drag plus the parasite drag plus the compressibility drag

$$T_{req} = D_P + D_i + D_{comp} \quad (2:72)$$

$$D_P = 1/2 \rho S V^2 C_{D_P} \quad (2:73)$$

$$C_{D_P} = f/s \quad (2:74)$$

At any altitude, then

$$D_P = \frac{\sigma f V^2}{296}, \quad V \text{ in knots} \quad (2:75)$$

$$D_i = 1/2 \rho S V^2 C_{D_i} \quad (2:76)$$

$$C_{D_i} = \frac{C_L^2}{\pi A Re} \quad (2:77)$$

$$C_L = \frac{W}{1/2 \rho S V^2} \quad (2:78)$$

At any altitude

$$D_i = \frac{94.1}{\sigma e} \left(\frac{W}{b}\right)^2 \frac{1}{V^2}, \quad V \text{ in knots} \quad (2:79)$$

$$D_{\text{comp}} = 1/2 \rho S V^2 C_{D_{\text{comp}}} \quad (2:80)$$

At any altitude

$$D_{\text{comp}} = \frac{\sigma S V^2}{296} C_{D_{\text{comp}}} \quad (2:81)$$

$$T_{\text{req}} = \frac{\sigma f V^2}{296} + \frac{94.1}{\sigma e} \left(\frac{W}{b}\right)^2 \frac{1}{V^2} + \frac{\sigma S V^2}{296} C_{D_{\text{comp}}} \quad (2:82)$$

However for most climbing speeds, $C_{D_{\text{comp}}}$ is negligible and the usual form for thrust required at climbing speed is

$$T_{\text{req}} = \frac{\sigma f V^2}{296} + \frac{94.1}{\sigma e} \left(\frac{W}{b}\right)^2 \frac{1}{V^2} \quad (2:83)$$

Figure 2:26 shows the variation with altitude of σ , the density ratio, δ , the pressure ratio and $\sqrt{\theta}$, the square root of the absolute temperature ratio. The last, $\sqrt{\theta}$, is also the speed of sound ratio.

Figure 2:27 presents the thrust available versus altitude for the J-1 engine.

The actual engine that will be used in the jet transport airplane being designed will hereafter be called the J.T.-1 engine. It will have the same specific fuel consumptions and the same variations in thrust with speed and altitude as the J-1 engine. Therefore the charts of the J-1 engine, with the required modification for difference in sea level, static take-off thrust, can be used for the J.T.-1 engine.

The time to climb in minutes is equal to the altitude in feet divided by the rate of climb in feet per minute. The range in climb is therefore the velocity in climb multiplied by the time to climb.

$$\text{Time}_{\text{climb}} = \text{altitude}/R/C \quad (2:84)$$

$$\text{Range}_{\text{climb}} = (V) (\text{time}) \quad (2:85)$$

Figure 2:28 presents the fuel consumption of the J-1 engine in terms of miles per pound of fuel versus velocity, for various

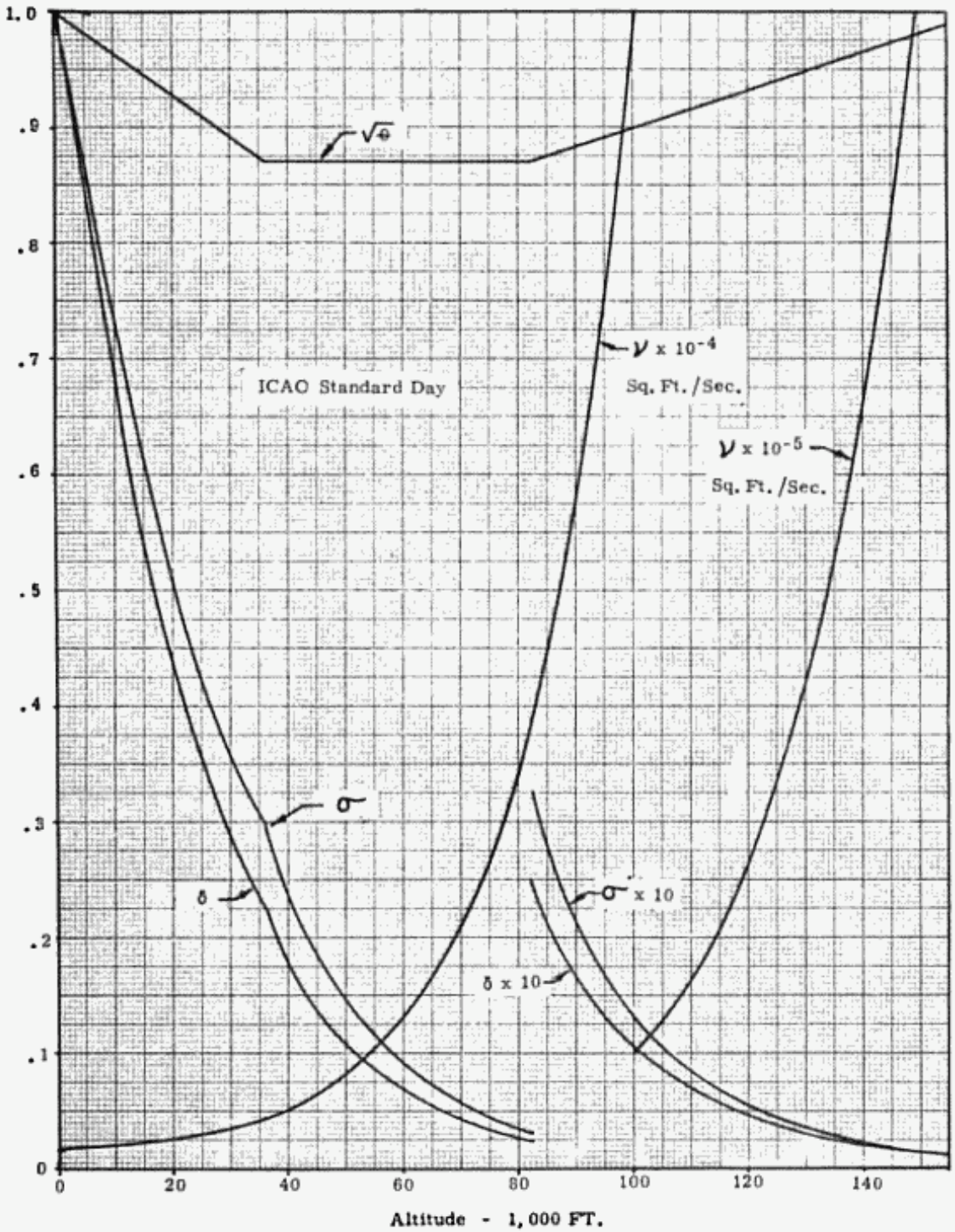


Fig. 2:26. Standard ICAO day characteristics.

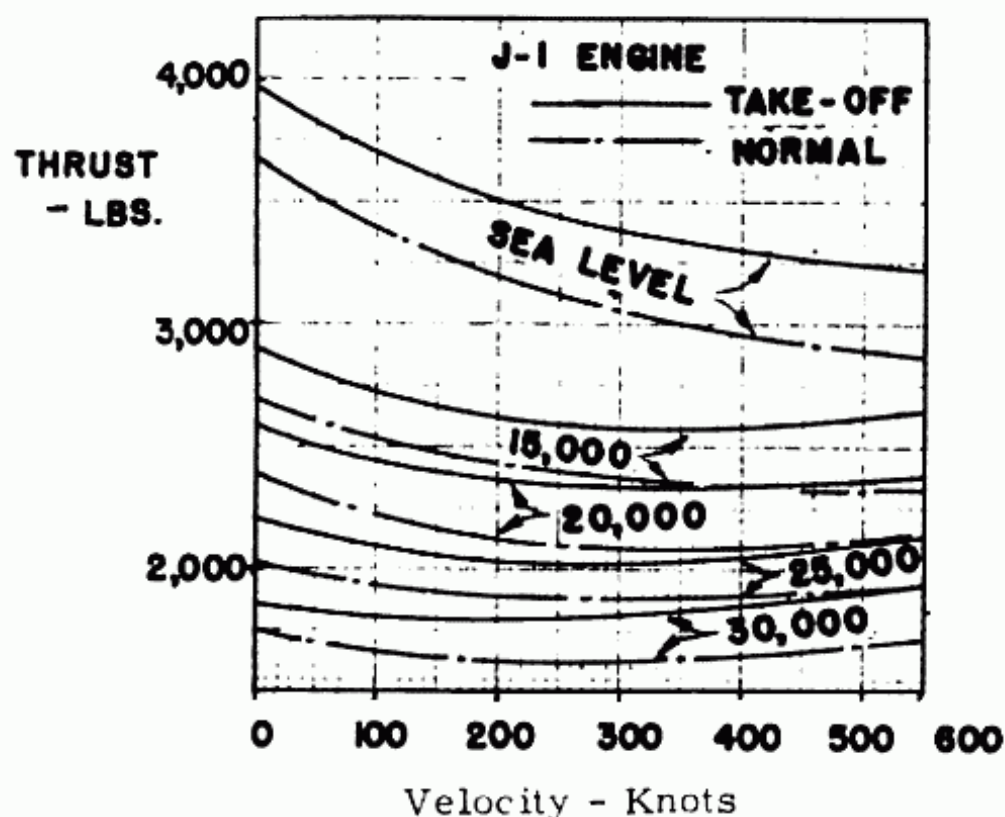


Fig. 2:27. Thrust available at altitudes below 35,000' for same engine as Figure 2:22.

altitudes for both normal and take-off thrusts. From this figure the miles per pound of fuel for the J.T.-1 engine can be determined for climb. The fuel consumed in climb is then equal to the range in climb divided by the miles per pound of fuel.

$$W_{f_{\text{climb}}} = \frac{R_{\text{climb}}}{\text{mi. per lb. fuel}} \quad (2:86)$$

For altitudes 35,000 feet and above, Figure 2:22 may be used.

The preceding method gives satisfactory results for preliminary design purposes. If more exact results are desired, a more rigorous method should be employed. The climb should be broken down into 5,000 foot increments and the rate of climb calculated for each increment, accounting for acceleration. From the rate of climb, the range in climb and the fuel to climb can be determined. The total fuel used in climb and the total range in climb can be obtained by adding all the increments calculated for each 5,000 foot interval.

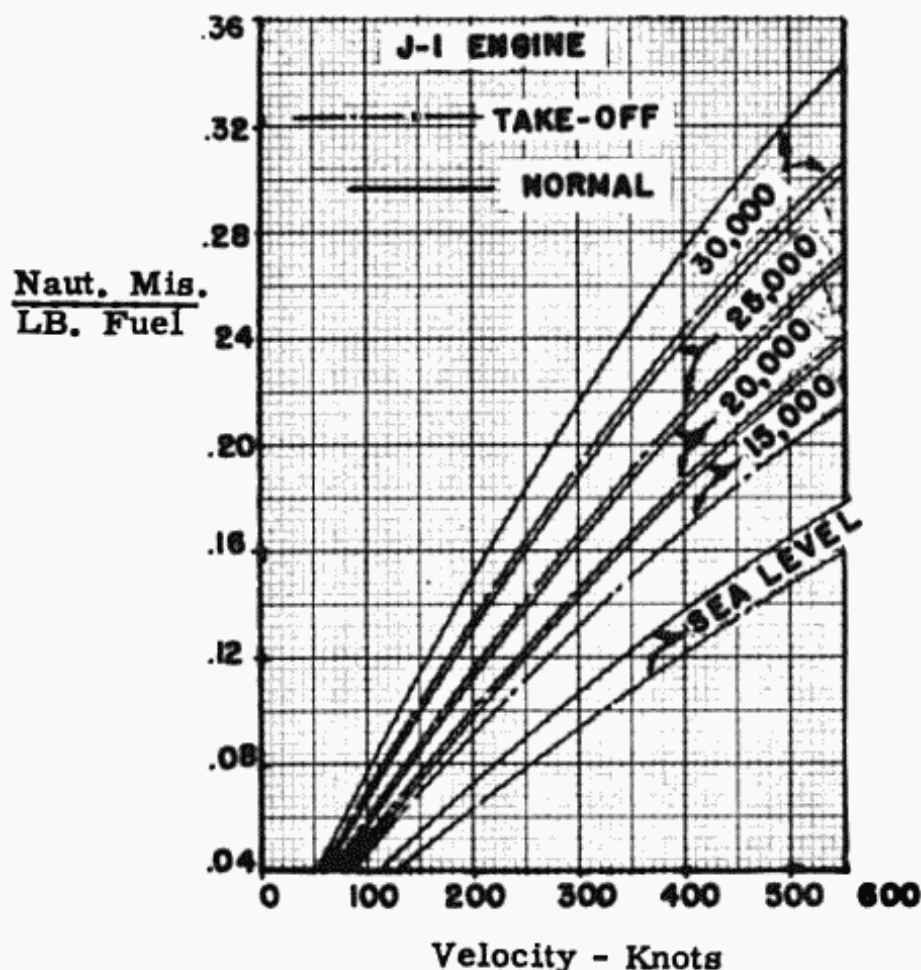


Fig. 2:28. Miles per pound of fuel at altitudes below 35,000' for same engine as Figure 2:22.

Total Range

The total range is equal to the range in cruise plus the range in climb. The range in cruise may be obtained from the mi/lb. calculated using the initial weight, W_0 , as the take-off weight minus the fuel weight used in climb, and the fuel weight, W_1 , as the take-off weight minus total fuel. This generally accepted method for determining all out range does not allow for descent. The range in descent can be calculated but depends on the assumption of the thrust used. It has generally been accepted that eliminating this extra assumption would give more standard results.

The range now calculated is based upon an approximate weight of fuel divided by take-off weight. If this is not the desired range, a new $W_{\text{fuel}}/W_{\text{take-off}}$ must be estimated and a new airplane calculated. It should be noted that this new fuel weight ratio must be used to determine a new W/S take-off from Equation 2:16, a

new W/T from Equation 2:23 and a new take-off weight from Equation 2:38. Since the take-off weight changes, so does the weight of fuel, the wing area and the thrust. It is therefore necessary to determine a new $mi\delta/lb.$ and a new range. The desired range can only be obtained by a few trials with estimated fuel weight/take-off weight ratios.

2-8 Fuel Storage

Internal

Up to this point the design has been based upon the assumption that there is sufficient internal space in the wing to store the required fuel.

The only possible places that fuel might be stored without adding any wetted area to the airplane, is the fuselage, the wing and the tail surfaces. The tail surfaces usually afford little capacity. In addition, because they are located so far from the center of gravity of the airplane, fuel variation in it would cause a large center of gravity movement of the airplane. For these reasons, the tail surfaces are neglected as a location to store fuel.

The fuselage of a transport airplane could be designed so that fuel could be stored in it efficiently and close to the center of gravity of the airplane. However in the event of a crash and the possibility of the fuel bursting into flames, it is undesirable to have fuel close to the passengers. For this reason, fuel is usually not stored in the fuselage of a commercial transport.

Therefore, if it is desirable to store the fuel internally, the only available space is in the wings. A rigorous method of obtaining the capacity of the wing involves a large amount of calculations. Sections of the wing must be drawn, their areas calculated allowing space for stringers, and a volume determined. For preliminary purposes an approximate method has been evolved which gives satisfactory results.

$$\text{Net fuel capacity} = K_2 \left(Q_1 K_1 \frac{t/c \text{ str.}}{.15} - Q_2 \right) \quad (2:87)$$

where Q_1 = capacity for a given area and aspect ratio with airfoil $t/c = .15$ streamwise, taper ratio = .5 and $d = 0$. (See Figure 2:29)

K_1 = correction factor for taper ratio variation. (See Figure 2:30)

K_2 = .91 for systems that use some type of fuel bag enclosed by smooth sheets over stringers, spars and ribs.
= 1.00 for integral fuel systems.

$\frac{t/c_{str}}{.15}$ = correction factor for thickness ratio variation.

Q_2 = quantity of fuel lost due to distance "d."
(See Figure 2:31)

d = distance from the outside of the wing skin to the inside of the fuel tank for either top or bottom. (See Figure 2:32)

Fuel capacity obtained from this formula is based upon the fuel being stored between the front and rear spars from wing tip to wing tip. If the tips are very thin and inefficient for carrying fuel, the error in assuming they do carry fuel is very small. The front spar is assumed to be at 15 per cent of the chord from the side of the fuselage outboard, while the rear spar is assumed to be at 65 per cent of the chord at the side of the fuselage and 50 per cent of the chord at the tip. The section of the wing passing through the fuselage is the same as at the side of the fuselage. Placing fuel in the portion of the wing passing through the fuselage seems contradictory to the statement that it is hazardous to have fuel in the fuselage for safety reasons. However it is felt that the wing structure through the fuselage is very rigid and strong and unlikely to spring a leak, and therefore safe for fuel storage. Nevertheless, if the wing is large enough to store all the fuel without using the portion through the fuselage it would be desirable from a safety point of view to do so.

Due to the need for large amounts of fuel space in many long range high subsonic aircraft, the space wasted by the plastic fuel tanks is intolerable, and by the special design of structural components fuel is carried integrally in the wing. For these designs of integral fuel tanks $K_2 = 1.0$, and Q_2 and d both equal 0.

If this estimate shows that there is not sufficient space to store all the fuel required there are a few possible solutions.

If it is feasible, increase the thickness ratio and sweepback so as to keep the same drag critical Mach number, but thereby increasing the fuel capacity. This may not be desirable due to the introduction of undesirable aeroelastic characteristics caused by excessive sweepback in conjunction with high aspect ratios. However if this method is possible it is the best since it does not add any wetted area.

External

In the event the above method is not feasible, there are two

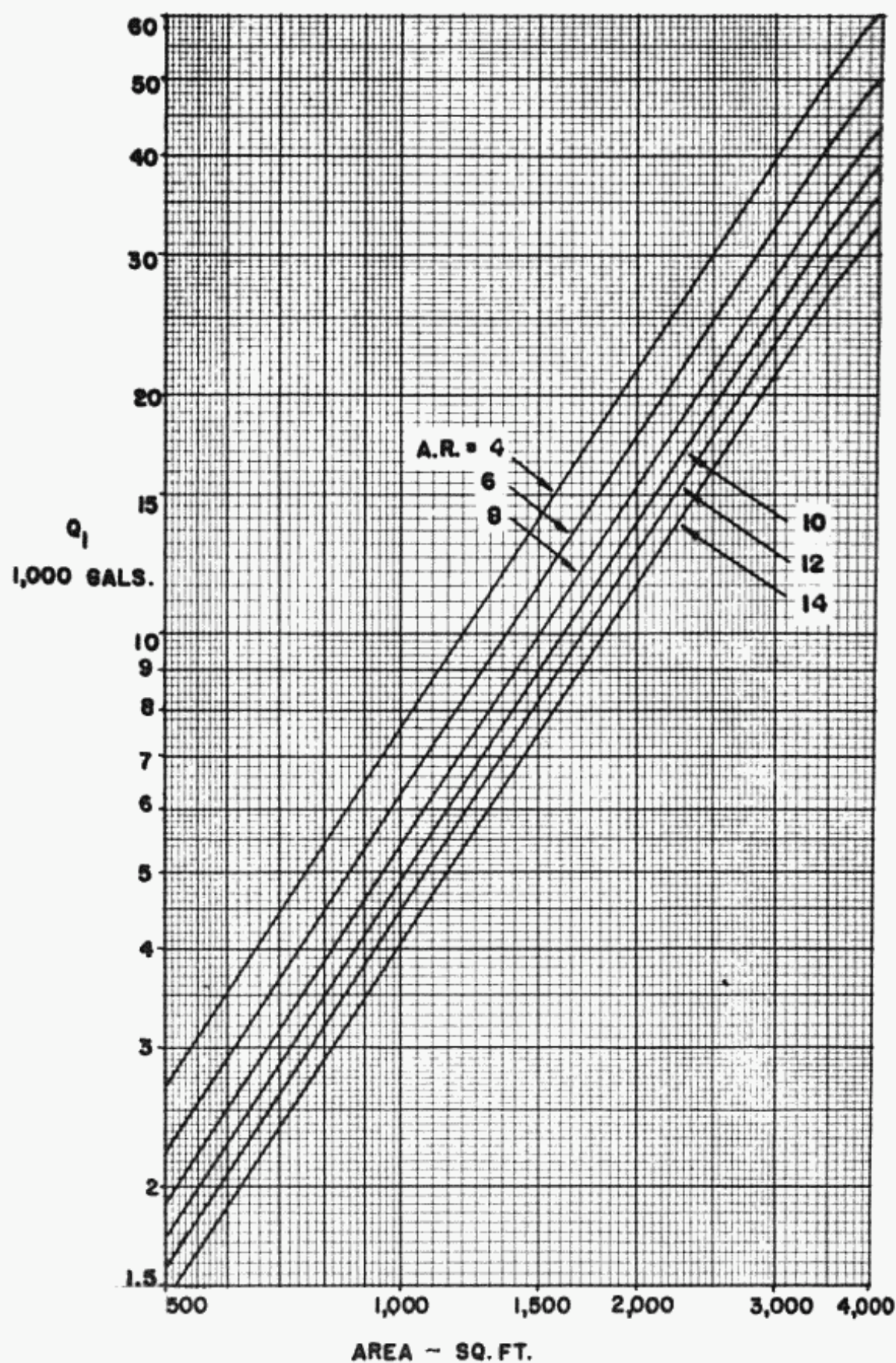


Fig. 2:29. Wing fuel capacity.

other ideas that might be studied. The first would be to add external tanks to carry fuel. It should be noted that adding the external tanks increases the weight and the wetted area and therefore will require more fuel for the same range. However if the wing has little sweep it might be possible to place the external wing tanks on the tips of the wing so as to reduce the induced drag. This is due to the fact the tanks may be made to act as end plates and thereby hinder the spilling of air over the tips. The external tanks might be added either to carry only the fuel that cannot be stored in the wing or made large enough to carry all the fuel. Although making the external tanks large enough to carry all the fuel obviously adds more wetted area, it does present some definite advantages. It is simpler to install than a series of small tanks and their necessary intertank piping. In addition, it can be placed far from the fuselage so that in case of fire it would present no hazard to the passengers. In fact it might be so designed so that it is droppable, and in the event of an impending crash the pilot could drop the tanks completely. These advantages have led some designers to the belief that it might be desirable to have only external tanks even if the wings are capable of storing all the required fuel.

The external tanks are usually a body of revolution with a fineness ratio of about five. For preliminary purposes the weight of tank can be assumed to equal about .6 of a pound per gal. of fuel. The weight of the fuel system for internal, pliocell tanks is approximately .5 of a pound per gallon of fuel, while the integral tank system weighs only approximately .13 pounds per gallon of fuel. Figure 2:33 presents the wetted area of the tank plotted against fuel capacity. For a tank supported below the wing as the nacelles are, C_f equals approximately .0030.

Increased Wing Area

Another alternative for adding fuel capacity is to increase the area of the wing, keeping all other factors the same, that is, decrease wing loading. The increase in wing area increases the parasite drag of the airplane, because of the larger wetted area,

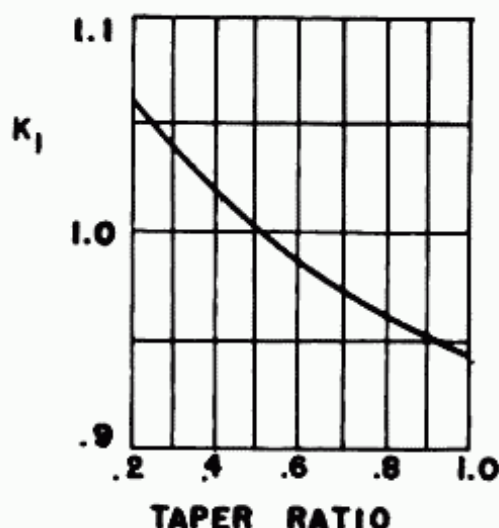


Fig. 2:30. Wing fuel capacity.

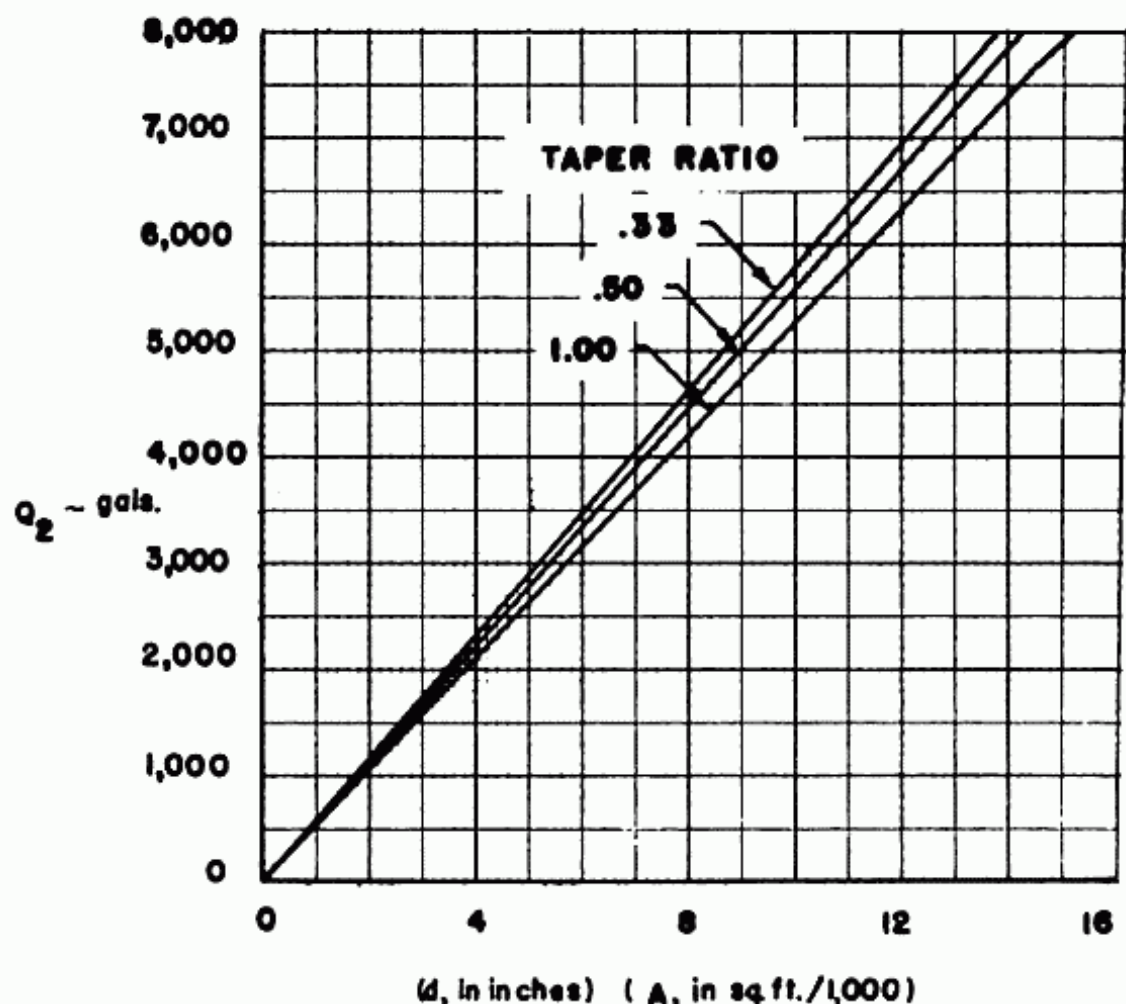


Fig. 2:31. Wing fuel capacity.

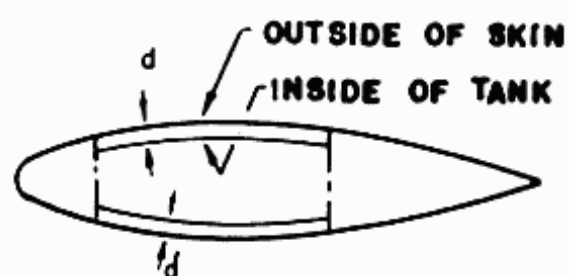


Fig. 2:32. "d," as used in Figure 31.

and also increases the weight of the wing. The lower wing loading decreases the landing field and the induced drag. To determine the optimum airplane this method should be compared with the external tank method.

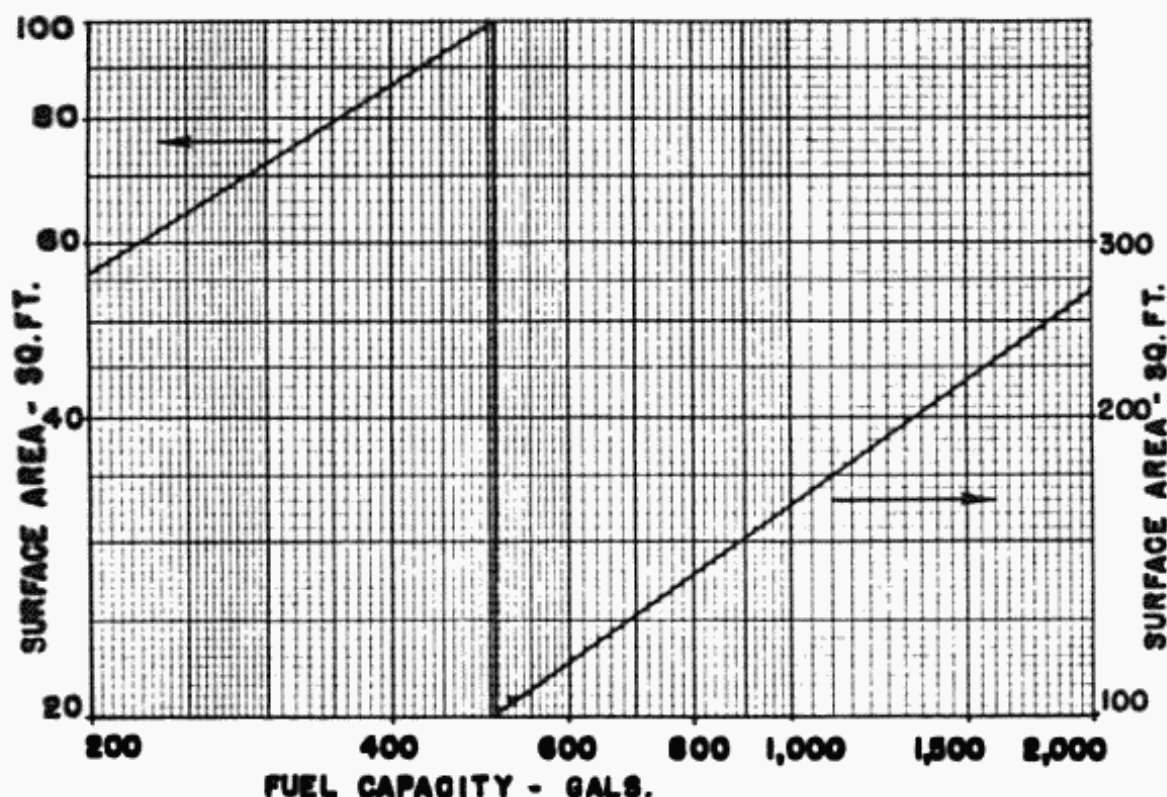


Fig. 2:33. External tanks: Surface area vs. fuel capacity.

2-9 Climb Requirements

The airplane has been designed and the thrust chosen so that the airplane can take-off in the required distance and cruise at the desired speed and altitude. However, the airplane must also be able to meet climb requirements as specified by the Civil Air Regulations. It is possible that these requirements will design the size of the engines and therefore must be investigated.

Special Civil Air Regulation No. SR 422, effective August 27, 1957, changes the Civil Air Regulations 4b as applied to "Turbine Powered Transport Category Airplanes of Current Design."

The climb requirements have essentially been broken down into 5 categories, 3 during take-off, 1 for approach and 1 for landing. Significant changes being made is that full temperature accountability is being introduced in all stages of performance, except the landing distance required. Another change is one in presenting the minimum requirements; previously these were specified as a certain value of R/C , usually as some function of stalling speeds, the new method is to specify climb gradients.

The new requirements are summarized as follows:

a) Climb Gradient Requirements

	Two Engines	Four Engines
First T.O. Segment	Positive slope	Positive slope
Second T.O. Segment	2.5%	3.0%
Final T.O. Segment	1.4%	1.8%
Approach	2.2%	2.8%
Landing	4.0%	4.0%

Condition	1st T.O.	2nd T.O.	Final T.O.	Approach	Landing
Engines inoper.	one	one	one	one	none
Thrust	T.O. at time gear is fully retracted	T.O. at 400' above take-off surface	Max. Cont. at 1000' above T.O. surface, or where trans. to enroute config. is comp., whichever is higher	T.O.	T.O.
Gear	Ext.	Retr.	Retr.	Retr.	Ext.
Flaps	T.O. pos.	T.O. pos.	Retr.	Set so that V_{S1} not greater than $1.10 V_{S0}$	Land. pos.
Weight	At time gear retraction is started	At time gear is fully retracted	At time flap retr. is started	Land. wt.	Land. wt.
Speed	V_2 , not less than $1.20 V_{S1}$	V_2 , not less than $1.20 V_{S1}$	not less than $1.25 V_{S1}$	Not greater than $1.5 V_{S1}$	Not greater than $1.4 V_{S0}$

To determine which condition is critical, each one would have to be investigated completely. However, it appears that the 2nd and final take-off segments, and the approach conditions are the most critical for 4 engine subsonic aircraft. It should be noted here that the low AR has a strong adverse influence on climb characteristics since C_{D1} is a large factor at these high C_L 's.

V_{S0} is defined as the stalling speed, or the minimum steady flight speed at which the airplane is controllable, in knots.

V_{S1} is the stalling speed, or the minimum steady flight speed at which the airplane is controllable in knots. The weight, flaps, landing, etc. shall correspond to the particular configuration for which V_{S1} is being used.

V_2 the minimum take-off safety speed shall be selected by the applicant so as to permit the gradient of climb

as required in the 1st and 2nd segment climbs, but shall not be less than

- 1) $1.2 V_{S_1}$ for 2 engine prop. driven airplanes, and for airplanes without propellers which have no provisions for obtaining a significant reduction in the one engine inoperative power-on stalling speed.
- 2) $1.15 V_{S_1}$ for propeller driven airplanes having more than 2 engines and for airplanes without propellers which have provisions for obtaining a significant reduction on one engine inoperative power-on stalling speed.

$$R/C = \frac{(T_a - T_r) 101V}{W} \quad (2:88)$$

Since the conditions of flight are specified, the velocity and weight are known, the thrust available can be obtained from the engine charts and the thrust required can be calculated. In determining the total drag, the drag of the deflected flap must be accounted for, as may be the reduced induced drag due to ground effects. Figure 2:34 presents the change in C_D due to flap deflection. Figure 2:35 presents the ground effect on the induced drag. Figure 2:36 presents the drag of the landing gears; this must be used in "landing gear extended" climb requirement.

$$V_{S_1} = \sqrt{\frac{296 W/S}{C_L \sigma}} \quad (2:89)$$

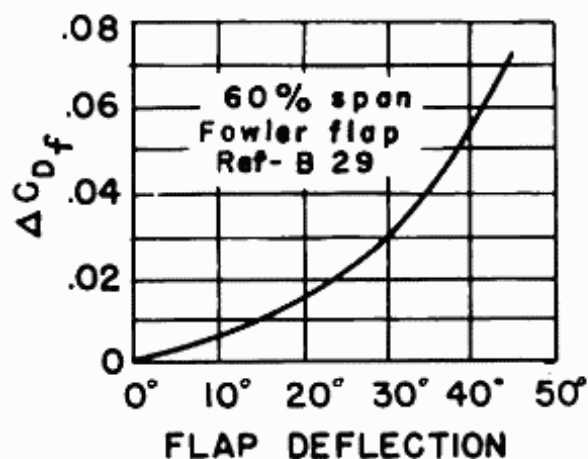


Fig. 2:34. Coefficient of drag for 60% Fowler flap. Ref.: B-29 flight tests.

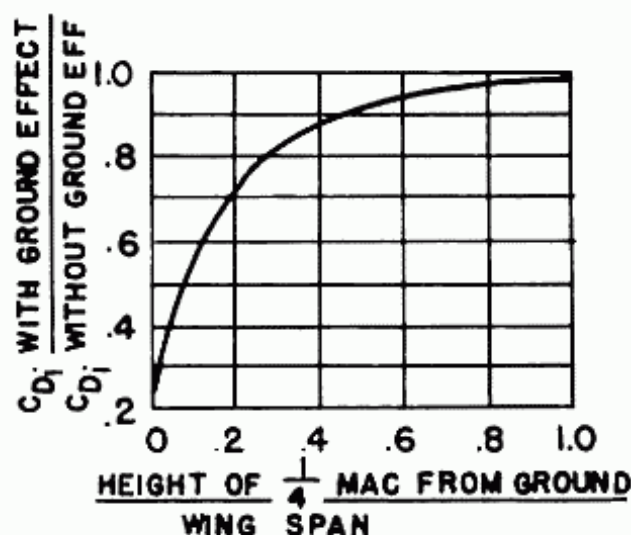


Fig. 2:35. Ground effect on induced drag coefficient. Ref.: "Engineering Aerodynamics" by W. S. Diehl, Ronald Press Co.

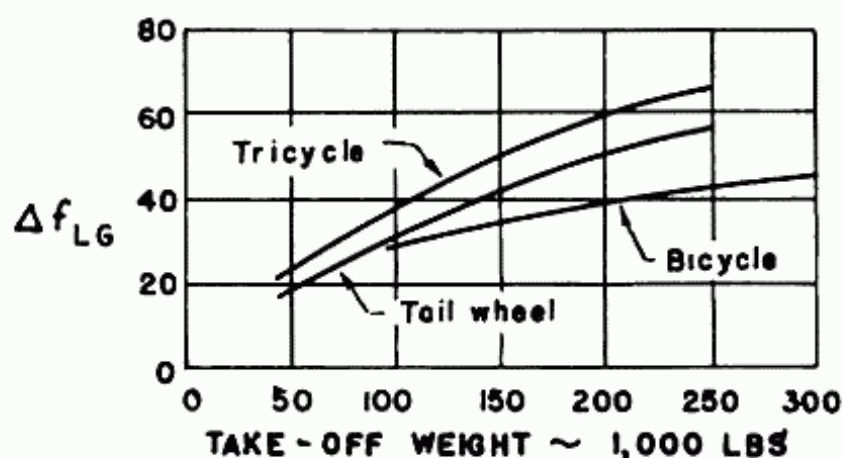


Fig. 2:36. Drag of landing gears. Ref.: "Airplane Performance, Stability and Control" by Perkins and Hage. John Wiley and Sons.

2-10 Optimum Airplane Selection of Criteria

By following the method outlined, an airplane can be designed to meet a set of requirements of field length, number of passengers, range, speed and altitude. However, since aspect ratio, and the combination of wing sweepback and thickness ratio were chosen arbitrarily, it is not the optimum airplane. It is necessary to choose a significant yet simply applied criterion for evaluating different designs so that an optimum airplane can be chosen. Since airlines are a private business, with their prime

motives being profit, probably the most significant criteria would be the per cent return on investment. To determine this criteria it is necessary to calculate the total operating costs and the investment. For an assumed total business in form of passenger miles per year, the investment can be estimated from past experience and present costs, as a function of the total airplane weight. The total operating cost is composed of the direct and indirect cost.

The direct operating cost is that cost which is directly associated to a specific flight. The cost of fuel, the pay of the crew, the overhaul time of engines, the insurance, the depreciation and the maintenance of engines and airframes are a direct function of each flight.

The indirect operating costs, which are all costs other than the direct, consist of office payroll, advertising, hangar costs, executive payroll and other miscellaneous items. These costs are difficult to determine with any degree of accuracy since they often vary drastically from one airline to another. For a very rough estimate, the indirect operating costs is often assumed to be equal to direct costs.

It is primarily because the indirect operating costs are such difficult items to determine with any degree of accuracy, that the per cent return on investment has not been chosen as the criteria for this presentation.

However some aspect of cost must be chosen as the criterion for the choice of planes, since it is the most important single item as far as the airline is concerned. The direct operating cost is the criterion that fits the specification of being significant and relatively simple to determine. It is significant because it is the cost that can be calculated for each flight and is a major factor in the total costs. Perhaps even more important is the fact that it is the cost that is most affected by the actual design of the airplane.

Since the engineer must choose the best design, and the direct operating cost has been designated as the best criterion, it is necessary for the engineer to be capable of determining this cost.

Direct Operating Cost

The latest publication of the Air Transport Association's "Standard Method of Estimating Direct Operating Costs of Transport Airplanes" in 1955 was presented to bring the method more up to date and particularly to include data and methods for gas turbine aircraft. The data for the reciprocating engines airplane is of course based on a wealth of experimental experience

while the "data specifically applicable to turbine powered airplanes are based largely on conjecture and the results therefrom should be used with caution".

The figures used in the following discussion are based upon the current costs of material and labor, the present practices in engine and airframe maintenance and overhaul, and some assumptions as to the life of the engine and airframe. Those items change from year to year, and if an accurate result is required at any time, the most up-to-date data must be used.

The direct operating cost has been broken down to the cost of five items; fuel, engine, airframe, crew and insurance. It is usually presented in terms of cents per ton mile.

1. Fuel

$$C_{\text{fuel}} = \frac{(\text{¢/lb.})(W_f)}{RP} \quad (2:90)$$

where

- R = range of flight (does not include range of reserve fuel)
- P = payload in tons
- W_f = weight of fuel in pounds for the range considered

The cost of fuel is estimated as 2.23 ¢/lb. domestic, and 2.92 ¢/lb. international. In addition turbine powered airplanes are assumed to use one quart/hr/engine. Therefore for a domestic turbine airplane with the cost of oil equal \$1.75/quart,

$$C_{\text{fuel}} = \frac{2.23 W_f}{R \cdot P} + \frac{175 N_e}{V_{BP}}; \quad \begin{array}{l} N_e = \text{number of engines} \\ = \text{number of quarts/hr.} \end{array}$$

2. Crew

The following is the pay schedule used for gas turbine transport airplanes.

Domestic base pay \$/block hr. (2 man, 18.07; 3 man, 26.14)

Int'l. base pay \$/block hr. (3 man, 28.03; 4 man, 39.95)

Hourly pay \$/n.m. (2 man, .040; 3 man, .051; 4 man, .052)

Gross wt. pay \$/block hr. (2 man .0286 G.W./1,000; 3 man or more .0341 G.W./1000)

For a domestic crew of 3 then the

$$C_{\text{crew}} = \frac{2,614 + (3.41 \text{ G.W./1,000})}{V_{BP}} + \frac{.051}{P}$$

The crew referred to above is the flight crew, and does not include hostesses.

$$V_B = \text{block speed}$$

$$= \frac{\text{range in n.m.}}{\text{time (to climb, cruise and maneuver) in hrs.}}$$

The entire flight should be based upon a 15 knot head wind. For simplification it has been assumed that the descent uses no fuel and covers no distance. Time to maneuver = .20 hrs. for 2 eng. aircraft and .25 hrs. for multiengined aircraft.

3. Insurance

The cost of insurance is simply the standard insurance rate based upon W_e plus a small factor depending on the range.

$$C_{\text{ins}} = 1.67 \frac{(\text{Cost of airplane})}{1000} \text{ per hour} + .10 \text{ per n.m.}$$

$$C_{\text{ins per ton mile}} = \frac{66.8 W_e}{1,000 V_B P} + \frac{.10}{P}$$

At the present time the cost of airplane for the jet transports, at the productions anticipated for them, is assumed to be \$40 per pound.

$$W_e = \text{weight empty}$$

4. Airframe

The cost of the airframe consists of two parts, the maintenance and the depreciation. The depreciation is based upon a depreciation period of seven years, cost of airframe equals \$40 per pound, utilization of ten hours per day, and a residual value of ten per cent at end of seven years.

The maintenance costs are based upon a study of actual maintenance costs of reciprocating engine aircraft used in service and projected estimates for the turbine powered aircraft.

$$C_{\text{maint/hr}} = \frac{627 + 31.57 W_a}{1000} + \frac{W_a(\text{cost/lb.})}{1000}$$

$$C_{\text{depr/hr}} = \frac{4.29 W_a(\text{cost/lb.})}{1000} + \frac{.43 W_a(\text{cost/lb.})}{1000}$$

$$C_{\text{¢/ton mile}} = \frac{627 + .261 W_a}{V_B P}$$

where W_a = weight of airframe
 = weight empty-weight of engines

5. Engine

The costs of the engine are also divided into maintenance and depreciation categories.

$$C_{\text{maint/hr}} = 264 K_{\text{He}_0} + \frac{19.6 N_e W_e (\text{cost/lb.})}{(1000 (K_{\text{He}_0}))} + \frac{91.5 N_e W_e}{1000 K_{\text{He}_0}}$$

$$C_{\text{depr/hr}} = \frac{7.5 N_e W_e (\text{cost/lb.})}{1000}$$

K_{He_0} is a factor dependent on the overhaul period. For an assumed overhaul period of 1,250 hours, $K_{\text{He}_0} = 1.42$. And assuming that engine cost is also equal to \$40/lb., then

$$\begin{aligned} C_{\text{¢/ton mile}} &= (375 + .55 N_e W_{\text{eng}} \\ &\quad + .065 N_e W_{\text{eng}} + .3 N_e W_{\text{eng}}) / V_{\text{BP}} \\ &= \frac{375 + .915 N_e W_{\text{eng}}}{V_{\text{BP}}} \end{aligned}$$

where W_{eng} = weight of one engine

Choice of Optimum Airplane

In designing the first airplane, a combination of wing sweepback and thickness ratio was chosen to meet the required M_{CRD} . However since there are various combinations that would result in the same M_{CRD} , it is therefore necessary to determine the optimum one.

Thickness ratio affects the airplane weight and the maximum lift coefficient. It also determines the wing fuel capacity. Sweepback also affects both the weight and maximum lift coefficient. When the thickness ratio and sweepback are varied in such relation so as to retain the same M_{CRD} , one factor will increase the weight and decrease the $C_{L_{\text{max}}}$, while the other will do the opposite. To obtain the optimum combination, the only solution is to design a series of three or four airplanes with different combinations and choose the one with the lowest direct operating cost. For this design, it has been established that sweepbacks of greater than 35° are undesirable because of the aeroelastic problems that they present in combination with high aspect ratios, and their unfavorable tip stall characteristics. Therefore if the direct operating cost decreases with increasing

sweepback beyond 35° , the latter is still considered the optimum. Figure 2:37 presents a curve of a typical design.

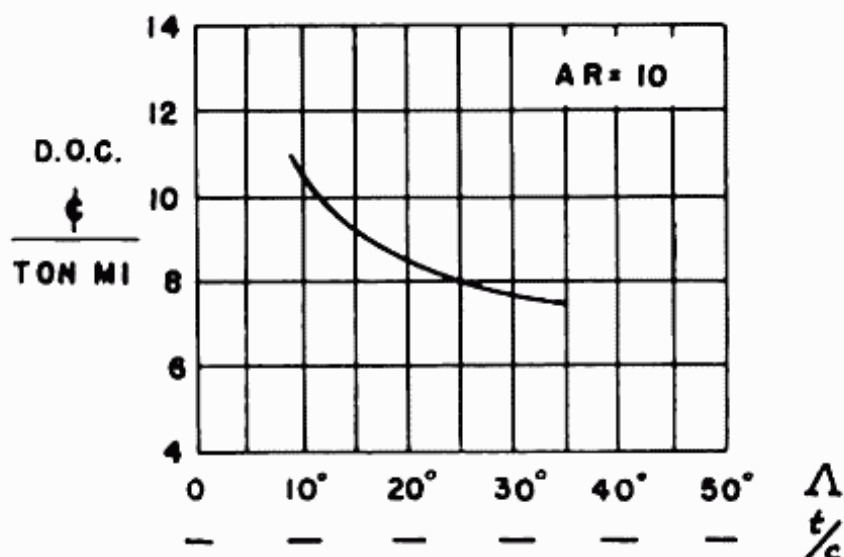


Fig. 2:37. Variation of direct operating cost with sweepback and thickness ratio for a typical jet transport.

Since a change in aspect ratio affects weight and induced drag in such a manner that one tends to improve the airplane while the other tends to reduce its efficiency, the optimum aspect ratio must also be determined by trial and error. In addition, aspect ratio affects M_{CRD} as shown in Figure 2:8. Using the optimum sweepback, airplanes are designed with various aspect ratios and direct operating costs calculated. Figure 2:38 presents a curve of a typical design.

The optimum aspect ratio is the one that results in the lowest direct operating cost. The airplane with the optimum aspect ratio and the optimum combination of sweepback and thickness ratio as calculated, is considered the best design.

It should be realized that to rigorously determine the optimum airplane, every combination of sweepback and thickness ratio should be studied with every aspect ratio. However this optimum airplane will rarely vary from the one obtained from the simplification presented.

2-11 Optimum Altitude

The airplane just designed is the optimum for the requirements specified if the cruise altitude starts at 35,000 feet and continues at a constant $W/\delta S$. However, there is probably some higher cruise altitude that would result in the highest mi/lb.,

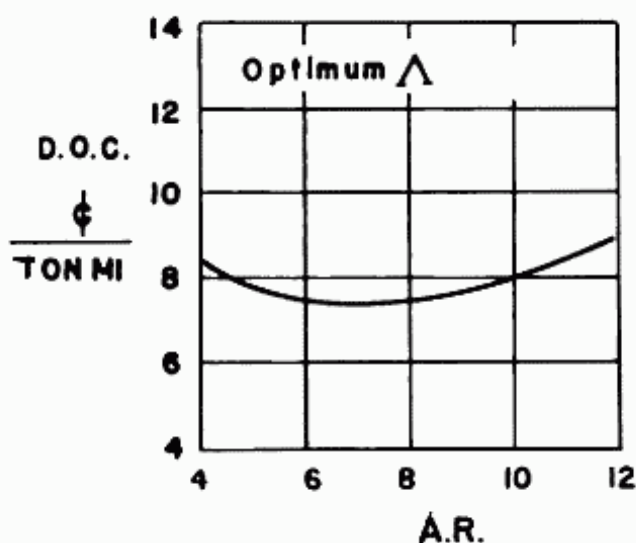


Fig. 2:38. Variation of direct operating cost with aspect ratio for a typical jet transport.

therefore the greatest range and the lowest direct operating cost. This optimum altitude is very simple to determine.

The weight of fuel required to climb to various altitudes can be determined, just as it was determined to climb to 35,000 feet. However, if it is calculated for just one high altitude, say 60,000 feet, accurate estimates can be made for the altitudes between it and 35,000 feet. If the 60,000 feet is near its absolute ceiling then the estimates would be inaccurate. The $\text{mi } \delta/\text{lb.}$ for each value of $W/\delta S$ corresponding to these starting cruise altitudes can be determined as outlined in Section 2:7. Since the weights at the beginning of cruise and the end of cruise are known, can be calculated for each $W/\delta S$. With $\text{mi } \delta/\text{lb.}$ and δ known, $\text{mi}/\text{lb.}$ can be determined and cruise range calculated. The total range, (cruise range plus climb range), can then be obtained and plotted.

As shown in Figure 2:39, total range will reach a maximum at one value of $W/\delta S$, which will indicate the optimum altitude. This optimum altitude, which will vary for each airplane, is discussed in greater detail in Section 7:6. It is possible that the optimum altitude for an airplane with a high wing loading could be 35,000 feet or even lower. However, a very long field length or very high maximum C_L would be necessary for this condition.

The direct operating cost of the airplane cruising at its optimum altitude would be less than the direct operating cost determined for 35,000 foot cruise due to the longer range possible because of the higher $\text{mi}/\text{lb.}$ However, a better comparison would result if a new airplane were designed with a lower fuel weight,

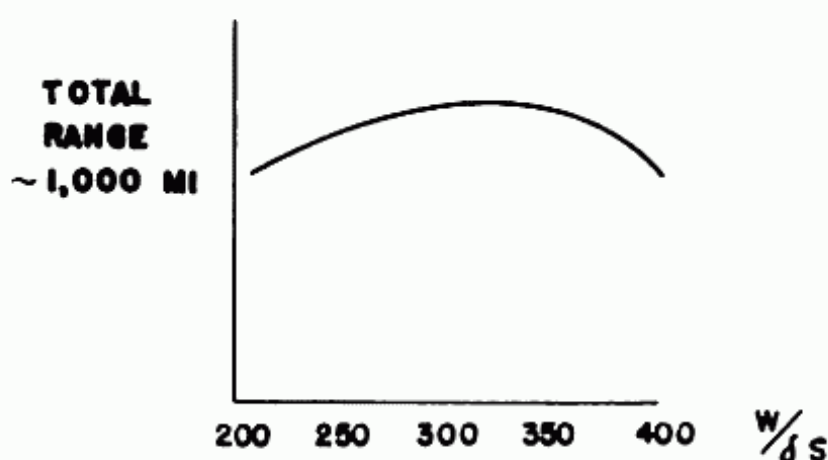


Fig. 2:39. Optimum altitude.

so that the same range was maintained while cruising at this optimum altitude. The comparison of the direct operating costs cruising at 35,000 feet and cruising at optimum altitude would then be only a result of the difference in altitude, and would include no effect of the difference in range.

It is possible that the airplane will not have enough thrust to reach a peak in the range versus $W/\delta S$ curve. In that case the direct operating cost of the airplane at the cruising altitude that does give the highest range should be determined. In addition, the thrust of the airplane should be increased, that is W/T lowered, to a value so that a peak in the range versus $W/\delta S$ curve can be obtained. The direct operating cost of this airplane with the lower W/T at this optimum altitude should be compared to the direct operating cost of the airplane with the original higher W/T to determine the optimum altitude.

PROBLEMS

Assign airplanes with varying specifications to the entire class, two students to one airplane. A partial list is:

<u>Allout Range</u> <u>Naut. Mis.</u>	<u>Cruise Speed</u> <u>Knots</u>	<u>No. of Passengers</u>	<u>Field Length</u>
2,000	425	100	8,000
"	450	"	"
"	475	"	"
"	500	"	"
"	525	"	"
3,500	500	60	8,000
5,000	"	"	"
2,000	500	60	8,000
"	"	140	"
2,000	500	100	6,000
"	"	"	7,000
"	"	"	9,000

- 1) Design airplane with $AR = 10$ and 35° sweepback to meet specifications. Altitude should be 35,000' at beginning of cruise and then at constant W/δ_s . Calculate direct operating cost.
- 2) Vary sweepback and thickness ratio maintaining same M_{CRD} . For each combination, determine direct operating cost. Choose the optimum sweepback and thickness ratio combination.
- 3) With this optimum sweepback, determine direct operating cost for aspect ratio equal to 6, 8 and 12. Choose the optimum aspect ratio. This will be the optimum airplane at the altitude specified.
- 4) With sweepback, thickness ratio and aspect ratio chosen from Problem 3, design one airplane to cruise at optimum altitude. Calculate direct operating cost and compare to airplane cruising at 35,000' at beginning of cruise.
- 5) Calculate range and direct operating cost of airplane of Problem 3, if it cruises at 35,000 feet throughout flight.

Problems 1 and 4 should be done by each student. The various characteristics investigated in Problems 2 and 3 may be divided among the students so as to reduce the amount of work for each student.

References

Ref. No.

- 2:1 Young, A. D., "Boundary Layers", Published in "Modern Developments in Fluid Dynamics - High Speed Flow", vol. I. Chapter X, Clarendon Press '53.
- 2:2 Van Driest, E. R., "Turbulent Boundary Layer in Compressible Fluids", J. Aero. Sciences, March '51.

Chapter III

AERODYNAMIC DESIGN - SUPERSONIC

3:1 Design Method - General

Much has been heard in the last few years of "Systems Analysis" or "Systems Design". Actually although the terms are comparatively new the method has been used in good preliminary design since the beginnings of airplanes. It essentially means that the concept of efficient design is a broad one; the lightest landing gear is not used because it leads to a poor ground handling airplane; the lowest drag fuselage is not used because the passengers will be too uncomfortable; the most efficient engine installation for drag purposes is not used because it leads to poor maintenance; and even the most efficient airplane, that is the one with the lowest direct operating cost, is not used because it leads to exceeding long runways. So as in subsonic design, this supersonic airplane will use the systems engineering, or good preliminary design, approach.

For supersonic transport design a new important factor arises. This is the effect of the supersonic boom on the ground. As can be seen from fig. 3:1, (obtained from ref. 3:1) it is evident that the transport airplane should not attain supersonic speed until it is at least 40,000 feet above populated areas. Although in many flights, with coast cities as the point of origin and destination, such as New York to Los Angeles or London, it may be possible to take-off and land over water, it is evidently desirable to have the airplane be able to take-off and land over populated areas, so that it can have much greater utility. This will be discussed in more detail in section 3:7 Range sub title Climb.

It is generally conceded that in supersonic airplane design it is necessary to develop all the airplane components together for optimum efficiency. The optimum airfoil section is not necessarily the section to be used with the optimum planform. The optimum plan form alone (that is without body) is not necessarily the wing plan form to be used in the optimum wing-body combination. However, in preliminary design, to eliminate the study of an infinite number of combinations it is helpful to indicate the optimum airfoil section, the optimum planform and the optimum fuselage. Using this knowledge with the interaction effects it is likely that the optimum combinations may be determined with

3:2 SUPERSONIC AND SUBSONIC AIRPLANE DESIGN

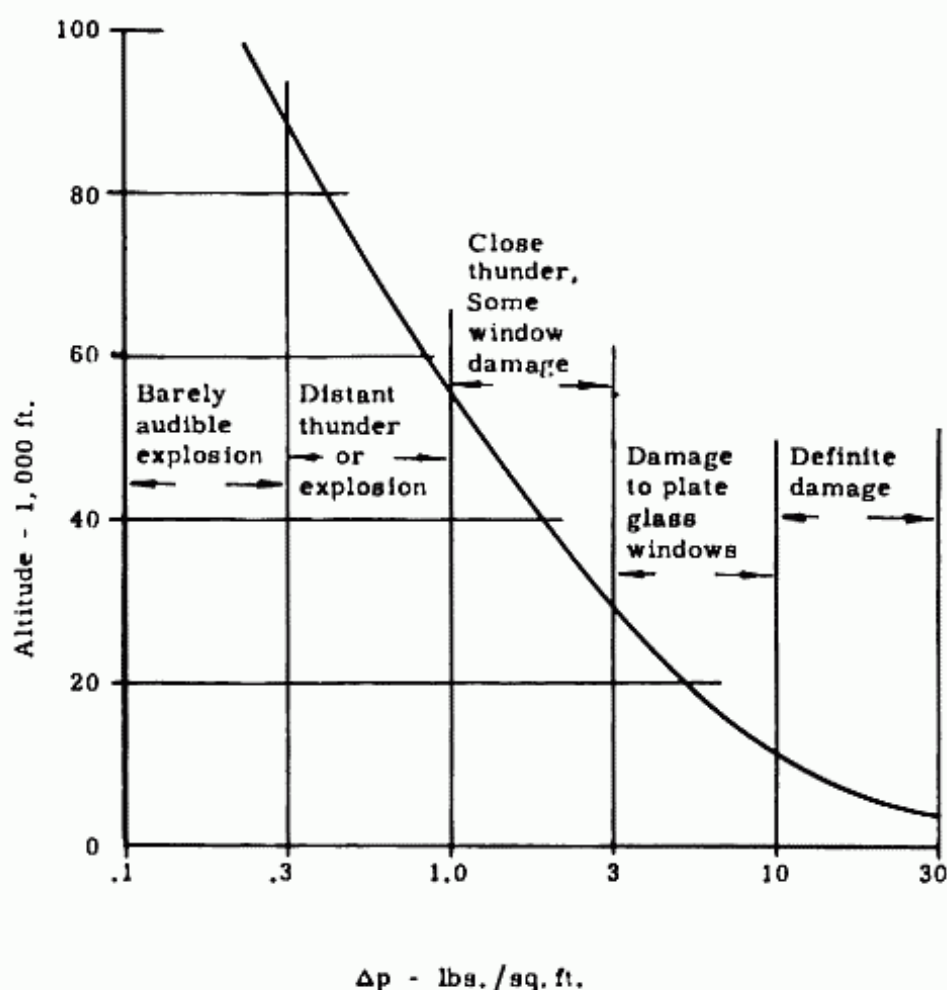


Fig. 3:1. Supersonic boom effects of a M3 transport.

less work and more certainty. After studying the characteristics of the components alone, interference effects are presented so that the components may be combined in the most efficient manner.

In general the method used in the supersonic design will be the same as used in the subsonic as described in section 2:1, that is the design characteristics will be dependent on the same principal specifications and will be discussed in the same order.

3:2 Choice of Taper Ratio and Aspect Ratio

Introduction:

The t/c and Λ chosen for the subsonic airplane was based upon the consideration that $C_{D_{comp}}$ should equal .0010. The effect of t/c and Λ on other factors that affect total C_D was assumed to be negligible.

In supersonic design, the choice of Λ is dependent both on

wave drag and on drag due to normal force, while the choice of t/c is dependent aerodynamically on wave drag only. As in subsonic design the final selection of t/c and Λ must also be tempered by the structural and fuel capacity effects.

There is also a difference in philosophy in approaching compressibility effects in the high subsonic and in the supersonic fields. In the design of the high subsonic airplanes the sweepback and thickness ratio are chosen to forestall the compressibility drag effects as the slope of the $C_{D_{comp}}-M$ curve is very steep. In supersonic flight the compressibility effects are accepted as inevitable and the wing is designed to be the most efficient compromise considering the combined aerodynamic and structural viewpoint.

As stated previously the t/c and Λ of the subsonic airplane were chosen so that $C_{D_{comp}}$ equalled .0010. It should be emphasized that this value is only an estimate. To actually obtain the most efficient combination of t/c and Λ , different combinations with corresponding values of $C_{D_{comp}}$ should be investigated, and the combination that results in the lowest direct operating cost is the optimum.

Source of Data

There are various sources of 3 dimensional wing data that can be used in choosing t/c and Λ . At this time it appears that the most systematic presentation is the theoretical data in ref. 3:2.

The data, based upon the linear theory and using the reversibility theorem, is presented in a series of curves of

$$\beta C_{L_{\alpha}} \text{ vs } \beta \cot \Lambda \text{ for various values of } \beta A$$

$$\beta C_{M_{\alpha}} \text{ vs } \beta \cot \Lambda \text{ for various values of } \beta A$$

and $\frac{\beta C_D}{(t/c)^2} \text{ vs } \beta \cot \Lambda \text{ for various values of } \beta A$

for double wedge and biconvex sections,

where $\beta = \sqrt{M^2 - 1}$, $\Lambda =$ sweepback of leading edge,

$$C_{L_{\alpha}} = dC_L/d\alpha, \quad C_{M_{\alpha}} = dC_M/d\alpha,$$

$A =$ aspect ratio of wing alone (no body)

Wings with taper ratios of 1.0, .5 and 0, are covered.

Method

In subsonic design the combination of Λ and t/c that resulted in the lowest D.O.C. for some arbitrary A.R. was assumed to be the best for all other aspect ratios. Although it was realized that this is not necessarily true, it was assumed to be accurate enough for the airplanes considered. In supersonic design it appears that the effects of Λ and A.R. cannot be separated as in the subsonic field and a slightly different approach is used.

Figs. 3:2 and 3:3, taken from ref. 3:2 present $\beta C_{L\alpha}$ and $\beta C_D/(t/c)^2$ vs $\beta \cot \Lambda$ for various values of βA for taper ratio = 0.

For the supersonic transport design the wing with taper ratio equal to zero and with either a trailing edge that is not swept, or is swept forward, has been considered. This taper ratio has been chosen because it results in the lowest wing weight, the largest fuel capacity, and no deleterious tip effects. The non-swept back trailing edge has been chosen because it probably results in the lightest and the least flexible wing. Actually the sweep of the wings to be investigated will vary from 0° at the midchord to those values resulting from an unswept trailing edge. For the case of the unswept trailing edge, $\cot \Lambda = A.R./4$, where Λ is the sweepback of the leading edge.

As an aid in choosing the wing plan form, the data from ref. 2 has been cross plotted to show the effect of A.R., and sweepback on L/D for M between 2.0 and 6.0. Although figs. 3:2 and 3:3 (taken from ref. 3:2) show peaks in the $\beta C_D/(t/c)^2$ and $\beta C_{L\alpha}$ curves at the values of sonic leading edge and max. thickness lines, these sharp breaks do not occur in actual flight. This phenomena is verified by test results reported in ref. 3:2 itself. In addition references 3:19 to 3:21 compare experimental results to theory for a great number of wing plan forms and Mach numbers, with varying degrees of agreement.

Fig. 3:4 a and b present L/D vs C_L (or W/S) for a double wedge airfoil wing with $t/c = 0.3$, $\lambda = 0$ and $\Lambda_{.5C} = 0$, cruising at 60,000 ft. for both $M = 2.0$ and 4.0. It shows that the optimum C_L varies from .10 to .11 for $M = 2.0$, and from .05 to .06 for $M = 4.0$.

Fig. 3:5 compares the L/D 's of the delta wing and the zero sweep .50 chord wing at $M = 2.0$ and 4.0, at their optimum C_L 's (as obtained from fig. 3:4) at $t/c = .03$. From these curves there is little to choose between the two plan forms, with the delta wing having a slight edge, up to 4%, at certain values of A.R. However these have been compared only at one value of C_L (the optimum for L/D), at one value of t/c , and only for the

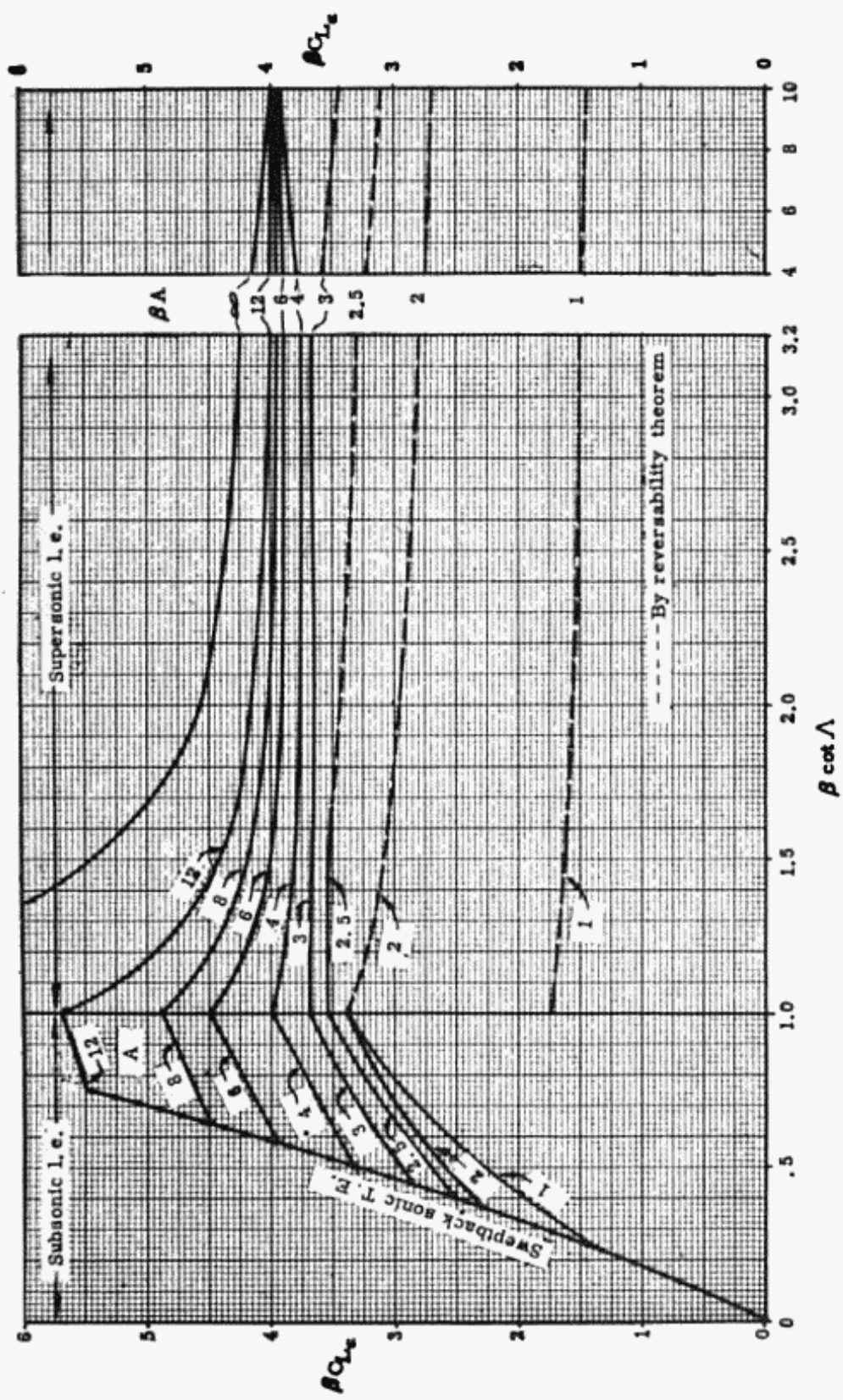


Fig. 3:2. $C_{L_{\alpha}}$ vs. $\beta \cot \Lambda$ for sweptback landing edge wings with double wedge air foil sections and taper ratio = 0.

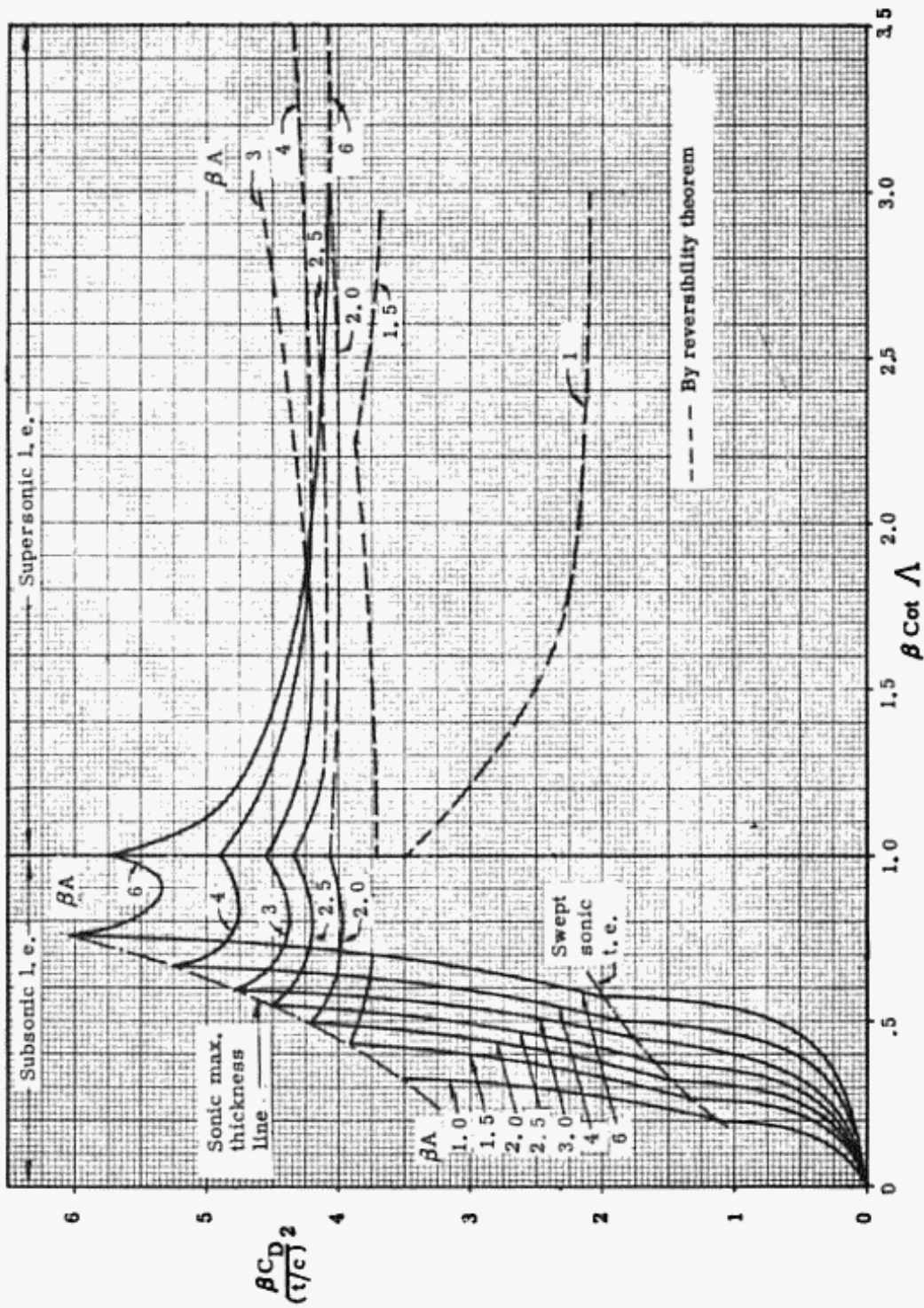


Fig. 3:3. Wave drag coefficient vs. $\beta \cot \Lambda$ for swept l.e. wings with double wedge air foils and taper ratio = 0.

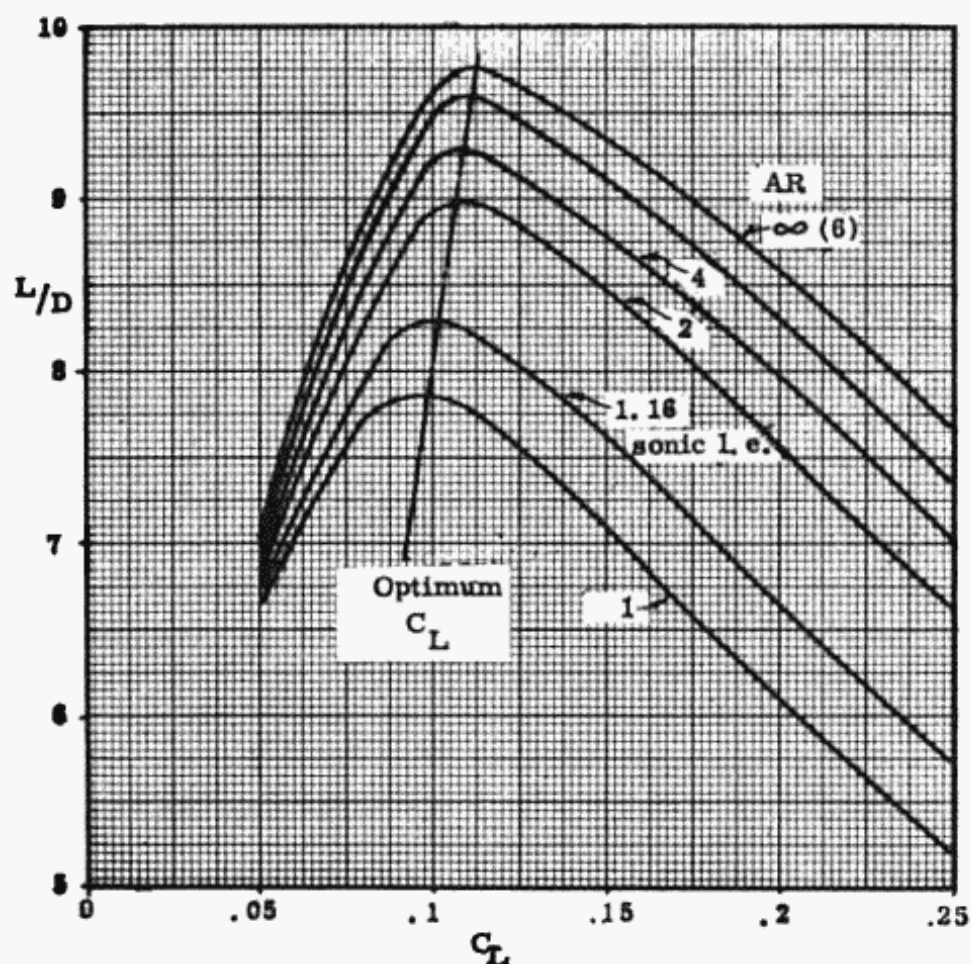


Fig. 3:4a. L/D vs. C_L for double wedge section wing $t/c = .03$, $\lambda = 0$, $\Lambda_{.5c} = 0$, at $M = 2.0$ and 60,000 ft.

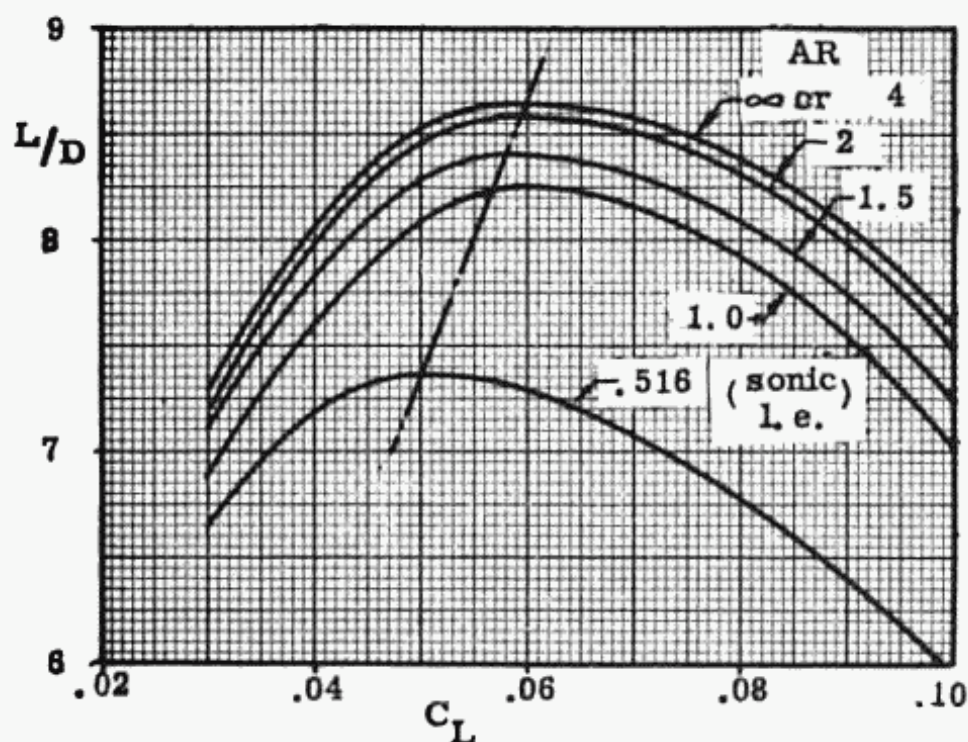


Fig. 3:4b. L/D vs. C_L for double wedge section wing $t/c = .03$, $\lambda = 0$, $\Lambda_{.5c} = 0$, at $M = 4.0$ and 60,000 ft.

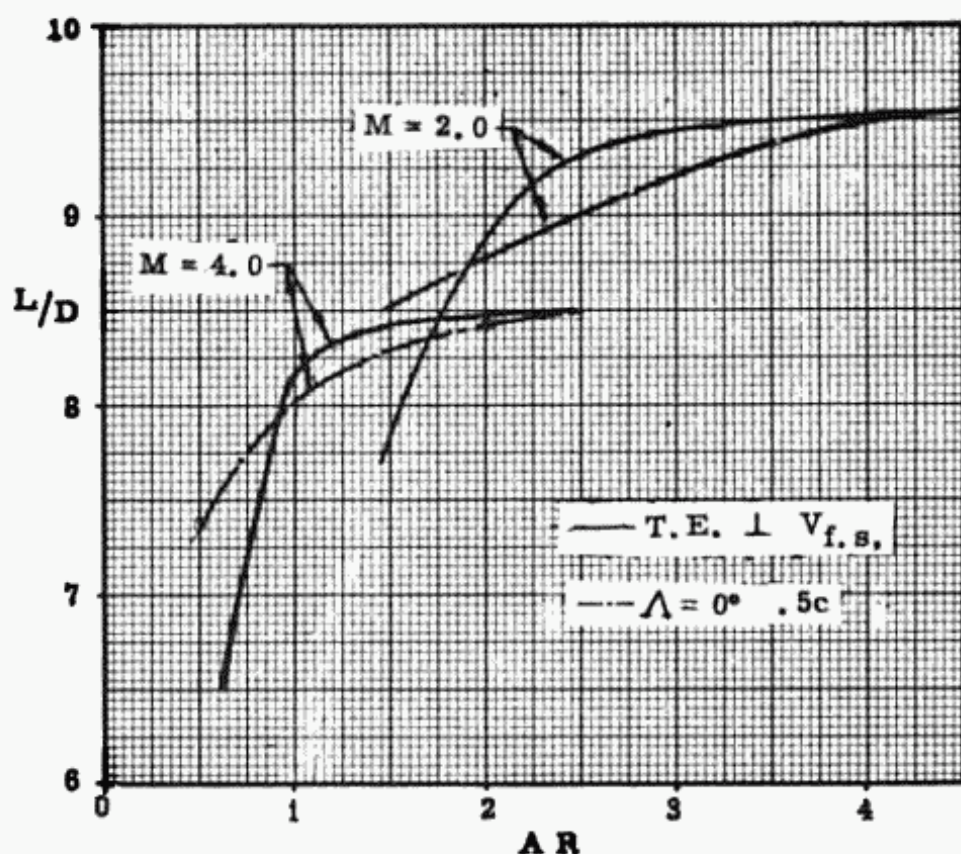


Fig. 3:5. L/D vs. AR for $M = 2.0$ at $C_L = .1$ and for $M = 4.0$ at $C_L = .05$; delta wings and zero $c/4$ sweep wings. $t/c = .03$

double wedge airfoil. Other values than those chosen will unquestionably change the relationships somewhat.

A very important advantage of the delta wing over the zero sweep wing is the much smaller shift in a.c. from subsonic to supersonic flight. In supersonic flight the a.c. is at approximately .50 MAC for both. However in subsonic flight the a.c. of the zero sweep wing is at .25 MAC, while the delta wing a.c. is at approximately .35 to .40 MAC. This smaller shift in a.c. is a great advantage in stability and control, as will be shown in part II "Stability and Control," and results in a more efficient airplane.

Because of the slight advantage in L/D , and decided advantage in stability and control, as well as the structural and mechanical advantages possible with the straight trailing edge, the delta wing has been chosen at this time for the supersonic transport. There is obviously a need for a more thorough investigation of the optimum planform. The one chosen is not necessarily

the best for any other design, or even for the one being investigated.

Ref. 3:22 shows that the max. C_L 's of low A.R. delta wings are surprisingly high. A 2.04 A.R. delta wing (63.03° leading edge sweep) with either a NACA 0005 (modified) wing section, or a 5% thick double wedge with its max. thickness at .20 chord (faired), has a max. C_L of 1.34 at $RN = 15 \times 10^6$. The angle for this $C_{L_{max}}$ is 34° with no flaps. At $RN = 32.3 \times 10^6$, a 2.0 A.R. delta wing with the same 5% thick double wedge with its maximum thickness at .20 chord has a max. C_L of 1.37 at $\alpha = 33^\circ$ with no flap. By adding a leading edge flap for 86% span max. C_L is increased to 1.62 at $\alpha = 37^\circ$. These wings have very low values of L/D at .85 max. C_L ; approximate 2.35 without flap, and 2.15 with flap. To use wings with these sections and such low A.R.'s it will probably be necessary to use some other devices to obtain higher values of max. C_L with higher values of L/D , so that the airplane will have satisfactory handling characteristics in landing.

For a supersonic transport that has the specifications of M , range, number of passengers and landing field, just as the subsonic, the solution is again one of minimizing the direct operating cost by first comparing different type wings. The wing plan form that results in the lowest direct cost, for one particular wing-body combination may be used as a basis to compare other wing-body combinations. Of course, here again it is possible that some other plan form in a different wing-body combination might prove most efficient. However, at this time this approach appears to be the best available for studying the subject of supersonic airplane design.

In the subsonic design the high speed jet transport was specified to start cruising at 35,000 feet. This altitude was specified because it was felt that the problems involved with explosive decomposition, or pressure leakage at higher altitudes did not make it desirable to try to derive the benefits of somewhat lower D.O.C.'s obtainable at some higher altitudes. However with supersonic flight it is accepted that the cruising altitudes must be considerably higher than 35,000 feet or the direct operating costs will be so high as to make the supersonic transport unacceptable. It will then be necessary to design the cabin structure so as to be as reliable as the wing structure. The studies used for ref. 3:1 indicate that the first supersonic transports will cruise at M approximately 3.0 at an altitude of 60,000 feet

3:10 SUPERSONIC AND SUBSONIC AIRPLANE DESIGN

or higher. It is then necessary to add another variable to this design problem and that is the optimum altitude.

It would appear that it might be desirable to first choose W/S , as outlined in 2:3, in which it is dependent on landing field and max. C_L primarily. The optimum altitude might then be approximated by choosing a likely delta plan form, i.e. A.R. and a likely thickness ratio, possibly .03, and determine the altitude that results in the highest L/D . Although this optimum altitude will vary with A.R. and t/c as shown in figs. 3:6 and 3:7, it may be used for a preliminary design estimate. Fig. 3:6, which shows the variation in L/D with altitude for a delta wing with $t/c = .02, .03$ and $.04$, aspect ratios, 2, 3 and 4, and wing loadings 60, 80 and 100, indicates the optimum altitudes for a M_2 transport. Fig. 3:7 presents the L/D variation with altitude for a $M = 4$ transport for $t/c = .02, .03$ and $.04$ at $AR = 3.0$ for $W/S = 60, 100$ and 160 .

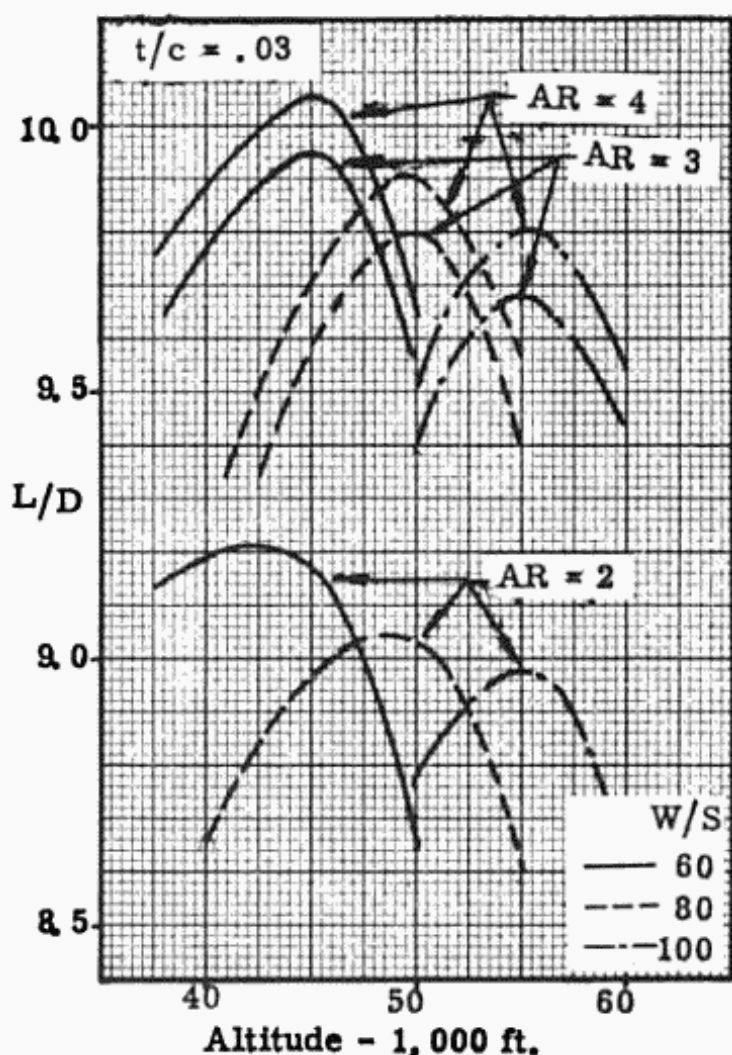


Fig. 3:6a. Effect of A.R., W/S and altitude on L/D for $t/c = .03$ delta wing at $M = 2.0$.

With the altitude chosen the problem is similar to the subsonic. The W/S and altitude, with the known M , will then determine the cruising C_L . As shown in fig. 3:5, it would appear that at $M = 2.0$ the minimum D.O.C. would occur at A.R. = approximately 2.5. Below this value L/D drops off rapidly, and the increase above this value is hardly great enough to offset the loss in range caused by the increased weight, i.e., the decrease in log of the weight ratio in Breguet's range equation.

Then airplanes may be designed at 3 values of aspect ratio, 2.0, 2.5 and 3, at the same t/c to determine the optimum A.R. for minimum D.O.C. This aspect ratio can then be used with four t/c 's to determine the optimum t/c .

As will be shown later other considerations will be taken into account in finally choosing A.R. and t/c . Other factors

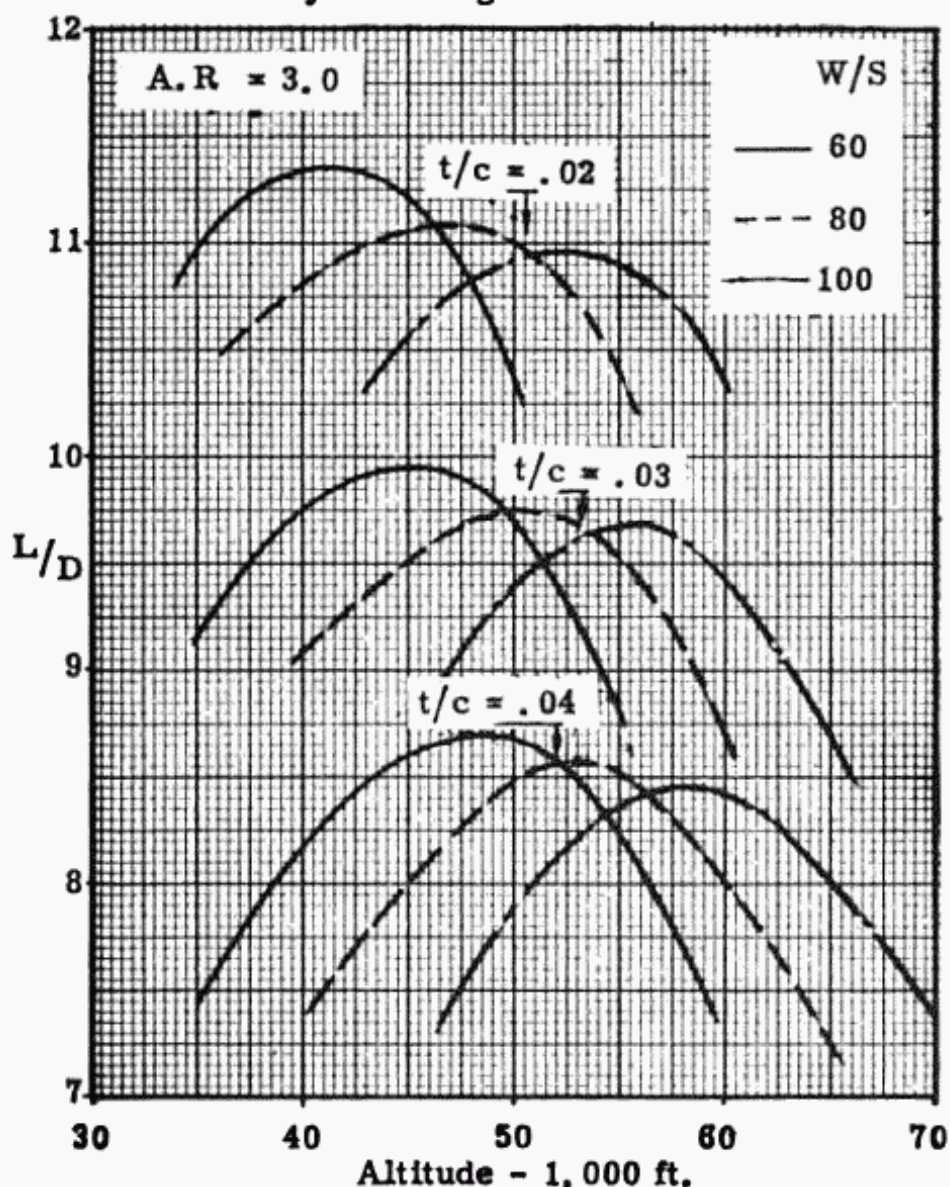


Fig. 3:6b. Effect of t/c , W/S and altitude on L/D for A.R. = 3.0 delta wing at $M = 2.0$.

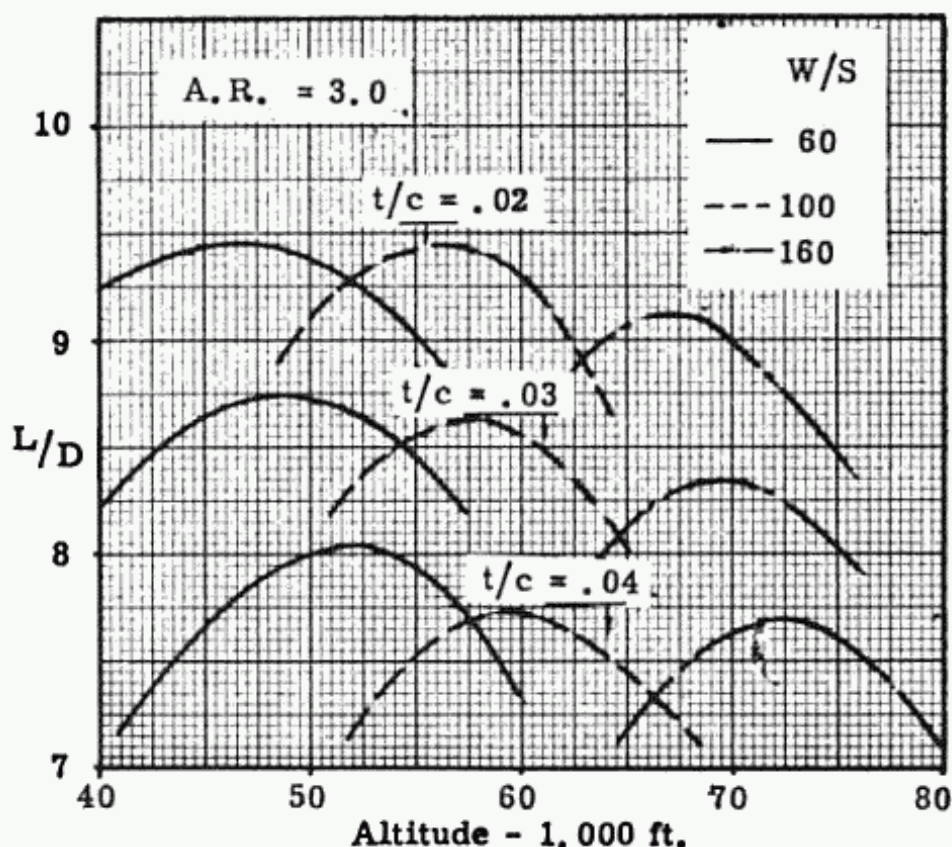


Fig. 3:7. Effect of t/c , W/S and altitude on L/D for $A.R.$ 3 delta wing at $M = 4.0$.

affecting choice of $A.R.$ are the effects of $dC_L/d\alpha$ on the gust load factors, on the angle of attack required for landing and on L/D in landing, and the effect of subsonic induced drag on climb and acceleration characteristics. The main factor affecting choice of t/c other than those mentioned, is the important criteria of fuel capacity. If a certain value of t/c results in the minimum D.O.C. and there is insufficient room in the wing to store the required fuel, it may be more efficient to increase the wing thickness than to either add external tanks, or use some other storage method.

The optimum wing plan form, airfoil thickness ratio and altitude may be chosen for any cruising M as outlined by the above method.

Before leaving this section it must be noted that the weight ratio is a very important factor in the supersonic transport, and therefore much emphasis must be placed on the structural weight. Actually the final calculation of the minimum direct operating takes into account all aerodynamic and weight factors, and indicates the most efficient combination.

3:3 Wing Loading

The problem of determining W/S for the supersonic airplane is the same as that for the subsonic, with different aspects of it being emphasized. The effect of W/S on optimum altitude has already been discussed in section 3:2, and some results plotted in figs. 3:6 and 3:7.

As in the subsonic airplane design, the W/S may be chosen as the highest value that would permit the plane to meet the landing field requirement. Because of the supersonic cruise condition the wing probably will have a very thin section, a very low aspect ratio and a high sweepback. All these characteristics tend to reduce the usable max. C_L , and therefore require a lower wing loading than the subsonic airplane for the same landing field. However, since the supersonic transports will probably be flown only on long flights, (it is only on these flights that substantial time is saved) and have large payloads of 125 to 150 passengers, they will use only the airports of the major cities, such as N.Y., Los Angeles, Chicago, London, Paris, etc. which have long runways. Therefore, the field lengths specified for the supersonic transports will be in the order of 9,000 to 10,000 feet.

Although the lower wing loadings of the supersonic airplanes present inefficiencies in friction and wave drags, the larger wing areas will allow more fuel to be carried in the wing; and internal fuel storage space may become a problem in the very thin winged supersonic airplanes.

The problem of obtaining high values max. C_L in landing for the supersonic airplanes, is that the α for max. C_L , at the low aspect ratios that are efficient, is so great that they are difficult to attain in landing. The values from fig. 2:11 which were used for subsonic airplanes would hardly apply to the airfoil sections, aspect ratios and R.N.'s likely to exist on supersonic aircraft. Values from data such as in Ref. 3:22 (shown in section 3:2) should be used.

In using fig. 2:12 for determining W/S landing it should be noted that this figure is based on equ. 2:14 and assumes $L/D = 9.0$ in landing. Since

$$\frac{L}{D} = \frac{C_L}{C_D} = \frac{C_L}{C_{D_P} + C_{D_i} + C_{D_{L.G}} + C_{D_{FLAP}}}, \quad (3:1)$$

and

$$C_{D_i} = \frac{C_L^2}{\pi A R e}$$

L/D in landing for the supersonic airplane will be much lower than the 9.0 used for the high subsonic airplanes, because of the

3:14 SUPERSONIC AND SUBSONIC AIRPLANE DESIGN

low values of A.R. As noted in section 3:2, the .05 t/c, A.R. 2, delta wing alone has an L/D of only 2.35 at .85 max. C_L . Although a very low A.R. might be efficient for cruise, that is have good structural and aerodynamic characteristics, the requirement of proper handling characteristics in landing might dictate a higher value of A.R.

Because of the problem of attaining a high usable $C_{L_{max}}$ by conventional methods for wings with low t/c, low A.R., low λ , and high sweepback, it may be necessary to resort to a more radical approach. Two possibilities are

- 1) variable incidence wing; one incidence for cruise and another for landing and take-off, so that the fuselage can be at $\alpha = 0$ for supersonic cruise and close to 0 for take-off and landing.
- 2) blowing over the wing to increase C_L at all α 's.

Each of these systems has disadvantages of added weight and complexity. It is then necessary to analyze the airplanes for the D.O.C. with these two systems and the conventional flap design, and then decide on the optimum design. It should be noted that the variable incidence wing does not increase the low value of L/D at landing, while a blowing system might. The low L/D is largely a function of the high induced C_D due to the low A.R.

The in-flight variable sweep wing shows promise of solving the max. C_L and L/D dilemma. However, it would not be used on a transport airplane until it has been shown to be safe by years of flight on a military airplane. The mechanical problems, the added flexibility, the added weight, and the usage of internal fuselage space for retraction, are the factors that inhibit the development effort.

3:4 Thrust Loading

For the supersonic transport, as in the subsonic, 3 conditions must be considered in choosing the thrust loading: take-off distance, rate of climb and cruising speed. It would appear that the high cruise speed required would cause this to be the critical condition. However, a first estimate of W/T based on take-off distance would be justified since it will insure this performance specification, and would otherwise require checking at some later time.

The same method and data as presented in section 2:4 for the subsonic airplane can be used for the supersonic. Fig. 2:14 should be used only as a rough approximation for supersonic aircraft as it is based on an average value of drag/thrust to be

expected during take-off for subsonic aircraft. As has been mentioned in connection with wing loading in section 3:3, the drag during take-off and particularly during climb, will be considerably higher due to C_{D_i} . It should be noted that during most

of the ground run C_L can be maintained very close to zero. A good check on ground run can be made as outlined in Chapter VI, section Take-off Distance.

Based upon experience it appears that the value of W/T required for the take-off field length is too high to attain the M_{cruise} desired. A lower value than the take-off W/T may be assumed at this stage.

Fig. 3:8 presents an estimate of the performance of a turbojet engine designed for $M = 3$ at 60,000 ft., with a sea level, static, standard day, max. A/B thrust of 15,000 lbs. This combination of Mach number and altitude was chosen because it appears that the first round of supersonic transports will be cruising under these conditions. See ref. 3:1. For engines of different sea level thrust rating and the same M , the thrust and fuel characteristics may be scaled up or down as in section 2:7 "Range".

Although this discussion has been based upon using a turbojet power exclusively, it has been suggested that other types of power plant may be more efficient for supersonic airplanes (see ref. 3:3). This reference suggests a combination of turbojets and ramjets, either mounted independently, or the turbojet installed in the ramjet. Ref. 3:4 also studies turbojet-ramjet combinations and concludes that "for large, long range vehicles where cruise performance is of prime importance and where Mach 3.0 gas generators will soon be available, the turbojet-ramjet appears to have considerable potential. On the other hand, the straight turbojet would be attractive for small, short and medium range vehicles where simplicity and good acceleration thrust-weight ratios are important."

A very important part of supersonic engine design for maximum overall efficiency is the intake and exit nozzle configuration. This subject is covered partially in courses in "Supersonic Aerodynamics" and in "Propulsion". Since the topic is also covered extensively in the literature it has been decided that the subject will not be included in this text but only some references presented. See refs. 3:24 to 3:28.

3:5 Weight Estimation

Again the same methods used for the subsonic design, section 2:5 may be used for the supersonic.

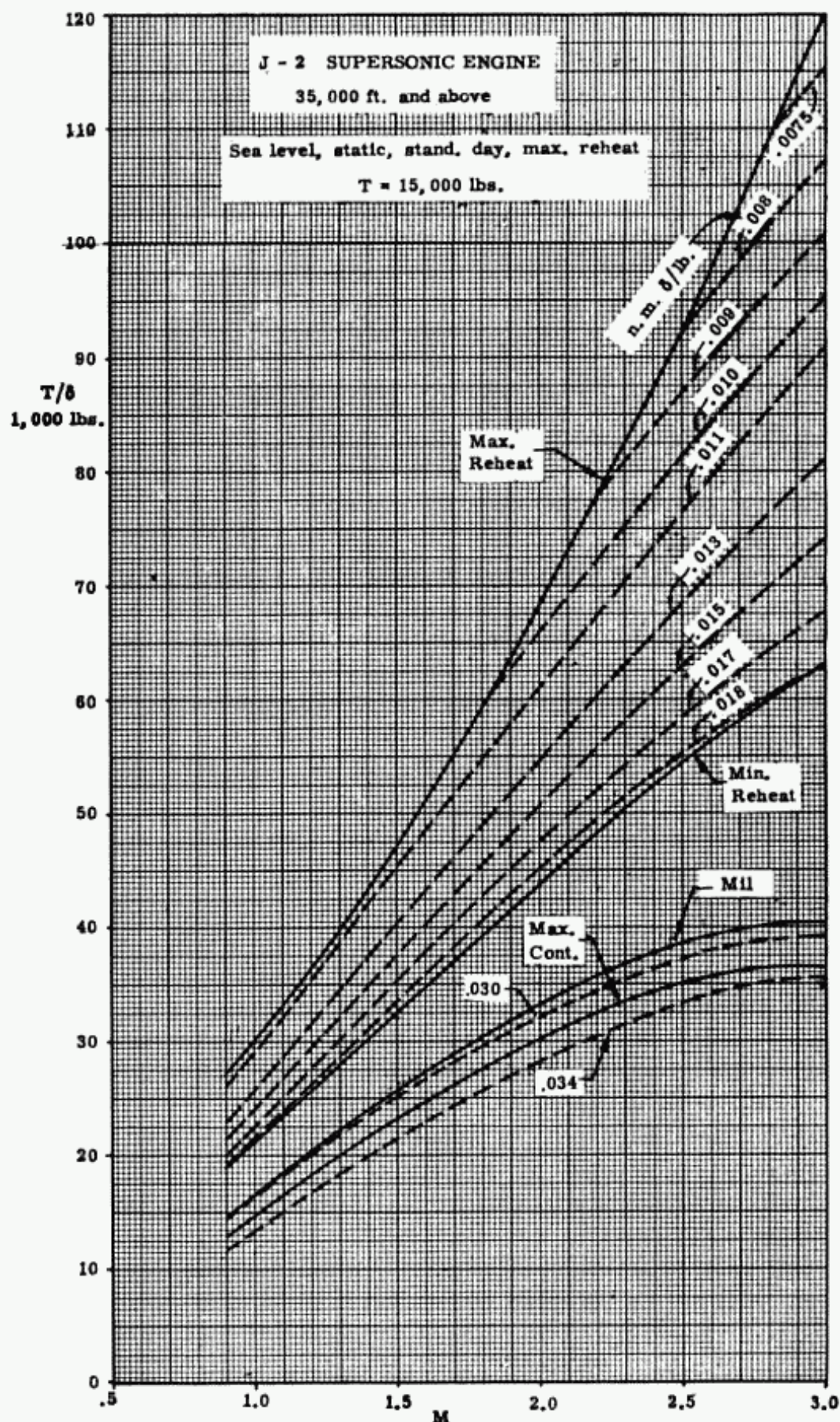


Fig. 3:8. Engine performance at 35,000' and above for a Typical Supersonic Jet Engine at 15,000 lbs. sea level, stat., max. reheat stand. day thrust.

The figures 2:19, 2:19a, and 2:20, correction factors for structural aspect ratio, thickness ratio and taper ratio have been extended to include the low values used in efficient supersonic designs. It is felt that the data should be satisfactory for supersonic preliminary design purposes.

It should be noted that fig. 2:19 uses structural A.R. as the variable. This criterion is satisfactory for wings with large values of both sweepback and aspect ratio, since the lengths of the spars are increased due to the sweepback. However, for the delta wing with high sweepback, low A.R., and straight trailing edge, the aft spar is not swept and therefore is not lengthened due to Λ . It would therefore appear more accurate to use the aerodynamic A.R. instead of structural A.R. in fig. 2:19 for high Λ , straight trailing edge wings.

The dry weight for the J-2 Supersonic engine with a 15,000 lb. sea level static, max, reheat, standard day thrust may be taken as 3,600 lbs., with standard equipment. For other size engines the weights may be scaled up or down by the scale factor shown in fig. 5:6.

3:6 Total Drag - Theory

The total drag is divided into three categories. Although the subsonic drag was also divided in three categories, the types of drag are not the same.

Skin Friction Drag

This drag is the same as the subsonic friction drag. (It should be noted that the subsonic parasite drag is actually friction drag, including the effects of the shape of the body.)

Wave Drag

Wave drag is the drag resulting from the normal pressures on the surfaces at zero lift. This is sometimes called form, or pressure drag, although pressure drag is misleading since other drags discussed here are also pressure drags. As can be noted from fig. 3:9 all chordwise components of the pressure forces of this wedge shaped airfoil section at 0° act aft. In subsonic flow the resultant drag due to pressures normal to the surface is equal to zero at zero lift.

Although fig. 3:9 shows only an airfoil section the same theory applies to a body of revolution. In supersonic flow, all theoretical formulas are based on the assumption that the shock wave is attached to the nose, and therefore do not apply to round nosed shapes. Whether the shock wave is attached to the nose or not depends on the $M_{f.s.}$ and the included angle of the body.

3:18 SUPERSONIC AND SUBSONIC AIRPLANE DESIGN

In fig. 3:10 are shown the detachment angle boundaries for a two dimensional airfoil and a body at revolution.

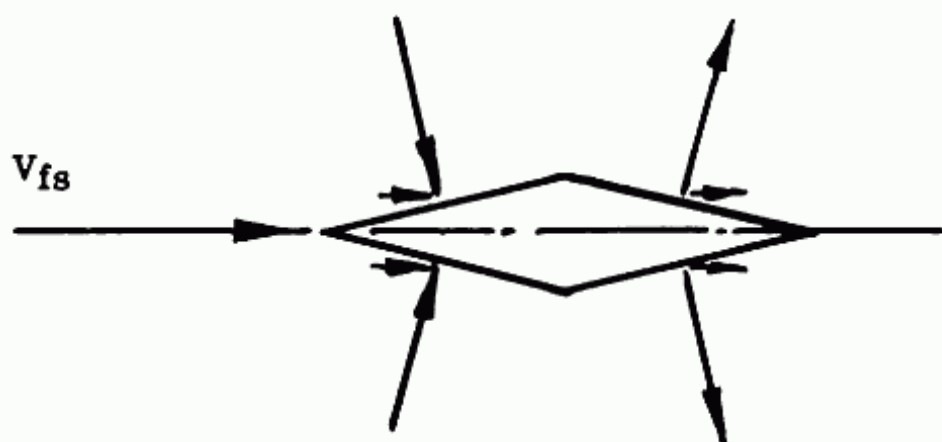


Fig. 3:9. Wave drag.

By the linearized theory the following formula is derived for the wave drag coefficient, for a two dimensional airfoil

$$c_{dW} = \frac{1}{c\sqrt{M^2 - 1}} \int \left(\frac{dt}{dx}\right)^2 dx$$

This formula is true for any section and M where the shock

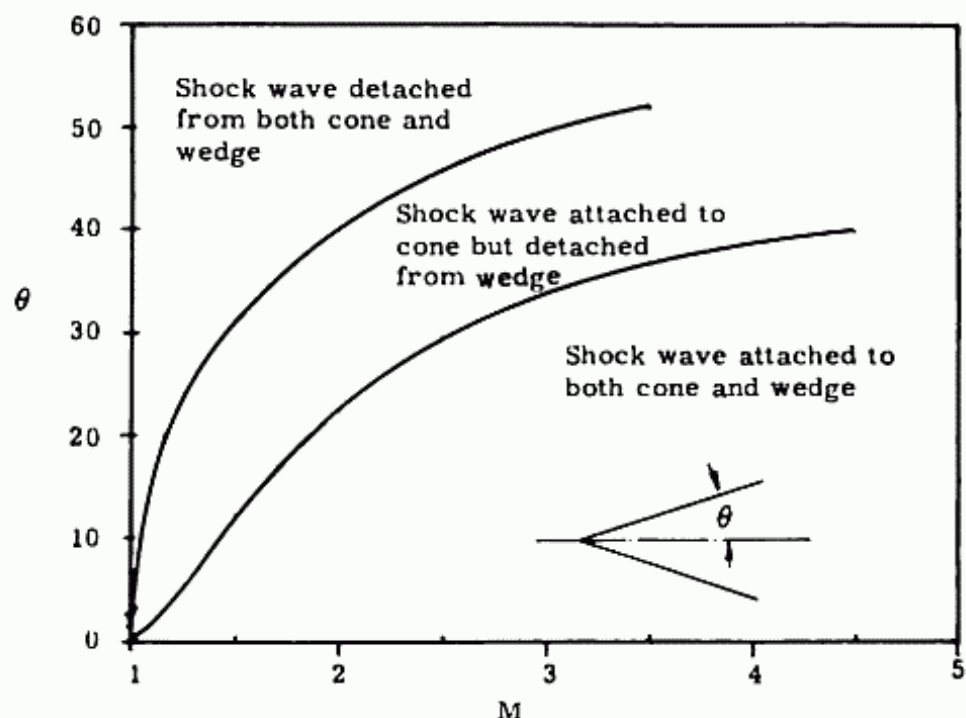


Fig. 3:10. Detachment angle vs. M for cones and wedges.

wave is attached to the nose, except where M is close to 1.0. This is useful in comparing the relative values for the double wedge, the biconvex and modified double wedge airfoils.

$$\text{Double wedge:} \quad c_{dW} = \frac{4}{\sqrt{M^2 - 1}} \left(\frac{t}{c}\right)^2 \quad (3:2)$$

$$\text{Biconvex:} \quad c_{dW} = \frac{16}{3\sqrt{M^2 - 1}} \left(\frac{t}{c}\right)^2 \quad (3:3)$$

$$\text{Modified double wedge:} \quad c_{dW} = \frac{6}{\sqrt{M^2 - 1}} \left(\frac{t}{c}\right)^2 \quad (3:4)$$

The C_{Dw} of a conical nose is shown in fig. 3:12 for various values of M and θ , the semivertex angle. These values are based on the Taylor Maccoll Method and the C_D is based on the base area of the cone.

Ref. 3:6 compared the C_D of various nose shapes given by the equation

$$\frac{y}{d/z} = \left(\frac{x}{l}\right)^n \quad (3:5)$$

Fig. 3:13 shows the variation of C_D for different values with M . Fig. 3:14 shows the nose shapes corresponding to the values of n , and a tangent ogive.

The drags indicated in fig. 3:13 include friction drag as well as wave drag. In fact it is the increase in C_F at $M = 5$ and 6 (due to the lower R.N. in this range in this test procedure) that causes the C_D to rise. Note that the body with $n = 1.0$ is a cone. It is obvious that for the sections tested, the body corresponding to $n = .75$ is the best from the drag standpoint, and is also better from both the internal space and structural considerations than the cone.

However the ogive and the $n = 1/2$ body are better than the $n = 3/4$ body from both internal space and structural considerations. The difference in the effect of the various nose shapes on the after body drag at $\alpha = 0^\circ$ is negligible.

From fig. 3:12, a study was made to see which of the cones had the least drag, wave plus friction, at $M = 1.5$ for a given base area. Fig. 3:15 shows that the cone with a semi-vertex angle of about 6° , is best from this viewpoint. The optimum angle, including structural considerations, but neglecting space available, will be greater. In all the above comparisons the variation in $C_{N\alpha}$ and stability effects are neglected. Similar

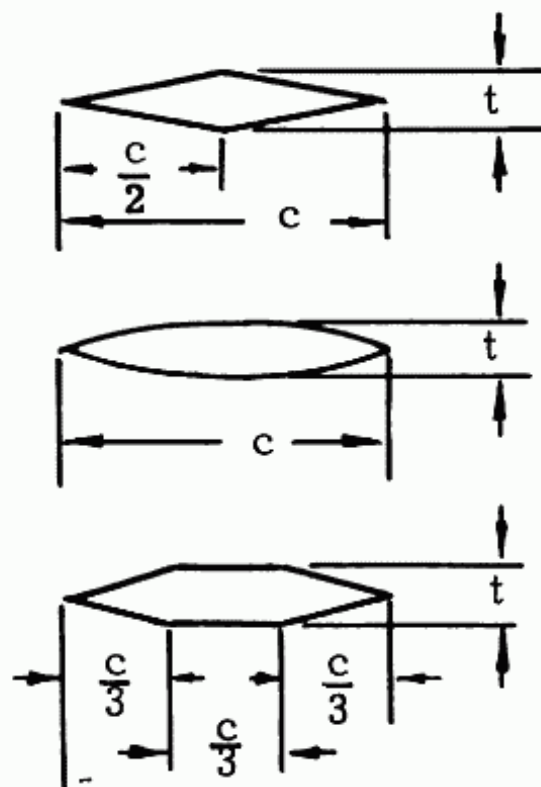
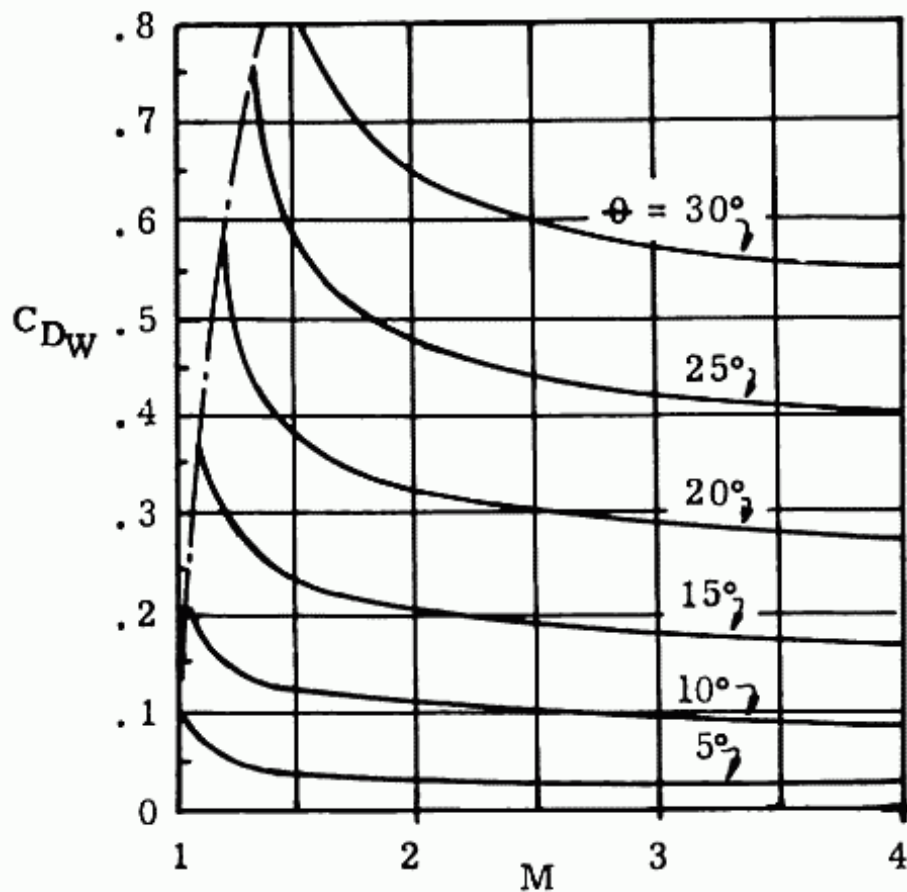


Fig. 3:11. Typical supersonic sections.

Fig. 3:12. C_{DW} vs. M for cones with various semivertex angles.

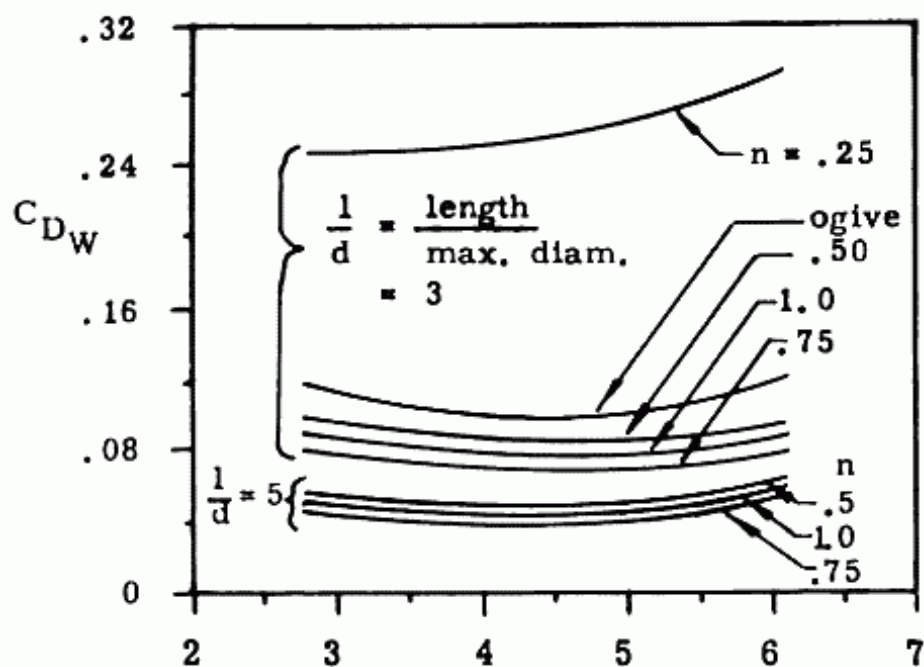


Fig. 3:13. C_{DW} (no base drag) with M for various bodies.

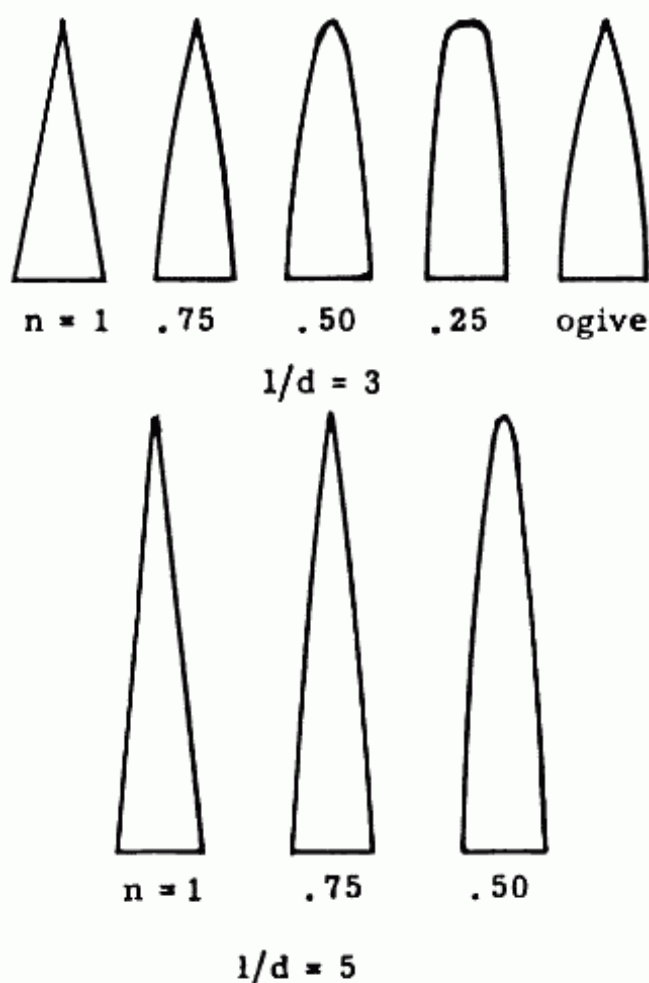
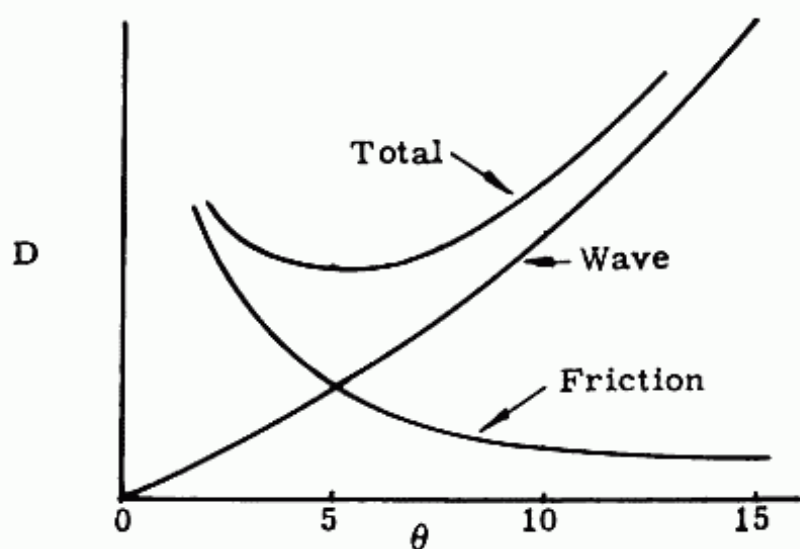


Fig. 3:14. Outlines of bodies used in fig. 3:13.

Fig. 3:15. Wave + Friction Drag vs. θ .

studies to show the minimum vertex angle that should be considered could be made for other M 's, and nose shapes better than cones.

Drag due Normal Force

Drag due to lift is the name often used for this third part of the total drag. Since this drag is the chordwise component of the normal force it would appear that it would more properly be called "drag due to normal force". In this text the term drag due to normal force will be used and the coefficient denoted by $C_{D_{NF}}$.

It has been shown that this drag due to normal force (or drag due to lift as used in ref. 3:7 from which the following data is obtained) should be considered as being composed of two components: one, the drag associated with trailing vortices, called

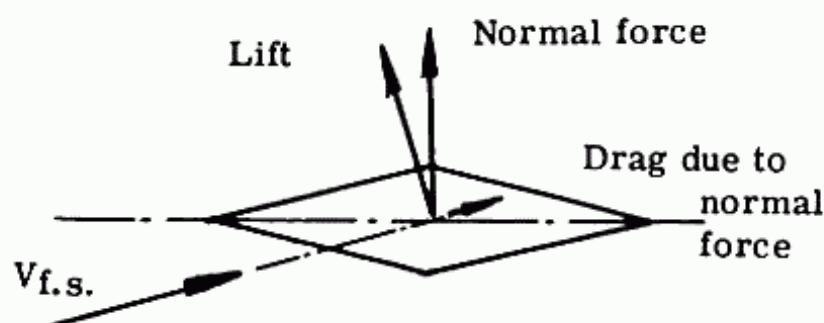


Fig. 3:16. Drag due to normal force.

vortex drag, and two, a drag associated with the chordwise distribution of lift, which may be interpreted as the wave drag due to lift. This viewpoint of drag due to normal force allows for minimization of each of the components separately since vortex drag is determined only by spanwise lift distribution, and the wave drag due lift only by chordwise distribution. Although this theory is now only limited to very low values of aspect ratio, i.e. $(\beta/2)A.R.$ less than .4, it is hoped that larger values of this slenderness ratio will be applicable. The reference shows that by proper contouring of fuselage and wing, that at $\beta A.R./2 = .4$ and for fuselage fineness ratio = 10, the drag due to normal force can be reduced by about 7% from a typical conventional configuration. Much research is being done by leading aircraft companies to develop this idea further and arrive at optimum chordwise distribution to reduce the wave drag due to lift for each design being investigated. It should be noted that the theory as shown in ref. 3:7 allows only for optimization at one M , and the drag reduction deteriorates at any off-design M . Another method of reducing the drag due to normal force is incorporation of conical camber in wings with subsonic leading edges. This device consists of using spanwise camber which develops a leading edge suction force that reduces the drag.

As shown in fig. 3:16 there is a drag due to normal force on lifting surfaces. Although in subsonic flow the drag due to lift on the fuselage is assumed to equal zero, in supersonic design the drag due to normal force must be calculated under certain conditions of high angle of attack. This is so since the converging and diverging sections do develop normal force as shown for the cones in fig. 3:17. However, since a supersonic transport will be designed so that the fuselage will cruise at zero angle of attack, the normal force will be zero in this condition. It should be noted that C_{N_α} is based on the maximum cross sectional area.

Base Drag

Base drag has not been presented up to now since in most airplane designs it is comparatively unimportant. It becomes significant in engine out operation. Because of its usually insignificant character on transport airplane design, and because it is most difficult to accurately predict, the base drag will only be discussed briefly here.

This base drag is the result of the separation of flow from a blunt trailing edge body. The flow along the body acts like a jet pump as it continues beyond the aft end, sucking the dead air

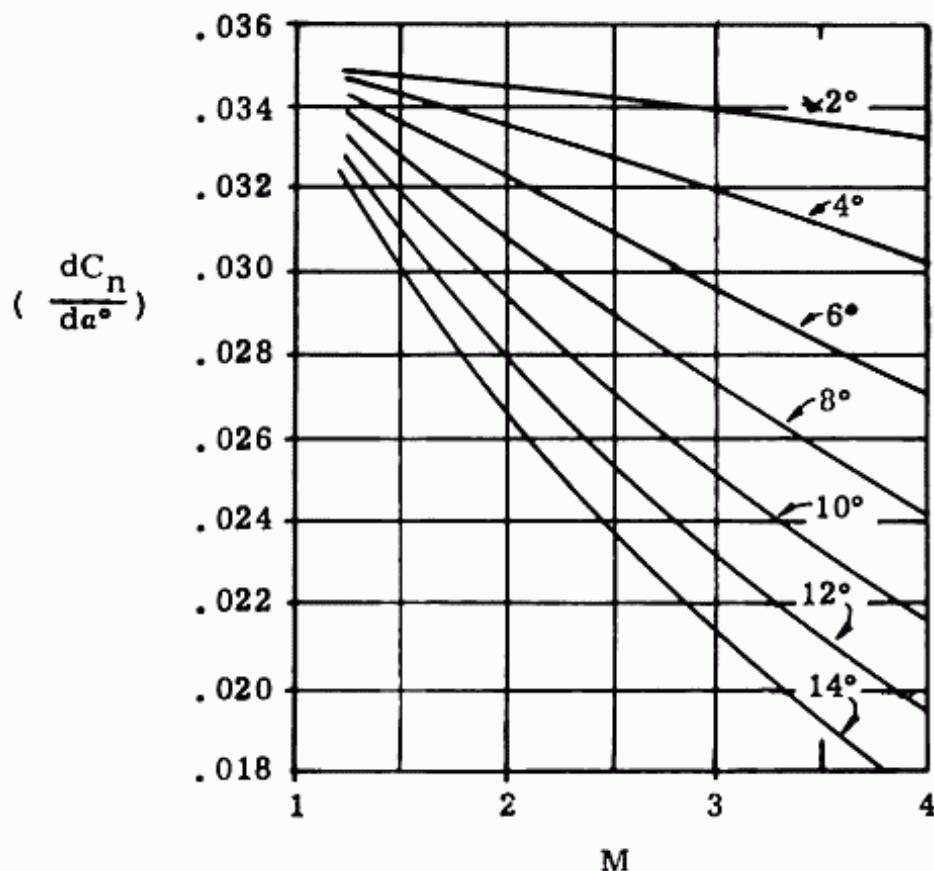


Fig. 3:17. $C_{n\alpha}$ vs. M for a cone by Tsien's theory.

behind the body with it. The pressure at the base therefore reduces, resulting in the base drag. Ref. 3:30 has a good presentation of the mechanics of the flow, and the resulting pressures, for supersonic flow in the "power-off" condition. Similar reasoning can be extended to "power-on" condition, which will be discussed later.

Airplanes are usually designed to eliminate base drag completely, as seen in the conventional shaping of the rear end of the fuselage. Fig. 3:18 shows a body that would encounter base drag, and approximately what must be done to eliminate this drag. Note that the added afterbody introduces additional friction drag, wave drag, and weight. However the faired design usually results in a more efficient airplane.

As stated previously base drag is important in cases where an engine is inoperative. In this case, with no flow through the engine, the aft end causes considerable drag. In designs where the jet exhaust area is less than the base area there is a base drag even with the engine operating.

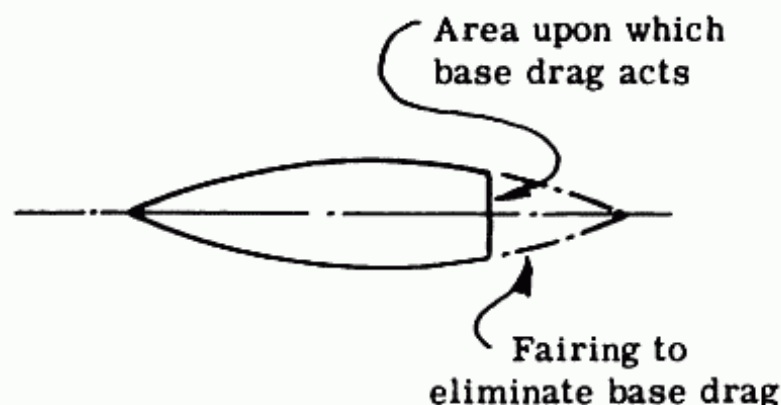


Fig. 3:18. Base drag.

The base drag problem can be divided into two categories "power-off" and "power-on". The significant parameters in determining the base drag coefficient for "power-off" are:

- (1) M and pressure at the free stream
- (2) afterbody shape: cylindrical, boat-tailed or flared; and variation in angle of convergence or divergence with length.
- (3) type and thickness of boundary layer
- (4) base diam./max. diam.
- (5) position and dimensions of fins
- (6) angle of attack

Additional factors to be included for "power-on" are:

- (1) jet area/base area
- (2) number of jet nozzles, and cross-sectional location
- (3) shape of nozzle; angle of divergence
- (4) fore and aft location of jet nozzle in reference to base plane
- (5) temperature and physical properties of exhaust gases
- (6) jet total pressure/static pressure

For the "power-off" case, which is significant on all airplanes, fig. 3:19a (from ref. 3:31) presents the base drag coefficient, C_{DB} , vs M for a cylindrical body of infinite length.

This report is a compilation of free flight test data of a large group of varied body and fin combinations, and has an extensive list of references. As shown in some tests this base drag is affected by the flow conditions ahead of the base in the fin and nose pressure fields, even when the boundary layer is turbulent

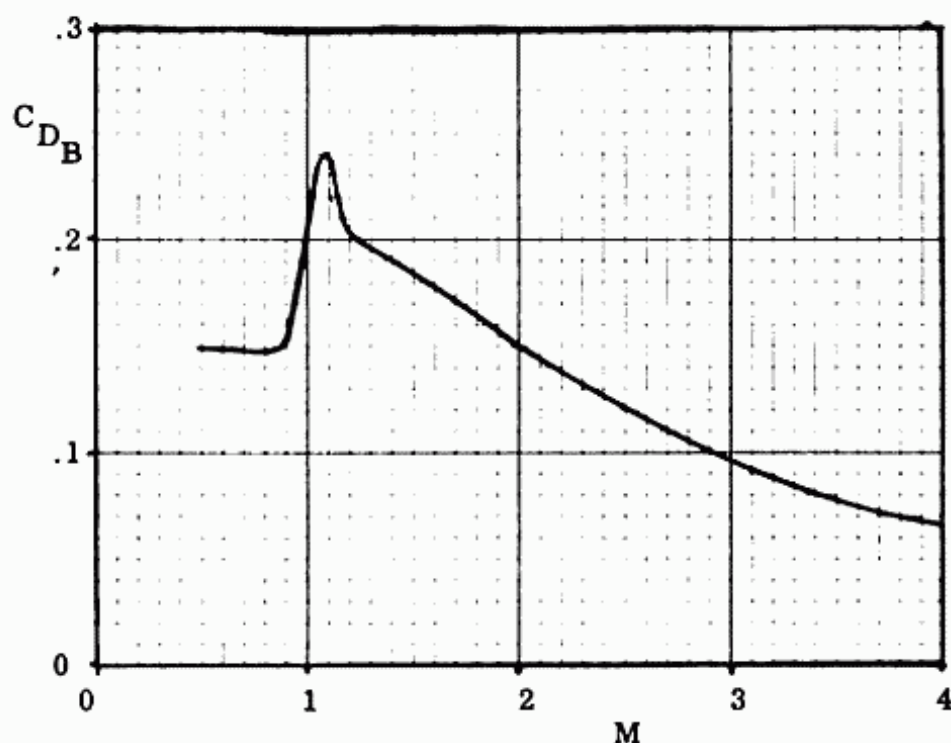


Fig. 3:19a. Base drag coefficient vs M for cylindrical bodies.

well ahead of the base. For transport type airplanes with cylindrical afterbodies, this effect is believed to be quite small at supersonic speeds, but may be more significant subsonically.

For bodies with boat-tails some wind tunnel tests on base drag indicate that the following relationship gives satisfactory results:

$$C_{D_{base}} = C_{D_{cyl. base}} \left(\frac{r_{base}}{r_{max}} \right)^3 \quad (3:6)$$

where r = radius.

This relationship is for the usual gradually faired afterbody and therefore does not account for variations in shape, which may have a significant effect in extreme cases. A particular design could be compared to one of the configurations tested in ref. 3:31 and possibly obtain more accurate data. If this report does not include a similar body then fig. 3:19a and equ. 3:6 may be used for a good preliminary estimate.

The "power-on" case is significant on designs where there is some base area around the jet exhausts as shown in fig. 3:19b and c. Condition 3:19c will exist on supersonic transport designs using multiple engines housed in the aft end of the fuselage.

As stated previously there are new and complex factors to be considered in the "power-on" case. Little experimental data is now available for presentation and it appears that a theoretical approach that includes all the necessary variables is impossible. A first approximation is to obtain the base drag coefficient from fig. 3:19a, power-off, and use it with the net area (base area minus jet area) as the reference area. Although it is evident from tests that the effect of the jet operating is usually to decrease the base drag coefficient

supersonically, and to increase it both transonically and subsonically, it is difficult to present a quantitative picture because of the large number of variables, and limited data. Ref. 3:32 presents some base pressure data for a single nozzle with jet operating in the transonic range, and Ref. 3:33 in the supersonic range. Although none of this data is directly applicable to a jet transport configuration, or operation, some order of magnitude values may be obtained.

Total Drag

In subsonic design the total drag of the airplane is assumed equal to

$$\begin{aligned}
 & C_{D_P} \text{ of wing, fuselage, tail and nacelles} \\
 & + C_{D_i} \text{ (} C_{D_i} \text{ of tail is accounted for by } e \text{) (See section 7:13} \\
 & \quad \text{for more detailed discussion of "e".} \\
 & + C_{D_{comp}} \text{ of wing (} C_{D_{comp}} \text{ of tail and fuselage is usually} \\
 & \quad \text{neglected)} \\
 & \quad 5\% \text{ for interference and miscellaneous excrescences}
 \end{aligned}$$

In supersonic design, the total drag of the airplane is assumed equal to

$$\begin{aligned}
 & C_F \text{ of wing, fuselage, tail and nacelles} \\
 & + C_{D_W} \text{ of wing, fuselage and tail} \\
 & + C_{D_{NF}} \text{ of wing and fuselage (at cruise } C_{D_{NF}} \text{ of tail can} \\
 & \quad \text{usually be neglected). It should be noted that the}
 \end{aligned}$$

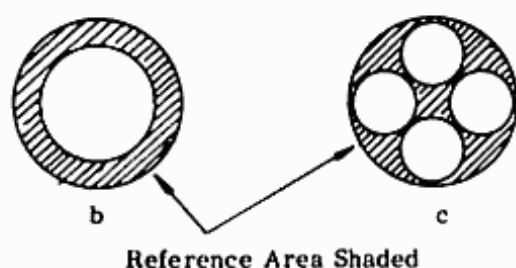


Fig. 3:19b,c. Base-drag reference areas shaded for jet-on condition.

fuselage does have a normal force at values of α greater than 0. At cruise the airplane is designed so that $\alpha = 0$ and $C_{D_{NF}}$ of fuselage alone = 0.

However the effect of a wing at some positive angle of attack on a fuselage at zero angle of attack increases the normal force of the wing-fuselage combination.

+ interference effects (See next section).

Interference Effects

In subsonic design the interference effects are accounted for by adding a certain percent to the parasite drag. It should be realized that even in subsonic flow the preliminary design of the airplane components are so arranged that interference effects are kept to a minimum, as limited by the overall efficiency of pods in relation to the wing. The nacelles are placed so that the flow around them does not adversely affect the flow around the wing to any marked degree, as it certainly would if its maximum section was directly below the maximum thickness point of the wing. In fact it is placed so that its maximum section is well ahead of the leading edge of the wing, with its trailing edge at the wing leading edge.

This design in subsonic flow, it will be noticed, is actually following the transonic area rule, except that it considers planes along the flow path, instead of perpendicular to it, as in the transonic rule.

For the design of a supersonic commercial transport, at a M of approximately 3.0, with their huge practically constant section fuselages and very thin wings and tail surfaces, it is generally agreed that disadvantageous interference effects can be kept very low by good preliminary design.

Area Rules, General

The method and philosophy of calculating wave drag at both transonic and supersonic speeds are essentially the same. It is based on the theory that the wave drag of a body going through a shock wave is a function of the cross-sectional areas of the body cut by a plane parallel to the shock, plotted against the length of the body. It has been determined that the minimum wave drag for a body can be obtained from the following formula:

$$\frac{D_W}{q} = \frac{128}{\pi} \left(\frac{\text{Volume}}{l^2} \right)^2 \quad (3:8)$$

This is only true for an optimum area distribution, which requires that the body have pointed nose and tail, and be a body of

revolution with no discontinuities in slope in the lengthwise direction. This body that results in the minimum wave drag is denoted as a Sears Haack body.

a. Transonic Area Rule

Since a true Sears Haack body is never attainable in a conventional airplane, due to wings, tails, etc., equ. 3:8 does not hold and another approach must be used. In the transonic area rule, ref. 3, which is applicable in the range of $M = .9$ to 1.2 , it is assumed that a normal shock occurs. It is for this reason that sections through the airplane perpendicular to the longitudinal x must be calculated and plotted.

It is then necessary to determine the slope of the area curve along its length. It is suffice to say, at this time, that the drag is a function of the slopes squared and its lengths. It can be seen that the slopes and length will determine the value of the total volume, so that it is related to the simple equation of the Sears Haack body.

In the application of the transonic area rule it is readily seen that elimination of bumps will reduce the slopes and thereby reduce drag. It is also obvious that the smaller the volume for the

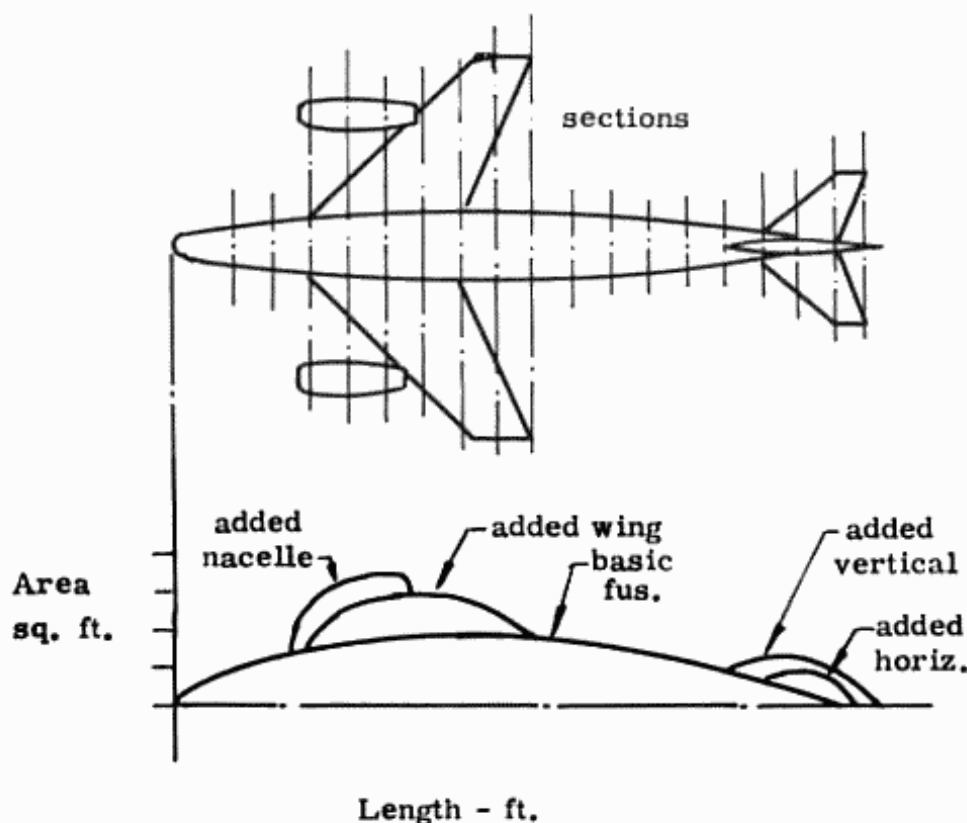


Fig. 3:20. Transonic area rule.

3:30 SUPERSONIC AND SUBSONIC AIRPLANE DESIGN

same length, the less the wave drag. It is because of these considerations that beneficial effects of the coke-bottle occur. The effects of the coke bottle shape can be explained also by the interference between the wing and fuselage. See fig. 3:21.

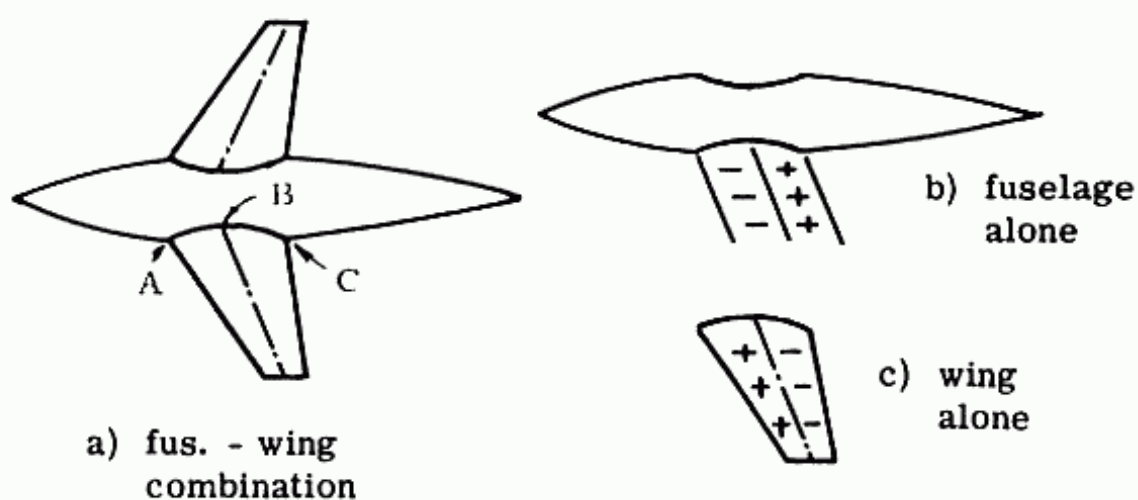


Fig. 3:21. Pressures acting on an indented body configuration.

Considering the fuselage acting alone, at point A, the slope of the fuselage changes sign and the flow expands causing a negative pressure. This negative pressure acts in the region between A and B along some Mach line as shown in (b), since expansive flow occurs between these two points. Between B and C the flow is compressed, causing a positive pressure, also shown in (b).

Considering the wing acting alone as shown in (c), due to the double wedge section the forward half experiences a positive pressure due to compression, and the aft half a negative pressure due to expansion. It can therefore be seen that the pressures from the coke-bottle fuselage tend to cancel the pressures on the wing which are contributing to the wave drag.

Ref. 3:9 in studying wings of rectangular plan form states that "It is found that the sonic zero-lift drag-rise data for the present family of wings can be successfully correlated on the basis of the area rule (transonic), provided the wing profiles are symmetrical and the product of the aspect ratio and the cube root of the thickness ratio is less than about unity" that is

$$A(t/c)^{1/3} < 1.0.$$

Ref. 3:10 in studying wings of triangular plan form states that "The results of an experimental investigation performed to determine the range of applicability of the transonic area rule

for wings with triangular plan form, with NACA 6300X airfoil sections in the streamwise direction, and centrally mounted on a simulated infinite cylindrical body, show that the data at sonic speed are in agreement with the transonic area rule for values of

$$A(t/c)^{1/3} \lesssim 1.3.$$

This result applies strictly for the conditions stated above. However it is to be expected that changes in wing section, or body diameter to wing span ratio (even for a body diameter to wing span ratio of zero) would not alter the result significantly."

Supersonic Area Rule

Just as in the transonic rule the wave drag is a function of the slope squared of the area curve, the same is true in the supersonic area rule. For development of supersonic rule area see Ref. 3:11. However, the supersonic rule is much more complicated since the shock is not normal and therefore a Mach cone exists.

It is then necessary to draw up area curves similar to the one in the transonic rule, except that there is a series of curves each representing a cutting plane tangent to the Mach cone, but at different angle around the circumference of the cone. The cutting planes shown in fig. 3:22 are parallel to the tangent of the Mach cone at $\theta = 90^\circ$, as shown in front view. The areas as cut by the planes must be plotted against x , the point where the cutting plane crosses the line of symmetry. In addition, it is necessary to obtain area curves for various values of θ . The usual practice is to take increments of $\theta = 30^\circ$, and since there is a plane of symmetry it is only necessary to go 180° , instead of 360° . The fuselage areas are usually taken perpendicular to θ of airplane at cutting plane intersection with θ airplane.

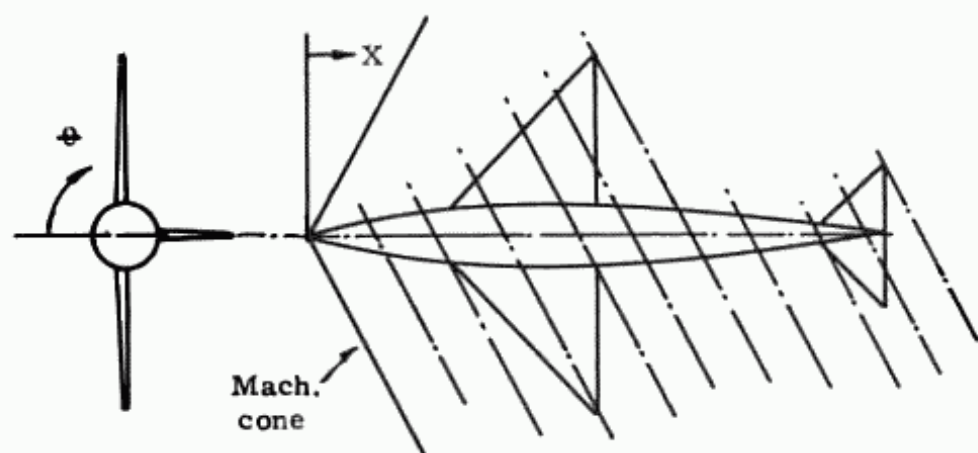


Fig. 3:22. Cutting planes for supersonic area rule.

The total drag is then dependent on the average of the drags of the area curves, as calculated by the supersonic rule. It is felt that this rule is only effective up to values of $M = 2.5$ or 3.0 . Ref. 3:12 develops the supersonic area rule further, comparing experimental results with the theoretical.

Methods of Reducing Interference Effect and Drag

The following discussion is to present some ideas that have been developed to reduce drag. Some, or all, of these ideas might, or might not, have some worthwhile practical applications to certain types of airplanes. It is hoped that students (in school or in industry) will realize that large horizons still loom for the improvement in both the science and art of supersonic flight.

Freedman and Cohen in Ref. 3:13 study the arrangement of bodies of revolution that taper from the middle toward the ends to reduce the wave drag at supersonic speeds. From a study of two-body and three-body arrangements they conclude "that in the frictional potential flow it might be possible to increase volume by as much as 25% (three-body arrangement) and at the same time actually decrease wave drag. In practice of course, the additional friction drag might easily nullify any such gain. Nevertheless, if there are to be auxiliary bodies, the importance of selection of the relative positions seems clear." And "The most favorable location appears to be one in which the maximum cross-section of the auxiliary body is slightly forward of the Mach cone from the tail of the main body. The least favorable is the region between the Mach cone from the nose and the fore cone from the tail of the main body." It should be noted that the addition of auxiliary bodies increases subsonic friction drag, and weight.

Baldwin and Dickey in Ref. 3:14 develop a moment of area rule, which is an extension of the transonic area rule. They show (fig. 3:23) that the addition of auxiliary bodies on the wing can reduce the C_{D_w} of the airplane below the value that can be obtained by the area rule, between $M = 1.1$ and 1.4 . They conclude "the concept of introducing auxiliary bodies along the wing span to effect decreases in wave drag promises to find important applications for aircraft intended to carry external stores. For such aircraft, the possibility exists of shaping the stores according to the moment of area rule so as to obtain drag reductions at transonic speeds with no friction penalty at lower speeds." Both references 3:13 and 3:14 are extensions of work done by R. T.

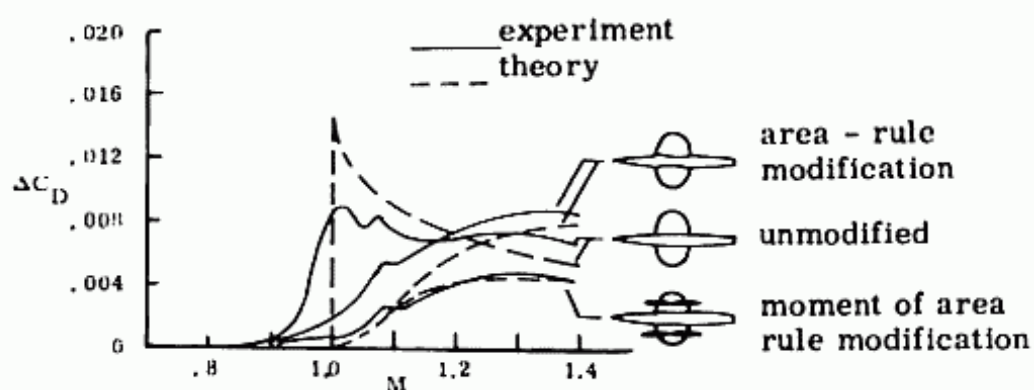


Fig. 3:23. Effect of area rule modifications on the ΔC_D of wing - body combinations.

Jones and R. Whitcomb, ref. 3:15 and 3:8. H. Lomax and M. A. Heaslet in ref. 3:16 "A Special Method for Finding Body Distortions That Reduce Wave Drag of Wing and Body Combinations at Supersonic Speeds," present experimental and theoretical results for an elliptic wing having a biconvex section, a thickness-chord ratio equal to .05 at the root, and an aspect ratio of 3.0.

Another very interesting method of reducing wave drag is the device called the Buseman biplane, as shown in figure 3:24. By the use of correct spacing of the wings it is shown (ref. 3:17) that it is theoretically possible to achieve zero wave drag on a biplane of finite thickness at one particular M . Although this theory was presented by Buseman in 1935 it has never been developed because of numerous difficulties. It has only this zero drag at one M and the increase in drag at off-design points might be large. The theory depends upon a certain relative position between the upper and lower wings, which will change

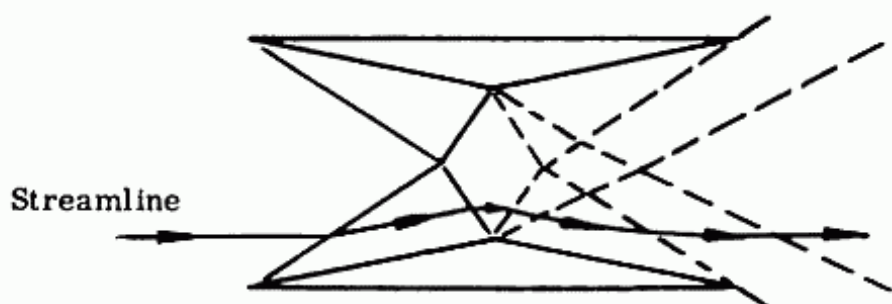


Fig. 3:24. Flow pattern around a Buseman bi-plane.

under load due to both bending and torsion. It would also be inefficient in subsonic and transonic flight.

A system, in ways similar to the Buseman biplane, but applied to a body of revolution, is the use of a cowl to reduce the pressure drag of the center body. This is accomplished by placing the cowl of the correct shape at the proper relative position to the center body so that the conical shock generated from the apex of the center body is reflected on to its boat-tailed rear part. Thus the pressure on the rear part of the body is increased and the pressure drag considerably reduced in comparison to that of the center body alone.

M. Visich Jr. and A. Martelucci in Ref. 3:18 present experimental data for a cowled boat-tailed body of revolution (fig. 3:25) to show that the wave drag of the body alone is reduced by approximately 83%, and that the total drag of the cowled body is about 62% less than the uncowled one. The total drag of the optimum cowled body was 47% less than that of a cone with same volume and length. The study was made at $M = 3.09$. Ref. 3:29 reports on the development of the ring-wing configurations, which are also cowled bodies as shown in fig. 3:25.

Total Drag - Calculation

Skin Friction Drag

The value of the skin friction drag coefficient, C_{D_F} is equal to f/S , where f equals the wetted area times C_f the coefficient of friction. The value of C_f is dependent on the Mach number and

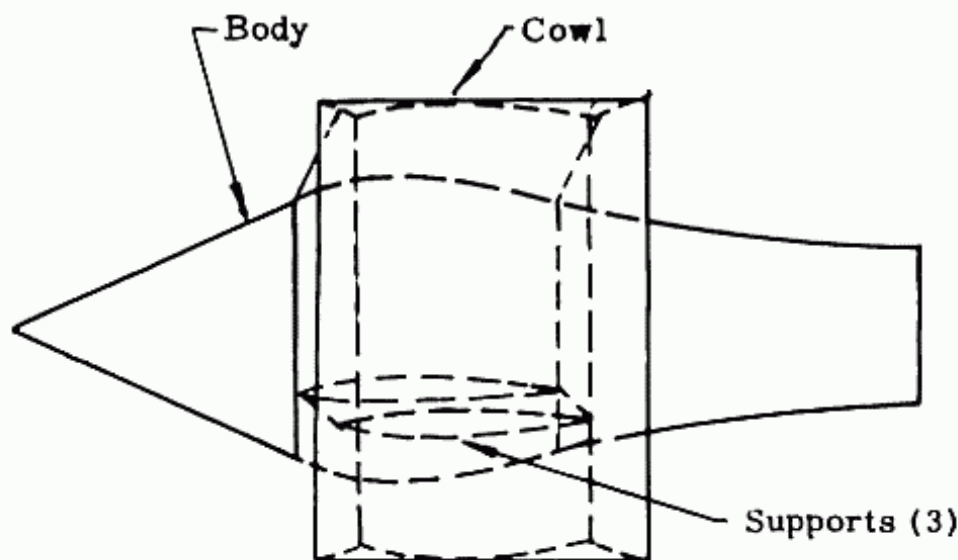


Fig. 3:25. Cowled body to reduce wave drag.

the type of boundary layer, laminar or turbulent. Fig. 2:21a and b show these values. Since there is a transition from laminar to turbulent boundary layer that may be correlated with Reynolds Number it is well to make some such estimate as it might have a significant effect on high altitude flight. At this time there appears to be no reliable method available to determine this transition R.N. for various M 's and body shapes. An assumption of an all turbulent boundary layer for the supersonic transport at $M = 3.0$ and 60,000 foot altitude will result in C_D 's very close to the actual values.

Since M is known the R.N.'s can be calculated and the C_{D_F} of the airplane can be obtained by using the C_f 's and their corresponding wetted areas. The values of C_f are based upon the surface being an insulated plate, i.e. heat transfer equal zero, which is close to reality for values of M up to about 3.0. Beyond this value of M , and depending on the altitude, this assumption of zero heat transfer should be investigated. It should be noted that for preliminary design work the assumption of turbulent boundary layer for the entire surface is justified since roughness caused by service and manufacturing practices would tend to trip the transition at a much lower R.N. than theoretically predicted for a smooth surface. It has been noted in many studies that the stability of the boundary layer becomes greater with increase in M , indicating that there would be this particular advantage of more laminar boundary layer for airplanes with increasing M .

The skin friction drag coefficient C_{D_F} must be calculated for the entire airplane.

Wave Drag

The value of the wave drag coefficient C_{D_W} , for the wing can be obtained from fig. 3:3, $\beta C_D/(t/c)^2$ vs $\beta \cot \Lambda$ for various values of $\beta \Lambda$. All characteristics except C_D are known, or can be calculated. The wave drag of the tail surfaces can be estimated from wing data.

As will be shown in Chapter V, some modified double wedge or biconvex airfoil is more efficient than the pure double wedge, from an aerodynamic and structural point of view. It appears at this time that the modified double wedge is the most desirable, with the biconvex being very close behind. Ref. 3:2 presents $\beta C_D/(t/c)^2$ of a biconvex section only with $\lambda = 1.0$. A comparison of the values of $\beta C_D/(t/c)^2$ of the biconvex (parabolic) to the

double wedge shows that the biconvex drag is just about 33 per cent greater at all values of βA , for $\beta \cot \Lambda$ greater than 1.0. Comparing equations 3:2 and 3:3 for the wave drag coefficient of a two dimensional double wedge and a two dimensional circular biconvex shows the biconvex drag is exactly 32.5% larger. The modified double wedge drag is exactly 50% larger than the double wedge drag for the same thickness from equations 3:2 and 3:4. This 50% factor may then be used for three dimensional wings also.

The wave drag of the fuselage may be calculated by the use of figs. 3:12 and 13. The afterbody, which may be a reversed ogive with the point being at the aft end, may be calculated from the same curve in the same manner. The total fuselage wave drag is then equal to the nose wave drag plus the afterbody wave drag.

Drag due Normal Force

From the linearized theory it can be shown that

$$C_N = \frac{4\alpha}{\beta} \quad (3:9)$$

Since C_{DNF} is the drag component of C_N , (see fig. 3:16)

$$C_{DNF} = C_N \sin \alpha \quad (3:10)$$

This equation is only true for a wing with a supersonic leading edge, that is $\beta \cot \Lambda > 1.0$, or $\tan \omega / \tan \mu > 1.0$; where ω is one half the apex angle of the wing, and μ is the Mach angle. For a wing with a subsonic leading edge, the drag may be less due to leading edge suction.

Assuming that in cruise the value of α is small enough so that $\sin \alpha$ is equal to α in radians and that equation 3:10 is accurate enough for subsonic leading edges also then,

$$C_{DNF} = \frac{4\alpha^2}{\beta} \quad (3:11)$$

C_L can then be obtained from

$$C_L = \frac{W/\delta S}{1481M^2} \quad (3:12)$$

Note that S is the exposed wing area only, and that W should really be the lift on the wing only. In preliminary design the load on the tail is assumed to equal zero at this stage. However even at this low speed there is some centrifugal force that reduces the lift required on the wing due to aerodynamic forces.

Since
$$\Delta nW = \frac{W}{g} \frac{V^2}{R} \quad (3:13)$$

an airplane cruising at $M = 3.0$ at 60,000 feet develops a $\Delta n = .0133$, or the lift due to centrifugal force on a 200,000 pound airplane = 2,660 pounds. Therefore knowing C_L from equation 3:12, α could be obtained from

$$\alpha = \frac{C_L}{C_{L\alpha}} \quad (3:14)$$

For a wing alone $C_{L\alpha}$ can be obtained from fig. 3:2, and therefore α and $C_{D_{NF}}$ determined. However, for a wing-body combination there is a definite effect of the body on the $C_{L\alpha}$ of the wing alone, even at fuselage $\alpha = 0$.

At $M = 3.0$ and aspect ratio = 3.0, ($\beta A = 8.5$) the interference effects between the wing and the fuselage, where body radius divided by body plus wing semispan is about .15 or .20 should be very small. However, ref. 3:23 presents data from which the interference effects calculated by the slender body theory and the linear theory compare favorably to some experimental points at values of βA for which the slender body usually does not apply. The report states: "It is well known that for wing-body combinations which are not slender, lift curve slopes are overestimated by slender body theory. However, this fact does not preclude the use of slender body theory for non-slender configurations, since, in certain instances, the ratio of the lift of the wing-body combination to that of the wing alone can be accurately predicted by slender body theory, even though the magnitude of the lift curve slope might be incorrect."

The method of ref. 3:23 is presented here for the case of the body at zero angle of attack with the wing at some positive α , as would be probably experienced in cruising on a supersonic transport. The report also presents the effects of the body at some positive α with the angle of incidence equal to zero. The effects of wing-body interaction on lift can be quite pronounced, particularly at large values of fuselage radius to wing + body semi-span.

$$C_{L_{total}} = C_{L_{W(B)}} + C_{L_{B(W)}} \quad (3:15)$$

where $C_{L_{W(B)}}$ is the C_L of the wing in the presence of the body and $C_{L_{B(W)}}$ is the C_L of the body in the presence of the wing

$$C_{L_{W(B)}} = k_{W(B)} (C_{L\alpha})_W \alpha_W \quad (3:16)$$

3:38 SUPERSONIC AND SUBSONIC AIRPLANE DESIGN

where $(C_{L\alpha})_W$ is the slope of the lift curve of the wing alone

α_W is the angle of attack of wing

$k_{W(B)}$ is the factor that is a function primarily of the fuselage radius, r , divided by wing + body semi-span, s . See fig. 3:26.

= Lift of wing in presence of body divided by the lift of wing alone.

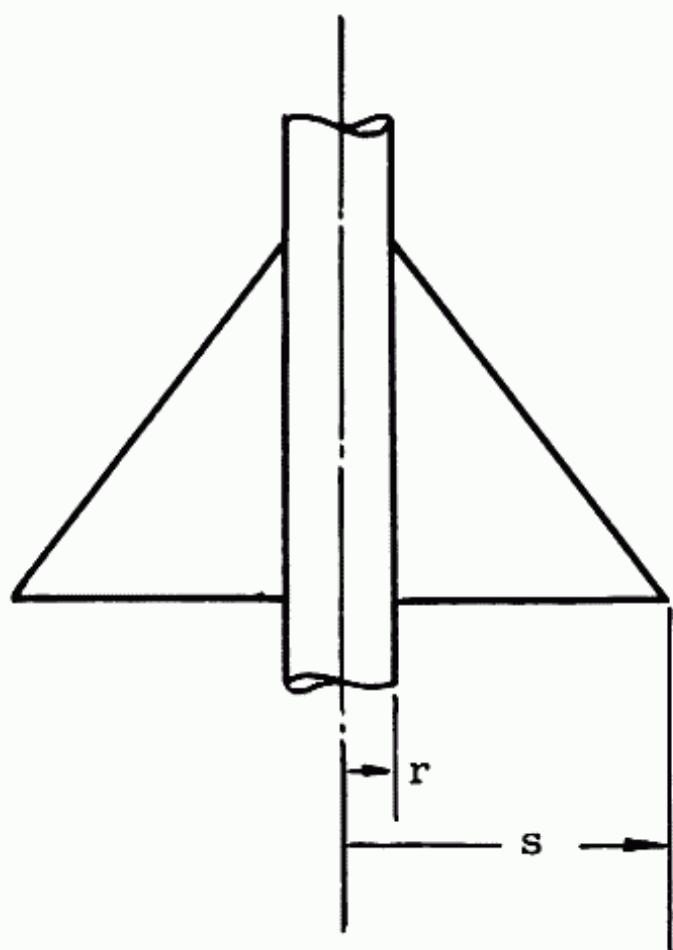


Fig. 3:26. Fus. radius and wing-fus. semi-span.

The value of $k_{W(B)}$ can be obtained by the slender body theory for slender triangular wings and body combinations, and by the exact linear theory for rectangular wing and body combinations. Fig. 3:27 shows $k_{W(B)}$ vs r/s by the slender body theory and the linear theory. For values of βA greater than 3.0 in the range of r/s that might be expected for a long range supersonic transport, about .15, the variation in $k_{W(B)}$ due to the theory used is very small.

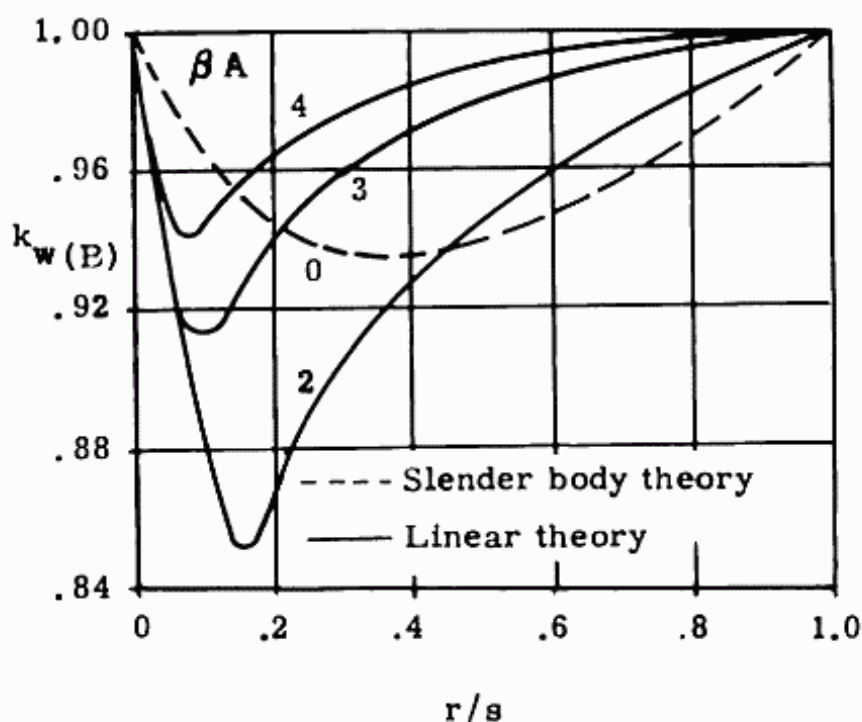


Fig. 3:27. Values of $k_w(B)$ by linear theory and slender body theory.

$$C_{L_{B(W)}} = k_{B(W)} (C_{L_\alpha})_W (\alpha_W) \quad (3:17)$$

where $k_{B(W)} = K_{W(B)} - k_{W(B)} \quad (3:18)$

$k_{W(B)}$ obtained from fig. 3:28

$K_{W(B)}$ is the lift of the wing in the presence of the body divided by the lift of the wing alone for a combination where the angle of incidence = 0 but the body is at an angle of attack.

Substituting equ. 3:16, 3:17 and 3:18 into 3:15 gives

$$C_{L_{total}} = k_{W(B)} (C_{L_\alpha})_W \alpha_W \quad (3:19)$$

This merely indicates that the entire effect can be presented as the effect of the body on the wing. $K_{W(B)}$ is shown in figure 3:28. By the use of this method an effective C_{L_α} equal to $K_{W(B)} (C_{L_\alpha})_W$ can be used in equation 3:14 to obtain α .

The airplane can be designed so that the lift on the horizontal tail surface is zero in the cruise condition, thereby eliminating $C_{D_{NF}}$ of the tail. However to attain this condition, requiring that the center of pressure of the airplane minus horizontal surface be at the c.g. of the airplane, might add other airplane

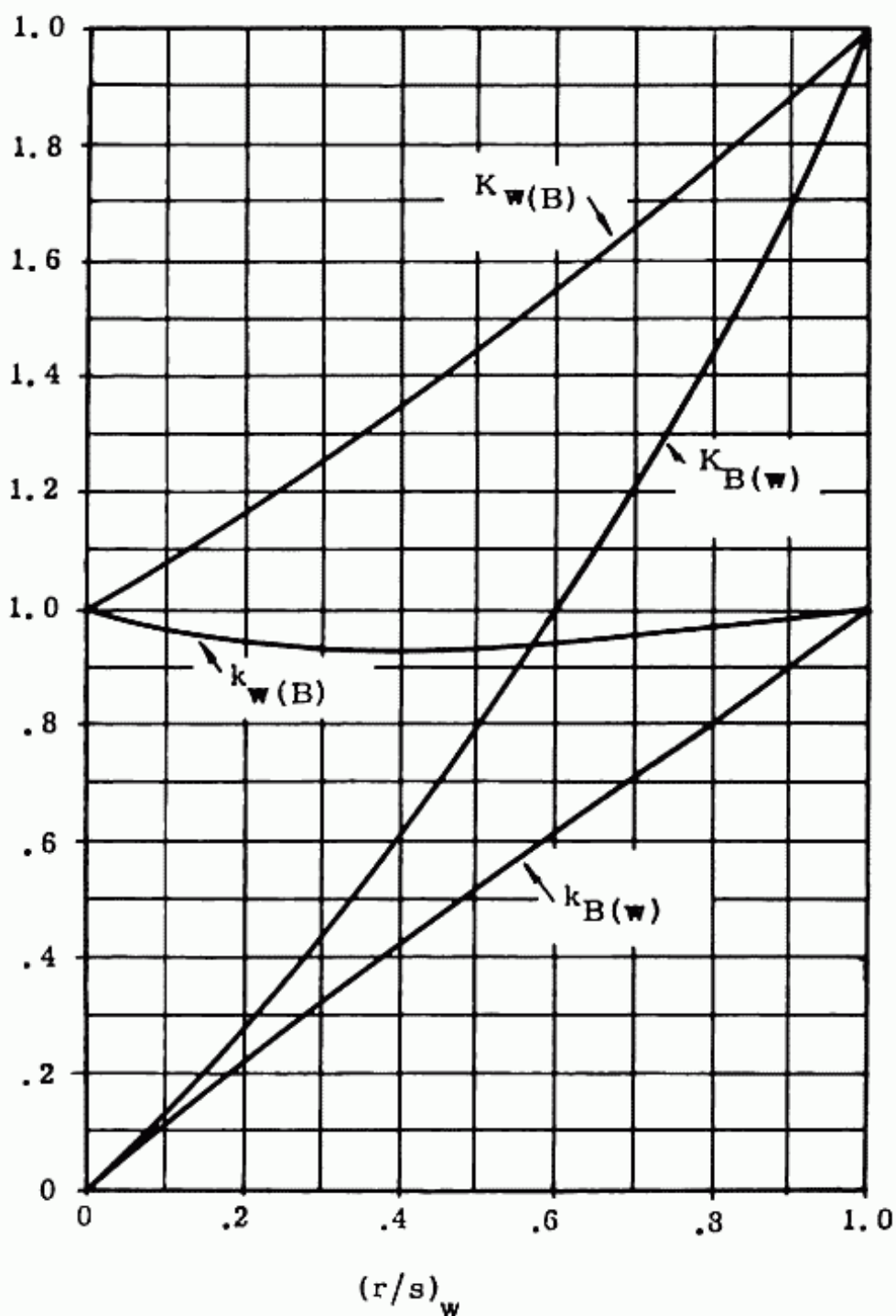


Fig. 3:28. Values of lift ratios based on slender body theory.

inefficiencies. Therefore the drag due to normal force on the horizontal control surface is not usually equal to zero at cruise, but is some small percent of the wing normal force drag perhaps about 5%. This value will vary depending upon many factors, such as canard or conventional horizontal surface, wing plan form and wing-body interference effects. For control surfaces that require an up load for cruise, $C_{D_{NF}}$ of surface can be neglected, and wing lift assumed equal to airplane weight.

The $C_{D_{NF}}$ of the fuselage forebody can be obtained from

$$C_{D_{NF}} = C_N \sin \alpha$$

where

$$C_N = C_{N_\alpha} \alpha$$

and C_{N_α} obtained from fig. 3:17.

At cruise where α of the fuselage is usually zero, the $C_{D_{NF}}$ of the fuselage forebody will be zero.

Total drag

The total drag is then the addition of all the wave drags, skin friction drags and drags due to normal force just calculated. Care should be taken that the correct areas are used with the coefficients used; the C_{D_w} of the fuselage is based on max. cross section area, while all others are usually based on projected exposed wing area.

It should be noted that many people working on missiles have changed all their coefficients so that they are based on the maximum fuselage cross-section area. Of course any system gives the correct answer as long as it is consistent, and there appears to be little difference in efficiency between using one system or another.

3:7 Range

Cruise

The principles and formulas that apply to range in the subsonic field also apply to the supersonic, and the cruise range can be obtained by the same Breguet formula:

$$R = 2.0 (L/D)(V/c) \log_{10} \left(\frac{W_0}{W_1} \right)$$

It would appear from looking at the Breguet formula that for the same initial weight, W_0 , the range of the supersonic airplane should be higher than the subsonic due to the large increase in V , from perhaps 500 knots to 1700 knots. However, due to the

decrease in L/D , the increase in c , and the likely increase in W_1 , the supersonic airplane at the same initial weight and payload will usually not have a greater range.

The decrease in L/D in the supersonic range for the same weight, i.e. the same lift, must of course be due to the increase in drag in pounds. This increase in drag is due primarily to the increased dynamic pressure, $1/2\rho V^2$, and the introduction of the wave drag. For a subsonic airplane cruising at $M = .85$ and 35,000 ft., $q \approx 250$, while for the supersonic airplane cruising at $M = 3.0$ and 60,000, $q \approx 950$. The wave drag in supersonic aircraft is an added factor that did not occur in the subsonic; the little compressibility C_D that might exist at $M = .85$ is much smaller. It is true that the friction drag coefficient, is lower supersonically than subsonically due to the increase in M and also the usual increase in Reynolds Number, as seen in fig. 2:21. The relative values of the induced drag coefficient and the drag coefficient due to normal force depends upon all the factors of M , altitude and wing loading, besides plan form. In discussing drag not only is q and C_D involved, but also the reference area, here used as wing area. This area depends on the wing loading which is dependent on landing field and also optimum cruising altitude.

The thin wings, and the large engines, required for efficient supersonic flight increase W_1 , the final weight. However the usual low aspect ratios and low taper ratios tend to decrease the structural weight. A completely new factor that increases the weight empty is the insulation and structural weight required to take care of the aerodynamic heating problems encountered in high supersonic flight. This problem will be discussed more fully in Chapter V.

The value of c for supersonic jet engines particularly with afterburners will be considerably higher than for the jet engines designed and operating at high subsonic speeds. The engine shown in Fig. 3:8, at $M = 3$, has a c of about 2.0 for maximum reheat, and only about 1.40 for normal continuous thrust. Note that

$$c = \frac{V}{(\text{mi. } \delta/\text{lb})(T/\delta)} \quad (3:20)$$

From considerations of only c it would appear that afterburners should be eliminated, and that the engines be designed and used at normal continuous thrust for cruise. However, it should be noted that the afterburner thrust above 35,000 ft., is over three times the normal continuous thrust at this M . It would therefore require three times as many engines, or engines three

times as powerful, to cruise supersonically at normal continuous thrust as compared to using an afterburner engine. The added weight, drag and complexity would probably offset the gain in s.f.c. However, two items should be kept in mind. One is that the comparison has been made on an engine that was designed to be most efficient at this condition of $M = 3.0$ and 60,000 feet for the afterburner condition, with the performance characteristics at normal continuous thrust of secondary importance. Secondly the decision of which is most efficient, the afterburner with higher c , or the normal continuous with lower c , depends on the airplane range as well as the engine characteristics.

The range of the airplane may now be determined by calculating the individual items, L , D , V , c , W_0 and W_1 as outlined in this chapter, and substituting in the Breguet formula; or as has been shown by calculating mi/lb and the weight of fuel.

For an airplane designed to cruise at $M = 3.0$ and 60,000 feet and with an engine with an equal value of T/D^2 , where D is the inlet diameter, the data from figure 3:8 may be used, scaling both the T/δ and the mi δ /lb to account for the new values of thrust. For airplanes with cruising speeds and altitudes other than $M = 3.0$ and 60,000 feet, this engine data would not hold as it was designed specifically for these cruising conditions. It has been shown theoretically that V/c is constant for a constant value of $M\sqrt{\delta}$ for constant thermal efficiency, constant T/D^2 and other ideal assumptions; and that V/c increases and decreases with $M\sqrt{\delta}$. The rate of change is quite variable depending on the value of $M\sqrt{\delta}$ and T/D^2 . Since the higher the M , the higher the optimum cruising altitude is likely to be, (therefore tending to keep $M\sqrt{\delta}$ constant) it would appear that the same engine data may be used for Mach numbers close to $M = 3.0$ for preliminary purposes, if no better data are available.

Climb

In subsonic flight, if the climb is broken down in increments, and each increment flown at its optimum V for climb, approximately $1.3 V_{L/D_{max}}$, it is found that at sea level this optimum R/C speed is not much higher than the required take-off speed, and at 35,000 feet this optimum R/C speed is not much lower than the cruise speed. It is therefore fairly obvious what is the best method of climbing, and the desired speed variation.

In supersonic flight a few possibilities that are vastly different exist, and must be investigated, before the optimum climb method can be established.

3:44 SUPERSONIC AND SUBSONIC AIRPLANE DESIGN

First, as explained in section 3:1, since it is assumed that the transports cannot reach $M = 1.0$ below about 40,000 because of the sonic boom effects on the civilization below, it would appear that some flight path up to this altitude, similar to that of the subsonic aircraft, would be most efficient. However, it must be realized that the main object of cruising at $M = 3.0$ is to reduce travel time, and that therefore it might be more desirable to sacrifice a little D.O.C. to get up to the point of high M as soon as possible.

From this point of 40,000 feet and approximately $M = 1.0$ there are still a few possibilities: (1) climb and accelerate concurrently to $M = 3.0$ and 60,000 feet; (2) climb at some M just below 1.0 to 60,000 ft. and then accelerate to $M = 3.0$; (3) accelerate to $M = 3.0$ at 40,000 ft. and then climb to 60,000 ft., or (4) some other combination of reaching 60,000 ft. at some M between 1.0 and 3.0 and then accelerating. Again the two factors of D.O.C. and flight time should be considered in choosing the optimum flight schedule.

Fig. 3:8 presented the performance at 35,000 feet and above, for an engine designed to cruise at $M = 3.0$ and 60,000 feet. Figs. 3:29 and 3:30 present the thrusts from sea level to 30,000 ft. This data is required for determining the climb characteristics of the supersonic aircraft.

3:8 Fuel Storage

Fuel storage problems on supersonic airplanes are probably more acute than in the subsonic due to the smaller t/c 's used in the wings, and the greater amounts of fuel required for the same range.

3:9 Climb Requirements

There is no reason to believe that the climb requirements for a supersonic airplane should be any different than a subsonic one. Therefore the specifications and reasoning of 2:9 should still apply. Due to the high thrust requirements for supersonic flight it would appear that these climb requirements should not be critical for the supersonic aircraft. However the low aspect ratios do decrease the induced drags, which in turn reduce the (T-D) term so important in R/C determination.

3:10 Optimum Airplane

For the supersonic transport airplane, the direct operating cost is still considered the best criterion in comparing airplanes to choose the optimum design. In addition the methods of calculating the direct operating costs should stay essentially

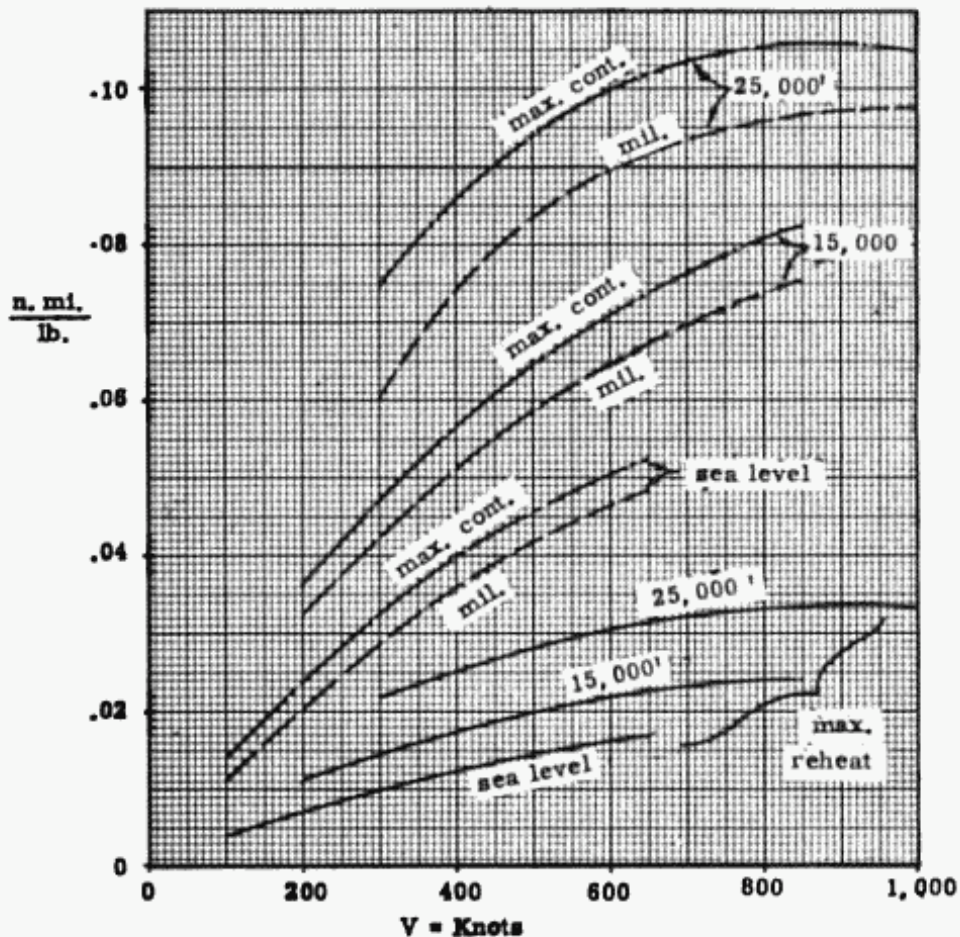


Fig. 3:29. Naut. mi. δ /lb. fuel vs. V from S.L. to 25,000 ft. for the turbojet of fig. 3:8.

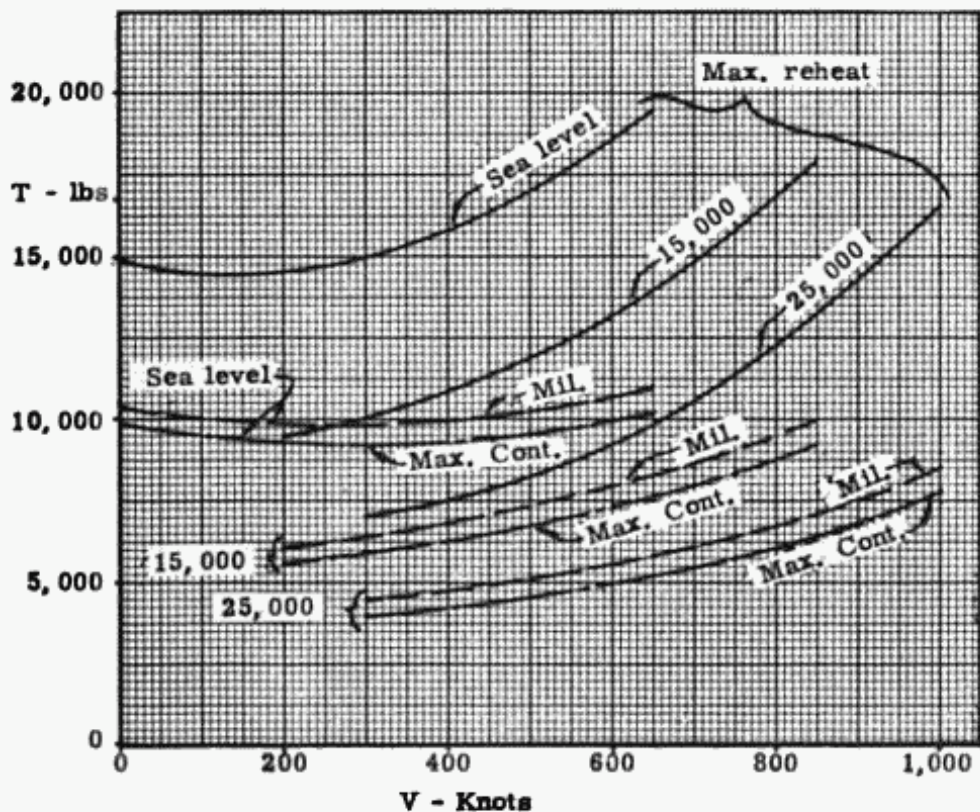


Fig. 3:30. Thrust vs. V from S.L. to 25,000 ft. for the turbojet of fig. 3:8.

the same. One item should be noted is that the maneuver time on the ground, .25 hours for multi-engined aircraft, becomes an increasingly large percent of the total block time, and decreases the block speed appreciably. In the subsonic airplanes, various combinations of aspect ratio, sweepback, and thickness ratio were compared to choose the optimum design. In the subsonic, Λ and t/c were chosen in combination to obtain a chosen value of M_{CRD_0} . However in the supersonic design this criteria of M_{CRD_0} does not exist and other criteria must be used. If a delta wing is chosen, as was done for the transport study, then A.R. is dependent on sweepback and the two main wing variables are A.R. and thickness ratio. However for a more complete analysis, other airfoil sections, taper ratios, trailing edge sweeps, and tip designs should be considered.

3:11 Optimum Altitude

The principles here again are similar to those for the subsonic airplanes in section 2:11. The optimum altitudes for the supersonic airplanes will be considerably higher than for the subsonic, as previously indicated.

References

Ref. No.

- 3:1 "Supersonic Transports", IAS Paper FF-20 Commercial Air Transportation beyond the Subsonic Jet, by R. C. Sebold.
- 3:2 Navord Report 1488 Vol. 3, Sect. 7, "Handbook of Supersonic Aerodynamics Three Dimensional Airfoils", Bu. of Ordn. Publ.
- 3:3 "Ramjet-Turbo jet Propulsion System for Supersonic Flight" by R. T. DeVault, presented at the S.A.E. National Aeronautics Meeting, April '57.
- 3:4 "Design and Application of M4 Turbine Engines" by N. A. Ziplin and R. E. Neitzec, IAS Preprint 859, presented at CAI-IAS meeting, Oct. '58.
- 3:5 "Engineering Supersonic Aerodynamics" by Ronny.
- 3:6 NACA T.R. 1306 "Bodies of Revolution having Minimum Drag at High Supersonic Speeds" by A. J. Eggers, Jr.
- 3:7 WADC Tech Report 57-316 Part I "Drag due to Lift of a Not So Slender Configuration" by H. K. Cheng. Part II, Application of Theory" by R. J. Vidal.
- 3:8 NACA RM L 52HO8 "A Study of Zero-Lift Drag-Rise Characteristics of Wing-Body Combinations Near the Speed of Sound" by R. T. Whitcomb, 1952.

Ref. No.

- 3:9 NACA TN 3673 "On the Range of Applicability of the Transonic Area Rule" by J. R. Spreiter, May '56.
- 3:10 NACA TN 3872 "Experimental Deformation of the Range of Applicability of the Transonic Area Rule for Wings of Triangular Planform", by Wm. A. Page, Dec. '52.
- 3:11 NACA RM L53H31a "Development of a Supersonic Area Rule and an Application to the Design of a Wing-Body Combination having High Lift-to-Drag Ratios" by R. T. Whitcomb and T. L. Fischetti, Oct. '53, Declassified, Sept. '58.
- 3:12 NACA TR 1284 "Theory of Wing-Body Drag at Supersonic Speeds" by R. T. Jones, '56.
- 3:13 M. D. Freedman and D. Cohen, NACA TR 1236 "Arrangement of Fusiform Bodies to Reduce the Wave Drag at Supersonic Speeds", 1956.
- 3:14 B. S. Baldwin, Jr. and R. R. Dickey, NACA RM A54J19 "Application of Wing-Body Theory to Drag Reduction at Low Supersonic Speeds", Jan. '55.
- 3:15 R. T. Jones, NACA TR 1284 "Theory of Wing-Body Drag at Supersonic Speeds", 1956.
- 3:16 H. Lomax and M. A. Hesslet, NACA TR 1282 "A Special Method for Finding Body Distortions That Reduce Wave Drag of Wing and Body Combinations at Supersonic Speeds", 1956.
- 3:17 W. F. Hilton, "High-Speed Aerodynamics", Longmans, Green and Co.
- 3:18 M. Visich, Jr. and A. Martellucci "Theoretical and Experimental Analysis of a Cowling as a Means of Drag Reduction for an Axisymmetric Center Body" AFOSR TN 58-760, Aug. '58.
- 3:19 M. Pittel, NACA TN 3697 "Flight Tests of Supersonic Speeds to Determine the Effect of Tapes on the Zero Lift Drag of Sweptback Low-Aspect-Ratio Wings", June '56.
- 3:20 S. Lampert, "Aerodynamic Force Characteristics of Delta Wings at Supersonic Speeds", Cal. Inst. of Tech., Jet Prop. Lab. Report No. 20-82, Sept. '54, Declassified Nov. '55.
- 3:21 E. S. Love, NACA TR 1238 "Investigations of Supersonic Speeds of 22 Triangular Wings Representing Two Airfoil Sections for Each of 11 Apex Angles", 1955.
- 3:22 G. C. Furlong and J. G. McHugh, "A Summary and Analysis of the Low Speed Longitudinal Characteristics of Swept Wing at High Reynolds Numbers", 1957, NACA TR 1339.
- 3:23 William C. Pitts, Jack N. Nielsen and George E. Kaattari, "Lift and Center of Pressure of Wing-Body-Tail Combinations at Subsonic, Transonic, and Supersonic Speeds" NACA Rept. 1307, 1957.

3:48 SUPERSONIC AND SUBSONIC AIRPLANE DESIGN

Ref. No.

- 3:24 J. C. Eppard, "Diffusers and Air Intakes", Sect. E. "Aerodynamic Components of Aircraft at High Speeds", High Speed Aerodynamics and Jet Propulsion Series, Vol. XII; Princeton Univ. Press.
- 3:25 A. Ferri, "Elements of Aerodynamics of Supersonic Flow", MacMillan.
- 3:26 A. H. Shapiro, "The Dynamics and Thermodynamic of Compressible Fluid Flow", Vol. II, Ronald Press.
- 3:27 F. H. Clausser, "Ramjet Diffusers at Supersonic Speeds", Jet Propulsion Vol. 24, No. 2, Journal of American Rocket Society.
- 3:28 R. Herman, "Supersonic Inlet Diffusers and Introduction to Internal Aerodynamics", Published by Minneapolis-Honeywell Regulator Co.
- 3:29 L. H. Schindel, "Supersonic Wind Tunnel Tests of Ring-Wing Configurations" NADC TR 58-220; ASTIA No. AD155534; Wright Air Development Center.
- 3:30 E. S. Love, NACA TN 3819, "Base Pressure at Supersonic Speeds on Two Dimensional Airfoils and on Bodies of Revolution With and Without Fins Having Turbulent Boundary Layers", Jan. '57.
- 3:31 W. E. Stoney Jr. NACA TN 4201, "Collection of Zero Lift Drag Data on Bodies of Revolution from Free-Flight Investigations", Jan. '58.
- 3:32 J. M. Cabbage, Jr. RML56C21 "Jet Effects on Base and Afterbody Pressures of a Cylindrical Afterbody at Transonic Speeds" May '56.
- 3:33 P. E. Purser, J. G. Thibodaux, and H. H. Jackson RML50I18 "Note on Some Observed Effects of Rocket Motor Operation on the Base Pressures of Bodies in Flight."

Chapter IV

AIRPLANE LAYOUT - SUBSONIC

4-1 Layout

The next step is to draw the airplane from the data that has been determined in Chapter II. A very important factor is the location of the center of gravity at take-off weight and the possible range of center of gravity for various loading conditions. It is desirable to keep this range of centers of gravity to a minimum and centered about the .25 mean aerodynamic chord. This will be discussed more fully in Part II, "Stability and Control."

4-2 Wing Plan Form

The plan form of the wing should be drawn independently of the other parts of the airplane and the location of mean aerodynamic chord shown.

From the method explained in Chapter II, wing area, aspect ratio, sweepback and thickness have been calculated. The only characteristic necessary for drawing the wing plan form that has not been calculated is the taper ratio.

Taper ratio is defined as the wing tip chord divided by the chord at the center line of the wing,

$$TR = \frac{C_t}{C_c} \text{ as shown in Figure 4:1} \quad (4:1)$$

It should be noted that the tip chord on a rounded tip is the distance between the leading and trailing edges of the wing extending to the actual wing tip.

The choice of taper ratio is based upon a compromise between structural and aerodynamic efficiencies. The smaller the taper ratio, the lighter the wing will be. Since the bending moments on the wing are largest at the side of the fuselage, it is important to have the depth of the wing greatest at that point. In such a configuration the material required to carry the bending

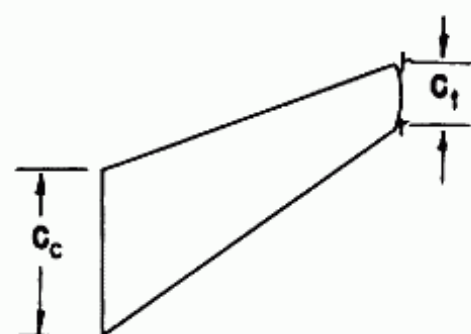


Fig. 4:1. Tip chord and center line chord.

moment loads will be a minimum. The smaller the taper ratio, the larger the chord at the side of fuselage and therefore the thicker the wing will be for the same thickness ratio. As shown in Figure 2:30, the space in the wing available for fuel is greater with a lower taper ratio. In addition, the bending moments along the span are less for the wing with the lower taper ratio, which again tends to reduce the weight of the wing.

A disadvantage of reducing taper ratio is that unfavorable tip stall characteristics are introduced. Actually the general usage of the term tip stall does not refer to the actual tip but to sections a little inboard of the tip. Any wing may at some time be stalled, the most preferred sequence of wing stalling is the inboard section first, progressing outboard. Although stalling of the root causes buffeting of the tail due to the turbulent wing wake of the root, this effect is desirable as it acts as a physical warning to the pilot that the tip stall is imminent.

The reason that stalling of the tip is undesirable is that the aileron becomes ineffective, and roll control is lost when it is most important, near max C_L , that is in take-off and landing.

There are two main reasons why reduced taper ratio tends to induce tip stall:

- 1) Smaller taper ratios mean smaller chords at the tip and smaller R. N. since $R. N. = V\ell/\nu$, where $\ell = \text{chord}$. (See fig. 2:26 for ν) Wind Tunnel tests have verified that max C_L and α for max C_L are both reduced at lower R. N. as shown in fig. 4:1 a.

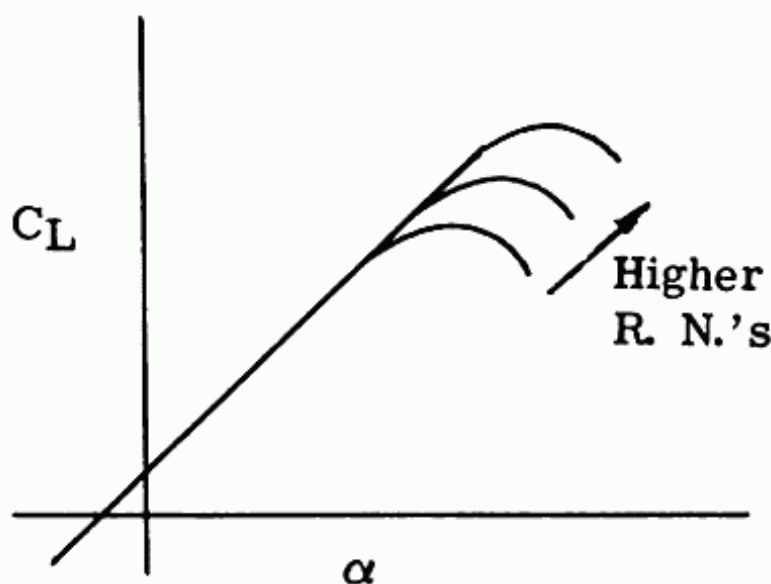


Fig. 4:1a. Effect of α on C_L .

- 2) As previously stated, an elliptical spanwise loading distribution results in a constant C_L along the span. For any other loading distribution C_L varies along the span. As taper ratio decreases the max C_L moves outboard, see fig. 12:21.

This combination of a higher operating C_L near the tip and a lower actual max C_L results in undesirable tip stall characteristics for wings of low taper ratio.

There are ways of delaying tip stall. The one used most on unswept wings is twisting the wing so that the tip is at a lower angle of attack than the inboard portion. Other methods are the use of slats in the leading edge of the outboard sections, or tip airfoil sections that have higher values of max C_L . The most effective method for sweptback wings is the use of fences. This is true because the most important cause of tip stall on a sweptback wing is the build-up of the boundary layer, and fences prevent this build-up.

The choice of the optimum taper ratio is mainly a compromise between these two effects of reduced weight and of tip stall characteristics, with the added factor of induced drag. For a wing of elliptical plan form the induced drag is a minimum. Wings with taper ratio equal to approximately .4 give approximately the same results as a wing of elliptical plan form.

$$\Delta C_{D_i} = \frac{C_L^2}{\pi AR} \phi \quad (4:2)$$

where ΔC_{D_i} is the increase in C_{D_i} due to spanwise loading distribution

and ϕ is a correction factor dependent on taper ratio, and = 0 for elliptical spanwise distribution. See fig. 4:2.

Figure 4:2 a, b shows the variation in ϕ with taper ratio and aspect ratio. Figure 4:2 a shows that for taper ratios between .3 and .6 at $AR = 6$ the increase in C_{D_i} over the elliptical plan form is in the vicinity of 1 percent.

It is impossible to try to choose analytically the taper ratio which is the optimum for each airplane, as has been done for aspect ratio, sweepback, and thickness ratio in Chapter II. However taking into consideration all the pertinent factors it has been decided that taper ratio equal to .33 is close to the optimum for this jet transport airplane.

Taper ratios from .2 to .6 are usual for high performance aircraft, although the extremes of zero and values greater than

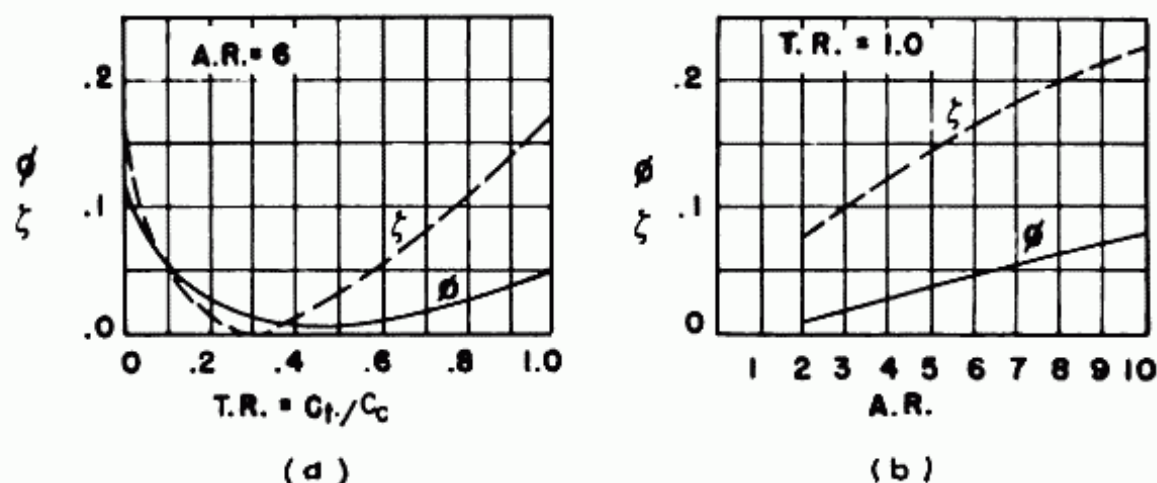


Fig. 4:2 a, b. Effect of T.R. and A.R. on induced drag coefficient and slope of the lift curve.

1.0 have been used on airplanes of special requirements. Taper ratio equal to 1.0 is often used on private airplanes since they are the cheapest to produce, especially if a constant airfoil section is used.

Mean Aerodynamic Chord

For the purpose of convenience it is generally assumed that any surface, wing or empennage, can be represented by a chord, the forces and moments on it representing those on the surface. This chord is called the mean aerodynamic chord. Equations 4:3 and 4:4 present the formulas for calculating the length and spanwise position of this chord.

$$M.A.C. = \frac{2}{3} \left(C_c + C_t - \frac{C_c C_t}{C_c + C_t} \right) \quad (4:3)$$

where C_c = root chord

C_t = tip chord

$$\frac{y}{b/2} = \frac{1}{3} \left(\frac{C_c + 2C_t}{C_c + C_t} \right) \quad (4:4)$$

where y = spanwise location of M.A.C.

b = wing span

The above formulas are true for wings with straight leading and trailing edges. In this case the mean aerodynamic chord is actually a chord of the wing.

Fig. 4:3 presents M.A.C./ C_c and $\frac{y}{b/2}$ for taper ratios from 0 to 1.0.

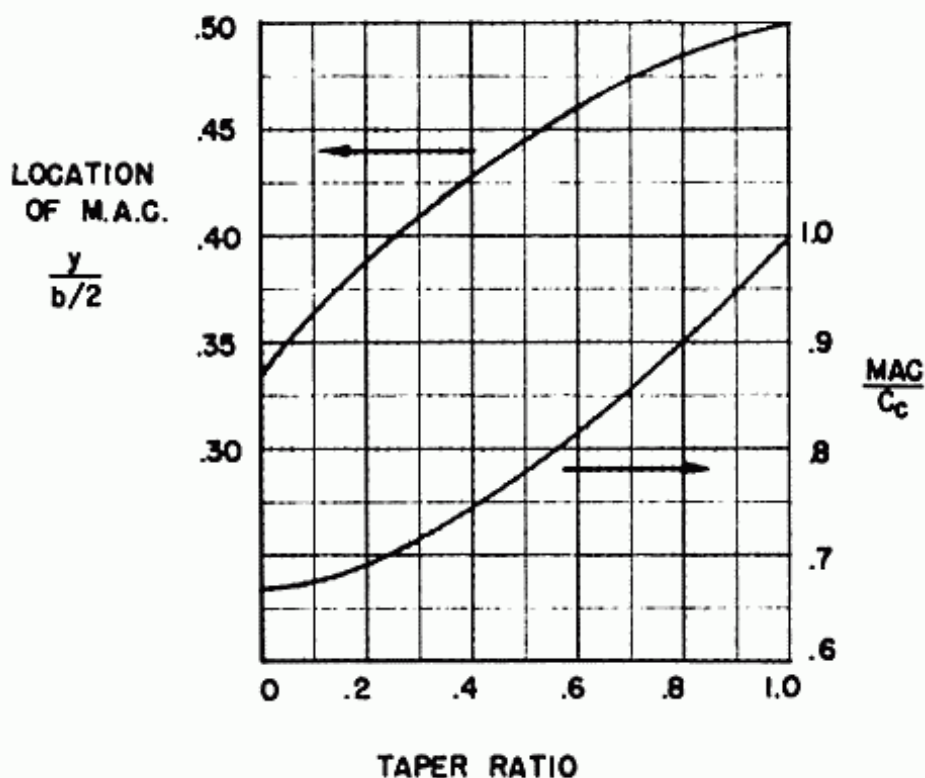


Fig. 4:3. Variation in M.A.C. length and location, with taper ratio.

The above data on mean aerodynamic chord length and spanwise location is for an unswept, rigid, untwisted wing. Wing sweepback, flexibility and twist do affect the spanwise loading distribution of the wing and therefore the mean aerodynamic chord. However, for balance consideration the method neglecting these factors is of sufficient accuracy and is usually used in preliminary design.

Mean Aerodynamic Center

The mean aerodynamic center of an airfoil section is the point at which the lift due to angle of attack acts. Fig. 4:4 a and b shows the C_L vs α curve, and the points at which the lift acts for a cambered airfoil.

It should be noted that the C_L due camber is a constant, i.e. does not vary with α . Therefore another definition of a.c. is that it is the point at which the C_m is constant, i.e. independent of α . The a.c. for the subsonic airfoil with no sweepback is at approximately the .25 MAC, usually between .23 and .26. It is for this reason, as stated in section 4-1, that the c.g. is usually centered about the .25 MAC.

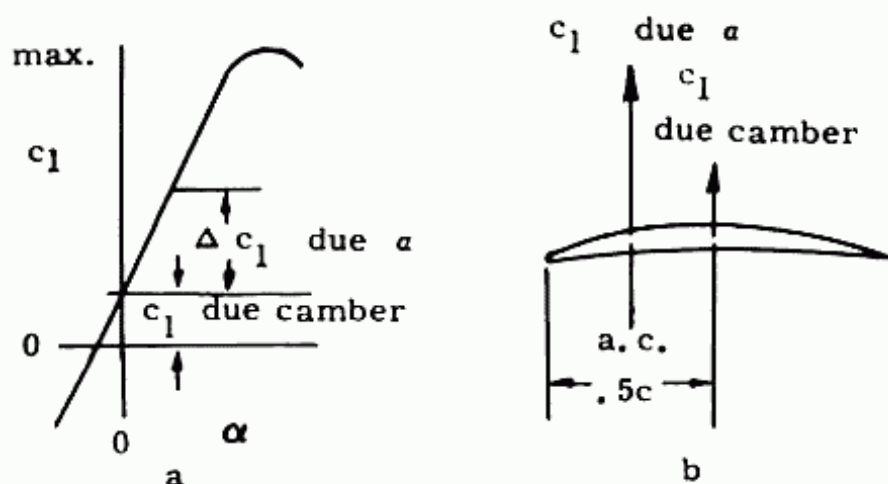


Fig. 4:4a, b. Effect of α and camber on c_l .

Location of Spars

The locations of the spars are influenced by many factors. The rear spar is usually placed as far aft as possible and its position is limited by the control surfaces and the mechanisms required to operate them. The further aft the rear spar is, the greater the space available for fuel storage and the larger the torsion box. The structural disadvantage to moving the rear spar too far aft is that its height becomes less and therefore is not as efficient in bending. The front spar location is determined by structural considerations as well as the items located in the nose of the wing. It must be aft of the entire anti-icing system and slot, if there is one. The further forward it is, the larger the fuel storage space and the torsion box are. However, the structural efficiency of the spar as affected by its height must be considered. Typical locations for the spars are 12 to 15% of the chord for the front spar and for the rear spar, 65% of the chord at the side of the fuselage and 50% of the chord from about 60% of the spar outboard. This variation in location of the rear spar with span is to allow for variation in flap and aileron requirements.

Ailerons and Flaps

The size of flaps and aileron will only be approximated. The ailerons are commonly about 30% of the chord and extend from about 65% of the span outboard. The size of aileron required varies with the type of airplane; an airplane with high maneuverability requirements should have a more powerful aileron. Flaps are used to increase the maximum lift coefficient of the

airplane. Since the higher the maximum C_L the better, particularly for a transport airplane with a limited landing field, an efficient flap is required.

There are numerous types of flaps. The plain flap and split flap are comparatively simple mechanically and yield a moderate increase in maximum C_L . The slotted flap and Fowler flap are much more complicated and yield a substantially larger maximum C_L . The choice depends upon the particular airplane being designed.

Figure 4:4 presents a table of high lift devices including both flaps and slats, showing maximum C_L , α at maximum C_L , $(L/D)_{\max}$ and C_m about a.c. A Fowler flap is very effective in increasing the lift on the wing as it increases the wing area as well as increasing the airfoil camber. The length of the chord of the flap is limited by such considerations as the fuel space in the wing, the size of torsion box and the efficiency of the flap both structurally and aerodynamically. Although the maximum C_L is increased by increasing the chord of the flap beyond 30% of the wing chord, it seldom increases the overall efficiency of the airplane to do so. Usually the span of the flap runs from the aileron to the side of fuselage; sometimes it is extended below the fuselage. There has been much work done on the design of full span flaps. These flaps actually require that the aileron act as either a flap or an aileron or both as required. However full span flaps are not efficient on highly swept wings as the outboard portion of the flap is far aft of the quarter mean aerodynamic chord of the airplane and causes a high diving movement. A Fowler flap is most efficient if its leading edge is parallel to the wing trailing edge and moves perpendicular to it. It is therefore usually desirable to break the flap into at least two pieces on each side of the wing to allow for the variation in the wing chord. Figure 4:5 shows a typical plan form of a sweptback wing with the spars, flaps and aileron outlined.

Both the Douglas DC-8 and Boeing 707 use the double slotted flap. Although this flap does not have as high a max C_L as the Fowler flap, it is felt that the higher drag associated with the double slotted flap results in about the same landing field, although it has a higher landing speed. The advantages of the double slotted flap is that it is less complicated and lighter, and due to its high drag the pilot can come in high and get down fast.

Incidence

The angle of incidence is defined as the angle that the wing chord makes with the center line of the fuselage. It is established by considering the take-off lift coefficient required, the




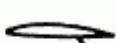









Designation	Diagram	$C_{L_{max}}$	α at $C_{L_{max}}$ (degrees)	L/D at $C_{L_{max}}$	$C_{m_{ac}}$	Ref. NACA
Basic airfoil Clark Y		1.29	15	7.5	-.085	TN 459
.30c Plain flap deflected 45°		1.95	12	4.0	-	TR 427
.30c Slotted flap deflected 45°		1.98	12	4.0	-	TR 427
.30c Split flap deflected 45°		2.16	14	4.3	-.260	TN 422
.30c hinged at .80c Split flap (Zap) deflected 45°		2.26	13	4.43	-.300	TN 422
.30c Fowler flap deflected 40°		2.82	13	4.55	-.660	TR 534
.40c Fowler flap deflected 40°		3.09	14	4.1	-.860	TR 534
Fixed slot		1.77	24	5.35	-	TR 427
Handley Page automatic slot		1.84	28	4.1	-	TN 459
Fixed slot and .30c plain flap deflected 45°		2.18	19	3.7	-	TR 427
Fixed slot and .30c slotted flap deflected 45°		2.26	18	3.77	-	TR 427
Handley Page slot and .40c Fowler flap deflected 40°		3.36	16	3.7	-.740	TN 459
Double slotted .78c flap deflected 55° 55 ₂ -415 airfoil		2.39	2 dim. test R: 6×10^6			TN 2149
NACA 7 by 10 ft. tunnel data AR = 6 RN = 609,000						

Fig. 4:4. Flap and slat characteristics.

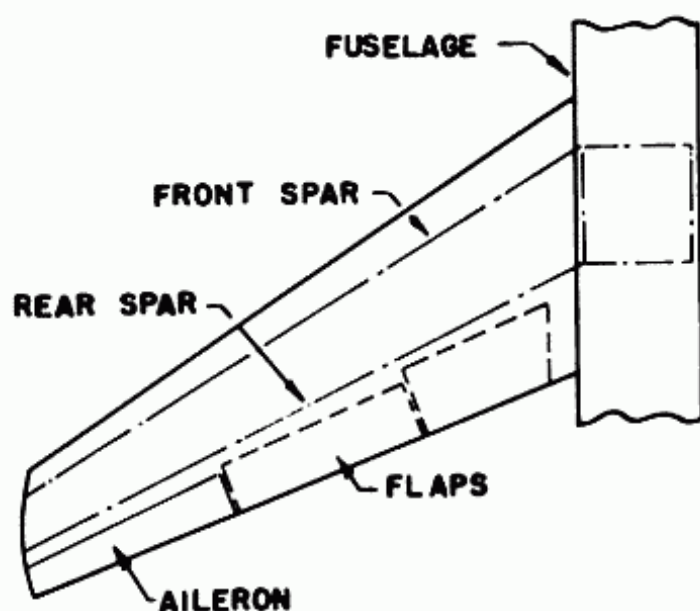


Fig. 4:5. Typical layout of a sweptback wing.

attitude of the cabin floor during cruise and on the ground, and the variation in drag of the fuselage with change in angle of attack.

An airplane with a bicycle landing gear usually makes its ground run in take-off with all the main wheels on the runway. Due to the large distance from the center of gravity of the airplane to the rear gear, an impractically huge horizontal tail surface would be required to rotate the airplane to raise the front gear. If the cabin floor is parallel to the ground and to the center line of the fuselage, it is most efficient in loading and unloading, and at the same time most comfortable for the passengers. The main gears are designed to be as short as possible and still perform their required function. A short landing gear is light and permits easy loading and unloading of the fuselage which will be close to the ground.

As previously stated the take-off coefficient of lift is equal to .75 times maximum C_L . This reduction is required as a safety factor so that the wing will not stall if the angle of attack is suddenly increased due to a gust. With flaps in take-off position and the main wheels on the ground, the angle of attack of the wing must be such that .75 maximum C_L is attained. For a given flap design this requirement determines the angle that the wing must make with the ground.

4:10 SUPERSONIC AND SUBSONIC AIRPLANE DESIGN

In obtaining the angle for the specified lift coefficient it is necessary to account for all the factors that affect the position and the slope of the lift curve. The airfoil data must be corrected for flap deflection, aspect ratio, sweepback and ground effects. Flap data is usually presented with the airfoil characteristics; variations due aspect ratio and sweepback are presented in Section 9:5 and the ground effect on slope of the lift curve, is shown in Figure 4:6. The influence of the ground on the forces on the airplane can be calculated. It has been shown that it is equivalent to increasing the aspect ratio which in turn increases the slope of the lift curve. Another ground effect is that the higher effective aspect ratio reduces the induced drag, as shown previously in Figure 2:35.

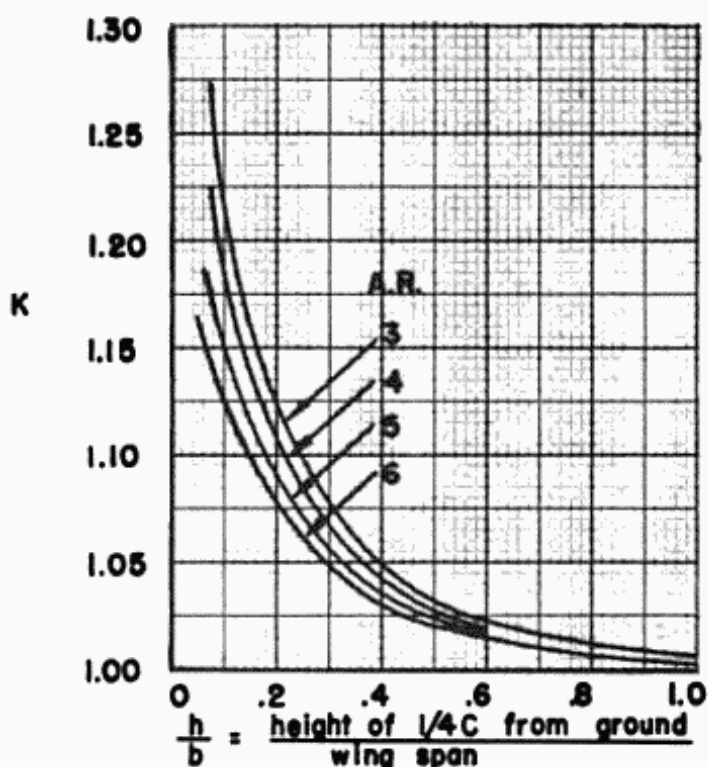


Fig. 4:6. Ground effect on slope of the lift curve. Ref.: NACA W.R.L. 95.

$$\left(\frac{dC_L}{d\alpha}\right)_{\text{ground effect}} = K \left(\frac{dC_L}{d\alpha}\right)_{\text{no ground effect}} \quad (4:5)$$

K obtained from Figure 4:6

It should be noted that Mach number also affects slope of the lift curve. However, at take-off speed the effect is negligible.

From the final curve of C_L versus angle of attack at take-off, the required angle that the wing must make with the ground is determined. If the center line of the fuselage is parallel to the ground, the angle of incidence is equal to the ground angle.

A new curve of C_L versus angle of attack must be plotted for cruise. In this condition, there is no ground effect or flap deflection, but the Mach number effect must be introduced. The variation of $dC_L/d\alpha$ with Mach number is shown in Figure 9:8.

If the angle of attack for cruise C_L is equal to the angle of incidence then the most satisfactory condition exists; the cabin floor is level in flight and on the ground, and the landing gear is at its optimum length. However, if these conditions do not exist, then a compromise must be made. If the angle of incidence is greater than the angle required for cruise, the cabin floor would slope downward in flight. A condition of zero slope is not required and a small slope would not be objectionable. However, it may be corrected by increasing the length of the front gear, thereby adding weight to the gear and requiring greater space for retraction in the fuselage. In addition, the floor would slope on the ground. The exact manner of solution and compromise depends on the particular airplane designer.

For the tricycle landing gear airplane the angle of incidence is easier to choose since this arrangement permits the airplane to be rotated on the ground before take-off, to the angle of attack required.

Dihedral

The dihedral is measured by the angle between the plane of the wing chord and the plane perpendicular to the plane of symmetry passing through the root chord. The dihedral angle is positive if the wing tips are above the root, for zero incidence. See Figure 4:7. For wings with sweepback and incidence the tip chord will be lower than the root chord with zero dihedral.

The dihedral effect is most important in the lateral stability and control of the airplane. The rolling moment variation with

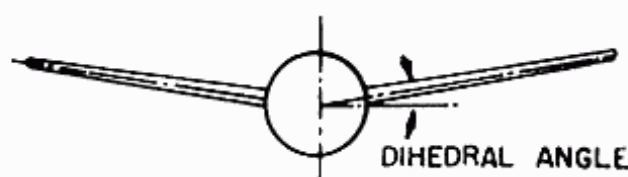


Fig. 4:7. Dihedral angle.

4:12 SUPERSONIC AND SUBSONIC AIRPLANE DESIGN

sideslip is called the dihedral effect. If an airplane with a dihedral angle sideslips, the forward wing is at a greater angle of attack than the trailing wing and a rolling moment is induced. Other factors that modify the dihedral effect are the vertical location of the wing on the fuselage, wing sweepback, flap deflection and power. See Chapter X for a more detailed discussion.

The criteria for dihedral effect has never been satisfactorily established. The pilot usually feels that some dihedral effect is desirable. However, it is possible to attain so much dihedral effect that it will be undesirable for directional control and in fast rolling maneuvers. Wings with zero sweepback usually require some dihedral to give satisfactory rolling moment characteristics. Sweepback results in the same effect as dihedral, particularly at high coefficient of lift.

As has been shown previously the force on a wing is a function of the velocity perpendicular to the quarter chord. From fig. 4:7a it is evident that in a sideslip the leading side of a swept wing has a higher velocity perpendicular to the $c/4$ than the trailing side, and therefore a higher lift, causing roll due to sideslip.

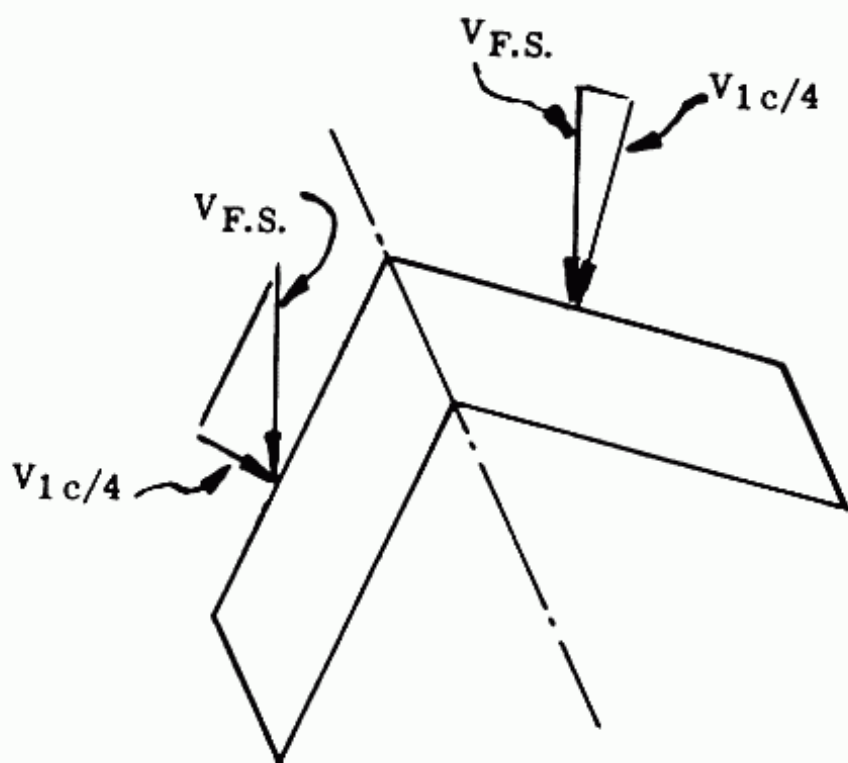


Fig. 4:7a. Effect of sweepback on dihedral effect.

It is for this reason that wings of high sweepback often have no dihedral or sometimes even negative dihedral. However, with a high angle of incidence and large amount of sweepback, zero or negative dihedral might present a wing tip-ground clearance problem.

Airfoil Selection

Some of the general data presented in Chapter II was based upon some typical airfoil being used. It is therefore desirable at this time to present the criteria involved in choosing an airfoil.

The choice of airfoil, although quite complex, has been greatly simplified by the work of the National Advisory Committee for Aeronautics. Through the years, they have developed and studied many series of airfoil sections and presented the information to the industry. The latest series is not necessarily the best for all airplanes. One may be best for one type of airplane while another best for a different type. In choosing an airfoil section for a particular design the following criteria must be considered:

- (1) $c_{l_{max}}$ - maximum lift coefficient with flaps. This is especially true in a jet transport where the landing field requirement is important. This maximum c_l is an important factor in landing field evaluation and should be as large as possible.
 - max. lift coeff. without flaps. This is important in maneuver. The ability of an airplane to maneuver is dependent on max C_L without flaps/cruise C_L . Therefore for airplanes that require a high degree of maneuverability max C_L without flaps is a very important criterion.
- (2) $c_{m_{ac}}$ - moment coefficient of the airfoil about the aerodynamic center. Since for any equilibrium condition the moment coefficient of the airplane about the center of gravity must equal zero, the $c_{m_{ac}}$ should be as small as possible. Zero moment coefficient is ultimately attained by horizontal tail deflection. The smaller the moment that must be balanced by the tail, the more efficiently the tail can be designed. For the all wing airplane, that is an airplane with no horizontal tail, it is most important to get $c_{m_{ac}}$ equal, or close to, zero as there is no horizontal tail to balance out the $c_{m_{ac}}$. This low value of $c_{m_{ac}}$ can be attained by using a reflex airfoil.

- (3) $c_{d_{\min}}$ - minimum coefficient of drag. It is important for this criteria to be as low as possible and furthermore that it should occur at the design lift coefficient. In a transport airplane, the design C_L is at cruising; in a fighter airplane, the design C_L is at high speed.
- (4) L/D - Lift divided by drag, or c_l/c_d . This is one of the most important criteria in airfoil designs and should be as high as possible. It is often used to judge the efficiency of the airfoil. Obtaining the maximum L/D at the design condition is accomplished by having $c_{d_{\min}}$ at design lift coefficient as explained in (3).
- (5) M_{cr} - critical Mach number is the Mach number of the free-stream at which the local speed over any point on the airfoil reaches the speed of sound. The increase in drag due to the compressibility of air is a function of the M_{cr} , for each airfoil. To keep this increase in drag to a minimum for high subsonic airplanes M_{cr} should be as high as possible.
- (6) $\left\{ \begin{array}{l} M_{crD} \\ M_{crL} \end{array} \right\}$ - For airplanes in the high speed range not only is the M_{cr} an important criteria, but the variation in c_d and c_l at Mach numbers higher than M_{cr} is also quite significant. These variations in c_d and c_l above M_{cr} determine M_{crD} and M_{crL} , which are vitally important in the design of the airplane. These factors are discussed in Chapter II.
- (7) Stall characteristics - Figure 4:8 shows the c_l versus angle of attack curve for two airfoils. If the angle of $c_{l_{\max}}$ is exceeded in airfoil A there is a sudden drop in c_l which is undesirable. Airfoil B represents more satisfactory stalling characteristics.

The NACA 6 series is a comparatively new airfoil that is efficient for jet transport design. The data for this series is presented in NACA T.R. 824. A typical airfoil of this group is

NACA 6 4, 2-3 15

where

- 6 - the series designation
- 4 - chordwise position of the minimum pressure, in tenths of chord behind the leading edge, for the basic symmetrical section at zero lift.
- 2 - range of c_l in tenths above and below design c_l , in which a favorable pressure gradients exist on both surfaces.
- 3 - design lift coefficient in tenths.
- 15 - maximum thickness ratio in percent of chord.

The actual choice of airfoil can now be made with the required thickness ratio known and the cruising C_L calculated.

An excellent reference in the field of airfoil sections and characteristics is "Theory of Wing Sections," by I. H. Abbott and A. E. Von Doenhoff.

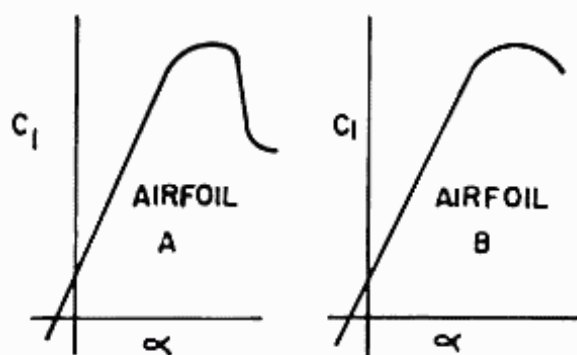


Fig. 4:8. Airfoil stall characteristics.

4-3 Landing Gear General

The conventional tail wheel arrangement is considered inadequate for commercial transports. The primary objection to this type of landing gear is its tendency to ground loop. The greatest advantage of this type of gear is that it is usually the lightest of all the types considered. Other disadvantages for commercial transport use are its poor ground handling characteristics and the slope of the floor relative to the ground. The latter condition is undesirable from comfort considerations for the passengers in loading and unloading during take-off and landing. Until recently the only alternative seemed to be the nose wheel configuration, usually called the tricycle. With this type of gear, the objections of ground looping, ground handling and sloping floor are eliminated. The tricycle configuration consists of a pair of main wheels supported out on the wings, usually retracted into the engine nacelles on multi-engined aircraft, and the nose gear retracted into the nose of the fuselage. This type has proven quite satisfactory for slow speed, reciprocating engine transports because the reciprocating engines are comparatively large and not sensitive to variations in shape of tail pipe. These characteristics

of the reciprocating engine allowed the designer to retract the main gears into the engine nacelles with little increase in drag.

However due to the facts that a jet engine is comparatively small and that the thrust of the engine is quite sensitive to tail-pipe variations from straight flow, it is difficult to store the wheels in the nacelle of a jet engine.

Bicycle Type Gear

In recent years many jet bombers have successfully used the bicycle type gear. In side view the main wheels of the bicycle gear are similar to the tricycle gear. The difference is that in the bicycle type, the front and rear wheels have been so located that the front gear takes a considerable portion of the total load, in some cases 50 per cent. In addition the main wheels of the bicycle type are retracted into the fuselage. This is usually quite satisfactory in a jet transport as there is space below the cabin floor into which to retract the gear. With the main wheels in the fuselage, a device is needed to stabilize the plane in turning maneuvers on the ground, and to provide means of accomplishing a wing low landing. For this purpose a gear is placed outboard on the wing. This gear, called the outrigger, is comparatively small and can be retracted into the nacelle or into the wing structure itself.

Some major problems deal with the outrigger wheels. Although the main purpose of these wheels is to stabilize the airplane in ground turning, the structure must also withstand the loads imposed on it during an outrigger first landing. These factors have led to considerable variation in design of the outrigger. The variables are the spanwise position, the position of outrigger tire relative to ground when main wheels are in the static position and the stiffness of the gear shock absorbing system. The next section presents a more detailed discussion of the problems involved in the layout of both the main and the outrigger gears.

Figure 4:9 shows a general arrangement drawing of an airplane using a nose wheel type landing gear and another with a bicycle type gear.

Bicycle and Tricycle Types - Landing Problems

Although the bicycle type has the advantages explained, it has definitely presented new problems. Probably the most serious is due to the inherent feature of the standard bicycle gear, that the rear tires are further aft of the airplane center of gravity than the main tires of the tricycle type.

The tricycle gear airplane is landed at a high angle of attack,

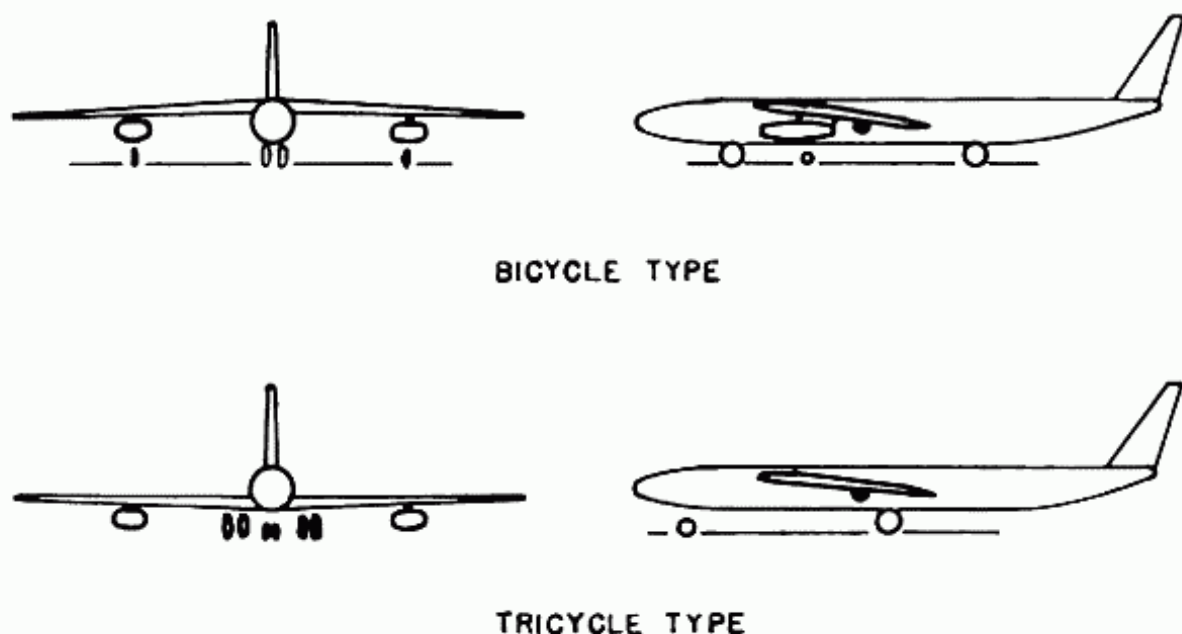


Fig. 4:9. Nose wheel and bicycle type gears.

the main tires making ground contact, with the nose tires still a considerable distance from the ground. At ground contact, the elevator is rotated down from the maximum up position so that the airplane weight is rapidly transferred from the wing to the tires. In this way, the brakes are more effective and the airplane can be handled in a cross wind.

If the bicycle gear is landed with the front tires high off the ground with the rear tires making contact, there is a very high pitching moment induced which causes the front gear to hit with a considerable bounce. This is due to the facts that the weight acting at the airplane center of gravity has a large arm to the ground contact point, which is the center of rotation, and the horizontal tail is not effective because it has a very short arm to the center of rotation. The tricycle gear airplane does not land with a bounce on landing because the distance from the center of gravity to contact point is very small and the rotation is controlled by the horizontal tail. The bicycle gear airplanes have usually been designed to land with both the front and rear gears making contact at the same time. In this type of landing, for a considerable period of time the airplane is floating close to the ground and then rolls with little load on the tires. While on the ground with little load on the tires, brakes are ineffective and the airplane is difficult to control if there is a cross wind.

These bicycle gear problems can be tackled in two ways. If landed with front and rear tires making contact simultaneously,

wing spoilers can be employed to decrease C_L so that the wing load is transferred rapidly to the tires, and a cross wind landing gear used to accomplish a cross wind landing. If the tricycle airplane type of landing, which is more desirable because it allows the airplane to have a higher angle of attack on landing, is to be considered, the severity of the front wheel bounce can be reduced in a number of ways. This can be accomplished by moving the rear tires closer to the airplane center of gravity, by using a long, soft front oleo and by making the horizontal tail more effective to reduce the high pitching moment. The most effective of these is to move the rear tires forward so that they are as close to the airplane center of gravity as the main tires of the tricycle gear airplane. However the tires would then be difficult to store efficiently in the fuselage. One method is to have two sets of tires close to the center of gravity, one rotating forward and the other aft, as shown in Figure 4:10.

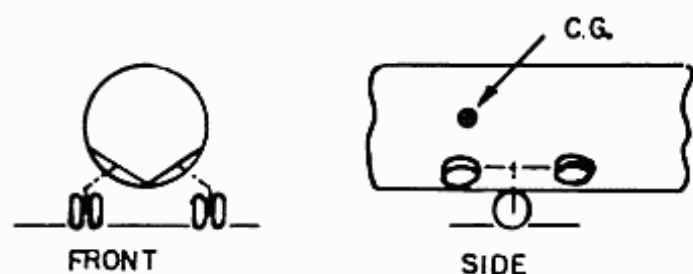


Fig. 4:10. Main wheels of bicycle type gear near center of gravity.

Choice of Type

To arrive at the best landing gear type for any airplane it is necessary to actually lay out the entire airplane with the best designs of each landing gear type and determine which design results in the most efficient airplane. One method of using a tricycle gear design is to support the main gears in the wing aft of the rear spar and retract them into the fuselage as is possible in the tricycle gear airplane shown in Figure 4:9.

This design requires a low wing airplane, reduces the size of wing flap and complicates the flap and aileron control systems.

Considering all the problems involved, the bicycle gear has been chosen for the jet transport studied in this text.

Landing Gear Layout

Main Wheels

For best efficiency it has been decided that a bicycle type landing gear will be used, with the main gears retracted into the fuselage and the outriggers somewhere out on the wing.

For the purposes of uniformity it would be desirable to place the front and rear wheels equi-distant from the center of gravity of the airplane at take-off weight. If this is done the front and rear tires can be the same size and the need for stocking more than one type of tire for replacements is eliminated. It would also be desirable to locate each gear at a distance from the center of gravity of the airplane equal to the radius of gyration of the fuselage taken about the airplane center of gravity. The critical loads on the front and rear gears will then be equal and a minimum in either a tail first or nose first landing.

However due to the fuselage design, these factors that tend to make the landing gear itself more efficient must sometimes be sacrificed to the overall efficiency of the airplane. Figure 4:19 shows how the landing gear has been shifted so that the rear gear can be retracted under the lavatories and the front gear can be retracted under the crew compartment. If they were to be placed equi-distant from the center of gravity of the airplane at a distance equal to the radius of gyration, the fuselage would have to have been made considerably larger to be able to enclose the tires. Figure 4:20 shows how the tires can be made to fit into the fuselage by using four wheels in each of the front and rear gears.

The size of the main tires is obtained by calculating the load on the tires by statics with the airplane resting on the ground at design weight and assuming all the weight is acting on the main tires. Using these loads and the tire ratings as presented by the tire manufacturers, the tire may be chosen. Again a compromise must be made. For the same load rating, higher tire pressures allow smaller tire sizes. Therefore, for efficiency of space, the higher pressures are more desirable. However, if the tire pressures and the total load on the tire are high, the resultant stresses on the airport landing fields and warming up strips may be prohibitive. Since landing fields vary in their capacity to withstand large tire loads due to different types of surfacing and thicknesses, the final combination of tire pressures and number of tires per gear, depends on the airports the plane is intended to service. Some present day commercial designs use pressures up to 165 pounds per square inch. Figure 4:11 presents a list of tires and ratings made by a prominent manufacturer.

Type VII - Extra High Pressure Tires Main Wheels

Tire Size	Ply Rating	Max Width inches	Max Diam. inches	Loaded Radius inches	Tire and tube wt. lbs.	Commercial		Military	
						Press lbs/sq.in.	Rated Load lbs	Press lbs/sq.in.	Rated Load lbs.
24 x 7.25	10	7.3	24.0	10.3	29.7	120	6,600		
29 x 7.7	12-16	7.6	28.0	12.2	36-44	160	9,800	220	13,800
34 x 11	18	11.0	33.0	13.9	84.1	125	15,500		
36 x 11	24	11.1	35.0	15.0	86.2			220	25,600
40 x 14	22	13.5	39.2	11.8	112	145	25,000		
44 x 13	26	13.4	43.2	18.4	141.5			200	35,000
44 x 16	26	15.6	43.1	18.0	151.6	165	35,500		
56 x 16	24	16.0	55.8	24.1	258.7			178	45,000
56 x 16	32	16.1	55.8	24.1	296.3			240	60,000
56 x 16	36	16.1	55.8	24.1	297.0			280	71,000

Fig. 4:11. Tire Ratings. Ref. U.S. Rubber Co.

Outrigger Wheels

The problems of the best location and the design loading on the outrigger are, in some aspects, more difficult than that of the main gear. Only an introductory discussion will be presented.

The loads on the outrigger due to ground turning are quite simple to determine. Figure 4:12 shows the front view of an airplane with a bicycle gear.

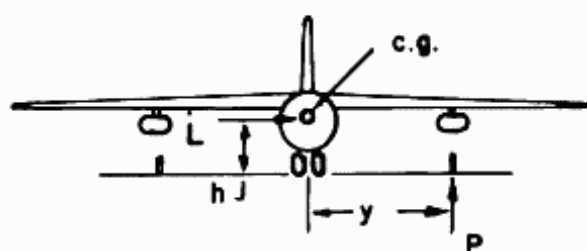


Fig. 4:12. Front view - bicycle gear.

$$P_{out} = \frac{Lh}{y} \quad (4:6)$$

where P_{out} = design load on outrigger gear due to ground turning

h = vertical distance from center of gravity to ground with airplane in static position

y = spanwise distance from center of main gear to center of outrigger gear

L = design side load acting at center of gravity in ground turning

= (take-off weight) x (load factor = .75)

The load imposed upon an outrigger gear due to an outrigger first landing involves a complicated calculation. It will depend upon the spanwise location of the outrigger, the flexibility of the shock absorbing systems of the main gears and the outrigger, and the flexibility of the wing itself. It has been established that the loads on the two outriggers will be equal and, therefore the minimum for an outrigger first landing, if they are placed at the radius of gyration of the airplane taken about the center line of the fuselage. This is true if the action of the main gears is neglected. If the gears are placed inboard of the radius of gyration the gear touching first will have the greater load; if the gears are placed outboard, the gear touching last will have the greater load. Whether the ground turning condition or the banked

4:22 SUPERSONIC AND SUBSONIC AIRPLANE DESIGN

landing condition is critical depends upon the factors that determine the landing loads mentioned above, in addition to the spanwise location of the gear. Inasmuch as these factors are not yet determined in the preliminary design it is satisfactory to estimate the tire size by the ground turning condition. In the actual design of the outrigger an effort should be made so that the loads in the banked landing should not exceed the ground turning loads.

The spanwise and chordwise location of the outrigger is dependent on many factors. The spanwise location as a factor in obtaining the lowest loads has just been discussed. However convenience in retraction and aerodynamic efficiency must also be considered. If the airplane has a nacelle slung under the wing with two small engines in it, it is possible to retract the outrigger into the nacelle between the engines. However it probably requires spreading the engines apart slightly to provide space for the tire and presents the problem of keeping the tire away from the hot exhaust. In addition the spanwise location of the gear is dictated by the location of the nacelle. This arrangement does provide the advantages of adding little, if any, additional wetted area, and of a short and therefore light landing gear. The loads can be carried from the nacelle support to the wing by the existing nacelle strut.

Another arrangement is one in which the outrigger is retracted spanwise into the wing structure behind the rear spar and forward of the control surface. The advantage is that it requires absolutely no additional wetted area, does not complicate the design of the nacelle and allows positioning the gear in its best location spanwise. It presents the problem of finding space in the wing for the tire. It can be accomplished by bending the rear spar so as to accommodate the tire. This might reduce space for fuel and add some structural weight. In addition, the long outrigger gear aft of the rear spar complicates the design of the aileron and flap control systems. Although a longer gear is normally heavier, in this case the extra length might be used efficiently in increasing the stroke of the oleo and reducing the loads in an outrigger first landing.

It can be seen that the choice of either of these arrangements, or of any other, depends on the particular characteristics of the airplane. What might be the optimum for one design need not be for another. For the airplane being considered the retraction into the nacelle has been chosen. (Figures 4:13 and 4:14 show the two possibilities.)

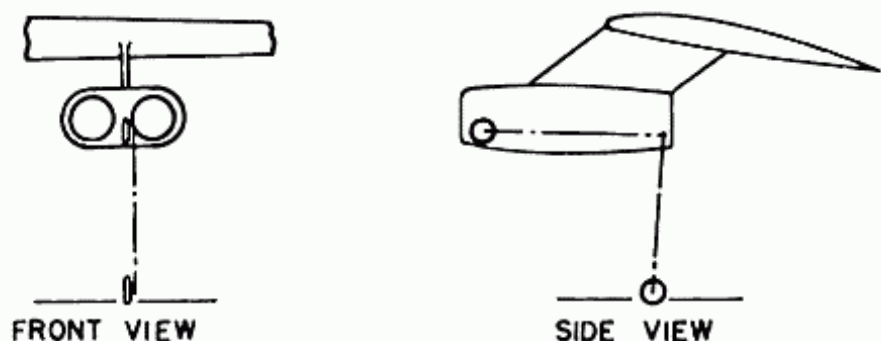


Fig. 4:13. Outrigger gear retracted into nacelle.

4-4 Vertical Location of Wing on Fuselage

General

The next choice to be made is whether the airplane should have a low wing, a midwing, or a high wing. Each type has its advantages and disadvantages. The mid-wing is the best aerodynamically but introduces the problem of keeping the fuselage clear for passengers while carrying the wing loads through. This has been done on some transport planes with varying degrees of efficiency. The low wing airplane has been most popular for transports primarily because the main gear structure, which has usually been retracted into the wing, could be made very short and efficient. The high wing airplane has one great asset for transport airplanes in that it allows the best vision for all the passengers. There is little to choose between the high wing and low wing airplanes aerodynamically.

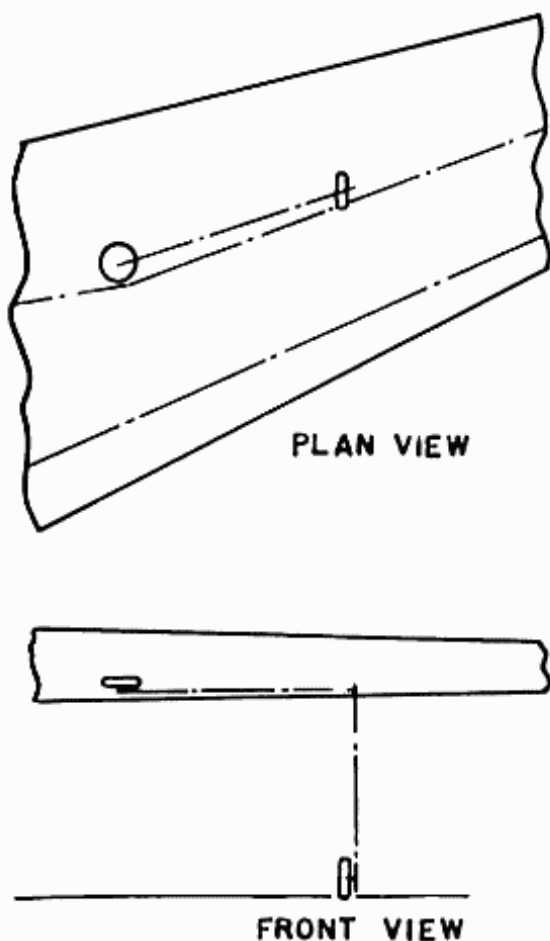


Fig. 4:14. Outrigger gear retracted into wing.

In the high speed jet transport a new factor has been introduced into the choice of type

of wing, high, low, or mid-wing. This is the fact that for a wing of zero dihedral, the tip chord of a wing with positive incidence and sweepback is closer to the ground than the root chord. For efficient design, high speed jet transports require wings with considerable sweepback. For the purposes of passenger comfort, as well as structural and aerodynamic efficiency as explained in "section 4:2 Incidence," transport airplanes require wing incidence; a bicycle type gear in particular, requires a high angle of incidence for take-off. As has been discussed in "section 4:2 Dihedral," a sweptback wing transport usually requires zero or even negative dihedral angle for satisfactory dihedral effect. Because of these factors, the problem of providing ground clearance for the wing tip of any structure supported by the wing, must be considered in the choice of wing location. Since the engine nacelles are usually supported by the wing, it is now necessary to choose the type of nacelle to be used in the jet transport design.

Nacelle Arrangement

In transport design there is the choice of placing all the power into either two engines or four engines. Although the nacelles of the two engine airplane can be made lighter and present less drag than the nacelles of a four engine airplane, they do not present the better alternative. The civil air regulations for one engine out performance and the appeal of greater safety to the passenger has set the pattern of four engine aircraft whenever possible. With the choice of four engines established, the grouping and placement of the engines is required.

If the four engines are placed in two nacelles with two engines in each nacelle, it has been found that they offer less drag than four nacelles with one engine in each.

In addition, the two nacelle design has other advantages over four nacelles. It can be located out on the wing so that the noise cone of the exhaust does not intersect the passenger cabin compartment. Flaps cannot be located in the area of jet blast. With two nacelles at approximately 60% of the wing span, this area is an efficient place to end the flap and begin the aileron. With four nacelles there are four areas in which a flap cannot be located, requiring some loss in efficiency. If the inboard nacelle of a four nacelle design is located so as not to cause an excessive amount of noise in the cabin, the outboard nacelle would probably be far enough outboard to cause an increase in size of vertical tail. With the two nacelle design the operating weight empty is less because of reduction in strut weight, and in wing

weight due to the outboard location of both engines.

The main disadvantage of the two engine nacelle design is the possible reduction in safety. In some instances, the failure of one engine due to a turbine blade failure, or to an engine seizure, or to an engine fire jeopardized the operation of the other in the same nacelle. For this reason primarily, many jet transport designs will use four single engine nacelles. However it is felt that with proper study and design this difficulty can be overcome. Service difficulty is another disadvantage claimed for the two engine nacelle design. Considering all the arguments presented, the two two-engine nacelles have been chosen for this transport.

Much research has been done on the placement of nacelles in reference to the wing. Positions in the wing, in front of, in back of, below and above the wing have been studied. There are advantages and disadvantages to each depending upon the type of airplane designed. Figure 4:15 shows a diagram of a nacelle slung under the wing.



Fig. 4:15. Nacelle supported on wing strut.

This arrangement has the advantages that (1) it is close to the ground and therefore easily serviced and (2) that the exhaust from the jet clears the flap when deflected. In addition, experiment shows that the underslung nacelle has less drag than any nacelle mounted on the wing. The disadvantage of this type of design is that if care is not taken, the heat of the exhaust might cause airport runways to deteriorate more rapidly than is acceptable. Considering all the advantages and disadvantages the underslung nacelle has been selected as the best choice for the jet transport.

Another engine arrangement that has obvious advantages is supporting the engines on horizontal supports from the aft end of the fuselage. The advantages are primarily that (1) in cruise the noise in the cabin is at a very low level, (2) the one engine out effects on yawing moment is negligible and (3) there is no wing-nacelle interference. For these reasons this arrangement has been adopted by the designers of the French Caravelle, and some American companies. Fig. 4:20 c shows a 3 view of the Caravelle.

The disadvantages that are inherent are that (1) the c.g. is moved aft causing a shorter tail arm and therefore larger tail surfaces, (2) the wing weight is greater due to the loss of the relieving engine dead weights, (3) the added danger of fuel lines running from the wing to the engines through a larger portion of the fuselage in the cabin compartment, and (4) the heavier fuselage weights due to a combination of horizontal down load and added engine dead weight and (5) the probable heavier nacelle strut, since it is in bending instead of in tension. Of a questionable nature is the comparison of the drags of the 2 installations and the effects on the tail surfaces.

Comparison of High Wing and Low Wing Designs

If the high wing and low wing designs are compared as shown in Figure 4:16, the high wing is unquestionably more efficient. The landing gear is shorter, therefore is lighter and requires less space for retraction, and the fuselage is closer to the ground for easier passenger and cargo loading and unloading.

However the disadvantage of having a long landing gear as shown for the low wing, can be eliminated by (1) using positive

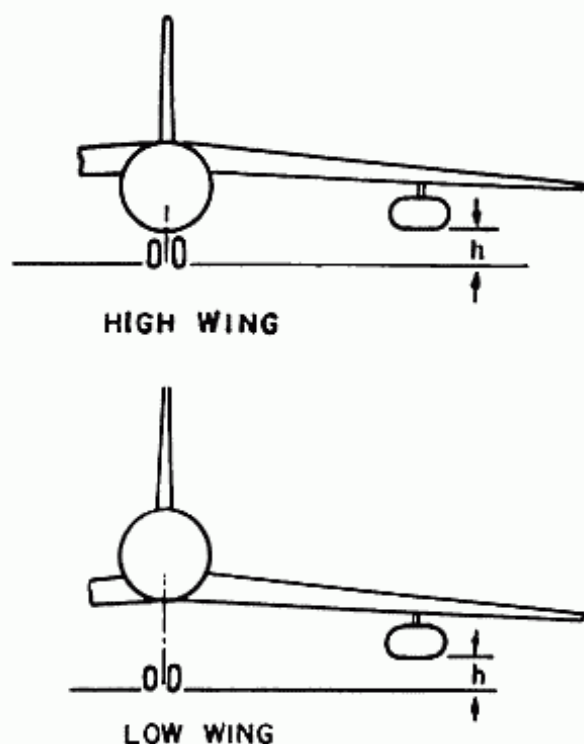


Fig. 4:16. High Wing and Low Wing Airplanes with Underslung Nacelles, and zero Dihedral with Incidence and Sweepback.

dihedral and (2) use a fuselage with a bottom lobe (as shown in Figure 4:17) with the wing directly below the floor. For large airplanes, with large wings, this fuselage would most likely be

required so that the wing can go through the fuselage under the floor. If a high wing were used with a very large wing, there would probably not be enough headroom in the portion of the fuselage underneath the wing. The 60 passenger airplane in Figure 4:20, shows how the space underneath the wing can be used for lavatories. However if the airplane had a larger range and required still larger wings, a bottom lobe would be required as shown in Figure 4:17.

For efficient over-all design, it is necessary to consider the choice of the type of nacelle support, the landing gear design and the location of the wing as one problem. The high wing airplane with underslung nacelles and bicycle type gear has been chosen for a small jet transport. Where the wing becomes so large that it must be stored below the floor, then a low wing must be used.

It should be noted that if a tricycle gear is decided upon, a low wing design is required; otherwise the disadvantages of the long main gears supported by the high wing would be prohibitive.

Typical of the high wing design for small transports is the turbo-prop Fairchild F-27, shown in fig. 4:20 a. Note that the high wing allows a fuselage close to the ground with ample prop clearance.

Typical of the low wing design for large transports is the Boeing 707, shown in fig. 4:20 b. This same design is used on the DC-8, Convair 600 and the English Comet IV.

4-5 Fuselage

The inboard profile of the fuselage should be drawn with all significant items shown. As a starting point the wing should be placed so that the quarter M.A.C. is at 40% of the length of the fuselage. This will be the approximate location in a jet transport to obtain the desired center of gravity location.

The actual layout of the inboard profile of the fuselage involves a lengthy and complex study of many factors. It is mainly a determination of the best compromise between two conflicting aims, airplane efficiency and passenger comfort. The bigger and more luxurious the seats and the more space allocated to each passenger, the greater is his comfort. However, this added comfort results in decreased aerodynamic and structural efficiency, which must eventually be reflected in the passenger fares.

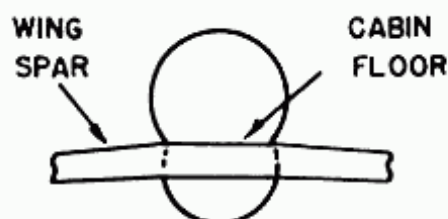


Fig. 4:17. Fuselage cross-section showing bottom lobe and wing spar.

The most efficient design will be one that utilizes as great a percentage of the space as possible; this involves the cross sectional area as well as the length of the fuselage. Since jet transports fly at high altitudes, they are all pressurized. Therefore for structural efficiency they must have either a circular cross-section or a combination of two circles, similar to a figure eight. The combination of circles is sometimes more efficient for a comparatively large airplane carrying a large pay load of passengers and cargo. The bottom lobe is efficient for carrying cargo, perhaps a lounge, the galley, large tires that might be required in a bicycle type landing gear, and possibly a low wing. For designs of medium range carrying 40 to 60 passengers the circular section has been found to be more efficient.

The number of passengers in a row, for airplanes with 30 to approximately 60 passengers, has been practically standardized at four. If less than four abreast seating is used, the fuselage tends to become too long and thin for structural efficiency. It is also difficult to use the cross sectional area efficiently. If more than four seats are used in one row, either another passageway must be provided or there must be more than two passengers sitting side by side. The added passageway is wasted space, and three abreast is undesirable when getting in and out of seats and when meals are being served. However, airplanes with five seats abreast, with one passageway separating the two groups are being used extensively on high density loadings as used in coach service; and occasionally on regular service as shown in Figure 4:20.

The above discussions of number of seats abreast, and fuselage section, is valid for airplanes with capacity up to 60 passengers standard first class. However on the larger capacity airplanes as the DC-8's and 707's, five abreast has become standard for first class travel and six abreast for the coach flights. These airplanes have also used the double lobe fuselage section to add space under the cabin floor for the fuselage structure to go through, and to house the retracted main wheels.

In determining the number of passengers in a row, besides considering the cross sectional area and the length of fuselage, the center of gravity movement must be taken into account. The more seats there are in a row, the closer to the center of gravity the passengers can be placed. This will keep the center of gravity movement small due to passengers being absent from the extreme seats. However, due to the fact that the longer fuselage makes for more efficient tail surfaces, concentrating the

passengers in a short space longitudinally either results in an inefficient tail arm or empty space in the rear of the fuselage.

Since the greatest width required by a person is at his elbows when he is sitting, the seats should be placed so that the passengers' elbows are at the maximum width of the fuselage.

From other considerations it has been decided that the airplane is to have a high wing. If the wing is placed high on the fuselage the fillets required between the wing and the fuselage become larger and more inefficient. Although some airplanes have been designed with the top of the wing higher than the top of the fuselage, it is felt that it should be done only as a last resort as it results in indefinite aerodynamic and structural inefficiencies. As a compromise between these disadvantages and the loss of space in the fuselage, the wing has been placed so that the top of the wing coincides with the top of the fuselage. Since the section of the wing between the spars is carried through the fuselage, this area in the fuselage becomes critical for headroom. In the drawing, Figure 4:18, the necessary headroom of approximately 76 inches from floor to ceiling has been obtained by dropping the floor in the aisle about 7" below the level of the seats.

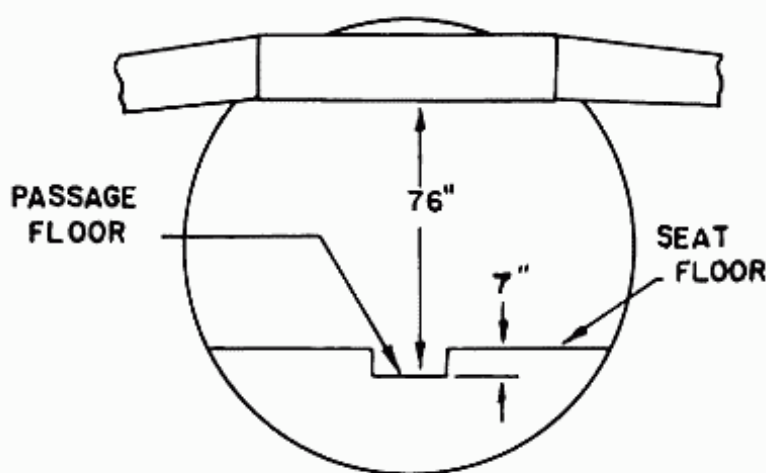


Fig. 4:18. Fuselage cross-section.

This arrangement has the slight disadvantage of requiring the passengers to step up and down between the seats and the aisle. However this is somewhat offset by the advantage that the hostess can serve meals with a little more comfort. This design is not as inefficient structurally as it might appear since the 7" risers can be used to carry the floor loads to the frames quite efficiently.

Although the location and spacing of the passenger seats are probably the most important problems in fuselage layout, the

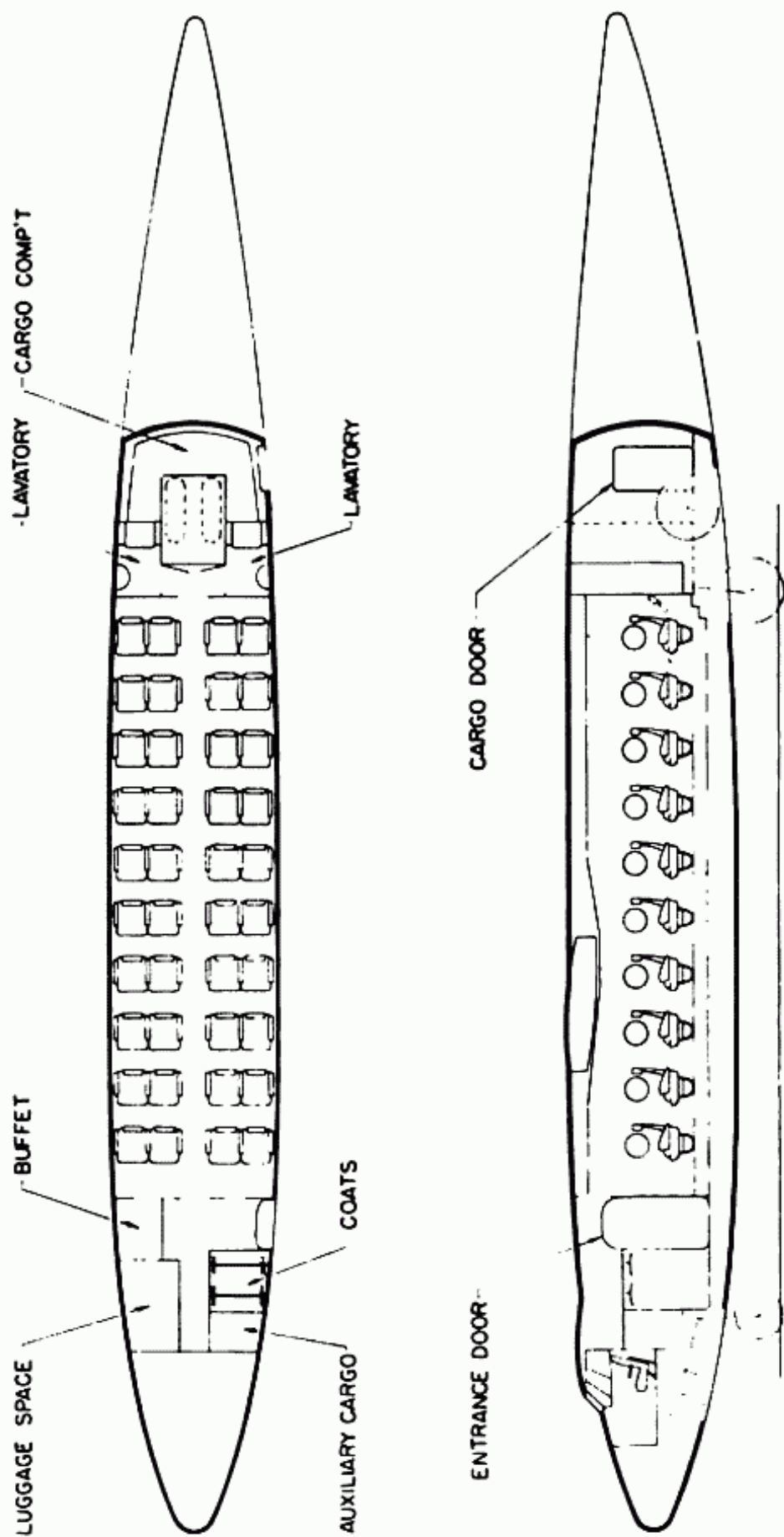


Fig. 4:19. Inboard profile - 40 pass. airplane.

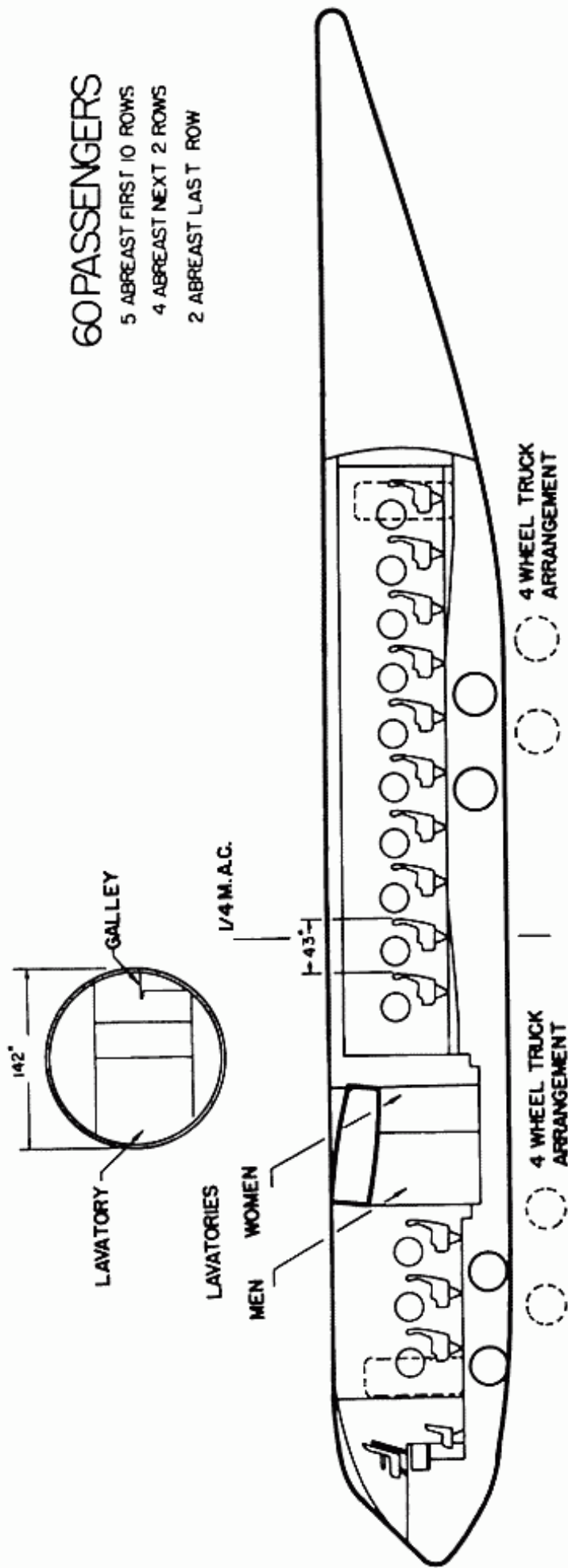
placing of the other items such as lavatories, buffet, baggage and cargo, as well as crew compartment do affect the over-all efficiency of the airplane. The location of crew compartment is, of course, in the front of the airplane. However the other items may be located as the designer sees fit, taking into account the airplane efficiency, center of gravity location and convenience to both passenger and crew. Another important item that is stowed in the fuselage, the landing gear, has been studied in Section 4:4.

As has been previously stated, the engineer, in designing the fuselage, must repeatedly make compromises between reducing the drag of the airplane and increasing the comfort of the passengers. Every extra passenger comfort must be paid for in added fuselage drag and weight, and ultimately in added cost to the passenger. This compromise is not an exact science. It is based upon airline studies, engineering cost studies and the opinion of experienced specialists. Figures 4:19 and 4:20 present two fuselage designs, one for 40 passengers, the other for 60 passengers. They are answers to a problem which has infinitely many solutions, each one depending upon the experience and preference of the individual designer. It is suggested that the student designing a jet transport in a "Design Course" use one of these fuselages. The purpose of this is to save him many hours of juggling seats, lavatories and buffets, so that he can concentrate on other more important subjects in Airplane Design. Fig. 4:20b shows the inboard profile of the Boeing 707-320 with the wheels and wing carry-through structure in the bottom lobe.

This design is satisfactory as shown if the thickness of the wing is not too great to allow sufficient headroom at the critical section. If the thickness is too great, then some modifications must be made.

It should be noted that if the seats are arranged facing rearward, the safety of the passengers in a crash is increased. In the case of a high deceleration due to an accident, the backs of the passengers would be pushed up against soft, large seat cushions instead of comparatively rigid, small safety belts. The resultant force on them would be smaller and better distributed, therefore resulting in less injury.

In cruising conditions there would be no reasonable objection to rearward seating. However since most people are not accustomed to traveling facing aft, the different effect of the accelerations in starting and stopping might raise some slight objection to this arrangement. Nevertheless, because of its obvious advantages one important airline is considering making rearward seating a requirement on all new designs.



60 PASSENGERS
 5 ABREAST FIRST 10 ROWS
 4 ABREAST NEXT 2 ROWS
 2 ABREAST LAST ROW

Fig. 4:20. Inboard profile - 60 pass. airplane.

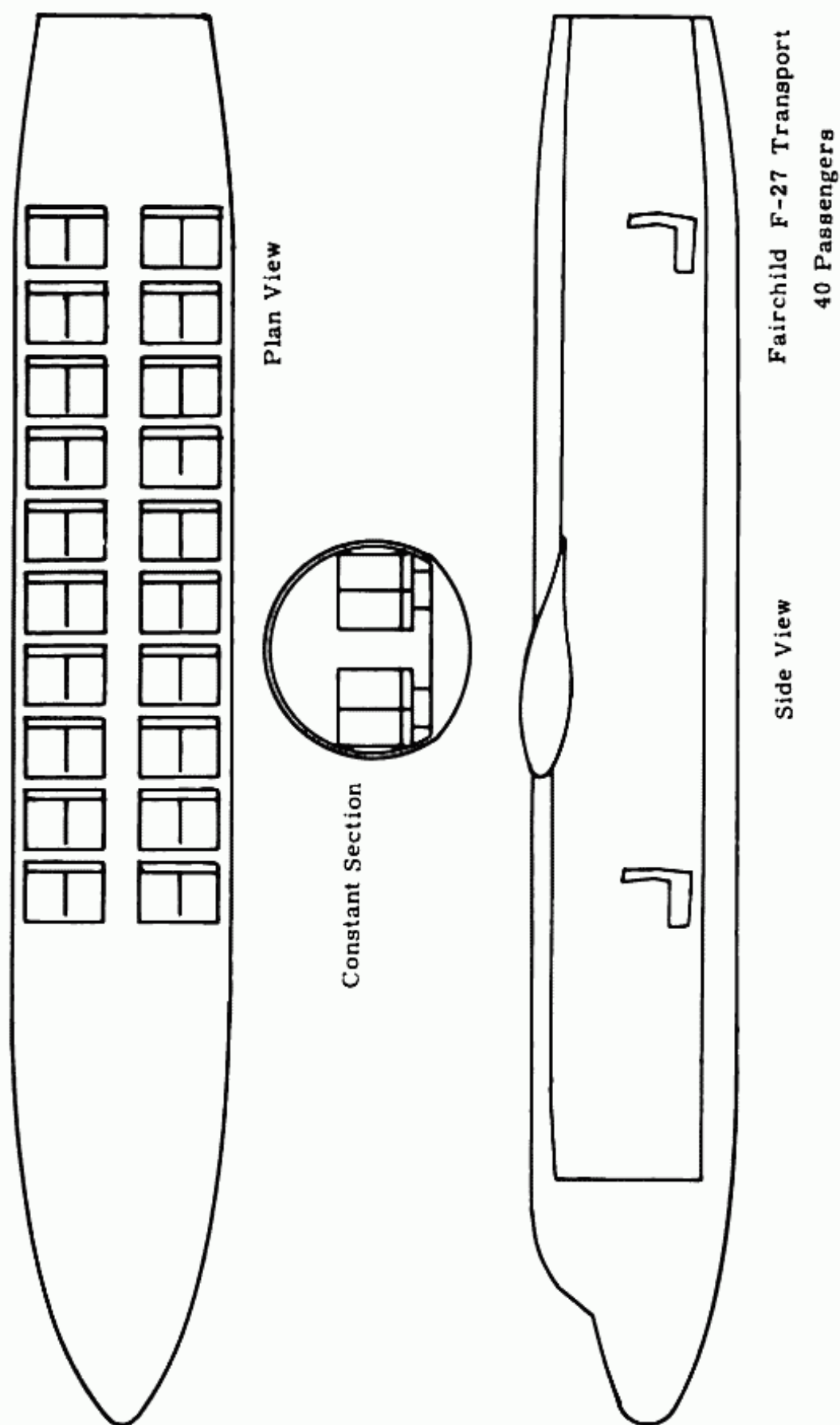


Fig. 4:20a. Fairchild F-27 Transport.

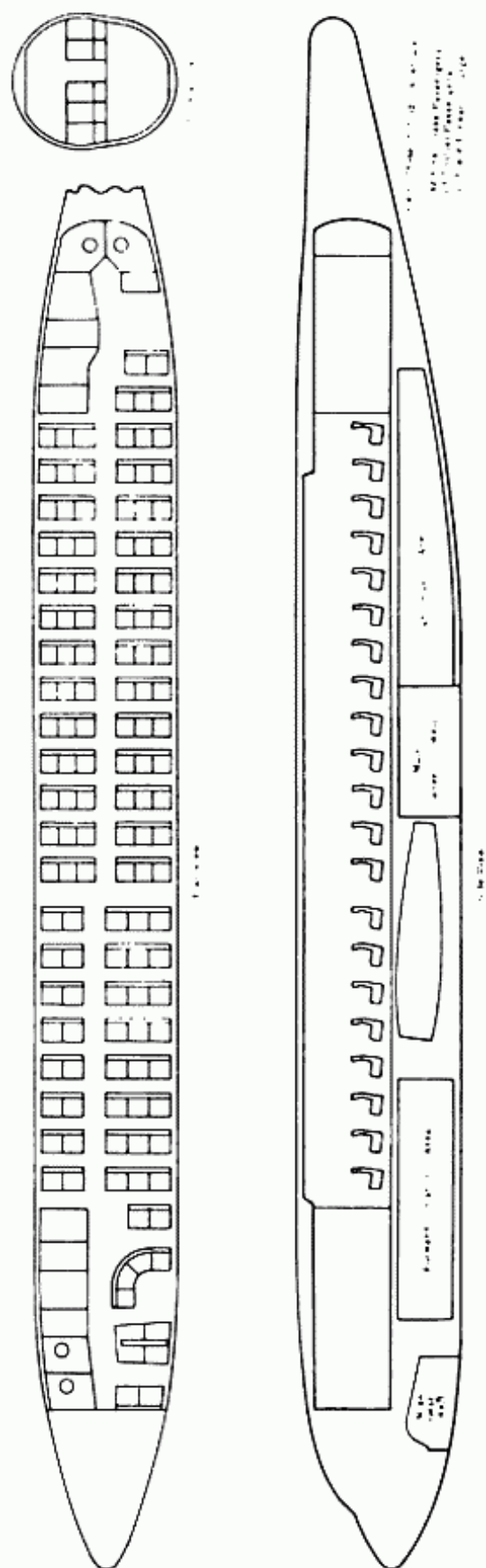


Fig. 4:20 b. Boeing 707-320.

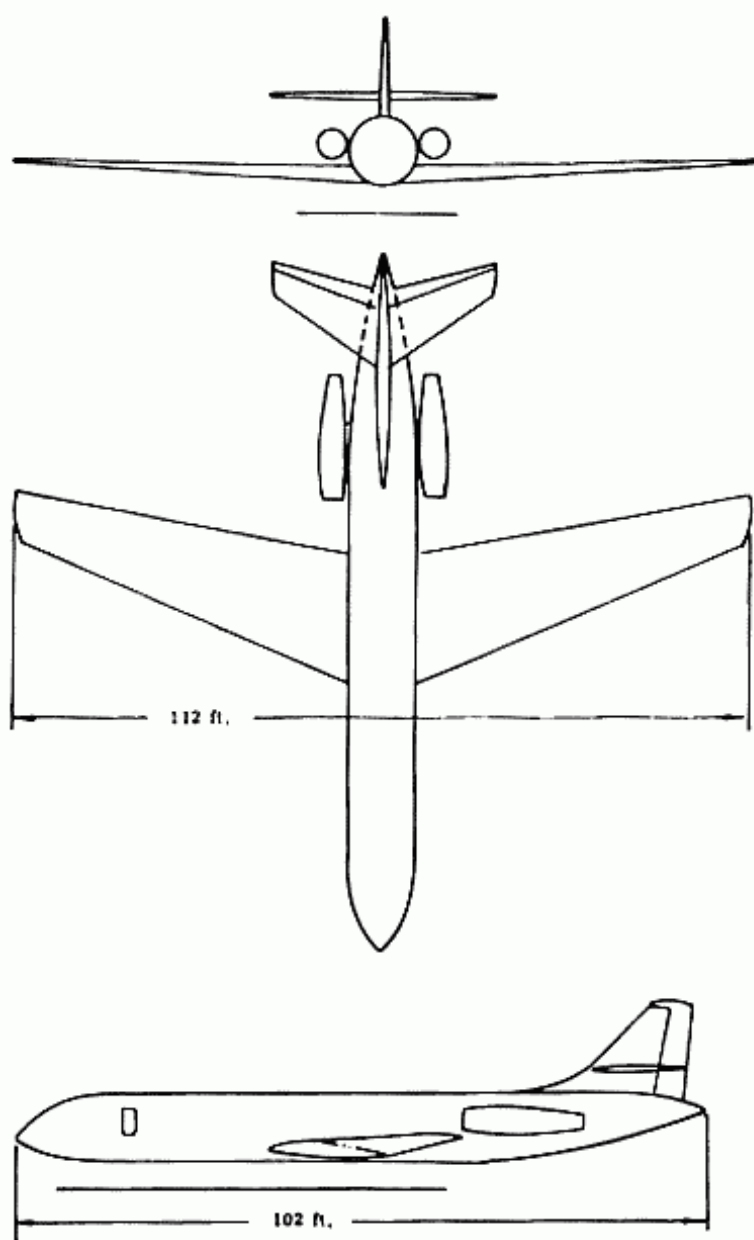


Fig. 4:20 c. Three views of the Caravelle.

4-6 Nacelles

The total drag of the airplane has been calculated on the premise that the thrust would be produced by four engines housed in 2 nacelles slung underneath the wing. The total drag should change very little if these 2 nacelles are supported from the aft end of the fuselage, or if there are 4 nacelles supported from the wing. If the nacelles are supported from the wing, the spanwise and chordwise positions must now be decided upon.

The fore and aft location is set by aerodynamic, structural and center of gravity considerations. For aerodynamic efficiency, that is low drag, the nacelle should be slung forward of and below the wing. Placing the nacelle forward is also beneficial to the flutter characteristics of the wing but adds weight to the strut and increases the moment on the wing rib supporting the nacelle. If the nacelle is located approximately one diameter below the wing, the nacelle plus the strut offer less drag than a higher position. However the strut becomes heavier and the problem of ground clearance may be introduced. As a compromise the nacelles have been placed longitudinally so that the aft end of the nacelle is in the same location as the leading edge of the wing chord at that point, and the vertical clearance is between one-half and three-quarters of the nacelle diameter. With this design good aerodynamic and flutter characteristics are maintained. Since the greatest problems are presented by the center of gravity being too far aft, this forward location of the nacelles is also advantageous in obtaining the desired center of gravity location.

The spanwise location is affected by four distinct considerations; wing weight, noise level in cabin, one engine out effect on tail surfaces, and the center of gravity location. A very important factor in passenger comfort is the noise level in the fuselage. On fast jet powered commercial aircraft it is possible to place the engines so that there is little noise in the cabin at cruising speeds, due to the engine. Since the greatest noise from a jet is from the exhaust, the noise cone from the exhaust should be made to miss the cabin compartment occupied by the passengers. Figure 4:21 presents a plan view of the fuselage showing the noise cone.

The location of the engines affects the wing weight in two ways, the dead weight reduces the shears and bending moments inboard but adds local concentrated loads. If the engines are located far outboard where the wing could be comparatively weak due to low airload bending moments and shear loads, weight must be added to support the high concentrated loads. However,

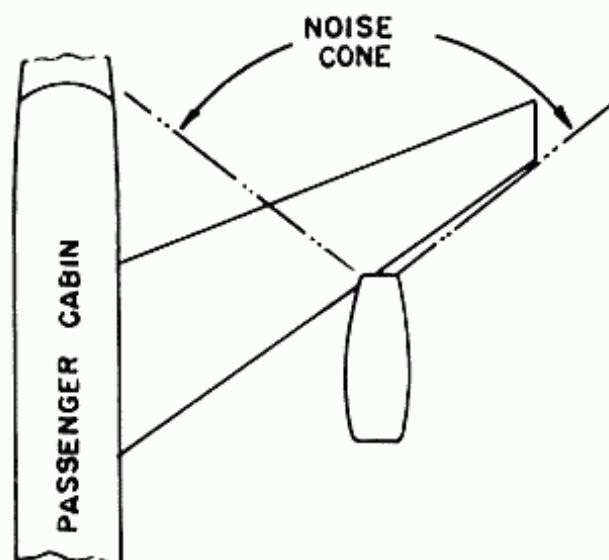


Fig. 4:21. Jet noise cone - passenger compartment relationship.

the reduction in weight due to the lower bending moments and shears inboard result in an overall weight saving for engines placed outboard on the wing.

In the case of an engine becoming inoperative in flight, the vertical tail must be powerful enough aerodynamically to produce a load that will balance the yawing moment due to the unbalanced thrust so that the airplane can fly without sideslip. Since the unbalanced moment is equal to the thrust times the distance of the engine to the center line of the fuselage, a greater moment is produced by engines that are further outboard. Therefore the requirement on the vertical tail is more critical for this condition. However since the thrust required has been divided into four small engines and the vertical tail must also meet other requirements of stability and control, this one engine out condition is usually not critical for the vertical tail, if the nacelle is approximately at 60% of the span.

Since the airplane has considerable sweepback, spanwise location of the nacelle affects the center of gravity location of the airplane. Later it will be shown that this spanwise location is one of the variables in changing the center of gravity location of the airplane.

Fig. 4:22 shows the approximate size of the nacelles required to house two British engines, the Bristol Orpheus with 4,850 lbs. S.L. Stat. T.O. thrust and Bristol Olympus B01-6 with 13,500 lbs. for civil use.

The same type of nacelles as shown in figure 4:22 can be

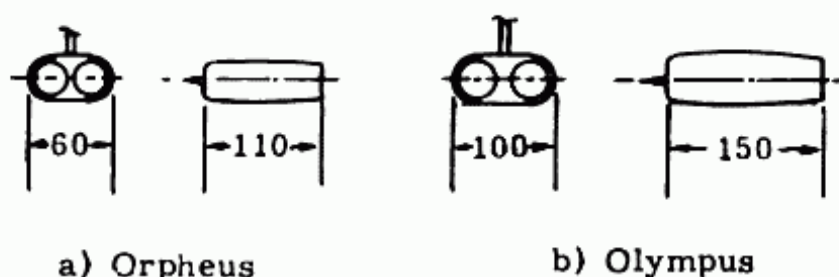


Fig. 4:22. Nacelle sizes.

used for aft-fuselage mounted nacelles. However the internal structure would be vitally different to be supported on the side, instead of on top. These require left and right hand nacelles, while the wing mounted ones do not.

4-7 Tail Surfaces

The purpose of the tail surfaces is to control the airplane in flight and to provide satisfactory stability characteristics. This control is accomplished by producing pitching and yawing moments about the center of gravity of the airplane. The magnitude of the moments produced is a function of the size of the surface, its efficiency in producing a coefficient of lift in the desired direction and the length from the tail surface to the center of gravity of the airplane. The moments it must balance are those produced about the center of gravity of the airplane by the other components of the airplane, mainly the wing in longitudinal control, and the fuselage in directional control. The calculation of the tail surface areas required is a complicated and complex one. They are not reliable and must be checked by wind tunnel tests, which also have not proven completely reliable because of scale effects. In practice they are often chosen by experience with similar airplanes. For preliminary purposes the following formulas may be used. In the discussion of stability and control, the basis of these formulas will be presented.

$$S_{H.T.} = C_{H.T.} \frac{(S_w) (M.A.C.)_w}{l_{H.T.}} \quad (4:7)$$

$$S_{V.T.} = C_{V.T.} \frac{(S_w) (b)}{l_{V.T.}} \quad (4:8)$$

where $S_{H.T.}$ = the horizontal tail area

$S_{V.T.}$ = the vertical tail area

S_w	= wing area
M.A.C. _w	= mean aerodynamic chord of wing
b	= wing span
$l_{H.T.}$	= distance from 1/4 M.A.C. of the horizontal tail to the 1/4 M.A.C. _w
$l_{V.T.}$	= distance from 1/4 M.A.C. of the vertical tail to the 1/4 M.A.C. _w
$C_{H.T.}$	= horizontal tail volume coefficient
$C_{V.T.}$	= vertical tail volume coefficient

The tail volume coefficients are the factors that must be determined from experience with other airplanes of the same type.

A list of the horizontal and vertical tail volume coefficients for various aircraft, is shown below:

		$C_{H.T.}$	$C_{V.T.}$
Constellation	L1039C	1.115	.089
Convair	240	1.025	.0593
Douglas	DC 4	.810	.051
	DC 6	.972	.056
Martin	404	1.195	.053
Boeing	Stratocruiser	.887	.0733
Boeing	B-47	.672	.0637
DeHavilland Comet	DH106, Series 1	.486	.032
A. V. Roe	Jet Liner	.673	.0598
Boeing	707-120	.642	.058
Boeing	707-320	.614	.045
Douglas	DC-8	.645	.046
Convair	600	.531	.067
Sud	Caravelle	.520	.041

It should be noted that the C_{HT} for all the jets is considerably lower than the reciprocating engine airplanes, while C_{VT} are all in the same range, except the Constellation with 3 vert. tail surfaces. The lower C_{HT} might be due to higher landing speeds on the jets making the tail surfaces more effective at minimum speeds. The variation in the tail volume coefficient for different airplanes may be due to many reasons, an obvious one being A.R. The higher the A.R. the more effective the surface is due to a higher $dC_L/d\alpha$, thus permitting a lower area. For the commercial high subsonic airplanes values of .600 for C_{HT} and .050 for C_{VT} seem reasonable estimates.

The tail surface areas must be calculated by estimating the tail arms, $l_{H.T.}$ and $l_{V.T.}$, from the drawing of the wing-fuselage combination. With these areas the surfaces should be laid out, the tail arms checked and the areas revised if required.

It is still necessary to determine the sweepback, thickness ratio, taper ratio and aspect ratio of the tail surfaces. The considerations are similar to the wing. Since the tail surfaces control the airplane it is imperative that they have a higher critical lift Mach number than the wing. To assure this, the tail must have either greater sweepback or a smaller thickness ratio than the wing. It is felt that with wings of high sweepback it is desirable to reduce the thickness ratio of the tail instead of increasing the sweepback. The exact amount required is difficult to determine. A reduction of a thickness ratio of .01 has been arbitrarily assumed; that is, if the thickness ratio of the wing is .10 the thickness ratio of the tail surfaces should be .09.

The choice of aspect ratio of the tail involves the same considerations as that of the wing; the higher the aspect ratio, the more effective the tail aerodynamically, but the less efficient structurally. This characteristic is also usually picked from experience, and for this type of airplane a horizontal tail surface aspect ratio of 4.0 and a vertical tail aspect ratio of 2.0 have proved to give the best results. As in the wing the taper ratio is 0.33.

The characteristics of airfoil section, dihedral and incidence are dependent on the specific requirements of the airplane. The airfoil section used in horizontal tail surfaces is often symmetrical since it must produce both up and down loads. For this same reason zero incidence is often used, although the down wash from the wing might require some tail incidence. In designs where it is necessary for the tail to produce loads in one

direction considerably higher than in the other, it is often more efficient to use either a cambered airfoil, or some incidence or both. Dihedral is seldom used in tail surfaces, although it may be used to reduce the downwash effect on the tips, or to miss the jet blast of the engines. The vertical tail has a symmetrical airfoil, and zero incidence as it must be able to produce equal forces in both directions.

4-8 Center of Gravity

The center of gravity of the airplane should be determined in both the vertical and longitudinal directions. Although the location in the vertical direction is significant in some calculations, the variation in position is small and usually of negligible importance. Therefore all the emphasis is placed on the center of gravity in the longitudinal direction since it is the most important factor in stability and control. It is found by locating all the items in the airplane in relation to some reference point, usually the nose of the fuselage, calculating the moment about this point, and then dividing by the total weight of the airplane. For this purpose it is necessary to break the airplane weight into factors that can be easily located or estimated on the airplane layout.

In Equation 2:37, the airplane weight is divided into five categories; structural, fuel, power plant, fixed equipment and payload. These weights must now be assigned to the component parts. The following estimate is satisfactory for a jet transport preliminary design. See Figures 8:8, 9 and 13 for comparison with other transports and military planes. A more accurate result could only be obtained from a rigorous layout of all component parts and a complete structural analysis.

Structural Weight

Component	$\frac{\text{Weight}}{\text{Weight}_{str}}$	Location of the center of gravity
Wing	.400	.22 M.A.C. for 35° sweepback .33 Chord at 40% b/2 for 0 sweepback
Fuselage	.306	.40 length of fuselage
Tail surfaces	.078	.25 M.A.C.
Nacelle	.056	.40 length of nacelle
Landing	.160	assume at center of gravity of airplane

4:42 SUPERSONIC AND SUBSONIC AIRPLANE DESIGN

The preceding breakdown gives the average values of the Boeing 707's, the Douglas DC-8's and the Convair 880, with all the values of the individual airplanes being very close to the average.

Payload

The payload, equal to 240 times the number of passengers is broken down as to weight and center of gravity location as shown:

<u>Item</u>	<u>Weight</u>	<u>Center of gravity location</u>
passengers	160 lbs. each	at seat
passenger baggage	40 lbs/passenger	in baggage compartment
cargo	40 lbs/passenger	in cargo compartment

Fixed Equipment

The fixed weight equals $160 N_p + 230 N_c + .045 W_{TO}$. Thirty pounds attributed to each passenger is due to the seats. The rest of the furnishings equal to 140 lbs/passenger is composed of lavatories, baggage racks, buffet equipment, food, water and air conditioning. These items may be estimated separately. However for a preliminary estimate only a small amount of error is introduced by assuming that they act at the center of gravity of the passengers.

The weight of the crew, 230 times the number of crew, is composed of the crew, their seats and baggage. A crew of four weighs 920 pounds. The breakdown is shown following. For an additional flight crew member add 260 pounds, and for an additional hostess, 170 pounds.

<u>Item</u>	<u>Weight</u>	<u>Center of gravity location</u>
Flight crew (3)	510 total	at seats
Hostess (1)	120 total	in buffet compartment
Seats (3)	180 total	at flight crew seats
Baggage	<u>110 total</u>	in crew compartment
	920	

The weight, .045 take-off weight, consists of many miscellaneous items, instruments, surface controls, and hydraulic, electrical, communicating and anti-icing systems. For the sake of simplicity they are all assumed acting at the center of gravity of the airplane. Where a somewhat more accurate estimate is

required the following center of gravity locations have been found to be typical.

Nacelles	15" Aft Engine C.G.
Power Plant Controls	40% Dist. from Pilot to Eng. C.G.
Instruments	40% Dist. from Pilot to Eng. C.G.
Surface Controls	100% M.A.C.
Hydraulic System	-10% M.A.C.
Electrical System	-10% M.A.C.
Communicating	Aft End Pilot's Compartment
Air Conditioning	40% Dist. from Pilot to Eng. C.G.

Fuel Weight

The fuel and fuel tank weights and locations are known, and the center of gravity can be determined accurately. For this purpose it is required that a rigorous method be used to obtain the location of fuel in the wing; that is, sections of the wing be drawn and the volume calculated.

Power Plant Weight

The power plant weight is equal to $(1.95)(10^{-3})N_eT_e^{1.55}$. If the actual engine used is known, the center of gravity can be obtained from the manufacturer. However if theoretical engines are used and the nacelles drawn, the center of gravity may be estimated at .40 length of the nacelle.

Center of Gravity Movement

The above calculations determine the center of gravity location of the airplane at take-off weight. For the purposes of stability and control calculations, it is required that the most forward and aft positions be known. This estimate consists of removing the items that could be omitted during flight to give the most critical conditions. If the center of gravity of the fuel is aft of the center of gravity of the airplane at take-off weight, it is assumed that the fuel has been used up for the most forward center of gravity calculation, but is still in the airplane for the most aft location. Care should be taken in not assuming extreme possibilities. It is possible, but not probable, that there will be only two passengers sitting in the two rear seats and there is a full load of baggage in a rear baggage compartment. Conditions such as this and others that give extreme center of gravity positions need not be considered as they are unlikely and if necessary could be modified.

It should be noted that the results obtained from the above method give only an approximate but satisfactory estimate of the center of gravity for preliminary purposes. However it is

important to investigate the possibilities of shifting the center of gravity if it is not in a desirable location.

Assume that the center of gravity is further aft on the M.A.C. than desired. If the wing is moved aft, and of course the M.A.C. with it, the center of gravity of the airplane moves in the same direction. The weight moved includes the weight of wing structure, the fuel in wing, the outrigger gears, and the power plant and nacelles, and adds up to approximately 50% of the total weight. If the center of gravity is 15 inches too far aft it would appear moving the wing about 30 inches aft would correct the condition. However by doing this the tail arm is reduced by 30 inches. For the same effectiveness of the tail surfaces, their size would have to be increased. This not only adds weight and drag to the airplane, but because it adds weight at a distance far aft of the center of gravity it again moves the center of gravity aft. Although this method of correcting center of gravity does not appear efficient it is sometimes used as a last resort.

Other possibilities of correcting a center of gravity position that is too far aft are:

1. Move engines forward. For engines mounted on the wing struts, if they are kept at the same spanwise position it requires a longer and heavier strut; if they are moved in-board, and therefore forward because of the sweepback, they would sacrifice the relieving dead weight advantage on the wing and introduce more noise in the cabin.
2. Modify the arrangement of seats, lavatories, baggage and cargo compartments, and buffet in the fuselage. This should be done but usually does not offer much possibility of great improvement.
3. Lengthen nose of fuselage, moving crew, passengers, etc., forward. This can be done but adds drag and weight to the airplane.
4. Moving the tail surfaces forward does not offer much help as they become heavier for the same effectiveness. A study may be made for any particular airplane to obtain the most efficient position of the tail surfaces. This involves a thorough study as the position of the tail effects the weight and drag of both the tail surfaces and fuselage, as well as the center of gravity position of the airplane.

The problem of correcting a center of gravity that is too far forward is not usually serious. Although it might require a large movement of the wing, this shift in the wing position is adding to the efficiency of the airplane by requiring a smaller tail.

This smaller tail will decrease the weight and drag of the airplane. Changes opposite to those suggested for the condition of the center of gravity being too far aft may also be investigated for an airplane with its center of gravity too far forward.

General

In assigning the weights and centers of gravity to each of the component parts, it was necessary to make many approximations for the sake of simplicity. It is not within the scope of this text to attempt an accurate determination of the airplane center of gravity. However, scanty treatment of the method of calculating the center of gravity should not be interpreted as an indication that the center of gravity location is not important. The location of center of gravity, because it is so important in stability and control, has such a considerable effect in limiting the airplane design that most airplane layouts are conventional in appearance.

PROBLEMS

- 1) Have students lay out airplanes designed in Chapter II.
- 2) Determine center of gravity as originally laid out.
- 3) Revise layout, if necessary, so that center of gravity is in satisfactory range.
- 4) Show final three view drawing and inboard profile.

Chapter V
AIRPLANE LAYOUT -
SUPERSONIC, AND AERODYNAMIC HEATING

5-1 Layout - General - Conventional or Canard

For the subsonic airplane it was assumed that a conventional tail surface would be used and it would be desirable to keep the c.g. movement centered around the aerodynamic center, which is at approximately .25 mean aerodynamic chord.

It is necessary at this point to discuss briefly some fundamental points in stability and control; Part II deals with the subject in more detail. A surface forward of the c.g. has a destabilizing effect since an increase in α results in a load and moment that further increase the α . A surface aft of the c.g. has a stabilizing effect since an increase in α results in a load and a moment that decrease the α , tending to return the airplane to its original position. The above statement neglects the effect of downwash. For longitudinal stability and control the wing and horizontal control surface are the predominant factors. Fig. 5:1a shows a conventional tail surface airplane, while 5:1b presents a canard type.

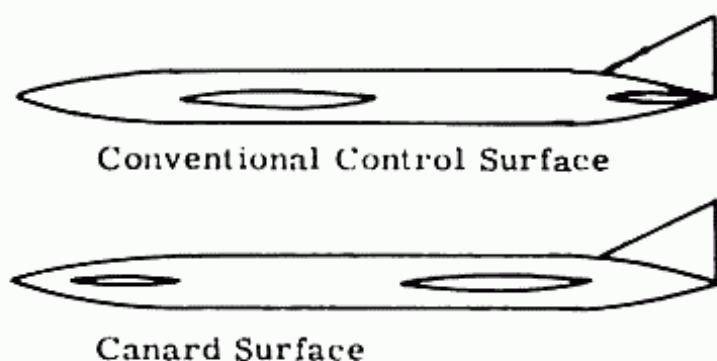


Fig. 5:1. Conventional Surface vs. Canard.

A. The conventional tail

Subsonic flight - a.c. at .25 MAC.

If the c.g. is far forward of .25 MAC, wing and tail are both very stable, a large horizontal tail is required for control in landing. If the c.g. is far aft of .25 MAC, the wing is very unstable and needs a large horizontal surface for stability.

Supersonic flight - a.c. at .50 MAC.

If the c.g. is near the .25 MAC, the wing is very stable. However, at supersonic speed the horizontal tail is very effective in control. The greatest disadvantage is that this condition requires a large download on the tail for equilibrium, i.e. C_M about the c.g. = 0, and introduces large amount of trim drag.

If the c.g. is near the .50 MAC, there is no large trim drag supersonically. But a very large tail would be required for stability subsonically, since the a.c. of the wing is far forward of the c.g. resulting in a very unstable wing.

B. Canard Type Airplane - fixed surfaceSubsonic flight - a.c. at .25 MAC.

The c.g. must always be forward of the wing a.c. since the wing must be stable enough to offset the instability of canard. Control is satisfactory.

Supersonic flight - a.c. at .50 MAC

With the c.g. forward of .25 MAC as required by subsonic stability, the airplane is very stable supersonically, and requires a large upload on the canard for equilibrium, i.e. C_M about the c.g. = 0. However, since an upload on a canard requires less lift on the wing there should be no significant trim drag, and the high degree of stability is no disadvantage as there is no requirement of high maneuverability for a transport airplane.

For canard type airplane - surface not fixed

There are possibilities of using a canard that either floats, or retracts, so that it does not add to the instability of the airplane, and at the same time maintains low trim drags throughout both speed regimes.

Choice of Control Surface

For these reasons, and others to be mentioned shortly, the canard type airplane has been chosen for the supersonic transport. Because of the added structural complexity and unknown characteristics of a floating or retractable canard, a fixed surface will be used for this design. A very important added disadvantage of a conventional tail surface for a supersonic airplane is that with the low aspect ratios that are efficient for supersonic design, the horizontal tail surface can become very ineffective stability-wise, (or might even become unstable) due to downwash from the wing. A canard also is more desirable in landing since the upload on the surface relieves the load on the wing, whereas the download on the conventional tail increases the wing load.

It should be noted that the B-58, the largest supersonic manned

airplane in operation at this time, has no separate horizontal control surface at all. The trailing edge wing flaps are used for pitch control. See fig. 8:21.

The vertical control surface is still at the aft end of the fuselage for directional stability.

5-2 Wing Plan form

The discussion of advantages and disadvantages of taper ratio of section 4:2 are still valid in the subsonic regime.

There would appear to be an added advantage to the zero taper ratio wing in supersonic flight since it would have no tip effects from the Mach wave. Ref. 5:1 presents experimental data to show that wings with $\lambda = 0$ have less wave drag than wings with $\lambda = .33$ or $.67$ from $M = 1.4$ up to 1.8 , the highest value tested. However, a comparison of values of $C_{L\alpha}$ for wings with $\lambda = .5$ and 0 (from ref. 3:2) shows that the wing with $\lambda = .5$ has a very slight edge in a higher $C_{L\alpha}$ for $\beta \cot \Lambda$ greater than 1.5 .

Considering the drag effects (wave and normal force), the large decrease in weight and the increased fuel capacity associated with $\lambda = 0$, the greater structural efficiency of a straight trailing edge, and the greater efficiency of the delta wing in stability and control, the delta wing has been chosen for this supersonic transport. It should be noted that a more rigorous study of all factors involved must be made for each type of aircraft before the correct selection of taper ratio can be made.

Some special devices to improve tip stall characteristics for subsonic flight, and to improve max. C_L and L/D in landing, may have to be incorporated. Although variable sweep, and possibly variable incidence may yet prove to be more efficient than a fixed surface, for this supersonic transport design a fixed surface will be used.

Mean aerodynamic chord and mean aerodynamic center.

See section 4:3 for discussion of these characteristics as applied to an airfoil section.

Location of Spars

These are affected by similar factors as in the subsonic wing, section 4:2. However, the final positions are usually different than in the subsonic due to the much greater sweepbacks, the straight trailing edge, and the different type airfoil sections used. For a delta wing an unswept straight-through aft spar appears to be the most efficient overall design primarily because of its structural efficiency.

Ailerons and Flaps

Flaps and ailerons, when used in the subsonic part of the flight, follow the same principles as outlined in 4:2. Although conventional ailerons on the trailing edge of the outboard wing may be incorporated in the design for the low speed regime they are not satisfactory for high speed flight as they might induce aileron reversal. (See sec. 10:3). For this high speed range either spoilers or leading edge ailerons may be used. The advantages of the leading edge ailerons in supersonic design are (1) the added lift might act far enough forward so that aileron reversal might not be a problem, (2) they are more effective than trailing edge surfaces in supersonic flight and (3) they may be used in landing as a high lift device while the trailing edge ailerons may be used for roll control. It should be noted that for supersonic flight the leading edge aileron must be deflected upwards to give an upload.

Because of the problem of obtaining a high max C_L with a wing that is efficient for supersonic flight, some type of blown flap may prove most efficient for supersonic transports. Ref. 5:2 presents very interesting data on the max. C_L , L/D and C_m characteristics for wings with various sweepbacks at subsonic speeds. For a double wedge .05 t/c airfoil wings with max. t/c at .20 chord and A.R. = 2.0 (delta wing), there is no increase in max. C_L due to deflecting a split flap 22° , but it does increase from 1.34 to 1.62 by using a leading edge flap. However for a similar wing with a rounded leading edge, .05 t/c section, max. C_L increased from 1.32 to 1.42 for a small deflection of a small trailing edge plain flap.

Incidence

The incidence angle problem is much greater for a supersonic airplane than a subsonic one, although the goals and the principles are essentially the same. The complication is due to the aforementioned fact that the characteristics of a wing that makes it efficient for supersonic flight (low A.R., low λ , low thickness ratio and high sweepback) result in both a lower max. C_L and a much higher α for max. C_L , as well as a low L/D in landing.

To be able to use even this lower max. C_L for landing at this very high α , it might be necessary to incorporate other devices as discussed in section 3:3.

Dihedral

The study of dihedral is the same as presented in section 4:4 subsonic, with the added emphasis on the dihedral effect of the usually high sweepback wings for supersonic flight.

Airfoil selection

The airfoils used in subsonic design have rounded leading edges as they result in high L/D 's in cruise and in high values of max. C_L for landing. Since round leading edges cause the shock wave in supersonic flight to be detached from the nose with a resulting decrease in L/D , sharp nosed sections are more desirable for a limited range of supersonic speeds because of L/D considerations. However, at the high supersonic speeds the problem of aerodynamic heating makes the rounded nose more efficient. In addition the rounded nose results in a higher value of max. C_L subsonically, which is an advantage for all manned aircraft that must land, as well as take-off, safely. It should be stated that at t/c 's in the order of 3%, because of the limitations set by manufacturing and servicing, the difference between a sharp leading edge and a rounded leading edge might be one more of degree than of quality. Nevertheless, keeping the distinction between rounded and sharp sections, there are 3 most widely used sharp nosed sections for supersonic flight. They are the double wedge, the biconvex, and the modified double wedge, fig. 5:2.

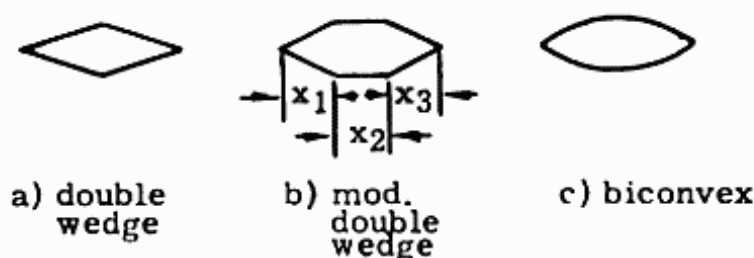


Fig. 5:2. Supersonic airfoil sections.

The biconvex can either have circular or parabolic arcs, the modified double wedge can have varying values of x_1 , x_2 , and x_3 , while the double wedge usually has the max. thickness at $.5c$ but can be varied, and becomes slightly more efficient for higher M 's with max. thickness aft of $.5c$.

For all these sections the value of c_{lmax} tends to be low since separation occurs at low α 's because of the sharp nose.

However the three dimensional and sweepback effects are so great in sharp-nosed thin sections with low aspect ratios and large values of sweepback, that the max. c_l of the two dimensional airfoil alone is not a good criteria for choosing the section. As noted previously leading edge flaps are helpful in increasing max. C_L . It should be noted again that the usable max

C_L for the supersonic airplanes might be considerably lower than the actual, due to the large value of C_{D_i} inherent in these wings with low values of A.R., and to the large α required.

Because of the usual radius and the general shape of the rounded leading edge subsonic airfoils, the values of c/I (where c = distance from neutral axis to outermost fibre of section) for different type airfoils of same thickness ratio varied very little, and the airfoil section was usually chosen predominately for aerodynamic reasons. This however is not true of the sharp nosed sections. Fig. 5:3 shows the values of c_d vs c_l for various thickness ratios for the double wedge, the modified double wedge and the biconvex sections. It should be noted that for all t/c 's the double wedge has the lowest drag and the modified double wedge the highest.

Now consider Fig. 5:4 that presents c_d vs c_l for the same sections as in fig. 5:3 but are compared on a c/I basis. The value of c/I is for a thin walled section with all its structure concentrated at the surface, which is close to reality for a large supersonic airplane. It should be noted that for equal values of c/I , an indication of the structural efficiency of the section, the c_d for the double wedge is by far the highest, with the modified double wedge and biconvex being very close, with a slight edge for the biconvex. However, the modified double wedge has been used more often due to manufacturing considerations.

It should be noted further that for the assumption that all the material is concentrated at the surface, for equal values of c/I the wetted areas and therefore the weights of the sections are within 0.3% of each other.

The comparisons presented are based on the premise that separation does not occur. For the same t/c 's, the biconvex is likely to maintain unseparated flow longest because of its more gradual changes in contour.

In subsonic flight, an airfoil with positive camber results in higher values of L/D and max. c_l than an uncambered one. Fig. 5:5 shows that the uncambered airfoil has the lowest value of c_d and therefore the highest value of L/D . It should be noted that at $\alpha = 0$, the section with positive camber has negative lift, and the section with negative camber has positive lift.

Although all sections discussed have pointed trailing edges, some tests indicate that some shapes with blunt trailing edges do result in higher values of L/D . However, at this time there is not enough coordinated substantiated data to report. See ref. 5:3, 5:4 and 5:5.

Ref. 5:6, "Two Dimensional Airfoils" Sect. 6 of the "Handbook of Supersonic Aerodynamics" published by the Bureau of Ordnance of the Navy Department is a good reference.

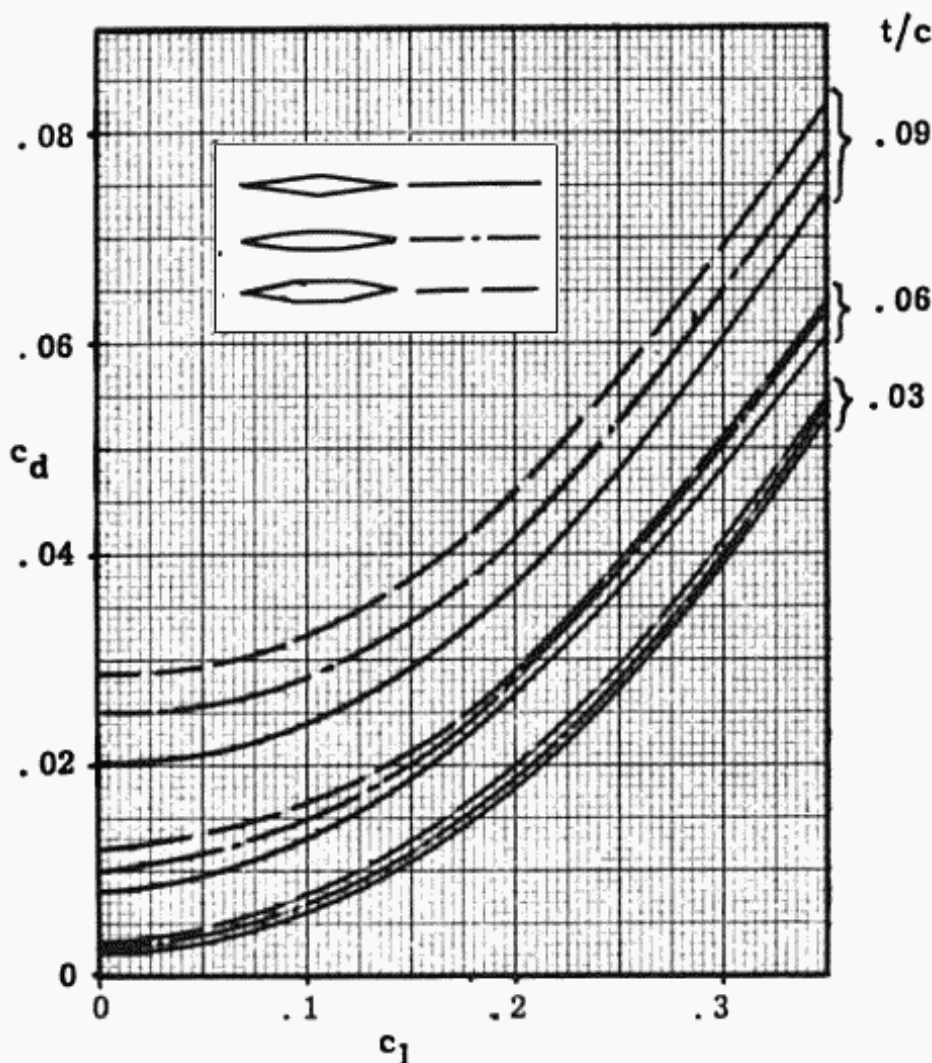
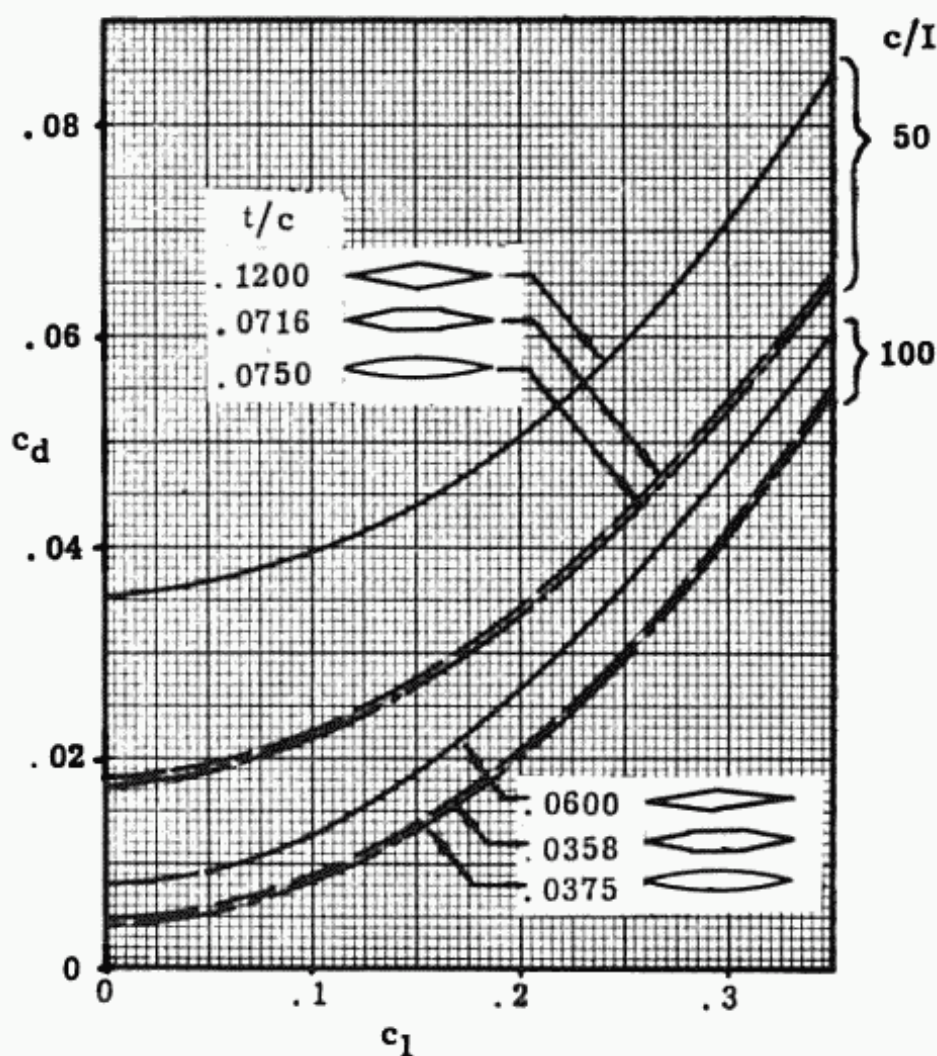


Fig. 5:3. c_d vs c_l ; constant t/c .

5-3 Landing Gear

The landing gear considerations are primarily the same for the supersonic airplane as the subsonic, since the gear is only used in landing and take-off, which is at subsonic speed.

However the problem is aggravated in supersonic design due to the facts that (1) wave drag is a function of frontal area and therefore it is more important to completely submerge the retracted landing gear in as small an area as possible (2) since the wings have a much lower t/c they might offer less space for retraction even though the chords are larger due to the lower aspect ratios and taper ratios, and (3) the low aspect ratios result

Fig. 5:4. c_d vs c_l ; constant c/l .

in high angles of attack for max. C_L and could affect the landing gear length.

5-4 Vertical Location of Wing on Fuselage

It is likely that a midwing airplane would show a greater aerodynamic advantage over the low or high wing designs in supersonic flight than in subsonic, particularly in the transonic range. For this reason and the fact that the supersonic transports will probably carry about 150 passengers, a double lobe fuselage with the wing going through just below the floor would probably be a very good compromise between structural and aerodynamic efficiency. Effects of the wing wake on the effectiveness of the horizontal control surface must also be considered in the final selection of the vertical position of the wing.

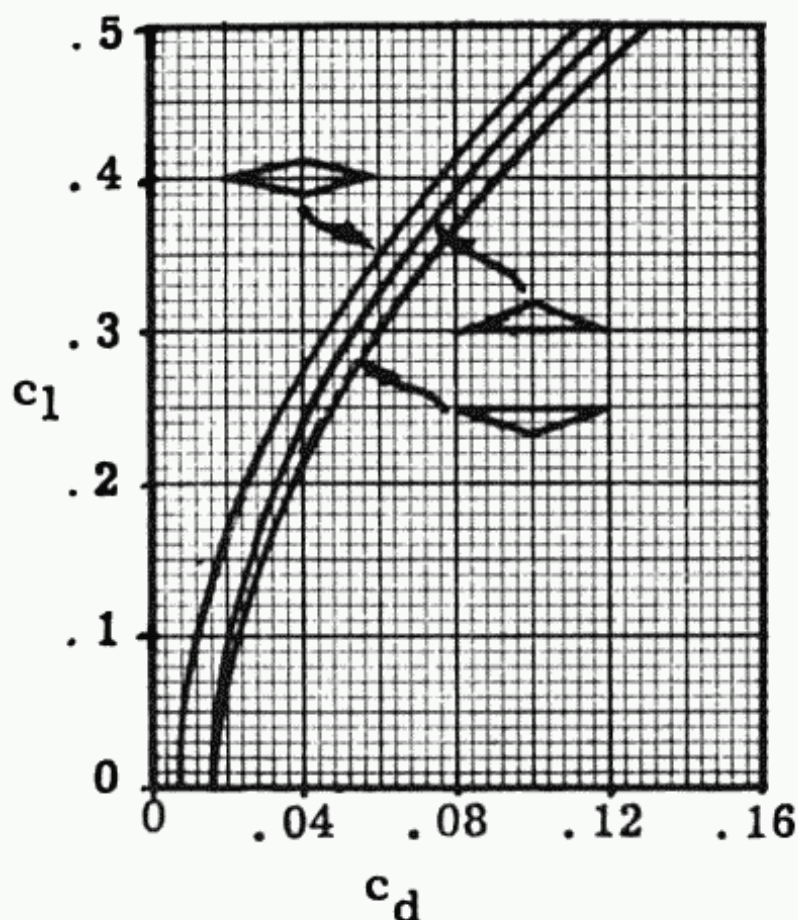


Fig. 5:5. Effect of camber on c_d .

5-5 Fuselage

The main problem in fuselage design, the compromise between comfort for the passenger and airplane efficiency, persists. The trend might be toward increasing the airplane efficiency, that is L/D , at the expense of the passenger comfort for two reasons. One is that at supersonic speeds the passengers will spend much less time in the airplane; at $M = 3.0$, N.Y. to Los Angeles will require a scheduled flight time of about 1-1/2 hours. Secondly, the L/D term is smaller in supersonic flight and therefore the decrease in D is likely to result in a larger percent increase in airplane efficiency.

To increase the airplane L/D it might be desirable to have a canopy that retracts into the fuselage, resulting in a smooth body of revolution, during supersonic cruise. For take-off and landing it can be extended for increased pilot visibility. Because of the higher altitude flight, and the resulting increase in pressure differential, the windows will probably have to be made smaller or eliminated completely, to save weight and for added safety. Due to the much shorter flight times, this feature should not inconvenience the passenger to too great an extent.

5-6 Nacelles and Number of Engines

The supersonic transport will have at least four engines. Because of the large amount of thrust required for these long range airplanes with a large pay load, it is possible that there will not be engines large enough to produce $1/4$ of the total thrust required, thus necessitating the use of more than 4 engines.

Even if sufficiently large engines are available it might be more efficient to use more than four engines as the W/T of the large engines might be too high and the large engines could be too difficult to store.

The design with engines in the aft end of the fuselage must be given serious consideration because of the possible increase in L/D and the reduced noise in the cabin. The increase in L/D over the separate under-wing, or fuselage-supported nacelles is due to the decrease in the skin friction drag, the elimination of the wave drag of the aft end of the fuselage, and the reduction in wave drag of the nacelles. Canard design makes this type of design even more attractive. The greatest problems involved are those involved with designing efficient intakes, good serviceability (particularly with a large number of engines), short tail arm from wing to vertical tail (partially offset by the large arm to the canard), and fuel lines in the fuselage, and added base drag.

For the design with engines in the wing the type of nacelles will of course depend on the number and size of engines. For high L/D's, engines submerged in the wing would probably be best. However, large engines and thin wings do not lend themselves to this type of design, even neglecting serviceability. Because of serviceability, and the greater importance of finesse ratio in supersonic flight, it is possible that a separate nacelle for each engine will be most efficient for the supersonic transport.

The 15,000 lb. S.L., static, standard day max a.b. thrust engine specified in fig. 3:8 has a length of approximately 100 inches and a max. diameter of approximately 60 inches. Fig. 5:6 presents curves showing how engine weight, length and diameter vary for similar engines with different thrusts.

5-7 Control Surfaces

The canard can no longer be called a "tail" surface as it is not on the tail end of the fuselage. As in subsonic design the control surfaces still maintain their same primary function, that is to control the airplane. When the control surface is aft of the c.g. it also contributes to the stability of the airplane. In a canard type airplane the horizontal control surface is forward of the

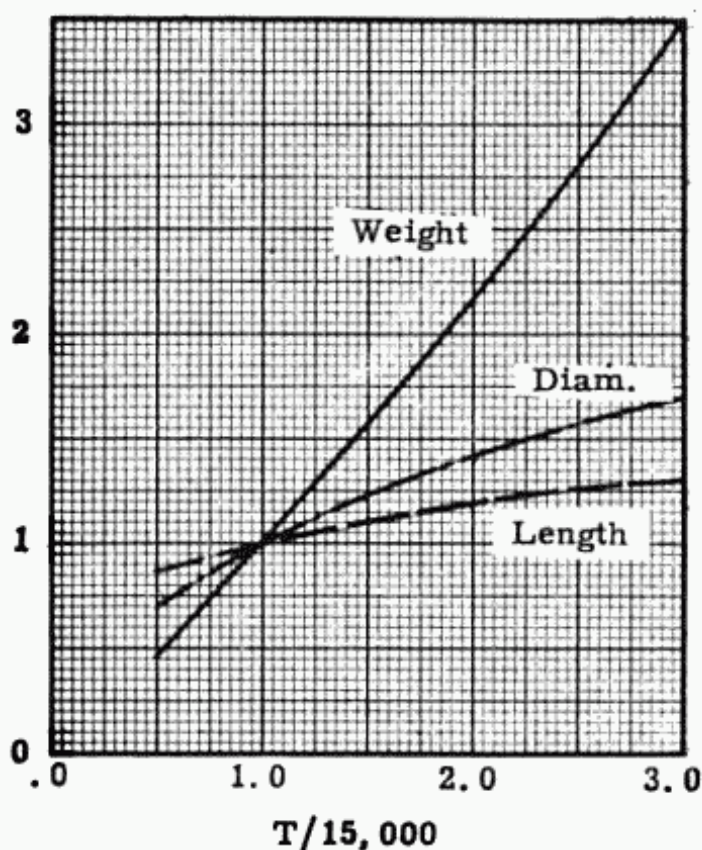


Fig. 5:6. Effect on thrust rating on engine size.

c.g. and is unstable, therefore requiring that the wing a.c. be sufficiently aft of the c.g. to result in a stable airplane.

Since the fuselage is generally a destabilizing factor in directional stability, the vertical control surface must be stabilizing, and therefore must be aft of the c.g. For this reason even on a canard type airplane the vertical surface is still as far aft as possible for maximum efficiency.

The values of C_{HT} and C_{VT} presented in section 4:7 are all for conventional control surfaces at the tail end of subsonic airplanes. Although many conditions that were critical for the subsonic airplane, such as longitudinal control in landing, critical engine out in directional control, and longitudinal stability with the c.g. in its most aft position, might still be critical for the supersonic canard, it is most unlikely that the C_{HT} 's and the C_{VT} 's that were efficient for the conventional subsonic airplane would be efficient, or even satisfactory, for the supersonic canard. This is true because of the possibility of control or stability becoming critical in the supersonic portion of the flight, (see Chapt XI) and because of the reverse downwash effect of a canard as compared to a conventional tail. The added effects of high sweepback and low aspect ratios certainly modify the values of the tail volume

5:12 SUPERSONIC AND SUBSONIC AIRPLANE DESIGN

coefficients. Therefore if data is available on the tail volume coefficients on supersonic, canard airplanes, with similar plan forms, the values should be used. Due to security regulations these are not for publication at this time. It is hoped that enough data will become available soon so that some rough estimates may be made.

5-8 Center of Gravity

The calculations are the same as the subsonic, of course, and the significance is similar. Since the airplane must maintain stability in the subsonic range, when the a.c. is at .25 MAC, it becomes very stable in supersonic flight when the a.c. is at approximately .50 MAC. Therefore satisfactory maneuverability and controllability are difficult to attain. It is therefore even more important in this type of design to keep the c.g. travel to a minimum, so that stability in subsonic flight can be maintained without penalizing control and maneuverability in supersonic flight. As mentioned previously the use of delta wings reduce the shift of the a.c. from subsonic to supersonic flight to about .10 to .15 MAC while the shift is approximately .25 MAC for more conventional wings of lower sweepback and higher taper ratio.

Structural Weights

The weights of the components presented in section 4:8 are based on the values of the Boeing 707, the Douglas DC-8 and the Convair 600. These airplanes all had fuselages for about 120 passengers, wings of $AR = 7$, taper ratio = .33, and effective thickness ratio approximately .10. For the supersonic airplane with $AR = 3$, taper ratio = 0 and thickness ratio of approximately .03, the structural weight of wing and tail will probably be a different percentage of the structural weight than for the subsonic airplanes. This change can be estimated from the factors K_t/c , K_{AR} , K_λ presented in chapter II. It will be noted that while the reduced t/c tends to increase the weight, the lower values of A.R. and T.R. tend to decrease it.

5-9 Aerodynamic Heating - General

It is felt that any text on supersonic airplane design would be incomplete without some discussion of aerodynamic heating. The following presentation relates some of the problems, and possible solutions, with special emphasis on transports.

A body flying in a viscous medium must overcome the effects of friction. In determining the thrust required for flight at any speed, the drag due to friction had to be considered. This is true

of course, in subsonic, as well as supersonic flight. This friction caused by the moving body in its surrounding medium results in the generation of heat as well as drag. In subsonic flow the heat produced was very low and presented no problem. In supersonic flow, this heat which can be appreciable at the higher M 's, is transferred to the airplane surface by convection through the boundary layer. Besides high temperatures being caused by friction, there is even higher temperatures produced at the stagnation point on a body where the air is brought to rest and all the energy of the air is converted to heat. This temperature is called the stagnation temperature, and depends upon the Mach number and altitude. This heat is also transferred to the body through convection. Actually the temperature that the body reaches, either due to friction or stagnation is a function of the local air density, the type and thickness of boundary layer, and the material properties of the body, as well as the M and altitude. Of course these temperatures can be modified by special methods which will be discussed later.

5-10 Nature of the Problem

The most important problems related to aerodynamic heating are:

1) The reduction in allowable stresses of the structural materials whose temperatures are elevated.

Figs. 5:7 shows strength weight ratio vs. temperature for a variety of metals that have been used or are being considered for use in aircraft. It is evident that the aluminum alloys, the standard structural material for subsonic aircraft becomes very inefficient beyond 400°F . The entire skin of a wing cruising at $M = 2.3$ and 35,000 feet would reach approximately this temperature, with no cooling or insulation. At $M = 3.0$, and even at 60,000 feet where the resulting equilibrium wall temperature is considerably less than at 35,000 feet, the wing would reach approximately 500°F . At the leading edge the temperature would be considerably higher. It is therefore evident that either cooling will have to be introduced to reduce the temperatures, or new materials used that can withstand the heat more efficiently. Ref. 3:1 indicates that at $M = 2.0$, aluminum will still be the most efficient structural material, being replaced by titanium at $M = 3$ and by steel at $M = 4$ or 5.

2) Introduction of thermal stresses.

Thermal stresses are defined as the stresses in a structural member due to temperature differences within the member.

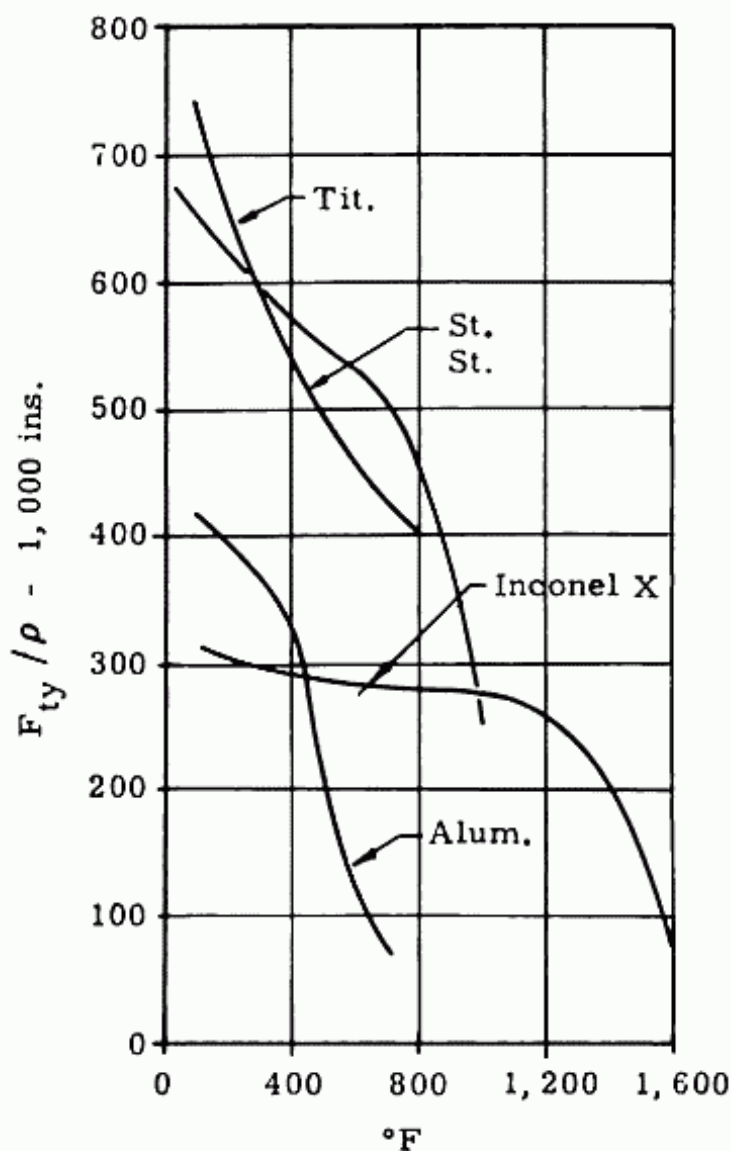


Fig. 5:7. Tensile yield stress/density vs. Temp. (Ref. 5:11)

Since the heat is being transferred from the outside inward, a temperature differential will exist between the surface exposed to the air and the inside surfaces.

The introduction of thermal stresses due to temperature difference may be simply explained by considering the I beam in fig. 5:8.

If the temperature of the top flange is higher than the rest of the beam, it tends to grow in length and tries to carry the entire beam with it. However, the rest of the beam resists, causing compression in the hot parts that are trying to stretch further, tension in the cooler parts that are being stretched, and shear due to the transfer of these loads. Ref. 5:7 states "This result indicates that large thermal stresses are to be expected when

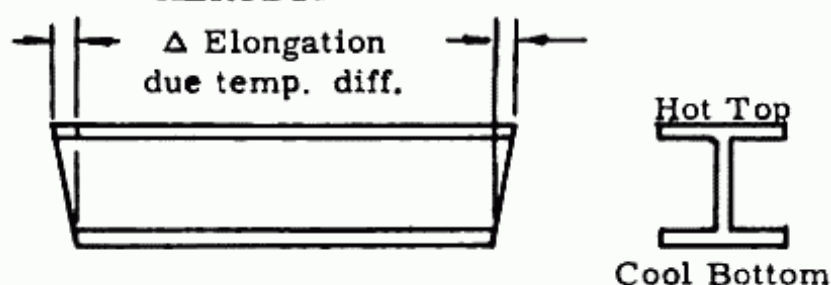


Fig. 5:8. Elongation thru temperature difference.

sandwich panels are heated. It appears that high core density, thin unheated faces, and thin panels will be necessary to prevent these stresses from being prohibitive."

3) Reduction in E

Fig. 5:9 presents curves of $E/\text{density}$ vs. temperature for the same metals shown in fig. 5:7. These changes with temperature are not as great as with the stress curves. The reduction in E presents one advantage and one disadvantage. The disadvantage is that the lower value of E results in a reduction in the rigidity of the structure for the same stress, i.e.

$$E = \frac{\text{stress}}{\text{strain}}$$

$$\text{or strain} = \frac{\text{stress}}{E}$$

The reduction in E however reduces the thermal stress for the same temperature difference, ΔT , and the same coefficient of thermal expansion, α , since

$$\text{thermal stress} = \alpha (\Delta T) E$$

4) Change in aerodynamic properties of lifting surface due to distortion of the lifting surface caused by temperature differences.

In all conditions of flight where $C_L = 0$, there is a difference in pressure between the upper and lower surfaces and a difference in temperature due to aerodynamic heating. In level flight this difference is usually small and may be neglected for preliminary design purposes. However, in a maneuver condition at high values of g where C_L is high, this temperature difference cannot be neglected, in fact can reach 600° and more, depending on g , altitude and M . In this condition the bottom surface which is hotter than the top, expands in the chordwise and spanwise directions relative to the top. This expansion introduces negative camber to the airfoil section and positive dihedral to the wing. These aerodynamic changes might be significant in the handling of the airplane.

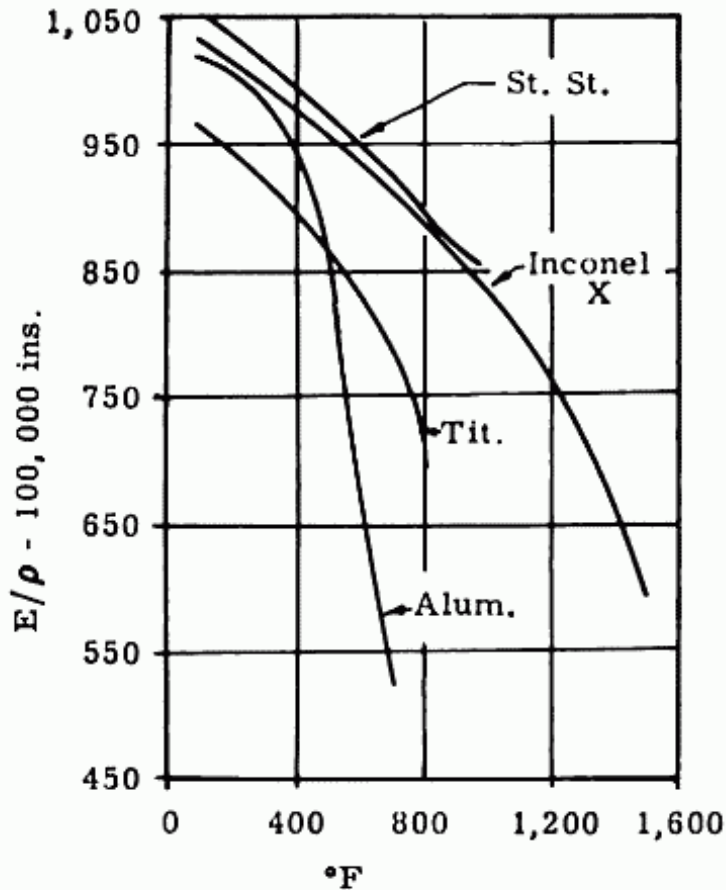


Fig. 5:9. Elastic Modulus/Density vs. Temp. (Ref. 5:11)

5) Creep due to repeated rise in temperature in structural elements.

The primary difference between creep and normal strain due to stress is that creep is dependent on time. Fig. 5:10 shows a typical curve of strain vs time as presented in ANC-5 with the accepted terminology.

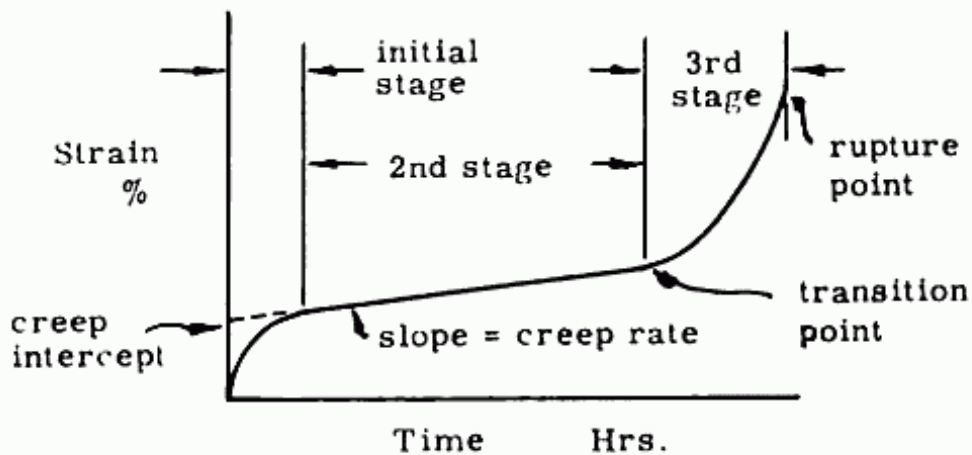


Fig. 5:10. Creep Curve.

This curve is only for a steady load. However, the fact that creep may also be critical for repeated loads, is important because airplanes experience loads, usually of a comparatively short duration, repeated many times during the airplane life. The creep effect from repeated loads, at this time, is the most difficult to analyze but very important in airplane design.

This creep effect is a similar phenomena to fatigue. Like fatigue, the failure due to creep can occur even though the loads repeatedly applied are each below the elastic limit.

Creep has come into prominence in aircraft in supersonic flight only because the elevated temperatures reached affect the ductility and possibly other characteristics of the normally used aircraft structural materials in such a manner that this creep phenomena might now be critical. It should be noted that creep could, and does, occur at room temperature in certain materials.

Fig. 5:11 (from Ref. 5:10) shows the variation in the stress to rupture vs. time at various temperatures for Inconel X.

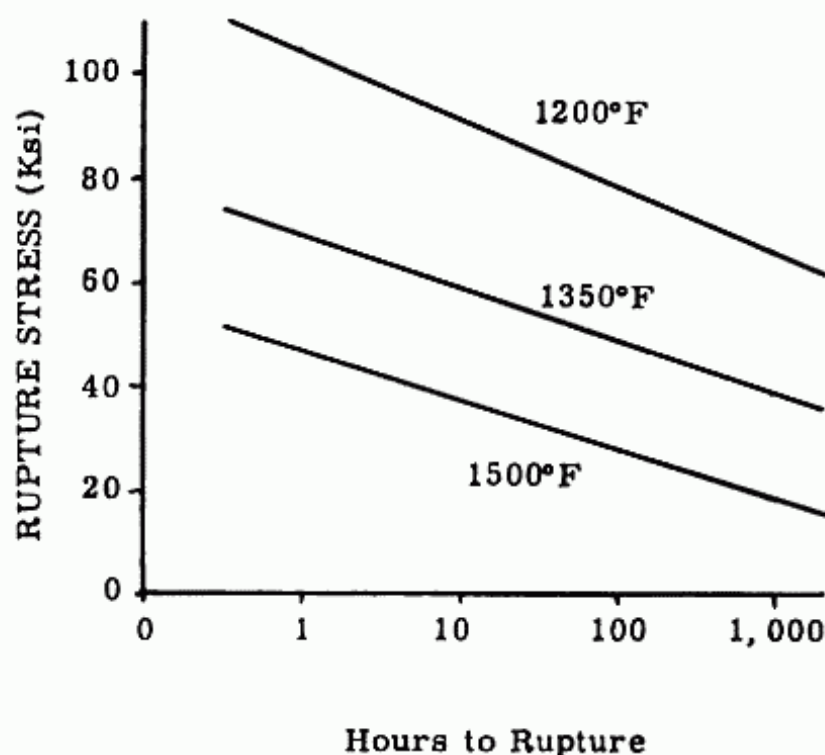


Fig. 5:11. Creep Effect on Inconel x.

6) Effect of high temperatures on the passengers, crew, fuel and equipment.

Since the temperature of the outside surfaces tends to rise to a very high temperature, possibly 1200°F at $M = 5.0$ and 60,000

5:18 SUPERSONIC AND SUBSONIC AIRPLANE DESIGN

feet, the temperature of the structure and air around it is raised by convection, conduction and radiation. If some precautions, such as insulation, or cooling, or both, are not taken the passengers and crew will be roasted, the fuel will tend to vaporize, and certain equipment will cease to operate.

5-11 Methods of Alleviation of the Aerodynamic Heating Problems

Before attacking the problem it is necessary to know the temperatures that will be encountered. Fig. 5:12 presents a curve of the equilibrium wall temperature, T_w , that would result accounting for radiation, at different M 's and altitudes, for a flat plate at zero angle of attack on a navy hot day. Fig. 5:13 shows the variation in T_s , T_r and T_w vs M at 60,000 feet. T_r , the recovery temperature, is the temperature corresponding to no radiation, and T_s is the stagnation temperature.

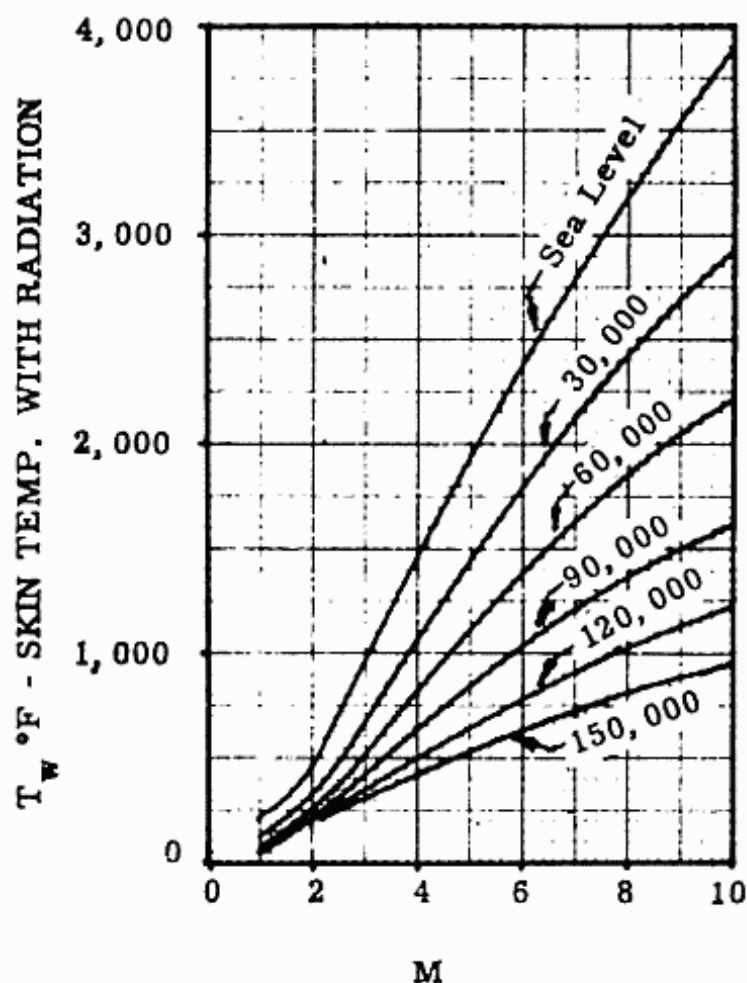


Fig. 5:12. T_w on A Flat Plate at 0° Angle of Attack 1 Meter from L.E. (coef. of emissivity = .8)

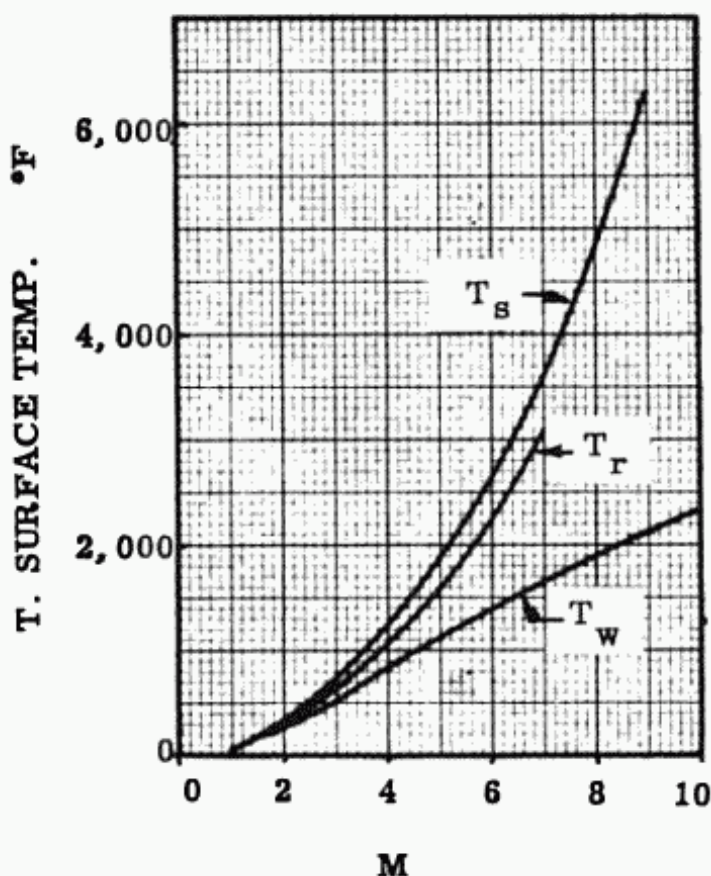


Fig. 5:13. Surface Temps. vs. M at 60,000 Ft.
(coef. of emissivity = .8)

These figures are taken from ref. 5:8, which presents all the assumptions used in their derivation. This problem of heating, as all other problems in airplane design, must be treated keeping in mind that the best solution is the one that results in the best airplane, considering direct operating costs, safety, and performance. An airplane can be designed to safely withstand the aerodynamic heating at almost any speed and altitude if it could have enough thrust to carry the water or material required to act as a heat sink to maintain safe structural temperatures. This brute force approach is hardly the most efficient. Although it is impossible here to present a rigorous study of the entire problem some approaches will be discussed.

1) Major Portion of Outside Surfaces

It would appear at this time that an efficient approach to the problem of the heating of the skins of most of the wing and fuselage is to choose an altitude, for the M chosen, so that an efficient structural material can be used that will require no cooling. That is, the material should be efficient at the equilibrium wall

temperature, as presented in figure 5:12. It should be noted that although this figure was determined for a flat plate, for all intents and purposes it applies equally well to bodies of revolution having radii which are large compared to the boundary layer thickness. For a transport cruising at $M = 3.0$ the choice of altitude is no problem by this criteria as there are many metals that are efficient stress/density wise at 500°F , which is the T_w at about 60,000 feet. A transport cruising at $M = 8$, presents more of a problem.

2) Leading edge of wing

The high temperatures likely to be encountered near the stagnation point presents a somewhat greater problem. However, it has been shown that the heat transfer to the leading edge surface is reduced by rounding the nose and sweeping the leading edge, so that the temperature of the leading edge is reduced considerably. Ref. 5:17 presents the variation in heat transfer coefficient, h , with sweepback for various M 's, as shown in fig. 5:14. These values are for certain assumed conditions and by one particular approach. The cosine Λ function closely approximates the curves of $M = 2.0$ and above, up to $\Lambda = 65^{\circ}$.

It should be noted that although rounding the leading edge tends to increase the C_D in supersonic cruise, it is distinct advantage in landing and take-off, and in subsonic flight. The high sweepback which is usually efficient from an aerodynamic and structural standpoint for a supersonic transport also proves efficient from a thermal point of view.

For aircraft cruising at very high Mach numbers it will be efficient to have either leading edge cooling or a heat sink, such as beryllium, as well as incorporating a rounded leading edge and a highly swept leading edge.

3) Nose of Fuselage

Here as in the leading edge of the wing a rounded nose will be necessary at high values of M . Of course there is no recourse to sweepback. However, since it is only a small area to be considered, as compared to the entire leading edge area of the wing, the weight required to maintain a satisfactory temperature will be comparatively small. This can be accomplished by evaporative or ablative cooling, or by a heat sink. Some insulation is also required to keep the heat from the nose from heating the crew compartment which is close behind.

4) Thermal Stresses

The problem of thermal stresses may be somewhat alleviated in a number of ways.

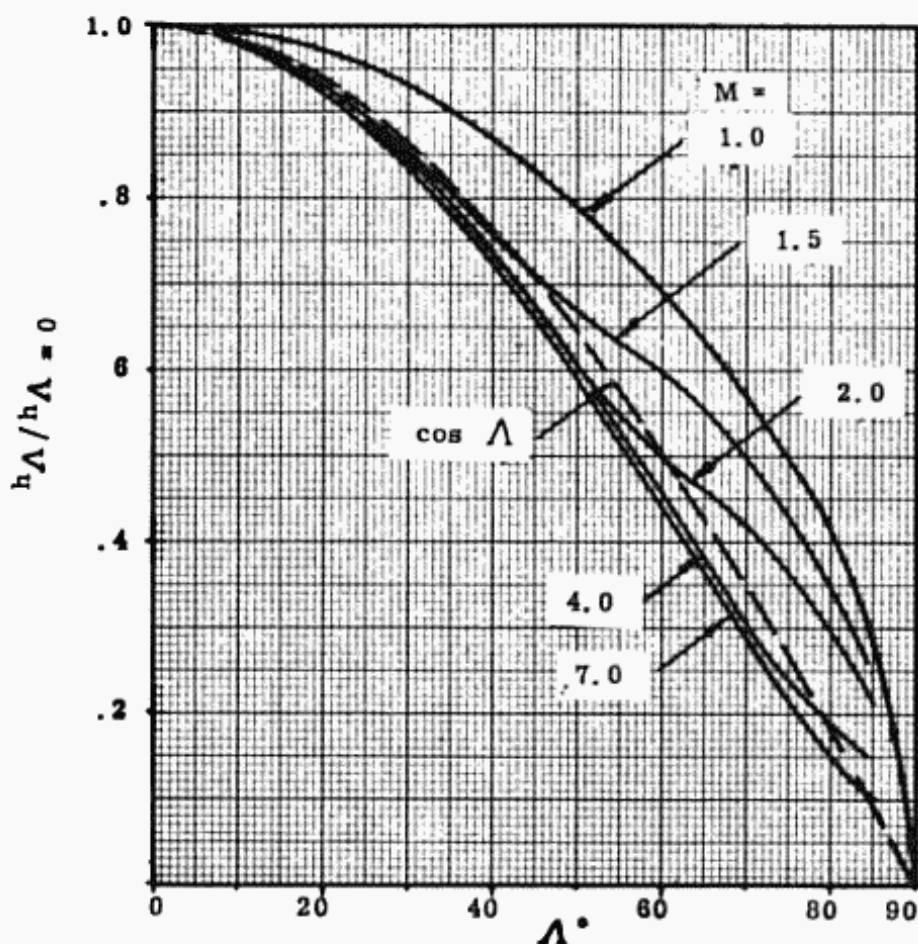


Fig. 5:14. Effect of yaw on heat transfer coef. at stagnation point of a circular cylinder with nearly insulated surface; Prandtl No. = 1.0

a) Have the inside of the structure, such as in a sandwich, or entire wing, treated so that it has a high value of emissivity and absorbtivity. In this way the hot surfaces with high emissivity will transfer their heat by radiation to the cool surfaces thereby keeping the temperature difference to a lower level. Of course this device is only effective at temperatures high enough so that radiation is a significant factor in the total heat transfer.

b) Have a sufficient number of members between the hot and cool surfaces to transfer the heat by conduction at the lower temperatures where radiation is ineffective. Notice, as stated on page 5-14, ref. 5:7 recommends sandwich construction of high core density.

c) Consider the use of materials with a low value of $E \alpha$ since

$$\sigma_{th} = \alpha E \Delta T$$

where σ_{th} = thermal stress

α = coeff. of thermal expansion

E = Young's modulus

ΔT = temperature difference

Titanium has a comparatively low value of $E\alpha$.

5) Reduction in Rigidity

The reduction in E and therefore in rigidity due to elevated temperatures must be considered along with the reduction in allowable stresses. Although this reduction in E results in lower thermal stresses, the resultant loss in rigidity can introduce serious problems in aileron reversal, flutter and other aeroelastic phenomena, especially on very thin wings.

6) Creep due to repeated rise in temperature in structural elements.

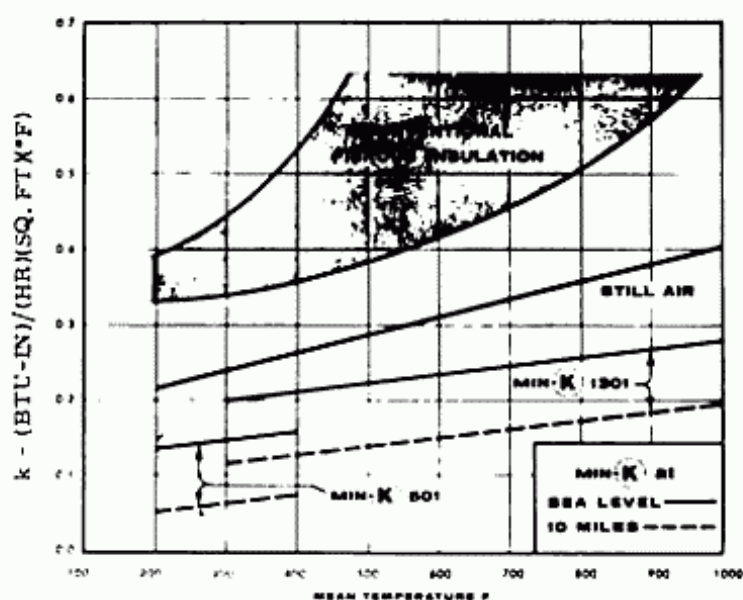
There is probably less data available on this subject than any other of the problems associated with aerodynamic heating, and therefore is a wide open field for research and study. It can become a serious problem because of the repetitive nature of aircraft loads, the severity depending upon the flight history. It should not be neglected in airplanes subject to high rates of acceleration and deceleration, and with a long life expectancy.

7) Effects of high temperature on the crew, and passengers

For a transport airplane it is most likely that the insulation or cooling system, or both, required to keep the crew and passengers comfortable, will introduce the largest weight penalty directly attributable to aerodynamic heating, with the possible exception of the outside structure. A method of determining this weight required for two systems is presented. System A consists merely of sandwich structure, a layer of insulation and a comparatively small and light weight refrigeration system to remove the little heat coming through the insulation, and generated by the passengers, to maintain 70°F in the cabin. System B is more complex, but having the same structure and refrigeration system. In addition it has a layer of insulation next to the structure, a water evaporative cooling system, and then another layer of insulation.

A newly developed insulation material is a Johns Manville product called MinK, which seems efficient for use in a supersonic transport. Fig. 5:15 shows the variation of the heat transfer

coefficient k with mean temperature, for 2 types of Min-K at sea level, and at 52,800 feet altitude. Also, included is the physical and thermal properties of this insulation.



Physical Property	Min-K 501	Min-K 502	Min-K 503	Min-K 504	Min-K 1301**	Min-K 1302
Maximum service temperature, F°	500	500	500	500	1300	1300
Nominal density, lbs/cu ft	10	12	14	16	20	20
Average transverse strength, psi	4	18	30	45	75	46
Compressive strength, psi						
5% compression	16.5	34.0	45.0	75.5	94.0	88.0
10% compression	32.5	67.5	99.0	180.0	200.0	161.0

Fig. 5:15. Physical and Thermal Properties of Min-K.

System B is shown in fig. 5:16

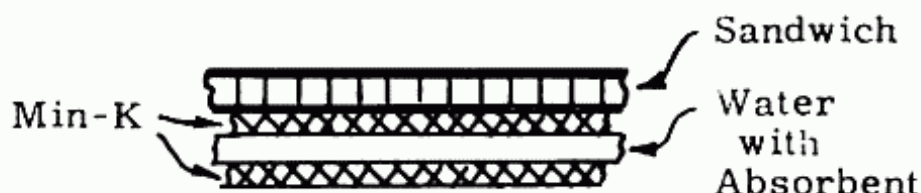


Fig. 5:16. System B.

The main structure is the outside sandwich, followed by insulation, some water for evaporative cooling and then more insulation. The outside minK will be type 1301 because of its high service temperature, while the inside will be type 501 (which is lighter and a better insulator) because of the low temperature it

encounters. In the cabin a refrigeration system is required. A jet transport cruising at $M = 3.0$ at 60,000 feet with 125 passengers in a 14 foot diameter cabin and 100 feet long, will be analyzed.

Obtain T_w at $M = 3.0$ and 60,000 from fig. 5:12. This value of 520°F is for a length of fuselage 10 feet long. For the fuselage 100 feet long obtain $c_k = .89$ (from fig. 5:17) and calculate the skin temperature for the entire fuselage; $(.89)(520) = 460^\circ\text{F}$. Note that the wall temperature decreases with increase in length.

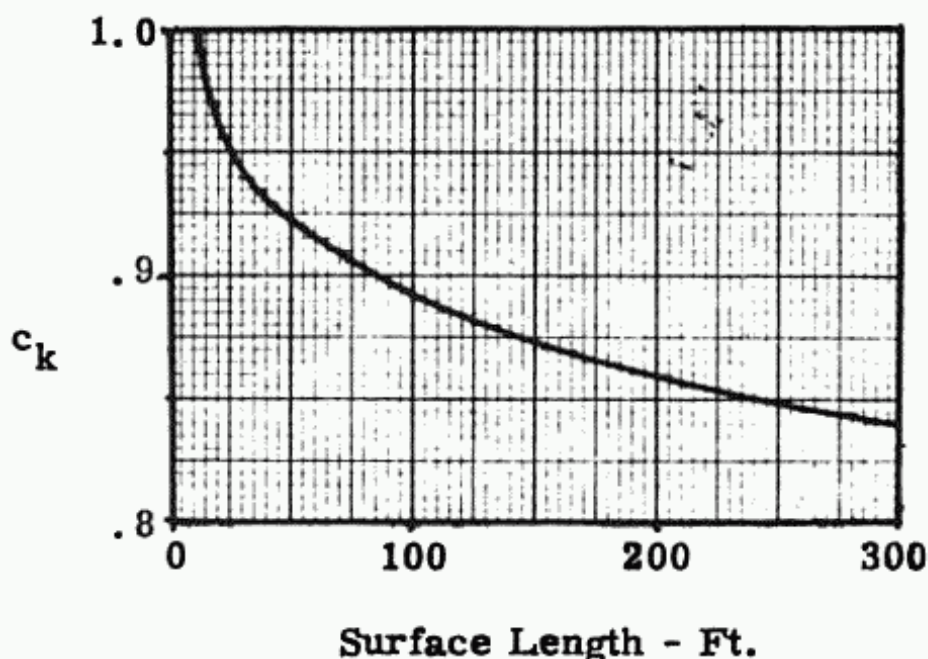


Fig. 5:17 a. Length Correction Factor on T_w .

The evaporative cooling requires that the evaporated water be exhausted to the atmosphere. The exhaust pressure may merely be the outside pressure, or a somewhat higher pressure regulated by a relief valve. At 60,000 feet on a ICAO standard day the pressure is 1.05 psi, at which point water boils at 103°F . See fig. 5:18. The lower the boiling point the more efficient this system becomes.

It is now necessary to determine the weight of the water and insulation required for this cruising flight so that passenger comfort is maintained. First the heat flow through the sandwich construction and the minK into the water must be calculated.

$$q = \frac{\Delta T}{\frac{t_1}{k_1} + \frac{t_2}{k_2}}$$

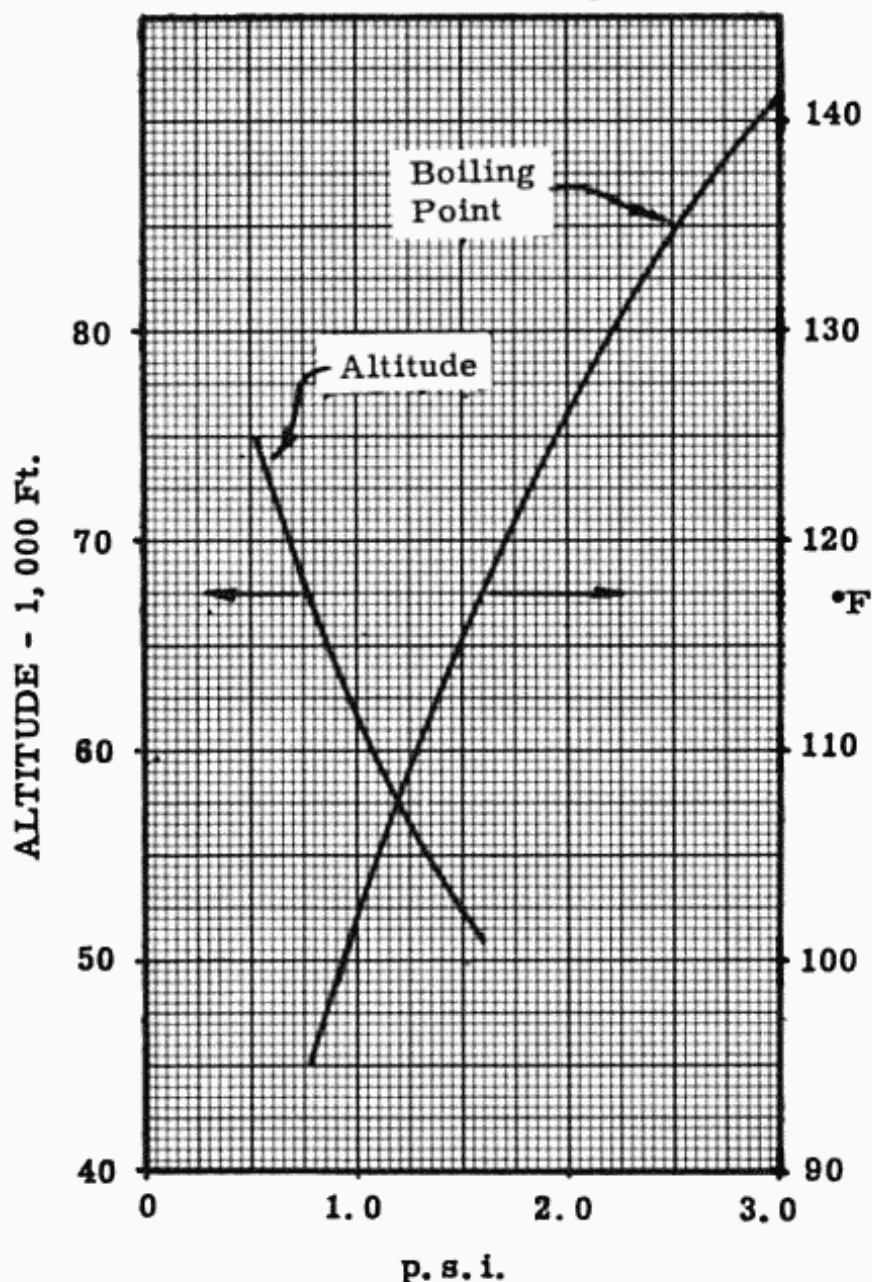


Fig. 5:18. Boiling Point of Water vs. p.s.i. and Altitude.

where q = heat flow in BTU/hr.-ft.²

ΔT = temperature change from outside of sandwich to inside of insulation

t_1 = thickness of sandwich, inches

t_2 = thickness of insulation, inches

k_1 = heat transfer coeff. of sandwich, in $\frac{\text{BTU, in.}}{\text{hr. ft.}^2 \text{ } ^\circ\text{F}}$

k_2 = heat transfer coeff. of insulation in "

$$\Delta T = 460 - 103 = 357^\circ\text{F}$$

k_2 is for an average temp. of 281.5 and equals .12 for minK 1301 exposed to air at 52,800 ft. altitude.

$\frac{x_1}{k_1}$ must be obtained experimentally for the sandwich being used. This value varies with temperature since the heat transfer by conduction and radiation varies radically with temperature. A 3/4 inch thick sandwich at this temperature might have a value of $x_1/k_1 = .10$, although it should be noted that this value varies with type of material, type of core, etc.

$$\therefore q = \frac{357}{.10 + (t_{\text{MinK}})/.12} ; \frac{\text{B.T.U}}{\text{hr.ft}^2} \text{ thru sandwich and minK}$$

Next the heat to vaporize the water must be known. The total heat required to vaporize one pound of water is equal to the heat required to raise the temperature to its boiling point plus the heat required to vaporize. Therefore this total heat per pound

$$\begin{aligned} &= (.45)(103 - 70) + 1,030 \\ &= 1,045 \text{ BTU/lb.} \end{aligned}$$

where

1,030 is the heat of vaporization of water at 103°F in BTU/lb.

70°F is the assumed temperature of the water at the start of the cruise.

.45 is c_p , the BTU/lb.-ΔT for water

Note that the initial temperature of the water has little effect on the total heat required, as long as it is kept below 103°F. Now to look into the weights of the components.

Weight of minK = $\frac{1.67 \text{ lbs.}}{\text{sq.ft.surface}}$ per inch thickness

Weight of water = 62.5 lbs/cu.ft.

So that the walls of the minK are always touched by water an absorbent for the water is required.

Weight of absorbent = 10 lbs./cu.ft. (assumed)

Also assume that there should be a reserve of 10% of the water at the end of cruise as a safety precaution.

If the heat flow into the water, in BTU/hr.ft.², is divided by the heat required to vaporize water, in BTU/pound, the weight of water in lbs./sq.ft.hr. is obtained. This weight of water must be multiplied by $\frac{62.5 + 10}{62.5}$ (1.10) to account for the absorbent and

reserve required. Therefore the weight of water, absorbent and reserve is

$$\frac{\text{lbs}}{\text{sq.ft.hr}} = \frac{(357) [(62.5 + 10)/62.5](1.10)}{[.10 + (t_{\text{minK}}/12)] (1,045)}$$

or

$$\frac{\text{lbs.}}{\text{sq. ft.}} = \frac{.0524 \text{ hrs.}}{.012 + t_{\text{minK}}}$$

Therefore for total weight of water system and minK,

$$W = (1.67 t_{\text{minK}} + \frac{.0524 \text{ hrs.}}{.012 + t_{\text{minK}}}) \text{ lbs/sq.ft.}$$

If W is differentiated in respect to t , and the result let equal zero, the value of t that results in the minimum weight will be obtained.

$$\text{let } t' = .012 + t_{\text{minK}}; t_{\text{minK}} = t' - .012$$

$$\text{then } W = 1.67 t' - .020 + \frac{.0524 \text{ hrs.}}{t'}$$

$$\frac{dW}{dt'} = 1.67 - \frac{.0524 \text{ hrs}}{t'^2}$$

Therefore letting $dW/dt' = 0$

$$t' = .176 \text{ (hrs)}^{1/2}$$

$$t_{\text{minK}} = .176 \text{ (hrs)}^{1/2} - .012$$

If the airplane is designed to cruise 3,460 n.mis., that is for two hours,

$$t_{\text{minK}} = (.176)(1.41) - 012 = .256$$

$$\text{Wt of minK} = (1.67)(.236) = .394 \text{ lbs/sq.ft.}$$

$$\text{Wt of water system} = \frac{(.0524)(2)}{.012 + .236} = .423 \text{ lbs./sq.ft.}$$

The water is now at 103°F and is separated from the cabin compartment by another layer of insulation. The heat flow thru this insulation with its inside surface temp. at 70°F must be cooled by a refrigeration unit. It is assumed that a unit to cool at the rate of 500,000 BTU/hr would weigh about 700 lbs., of

which 200 lbs. is fixed and the other 500 lbs. is a function of the cooling rate. In addition the weight of power input required was assumed to be in the order of $(.0002)(\text{BTU/hr. cooling})$. Therefore,

$$\text{Wt of refrigeration} = 200 + (.001 + .0002) \text{ BTU/hr.}$$

The heat input to the cabin thru the minK 501 is

$$\frac{(103 - 70)(.05)}{t_{\text{minK}}} = \frac{1.65 \text{ BTU}}{t \text{ hr.ft}^2}$$

$$\text{or} = \frac{1.65 \text{ ft}^2}{t} \text{ in BTU/hr}$$

Assuming passengers release 400 BTU/hr., the added heat flow to be cooled is $(400)(125) = 50,000 \text{ BTU/hr.}$

$$\text{Wt of refrigeration} = 200 + .0012 \left(\frac{1.65 \text{ ft.}^2}{t} + 50,000 \right)$$

Therefore, adding minK 501 which has a density of 10 lbs./sq.ft.

$$\frac{\text{Total Wt}}{\text{ft}^2} = .835 t + 260 + \frac{.00198}{t}$$

$$\frac{dW}{dt} = .835 - \frac{.00198}{t^2}$$

Letting $dW/dt = 0$

$$t = .0486$$

$$\text{Wt of minK} = (.0486)(.835) = .0406 \text{ lbs./sq.ft.}$$

$$\text{Wt of refrig.} = 260 + \frac{.00198}{.0486} = 260 + .0406 \text{ lbs./sq.ft.}$$

$$\text{heat flow thru the minK} \frac{1.65}{.0486} = 34 \frac{\text{BTU}}{\text{ht.ft.}^2}$$

Therefore the total weight of the insulation and cooling is equal to

$$\text{outside minK} = .394 \text{ lbs./sq.ft.}$$

$$\text{water system} = .423 \text{ lbs./sq.ft.}$$

$$\text{inside minK} = .0406 \text{ lbs./sq.ft.}$$

$$\text{Refrig. system} = .0406 \text{ lbs./sq.ft.} + 260$$

$$\text{Total weight} = .898 \text{ lbs./sq.ft.} + 260$$

For a 14 ft. dia. and 100 ft. long cabin, the surface area equals 4,400 sq. ft.

$$\text{Therefore weight} = (.898)(4,400) + 260$$

$$= 3,950 \text{ lbs. for 2 hour flight}$$

Before going to system B which is much simpler, attention must be called to the most important simplifications, and assumptions made in system A. They are (1) the weight of the exhaust system for the steam, and its mechanics, were neglected, (2) the ends of the cabin were completely neglected (3) the entire cylinder was assumed cooled, (4) the heat transfer coefficient of the sandwich structure, which was assumed to be designed primarily for strength, was assumed (5) the temperature of water was assumed to be 70°F at beginning of cruise and (6) the pressure vessel required between the exhaust steam system at 1.05 psi and the higher pressure passenger compartment, was neglected. Actually the ΔT and the hours could be kept as unknowns thru the final equations so that weight could be kept as a function of these factors. However, since the k of the sandwich and the k of the minK vary with temperature, the calculations are only valid for one T_w .

System A consisting of the outside sandwich construction, a layer of minK for insulation and the refrigeration unit to maintain 70°F in the cabin is shown in fig. 5:19. The minK for this system will be maintained at cabin pressure which will be close to sea level conditions.



Fig. 5:19. System A

To keep the systems on a comparative basis the same refrigeration unit size that proved to be the optimum for system B will be used for system A.

$$\begin{aligned} Wt_{\text{refrig}} &= 260 + .0406 \text{ lbs/sq.ft.} \\ &= 260 + .0406 (4,400) \\ &= 440 \text{ lbs.} \end{aligned}$$

Since $Wt = 440 = 200 + .0012 \text{ BTU/hr}$, the cooling capacity of refrigeration unit equals 200,000 BTU=hr. For heat flow thru the sandwich and the minK 501

$$q = \frac{\Delta T}{\frac{t_1}{k_1} + \frac{t_2}{k_2}}; \frac{\text{BTU}}{\text{hr-ft.}^2}$$

$$= \frac{(460 - 70)(4,400)}{.10 + (t_{\text{minK}}/.15)} = \frac{1,720,000}{.10 + (t_{\text{minK}}/.15)} \frac{\text{BTU}}{\text{hr.}}$$

Since the total heat flow thru the minK and generated by the passengers must be cancelled by the cooling of the refrigeration unit, then

$$200,000 = 50,000 + \frac{1,720,000}{.10 + (t_{\text{minK}}/.15)}$$

$$t = 1.72 \text{ inches}$$

Therefore the weight of the refrigeration unit and the minK insulation

$$= (1.72)(.835)(4,400) + 440$$

$$= 6,740 \text{ lbs.}$$

It should be noted that only minK 501 has been used in system A although it is marginal for maximum service temperature. If this minK was used in system B instead of the minK 1301, system B would be considerably lighter. It is possible in system A to use a thin outside layer of minK 1301 and a heavier inside layer of minK 501.

In either case system A can be improved considerably by using a size of refrigeration unit that is optimum for the system, instead of the size that was optimum for system B. It should also be remembered that system B has a water and steam exhaust system which is of questionable safety for a transport airplane, adds weight that has not been accounted for, and requires servicing for each flight.

A modification of system A might prove to be most efficient for airplanes with a high T_w . This system consists of a thin sheet of smooth material that can resist high temperatures but is not structural, a layer of insulation such as minK, and then the sandwich honeycomb in structure. The advantages of this system is that (1) the structure is kept comparatively cool, therefore has higher allowable stresses and is hence lighter, and (2) the sandwich construction at lower temperatures is a much better insulator than at the high temperatures. The main disadvantage is the added weight of the outside skin. Stainless steel sheet .010 in. thick, required to cover a cylinder 100 ft. long and 14 ft. in diameter weighs about 2,300 lbs.

Lastly it must be emphasized that the systems and methods used here are by no means accurate and have been presented primarily to show some methods by which this problem of cabin cooling might be attacked.

8) Effects of high temperatures on fuel

It has been suggested that the large amount of comparatively cool fuel aboard the airplane can be used as a coolant. This can be accomplished by cooling the hot surfaces, perhaps the wing leading edge, by pumping the fuel past these surfaces on its way to the engine. This system should be evaluated keeping in mind that the fuel is being heated by the hot skins before it even leaves the tank, and that there is an upper limit of temperature to which the fuel can be raised before it causes cavitation in the pump.

However it might prove necessary to use some insulation, around the tank merely to keep it at a usable temperature. Again a brief example will be presented. Assume that the airplane cruises at $M = 3.0$, at 60,000 feet for 2 hours, uses a total of 120,000 lbs. of fuel (or 1,000 lbs. per min) with a 20,000 lb. reserve, has an exposed tank area of 6,000 sq. ft., and an equilibrium wall temperature of 500°F . If the tank is insulated with minK, t inches thick

$$q \text{ into the tank} = \frac{(k \text{ minK})(\Delta T)(\text{ft}^2)}{t \text{ minK}} = \frac{\text{BTU}}{\text{hr}}$$

Starting at $T_w = 500^{\circ}\text{F}$ and $T_{\text{fuel}} = 100^{\circ}$, assuming a certain value of thickness of minK, and dividing the flight into 10 minute intervals, the heat flow into the fuel can be determined for the first 10 minute period. Using the c_p of the fuel as .5 BTU/lb. $^{\circ}\text{F}$, the increase in fuel temperature during this 10 minute period can be calculated, i.e.

$$\Delta F = \frac{\text{B.T.U. input}}{(c_p)(\text{fuel weight})}$$

With this new temperature, $100 + \Delta^{\circ}\text{F}$, the new fuel weight, and the slightly changed k and ΔT , another increase in fuel temperature can be calculated for the second interval. This can be repeated until the cruise is over. It will be noted that the amount of reserve fuel is the critical factor in the results since the temperatures rises the most during the period when the fuel is lowest. Of course in a rigorous solution the heating that occurs in descent must be accounted for, and may or may not be significant depending on the variation of M with altitude.

The critical factor to be considered is the temperature to

which the fuel can be raised before it causes cavitation in the pumping system.

REFERENCES

- 5:1 M. Piffel, NACA TN 3697 "Flight Tests at Supersonic Speeds to Determine the Effect of Taper on the Zero Lift Drag of Sweptback Low Aspect Ratio Wings, June '56.
- 5:2 G. C. Furlough and J. G. McHugh NACA TR 1339 "A Summary and Analysis of the Low Speed Longitudinal Characteristics of Swept Wings at High Reynolds Number"
- 5:3 J. D. Murrow NACA TN 3550 "Measurements of the Effect of Trailing Edge Thickness on the Zero-Lift Drag of Thin Low-Aspect Ratio Wings", Nov. 1955.
- 5:4 J. D. Murrow and E. Katz, NACA TN 3548 "Flight Investigations at M from .6 to 1.7 to Determine Drag and Base Pressures and Blunt-Trailing Edge Airfoil and Drag at Diamond and Circular Arc Airfoils at Zero Lift", Nov. 1955.
- 5:5 D. R. Chapman and R. H. Kester, TN 3504 "Effect of Trailing Edge Thickness on Lift at Supersonic Velocities, June 1955
- 5:6 Handbook of Supersonic Aerodynamics, NAVORD Rept. 1488, Vol. 3 Sect. 7 "Three Dimensional Airfoils"
- 5:7 E. Reshotko and J. E. Beckwith, NACA TN 3986 "Compressible Laminar Boundary Layer over a Yawed Infinite Cylinder with Heat Transfer and Arbitrary Prandtl Number", June 1957
- 5:8 H. W. Woolard and R. H. Cramer "Equilibrium Surface Temperature Resulting from Aerodynamic Heating and Radiant Cooling for Turbulent Boundary Layer Flow over a Flat Plate", Appl. Physics Lab., Johns Hopkins Univ., CF-2701
- 5:9 Aero-Space Engineering, April 1959 "Aeronautical and Space Applications for Ceramics", J. D. Welterlen
- 5:10 R. Goldin "Thermal Creep Design Criteria", IAS Preprint No. 730.
- 5:11 W. C. Caywood and R. M. Rivello - "Material Strengths under Missile Load Conditions" Johns Hopkins Applied Physics Lab Bumblebee Report No. 270.

Chapter VI

SPECIAL PROBLEMS

6-1 Introduction

The airplane has now been designed and drawn up based upon the best estimates possible during the design period. It is now convenient to check some of the assumptions and present another approach to obtaining performance characteristics.

6-2 Navaer Method of Performance Calculation

Breguet's formula for range calculation and the method using $mi \delta/lb.$ directly have been presented and found very useful for design purposes. The Navaer method of determining performance is most useful after the airplane design has been set. From

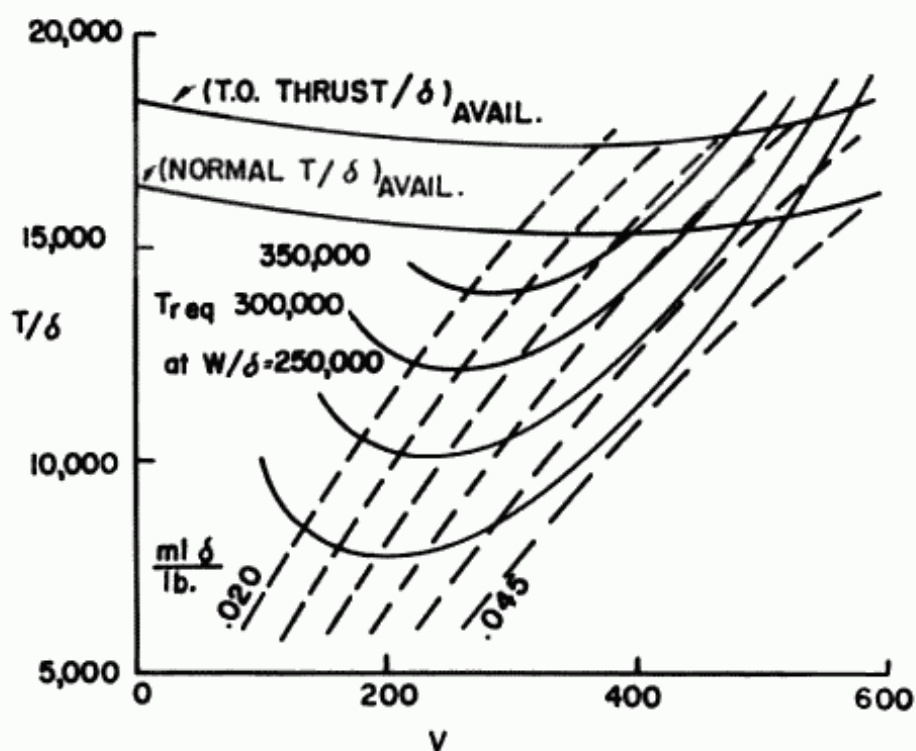


Fig. 6:1. Navaer graph for performance calculation.

one graph, the following data can be obtained for altitudes above 35,000 feet:

1. maximum speed for any weight at any altitude at any available thrust

6:2 SUPERSONIC AND SUBSONIC AIRPLANE DESIGN

2. range at any speed at any altitude, therefore maximum range and optimum speed and altitude
3. rate of climb

The necessary data to draw the curves require somewhat lengthy calculations. However once the curves are established, the data is obtained quickly and easily. The method consists of plotting the curves of thrust required as a function of W/δ , fuel consumption in the terms $mi\delta/lb.$ fuel, and thrust available in T/δ , with V , the velocity, as abscissa. A typical plot is shown in Figure 6:1. Thrust required is a function of the airframe characteristics while thrust available and fuel consumption are engine characteristics.

Thrust required - subsonic

$$T = D = 1/2 \rho S V^2 C_D \quad (6:1)$$

$$= \frac{\sigma V^2}{296} S C_D; \text{ for } V \text{ in knots} \quad (6:2)$$

Dividing by δ

$$T/\delta = \frac{\sigma}{\delta} V^2 \frac{S C_D}{296} \quad (6:3)$$

Since

$$\delta = \theta \sigma \quad (6:4)$$

$$T/\delta = \frac{V^2}{\theta} \frac{S C_D}{296} \quad (6:5)$$

$$C_D = C_{Dp} + C_{Di} + C_{Dcomp} \quad (6:6)$$

$$T/\delta = \left(\frac{S C_{Dp}}{296} \right) \left(\frac{V}{\sqrt{\theta}} \right)^2 + \left(\frac{S C_{Di}}{296} \right) \left(\frac{V}{\sqrt{\theta}} \right)^2 + \left(\frac{S C_{Dcomp}}{296} \right) \left(\frac{V}{\sqrt{\theta}} \right)^2 \quad (6:7)$$

$$1) \text{ From } C_{Dp} = f/S \quad (6:8)$$

$$\frac{S C_{Dp}}{296} \left(\frac{V}{\sqrt{\theta}} \right)^2 = \frac{f}{296} \left(\frac{V}{\sqrt{\theta}} \right)^2 \quad (6:9)$$

$$2) \text{ From } C_{Di} = \frac{C_L^2}{\pi A Re} \quad (6:10)$$

$$\text{and } C_L = \left(\frac{296}{\sigma} \right) \left(\frac{W}{S} \right) \left(\frac{1}{V^2} \right); V \text{ in knots} \quad (6:11)$$

$$C_{D_i} = \frac{\left(\frac{296}{S}\right)^2 \left(\frac{W}{\delta}\right)^2 \left(\frac{1}{V/\sqrt{\theta}}\right)^4}{\pi A Re} \quad (6:12)$$

$$\frac{SC_{D_i}}{296} \left(\frac{V}{\sqrt{\theta}}\right)^2 = \frac{296}{\pi b^2 e} \left(\frac{W}{\delta}\right)^2 \left(\frac{1}{V/\sqrt{\theta}}\right)^2 \quad (6:13)$$

$$3) \text{ From } M = \frac{V}{c} = \frac{V}{662\sqrt{\theta}} \quad (6:14)$$

$$M = \frac{V}{\sqrt{\theta}} \frac{1}{662} \quad (6:15)$$

Therefore M_{cruise} can be determined for each $V/\sqrt{\theta}$. With C_L known, the M_{crD} for each speed and altitude can be calculated.

From Figure 2:23 the $C_{D_{\text{comp}}}$ can be obtained.

Summing up 1, 2 and 3

$$T/\delta = \frac{f}{296} \left(\frac{V}{\sqrt{\theta}}\right)^2 + \frac{296}{\pi b^2 e} \left(\frac{W}{\delta}\right)^2 \left(\frac{1}{V/\sqrt{\theta}}\right)^2 + \frac{SC_{D_{\text{comp}}}}{296} \left(\frac{V}{\sqrt{\theta}}\right) \quad (6:16)$$

This formula is true for any altitude. For altitudes above 35,000 feet, $\sqrt{\theta}$ is constant and T/δ may be plotted versus V .

Thrust required - supersonic

The thrust required for supersonic flight can be developed in exactly the same manner as in subsonic flight. All that is required is obtaining the values of C_{D_F} , $C_{D_{NF}}$ and C_{D_w} instead of C_{D_P} , C_{D_i} and $C_{D_{\text{comp}}}$.

Engine Characteristics

As can be seen from Equation 6:16, the thrust required divided by the pressure ratio, δ , can be determined as one function of $V/\sqrt{\theta}$ at any altitude, from sea level up. It would therefore be convenient if the engine characteristics, thrust available and fuel consumption, could be obtained as one function of $V/\sqrt{\theta}$ for all altitudes. However this is not possible as the thrust available is directly proportional to δ above 35,000 feet, and a varying function of $\delta\sqrt{\theta}$ below. Therefore one curve cannot be plotted that would be valid for all altitudes. Since the airplanes

6:4 SUPERSONIC AND SUBSONIC AIRPLANE DESIGN

under consideration and most jet powered aircraft cruise at altitudes 35,000 feet and above, a graph representing conditions 35,000 feet and above will be satisfactory.

Method

From Equation 6:16, T/δ can be calculated for various values of W/δ at various speeds, and plotted as shown in Figure 6:1. The engine characteristics, T/δ available and $mi\delta/lb.$ fuel, can be determined from the engine characteristic chart, Figure 2:22 for subsonic airplane, and Figure 3:8 for supersonic.

To obtain the maximum speed at any weight and altitude, calculate the corresponding W/δ . The speed at which the thrust required curve of the desired W/δ crosses the thrust available curve is the maximum speed at that W/δ .

The method of determining the maximum range and the corresponding optimum altitude is not quite as direct. At each speed the maximum range will be at the W/δ that results in the highest $mi/lb.$, not the highest $mi\delta/lb.$ From the weights at the beginning and end of cruise, and the optimum W/δ just determined, the corresponding altitudes can be calculated. Therefore for each speed there will be a maximum range and a corresponding altitude. The speed with the greatest range will be the optimum speed and the corresponding altitude will be the optimum altitude.

A more direct way of finding maximum range and altitude is to determine the maximum $mi\delta/lb.$ for each W/δ . See Figure 6:1. Knowing the W at beginning and end of cruise, the corresponding $mi/lb.$ can be calculated and the range determined. The W/δ that results in the longest range, and the corresponding speed and altitude, will be the optimum values.

The determination of the maximum rate of climb at any W/δ is also a matter of trial and error. Since the rate of climb is a function of $(T_a - T_r)V$, not just $(T_a - T_r)$, it must be calculated at the speeds equal to and greater than the speed where $(T_a - T_r)$ is a maximum. These calculations are important as one of the climb requirements of the Civil Aeronautics Regulations is specified "at any altitude at which the aircraft is expected to operate."

6-3 Calculation of "f"

In the design calculations, f was obtained from formula 2:44

$$f = 1.10 + .128 N_p + .0070 S + .0021 N_e (T_e)^{.7}$$

With the airplane drawn it is now possible to calculate f more accurately, using the C_f of each component separately.

From the general arrangement drawing of the airplane the

net wetted area of each component must be calculated. The net wetted area is the surface of the part actually exposed to the air. The f of the airplane is then the wetted area of each component part multiplied by its corresponding C_f , plus .10 times the total f to account for miscellaneous excrescences and interferences. C_f of each component part can be obtained from figure 2:21b using the correct R.N. for each component.

Figure 6:2 shows diagrams of typical airplane components with the areas that are normally blanketed.

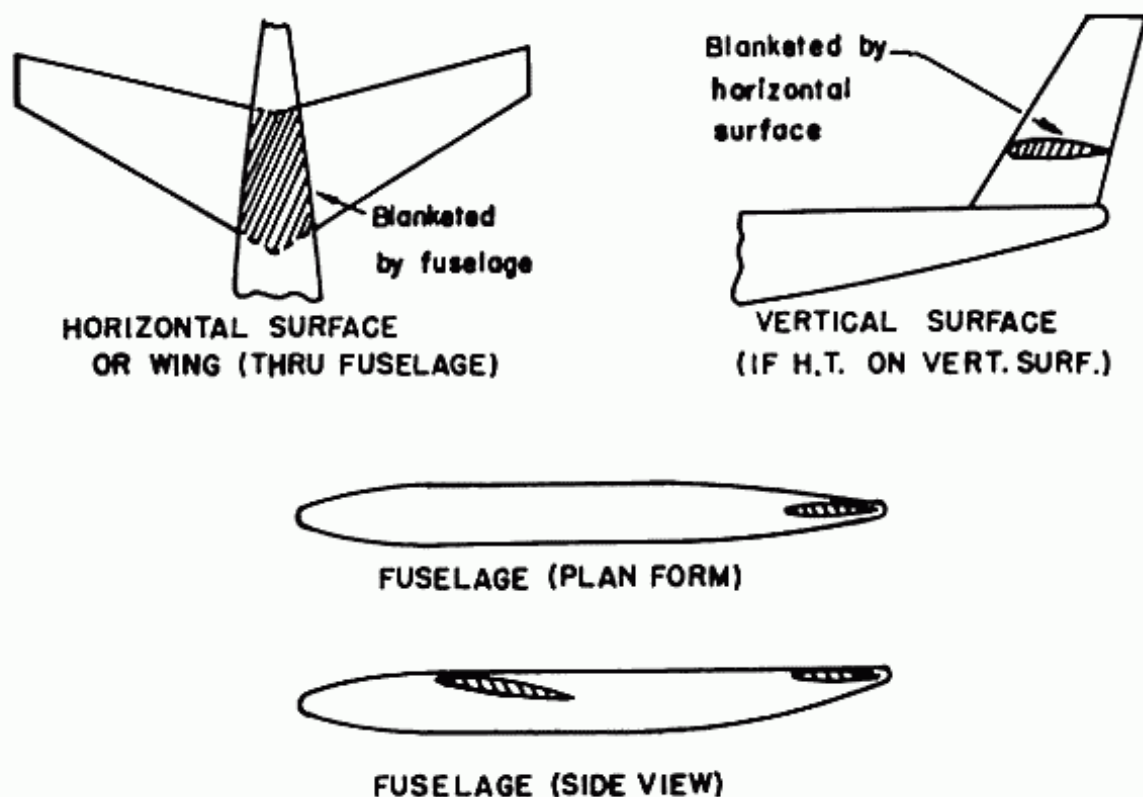


Fig. 6:2. Wetted areas of empennage wing and fuselage.

In determining the wetted area of an airfoil section, the effect of thickness must be accounted for. Figure 6:3 presents a factor K_p as a function of section thickness ratio, by which the chord may be multiplied to determine the perimeter of the airfoil. For sections with $t/c = .05$ and below, use K_p as 2.0.

A simplified method is suggested for determining the gross wetted area of the fuselage. The area of a cylinder, neglecting the front and rear flat plates is equal to the circumference of the circle times the length, that is

$$A = \pi DL$$

This may be presented as the area of the cylinder in side view, DL , times π . For a fuselage which has circular sections

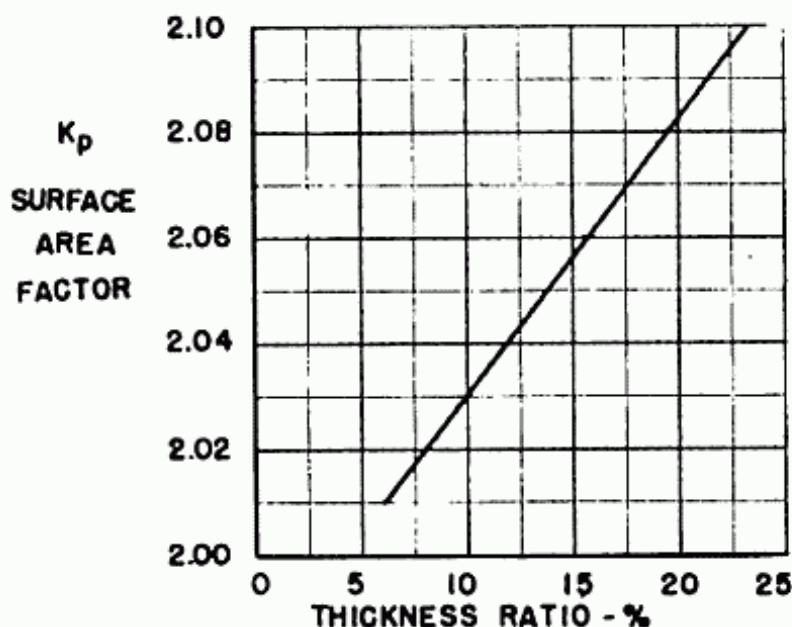


Fig. 6:3. Surface area factor as a function of thickness ratio. From N.A.C.A. 65 series of symmetrical airfoils.

throughout, an exact value of the wetted area may be obtained by multiplying the area in a side view by π .

This method gives good results with sections other than circular, if the average value of the areas in side and plan views is used.

6-4 Take-off Distance

In designing the airplane, the take-off distance requirement was used as one of the criteria for obtaining the thrust required for the airplane. From the derivation of the formula used to plot the curve Figure 2:14, it is seen that it is not a correct mathematical solution. It is now possible to make a more accurate check. This will be done for the ground run only, as it is the major portion of the take-off distance.

$$S = 1/2 at^2 = \frac{V^2}{2a} \quad (6:17)$$

where S = ground run

Therefore if a , the acceleration, was known as a function of the speed of the airplane from zero to take-off, the ground run could be obtained by $\int_0^{T.O.} \frac{V}{a} dV$. This can also be done by summing up the ground runs between finite values of velocity, if each acceleration is known. This is the method that will be used.

$$F = ma, \quad a = \frac{F}{m} \quad (6:18)$$

$$F = T_a - \text{Drag}_{\text{total}} \quad (6:19)$$

$$\text{Drag}_{\text{total}} = R + D \quad (6:20)$$

where R = friction drag

D = aerodynamic drag

$$\therefore \text{Drag}_{\text{total}} = \mu W_{\text{gr}} + \frac{\rho}{2} C_D S V^2; \quad V \text{ in ft/sec} \quad (6:21)$$

where μ is the rolling coefficient of friction

= .020 for rubber on concrete

$$\text{and } W_{\text{ground}} = W_{\text{TO}} - \frac{\rho C_L S V^2}{2} - \text{lift component of T} \quad (6:22)$$

$$F = T_{\text{avail}} - \left(\mu W_{\text{TO}} - \frac{\mu \rho C_L S V^2}{2} \right) - \frac{\rho C_D S V^2}{2} \quad (6:23)$$

$$C_D = C_{D_p} + C_{D_i} \quad (6:24)$$

$$C_{D_p} = f/S + C_{D_{\text{flaps}}} + \frac{f_{l.g.}}{S} \quad (6:25)$$

f/S is known

$C_{D_{\text{flaps}}}$ (flaps at max. deflection, and airplane at such a value of α so that $C_L = .75 C_{L_{\text{max}}}$)

$f_{l.g.}$ - from Figure 2:36

$$C_{D_i} = \frac{C_L^2}{\pi A \text{Re}} K \quad (6:26)$$

where K is the correction factor for ground effects and may be obtained from Figure 2:35

$$a = \left[T_a - \mu W_{\text{TO}} - \frac{\mu \rho C_L S V^2}{2} - \frac{\rho S V^2}{2} \left(f/S + C_{D_{\text{flap}}} + C_{D_{l.g.}} + \frac{C_L^2}{\pi A \text{Re}} K \right) \right] / m \quad (6:27)$$

It is now possible to obtain a , the acceleration, for any speed. Table 6:1 can be used to facilitate these calculations and the results plotted as shown in Figure 6:4.

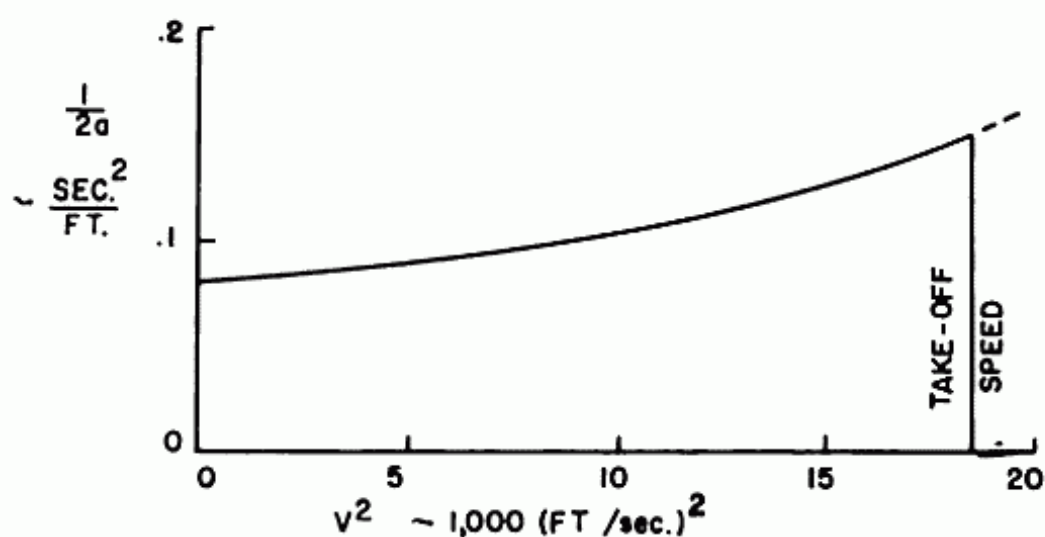


Fig. 6:4. Curve for determining ground run.

Table 6:1

- | | 0 | 40 | 80 | 120 |
|-------------------------------------------------------------|---|----|----|-----|
| 1. V | | | | |
| 2. V^2 | | | | |
| 3. μW_{TO} | | | | |
| 4. $\mu \rho C_L S V^2 / 2$ | | | | |
| 5. $R = (3) - (4)$ | | | | |
| 6. $D = \frac{\rho}{2} C_D S V^2$ | | | | |
| 7. $R + D$ | | | | |
| 8. $T_{avail}/plane$; obtained from engine characteristics | | | | |
| 9. $F = T - (R + D)$ | | | | |
| 10. $a = \frac{32.2 F}{W}$ | | | | |
| 11. $\frac{1}{2a}$ | | | | |

The area under the curve from $V = \text{zero}$ to V_{TO} is the ground run. V_{TO} is in knots.

$$V_{TO} = \sqrt{\frac{(W/S)_{T.O.} (296)}{\sigma C_{L_{TO}}}}$$

6-5 Cruise at Constant Altitude

The range of the airplane designed was calculated at a constant $W/\delta S$, that is, as the airplane weight decreased due to the use of fuel, the airplane climbed steadily. Under these conditions the airplane is flying at a constant $mi\delta/lb.$ and a constant T_r/T_a . Both these factors could be chosen as the optimum for the airplane.

It is interesting to study the possibility of flying at constant altitude. The range may be calculated readily by the $mi\delta/lb.$ method. Since the altitude is constant while W is changing, $W/\delta S$ is varying for the entire flight. For each value of $W/\delta S$, there will be a different value of $mi\delta/lb.$ The flight should be divided into four or five segments, and the range of each segment calculated by using the average $mi\delta/lb.$ times the increment of weight. The sum of these ranges will give the total range. The range at constant $W/\delta S$ will be greater than that at constant altitude, if the constant altitude is equal to the altitude at the beginning of the cruise at $W/\delta S$. This is true as long as the $W/\delta S$ cruising is not greater than the optimum $W/\delta S$, because then, at the lower altitude, $mi\delta/lb.$ will be smaller.

If the airplane is flying at constant altitude, the cruising speed can be increased if desired. This is due to the fact that at lower weights, subsonically the induced drag is lower and supersonically the normal force drag is lower, and there is less thrust required. The limit of the increase in speed is determined by two factors: the thrust required must not exceed the normal thrust available, and $C_{D_{comp}}$ should not exceed .0010. Since the M_{crD} is increasing as weight is decreasing (due to the decrease in C_L) the cruise speed can be increased to keep pace with it.

For airplanes with 2,000 n.m. all-out range and constant speed, the decrease in the range of a subsonic airplane due to flying at 35,000 feet constant instead of 35,000 at the beginning to approximately 38,000 at the end of cruise, was equal to approximately 10%. For a supersonic aircraft flying at its optimum altitude, a decrease in cruise altitude will likewise reduce its range.

6:10 SUPERSONIC AND SUBSONIC AIRPLANE DESIGN

PROBLEMS

- 1) By Navaer method, calculate range at design speed and at optimum speed.
- 2) Calculate actual take-off distance.
- 3) From the airplane drawing check " f " of airplane by C_f for each component. Compare result with f calculated from Equation 2:44.
- 4) Calculate the range of the subsonic and supersonic aircraft flying at constant altitude instead of in a climbing cruise.

Chapter VII
DISCUSSION AND RESULTS

7-1 General

The discussion of sections 7:1 thru 7:13 is presented as applying to subsonic aircraft, although some of the general trends would apply to supersonic aircraft. Section 7:13 will present some comments as to specific effects of supersonic aircraft design.

A series of airplanes were designed using the method and data presented in the preceding chapters. In all cases the airplanes climbed to 35,000 feet and then cruised at constant $W\delta/S$. The study was made to determine the effect of various specifications

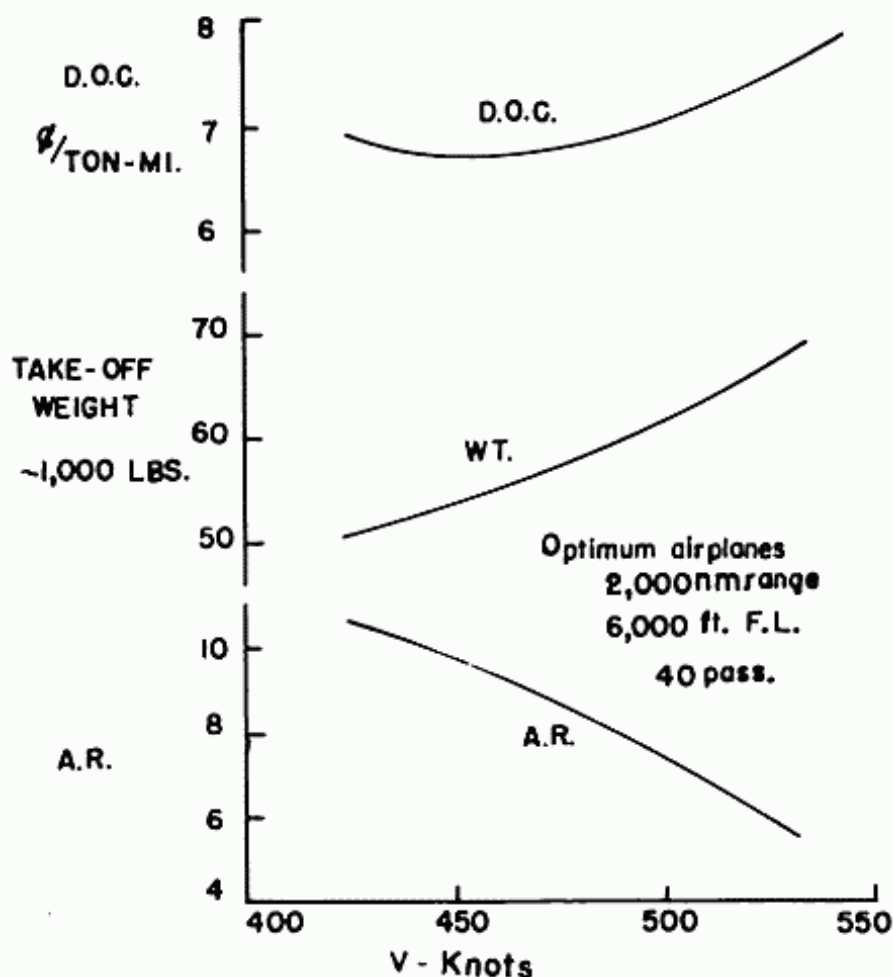


Fig. 7:1. Effect of Cruising Speed on Take-off Weight, Optimum A.R. and D.O.C.

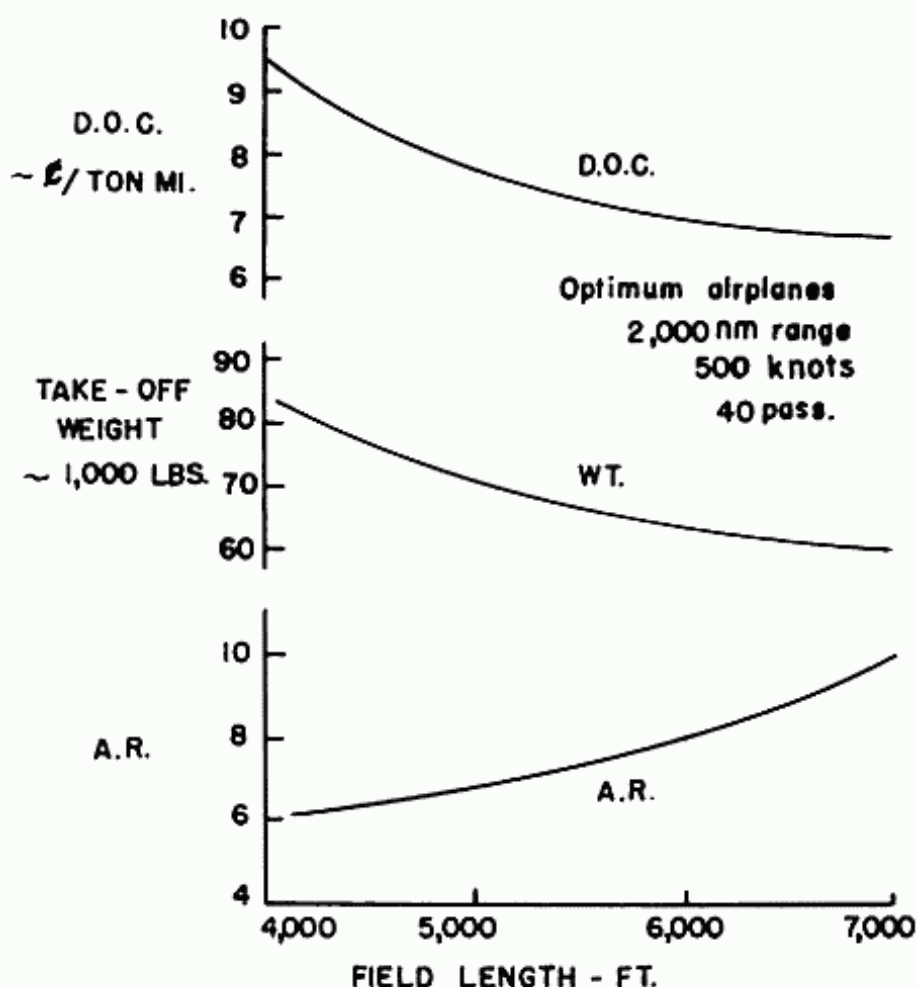


Fig. 7:2. Effect of Field Length on Take-off Weight, Optimum A.R. and D.O.C.

on the direct operating costs. Figures 7:1 and 7:2 present the variation of take-off weight and optimum aspect ratio as well as the direct operating costs, with cruising speed and field length. The discussion of these results and the effects of range and number of passengers compose a large portion of this chapter.

7-2 Effect of Speed

Figure 7:1 presents the trend of take-off weight, optimum aspect ratio and direct operating cost with variation in speed from 425 to 525 knots.

Take-off Weight

From Figure 7:1, it is noted that the take-off weight increases with increase in speed. To keep the difference between the M_{cruise} and the M_{CRD} of the wing at cruise constant, it is necessary that the thickness ratio decrease at constant sweepback at higher speeds. Since higher speeds cause higher drags, more thrust

and therefore a lower thrust loading is required. Both effects of thinner wing and lower thrust loading increase the take-off weight of the airplane.

Optimum Aspect Ratio

As can be seen from Figure 7:1, the optimum aspect ratio decreases with increase in speed. Aspect ratio directly affects the wing weight and the induced drag coefficient. As the speed of the airplane increases, the weight of the wing increases due to the required lower thickness ratio for the same $\Delta C_{D_{comp}}$. As the aspect ratio decreases it reduces the weight of the wing and therefore at the higher speeds where the decreased thickness ratio causes a high wing weight, the advantages of the low aspect ratio is the greatest.

The aspect ratio effect on the drag of the airplane is primarily due to the variation in the induced drag coefficient, C_{D_i}

$$C_{D_i} = \frac{C_L^2}{\pi A R e} \quad (7:1)$$

$$C_L = \frac{W/\delta S}{1481 M^2} \quad (7:2)$$

$$C_{D_i} = \frac{(W/\delta S)^2}{1481^2 M^4 \pi A R e} \quad (7:3)$$

From equation 7:3 it is seen that C_{D_i} is inversely proportional to the speed to the fourth power, if altitude is constant.

The parasite drag coefficient, C_{D_p} , which equals f/S , will decrease slightly with increase in speed. For the same wing loading and fuselage size, the wing area will increase faster than the equivalent parasite drag area, f , due to higher gross weight.

In the designs considered, the change in drag coefficient due to compressibility effects, $C_{D_{comp}}$, is constant.

Because C_{D_i} decreases rapidly with increase in speed, while C_{D_p} and $C_{D_{comp}}$ remain practically constant, C_{D_i} becomes a relatively less important factor in the total drag at the higher speeds. Therefore the disadvantage of increased C_{D_i} at low aspect ratio becomes less as the speed increases. It is the combination of the following two effects:

7:4 SUPERSONIC AND SUBSONIC AIRPLANE DESIGN

- (1) the advantage of decreasing the wing weight with low aspect ratio increases with higher speeds and
- (2) the disadvantage of increasing the C_{D_i} with low aspect ratio decreases with higher speeds,

that causes the reduction in optimum aspect ratio with increase in speed.

Direct Operating Costs

For a constant payload, the direct operating costs is mainly a function of fuel weight, empty weight and speed. It varies directly with the weights and inversely as the speed. As can be seen from Figure 7:1 the weights increase as the speed increases. Therefore the shape of the direct operating cost curve is dependent on the rate of change of the weight with speed. From this study the costs varied a little between 425 and 475 knots and then definitely increased at 500 knots. It should be realized that the actual shape of the curve depends upon the assumptions made in the performance and the direct operating cost calculations. Therefore, any modifications in the assumptions, formulas or charts, affecting the direct operating costs, can change the shape of the curve and the speed for minimum direct operating costs. However this study shows that there is an optimum speed for direct operating cost for any specified range, field length and payload. Variation in costs due to range, field length and payload will be studied in later sections.

7-3 Effect of Field Length

Take-off Weight

Figure 7:2 shows that as the required field length increases from 4,000 to 7,000 feet the take-off weight decreases, although the difference between 6,000 to 7,000 feet is quite small. An increase in specified field length allows a higher wing loading in landing. A higher wing loading, everything else being equal, reduces the weight of the wing and therefore the airplane. The higher wing loading, by reducing the wing area, decreases the parasite drag. This lower drag reduces the airplane weight by requiring smaller engines and less fuel for the same speed and range. However high wing loadings result in high cruising coefficients of lift, if altitude and speed is constant. This increase in C_L increases the induced drag coefficient, C_{D_i} , and the ΔM_{CR_D} due C_L . This larger ΔM_{CR_D} requires a wing of lesser thickness ratio for the same sweepback and therefore increases wing weight. The relative values of the decrease in weight caused by higher wing loading, and the increase in weight due to

the higher induced drag coefficient and the lower thickness ratio, determine the amount of change with field length.

It should be noted that the weight need never increase with higher specified field length. At field lengths greater than 7,000 feet this method might result in higher take-off weights. However since a field length specification only requires that it not be exceeded, evidently an airplane that meets a 7,000 foot field length requirement will meet the 8,000 foot requirement. It is quite unlikely that any transport that expects to be used in any but a few airports would have a field length requirement greater than 7,000 feet.

Aspect Ratio

The determination of the optimum aspect ratio is again one of comparing the effects of wing weight with the effects of C_{D_i} .

As field length increases, wing loading increases, wing weight decreases, while C_L and C_{D_i} increase. As C_{D_i} increases, its reduction due to increased aspect ratio is of greater importance. The wing weight decreases due to increased wing loading and increases due to the ΔM_{CR_D} effect of increased C_L , but the net ef-

fect is a decrease in wing weight. Since the wing weight decreases with increase in field length, the disadvantage of increasing it by increasing aspect ratio becomes less important with this increase in field length. Due to the facts that with increased wing loading

- (1) the advantage of reducing the induced drag coefficient by increasing aspect ratio is more important and
- (2) the disadvantage of increasing the wing weight by increasing aspect ratio is less important

the higher field lengths have a higher optimum aspect ratio.

Direct Operating Costs

Since speed and payload are constant, the costs vary directly with the fuel weight and the empty weight. Since they both decrease with an increase in field length from 4,000 to 7,000 feet the direct operating costs decrease.

7-4 Effect of Payload

Although a study to determine the quantitative effect of payload on the direct operating cost was not made, the qualitative results are known. As the payload increases, assuming that the number of passengers, baggage and cargo maintain a constant relationship, the size of fuselage must be enlarged. The result is greater weight and more drag of the fuselage. This effect, in turn, requires larger wings, engines and tail surfaces. However for

7:6 SUPERSONIC AND SUBSONIC AIRPLANE DESIGN

small and medium sized transports a 100% increase in payload does not result in an equivalent rise in all other factors, if speed and range are kept constant. Therefore the direct operating costs decrease with an increase in payload. The exact decrease depends upon the airplane specifications of range and speed.

Since it is obvious that the lower direct operating costs are more desirable, the change in costs with variation in payload would indicate that greater payloads should be used. However high payload, that is large numbers of passengers, present some definite disadvantages. Its greatest effect is on airline schedules. The greatest advantage of airlines over other modes of travel is that it is the fastest, and therefore saves the passenger valuable time. However for any means of transportation to be efficient and be of service to the public, it must also have frequent departures so that it is available when needed. If it is assumed that the airline business was constant, that is passenger miles per years did not vary, then an increase in passengers per plane would require a proportionate decrease in airplane departures. This reduction in the amount of airline flights could decrease the amount of passengers, since they would use other modes of travel that would be more convenient for them. It must be stated that there is another possibility. The reduction in direct operating costs due to larger payloads per airplane should be reflected in lower fares to the passenger. This reduction in fares would tend to increase airline business, perhaps enough to keep airline schedules the same as required with a lower payload. However it is not felt that a 50% increase in payload per airplane and the resulting decrease in costs could possibly result in a 50% increase in passenger miles.

Another disadvantage of greater number of passengers per airplane is the added difficulty that would be presented in the handling of passengers and baggage efficiently. Even at present, the loss of time in loading and unloading passengers and baggage, particularly in comparatively short flights, decreases the time saving that airlines offer. An increase in the payload per airplane would aggravate this problem.

There is one intangible advantage to larger airplanes and one disadvantage. The advantage lies in the fact that a large airplane, as a large boat, seems to have more appeal to the public. The disadvantage is that a huge number of casualties due to one accident presents spectacular and undesirable publicity.

7-5 Effect of Range

The results presented in Figure 7:1 and 7:2 are for an allout range of 2,000 n.m. As previously stated this is equivalent to

approximately 1,115 n.m. scheduled airline distance with no allowance for headwind. A study to determine the effect of range on the direct operating costs shows that for a forty passenger airplane the lowest cost is obtained for about 1,000 n. m. scheduled distance, in the speed range of 425 to 525 knots. However many other factors aside from costs must be considered in determining what range the jet transport should be designed for.

It is obvious that an airplane designed for 1,000 n.m. range could be used for a lesser range. However costs for a jet transport increase quite rapidly if flown at a range lower than its design range, particularly below 1,000 n. m. Therefore if a jet transport is to be used for 500 n. m. flights exclusively, a much more efficient airplane would be one designed for this range. The range of a jet transport can seldom be flown at ranges above its design range without reduction in payload, which causes an excessive increase in costs per passenger mile. However for routes over land, flights may be broken up to pick up fuel, and to load and unload passengers. For routes over water, there is at this time no reliable or economical refueling method available to transport airplanes.

If it were desired to design one jet transport to service all of continental United States, the maximum allout range required would be approximately 3,400 n. m. This would be for a east-west non-stop flight from New York to Los Angeles with 700 n.m. range reserve and allowing for a 100 knots headwind cruising at 500 knots. The minimum allout range required would probably be about 500 n. m. This would be equivalent to a New York to Washington, D. C. flight with reserve equal to the airline distance and an allowance for maneuvering. Obviously the minimum is far too low as it would be only available for short flights and would require too many stops transcontinental. The maximum allout range airplane would be extremely uneconomical on short flights. However it could be used for trans Atlantic flights with a stop at either the Azores or Gander on the East-West trip. To make a jet plane for this range economical, in fact feasible, would require a large payload and introduce the inherent disadvantages. It should be realized that although the high specific fuel consumption of jet engines make long range flights appear quite costly as compared to reciprocating engined airplanes, it is in the longer ranges that the advantages of the high speed and greater comfort of the jet transport are accentuated. At this time it appears that a jet transport of a little more than 2,000 n. m. all out range presents the best compromise for continental United States use. It would still be economical for

7:8 SUPERSONIC AND SUBSONIC AIRPLANE DESIGN

500 - 600 n. m. scheduled flights, be able to make many flights between important cities non-stop and cross the country with two or three stops to add fuel, and load and unload passengers.

Although it might be more economical in direct operating cost to have a medium range jet transport instead of a long range one, the long range transports have been developed by Boeing and Douglas because of the huge trans-Atlantic market. This same airplane can be used economically on the non-stop trans-continental flights. The French Caravelle is trying to fill the medium range market and the other companies have been interested in this field also.

7-6 Effect of Altitude

It was previously stated that the determination of the desired flight altitude presented complex problems but that probably a higher cruise altitude resulted in a lower direct operating cost. A study was made to obtain the difference in direct operating costs between airplanes cruising at 35,000 to 38,000 feet and others at the optimum altitude for the same wing loading. This wing loading was the maximum that would result in the required field length. The optimum altitude was defined as the altitude at which range is a maximum. The method of calculating the optimum altitude is presented in Section 2:11.

As the required landing field decreased, the maximum permissible wing loading decreased, and the optimum altitude became higher. For the 4,000 foot field length, it was from 50,000 to 53,000 feet. The direct operating cost at this altitude was approximately 15% lower than at the 35,000 to 38,000 foot altitudes, for the same field length. This airplane cruised at 500 knots and had a payload of forty passengers. For the field length of 6,000 feet the percent reduction in costs was lower. In fact for some combination of requirements the 35,000 to 38,000 foot cruising altitude proved to be the same as the optimum. It is even possible that cruising at the optimum altitude, as defined, will result in a higher direct operating cost than the 35,000 foot cruise. This is due to the fact that higher n.m./lb. is counteracted by the lower thrust loading that might be required. That is, the increase in direct operating cost due to the larger engines might be greater than the decrease in cost due to lower fuel consumption. From the results of the study of one particular set of specifications, the designer can decide if the economics, presented by high altitude flight, justify its use in the face of the added problems it presents.

Wing loadings lower than the maximum required for landing

field may be used to improve the high altitude conditions. The low wing loading reduces the C_L caused by low density at high altitude and therefore decreases the C_{D_i} . It is possible that in some designs, the inefficiency of adding weight and profile drag caused by lower wing loading may be offset by the resultant reduction in C_{D_i} at very high altitudes. However this is not usually the result and the most economical airplane is the one with the highest wing loading consistent with field length requirement, cruising at its optimum altitude.

Before a final choice of cruising altitude is made, the variation in head winds and turbulence with altitude must be studied. The disadvantages of high head winds and high turbulence at a certain altitude might offset the advantages previously calculated.

7-7 Theory of Maximum W/S and W/T

The design method presented is based upon the theory that the airplane that has the highest W/S and the corresponding W/T required to meet the specifications will be the optimum airplane. The wing loading is determined by the landing field requirement, and the maximum that will meet this specification is used. The maximum thrust loading that will then provide sufficient thrust to meet the climb, cruise and take-off requirements is used in conjunction with this wing loading.

If a wing loading lower than the maximum required for landing field is used, the airplane will still meet the field length specification. With this lower wing loading a higher thrust loading may be used if the take-off field is critical for thrust. The advantage of this higher thrust loading will tend to offset the disadvantage of the lower wing loading. A similar condition would exist if the airplane were critical for climb. However for the airplanes that are critical for cruise, as most high performance jet transports are, the added parasite drag of the lower wing loading would offset the advantage of the lower induced drag and require a lower thrust loading.

The results of the effect of required field length is actually the effect of varying wing loading. As the field length required decreased, the maximum wing loading was reduced. Therefore as can be seen from Figure 7:2, a decrease in wing loading resulted in an increase in direct operating costs. This proves that for the airplanes being investigated at 35,000 foot cruise, the

maximum wing loading theory is correct. The effect of lower wing loadings on very high altitude is discussed in Section 7-6.

Aside from the aerodynamic advantages of the higher wing loading and the reduced wing weight for the same airloads, there is a definite advantage in gust load factor and passenger comfort. This aspect is discussed more thoroughly in Chapter XII. However it should be stated here that gust load factors are usually critical for high speed jet transports and high wing loadings result in lower gust load factors. These smaller load factors decrease the airplane weight and increase passenger comfort.

7-8 Effect of Ground Deceleration

Wing loading, one of the most important factors in the direct operating costs of an airplane, is based upon the landing field requirement. The greatest portion of this distance is the landing ground run, which is a function of the deceleration as well as wing loading. From Section 2:3, the ground run,

$$S_G = \frac{925 W/S}{-a \sigma C_{L_{\max}}}$$

where $-a$ is the average deceleration

From Figure 7:2, it is seen that the direct operating cost of the airplane with the 4,000 feet landing field is approximately 20% higher than the 5,000 foot one. The difference in these costs is due to the wing loadings of the airplane. Therefore if the deceleration of the 4,000 foot airplane could be increased so that the same wing loading could be used as the 5,000 foot airplane, equal direct operating costs would result. As the required landing field increases, the variation in costs diminish until about 7,000 feet, where an increase in landing field would have no effect on direct operating costs. Therefore, the deceleration which affects the landing field is most important for airplanes with small field length requirements. In fact it is important to note at a field length requirement of 7,000 feet an added deceleration device might not reduce the direct operating cost at all by allowing a higher wing loading.

The maximum deceleration obtainable is dependent on many factors, size and type of brakes, type of landing gear, pilot technique and special devices such as reversible pitch propellers and landing chutes. New mechanisms are being devised to eliminate the pilot technique factor. These consist of an automatic device which will decrease pressure on the brake as soon as the tire begins to skid. The jet transport does not have the reversible pitch propeller alternative to increase its deceleration. This

method has been very effective on propeller airplanes and in some cases has increased the deceleration from 6 feet/sec.² without reversible pitch, to 10 ft./sec.² with it. As a substitute the jet airplanes now have reverse thrust mechanisms which should prove as effective as reverse pitch props. See Fig. 2:10a.

7-9 Take-off Distance

In the first attempt at determining the thrust loading required for the airplane, the take-off distance was used as the criterion, and Figure 2:14 was the basis for it. As can be seen from the derivation of the formula, upon which the curve was based, the take-off field obtained is not very accurate. After the airplane is designed the more accurate method, as described in Section 6:4, may be used.

The results showed that for all the airplanes designed, the maximum error ranged between -10% and 5%. In the few cases where take-off field was critical, a modification of the airplane could be made, if necessary.

7-10 Equivalent Parasite Drag Area, "f"

The equivalent parasite drag area used in design was based upon Equation 2:44

$$f = 1.10 + .128 N_p + .0070 S + .0021 N_e (T_e)^{.7}$$

After the airplane has been completely drawn up, a more exact answer may be obtained from the method presented in Section 6:3. The results from Section 6:3 only varied by approximately 5% from the original calculation.

7-11 Engine Choice

In determining the engine size for variation airplanes, the J-1 engine characteristics were used as typical. These characteristics represent an advanced theoretical engine and should be representative of a good production jet engine for a number of years. The minimum fuel consumption in cruise occurs between .70 and .80 normal thrust. This characteristic indicates that the most efficient airplane is one that cruises at some figure greater than 70% to 80% normal thrust. Since engine repairs and overhaul periods are a function of the temperature and r.p.m. the engine is running at, this high cruise thrust is comparatively inefficient in this respect. The engine manufacturers have pointed

7:12 SUPERSONIC AND SUBSONIC AIRPLANE DESIGN

out that it is possible for the thrust at minimum specific fuel consumption to be at a lower percentage of the normal thrust. If the airplanes were flown at this lower thrust, the engine life and overhaul period could be increased, thereby decreasing the engine cost. This possibility adds another variable to those already existing in jet transport design.

The use of a cruise thrust that is a lower percentage of the normal thrust, requires a larger engine and therefore increases the engine cost as well as the costs of all the other components. If the decrease in cost due to increased engine life and overhaul period, is greater than the increase in costs due to large engines, the larger engine would be desirable. The full effect of such a change should be studied before a cruise thrust that is a lower percentage of normal thrust is used, as it effects many factors, intangible ones as well as the direct operating costs.

7-12 Airplane Efficiency Factor "e"

An established accepted formula for calculating the induced drag coefficient, C_{D_i} is

$$C_{D_i} = \frac{C_L^2}{\pi A R e}$$

where "e" is the airplane efficiency factor

This factor is determined empirically only, although there is some good theoretical basis. Since e is practically always less than one, it represents an increase in drag. There are three main factors that it accounts for. They are: the increase in drag due to a non-elliptical spanwise airload distribution on the wing; the increase in trim drag; and the increases in drag on all the airplane components that might be attributed to angle of attack.

Non-Elliptical Spanwise Air Distribution

The effect of the non-elliptical spanwise airload distribution on C_{D_i} for low speed airplanes has been fairly well established. However, for most designs it is a comparatively unimportant factor. Figures 4:2a and 4:2b show the variation in ϕ with aspect ratio and taper ratio, where ϕ is the induced drag correction factor for the non-elliptical distribution.

$$C_{D_i} = \frac{C_L^2}{\pi A R} (1 + \phi)$$

It is seen that for taper ratios from .2 to .7, ϕ does not exceed .025, and from .3 to .5 it is approximately .010. Since

many airplanes with taper ratios between .3 and .5 have an "e" equal to .80, it is evident that this effect is relatively unimportant.

For high speed airplanes this effect may be somewhat higher. Figure 7:3 shows the variation in C_1 with span for a wing with elliptical spanwise distribution and one that has not. For an airplane flying at $C_L = .2$, the wing with the elliptical spanwise loading distribution will have a C_1 equal to .2 throughout the span, while the C_1 of the non-elliptical loaded wing will exceed the value of .2 along some portion of the span. From Figure 2:7 it will be seen that in this case the non-elliptical loaded wing will encounter some compressibility drag due to C_L , while the wing with the elliptical spanwise loading will not. This effect however is admittedly quite small.

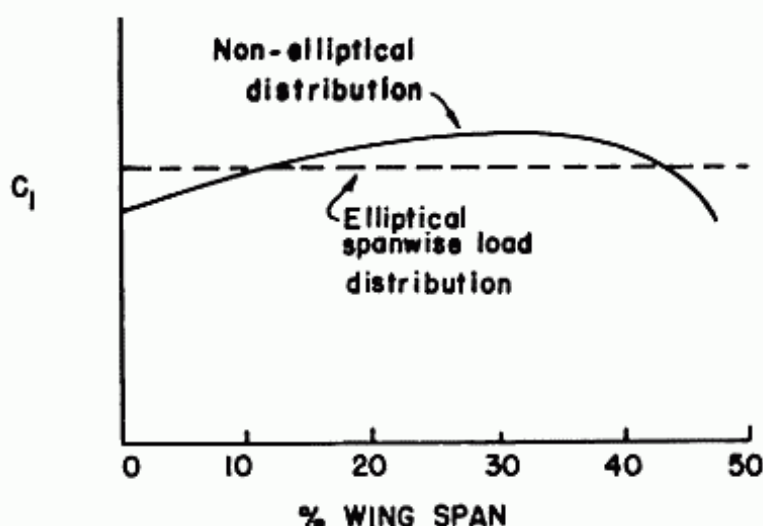


Fig. 7:3.

Trim Drag

Another factor is the variation in airplane drag due to elevator deflection. At each C_L a different elevator position is required to keep the airplane in equilibrium. The change in elevator deflection results in a different tail load and therefore a change in the induced drag of the tail.

Drag Due to Variation in Angle of Attack

The largest factor in the value of "e" is that portion of the drag of the airplane that is increased with angle of attack. This includes the change in the drag of the fuselage, nacelle, tail surface and interference effects. Since C_L is a function of angle of

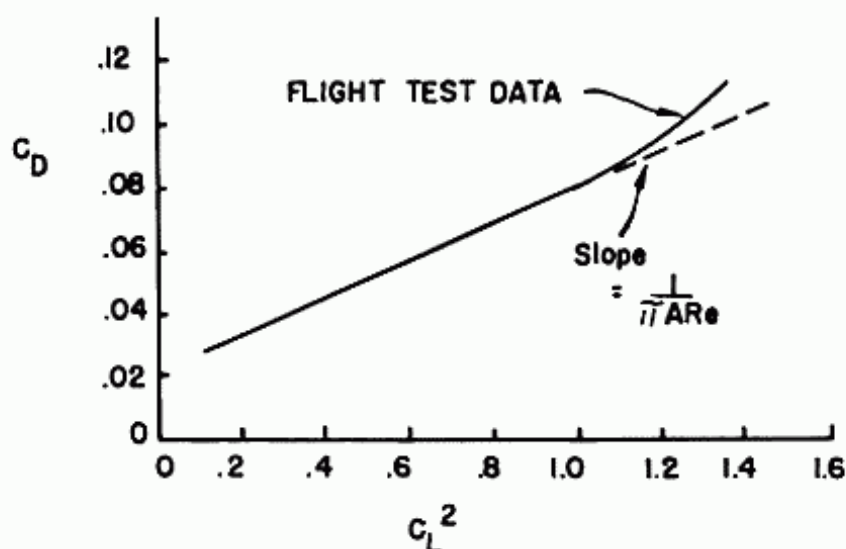


Fig. 7:4.

attack this factor has been introduced in C_{D_i} which is a function of C_L .

Determination of "e"

The determination of "e" from flight tests is based upon plotting the curve of C_D vs. C_L^2 as shown in Figure 7:4.

Neglecting compressibility effects

$$C_D = C_{D_p} + \frac{C_L^2}{\pi A R e}$$

From Figure 7:4 it is evident that the slope of the curve that is approximated by a straight line is equal to $\frac{1}{\pi A R e}$. From this relation "e" can be obtained.

The airplane efficiency factor "e," as actually determined from flight test, usually varies between .70 and .95. The value of .8 is usually used for preliminary design purposes, if there is no basis upon which to use another value.

Variation of "e" with A.R.

As aspect ratio was varied on each airplane, the induced drag coefficient, C_{D_i} was assumed to equal $C_L^2 / \pi A R e$. Although this is general practice, this method can be refined somewhat. The factor "e," as explained above, primarily accounts for the wing drag variation due to non-elliptical spanwise lift distribution, the variation in drag of other parts of the airplane due to change in angle of attack, and the variation in trim drag. Therefore the induced drag coefficient may be written as:

$$C_{D1} = \underbrace{\frac{C_L^2}{\pi AR} (1 + \phi)}_{\text{due to wing}} + \underbrace{\left[\frac{C_L^2}{\pi ARe} - \frac{C_L^2}{\pi AR} (1 + \phi) \right]}_{\text{due to all factors except wing}} \quad \text{Equ. 7:4}$$

It is generally accepted that for one airplane the part of the drag due to all factors except the wing is essentially independent of aspect ratio. Therefore as the aspect ratio changes the first term of Equation 7:4 changes but the second term remains essentially constant. Actually as aspect ratio increases and the mean aerodynamic chord decreases, the horizontal tail area decreases since it is proportional to the wing M.A.C. However since this factor accounts for only part of the trim drag, and trim drag is only part of "e," the second term can still be assumed as approximately constant.

Therefore, if this second term is to remain constant, e must be decreased as aspect ratio is increased. This is significant since the optimum aspect ratio for each set of specifications will be lower if this method of varying e with aspect ratio is used, instead of the usual practice of maintaining e constant while changing aspect ratio.

7:13 Supersonic Airplanes

The best trends in the effect of cruising M and ranges for supersonic transports are available from ref. 3:1. As in the subsonic studies the use of Breguet's range formula is most helpful.

Effect of Gross Weight on Range

Fig. 7:5 presents a curve of W_0/W_1 versus cruise M for various gross weights. This shows that from M = 2 to M = 5 there are large gains to be made in W_0/W_1 by increasing gross weight. This shows up particularly in the range since range is proportional to $\log(W_0/W_1)$. Note that for $W_0/W_1 = 1.4$ and 2.2, $\log(W_0/W_1)$ is respectively .147 and .343.

Although the data in figure 7:5 may be conservative it does indicate the importance of increasing gross weight to increase range, and the discussion indicates the importance of obtaining a high value of W_0/W_1 .

Effect of Cruise M on Gross Wt. and D.O.C.

Fig. 7:6a presents gross weight vs cruise M, and 7:6b D.O.C. vs. cruise M. For both cases two ranges are considered, as well as afterburner and non afterburner engines.

It is interesting to note that for the assumptions made and the

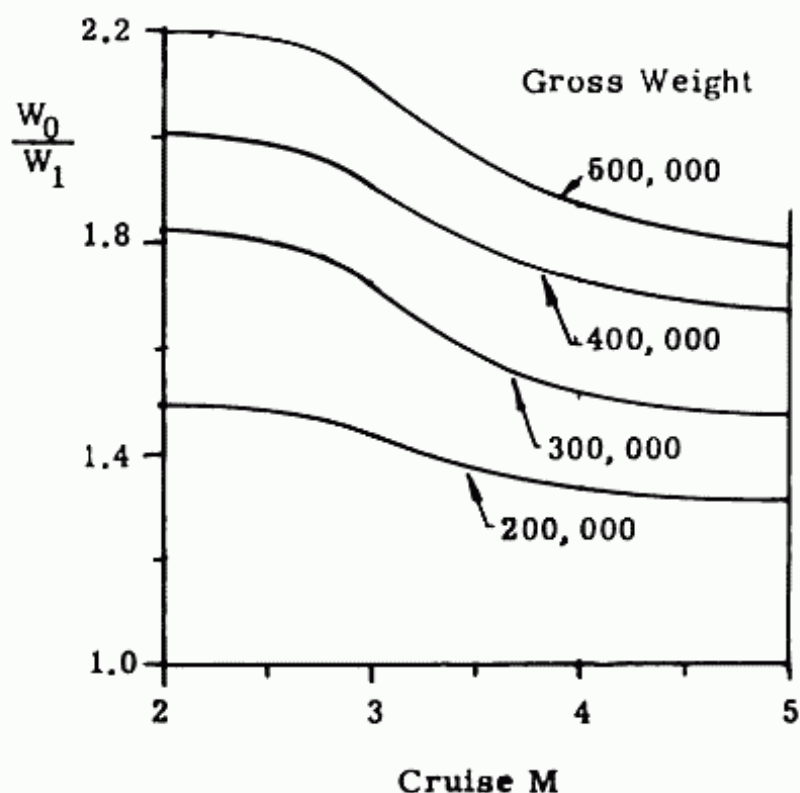


Fig. 7.5. Weight ratio vs. cruise M

engine characteristics used, below $M = 3.0$ the non afterburner engine is more efficient than the afterburner engine, since D.O.C. is still the best criteria. If the results of these studies are correct it would appear that a non afterburning engine airplane with about 4,000 n.m. range and a cruising M of somewhat over 2.5 will be the first supersonic transport to be sold. This airplane will weigh about 300,000 lbs. and have a direct operating cost of about 1.25 ¢/seat mile. At M greater than 2.5, the D.O.C. increases rapidly, and aerodynamic heating problems increase. Non-afterburning engines are much more desirable than the afterburning variety since they are much quieter. However, if the A/B is not required for take-off it is unlikely that the noise at altitude will be a problem.

The 4,000 n.m. range has been selected since N.Y. to London is 3,000 n.m. without reserve or head wing allowances and it would appear that a supersonic airplane should have at least this range, and more.

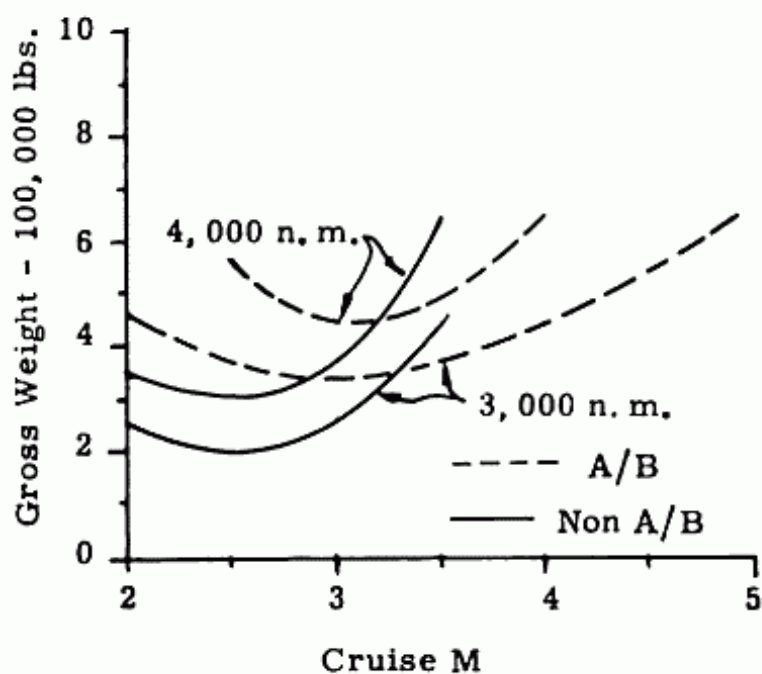


Fig. 7:6a. Gross Wt. vs. cruise M.

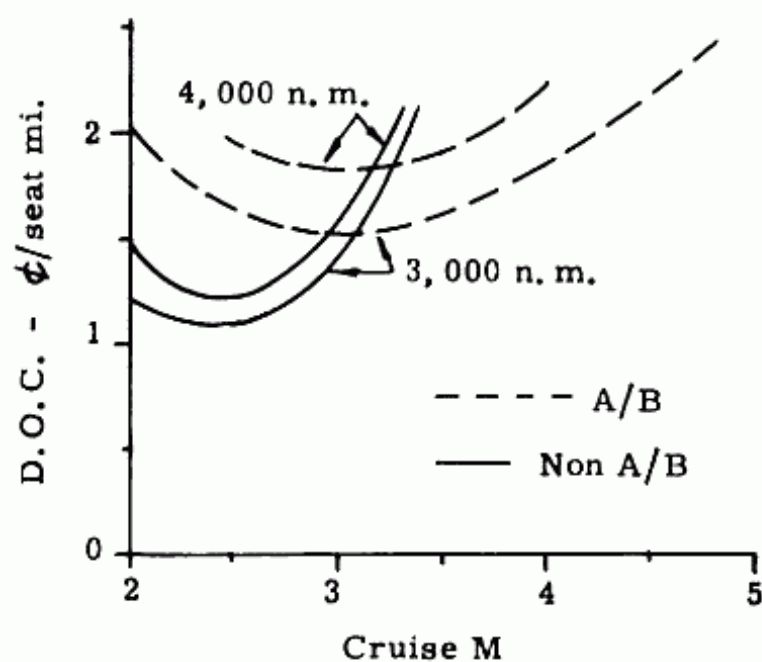


Fig. 7:6b. D.O.C. vs. cruise M

Chapter VII

APPLICATION OF METHOD TO OTHER TYPES OF AIRCRAFT

8-1 Introduction

The method of design presented in Chapter II is presented with the jet commercial transport as an example. However the ideas and method can be used in the design of any type of airplane. This chapter will show how this method must be revised to design other aircraft and will also present the additional data required.

8-2 General

The most important principle involved in this preliminary design method is the isolation of airplane characteristics that are dependent on one performance specification, or a combination of these specifications.

Landing field is one very important specification since it sets the maximum landing wing loading immediately, if a few characteristics such as maximum C_L , ground deceleration and lift/drag for landing can be established or estimated. Take-off field length is one criteria for thrust loading, if take-off wing loading has been determined. However other specifications and requirements, such as speed and climb, can be critical for thrust loading.

The number of passengers designs the fuselage. The speed and altitude specifications determine the wing sweepback and thickness ratio. These same specifications or others as required by various type airplanes can be used in many designs.

Before discussing aircraft powered with reciprocating or turbo-prop engines, it is necessary to have a brief discussion of propellers and propeller efficiency.

8-3 Propellers

General - Maximum Efficiencies

For both reciprocating and turbo-prop engines, it is necessary to choose suitable propellers and determine their propulsive efficiencies. The thick-bladed propellers used for reciprocating engine airplanes during the early 1940's were designed for maximum efficiency at about Mach number 0.5. The efficiency of these propellers dropped off rapidly with increase in Mach number. For this reason it was necessary to change the design so that high efficiency could be maintained at high Mach

8:2 SUPERSONIC AND SUBSONIC AIRPLANE DESIGN

numbers. Figure 8:1 represents the maximum propeller efficiency vs. airplane Mach number, and on this basis each curve is a plot of optimum design points, and does not represent the performance of a single propeller.

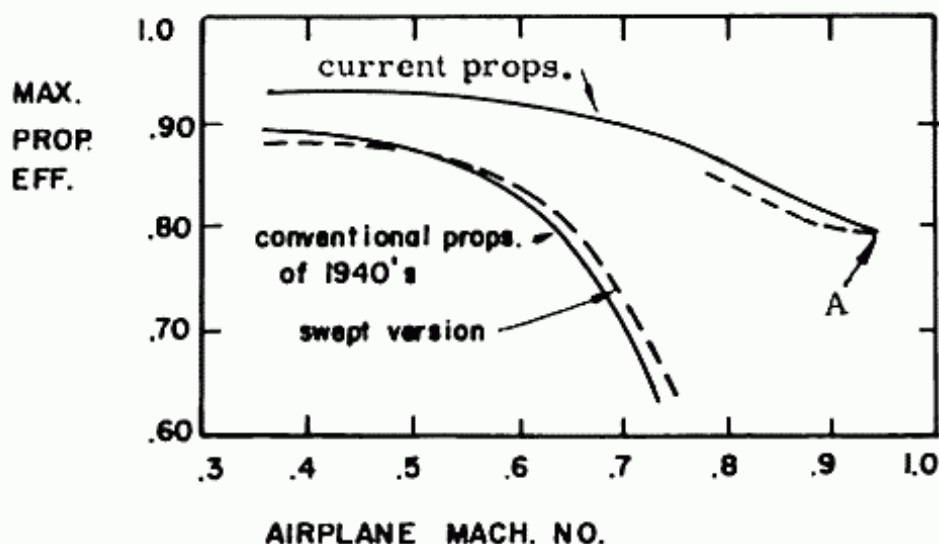


Fig. 8:1. Maximum Propeller Efficiency vs. Airplane Mach Number.

The curve labeled current props ends at point "A" at $M = .94$. This point and the dotted line connected to it, are the efficiencies obtained from one extremely thin propeller tested in Ref. 8:1.

Comparative Efficiencies of Individual Propellers

Figure 8:2 presents propellers designed for operation at .5, .7 and .9 Mach numbers.

Propeller "A" indicates the kind of propeller which was commonly designed in the early '40's. The propeller is characterized by cylindrical blade shanks and by working blade sections about 10% thick. Such a propeller is intended for application at speeds up to approximately .5 Mach number, and for this speed range it is still the type of propeller most commonly used. A typical application of this type would be a three bladed propeller of between 11 and 13 feet in diameter, which would absorb 1500 to 2000 horsepower at a rotational speed of between 1200 and 1500 RPM.

Propeller B was developed in the late '40's for cruising speeds of about $M = 0.7$. Through this design, the major faults of the earlier propeller have been eliminated. For this propeller, the thickness ratio of the working sections have been reduced to about 6% and the cylindrical shanks have been replaced by airfoil sections which extend to the spinner surface. The

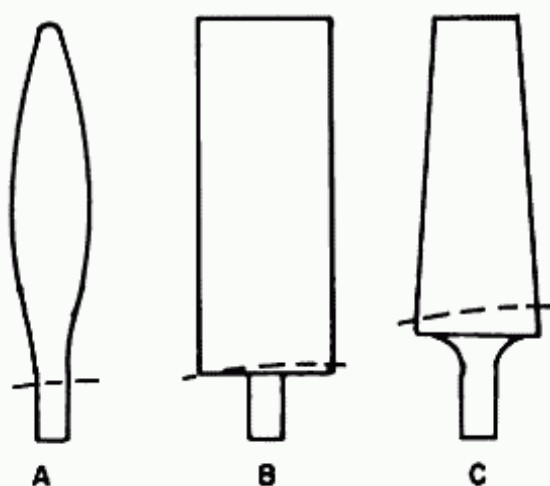


Fig. 8:2. Typical propellers.

essential feature of this propeller is that it operates at relatively low values of rotational speeds by which means the adverse effects of compressibility are delayed until higher forward speeds are obtained. These changes have resulted in a propeller which will operate efficiently at flight speeds of .7 Mach number and still remain as efficient as the older type propeller in the lower speed range.

In this case, a practical application would be represented by the use of a 14 foot diameter, 4 blade single or 6 blade dual rotational propeller turning at a rotational speed of between 800 and 1000 RPM and absorbing approximately 5000 horsepower at 500 MPH.

Propeller "C" is essentially a highly refined version of the best modern propeller previously described, and its characteristic feature is its extremely thin blades. For this type of propeller, the fact is accepted that adverse compressibility effects can no longer be avoided by reduction of blade section speed and, therefore, every effort is made to reduce the magnitude of loss which is known to occur. Reduced blade thickness has been found to be the most effective means of minimizing compressibility losses at high speeds and therefore a very thin bladed propeller results. Fig. 8:2a presents the physical characteristics of the propeller whose efficiency is shown by the dotted line in fig. 8:1.

The comparison of propeller efficiency is presented in Figure 8:3. The break in efficiency curves, which occurs for the various propeller types, denotes the speed at which the adverse effects of compressibility cause an increase in drag, leading to a rapid loss of efficiency with further increase in speed. As is also noted, the propeller with the thin blade sections not only delays the onset of compressibility losses, but also reduces the rate of efficiency losses with increased forward speed. Thus, through the use of properly designed propellers, efficiencies of

8:4 SUPERSONIC AND SUBSONIC AIRPLANE DESIGN

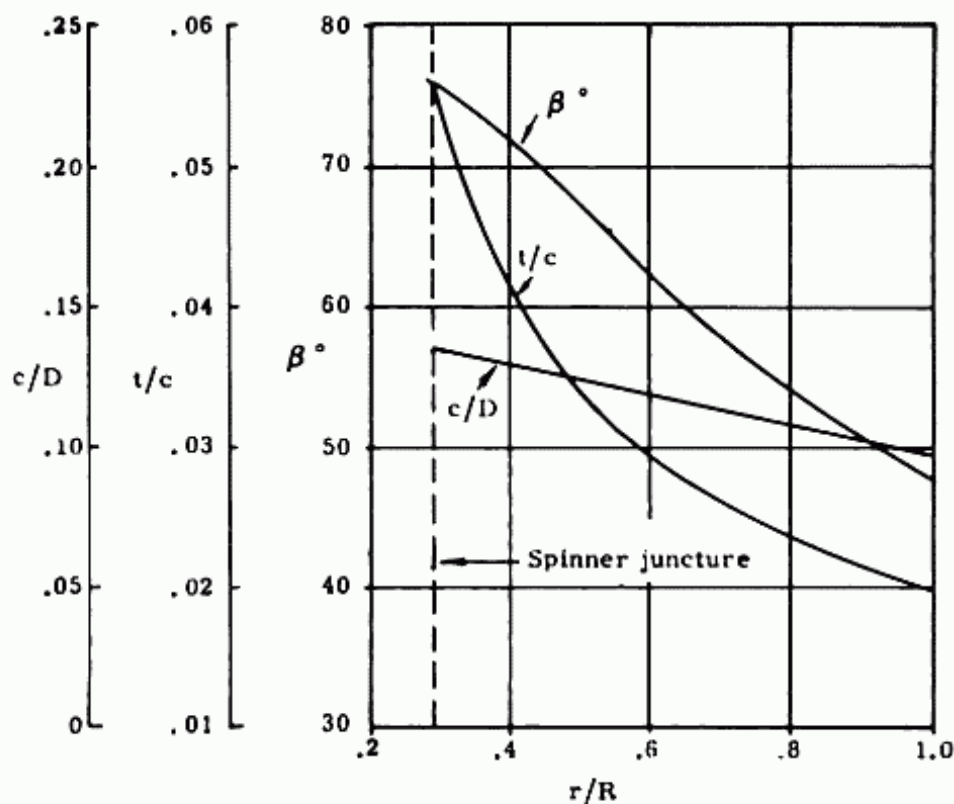


Fig. 8:2 a. Physical Characteristics of Supersonic Prop. (Ref. 8:1)

the order of 80% and greater can be maintained in subsonic, transonic, and supersonic flight regimes.

Figure 8:3 shows the comparative propeller efficiencies for these propellers.

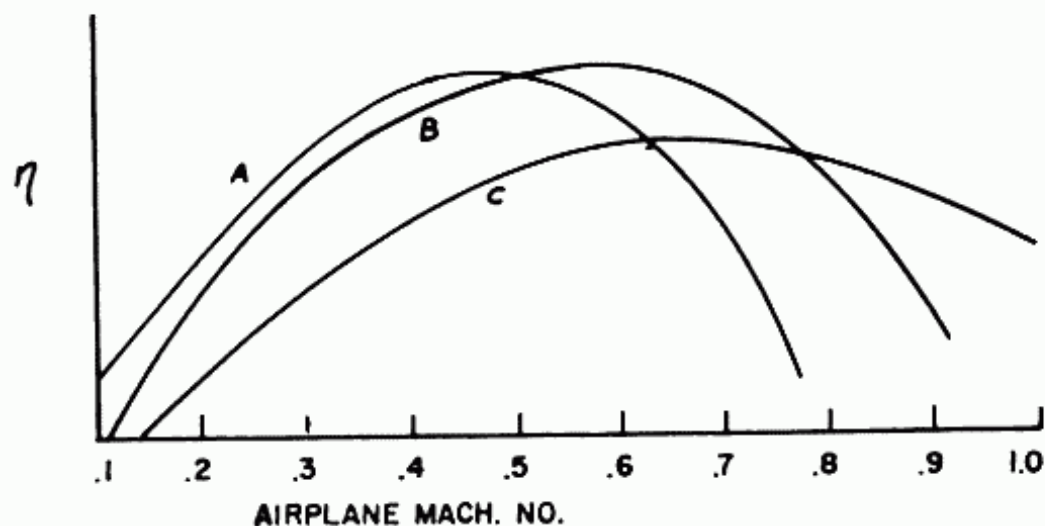


Fig. 8:3. Comparative Propeller Efficiencies vs. Mach Number, courtesy Aero Products.

Propeller Weights

The weight of these propellers designed for Mach numbers from .5 to .9 is between .17 and .20 pounds per horsepower at the static take-off condition. This approximately equal weight condition arises through a progressive reduction in propeller diameter as airplane Mach number increases. Actually the weight per horsepower has decreased with increase in airplane Mach number.

Definition of Propeller Efficiency

Before going into the selection of a propeller for optimum efficiency, the efficiency of a propeller is defined.

A propeller is a means of converting the work done by a power plant into useful work to drive the airplane. The propeller efficiency, η , is the ratio of these items, that is;

$$\eta = \frac{\text{Useful work done on airplane}}{\text{Work output of power plant}} = \frac{\text{THP}}{\text{SHP}}$$

Where THP = Thrust horsepower

SHP = Shaft horsepower

Shaft horsepower (often referred to as brake horsepower) is the power delivered to the engine shaft. The propeller takes the power from the shaft and converts it to thrust horsepower.

In turbine-propeller engines a term, equivalent shaft horsepower, ESHP, is used.

Although a turbo-prop engine delivers most of its power to the shaft, there is still some thrust derived from its jet exhaust, which can be converted to horsepower.

In order to establish a proper equivalency between direct shaft horsepower and jet output, the power plant manufacturers have set a standard practice of accounting for propeller efficiency. They have set an efficiency of 80% for all conditions above 105 knots, and a static thrust propeller effectiveness value of 2.5 lbs. of thrust per horsepower for the zero air-speed condition, up to 105 knots.

Therefore,

For airspeeds above zero m.p.h.

$$\text{E.S.H.P.} = \text{Direct S.H.P.} + \frac{(\text{Net Thrust})(\text{Velocity in knots})}{(326)(.80)}$$

For static condition,

$$\text{E.S.H.P.} = \text{Direct S.H.P.} + \frac{T}{2.5}$$

It should be noted that the factor 2.5 in the $T/2.5$ term is strictly an average empirical value. The exact factor must be obtained by a test of the particular propeller at the r.p.m. and forward speed being considered, or by a theoretical approach utilizing the propeller characteristics and speeds.

Determination of Propeller Efficiencies

The momentum theory of propellers is the basis of these charts. The development of this theory is available in many texts. In this section only the method of determining the efficiencies will be presented. The following terms and their definitions are required for the use of these charts:

$$J = \frac{101V}{ND}$$

$$C_p = \frac{(\text{SHP}/1000)}{2(N/1000)^3 (D/10)^5 \sigma}$$

Where D = propeller diameter in feet

V = forward velocity in knots

N = rotational velocity in revolutions per minute

$$C_{px} = \text{effective power coefficient} = \frac{C_p}{X}$$

Where X is an adjustment factor dependent on activity factor AF , and whether single or dual rotation is used.

$$AF = \frac{100,000}{16} (\text{No. of blades}) \int_{0.2}^{1.0} \left(\frac{r}{R}\right)^3 \left(\frac{b}{D}\right) d\left(\frac{r}{R}\right)$$

Where R = propeller radius

D = propeller diameter

r = radius of point being considered

b = blade width at given r

Activity factor is a non-dimensional form which is an indication of the capacity of the propeller to absorb power. The activity factor can be determined by numerical integration. That is, if $(r/R)^3 (b/D)$ is plotted against r/R , the area under the curve between .2 and 1.0, multiplied by $(100,000/16)$ (No. of blades) is the activity factor. Activity factors usually vary between 80 and 150.

Figure 8:4 shows propeller efficiency η , plotted against $J/(C_p)^{1/3}$ for various values of C_{px} ; and X versus total activity factor for single and dual rotation propellers. This adjustment factor, X , is necessary to determine C_{px} .

Two other corrections are required for maximum accuracy in determining efficiency; one accounts for the profile drag

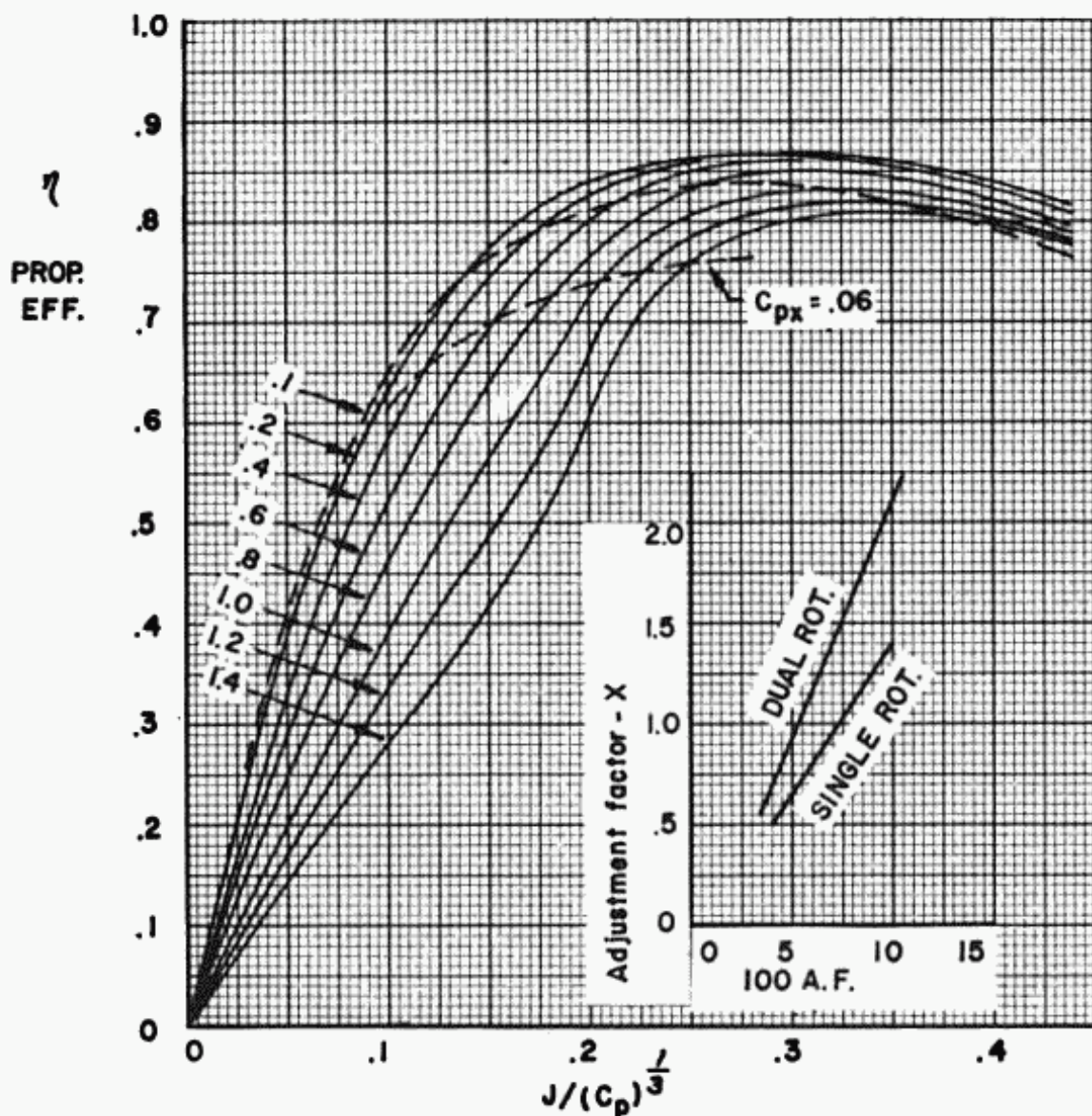


Fig. 8:4. Power Coefficient Adjustment Factor, X , and η .

8:8 SUPERSONIC AND SUBSONIC AIRPLANE DESIGN

losses for the blade; the second takes into account compressibility effects. The first can be expressed as a function of activity factor and $J/(C_p)^{1/3}$, and is determined by the following formula:

$$\Delta \eta = \frac{1}{200} \left(100 \frac{F_S}{D^2} \right) \left(\frac{J}{C_p^{1/3}} \right)^3$$

where F_S = increment of flat plate drag area

The General Propeller chart, Figure 8:4, is based upon an activity factor of 450. Therefore Figure 8:5 shows the variation in efficiency with variation in activity factors. For values less than 450 there is an increase in efficiency.

The second correction, for compressibility effects, is a more serious and complex one. All the factors that affect the compressibility drag on the wing, thickness ratio, aspect ratio, taper ratio, lift coefficient, sweepback and airfoil section, also effect a propeller blade. The propeller blade is further complicated by the variation of speed along its span and rotational effects. To obtain an accurate estimate of this correction a rigorous analysis must be made. For the purposes of preliminary design, Figure 8:6 will give an approximate result.

Two items should be noted about Figure 8:6. First, the tip speed is the speed in feet/sec. due to rotational plus forward speed. Second, that although the curve is plotted against tip speed only, the compressibility effects are a function of the speeds throughout the span. For different combinations of rotational and forward speeds that result in the same tip speed, different compressibility effects will result. However the results of Figure 8:6 are satisfactory for preliminary design.

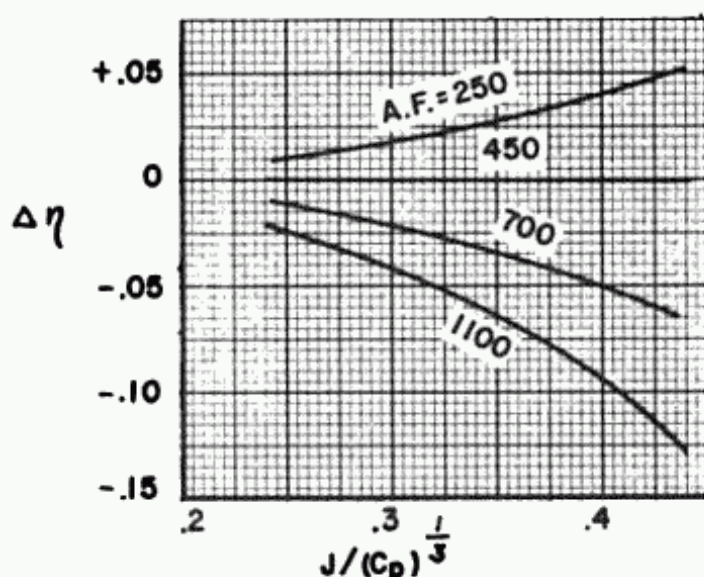


Fig. 8:5. Effect of Profile Drag Losses on Propeller Efficiency.

The following steps are required to determine propeller efficiency:

- (1) Determine $J/(C_p)^{1/3}$
- (2) Use Figure 8:4 to obtain uncorrected η .
- (3) Determine C_{px} ; requires calculation of activity factor and Figure 8:4.
- (4) For high values of $J/(C_p)^{1/3}$, determine correction for profile drag losses; Figure 8:5.
- (5) For high tip speed, obtain reduction in propeller efficiency due to compressibility effects; Figure 8:6.

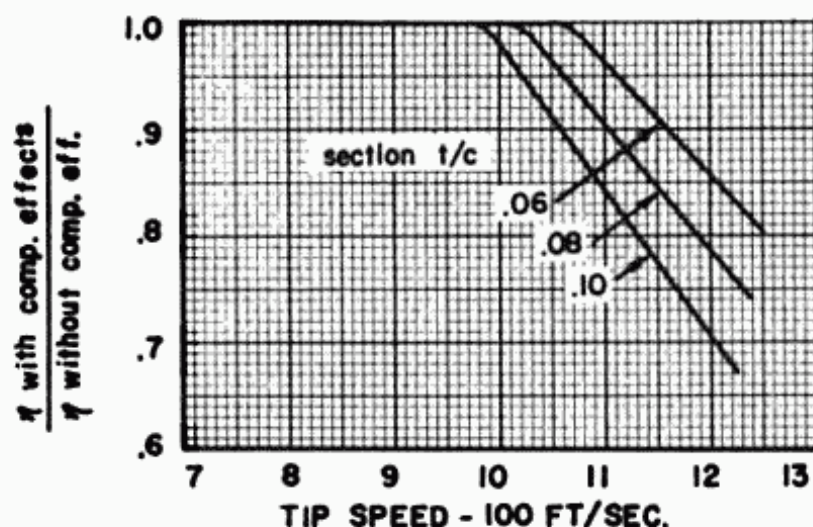


Fig. 8:6. Compressibility Effect on Propeller Efficiency.

$$\text{Resultant tip speed} = \sqrt{V^2 + \left(\frac{\pi}{60} DN\right)^2}$$

Where V = forward velocity in ft/sec.

N = rotational velocity in rev/min.

D = propeller diameter in ft.

- (6) Add corrections due to compressibility and drag effect to uncorrected η for final propeller efficiency.

8:4 Reciprocating and Turbo-prop Transports (Subsonic)

General

The method for the jet transport can be converted with ease for use in either propeller driven transport. Since the specifications required, speed, range, number of passengers and field length will be the same, the method will be followed through step by step.

8:10 SUPERSONIC AND SUBSONIC AIRPLANE DESIGN

Thickness Ratio and Sweepback

The determination of the wing thickness ratio and sweepback is identical with the method used for the jet transport. The same figures and formulas may be used.

Wing Loading

The formula, Equation 2:14, which was used to determine the landing wing loading still holds. However the values of the ground deceleration and L/D in landing must be revised. The average deceleration on the ground can be increased, up to about 10 ft/sec.^2 , for 4 engine aircraft by the use of reversible pitch propellers. This can be a large factor on airplanes that must land in short distances. Lastly the lift/drag of a propeller engine in descent is a little lower than that of a jet airplane. Instead of assuming $L/D = 9$, a better value for propeller airplanes would be 8.0.

Thrust Loading

In obtaining the power loading required for take-off, similar modifications must be made. The C_L for take-off can be used equal to $C_{L_{\max}}$ with no power. In addition, a propeller driven engine is more efficient at low speeds than a jet engine. Therefore for a required take-off distance, all other factors being the

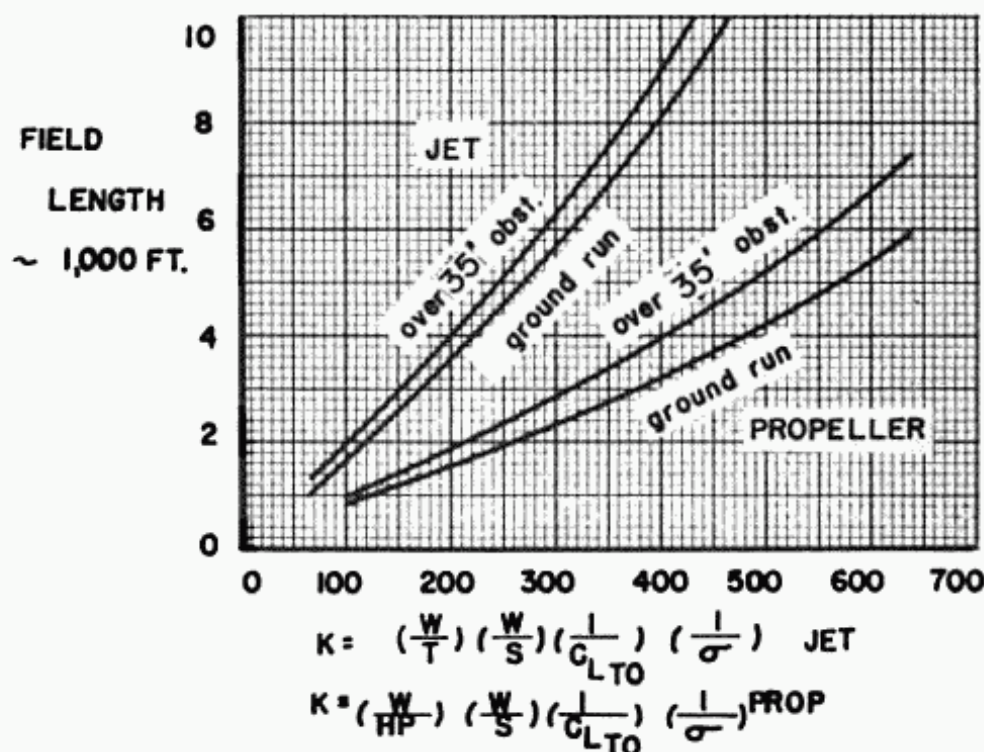


Fig. 8:7. Take-off Chart for Jet and Propeller Airplanes.

same, the power loading of a propeller airplane will be greater than the thrust loading of a jet airplane. Figure 8:7 shows the comparison between the jet and propeller driven airplanes.

Weight by Formula

For the jet transport, the take-off weight was determined from Equation 2:38. A similar formula can be used for either propeller engine airplane if the weight of engine and propeller is substituted for the weight of the jet engine alone. This may be done by plotting the weight of various props and engines against horsepower and determining a formula for the curve connecting the points. The formula for structural weight, fixed weight, and variation of structural weight with thickness ratio and aspect ratio do not vary significantly.

Weight - by Comparison with Other Transports

Figures 8:8 a, b and 8:9 present the weight of all the airplane components versus take-off weight for the existing U.S. reciprocating engine aircraft. It should be noted that the 8:8 a, b is the weight empty and 8:9 is the useful load. The take-off weight is the addition of these two weights. The structural weight is the sum of the wing, fuselage, landing gear, nacelles and tail surface weights.

It is quite unexpected that there should be so little scatter of points if the airplanes are broken into two groups, short range two engine airplanes and long range four engine airplanes. In a few cases where the DC-3 weights were a considerable distance from the estimated line, these values were neglected due to the obsolescence of the model. The lines of the long range and short range airplanes are connected by a jagged line for convenience and have no significance.

To obtain the take-off weight by this method, a take-off weight must first be assumed and the component weights obtained from the figures. The range must then be calculated to check the fuel weight. If the fuel weight must be modified, then the take-off weight and component weights change with it.

The weights of the high subsonic jet transports, the DC-8, the Boeing 707 and the Convair 600 are presented on curves separate from the propeller airplanes.

Drag

A very important change goes occur in the drag calculation. The induced and compressibility drag coefficients may be calculated in the same manner, the important difference being in

8:12 SUPERSONIC AND SUBSONIC AIRPLANE DESIGN

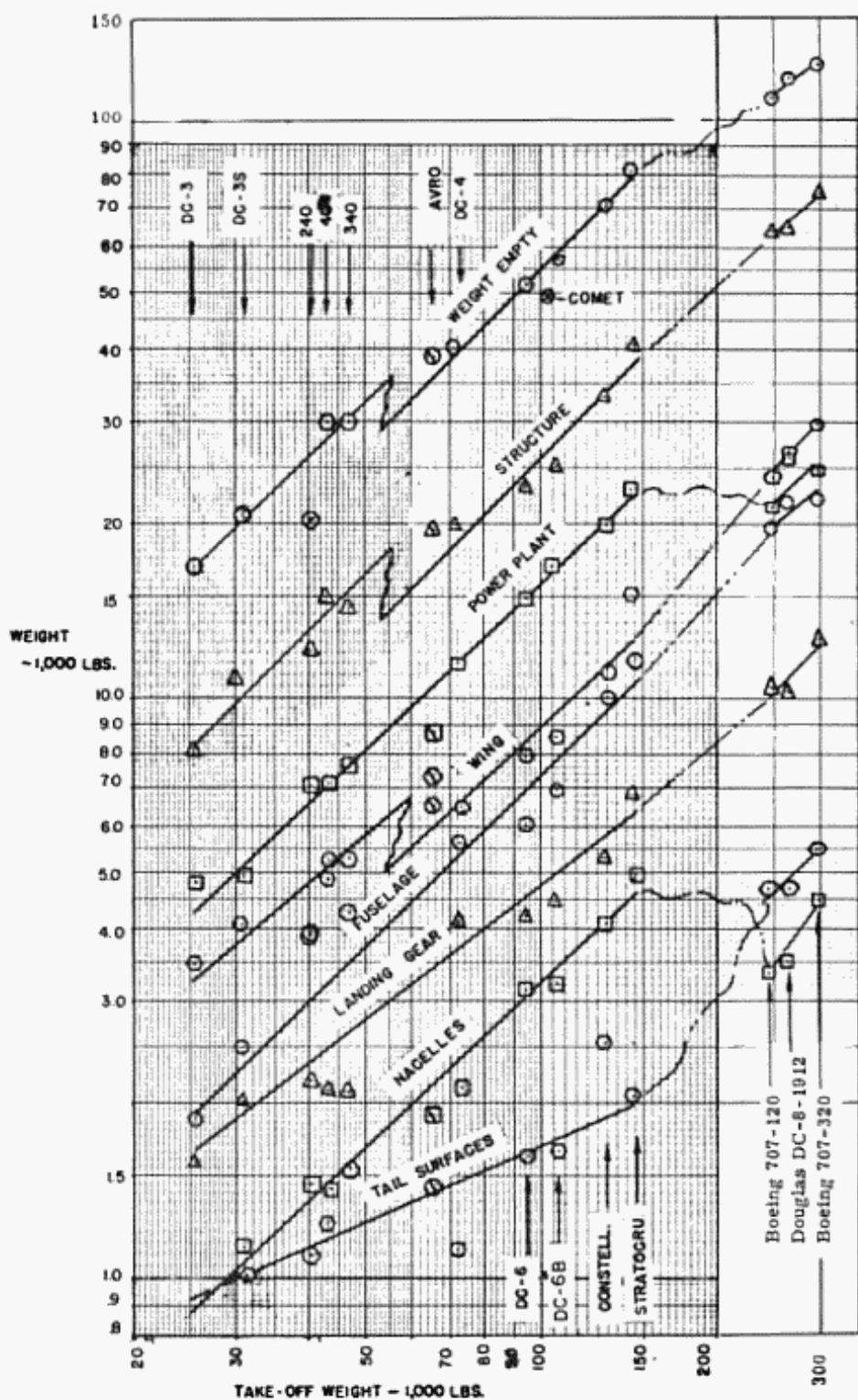


Fig. 8:8 a. Components of Empty Weight vs. Take-off Weight (Transports).

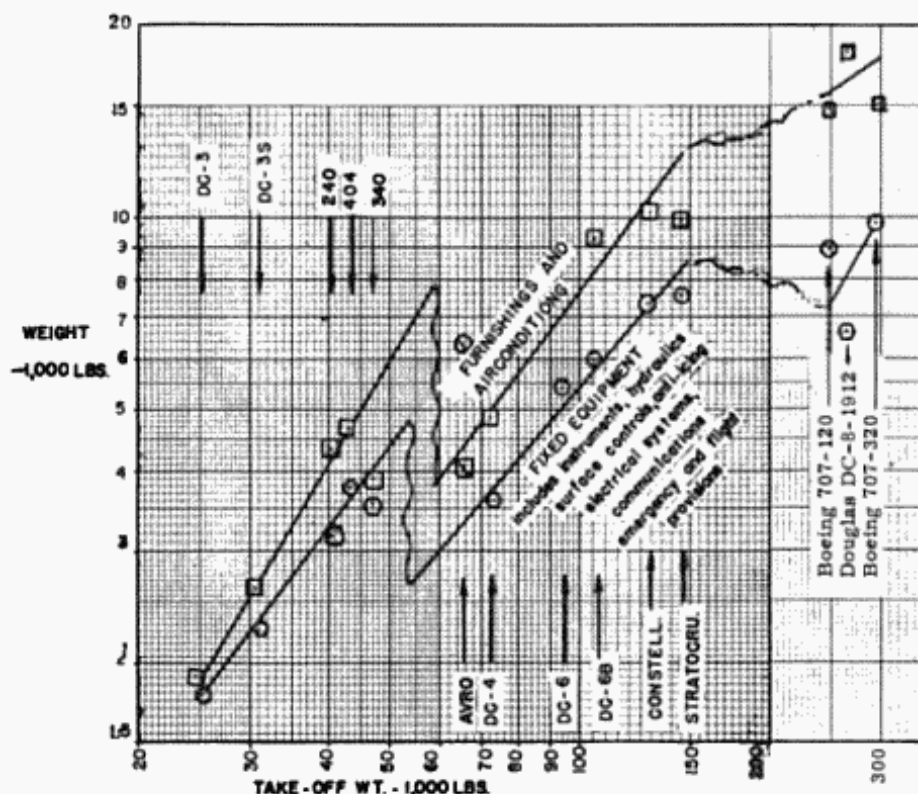


Fig. 8:8 b. Components of Empty Weight vs. Take-off Weight (Transports).

the parasite drag coefficient. Wind tunnel tests have shown that for a clean jet airplane, C_f average is equal to about .0030 to .0033; for a clean propeller driven four engine airplane, C_f average increases about 33% to approximately .0040 to .0044. This difference is due to the slipstream of the propellers practically enveloping the whole airplane except fuselage nose. It is this increase in the parasite drag of the propeller driven airplane that offsets a large part of its advantages of a lower specific fuel consumption than the jet airplane. This is one of the reasons why a jet transport compares favorably with the propeller driven airplanes at medium ranges.

Figure 8:10 shows the values of C_f obtained from flight test for some clean air-cooled and liquid-cooled reciprocating engine airplanes and some jet engine airplanes.

To determine "f", Equation 2:44 may be used as for the jet airplanes, except that the result should be multiplied by 1.33.

Range

The cruise range can be calculated by Breguet's formula since it was originally derived for propeller driven airplanes.

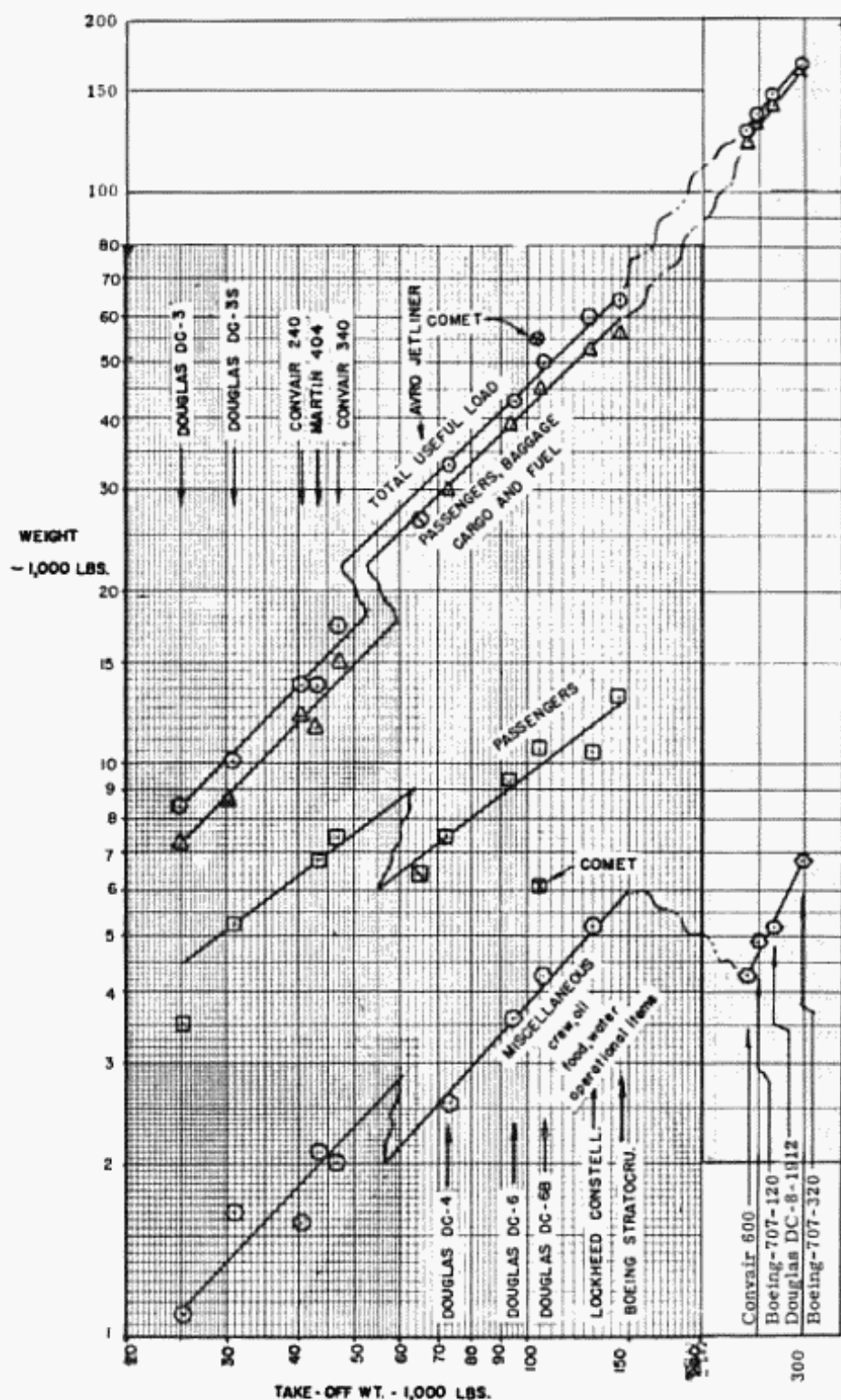


Fig. 8:9. Components of Useful Load vs. Take-off Weight (Transports).

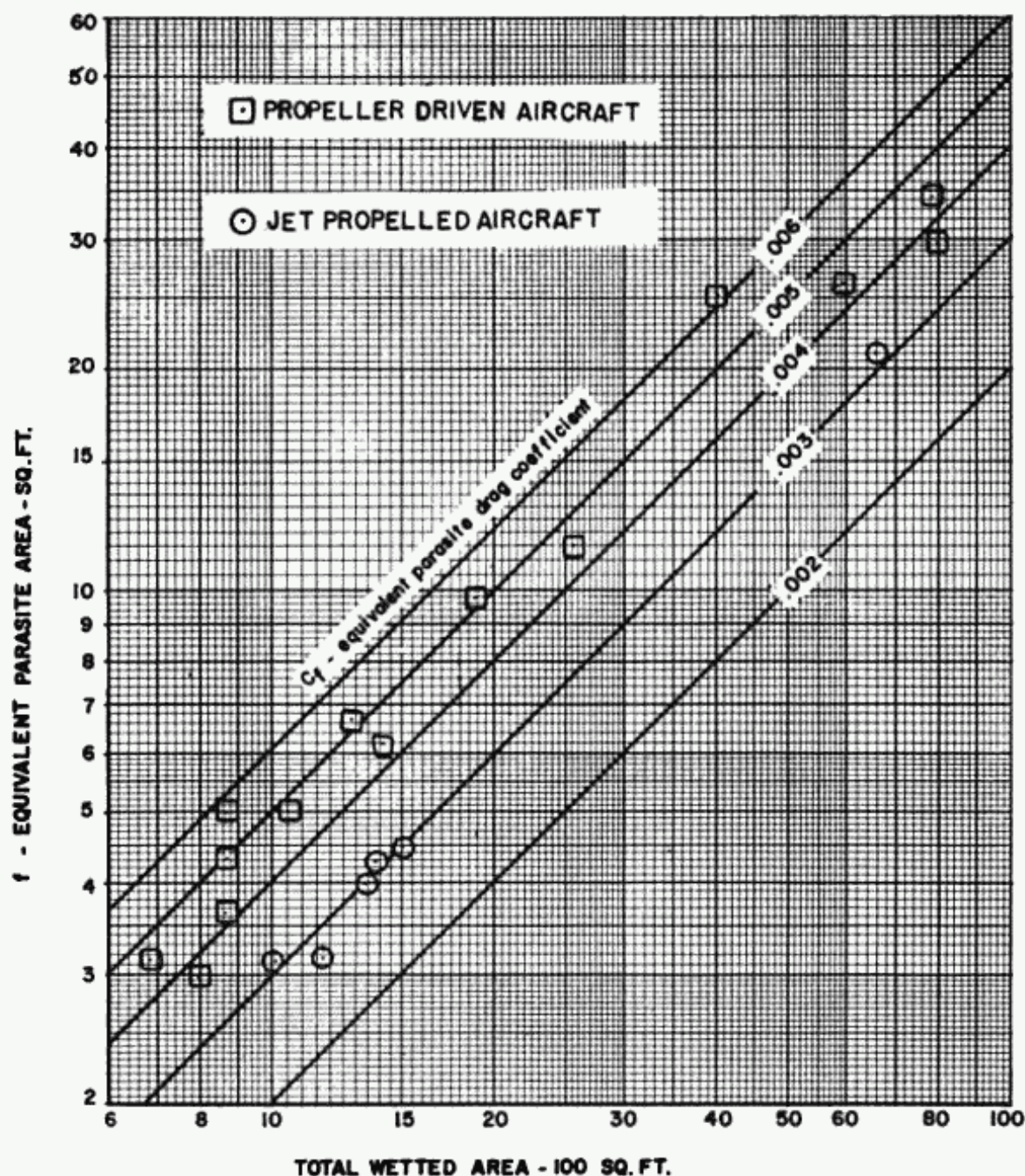


Fig. 8:10. The Equivalent Parasite Drag Coefficient.

$$R = 863.5 \frac{L}{D} \frac{\eta}{c} \log \frac{W_0}{W_1}$$

The lift-drag ratio L/D can be determined in a similar manner as was done for the jet transport; that is

$$L/D = C_L/C_D$$

The propeller efficiency, η , can be determined by Figure 8:4 to 8:6, or can be estimated from Figure 8:1. The specific fuel consumption, c , can be determined from the engine data.

PRATT & WHITNEY WASP MAJOR

PERFORMANCE - T.O. WET HP = 3,500 - SOLID LINES

ARE FOR UNSUPERCHARGED ENGINE AS PROVIDED BY

P&W. DOTTED LINES SHOW ESTIMATED PERFORMANCE

POSSIBLE WITH SUPERCHARGER

WEIGHT AND DIMENSIONS

DRY WT. WITH STANDARD ACCESSORIES

• 3,682 LBS.

ENGINE LENGTH - MAXIMUM

• 96.5 IN.

ENGINE DIAMETER - MAXIMUM

• 55 IN.

MAX. OIL CONSUMPTION AT NORMAL POWER AND SPEED

• .025 LB./SHP-HR

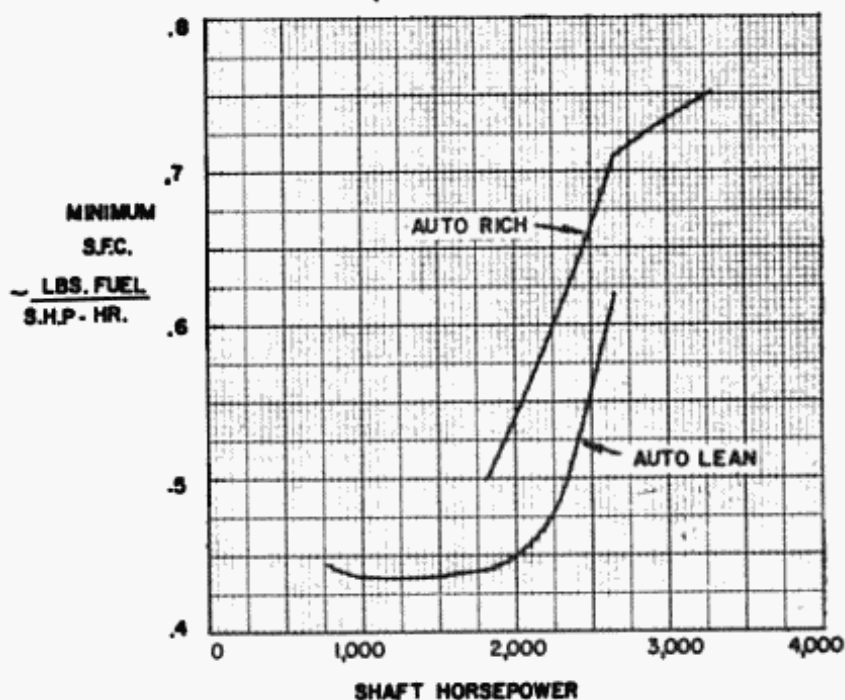
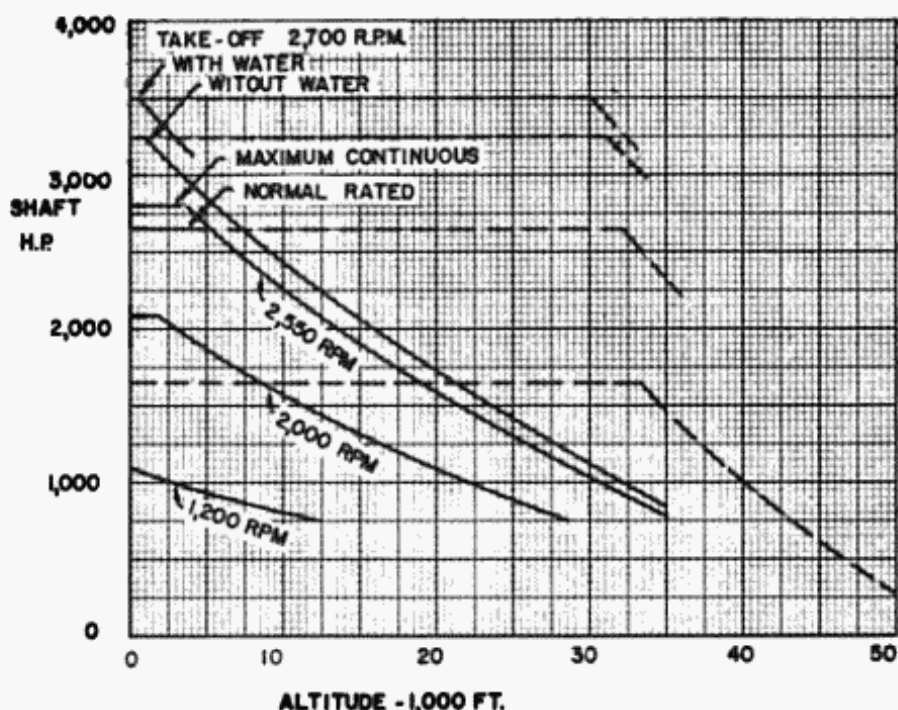


Fig. 8:11. "Characteristics and Performance of the P. and W. Wasp Major," courtesy of Pratt and Whitney.

Figure 8:11 presents the performance and physical characteristics, of the Pratt and Whitney Wasp Major engine. This reciprocating engine has a wet take-off rating of 3,500 HP and a normal rating of 2,650 HP. For transport studies similar to the jet study presented in the text, the characteristics of this engine can be scaled up or down to fit the needs of the airplanes. However for a specific airplane, there is a wide choice of reciprocating engines available in a large range of powers.

The specifications of the turbo-prop engines, Models "500" and "501" are listed on page 8:17, by courtesy of Allison Division of the General Motors Corporation. The performance characteristics of these engines are restricted.

The Allison Model "500" turbo-prop engine consists of two axial flow gas turbine power sections driving a dual rotation propeller through a common reduction gear. The power sections are connected together so that in effect they form a single unit and are connected to the reduction gear by extension shafts. The power sections can be operated together or one may be shut down in flight for economical cruise. When this is done the single unit still operates both contrarotating propellers through a special clutching arrangement.

The Model "501" engine is the same type, but consists of only one of the two power sections, fitting a lower power range and operating a single propeller through its own reduction gear.

	Model 500	Model 501
Takeoff, static ESHP	5500	2750
Takeoff, RPM	14,300	14,300
Takeoff, fuel consumption	.603	.603
Takeoff, oil consumption	4 lb/hr	2.5 lb/hr
Basic weight (inc. shaft and gear)	2575 lbs.	1650 lbs.
Overall length " " " "	185 in.	149 in.
Width	45 in.	40 in.
Height	45 in.	--

Figures 8:12a and b present the performance of a theoretical turbo-prop engine that may be used for classroom work.

The take-off weight and the final weight, W_1 , are known. Before W_0 , the initial weight for cruise can be established, the fuel

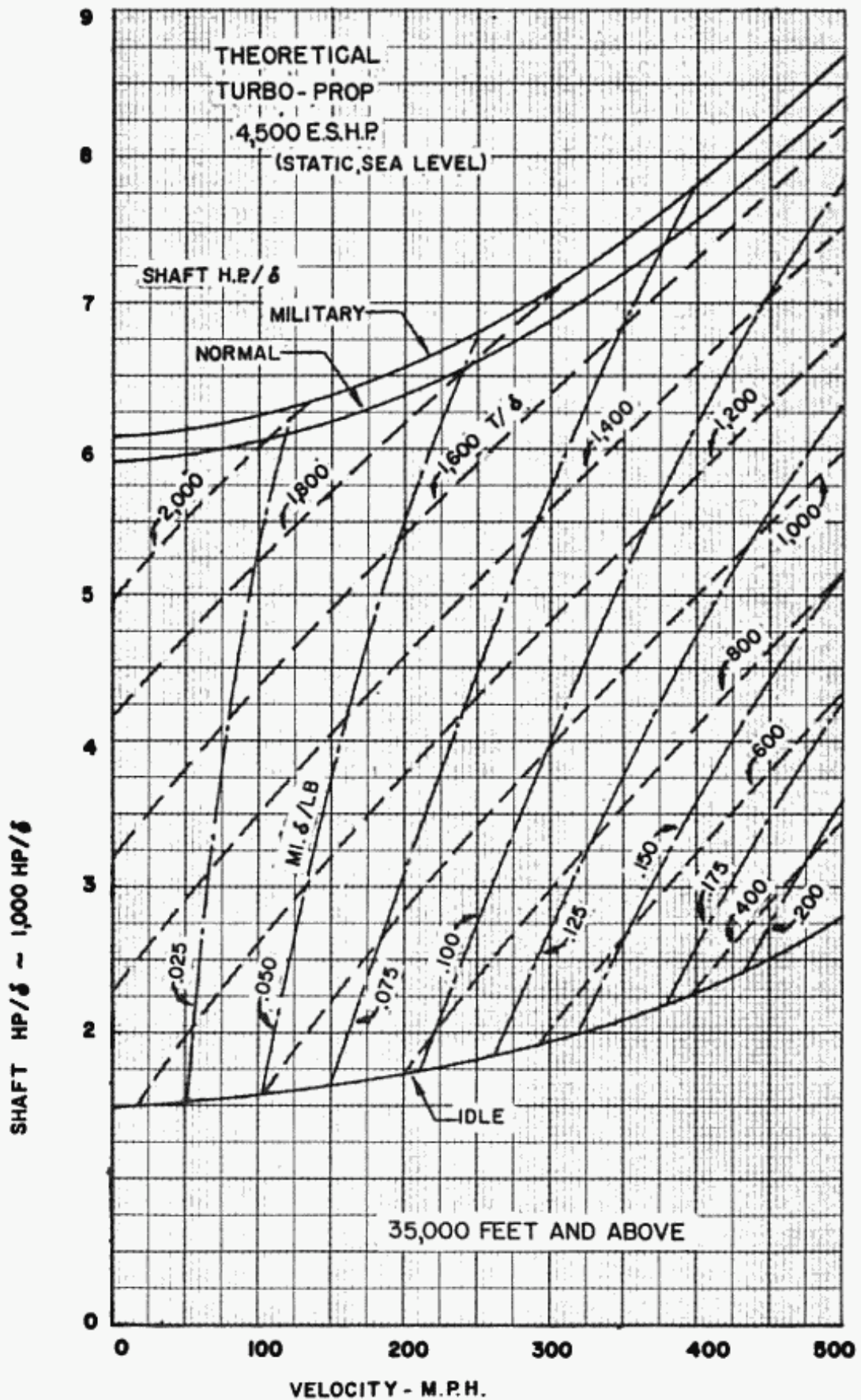


Fig. 8:12 a. Turbo-prop Performance; 35,000 ft. and above.

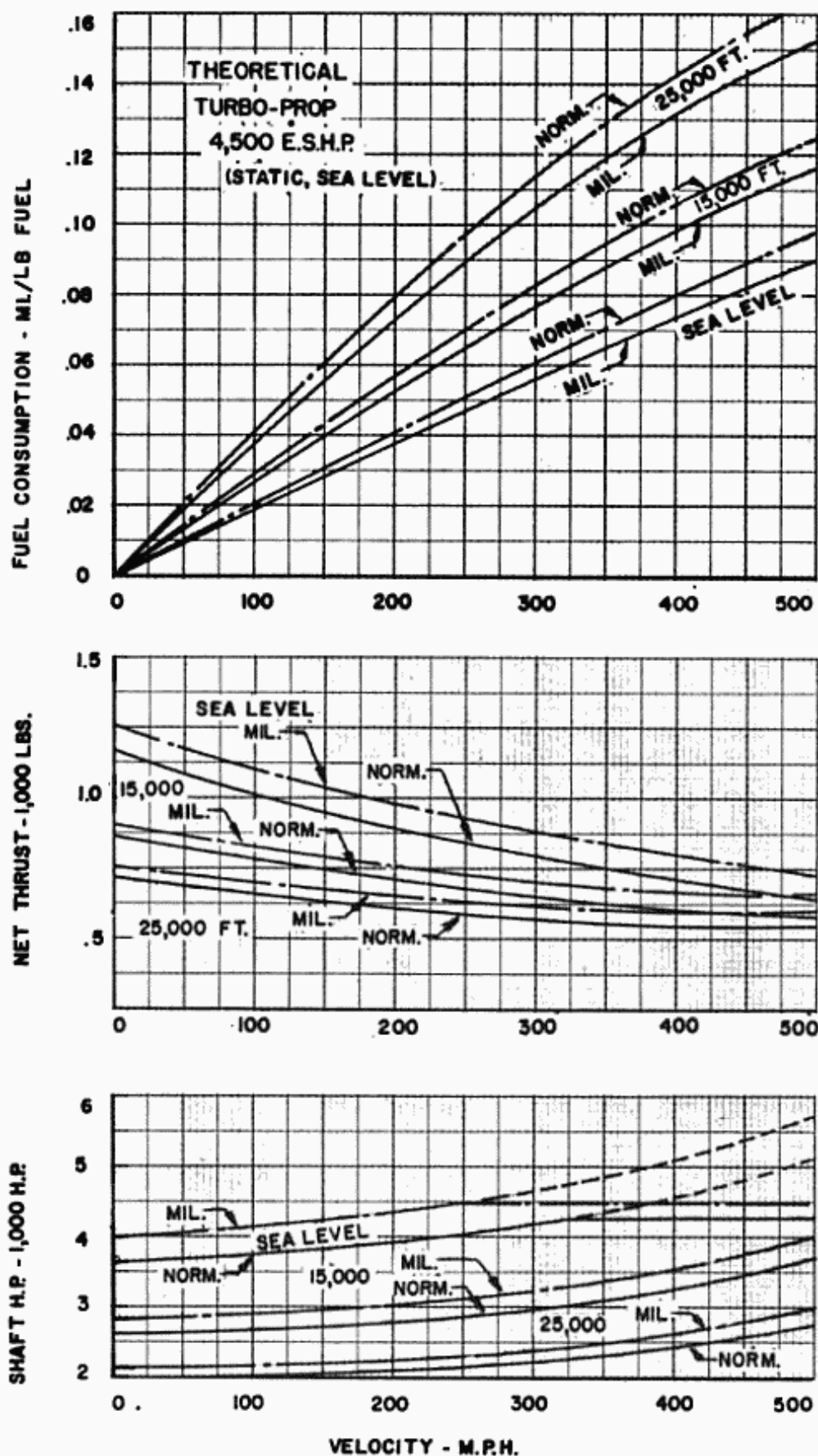


Fig. 8:12 b. Turbo-prop Performance; sea level to 25,000 ft.

used in the climb must be determined. The climb characteristics can be calculated by exactly the same method as used in the jet transport.

If the range calculated is not equal to the range required, the weight of fuel, and the gross weight must be revised until the required range is met.

Climb

As with the jet transport, the propeller airplanes must be checked to determine if they meet the C.A.M. climb requirements. If they do not, and the engine power must be increased, the entire airplane design must again be revised to meet all requirements.

Fuel Storage

Because of the lower specific fuel consumptions of the propeller engines and the greater wing thickness ratios allowed by the lower cruising speeds, the wing is usually large enough to store all the fuel required. Tending to offset the facts indicating sufficient fuel storage space in the wing, is the fact that the propeller airplanes can have a higher wing loading, therefore a smaller wing, for the same field length. This is due to the higher maximum C_L 's attainable with wings designed for lower cruising speeds, the greater decelerations possible with reversible pitch propellers and the lower L/D in landing. If there is not sufficient fuel space in the wing, the same alternatives exist as with the jet transport. See Section 2:8.

8-5 Bombers

Specifications

The specifications of a bomber are of necessity quite different than that of a transport. They usually consist of the bomb load required, in both sizes and weights, the high speed at military power, altitude over the target and the range. The range may be specified in a number of ways; at a required altitude and cruising speed through the flight; at an altitude and speed within a certain range of the target, without specifying requirements for the rest of the flight, or other possibilities. Sometimes, especially if it is to be launched from an aircraft carrier, the total weight is specified. This however only works as a squeeze on the other requirements. Although field length is not as important a factor for the bomber as for the commercial transport, it is given due consideration. However special means, such as rockets for take-off, and chutes for landing, may be used to reduce required field length.

Design Factors

As the payload, passengers, cargo, and crew designed the fuselage of the transport, the bomb load and crew design the fuselage of the bomber. In addition, bomber fuselages are usually required to carry fuel. Again the speed requirements design the thickness ratio of the airfoil and the sweepback of the wing. Whereas the landing field set the maximum wing loading for the transport it is not the critical factor for the bomber. For high speed condition the wing loading should be as high as possible, but the minimum is set by the altitude and speed requirements at the target. Since

$$W/\delta S = 1481 M^2 C_L$$

and δ and M are known, W/S can be obtained by estimating C_L . A few airplanes may be designed with different combinations of C_L and W/S at target, and the optimum combination chosen.

With the chosen wing loading, a power loading may be estimated for the speed requirements at altitude. With the W/S and either W/P or W/T chosen the airplane can be designed as the transport was.

The formulas for both f and take-off weight used on the jet transport must be modified to account for the bomb load instead of the payload, and any change in power plant. However instead of using the weight formula, a weight estimate can be made from Figure 8:13. This graph shows the weight of each component part against take-off weight for a large number of military aircraft, some of which are jet powered. Although the type of aircraft is not designated, the smaller ones, up to about 40,000 lbs. take-off weight are fighters and those above are bombers, transports and cargo aircraft.

The power plant may be either the reciprocating, the turbo-prop or the turbo-jet engine. The characteristics of the propeller engines are shown in Figures 8:11 and 8:12. The performance of a typical jet engine is given in Chapter II. Figure 8:14 shows the performance of a jet engine already in production, the Pratt and Whitney JT6B, with take-off thrust equal to 5,000 lbs. For the supersonic airplanes up to $M = 2.0$, the performance of the P. and W. JT12A-21 turbujet, rated at 4,025 lbs. T, sea level static standard day with A.B., and the JT4A-28 rated at 24,500 lbs. T under the same conditions is presented in figures 8:14a and 8:14b.

Criteria for Choosing Optimum Design

The criteria for deciding the optimum for a bomber is fundamentally different than those of a transport. For a transport, the

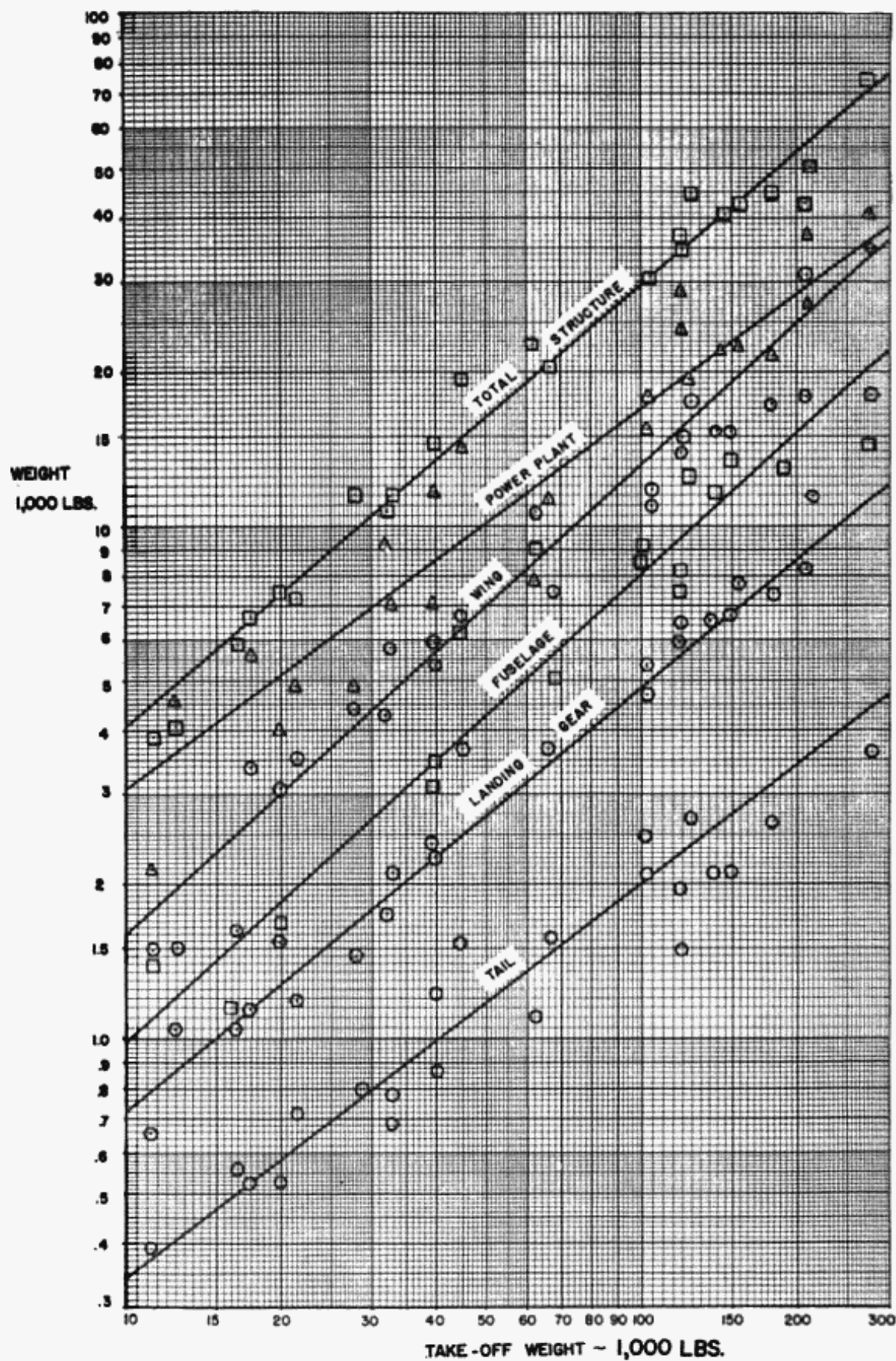


Fig. 8:13. Weight Breakdown of Military Aircraft.

AERODYNAMIC DESIGN

8:23

PRATT & WHITNEY JT6B TURBO-JET
PERFORMANCE - TAKE-OFF THRUST - 5,000 LBS.
S.F.C. - 1.12 LB/LB-HR.

WEIGHT AND DIMENSIONS
DRY WT. INCLUDING STANDARD EQUIP. - 1,729 LBS.
LENGTH, NO EXT. PIPE OR JET NOZZLE - 103.3 IN.
DIAMETER - 49.5 IN.

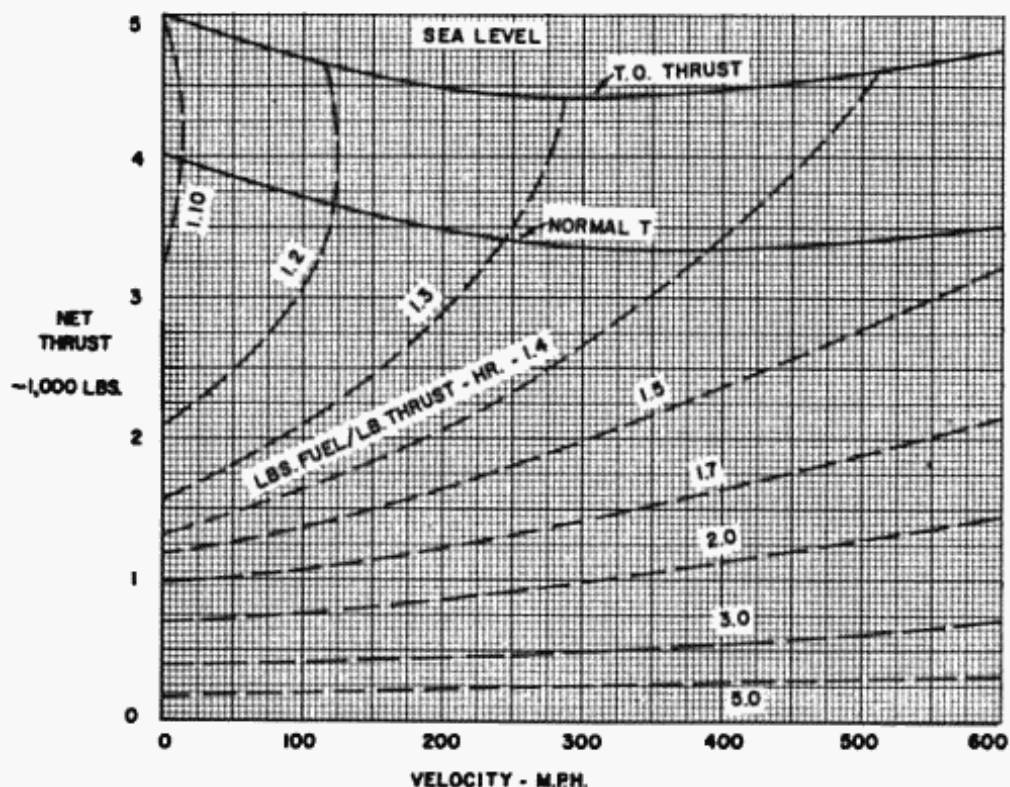
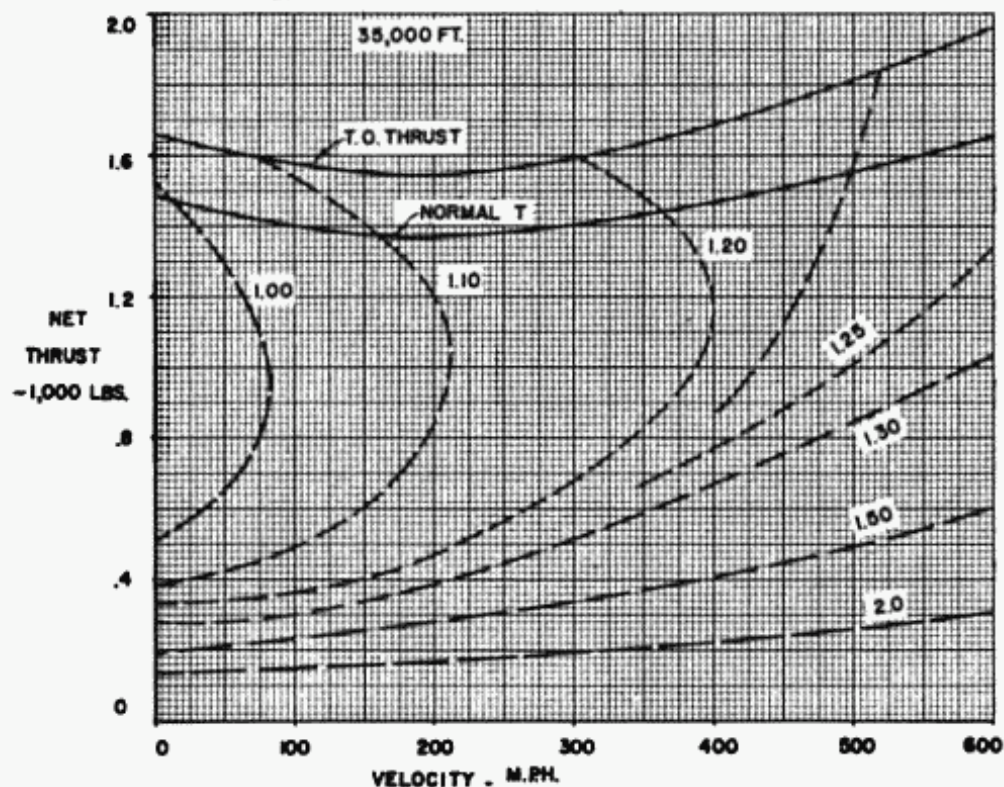


Fig. 8:14. "Characteristics of the P. and W. JT6B Turbo-Jet Engine," courtesy Pratt and Whitney.

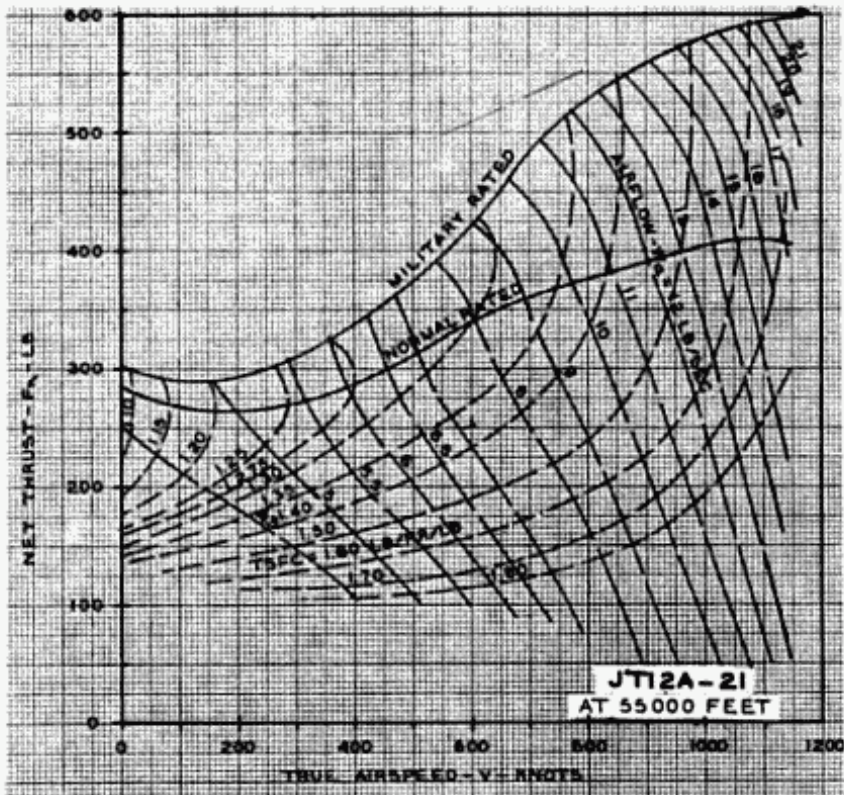
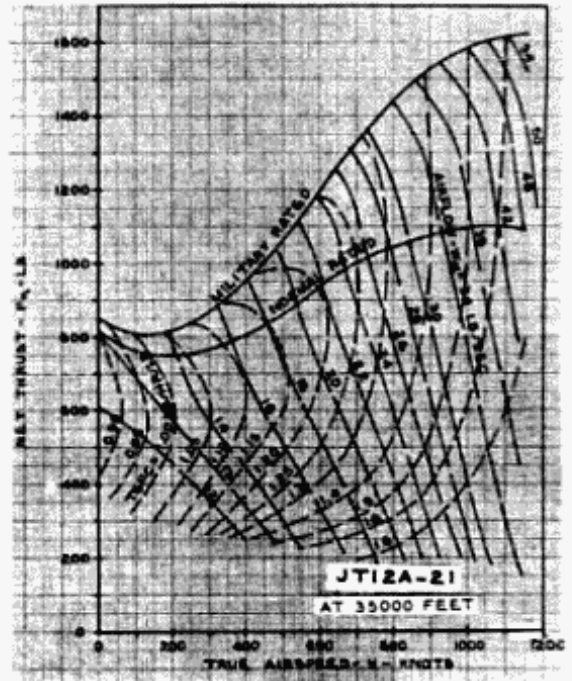
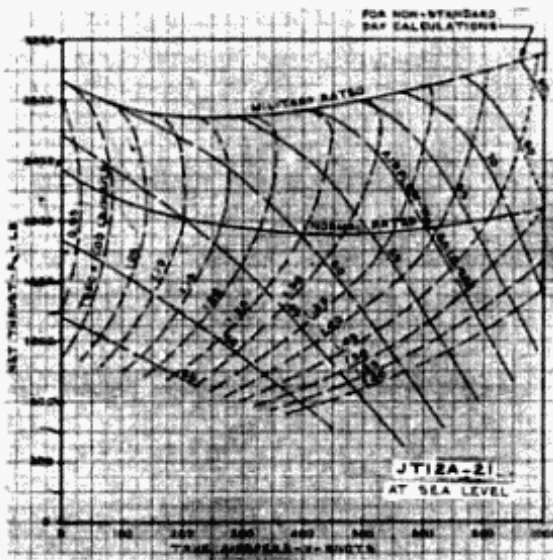


Fig. 8:14a. Performance of P.W. JT 12 A-21 Supersonic Jet S.L., Static, St. Day, $T = 4,005$ lbs. with A/B.

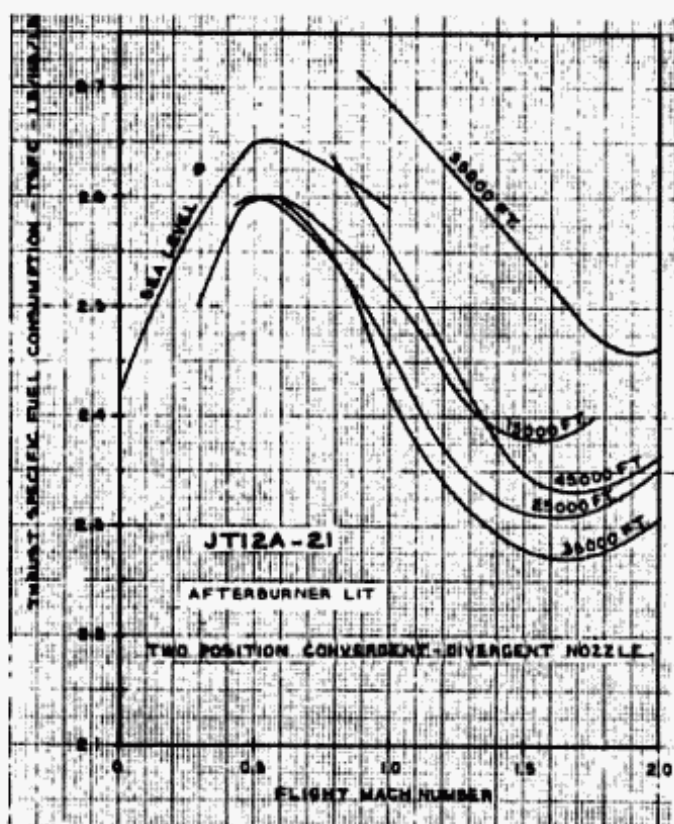
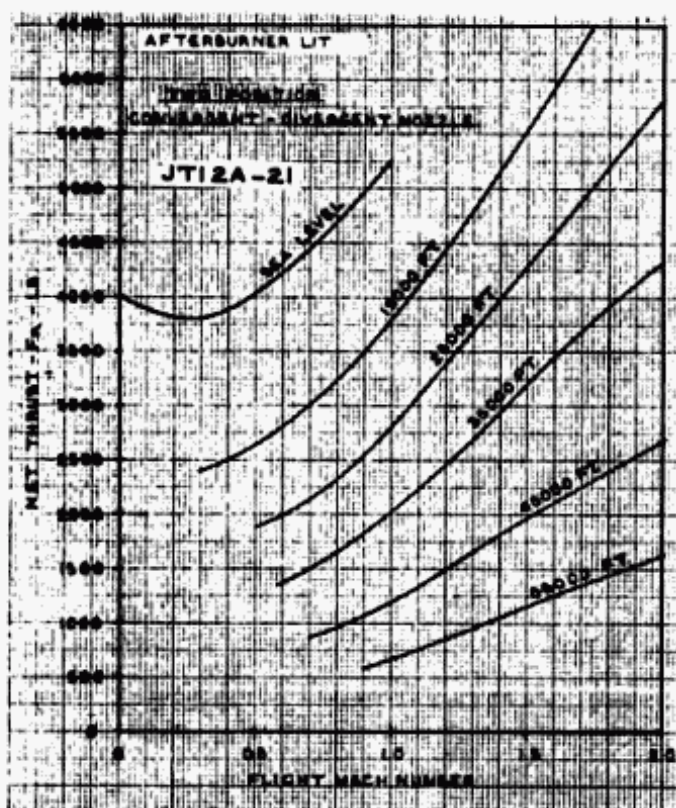


Fig. 8:14a. (cont'd)

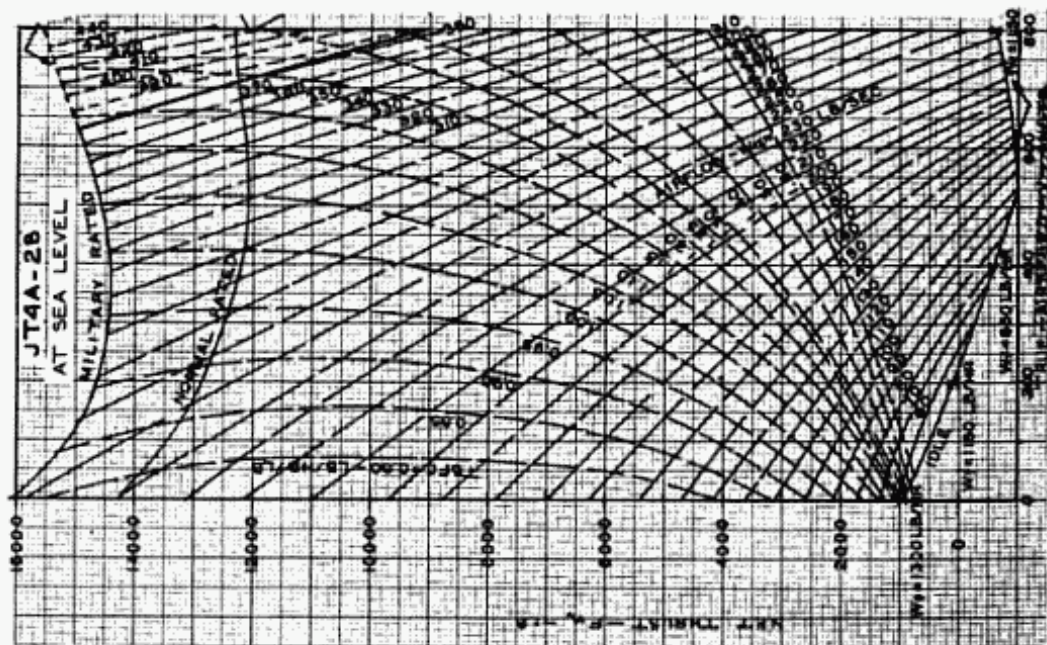
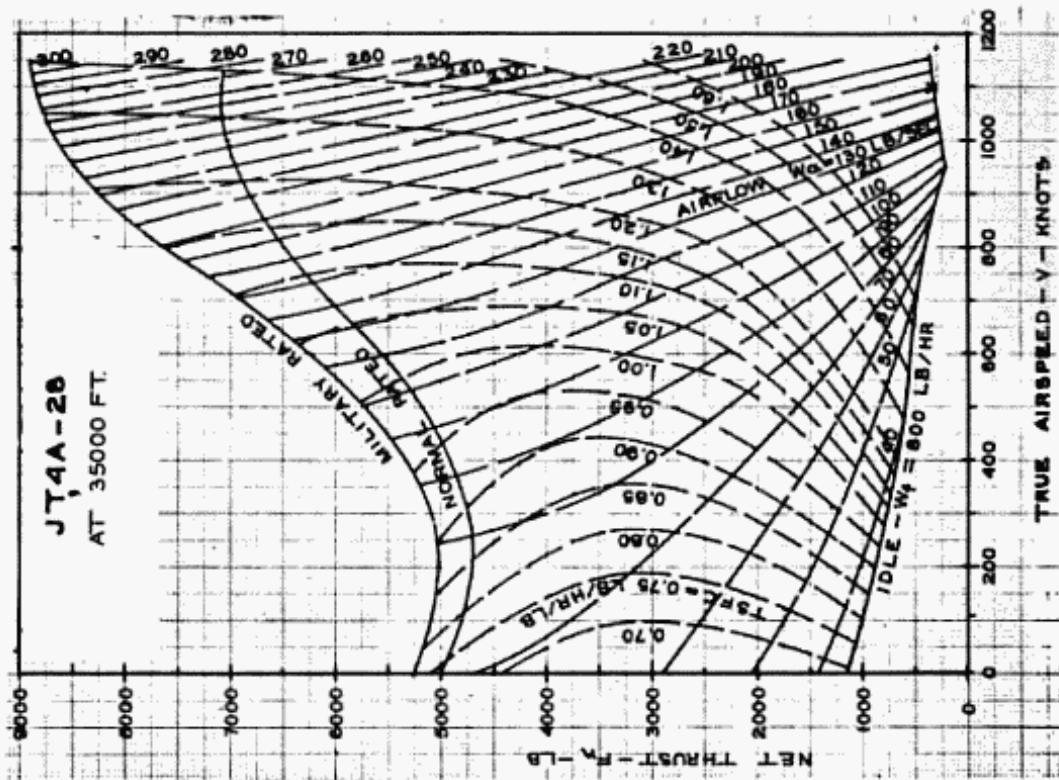


Fig. 8:14b. Performance of the P. W. JT4A-28 Supersonic Jet S.L., Static, Stand. Day, T = 24,500 lbs. with A/B.

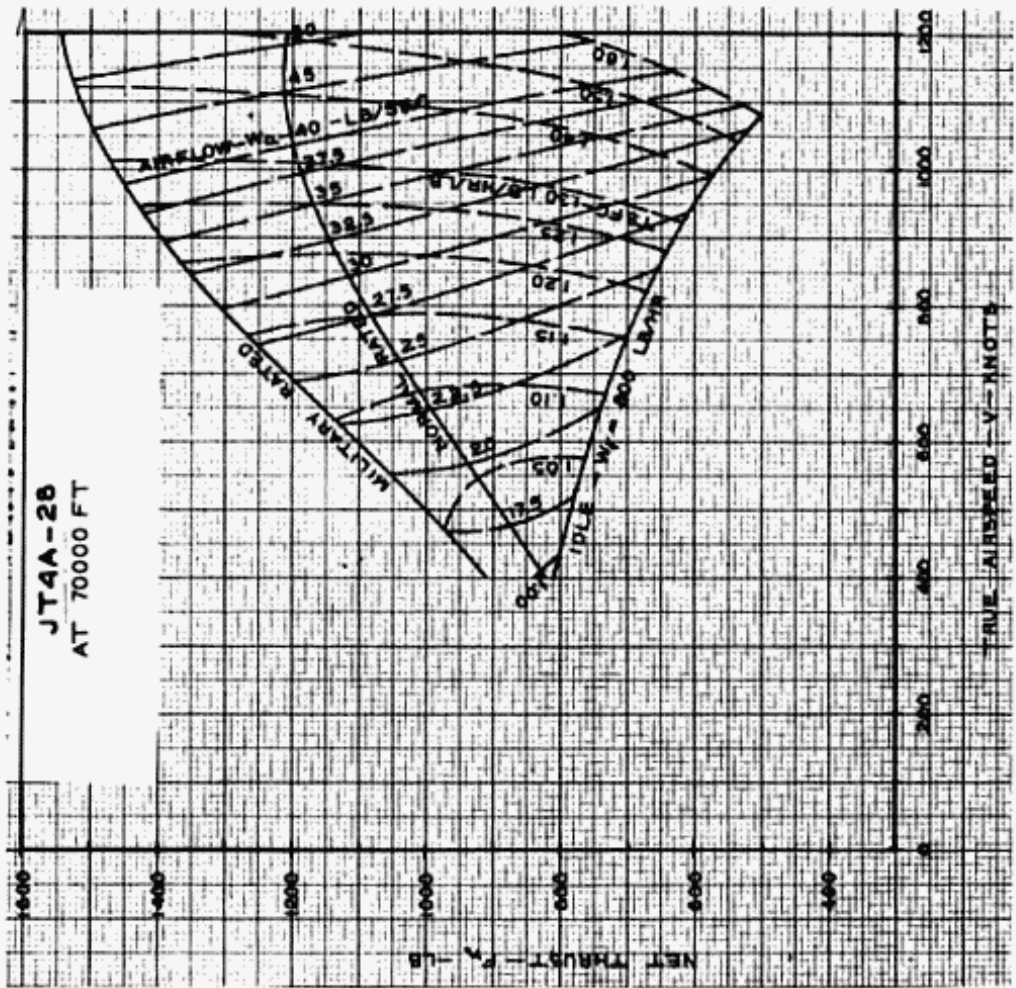
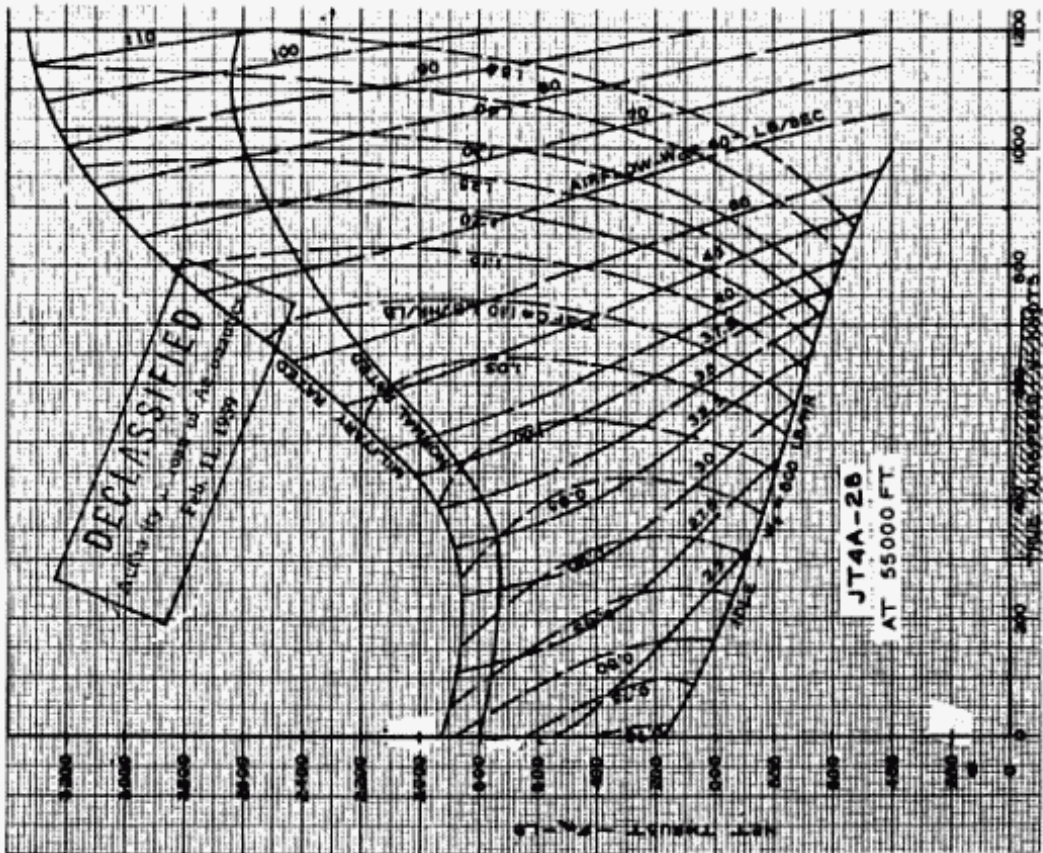


Fig. 8.14b. (cont'd)

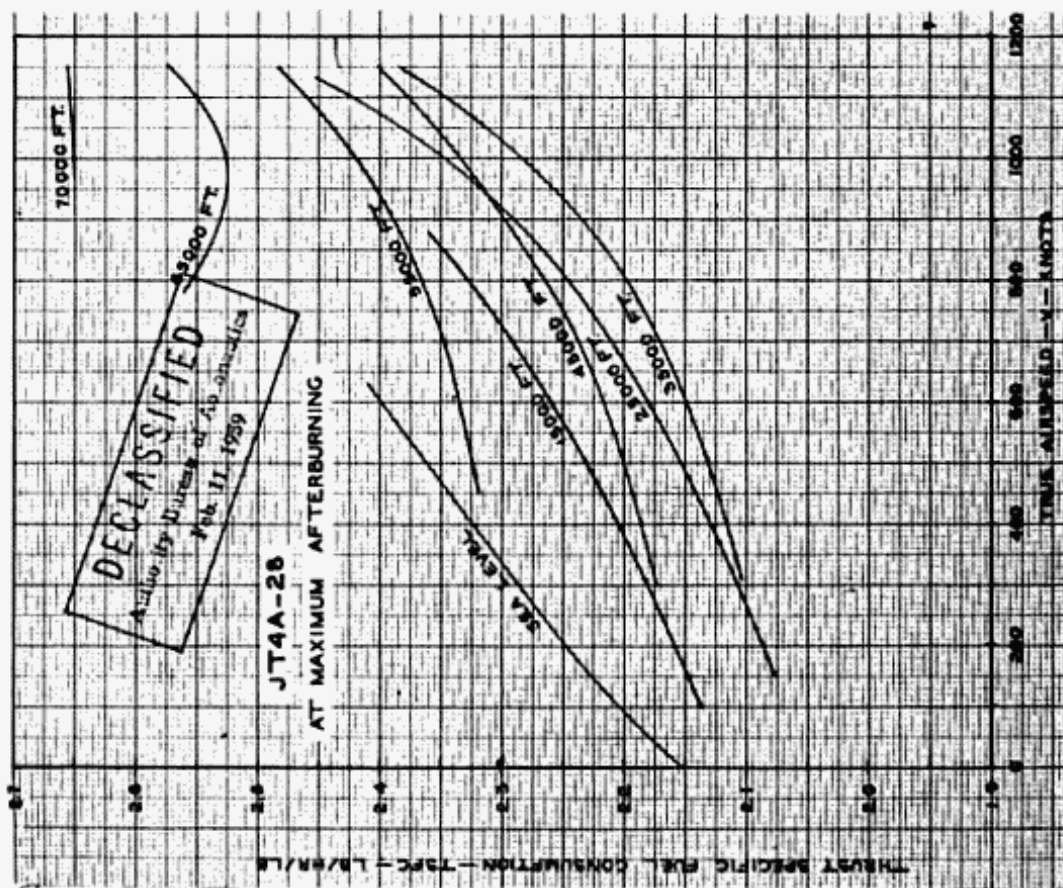
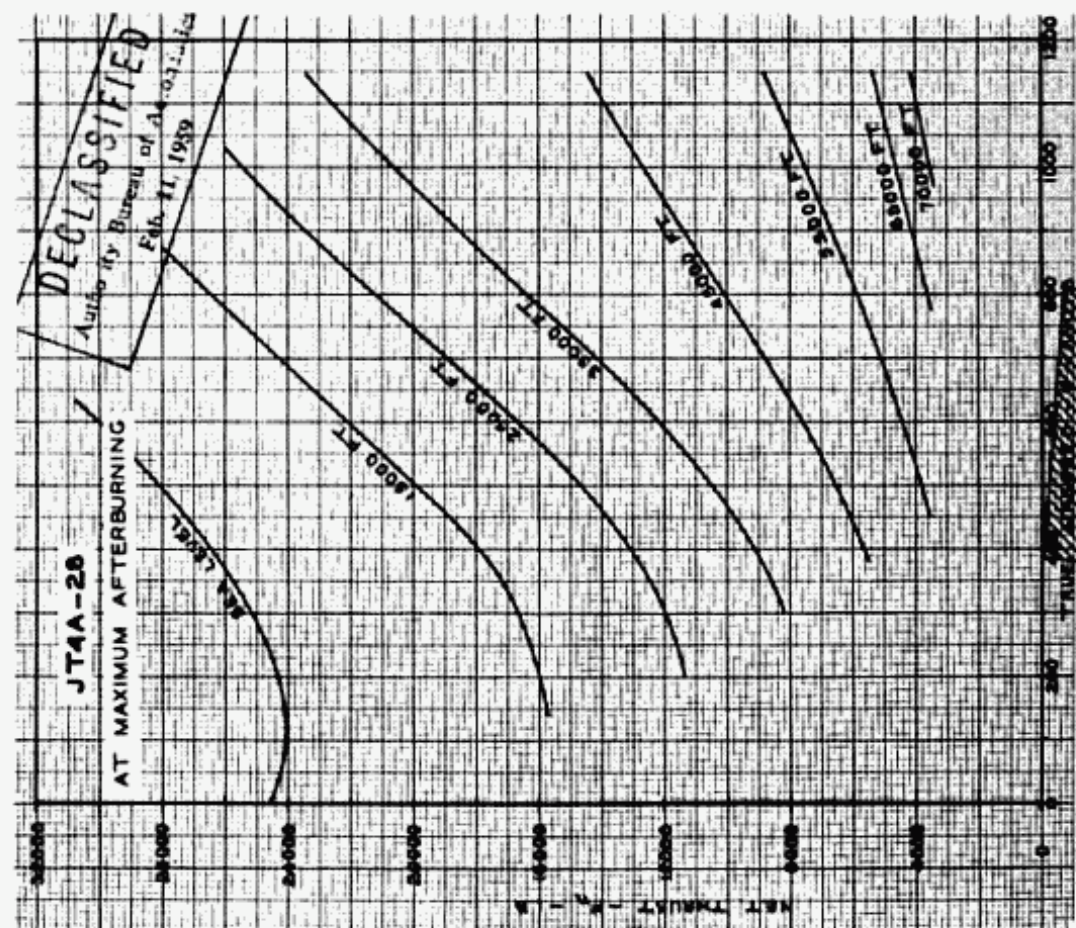


Fig. 8:14b. (cont'd)

range and speed are specified and the prime purpose of the design is to meet these requirements for the lowest operating cost. However in a bomber every additional mile of range and increase in speed is quite useful. Therefore if it is possible to exceed the requirements by increasing the size of the airplane, thereby the cost, it is up to the designer to decide the issue. However for the set requirements, the smaller airplane, and the lighter one is the best one. The size factor, in terms of projected area, is particularly important because the smaller airplane not only presents a smaller target but is also more difficult to detect on a radar screen. The lighter airplane will cost less, and therefore the same money appropriation will buy more airplanes.

8-6 Fighter or Interceptor

General

The fighter or interceptor, although used for different purposes are essentially high speed, short range airplanes. Whereas the fighter primarily requires high speed and maneuverability to combat other fighters and bombers, endurance is an important factor so that it can be effective for a long period. The interceptor, in addition to doing all that a fighter is required, has the prime requirement of climbing rapidly to intercept enemy planes.

The minimum rate of climb specified is based upon the speed and altitude of the enemy plane, and the amount of warning the interceptor is given. Since the important factor in climb is the excess of the power available over the power required divided by the weight, the thrust loading will be designed by this criteria. Wing loading is also important in climb, since it is an important factor in thrust required.

Since the bomber and transport are multiengined aircraft, the fuselage was designed by the bombload and crew, or payload and crew. The bomber also carried fuel in the fuselage. However both the fighter and interceptor might be either single or twin engined. If the plane has one engine, the fuselage must be designed to carry the crew and the engine, in addition to the specified armament. On a twin engined plane, the engines are usually carried on the wings, and the fuselage carries the crew and armament.

Since the interceptor and fighter are comparatively small airplanes the fuel storage space for the required range is a large factor in design. All these factors make standardization of design methods for these types of airplanes almost impossible.

Design

Because no general method is convenient for designing this type of aircraft, a large amount of time must be spent on trial and error methods. The weights can be estimated by Figure 8:13 as used in the bomber design. The lower weight airplanes in this figure represent the fighters and interceptors. The f of the airplane can be estimated from Figure 8:10 after the airplane is laid out. The wing loading and thrust loading will have to be determined purely by trial and error. If the requirements of the airplane being designed is not radically different from some existing airplane, the values from the existing airplane can be used as a guide. The performance must then be checked for the values estimated, W/T , W/S and fuel weight, and these parameters varied until the most efficient combination is attained. The wing sweepback and thickness ratio can be determined in the same manner as the jet transport. The power plant characteristics can be obtained from Figures 8:11, 12 or 14. The criteria for choosing the optimum fighter or interceptor is both size and weight, the same as a bomber. Figs. 8:19 and 8:20 show 3 View drawings of 2 supersonic fighters the McDonnell F4H-1 and the Convair F106A. Fig. 8:21 shows the 3 view of the Convair B58 M=2 bomber.

8-7 Private PlanesGeneral

The private plane is very similar to the commercial transport in both specifications and criteria for judging the optimum. An added important factor in judging the optimum is one of the items that go into determining the direct operating cost, the first cost. For this reason any design that leads to low production costs is most desirable.

Where the private plane specifications usually do include number of passengers, range and cruising speed, the landing speed is specified instead of the field length. Just as the landing field set the wing loading for the transport, the landing speed will decide the wing loading for the private airplane. The thrust loading will be designed by the speed and climb requirements but again the choice of the number of engines must be based on other factors. Although two engines are safer than one engine for private planes, the added first cost and operating costs is such a large factor that most private planes have kept to one engine.

The fuselage, in a single engine airplane, is then designed by engine and passenger requirements. The wing plan form is arrived at by a combination of aerodynamic and manufacturing

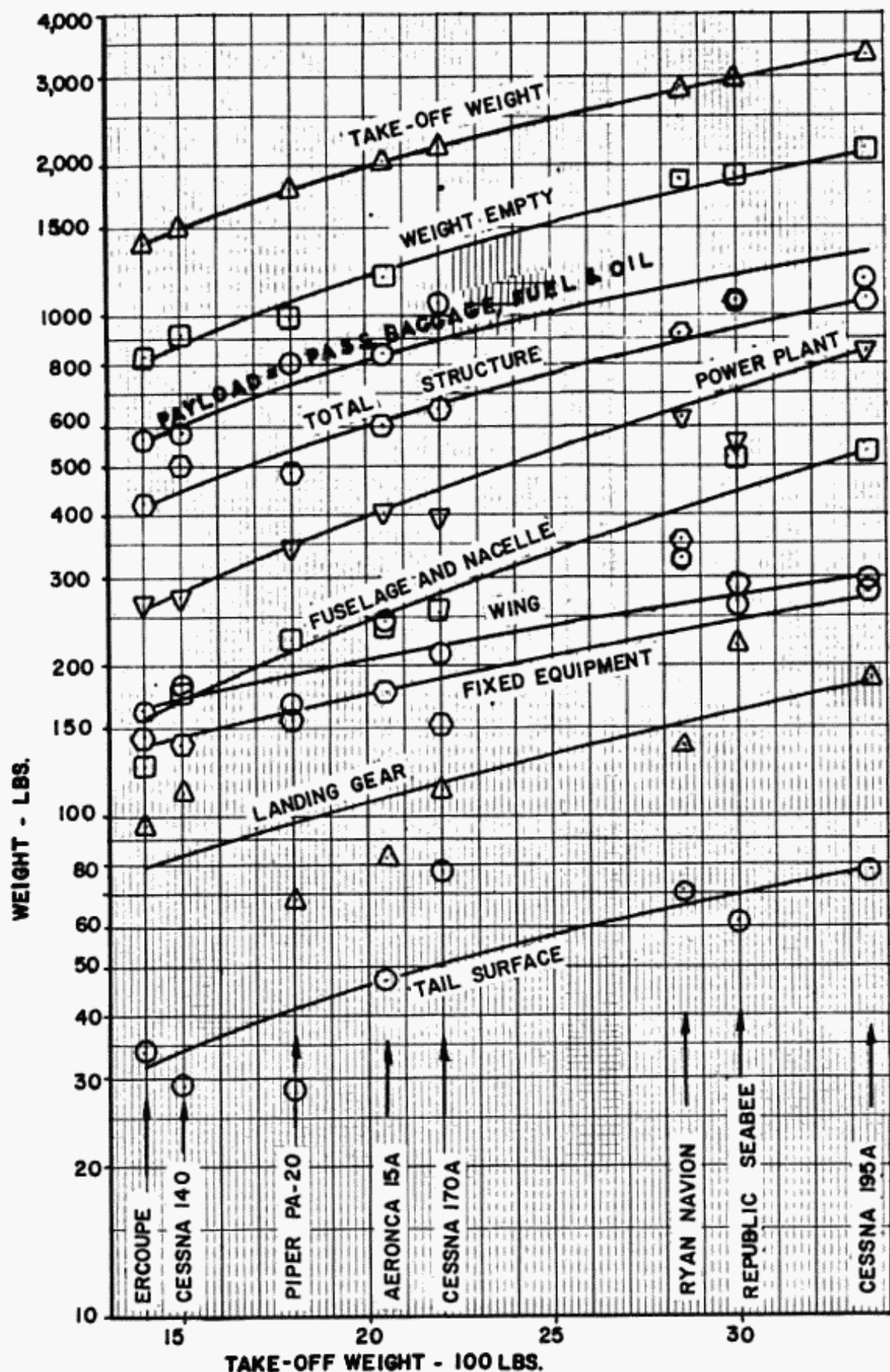


Fig. 8:15. Weight Breakdown of Private Airplanes.

CONTINENTAL ENGINE MODEL 185

PERFORMANCE

MAX. CONT. RATING - 185 HP
 TAKE-OFF RATING - 208 HP (ONE MINUTE)

WEIGHT AND DIMENSIONS

DRY WT. WITH STANDARD ACCESSORIES - 328 LBS.
 OIL CONSUMPTION AT RATED COND. - .08 LBS./HP-HR.
 LENGTH WITH SAE NO. 20 SPLINE - 48.40 IN.
 WIDTH - 33.38 IN.
 HEIGHT (DRY SUMP) - 21.66 IN.
 (WET SUMP) - 25.63 IN.

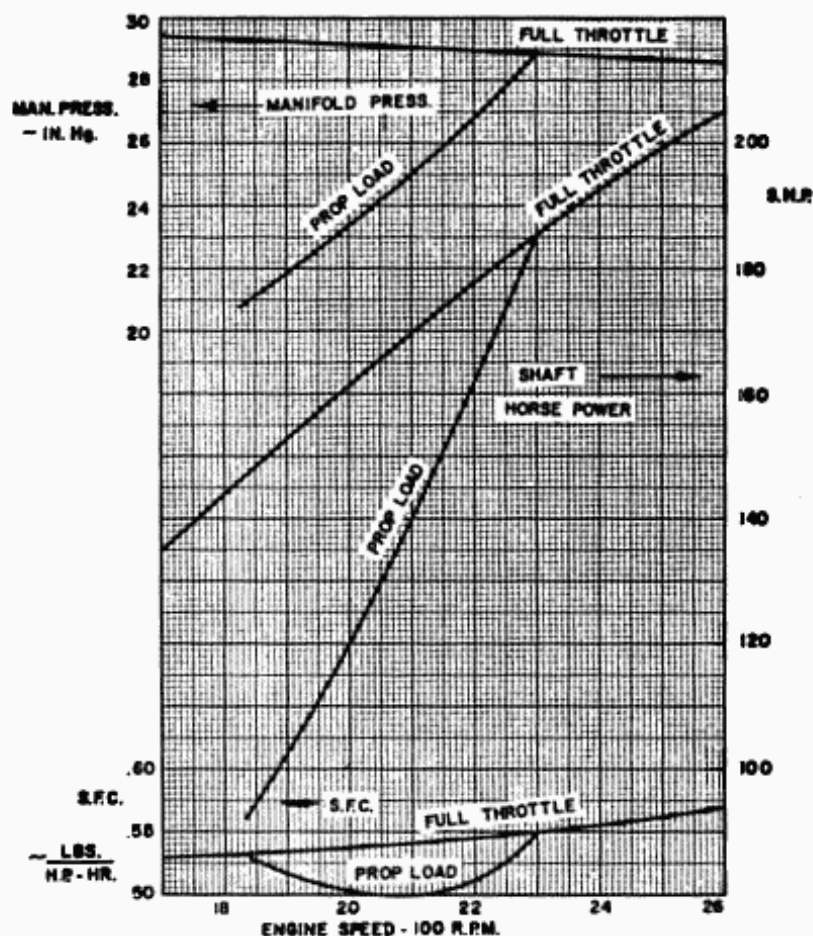
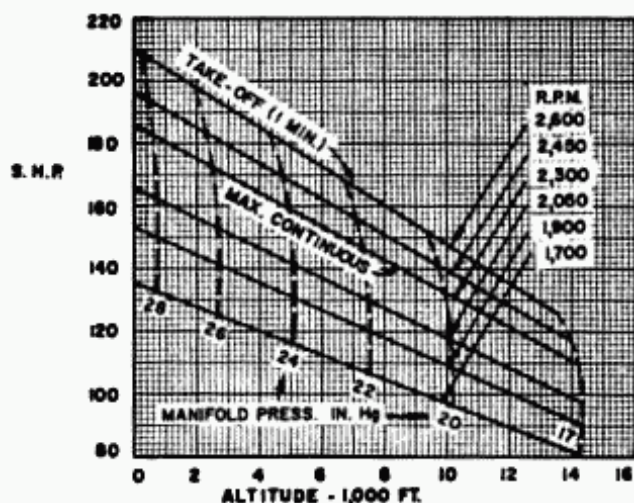


Fig. 8:16. "Characteristics of the Continental 185 H.P. Reciprocating Engine," courtesy Continental Engines.

BOEING 500-2 TURBO-JET

PERFORMANCE RATED THRUST	= 175 LBS.
S.F.C.	= 1.37 LB/LB-HR.
WEIGHT AND DIMENSIONS	
DRY WT. WITH STANDARD ACCESSORIES	= 120 LBS.
MAX. LENGTH	= 31.7 IN.
MAX. HEIGHT	= 22.2 IN.
MAX. WIDTH	= 21.0 IN.

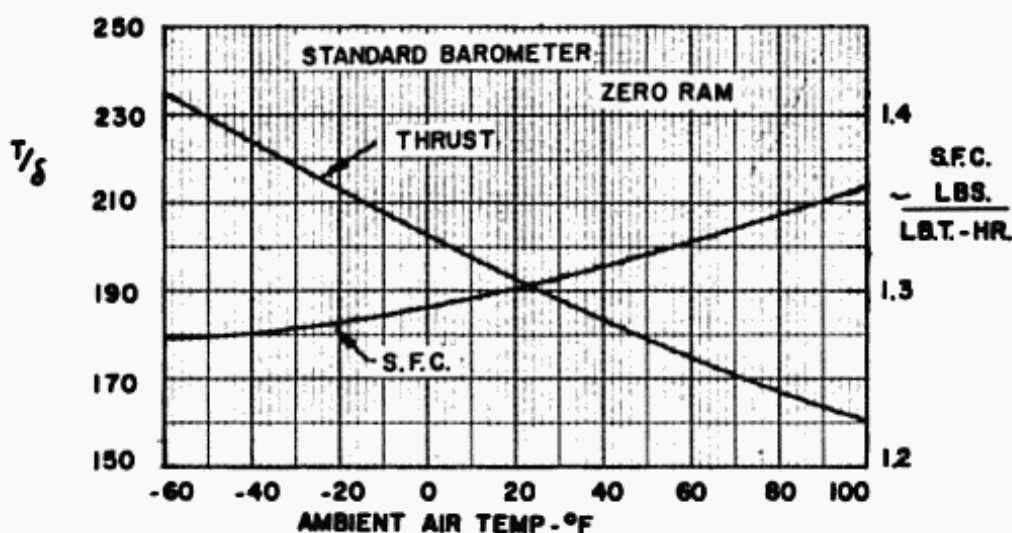
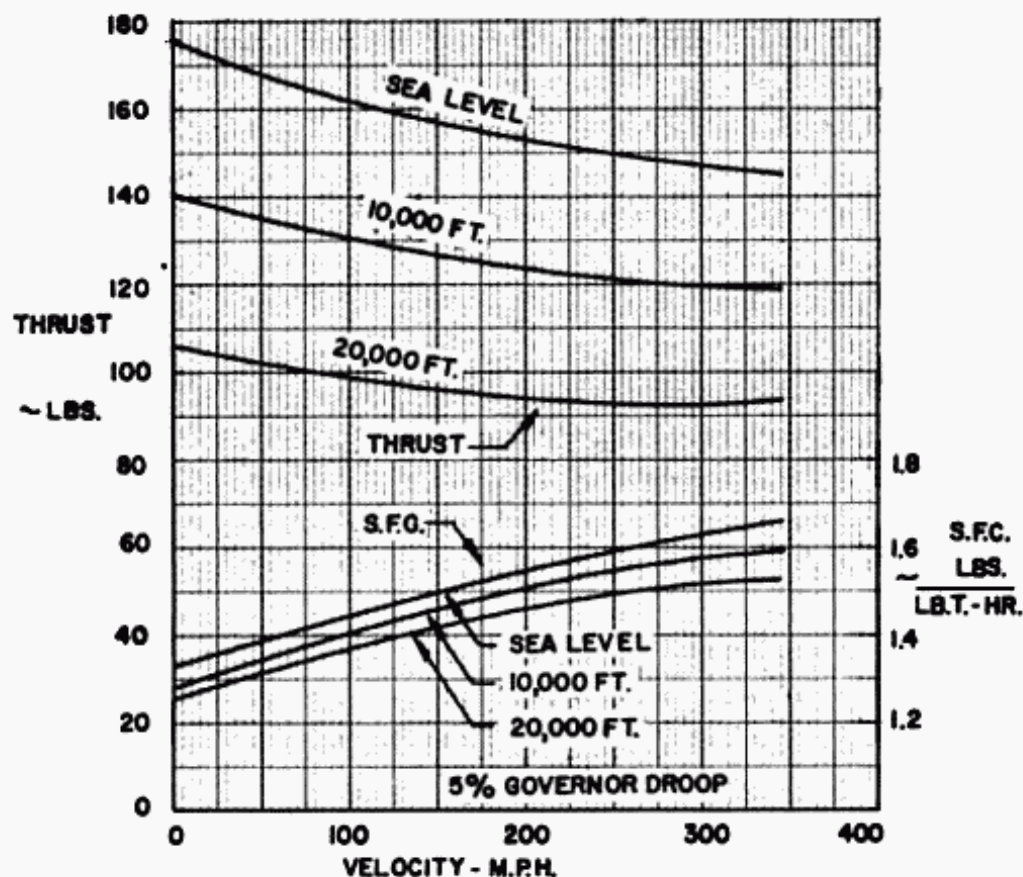


Fig. 8:17. Characteristics of Boeing 500-2 Turbo-Jet, courtesy of Boeing Aircraft.

BOEING 502-2E TURBO-PROP
 PERFORMANCE - RATED POWER - 175 S.H.P.
 S.F.C. = 1.3 LB/HP-HR

WEIGHT AND DIMENSIONS

DRY WT. WITH STANDARD ACCESSORIES	= 230 LBS.
MAX. LENGTH	= 39.9 IN.
MAX. WIDTH	= 25.2 IN.
MAX. HEIGHT	= 23.0 IN.

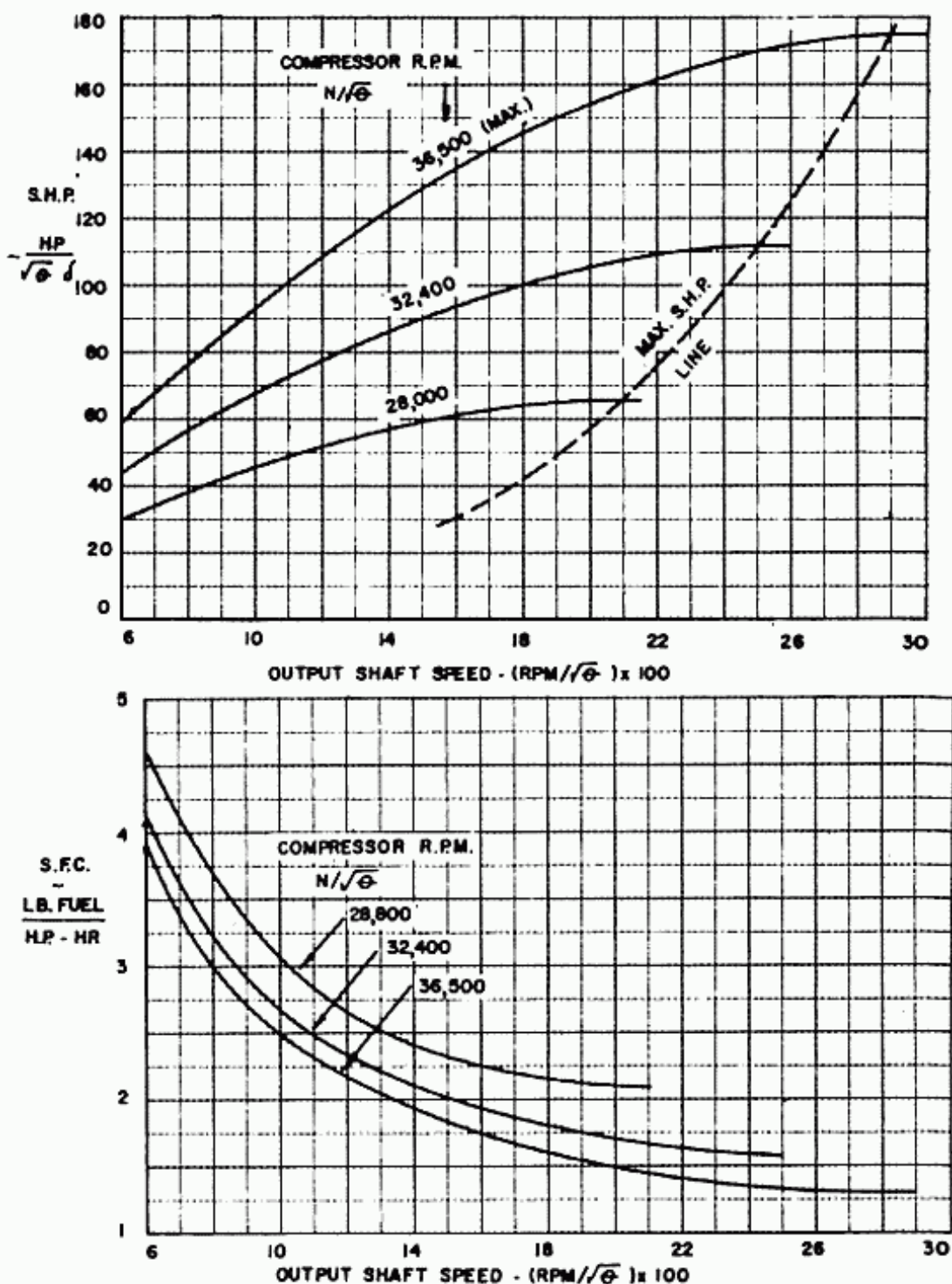


Fig. 8:18. Characteristics of Boeing 502-2E Turbo-Prop, courtesy of Boeing Aircraft.

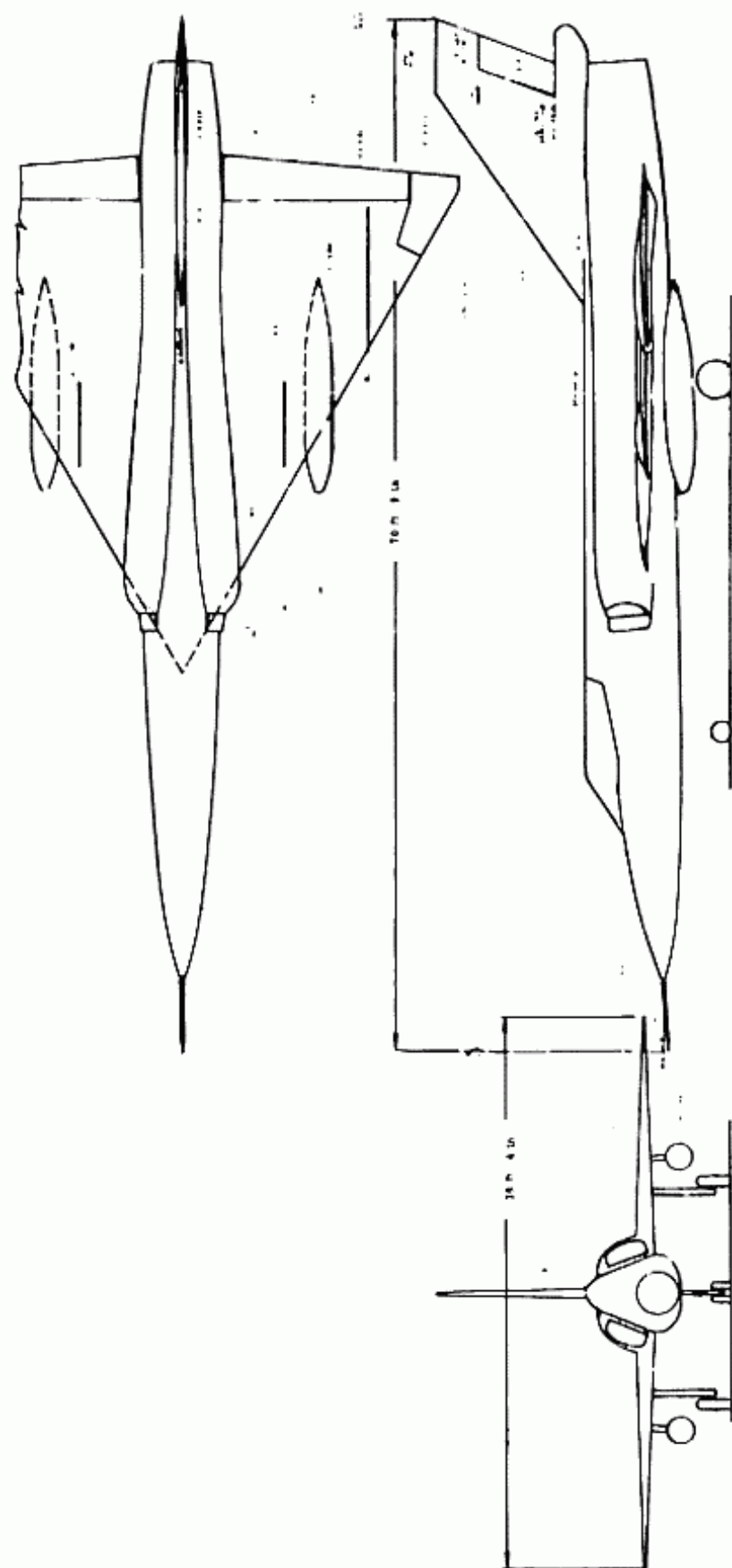


Fig. 8:19. Convair F 106 Supersonic Fighter.

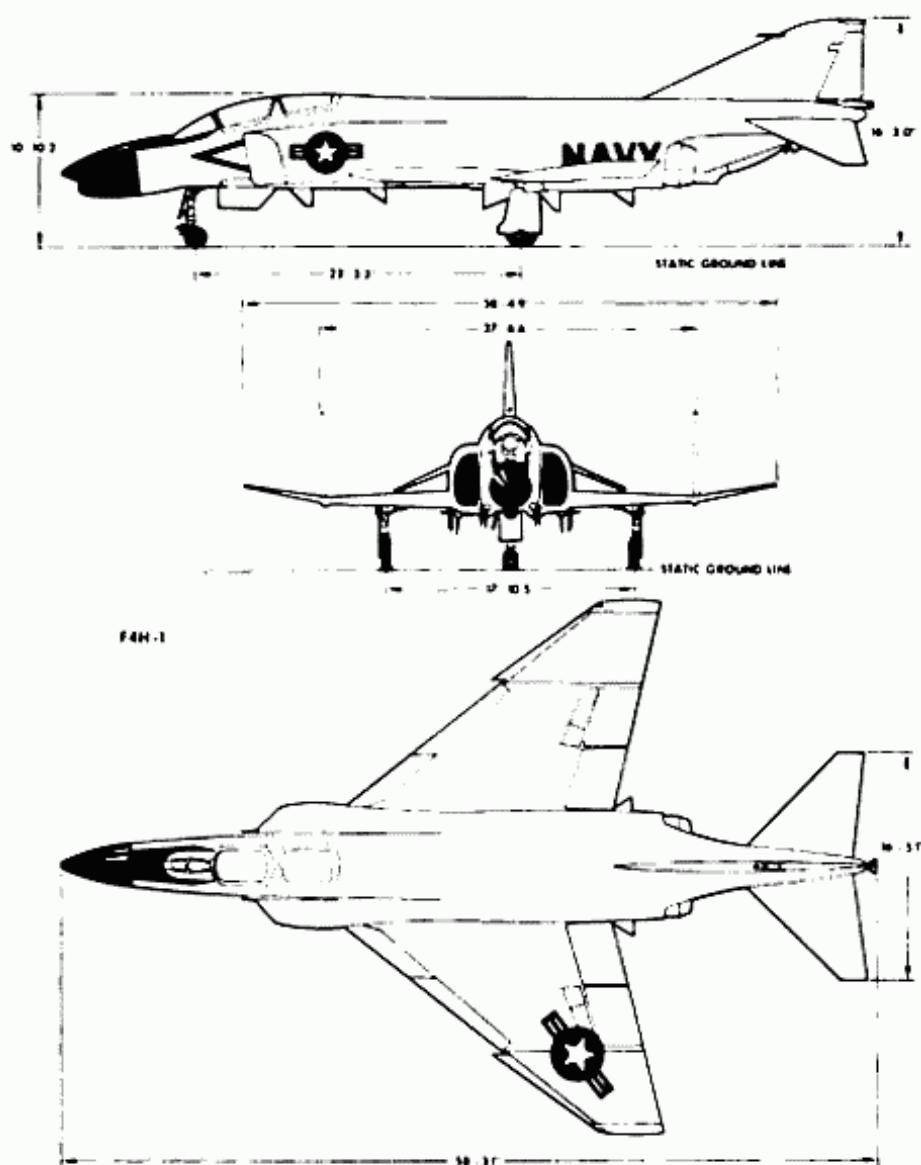


Fig. 8:20. McDonnell F4H-1 Supersonic Fighter.

factors. The cost factor is responsible for the lack of taper and for the constant airfoil sections in most private planes. The aspect ratio is, as before, a choice between aerodynamic and structural efficiency.

The design method outline of the jet transport can be followed for a private plane if the required changes to the weight and profile drag formulas are made, in addition to first choosing whether one or two engines are to be used. However since the private airplane is so small this preliminary work is usually not justified. In addition, private planes are often designed about a specific engine available at the time and there is not much need for varying engine sizes. However the ideas of choosing the wing

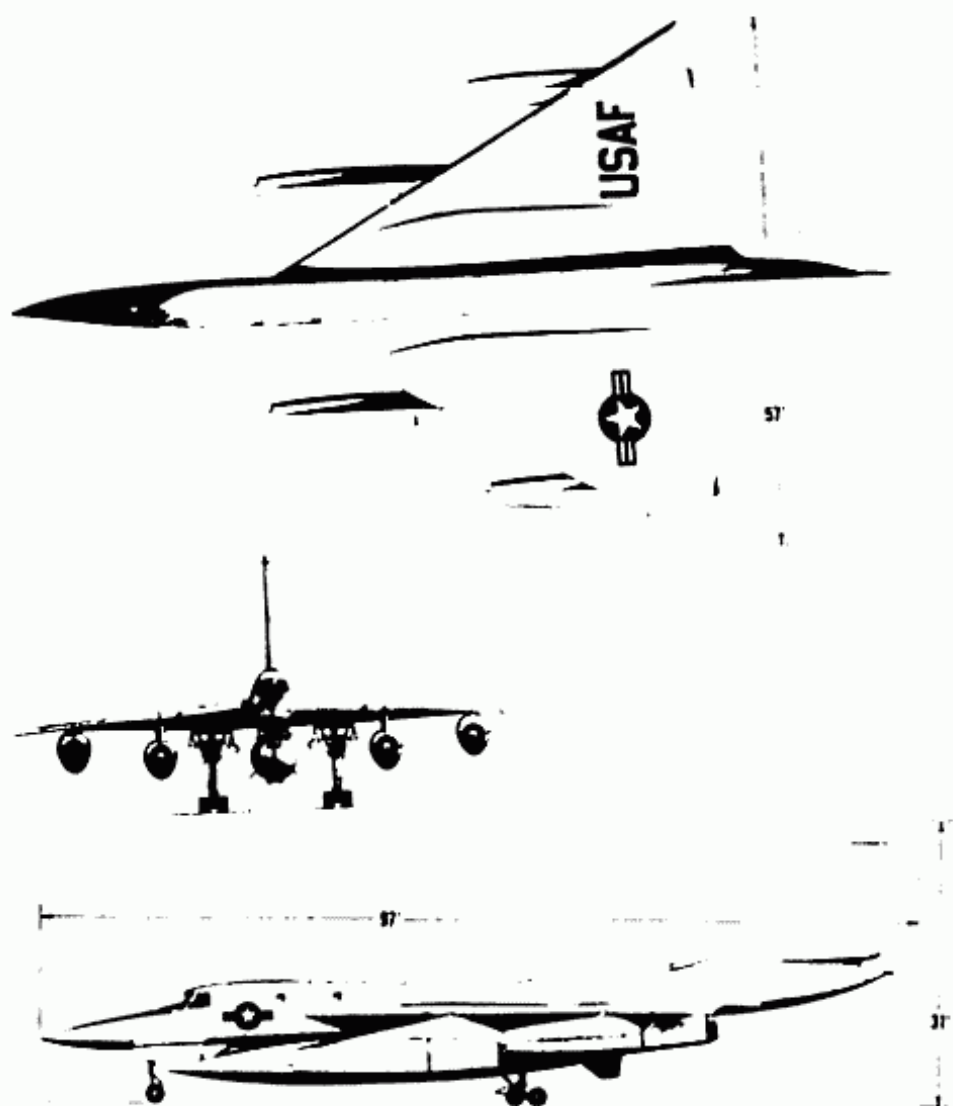


Fig. 8:21. Convair B 58 Hustler.

loading and thrust loading based upon the requirements might aid in simplifying the amount of work required in a trial and error method.

Design

The weight breakdown of a variety of private airplanes powered by reciprocating engines is presented in Figure 8:15. This data can be used in making preliminary weight estimate. The weights of the Republic Seabee were included. However they were not used to determine the curves since it is an amphibious aircraft and therefore is not comparable to the strictly land based aircraft.

Figure 8:16 presents the engine characteristics of the Continental Engine Model 185, with a take-off rating of 205 horsepower and a continuous rating of 185 horsepower.

The introduction of a small turbo-prop and a small turbo-jet by Boeing Aircraft into the engine field, increased the choice of

8:38 SUPERSONIC AND SUBSONIC AIRPLANE DESIGN

engine for the private plane designer. Figures 8:17 and 8:18 present the characteristics of the Boeing Model 500-2 turbo-prop and the Boeing Model 502-2E turbo-jet engines. The outstanding characteristics at these power plants, as compared to the reciprocating engines, are their low weight and small size.

A turbo prop engine much newer than the Boeing 501 is the G.E. T-58. Although this engine has a rating of 1,050 H.P., it weighs only 250 lbs. Its length is 55 inches and the diameter about 16 inches.

Chart 8:1 presents the tail volume coefficients for some existing private airplanes. These can be used as a guide in determining the tail surface areas for new designs.

<u>Airplane</u>	<u>T.O. Wt.</u>	<u>C_{HT}</u>	<u>C_{VT}</u>
Ercoupe	1,400	.36	.028
Cessna 140 A	1,500	.49	.037
Aeronca 15 A	2,050	.56	.033
Cessna 170 A	2,200	.76	.055
Ryan Navion	2,590	.62	.036
Cessna 195	3,350	.44	.037

8:8 Executive Airplanes

In the last few years, private airplanes of a much larger size than the ones presented in section 8:7 have been used for business by large corporations for their executives, and also for salesmen. These have come to be called executive airplanes.

These planes are essentially the same as the private planes only larger, with 2 engines, much greater equipment and more space. They might even be classed as small transports. They of course would be designed in the same manner as a private airplane or the transport. One of the newest and largest in its field is the Lockheed Jet Star which is presented in figure 8:22.

8:9 Missiles

The problem of designing a missile is, in many ways, similar to that of designing any other aircraft, particularly if only winged missiles are considered. The primary difference is in the replacement of the pilot by electronic control to fly the vehicle. The cruising performance can be calculated exactly as the

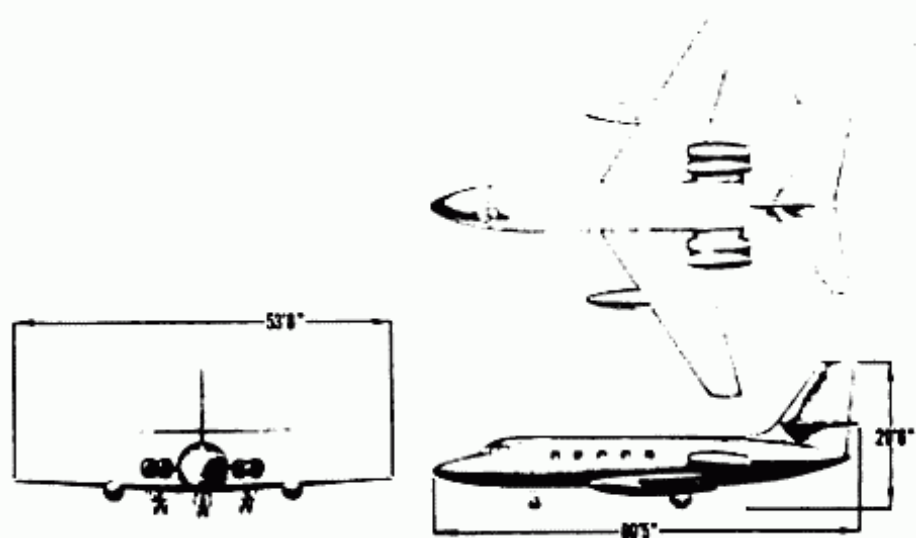


Fig. 8:22. Lockheed Jet Star - Executive or Utility Transport.

manned aircraft was, if the weight and volume requirements of the black boxes and warhead are known.

The fact that the take-off and landing problem of the manned aircraft is replaced by a launching problem for a ground-based missile, results in a change in the structural and propulsive design of the vehicle.

Due to the above differences and the added factor that a missile only has a life of one flight, the final configuration of a missile often looks radically different than that of a manned aircraft. A major difference between the missile and manned aircraft analysis is in stability and control. This is due to the fact that many missiles are symmetrical about both the XZ and XY planes, whereas the manned vehicles are only symmetrical about the XZ plane. The facts that the pilot has been replaced by electronic controls and that there are different stability and control requirements also, affect the stability and control problem.

There are separate texts that present the entire problem of missile design in an extensive and rigorous manner.

Ref. 8:1

J. B. Hammack and T. C. O'Bryan, "Effect of Advance Ratio on Flight Performance of a Modified Supersonic Propeller." NACA TN 4389, Sept. '58.

PART II
STABILITY AND CONTROL

Chapter IX

STABILITY AND CONTROL

9-1 Introduction

Every airplane must have satisfactory stability and control characteristics. For each type of airplane, commercial transport and private, the requirements are different and are set up by the controlling agency. However the fundamental theories behind the calculations of stability and control are the essentially the same. For this reason a general discussion of the problem, and a theoretical analysis of stability and control gives only an approximate solution to the problem. Actual preliminary design is more often based on previous experience and some wind tunnel testing than theoretical analysis. The final solution is obtained from complete wind tunnel, and full size model, tests. The unsatisfactory results of even wind tunnel tests is evidenced often by the modifications to tail surfaces after the first airplane is designed and flown. Nevertheless theoretical analysis is important since it indicates the significant criteria and the relative importance of each.

Since a jet transport airplane has been designed a brief outline of the stability and control requirements of the Civil Aeronautics Board is presented. The full text is not stated since it is very lengthy and may be obtained from the Civil Air Manual, Part 4B, Airplane Airworthiness, Transport Categories. The requirements are specified under two headings:

Controlability

"The airplane shall be safely controllable and maneuverable during take-off, climb, level flight, descent and landing for any center of gravity position that the airplane is liable to encounter." The specific details are then listed under the headings of longitudinal, directional and lateral control, and minimum control speed.

Stability

"The airplane shall be longitudinally, directionally and laterally stable in accordance with requirements under the following headings:

- Static longitudinal stability
- Stability during landing

Stability during approach

Stability during climb

Stability during cruising, landing gear extended and retracted

Dynamic longitudinal stability

Static directional and lateral stability

Dynamic directional and lateral stability."

Definition of Stability and Equilibrium

For an airplane to be in equilibrium the moment about the center of gravity must equal zero. If an airplane in equilibrium is acted on by outside forces so that equilibrium no longer exists, i.e., the summation of moments about the c.g. does not equal zero, it is truly stable if it ultimately returns to its original equilibrium position.

If the airplane that is disturbed from its equilibrium position initially tends to return to its original position it is said to be statically stable. If it then actually does return to its original equilibrium position it is said to be dynamically stable.

In considering the stability of an airplane, that is, both static and dynamic, there are four possible conditions. These are shown graphically in Figure 9:1.

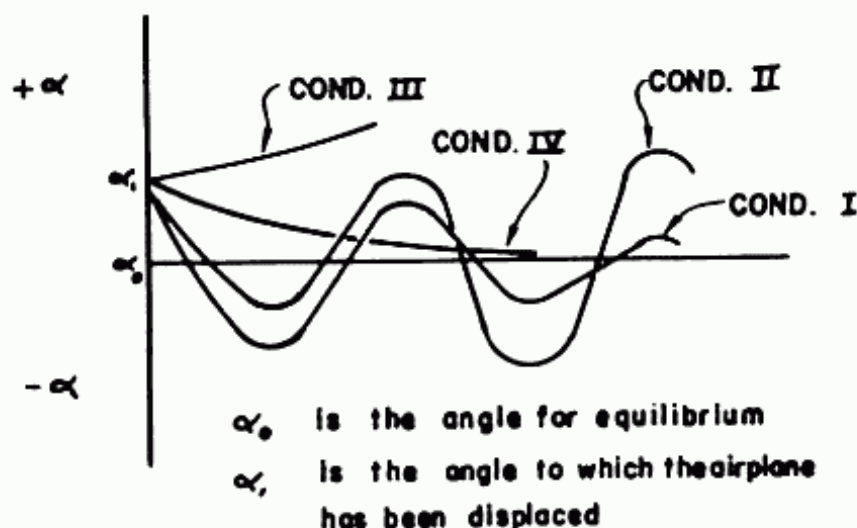


Fig. 9:1. Stability as defined by airplane motions.

- Cond. I Statically stable and dynamically stable. The airplane initially tends toward equilibrium and after a number of oscillations actually does reach the equilibrium state.
- Cond. II Statically stable but dynamically unstable. The airplane initially tends toward equilibrium but with each

oscillation diverges further and further from the equilibrium state.

Cond. III Statically and dynamically unstable. The airplane does not initially tend toward equilibrium, nor ever reach the equilibrium state.

Cond. IV Statically stable and extremely dynamically stable (similar to I); direct convergence. The airplane initially tends toward equilibrium and reaches it with no oscillations.

General

The study of stability has often been divided into two separate categories, static and dynamic, and each presented separately. Usually static stability has been presented first as it is fundamentally much simpler, and in the past, not only was the methods of determining dynamic stability not greatly developed, but also an airplane that was statically stable was usually satisfactory as far as dynamic stability was concerned.

However since the theory of dynamic stability has been further developed, and its greater importance realized, it is felt that a more general presentation of stability should be made, with static stability presented in its proper place as one facet of the stability problem.

Since stability is a function of the motion of the airplane, the equations of motion of the airplane must be set up and analyzed. In deriving these equations, the following assumptions are made:

1. only very small displacements from equilibrium position are considered.
2. changes in external forces and moments depend upon these changes in displacement, and speeds, not upon accelerations.
3. the coupling effects between the motions along the X and Z axis and about the Y axis, and the motions along and about the Y axis, and about the X axis, are assumed to be either zero or negligible. Although the following derivation is based upon this assumption, the configurations that have developed for high subsonic, and particularly supersonic, airplanes are such that in many cases the cross coupling effects cannot be ignored.

Since in considering dynamic stability the airplane is considered a rigid body, there are six equations of motion for fixed controls, three along the axes, and three about the axes. The equations along the axes involve forces while those about the axes

9:4 SUPERSONIC AND SUBSONIC AIRPLANE DESIGN

involve moments. For free controls there is an additional equation for the movement about the hinge line of each control surface, and is therefore in terms of moments.

Fig. 9:2 shows the three axes of the airplane, the symbols of the angular velocities about them, and the symbols of the velocities along the axes.

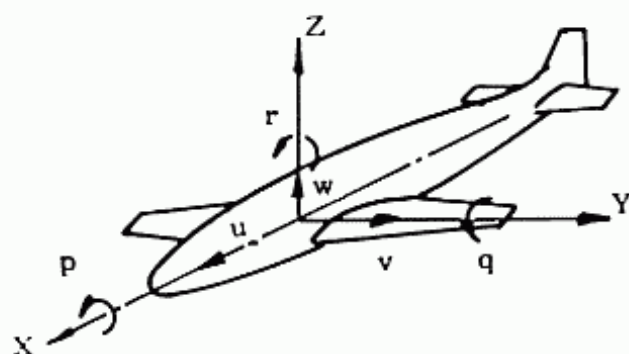


Fig. 9:2. Airplane axes.

where p is the angular velocity about the X axis
 q is the angular velocity about the Y axis
 r is the angular velocity about the Z axis
 u is the linear velocity along the X axis
 v is the linear velocity along the Y axis
 w is the linear velocity along the Z axis

It should be noticed here that the X-Z plane is the usual plane of symmetry in an airplane. All motions in the plane, that is along the X and Z axes and about the Y axis, are considered in longitudinal control and stability. All motions outside of this plane, that is about the X and Z axes and along the Y axis, are considered in lateral control and stability.

Since stability and control is only a part of the design problem it will be presented here only briefly. A more detailed discussion may be obtained in the literature, see references at end of chapter. The longitudinal stability problem will be discussed in some detail, while directional and lateral stability will be only touched upon.

9-2 Longitudinal Dynamic Stability

A. Longitudinal Equations of Motion

Longitudinal stability is dependent only upon the airplane motions along the X and Z axes, and about the Y axis, if the stick is fixed. In the case where the stick is free, the motion of the

elevator about its hinge line must also be considered. The choice of axes to use in these equations of motion is most important as it is instrumental in determining the ease with which the resulting equations may be solved. One set of axes, those fixed to the body, are called the body axes, and usually has the X axis along the fuselage reference line, with the Y and Z axes perpendicular to it. Another possibility is the set of axes with the X axis pointing into the relative wind and is therefore called the wind axes. It is shown in figure 9:3, where α , γ , and θ are shown positive. The formulas presented here, are based upon the wind axes as they are more convenient, and upon the assumptions that the changes of moments of inertia and products of inertia are negligible for the small disturbances.

$$\Sigma F_x = m\dot{V} \quad (9:1)$$

$$\Sigma F_z = mVq \quad (9:2)$$

$$\Sigma M = I_y\dot{q} \quad (9:3)$$

$$\Sigma HM_e = I_e\ddot{\delta}_e \quad (9:4)$$

For the sake of simplicity the study of the stick-fixed condition is made first and then modified for the stick-free condition. Therefore in the stick fixed condition equation 9-4 is eliminated since $\ddot{\delta}_e = 0$.

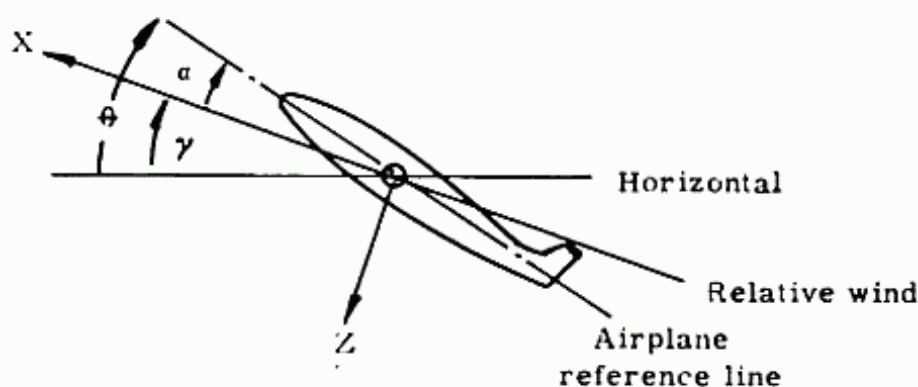


Fig. 9:3. Wind axes.

B. The Differential Equations

To solve these equations of motion for the stability characteristics of the airplane it is necessary to develop them further. The left sides of the equations are first partially differentiated with respect to the variables that affect this particular characteristic. Equation 9:1 will be used as an example.

9:6 SUPERSONIC AND SUBSONIC AIRPLANE DESIGN

The 3 major variables that appear to affect F_x are:

V - forward speed

α - angle of attack

θ - attitude of airplane as referred to the horizontal

The change in F_x due to the change of these variables and of their derivatives in respect to time is shown in equ. 9:5.

$$\Sigma F_x = \frac{\partial F_x}{\partial V} dV + \frac{\partial F_x}{\partial \alpha} d\alpha + \frac{\partial F_x}{\partial \theta} d\theta + \frac{\partial F_x}{\partial \dot{\alpha}} d\dot{\alpha} + \frac{\partial F_x}{\partial \dot{\theta}} d\dot{\theta} \quad (9:5)$$

It should be noted that equ. 9:5 is the change in motion from the equilibrium condition due to changes in α , θ and V from the equilibrium values of α , θ and V .

The variation in F_x with respect to the 2nd derivative of the velocity has not been included as one of the assumptions is that the change in external forces is independent of acceleration. Since the displacements have been assumed to be small and the partial derivatives linear, dV can be changed to ΔV , $d\alpha$ to $\Delta\alpha$, etc. Taking into account that $\partial F_x/\partial \dot{\alpha}$ and $\partial F_x/\partial \dot{\theta}$ are negligible, ΣF_x then becomes

$$\Sigma F_x = \frac{F_x}{V} \Delta V + \frac{F_x}{\alpha} \Delta\alpha + \frac{F_x}{\theta} \Delta\theta = m\dot{V} \quad (9:6)$$

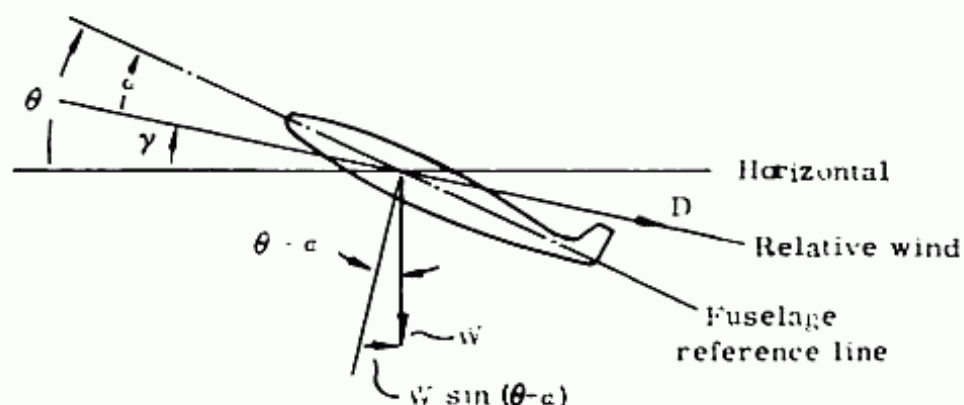


Fig. 9:4. Changes in forces along X axis.

It should be noted that F_x is + in the forward direction and - in the aft direction.

From fig. 9:4, (again these are changes in forces due to changes from equilibrium) assuming $(\theta - \alpha)$ is small enough so that $\sin(\theta - \alpha) = \theta - \alpha$, and assuming a glide with thrust = 0;

$$\Sigma F_x = 1/2 \rho S V^2 C_D - W (\theta - \alpha) \quad (9:7)$$

$$\frac{\partial F_x}{\partial V} = -\rho S V C_D - \frac{\rho}{2} V^2 S \frac{dC_D}{dV} \quad (9:8)$$

$$\frac{\partial F_x}{\partial \alpha} = -1/2 \rho V^2 S \frac{dC_D}{d\alpha} + W \quad (9:9)$$

$$\frac{\partial F_x}{\partial \theta} = -W \quad (9:10)$$

Substituting the values of $\partial F_x/\partial V$, $\partial F_x/\partial \alpha$ and $F_x/\partial \theta$ into equ. 9:6, and assuming $dC_D/dV = 0$, equ. 9:11 results. For subsonic airplanes dC_D/dV may be considered equal to zero except possibly at V_{cruise} in high subsonic designs where dC_D/dV might not be negligible due to compressibility effects. For supersonic aircraft where wave drag is an appreciable factor and is dependent on M , which is dependent on V , dC_D/dV cannot be assumed equal to zero.

$$-\rho S C_D V \Delta V - (\rho/2) S V^2 \frac{dC_D}{d\alpha} \Delta \alpha + W \Delta \alpha - W \Delta \theta = m \dot{V} \quad (9:11)$$

To ultimately eliminate W first divide thru by $\rho S V^2$.

$$-C_D \frac{\Delta V}{V} - \frac{1}{2} \frac{dC_D}{d\alpha} \Delta \alpha + \frac{W}{\rho S V^2} \Delta \alpha - \frac{W}{\rho S V^2} \Delta \theta = \frac{m}{\rho S V^2} \dot{V} \quad (9:12)$$

Letting $\Delta V/V = u$ and $V/V = \dot{u}$, and knowing $\frac{2(W/S)}{\rho V^2} = C_L$,

(Note that u here is the non dimensional velocity in the X direction, that is the change in u (as shown in fig. 9:2) divided by the equilibrium velocity in the X direction, V),

then

$$-C_D u = \left(\frac{1}{2} \frac{dC_D}{d\alpha} - \frac{C_L}{2} \right) \Delta \alpha - \frac{C_L}{2} \Delta \theta = \frac{m}{\rho S V} \dot{u} \quad (9:13)$$

Note that both sides of the above equation are non-dimensional. On the right hand u has the dimension of $1/T$, while $m/\rho S V$ has the dimension of T . For simplification τ is used for $m/\rho S V$, and time is used as the non-dimensional time, t/τ . Then the right hand side of the equation, $(m/\rho S V) u$, is equal to

$$\tau \frac{du}{dt} \text{ or } \frac{du}{d(t/\tau)}$$

Now if the term $\frac{d}{d(t/\tau)}$ is called the operator \underline{d} , the right hand sides become $\underline{d}u$. Using the usual notation that $dC_D/d\alpha$ is $C_{D\alpha}$ and letting α and θ be used for $\Delta\alpha$ and $\Delta\theta$, equ. 9:13 becomes

$$\left(C_D + \underline{d}\right)u + \left(\frac{C_{D\alpha}}{2} - \frac{C_L}{2}\right)\alpha + \frac{C_L}{2}\theta = 0 \quad (9:14)$$

This is the differential equation developed from the equation of motion along the X axis, equ. 9:1.

Following the same procedure for eqs. 9:2, and 9:3, (the equations of motion along the Z axis and about the Y axis respectively), the following differential equations may be developed:

$$C_L u + \left(\frac{C_{L\alpha}}{2} + \underline{d}\right)\alpha - \underline{d}\theta = 0 \quad (9:15)$$

$$\left(C_{M\alpha} + C_{M\underline{d}}\alpha\underline{d}\right)\alpha + \left(C_{M\underline{d}}\theta\underline{d} - h\underline{d}^2\right)\theta = 0 \quad (9:16)$$

Note that

$$h = \frac{2K_y^2}{\mu c^2}$$

where

K_y = the radius of gyration about the Y axis

$\mu = \frac{M}{\rho S c^2}$ called the airplane relative density factor and is dimensionless.

c = the mean geometric chord

These equations 9:14, 9:15 and 9:16 are now simultaneous differential equations with constant coefficients which are made up of the airplane mass and inertia parameters as well as the stability derivatives, $C_{L\alpha}$, $C_{D\alpha}$, $C_{m\alpha}$, $C_{Dd\theta}$, etc. These derivatives must eventually be evaluated by either analytical or wind tunnel methods, before the dynamic motion of the airplane can be determined. The mass and inertia parameters can be calculated from the airplane's physical characteristics.

C. Solutions to the simultaneous differential equations (stick fixed).

These simultaneous differential equations can be solved by assuming the solution in the form:

$$\begin{aligned}
 u &= u' e^{\lambda t/\tau} & \alpha &= \alpha' e^{\lambda t/\tau} & \theta &= \theta' e^{\lambda t/\tau} \\
 \frac{du}{dt} &= \lambda u' e^{\lambda t/\tau} & \frac{d\alpha}{dt} &= \lambda \alpha' e^{\lambda t/\tau} & \frac{d\theta}{dt} &= \lambda \theta' e^{\lambda t/\tau} \\
 \frac{d^2 u}{dt^2} &= \lambda^2 u' e^{\lambda t/\tau} & \frac{d^2 \alpha}{dt^2} &= \lambda^2 \alpha' e^{\lambda t/\tau} & \frac{d^2 \theta}{dt^2} &= \lambda^2 \theta' e^{\lambda t/\tau}
 \end{aligned} \tag{9:17}$$

where u' , α' , θ' and λ' are constants, either real or complex. If substitutions of u' , α' , θ' and their derivatives, of equ. 9:17, are made in equs. 9:14, 15, and 16, they reduce to 3 new equations with the unknown λ and the new variables u' , α' and θ' .

$$(C_D + \lambda)u' + \left(\frac{1}{2} C_{D\alpha} - C_L\right) \alpha' + \frac{C_L}{2} \theta' = 0 \tag{9:18}$$

$$C_L u' + \frac{1}{2} (C_{L\alpha} + \lambda) \alpha' - \lambda \theta' = 0 \tag{9:19}$$

$$(C_{m\alpha} + C_{m\dot{\alpha}}) \alpha' + (C_{m\dot{\theta}} \lambda - h\lambda^2) \theta' = 0 \tag{9:20}$$

If values of u' , α' , and θ' are to be obtained by the methods of determinants then the following procedure must be followed. Set equations in this manner, with _____ denoting a coefficient:

$$\begin{array}{rcl}
 \text{_____ } u' & + & \text{_____ } \alpha' & + & \text{_____ } \theta' & = & a \\
 \text{_____ } u' & + & \text{_____ } \alpha' & + & \text{_____ } \theta' & = & b \\
 \text{_____ } u' & + & \text{_____ } \alpha' & + & \text{_____ } \theta' & = & c
 \end{array}$$

Then,

$$\alpha' = \frac{\begin{array}{c} \text{_____ } a \text{ _____} \\ \text{_____ } b \text{ _____} \\ \text{_____ } c \text{ _____} \end{array}}{\begin{array}{c} \text{_____} \\ \text{_____} \\ \text{_____} \end{array}} \tag{9:21}$$

Since in equations 9:18, 9:19 and 9:20, a, b, and c are equal to zero the numerator determinant in 9:21 = 0. If α' , u' and θ' are to be finite numbers, then the denominator determinant of equ. 9:21 must also be zero. This result can now be used to obtain the values of λ .

$$\begin{array}{rcl}
 C_D + \lambda & & 1/2 (C_{D\alpha} - C_L) & & 1/2 C_L \\
 C_L & & 1/2 (C_{L\alpha} + \lambda) & & - \lambda \\
 0 & & C_{m\alpha} + C_{m\dot{\alpha}} & & C_{m\dot{\theta}} \lambda - h\lambda^2
 \end{array} \tag{9:22}$$

By expanding this determinant, a quartic in λ is obtained:

$$A\lambda^4 + B\lambda^3 + C\lambda^2 + D\lambda + E = 0 \quad (9:23)$$

From the values of λ alone the character of the motion can be determined, and the values of α' , u' , and θ' are not necessary. Usually all that is required is to determine if the airplane is longitudinally stable, its period, and its time to damp to half amplitude if the motion is oscillatory. However, it is also possible to determine the entire motion of the airplane, that is plot up u , α and θ as a function of time. This may be done by first solving equ. 9:23 for λ , and thereby obtain 4 values of λ : λ_1 , λ_2 , λ_3 and λ_4 .

Substitute λ_1 in eqs. 9:18, 9:19 and 9:20 with u_1 , α_1 , and θ_1 and solve these simultaneous equations for u_1 , α_1 , and θ_1 . Using λ_2 obtain u_2 , α_2 , and θ_2 etc. Then,

$$\begin{aligned} u &= u_1 e^{\lambda_1 t/\tau} + u_2 e^{\lambda_2 t/\tau} + u_3 e^{\lambda_3 t/\tau} + u_4 e^{\lambda_4 t/\tau} \\ \alpha &= \alpha_1 e^{\lambda_1 t/\tau} + \alpha_2 e^{\lambda_2 t/\tau} + \alpha_3 e^{\lambda_3 t/\tau} + \alpha_4 e^{\lambda_4 t/\tau} \\ \theta &= \theta_1 e^{\lambda_1 t/\tau} + \theta_2 e^{\lambda_2 t/\tau} + \theta_3 e^{\lambda_3 t/\tau} + \theta_4 e^{\lambda_4 t/\tau} \end{aligned} \quad (9:24)$$

Now since the u 's, α 's and θ 's are known, as well as the λ 's, the motions can be plotted as a function of t/τ . The value of τ can be calculated at any velocity and altitude.

D. Significance of λ .

Although the motions can be evaluated as a function of time as explained above, it is unnecessary. The values of λ alone are enough to determine the airplane stability, and, if oscillatory, its periods and times to damp to half amplitude. It is assumed that the quartic equation is solved by one of the numerous methods, normal algebraic analytics, graphics, or refined trial and error. Ref. 9:1 presents a graphical method of solution while ref. 9:13 presents a refined trial and error procedure.

Now, if all λ 's are real numbers the motion is aperiodic; convergent if negative, divergent if positive. This is readily seen from studying the term $e^{\lambda t/\tau}$. If λ is positive the e term increases with time, and α , u and θ eventually become infinite. If λ is negative, the e term decreases with time, and therefore α , u and θ tend to approach zero. Note that α , u and θ are changes from the equilibrium position. It is important to realize that from $e^{\lambda t/\tau}$, with λ being negative no matter how large, the

disturbances α , u and θ are not completely damped out, i.e. reach zero, until t is infinite. It is for this reason that the criteria for damping is the time required to damp to half amplitude, which is a function of λ , and not the time to be damped to zero amplitude, which is independent of the magnitude of λ and can only occur at t equal infinity. If any of the values of λ form a complex pair, the motion is oscillatory; positively damped if the real part is negative, and negatively damped if the real part is positive. The term, neutrally damped, will be used for the condition where the real part is zero, that is the oscillation neither converges as when positively damped, nor diverges as when negatively damped. The term undamped is sometimes used for neutrally damped.

For a complex value of λ

$$u = u_1 e^{(a + ib) t/\tau} + u_1 e^{(a - ib) t/\tau} + \text{etc.} \quad (9:25)$$

or
$$u = u_1 e^{at/\tau} \left[e^{ibt/\tau} + e^{-ibt/\tau} \right] \quad (9:25a)$$

Since
$$e^{ibt/\tau} + e^{-ibt/\tau} = 2 \cos (bt/\tau) \quad (9:25b)$$

it is obvious that the variation in u with time is an oscillatory motion of the simplest kind, an harmonic. The positive real part of a complex pair of roots results in a divergent oscillation, while a negative real part results in a convergent oscillation. These results are shown graphically in figure 9:5.

E. Significance of Coefficients of Quartic:

The section above has shown how the motion can be studied if the quartic has been solved for the values of λ . However, valuable information can be obtained merely by inspection of the coefficients of the quartic.

- 1) If all coeff. are +, there can be no + real roots and therefore no pure divergence.
- 2) If one of the coefficients is -, there will be either an increasing oscillation or a pure divergence, in one of the modes. (opposite of 1)
- 3) If Routh's discriminant $(BCD - AD^2 - B^2E)$ is +, there is no possibility of the real part of any complex pair being positive, and there will be no negatively damped oscillation.
- 4) If Routh's discriminant is -, there will be one complex pair with a positive real part, implying an negatively damped oscillation.
- 5) If Routh's discriminant is = 0, a neutrally damped oscillation will result.

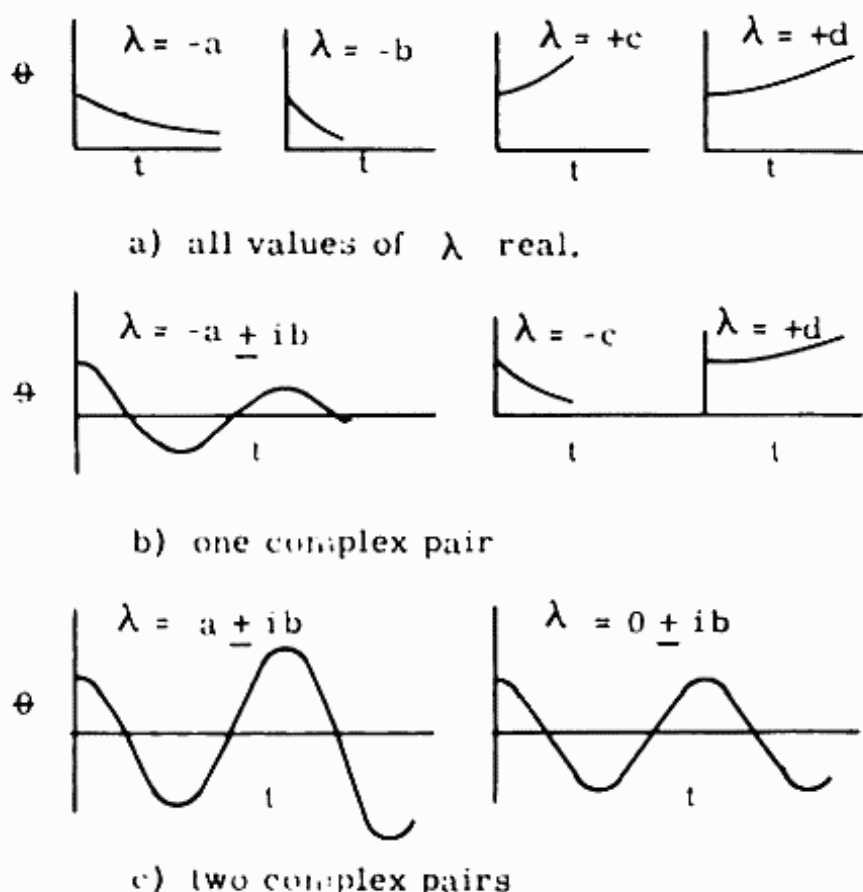


Fig. 9:5. Airplane motions:

- 6) If $E = 0$, then one of the roots is 0 and one of the modes can continue unchanged indefinitely.

It should be noted here that for the quartic

$$A\lambda^4 + B\lambda^3 + C\lambda^2 + D\lambda + E = 0$$

where A is positive a necessary condition for stability is that E be positive. In the derivation of this formula (ref. 9:1)

$$E = -\frac{C_L^2}{2h} C_{m\alpha} \quad (9:26)$$

Since h is always positive it is necessary for $C_{m\alpha}$ to be negative for E to be positive. Since

$$C_{m\alpha} = \left(\frac{dC_m}{dC_L} \right) \left(\frac{dC_L}{d\alpha} \right) \quad (9:27)$$

and $dC_L/d\alpha$ is always positive below the stall, dC_m/dC_L must be

negative for stability. It is therefore seen that maintaining dC_m/dC_L negative is one condition for dynamic stability, and this criteria of negative dC_m/dC_L is the requirement for "static stability". This static stability and the physical implications of a negative dC_m/dC_L will be discussed later. However note here that if $E = 0$ as stated in (6) above, $dC_m/dC_L = 0$, (there is no moment induced by a change in C_L) and the airplane will stay in this displaced position of C_L , or α , indefinitely.

The Determination of the Period and Damping:

The values of λ must be known before the period and damping characteristics can be evaluated. If the solution of the quartic yields two complex pair for λ , i.e.

$$\lambda_{1,2} = -a_1 \pm ib_1, \quad \lambda_{3,4} = -a_2 \pm ib_2$$

then there are two oscillatory modes,

$$e^{at/\tau} (e^{ibt/\tau} + e^{-ibt/\tau}) = e^{at/\tau} [2 \cos (bt/\tau)].$$

From the above harmonic motion, it follows that

$$\text{period} = \frac{2\pi}{b} \tau \quad (9:28)$$

The time to damp to half amplitude may be derived by finding t when

$$e^{at/\tau} = 1/2$$

then $\ln e^{at/\tau} = \ln 1/2$

$$at/\tau = -.693$$

$$t/\tau = -.693/a$$

$$t_{1/2} = \frac{-.693}{a} \tau \quad (9:29)$$

Note that 'a' must be negative for a positively damped motion, and therefore results in a positive t .

F. Stick Free Longitudinal Stability

From the above information, it is possible to understand the method of obtaining the longitudinal characteristics of the airplane in the stick fixed condition. For the stick free condition it is necessary to introduce the equation of motion about the elevator hinge line, equ. 9:4. Although the 4 equations of motion may be solved the work involved is quite time consuming. For

simplification, and ease of understanding it is often assumed that the change in velocity is negligible, that is the motion along the X axis is constant, and therefore equation 9:1 can be neglected.

Then using equations 9:2, 9:3 and 9:4, in a similar manner as shown above for 9:1, 9:2, and 9:3 another quartic in λ is obtained, and analogous information determined, i.e., stability characteristics, periods and damping.

G. Stability Derivatives

To solve the quartic equation for λ it is necessary to know the value of the coefficients. These coefficients which involve C_{m_α} , C_{L_α} , $C_{m_{d\theta}}$, etc. are called stability derivatives. These terms may be obtained analytically, experimentally or by a combination of the two methods. Ref. 9:1 presents analytical methods for obtaining the derivatives required. The analysis does not include effects of sweepback, compressibility or interference. Refs. 9:2 to 9:11 present analytical and experimental values of stability derivatives for swept wings, for effects of high subsonic, and supersonic speeds, for cones at supersonic speeds, for delta wings, and for full airplane models.

H. Outline of Stability Analysis

It would be worthwhile now to go back briefly to the steps that were taken to determine the stability characteristics of the airplane, and see the reasoning and procedures involved.

The purpose of the analysis is to observe the motion of an airplane, after it has been displaced from its equilibrium position. Since we are concerned with motions, and motions are only caused by forces and moments it is necessary to write equations of the summation of forces and moments along and about the axes concerned. In the longitudinal case it is along the X axis, along the Z axis, and about the Y axis. These are called the equations of motion.

Now that we have the equations of motion, i.e. $\Sigma F = ma$, etc. how do we determine the manner in which a displacement from the equilibrium position affects the motion? If we know that certain displacements have an effect on this motion, say α , θ , and V , and we are interested how these displacements vary with time after the initial disturbance, it is necessary to rewrite the equation of motion with $\Delta\alpha$, $\Delta\theta$ and ΔV as the variables, i.e.

$$\Delta F_x = \frac{\partial F_x}{\partial V} \Delta V + \frac{\partial F_x}{\partial \alpha} \Delta \alpha + \frac{\partial F_x}{\partial \theta} \Delta \theta = \Delta m \dot{V} \quad (9:30)$$

Writing out the values of $\partial F/\partial V$, etc. in this equation and in the

other 2 equations of motions, results in 3 simultaneous equations with the 3 variables ΔV , $\Delta\alpha$ and $\Delta\theta$. These equations then compromise the solution to the problem of replacing the physical problem by a mathematical one. The rest is merely the mathematical solution to the problem. The setting up of the equations is the most important and challenging problem for the aeronautical scientist.

The mathematical solution is then followed as explained in the previous presentation. The simultaneous equations are solved by assuming that α , θ , and u , are a function of time in the form of $\alpha = \alpha_1 e^{\lambda t/\tau}$, substituting in the simultaneous equations, and solving for λ . Once the values of λ are known, the variation of the change in α , θ and u with respect to time are known. The stability characteristics can then be obtained.

9-3 Motions of the Airplane

The oscillatory motions usually encountered in airplane flight are as follows:

A. Longitudinal

a) Stick fixed

1. a long period mode, called the stick fixed Phugoid
2. a short period mode, very heavily damped

b) Stick free

1. a long period mode, called the stick free Phugoid
2. a very short period mode, heavily damped
3. a short period mode, sometimes negatively damped

B. Lateral

a) Stick fixed

1. a spiral divergence is sometimes tolerated although if not corrected it can tighten to a steep highspeed spiral dive.

Note: Spin - airplane descends vertically along a helical path of large pitch and small radius at α greater than stall

Spiral - airplane descends vertically along a helical path of small pitch and large radius at α in usual flight range.

2. a direct convergence, very heavily damped
3. a short period mode, called Dutch roll, usually heavily damped.

b) Rudder free (aileron locked)

1. spiral divergence - usually very slow (similar to stick fixed)

2. a direct convergence - very heavily damped (similar to stick fixed)
 3. short period oscillation - heavily damped
 4. oscillatory motion, similar to Dutch Roll but no rolling, called snaking
- c) Aileron free - (rudder locked)
1. spiral divergence - (similar to stick fixed, and rudder free)
 2. a direct convergence - very heavily damped (similar to stick fixed and rudder free)
 3. short period mode, Dutch Roll aileron free
 4. two convergences - heavily damped, can change to a heavily damped short period oscillation by extreme aerodynamic balancing.

9-4 Significance of the Usual Motions

A. Longitudinal

a) Stick fixed

1. The phugoid mode is a long period mode that may be considered as the attempt of the airplane to return to its equilibrium condition of $C_L V^2 = a$ constant, with C_L remaining essentially constant. Therefore the motion is due to the variation in V (climbing as V exceeds the equilibrium V , and sinking when it is lower than equilibrium V) with the damping primarily due to drag. Other parameters affecting mode are c.g., C_L , C_D , C_m , and inertia. It is usually of such a long period that neither the Air Force nor the Navy require that it be positively damped, although the CAA does.
2. This short period oscillation is very heavily damped, with V essentially constant.

b) Stick free

1. The phugoid and the very heavily damped short period mode are similar to the stick fixed motions.
2. 3rd stick free mode called "Porpoising" when neutrally damped. It can be a serious problem for fast heavy airplanes because of its short period. The oscillation of the normal acceleration has resulted in injuries to pilot and damage to aircraft. The major variables to correct this condition are $C_{h\delta}$ and

$$C_{h\alpha}$$

$C_{h\delta}$ is the change in elevator hinge moment coefficient with change in elevator deflection.

$C_{h\alpha}$ is the change in elevator hinge moment coefficient with change in angle of attack.

B. Lateral

a) Stick fixed

1. The spiral divergence is usually so mild that it can be easily corrected by pilot. In some cases it is often tolerated to obtain a desirable relationship between direction α stability and stable dihedral effect. (See fig. 9:8)
2. The heavily convergent motion is no problem as it is usually damped out so rapidly that it is not discernible.
3. The short period oscillation, the Dutch roll, is usually not objectionable as the damping is usually heavy. It is a combination of yawing and rolling while the airplane is trying to return to its equilibrium position. It can become objectionable, sometimes because of excessive stable dihedral effect. Dihedral effect is, of course, the rolling caused by sideslip, and it can readily be seen how it would contribute to this Dutch Roll oscillation. The important parameters are $C_{n\beta}$ and $C_{l\beta}$.

$C_{n\beta}$ and $C_{l\beta}$ are the changes in yawing moment and rolling moment coefficients respectively, with sideslip.

b) Rudder free

1. The spiral divergence and heavily convergent motion are similar to the stick free motions. The short period oscillation, which is heavily damped is usually no problem.
2. The oscillatory motion that is similar to the Dutch Roll but has no roll, is called Snaking. In this mode the airplane c.g. flies in an essentially straight path, while the airplane oscillates about the Z axis, so that sideslip varies from positive to negative. This mode can have neutral or even negative damping. The important parameters are $C_{h\delta}$ and $C_{h\alpha}$. The trend of aerodynamic balancing toward positive values of $C_{h\alpha}$ makes this mode a problem as it causes low damping of this snaking mode.

c) Aileron Free

These modes are similar to previously mentioned modes and seem to present no problem. This is due primarily to the fact that normal mass balanced ailerons do not present any dynamic complications when freed, and all controls are usually mass balanced.

9-5 Variation of Parameters - Stability Diagrams

The effect of the variation of only one parameter, or of a combination of parameters on dynamic stability can be shown most effectively by the use of graphs, sometimes called stability diagrams. A few examples will be shown.

A. Longitudinal, Stick Fixed - Phugoid Mode

Probably the simplest curve would be of the type showing the effect of c.g. location on the stability of the stick fixed longitudinal, phugoid, mode. The quartic equation is solved for the values of λ , and is found to be $a \pm ib$. The values of a , the damping constant, is plotted against b , the period constant, for different values of c.g. location. Since the motion is stable when a is $-$, and unstable when a is $+$, the line where a is $= 0$, is the boundary between stability and instability.

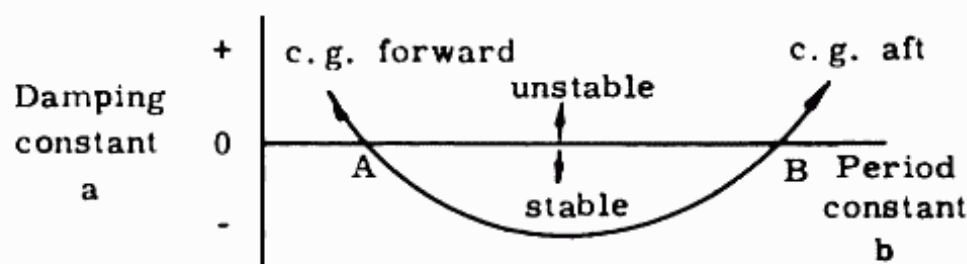


Fig. 9:6. Typical effect of c.g. on phugoid mode.

It should be noted that this curve is drawn for a definite equilibrium condition, with one value of C_L . A different curve should be drawn for each value of C_L . Also only values of c.g. that result in static stability, i.e. where dC_m/dC_L is negative, are shown. This plot also indicates the values of b , the period constant, which determines the length of period associated with each c.g. location. The values of period, and time to damp to $1/2$ amplitude can be obtained by the use of equations 9:28 and 9:29. Note that only values of c.g. between points A and B result in a stable phugoid mode, for this C_L . The effect of the parameters $C_{m_{d\theta}}$ and $C_{m_{\alpha}}$ are shown in fig. 9:7. Since here only the stability boundary of an oscillatory mode is desired, it is only necessary to determine where Routh's discriminant is equal to 0 to

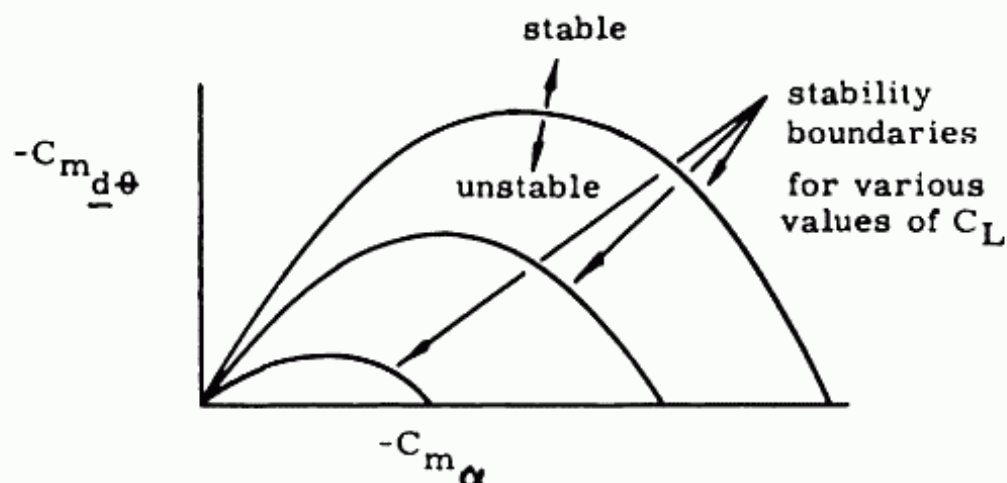


Fig. 9:7. Effects of $C_{m d\theta}$ and $C_{m \alpha}$ on phugoid mode for one value of c.g.

ascertain this boundary. It still requires a considerable amount of work to obtain this condition for a combination of $C_{m d\theta}$, $C_{m \alpha}$ and C_L . However the final result does present clearly the effects of these parameters.

B. Lateral - Stick Fixed, Spiral Mode and Pure Divergence

In the previous examples, the stability diagrams were based on solving the quartic for λ and making use of the fact that the stability boundary occurs when the damping constant $a = 0$, or when Routh's discriminant = 0. For the following example, the solution of the quartic is not required, but use is made of Routh's discriminant, and the sign of the constant E. Fig. 9:8 shows the effect of degrees of directional stability $C_{n\beta}$, and degrees of stable dihedral effect, $C_{l\beta}$ on the pure divergence and the spiral modes. Note that only the area between the curves is stable considering both the spiral mode and pure convergence. However only where $C_{n\beta}$ is positive is the airplane statically directionally stable as well. It can also be seen from the figure 9:8 that if it were desired to have a large degree of directional stability, i.e. $C_{n\beta}$ be high, a certain degree of stable dihedral effect is required to avoid pure divergence. If this required stable dihedral effect is more than is desired, from the pilots point of view, it might be less objectionable to allow some small degree of pure divergence, and maintain the desired dihedral effect.

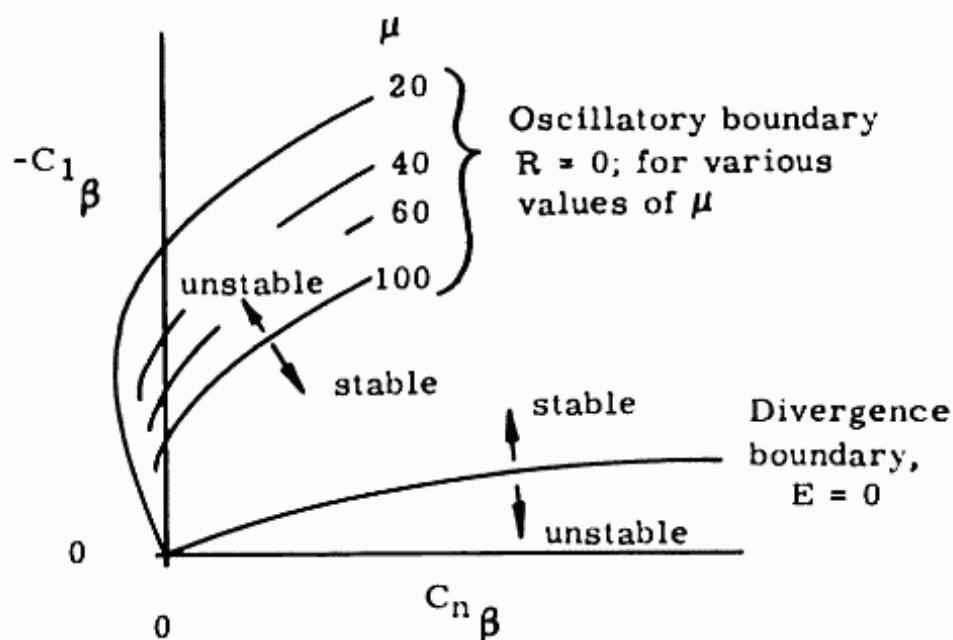


Fig. 9:8. Effect of static directional stability and dihedral effect on lateral stability.

9-5a Effects of Flexibility

Up to this point in the discussion of stability there has been no mention of flexibility of the structure, and how it might affect the motions of the airplane.

The way that flexibility makes itself felt in stability calculations is in the distribution of the loads on the wing, that is, the effect on the a.c. and $dC_L/d\alpha$ of the 3 dimensional wing and control surface, and in the loss in effectiveness of the control surface.

The change in a.c. of the wing is an important factor in stability for highly swept wings. This is due to the fact that the flexibility of the wing tends to throw the loads inboard, as explained in section "Spanwise Load Distribution" Chapt. XII, thereby moving the a.c. forward.

The loss in effectiveness of the control surfaces due to flexibility is important for the aileron, rudder and elevator. The loss in aileron effectiveness, which can lead to aileron reversal, is discussed in section 11:3. Fig. 9:9 shows the decrease in aileron effectiveness that might be expected for a fighter airplane at sea level. The loss in elevator effectiveness is caused by the bending of the fuselage as well as the twisting of the stabilizer. If the elevator is deflected down to give an increase in upload, a twisting of the stabilizer results that decreases the α thereby introducing a down load. In addition the upload resulting from the

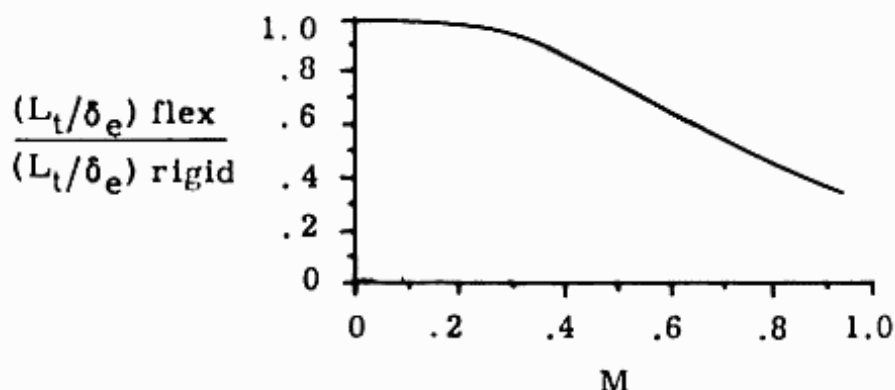


Fig. 9:9. Elevator control effectiveness vs. M for a particular airplane.

control surface bends the fuselage upward, again decreasing the α of the surface and introducing a down load. This fuselage effect is only true for a conventional surface aft of the c.g. For a canard the fuselage flexibility will increase the elevator effectiveness. Similar reasoning will show the loss in effectiveness of a rudder due to flexibility of fuselage and fin.

The changes in $dC_L/d\alpha$ of both the wing and control surface are caused by the twisting of a flexible surface when the loads are not applied at the shear centers.

9-6 Static Stability - Introduction

As has been stated previously, static stability is defined as the initial tendency of the airplane to return to its equilibrium position. In longitudinal stability this is equivalent to having the parameter dC_m/dC_L negative, and in directional stability having $dC_n/d\beta$ positive. There is no phenomena as static stability in roll, as there are no moments set up in an airplane that directly tend to make the airplane return it original equilibrium position about the X axis. The effect of dihedral on roll will be discussed later.

In analyzing the quartic equation in longitudinal dynamic stability it was noted in eq. 9:26 and 9:27 that dC_m/dC_L must be negative to have dynamic stability. This same dC_m/dC_L term is the criteria for static stability and is the change in moment coefficient about the Y axis with the change in lift coefficient. The evaluation of this term is the study of static longitudinal stability.

It should be realized, really, that it is only the dynamic and not the static stability that is important. This is so since static stability indicates only a tendency to return to equilibrium, it does not indicate if equilibrium is ever reached, what the period

of oscillation is, or the amount of damping. And these latter factors are the most important.

In fact, some forms of instability are permitted if the divergence in amplitude is slow, or if the period is long. Therefore not only is it important to determine if an airplane is stable or unstable, but the period and damping of the airplane as well.

For some time only the static stability was investigated, as not too much was known about dynamic stability and it was felt that if an airplane was statically stable it would be dynamically satisfactory. This is generally true, but with changes in design caused by a search for greater efficiency in high speed aircraft (higher airplane densities, greater aerodynamic surface balance, etc.) this picture is beginning to change. With more radical designs it is possible that static stability will no longer be an indication of dynamic stability.

As designs stand now, static stability still indicates that the airplane may be dynamically satisfactory, although it is by no means a guarantee. It is general practice that the dynamic stability of every airplane be investigated to determine the periods and damping of the modes, in addition to determining if it is stable or not. Static stability is still of importance, not only because it is an indication of dynamic behavior, but because it can be much more easily and accurately determined. For these reasons static stability is investigated in preliminary design, while dynamic stability often is not.

9-7 Method

When analytical methods are used, one approach to the problem is to estimate the control surface characteristics and then calculate whether the requirements are satisfied. If each requirement is treated as placing a limit on the center of gravity location, a range of centers of gravity will be determined that satisfies all the requirements. The airplane must then be designed so that the center of gravity of the airplane never moves outside of this range. It will be shown that certain requirements place an aft limit on the center of gravity while the others place a forward limit. A diagram of a mean aerodynamic chord showing typical locations of the center of gravity as limited by certain requirements is shown in figure 9:10.

9-8 Longitudinal Stability

The study of longitudinal stability is based upon the forces of the airplane and their effect on the moment about the center of gravity. Equilibrium is the condition that exists when the moments about the center of gravity equal zero. For a plane to be

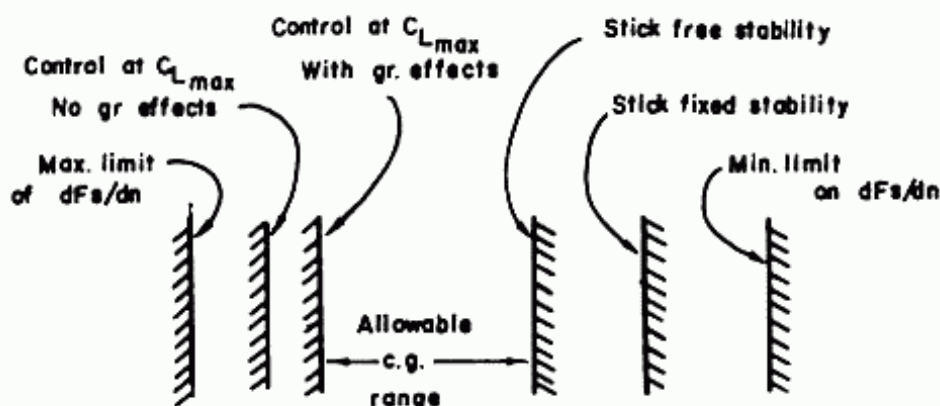


Fig. 9:10. Effect of requirements on center of gravity location.

statically stable, a diving moment must result from an increase in lift coefficient from the state of equilibrium, and a stalling moment from a decrease in lift coefficient. This may be illustrated by presenting the curves of the C_m , the moment coefficient, versus C_L , the lift coefficient for two airplanes as shown in Figure 9:11.

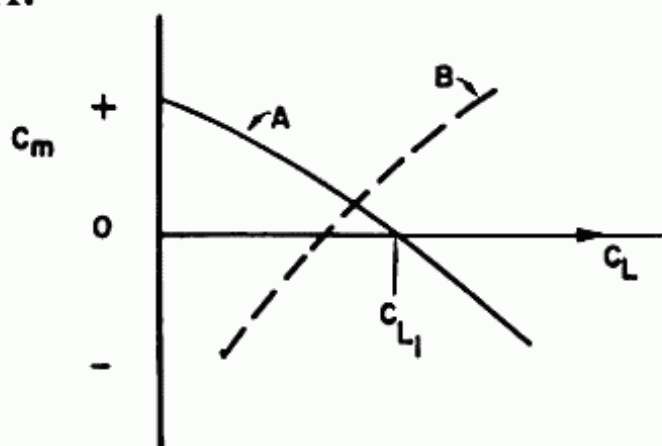


Fig. 9:11. Stability as defined by the slope of the C_m vs. C_L curve.

It is seen from Figure 9:11 that at C_{L_1} , airplane A is in equilibrium since $C_m = 0$. However as C_L increases beyond C_{L_1} , the C_m becomes negative and induces a diving moment. Since an increase in C_L is caused by an increase in angle of attack and a diving moment will decrease the angle of attack, the airplane will tend toward the equilibrium state. If C_L decreases from C_{L_1} , the C_m becomes positive and induces a stalling moment

which again tends to return the airplane to equilibrium. It is therefore evident that a negative slope of the dC_m/dC_L curve is evidence of static stability.

Airplane B which has a dC_m/dC_L curve that is positive, is unstable. That is, if a gust strikes the airplane so that the angle of attack is increased, the variation in C_m with C_L is such that a stalling moment is induced which further increases the angle of attack. And conversely, if the angle of attack is decreased, a diving moment is induced which further decreases the angle of attack. It is therefore evident that a positive slope of the dC_m/dC_L curve is equivalent to static instability. Further that the degree of stability or instability is a function of the value of the slope of the curve, the higher the negative value the greater the stability, the higher the positive value the greater the instability.

The condition where $dC_m/dC_L = 0$ is called neutral stability. If a neutrally stable airplane is displaced from equilibrium, it will neither tend to return to equilibrium nor diverge from it, but remain in the new attitude until acted upon by some other force.

For convenience in presentation, stability discussions are usually divided into two parts, stick free and stick fixed. The condition in which the stick is locked in place and cannot move due to either change in control surface force or pilot force is called stick fixed. If the stick is free to rotate due to aerodynamic surface force it is called the stick free condition. It is more convenient to present the stick fixed condition first, as some of the stick-fixed results can be used in the stick free study.

9-9 Stick Fixed Longitudinal Stability

General

The dC_m/dC_L of the airplane curve is a function of the dC_m/dC_L curve of each of the component parts, the wing, fuselage, nacelles and tail surfaces, and of power effects. However the effects of the wing and tail surfaces are by far the largest. Figure 9:12 shows the aerodynamic forces on an airfoil section, either of wing or tail surface.

Since the lift and drag always act perpendicular and parallel to the wind direction and their moment arms to the center of gravity change with variation in angle of attack, it is more convenient to use forces, N and C , which are parallel and perpendicular to the airplane reference line.

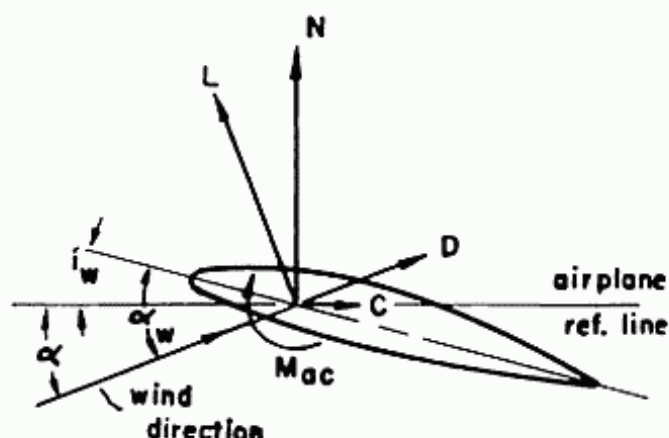


Fig. 9:12. Aerodynamic forces on an airfoil section.

$$N = L \cos \alpha + D \sin \alpha$$

$$C = D \cos \alpha - L \sin \alpha$$

Figure 9:13 shows the forces and moment on the airplane that are significant in affecting the moment about the airplane center of gravity. The forces and moments that have been omitted because of their negligible effect are the chordwise force of the tail, the moment about the aerodynamic center of the tail and the parasite drag of all the component parts of the airplane.

The chordwise force of the wing has a stabilizing or destabilizing effect depending on whether it is acting above or below the airplane center of gravity. If the chordwise force is above the center of gravity, it produces a stabilizing effect and if it is below the center of gravity, it produces a destabilizing effect. This is based on the assumption that $dC_C/d\alpha$ is negative; that is, an increase in α increases the value of C_C in the forward direction. Therefore for a high wing monoplane the effect of C_C is stabilizing and for a low wing monoplane it is destabilizing. However, since at low C_L the effect is completely insignificant and at high C_L it has only a small effect, the term is omitted in most analyses.

It has been found more convenient to work in terms of moment coefficient instead of moments, and therefore Equation 9:31 is divided by $q S_w (\text{MAC})$ where q is the dynamic pressure in pounds per square foot, S_w the wing area in square feet, and MAC the mean aerodynamic chord of the wing, in feet.

$$M_{Cg} = N_w X_w + M_{ac} + M_{fus} - N_t l_t \quad (9:31)$$

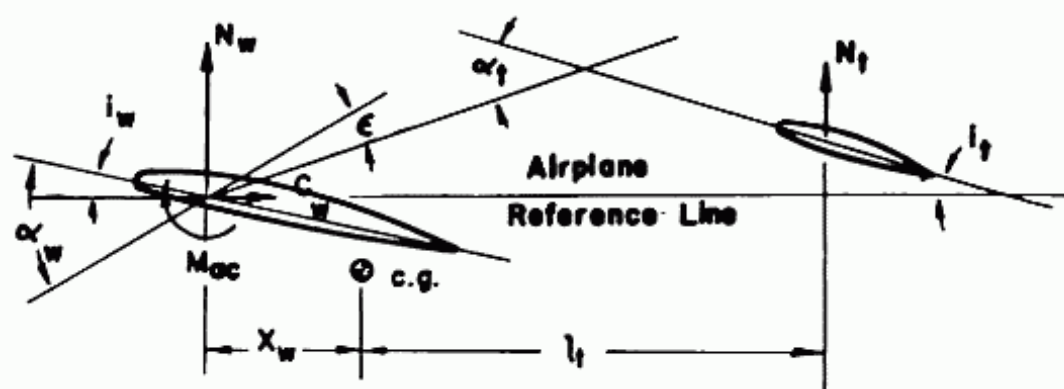


Fig. 9:13. Significant forces on the airplane.

$$C_{m_{cg}} = C_{N_w} \frac{X_w}{MAC} + C_{m_{ac}} + C_{m_{fus}} + C_{m_{nac}} - C_{N_t} \frac{S_t}{S_w} \frac{l_t}{MAC} \frac{q_t}{q} \quad (9:32)$$

In conventional airplanes, the tail surfaces are aft of the wing, fuselage and nacelles. Due to fuselage and wing interference the air producing lift on the tail is moving substantially slower than the freestream velocity. Therefore for an airplane in flight without power, q_t/q is less than one. In addition, the force on the tail is affected by the horizontal tail being partially immersed in the boundary layer of the fuselage and vertical tail. The effect of both q_t/q and the boundary layers are combined in η_t , the tail efficiency factor. In general η_t has been found to vary between .60 and .80. (Ref. NACA TR 521.)

Since it has previously been shown that the slope of the C_m versus C_L curve is the criteria for longitudinal stability, it is now necessary to differentiate $C_{m_{cg}}$ with respect to C_L .

$$\frac{dC_{m_{cg}}}{dC_L} = \underbrace{\frac{dC_{N_w}}{dC_L} \frac{X_w}{MAC}}_{\text{wing effect}} + \frac{dC_{m_{ac}}}{dC_L} + \underbrace{\frac{dC_{m_{fus}}}{dC_L} + \frac{dC_{m_{nac}}}{dC_L}}_{\text{fus. and nacelle effect}} - \underbrace{\frac{dC_{N_t}}{dC_L} \frac{S_t}{S_w} \frac{l_t}{MAC}}_{\text{tail effect}} \eta_t \quad (9:33)$$

Wing Effect

Since by definition $C_{m_{ac}}$ does not change with change in C_L , $dC_{m_{ac}}/dC_L = 0$. For small angles of attack C_N can be assumed to be equal to C_L and therefore $dC_{N_w}/dC_L = 1$.

$$\text{Therefore } \left(\frac{dC_{m_{cg}}}{dC_L} \right)_{\text{wing}} = \frac{X_w}{MAC} \quad (9:34)$$

However, since $X_w/MAC = X_{cg} - X_{ac}$, where X_{cg} and X_{ac} are the distances of the center of gravity of the airplane and the aerodynamic center of the wing from the leading edge of the M.A.C. divided by the M.A.C.; then

$$\left(\frac{dC_{m_{cg}}}{dC_L}\right)_{\text{wing}} = X_{cg} - X_{ac} \quad (9:35)$$

It can therefore be seen that the relationship of the positions of the aerodynamic center and the center of gravity of the airplane is the largest single factor in the stability of the wing. If the center of gravity is aft of the aerodynamic center the term is positive and therefore destabilizing. If the center of gravity is forward of the aerodynamic center the term is negative and therefore stabilizing.

Tail Effect

$$\left(\frac{dC_m}{dC_L}\right)_{\text{tail}} = -\frac{dC_{N_t}}{dC_L} \frac{S_t}{S_w} \frac{l_t}{MAC} \eta_t \quad (9:36)$$

However, dC_{N_t}/dC_L does not equal one as dC_{N_w}/dC_L did, because of the effects of wing downwash. It is therefore necessary to put dC_{N_t}/dC_L in terms that can be readily determined.

$$C_{N_t} = \left(\frac{dC_N}{d\alpha}\right)_t \alpha_t \quad (9:37)$$

where $\alpha_t = \alpha_w - \epsilon + i_t - i_w$; as shown in Figure 9:13. (9:38)

therefore

$$C_{N_t} = \left(\frac{dC_N}{d\alpha}\right)_t (\alpha_w - \epsilon + i_t - i_w) \quad (9:39)$$

since i_t and i_w are constants

$$\frac{dC_{N_t}}{dC_L} = \left(\frac{dC_N}{d\alpha}\right)_t \left(\frac{d\alpha_w}{dC_L} - \frac{d\epsilon}{dC_L}\right) \quad (9:40)$$

simplifying:

$$\frac{dC_{N_t}}{dC_L} = \frac{(dC_N/d\alpha)_t}{(dC_L/d\alpha)_w} \left(1 - \frac{d\epsilon}{d\alpha}\right) \quad (9:41)$$

then

$$\left(\frac{dC_{m_{cg}}}{dC_L}\right)_t = - \frac{(dC_N/d\alpha)_t}{(dC_L/d\alpha)_w} \frac{S_t}{S_w} \frac{l_t}{MAC} \eta_t \left(1 - \frac{d\epsilon}{d\alpha}\right) \quad (9:42)$$

For simplification in notation, and since $dC_N/d\alpha = dC_L/d\alpha$

$$(dC_N/d\alpha)_t = a_t$$

$$(dC_L/d\alpha)_w = a_w$$

then

$$\left(\frac{dC_{m_{cg}}}{dC_L}\right)_t = - \frac{a_t}{a_w} \frac{S_t}{S_w} \frac{l_t}{MAC} \eta_t \left(1 - \frac{d\epsilon}{d\alpha}\right) \quad (9:43)$$

The slope of the lift curve, corrected for aspect ratio, sweep-back and Mach number, must now be calculated.

Aspect Ratio Effect on Slope of Lift Curve

The effect of aspect ratio on slope of lift curve can be very easily derived for a wing with an elliptical spanwise load distribution.

$$\alpha = \alpha_0 + \frac{C_L}{\pi AR} \quad (9:44)$$

where

α = angle of attack in radians for any A.R.

α_0 = angle of attack in radians for infinite A.R.

$\frac{C_L}{\pi AR}$ = downwash angle in radians

Differentiating with respect to C_L

$$\frac{d\alpha}{dC_L} = \frac{d\alpha_0}{dC_L} + \frac{1}{\pi AR} \quad (9:45)$$

For simplification, let

a = slope per radian = $dC_L/d\alpha$

a_0 = slope per radian = $dC_L/d\alpha_0$

Then

$$\frac{1}{a} = \frac{1}{a_0} + \frac{1}{\pi AR} \quad (9:46)$$

$$a = \frac{a_0}{1 + \frac{a_0}{\pi AR}} \quad (9:47)$$

The above relationship is true for an elliptical spanwise loading distribution where the downwash angle is constant along the span. For other than elliptical spanwise load distribution, where the downwash angle is not constant, the following formula has been developed:

$$a = \frac{a_0}{1 + \frac{a_0 (1 + \zeta)}{\pi AR}} \quad (9:48)$$

where

ζ is a factor accounting for variation from elliptical lift distribution. For taper ratios between .2 and .4 with aspect ratio equal to 6, ζ is between 0 and .015. See Figure 4:2.

Sweepback Effect on Slope of Lift Curve

The effect of the wing sweep on the slope of the lift curve is easily determined from theory and is verified by wind tunnel tests. A wing with taper ratio equal one is used in the derivation. In this case the quarter chord is parallel to the leading edge. For the Unswept Wing,

$$L_{\text{unsw}} = 1/2 \rho S V_{f.s.}^2 C_{L_{\text{unsw}}} \quad (9:49)$$

where $V_{f.s.}$ = freestream velocity

For the swept wing, since the lift is a function of the velocity perpendicular to the quarterchord,

$$L_{\text{sw}} = 1/2 \rho S V_{f.s.}^2 \cos^2 \Lambda C_{L_{\text{sw}}} \quad (9:50)$$

The C_L of the swept wing is a function of the angle of attack between the chord and the velocity perpendicular to the quarter chord. It can be seen from Figure 9:14 that this effective angle of attack for the sweptwing is equal to the angle of attack of unswept wing divided by $\cos \Lambda$.

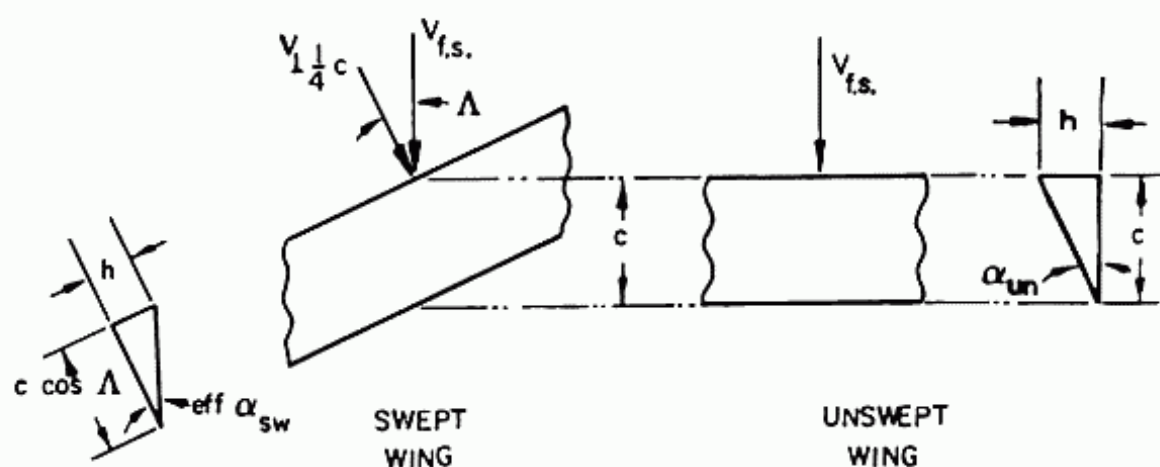


Fig. 9:14. Effective angles of attack for swept and unswept wings.

That is,

$$\alpha_{\text{unsw}} = \frac{h}{c}$$

$$\text{eff } \alpha_{\text{sw}} = \frac{h}{c \cos \Lambda} = \alpha_{\text{unsw}} / \cos \Lambda \quad (9:51)$$

Assuming that the airfoil section perpendicular to the quarter chord is the same for the swept and unswept wing, and that the airfoil is symmetrical, it can be seen from Fig. 9:15 and equ. 9:51 that

$$C_{L_{\text{sw}}} = C_{L_{\text{unsw}}} / \cos \Lambda; \text{ for airfoil perpendicular to } 1/4 \text{ chord} \quad (9:52)$$

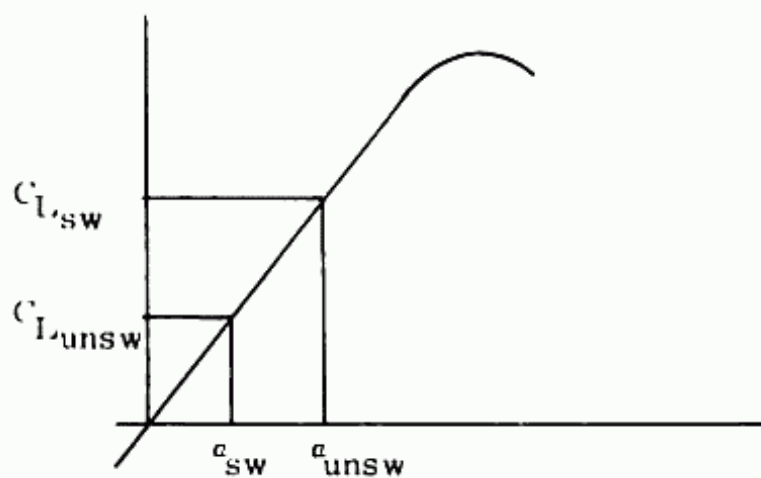


Fig. 9:15. C_L vs. α .

Substituting equ. 9:52 in equ. 9:50

$$\begin{aligned} L &= 1/2 \rho S V_{f.s.}^2 \cos^2 \Lambda C_{L_{unsw}} / \cos \Lambda \\ &= 1/2 \rho S V_{f.s.}^2 C_{L_{unsw}} \cos \Lambda \end{aligned} \quad (9:53)$$

From eqs. 9:49 and 9:53

$$L_{sw} = L_{unsw} \cos \Lambda \quad (9:54)$$

From the basic concept of C_L , i.e.

$$\begin{aligned} C_L &= \frac{L}{1/2 \rho S V_{f.s.}^2} \quad \text{- by definition} \\ C_{L_{unsw}} &= \frac{L_{unsw}}{1/2 \rho S V_{f.s.}^2} \\ C_{L_{sw}} &= \frac{L_{sw}}{1/2 \rho S V_{f.s.}^2} = \frac{L_{unsw} \cos \Lambda}{1/2 \rho S V_{f.s.}^2} \end{aligned} \quad (9:55)$$

$$\therefore C_{L_{sw}} = C_{L_{unsw}} \cos \Lambda; \text{ for chord parallel to free stream} \quad (9:56)$$

And since the geometric angle of attack has been kept constant, and $dC_L/d\alpha$ is based upon this geometric angle of attack

$$\left(\frac{dC_L}{d\alpha} \right)_{sw} = \left(\frac{dC_L}{d\alpha} \right)_{unsw} \cos \Lambda \quad (9:57)$$

The preceding derivation for $dC_L/d\alpha$ of swept wings, which shows that the slope of the lift curve for swept wings equals $(dC_L/d\alpha)_{un} \cos \Lambda$, is for no taper and no tip or center effects.

For large aspect ratios this relation is essentially true as the tip and center effects are small relative to the sweepback effect. As the A.R. becomes smaller, the tip and center effects become larger and the sweepback effect relatively unimportant. In fact at aspect ratio equal 1.5 and taper ratios of .4 and .2 there is no appreciable change in $dC_L/d\alpha$ from zero up to 40° sweepback.

Figures 7:16a and 7:16b show the variation of slope of the lift curve with sweepback for two taper ratios at aspect ratios from 1.0 to 10.0. This data has been derived from NACA Technical

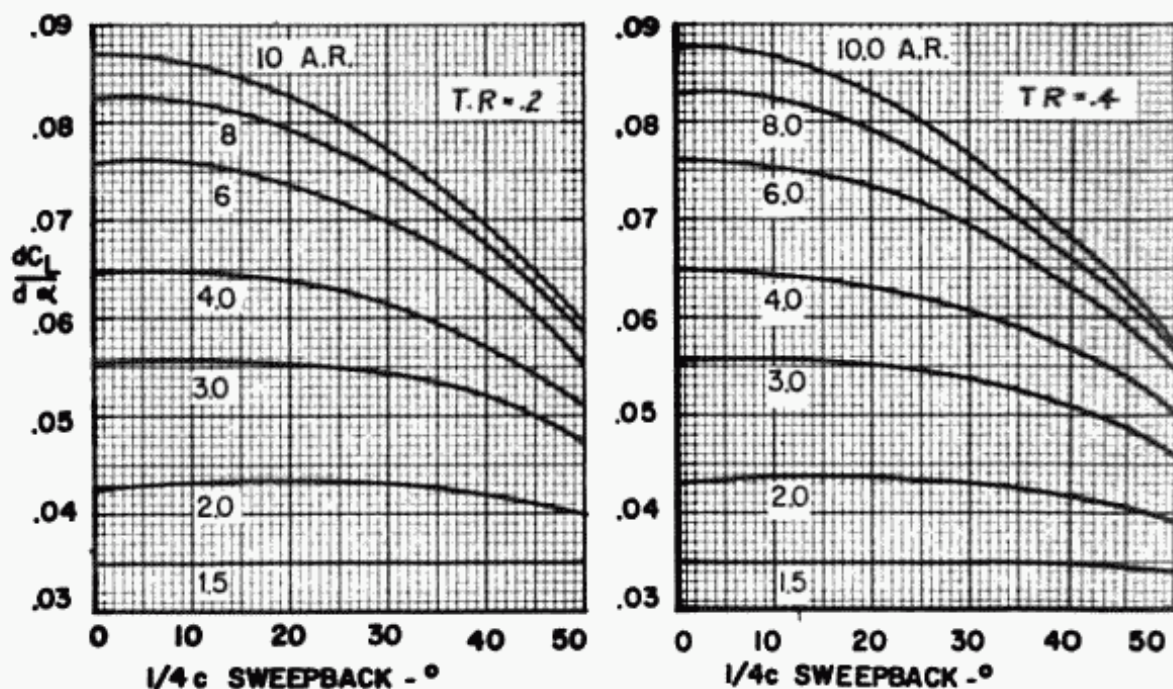


Fig. 9:16. Variation of $dC_L/d\alpha$ with sweepback and aspect ratio.

Note 1491, "Theoretical Additional Span Loading Characteristics of Wings with Arbitrary Sweep, Aspect Ratio and Taper Ratio" by J. De Young.

Mach Number Effect on Slope of Lift Curve

The slope of the lift curve must still be corrected for Mach number. Figure 9:17 presents a factor j , where

$$\frac{dC_L}{d\alpha} \text{ (at any } M) = (j) \frac{dC_L}{d\alpha} \text{ at } M = 0$$

The data for Figure 9:17 is derived from T.N. 1739, "Comparison with Experiment of Several Methods of Predicting the Lift of Wings in Subsonic Compressible Flow" by H. E. Murray. The wing model had an NACA 65₂-215 airfoil, a taper ratio equal to 0.5, and an aspect ratio equal to 6.0. Both experiment and theory show that this variation in $dC_L/d\alpha$ with Mach number is little affected by thickness ratio. As can be seen from Figure 9:17, the correction factor for this 15% thick wing at $M = .7$ and $\Lambda = 30^\circ$ is 1.26. The value for similar wing only 10% thick is 1.22. The test results up to $M = .7$ agree very well with those from analytical methods. Above this Mach number through the transonic range, it is difficult to develop a theory that will compare with test. It should be noted that extending the curve beyond $M = .7$ as determined by test, indicates the M_{CR_L} , lift critical Mach

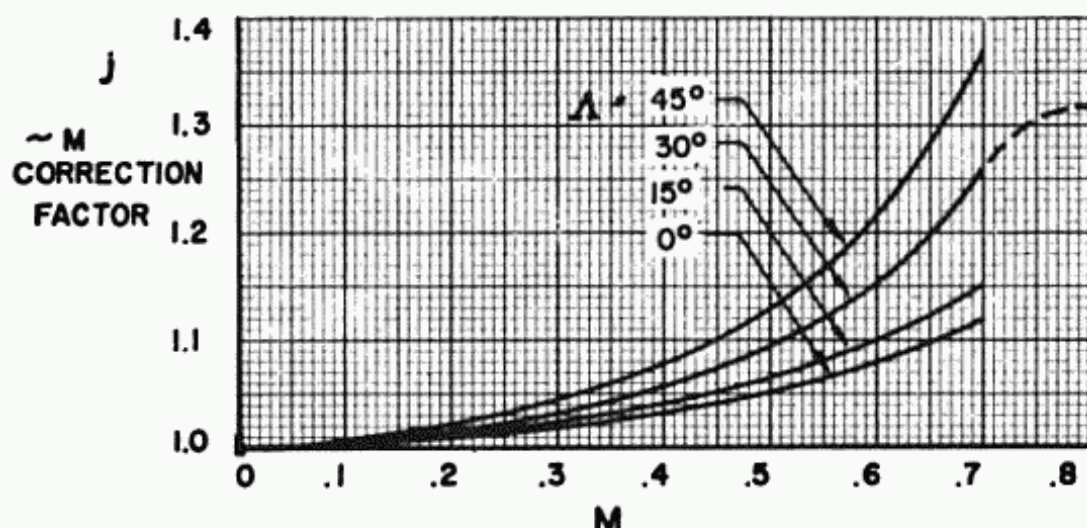


Fig. 9:17. Mach number correction factor for $dC_L/d\alpha$.

number. Since M_{CR_L} depends on the change in C_L at constant angle of attack, the $dC_L/d\alpha$ and the C_L curves vs. M are identical.

The final slope of the lift curve is determined by accounting for all the factors, aspect ratio, Mach number and sweepback.

$$a = \left(\frac{a_0}{1 + \frac{a_0 [1 + \zeta]}{\pi AR}} \right) (j) \text{ (sweepback factor)}$$

The sweepback factor = $\frac{dC_L/d\alpha \text{ at sweepback desired}}{dC_L/d\alpha \text{ at } 0^\circ \text{ sweepback}}$

for the aspect ratio being considered. (From Figure 9:16.)

Evaluation of $d\epsilon/d\alpha$

The term $d\epsilon/d\alpha$ must now be evaluated. Figure 9:18 shows the theoretical values and an approximation of true downwash, ϵ , before and behind a wing.

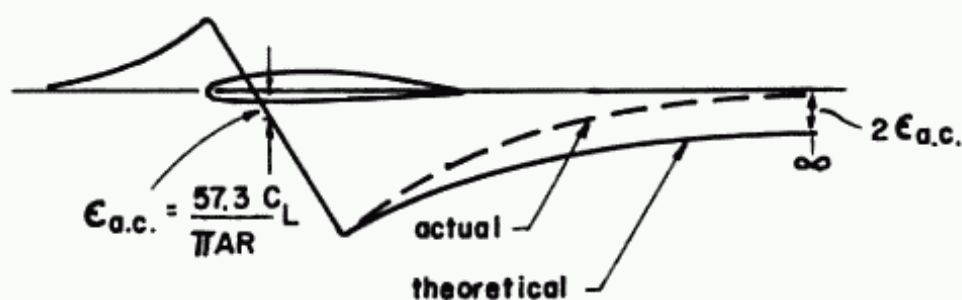


Fig. 9:18. Downwash angle variation.

TR = 1.0

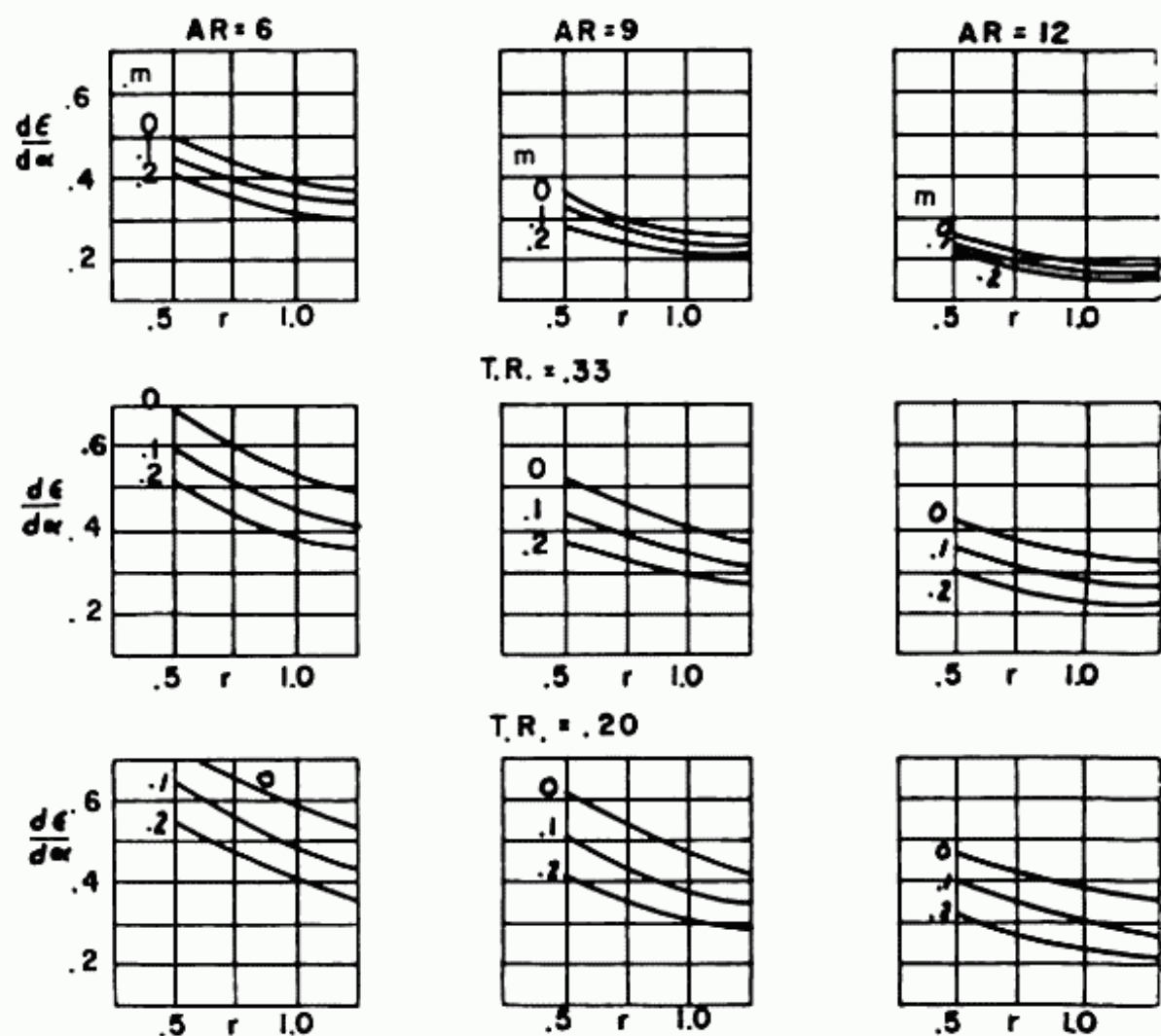
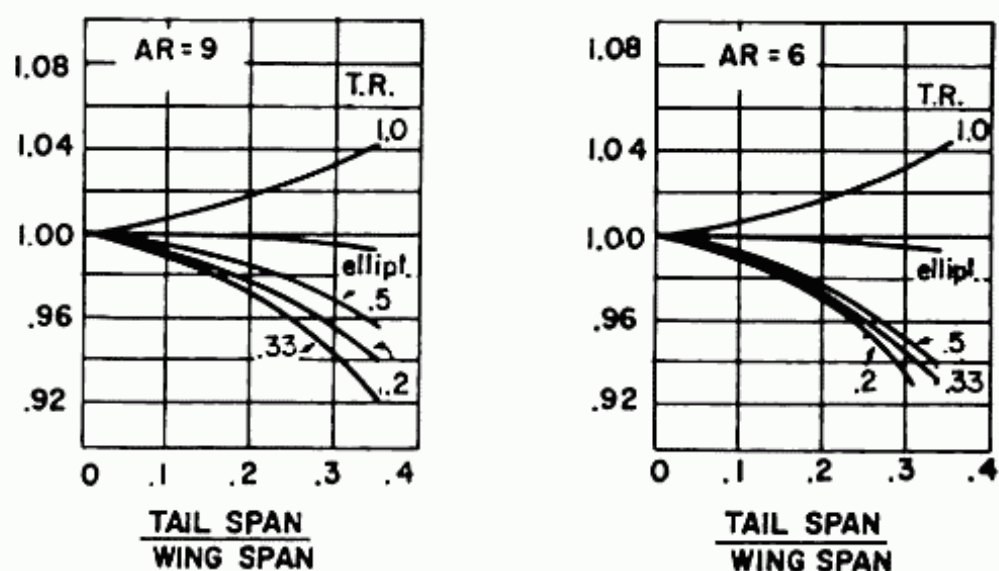
Fig. 9:19. $d\epsilon/d\alpha$ for various A.R.'s and T.R.'s.

Fig. 9:20. Correction factor for ratio of tail span to wing span.

Although theoretically the downwash at infinity equals twice the downwash at the aerodynamic center, actually, the downwash will eventually disappear due to viscosity. The true downwash at the tail varies substantially from the theoretical and is a function of the position of the tail with respect to the wing wake, which in turn is a function of the location of the tail in respect to the wing. If the tail is kept free of the wing wake, which is usually done, $d\epsilon/d\alpha$ may be obtained with a reasonable degree of accuracy from the following data obtained from T.R. 648, "Design Charts for Predicting Downwash Angles and Wake Characteristics behind Plain and Flapped Wings," by A. Silverstein and S. Katzoff.

The value of $d\epsilon/d\alpha$ to be used in Equation 9:43 is the value obtained from Figure 9:19 multiplied by the factor as determined from Figure 9:20. Figure 9:21 explains the terms m and r used in Figure 9:19. The tail contribution to stability can then be calculated.

Fuselage and Nacelles

The effect of the fuselage and nacelles on airplane stability is difficult to obtain especially when wing interference is accounted for. However since the effect is practically always destabilizing and in many cases it is quite sizable, some approximation to its magnitude must be made.

A fuselage flying at an angle of attack in an ideal fluid has a pressure distribution over it that results in a pure couple with the center of pressure at infinity. In an actual fluid the center of pressure is usually a little ahead of the nose of the fuselage. The lift and drag forces are usually neglected in the calculations of stability.

A fairly comprehensive method of computing fuselage and nacelle effects on $dC_{m_{cg}}/dC_L$ is presented by H. Multhopp in NACA T.M. 1036, "Aerodynamics of the Fuselage." However for normal arrangements a much simpler method by Gilruth and

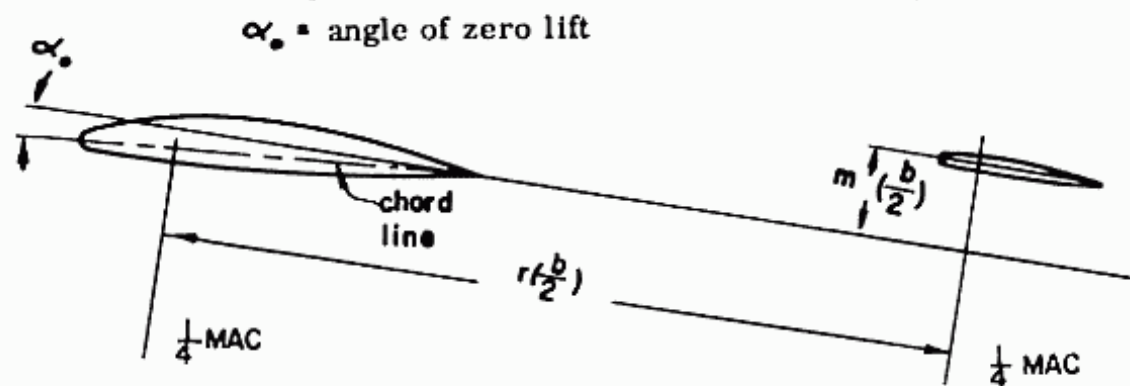


Fig. 9:21. Diagram of m and r .

White in NACA T.R. 711 "Analysis and Prediction of Longitudinal Stability of Airplanes," gives reliable results. It is accomplished by the Equation 9:58 and Figure 9:22.

$$\left(\frac{dC_m}{dC_L}\right)_{\text{fus or nac}} = \frac{K_f w_f^2 L_f}{S_w a_w \text{MAC}} \quad (9:58)$$

where L_f is the overall fuselage length

w_f is the maximum width of fuselage

K_f is an empirical factor shown in Figure 9:22

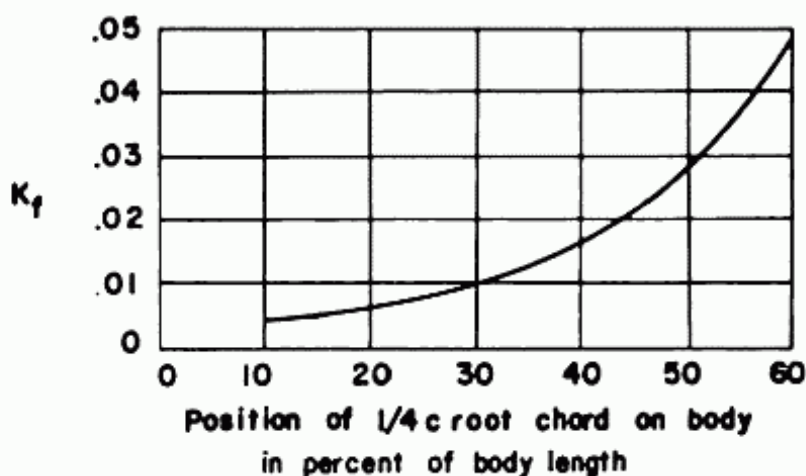


Fig. 9:22. Factor for dC_m/dC_c of fuselage and nacelle.

Stick Fixed Neutral Point

As previously shown

$$\frac{dC_m}{dC_L} = X_{cg} - X_{ac} + \left(\frac{dC_m}{dC_L}\right)_{\text{nac.}} - \frac{a_t}{a_w} \frac{S_t}{S_w} \frac{l_t}{\text{MAC}} \eta_t \left(1 - \frac{d\epsilon}{d\alpha}\right) \quad (9:59)$$

$$C_{m_{cg}} = C_L \frac{X_w}{\text{MAC}} + C_{m_{ac}} + C_{m_{fus}} + C_{m_{nac}} - C_{N_t} \frac{S_t}{S_w} \frac{l_t}{\text{MAC}} \eta_t \quad (9:60)$$

The stability Equation, 9:59, shows that except for center of gravity location all the items are fixed. The tail arm, l_t , changes with the center of gravity but since the percentage change is negligibly small, dC_m/dC_L is a direct function of the center of gravity position. For every movement of the center of gravity equal to .01 times the mean aerodynamic chord, the dC_m/dC_L of the airplane changes by .01. The further aft the center of gravity moves, the more positive dC_m/dC_L becomes and therefore the

more unstable the airplane becomes. The center of gravity location at which dC_m/dC_L equals zero is called the neutral point, N_0 . If the center of gravity moves aft of N_0 , the dC_m/dC_L becomes positive and the airplane becomes unstable. The neutral point is therefore one criterion for the most aft location of the center of gravity for a stable airplane.

From Equation 9:59 letting $dC_m/dC_L = 0$ and $N_0 = X_{cg}$ when $dC_m/dC_L = 0$.

$$N_0 = X_{ac} - \left(\frac{dC_m}{dC_L} \right)_{\substack{\text{fus.} \\ \text{nac.}}} + \frac{a_t}{a_w} \frac{S_t}{S_w} \frac{l_t}{MAC} \eta_t \left(1 - \frac{d\epsilon}{d\alpha} \right) \quad (9:61)$$

Power Effects, General

The effect of power on the static longitudinal stability of an airplane is quite pronounced. However a complete accurate analysis of this effect is not possible and therefore only limited results can be obtained. The calculations, even simplified, for propeller engines are quite complicated and of questionable accuracy, whereas the effects of a jet engine is somewhat simpler because of the absence of the propeller and the resulting slipstream. There are texts¹ that present the analysis of the propeller engine effects. Since the airplane designed in this text is jet powered, the effect of the jet engine operation on stability will be discussed.

The moment about the center of gravity of the airplane due to the jet engine is caused by three effects. They are the normal force at the duct inlet, the direct thrust and the jet induced downwash at the horizontal tail.

Direct Thrust

The moment coefficient, $C_{m_{cg}}$, due to direct thrust can be obtained directly from

$$C_{m_{cg}} = \frac{TY_t}{q S_w MAC} = \frac{TY_t C_L}{W (MAC)} \quad (9:62)$$

where Y_t = distance from line of thrust to the center of gravity location (see Figure 9:23).

1. "Airplane Performance, Stability and Control," Perkins and Hage.

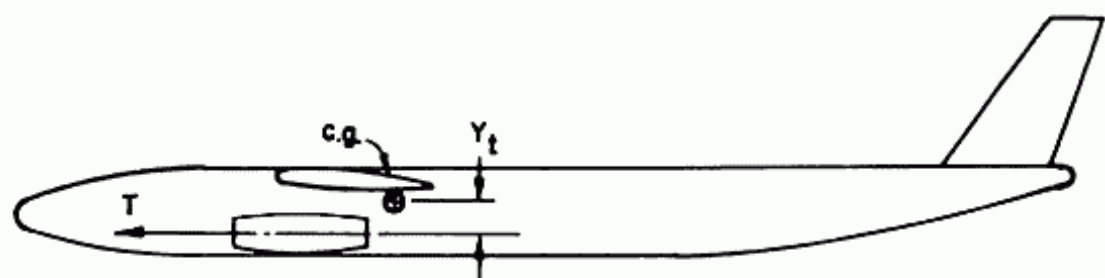


Fig. 9:23. Thrust line in relation to center of gravity.

If the thrust, T , for a jet airplane is assumed to be constant with speed, then

$$\left(\frac{dC_{m_{cg}}}{dC_L} \right)_{\text{eng. thrust}} = \frac{TY_t}{W(MAC)} \quad (9:63)$$

As can be seen from Equation 9:63, for unaccelerated flight, $C_{m_{cg}}$ due to thrust does vary with C_L . From the facts that

$$L = 1/2 \rho SV^2 C_L$$

and $L = \text{weight}$ for unaccelerated flight, it can be seen that for any weight, $V^2 C_L$ must be constant. Therefore as C_L increases, q decreases, and from Equation 9:62, $C_{m_{cg}}$ increases.

For airplanes which have a large variation in thrust with speed, Equation 9:63 will not hold. For these airplanes, C_m would have to be calculated for various values of C_L , and the C_m versus C_L curve plotted. The dC_m/dC_L due thrust can then be obtained. For many jet airplanes this effect of variation in thrust with speed would be appreciable.

Normal Force at Duct Inlet

Because of the change in flow from the free-stream direction to the duct axis, a normal force is produced at the jet engine inlet. (See Figure 9:24).

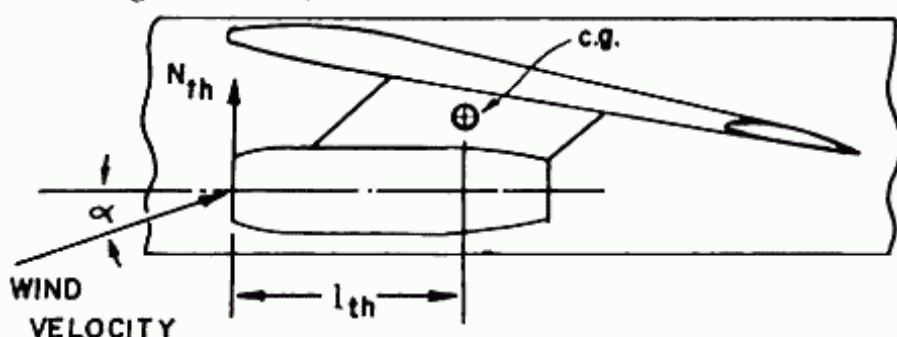


Fig. 9:24. Normal force at duct inlet.

$$C_{m_{cg}} \text{ due } N_{th} = \frac{N_{th} l_{th}}{q S_w MAC} = \frac{N_{th} l_{th} C_L}{W (MAC)} \quad (9:64)$$

therefore,

$$\left(\frac{dC_{m_{cg}}}{dC_L} \right)_{N_{th}} = \frac{N_{th} l_{th}}{W (MAC)} \quad (9:65)$$

Jet Induced Downwash at Horizontal Tail

A thorough analysis of the effect of the jet induced downwash at the horizontal tail is in the literature, but due to its length it is omitted from this text. However it is seen that the exhaust from the jet, due to turbulent mixing, will suck the air into the jet, thus causing an inclined flow about the jet. If the jet exhaust is aft of the horizontal tail it will have no effect on the flow about the tail. However if it is forward of the horizontal tail as in a jet transport, it will change the effective angle of attack at the horizontal tail and thereby affect both stability and equilibrium. A jet exhaust under the horizontal tail will reduce the effective angle of attack of the tail, decreasing the upload, inducing a stalling moment and thereby adding to the instability of the airplane.

Net Effect of Thrust

The effect of the direct thrust on stability can be obtained analytically from Equation 9:63. However the effects of both the normal force and the induced downwash involve lengthy calculations and the inaccuracy of results do not warrant the required work. An approximate value that may be used from jet planes tested indicate that for the normal force a dC_m/dC_L of .01 to .03 may be used, the higher value being for single engine airplanes with duct inlet at the nose of the fuselage. A value of $dC_m/dC_L = .04$ for the induced downwash effect was obtained from airplanes with jet flow under the tail. Since the thrust effect is usually destabilizing the neutral point with thrust will be critical for aft center of gravity position.

Equations 9:66 and 9:67 present the dC_m/dC_L and the neutral point including thrust effect.

$$\left(\frac{dC_m}{dC_L} \right)_{\text{thrust}} = X_{cg} - X_{ac} + \left(\frac{dC_m}{dC_L} \right)_{\text{nac}} \frac{a_t S_t l_t}{a_w S_w c} \eta t \left(1 - \frac{d\epsilon}{d\alpha} \right) + \frac{T Y_t}{W (MAC)} + \left(\frac{dC_m}{dC_L} \right)_{NF} \quad (9:66)$$

fus ID

$$\text{where } \left(\frac{dC_m}{dC_L} \right)_{NF} = \frac{dC_m}{dC_L} \text{ due normal force}$$

$$= .01 \text{ to } .03$$

$$\left(\frac{dC_m}{dC_L} \right)_{ID} = \frac{dC_m}{dC_L} \text{ due induced downwash}$$

$$= \text{approx. } .04 \text{ for exhaust forward}$$

$$\text{and below horizontal tail}$$

$$(N_0)_{\text{thrust}} = X_{ac} \left(\frac{dC_m}{dC_L} \right)_{fus} + \frac{a_t}{a_w} \frac{S_t}{S_w} \frac{l_t}{MAC} \eta_t \left(1 - \frac{d\epsilon}{d\alpha} \right) - \frac{T Y_t}{W(MAC)} \left(\frac{dC_m}{dC_L} \right)_{NF} \quad (9:67)$$

$$\text{nac} \quad \text{ID}$$

9-10 Controlability in Landing

The aft center of gravity location has so far been established by requiring the airplane be stable either in power on or power off condition with stick fixed in unaccelerated flight. Later it will be shown that there are also limitations on the aft position of the center of gravity imposed by requiring the airplane to be stable, stick free in unaccelerated flight and by the change in stick force with change in load factor in accelerated flight, usually called maneuvering flight.

Limitations on the forward center of gravity location of the airplane is set by other conditions. Probably the most critical is that set by the requirement that the airplane be controllable in landing. This requirement means that the elevator must be powerful enough aerodynamically to keep the airplane in equilibrium at $C_{L_{max}}$. From the curve of C_m vs. C_L for a typical airplane, Figure 9:25, it can be seen that the airplane is in equilibrium at $C_L = 0.4$, stick fixed at elevator deflection equals zero.

It can also be seen that if the airplane is displaced to maximum C_L with stick fixed, a $C_m = -.10$ is created which is tending to return the airplane to equilibrium. Therefore if the airplane is to fly at $C_{L_{max}}$, some control must be provided that can equalize this C_m . It is this requirement that limits the amount of stability desired. The more stable the airplane is, the more powerful the control must be to attain equilibrium at maximum

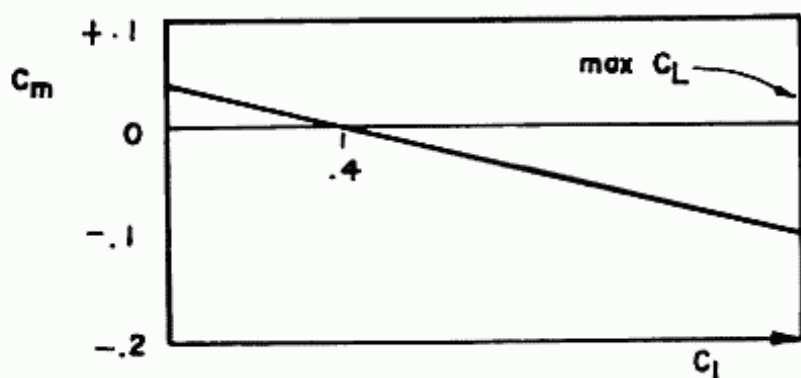


Fig. 9:25. Typical C_m vs. C_L curve, stick fixed.

C_L . The engine off equilibrium Equation 9:60 can be written as:

$$C_{m_{cg}} = C_{m_{ac}} + C_L (X_{cg} - X_{ac}) + C_{m_{fus}} + C_{m_{nac}} - \left(\frac{dC_L}{d\alpha} \right)_t \alpha_t \frac{S_t}{S_w} \frac{l_t}{MAC} \eta_t \quad (9:68)$$

if X_w/C is written as $X_{cg} - X_{ac}$
and C_{N_t} is written as $(dC_L/d\alpha_t) \alpha_t$

The only factors that can be used to control the airplane are the $C_{m_{ac}}$, the location of the center of gravity and α_t . $C_{m_{ac}}$ can be changed by deflecting the flaps of the wings. Although this is inefficient for a conventional airplane, it is the only practical available means of an all wing airplane. Moving the center of gravity of the airplane in flight is completely impractical. However the effective angle of attack of the tail, α_t , can be changed by deflecting the elevator. This method is much more efficient than deflecting a wing flap due to the large distance from the airplane center of gravity to the tail surface, as compared to the distance from the center of gravity to the wing flap.

The effective angle attack of the tail can be changed by either rotating the entire surface or just a part of it about some axis along the span. This movable surface in the aft end of the horizontal tail is called the elevator. A typical elevator is shown in Figure 9:26.

If the entire surface were rotated it would be a very powerful controlling factor. However there are a few other considerations involved that indicate that a fully rotatable surface should not be used. Because it is so powerful it is difficult to control for proper stick forces. Also there are the problems of flutter and weight. However in some designs it might be possible to have a

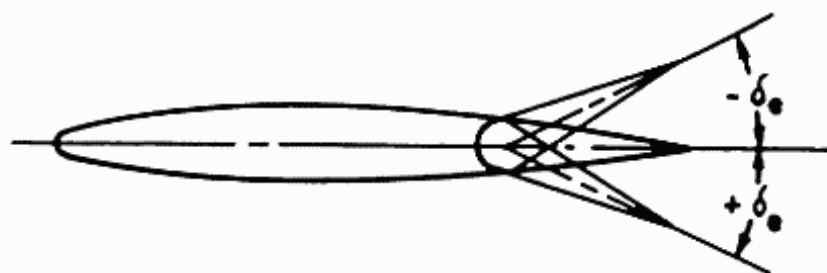


Fig. 9:26. Typical elevator section.

lower weight with an all movable tail instead of one with the conventional elevator since there are some decided savings. The need for the hinge fittings, the structure that ties to it and the duplication of spars and torsion boxes in both elevator and fixed surface is eliminated. Lastly, it is possible that the size of movable surface is not critical, that is, a very powerful control is not required. The only factor affected by the size of the elevator is $d\alpha_t/d\delta_e$. Figure 9:26 shows the signs of δ_e , the elevator deflection. It should be noted that some large high subsonic aircraft and most supersonic aircraft now use all movable control surfaces for a more efficient surface.

When the elevator is deflected it changes the angle of attack and therefore the lift of the tail surface, causing a change in moment about the airplane center of gravity. Differentiating the Equation 9:68 with respect to δ_e , results in

$$\frac{dC_m}{d\delta_e} = - \frac{dC_L}{d\alpha_t} \frac{S_t}{S_w} \frac{l_t}{MAC} \eta_t \frac{d\alpha_t}{d\delta_e} \quad (9:69)$$

This is termed elevator power. The last term $d\alpha_t/d\delta_e$ can be obtained from empirical data. Figure 9:27 shows the variation of $d\alpha_t/d\delta_e$ with S_e/S_t , where S_e is the elevator area and S_t the total tail area. It will be noted that $d\alpha_t/d\delta_e$ is not a linear function of S_e/S_t , and that if the entire surface is movable $d\alpha_t/d\delta_e = 1.0$.

Figure 9:25 shows the variation in C_m with C_L for an airplane with stick fixed and $C_m = 0$ at $C_L = .4$. As C_L increases from .4, C_m becomes negatively larger, and therefore a larger negative deflection of the elevator is required to maintain equilibrium. As C_L decreases from $C_L = .4$, an increasing positive deflection is required. If the airplane was designed so that the elevator deflection, δ_e , equaled zero to maintain equilibrium at

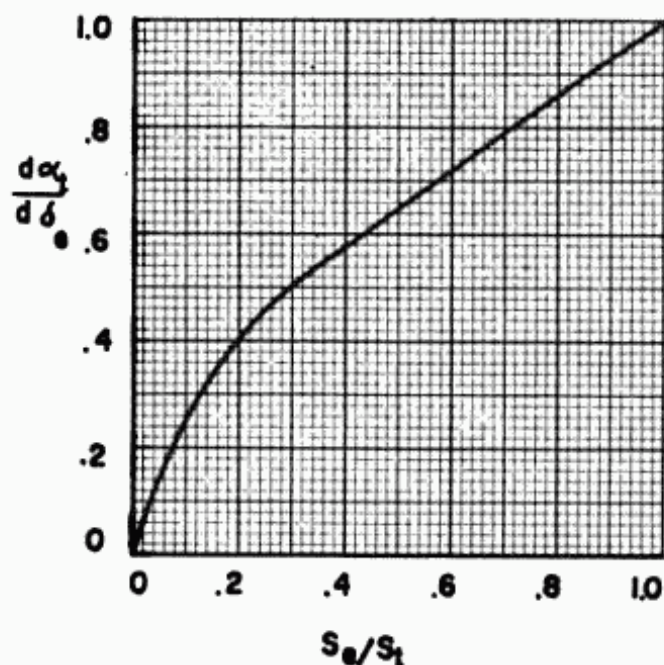


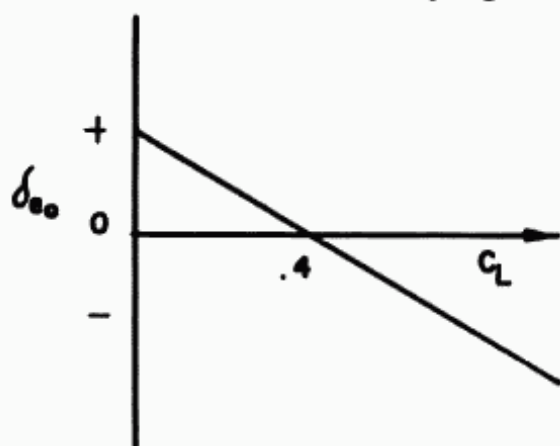
Fig. 9:27. Variation of $d\alpha_t/d\delta_e$ with S_e/S_t . Ref., N.A.C.A. - L-95 "A Method of Predicting the Elevator Deflection Required to Land" R. F. Goranson.

$C_L = .4$, the variation in δ_e required to maintain equilibrium versus C_L is shown in Figure 9:28.

Since the airplane becomes more stable as the airplane center of gravity moves forward, greater elevator power is required to keep the airplane in equilibrium at the more forward center of gravity locations. That is, from Equation 9:68, it can be seen that to keep $C_{m_{cg}} = 0$ as X_{cg} moves forward, the tail contribution term must become larger positively for positive values of C_L . Therefore the condition with the airplane center of gravity furthest forward and flying at $C_{L_{max}}$ is the critical condition

for elevator power. This requires the maximum up deflection of the elevator. The derivation of the formula for the most forward center of gravity can be developed with the data already known.

Fig. 9:28. Elevator deflection required for equilibrium for values of C_L .



9:44 SUPERSONIC AND SUBSONIC AIRPLANE DESIGN

Equation 9:68 can be written as,

$$C_{m_{cg}} = C_{m_{nac}} + C_L (X_{cg} - X_{ac}) + C_{m_{fus}} - \left(\frac{dC_L}{d\alpha} \right)_t \frac{S_t}{S_w} \frac{l_t}{MAC} \eta_t (\alpha_w - \epsilon - i_w + i_t + \frac{d\alpha}{d\delta_e} \delta_e) \quad (9:70)$$

Setting $C_{m_{cg}} = 0$, δ_e , the elevator deflection required for equilibrium becomes

$$\delta_e = \frac{C_{m_{nac}} + C_L (X_{cg} - X_{ac}) + C_{m_{fus}} - \frac{dC_L}{d\alpha} \frac{S_t}{S_w} \frac{l_t}{MAC} \eta_t (\alpha_w - \epsilon - i_w + i_t)}{\left(\frac{d\alpha_t}{d\delta_e} \right) \left(\frac{dC_L}{d\alpha} \right)_t \frac{S_t}{S_w} \frac{l_t}{MAC} \eta_t} \quad (9:71)$$

Letting δ_e equal maximum deflection and C_L equal $C_{L_{max}}$, solving for the most forward X_{cg} results in Equation 9:72.

$$X_{cg_{fwd}} = X_{ac} - \left(\frac{dC_m/d\delta_e}{C_{L_{max}}} \right) \left[\delta_{e_{max}} + \frac{(\alpha_w - \epsilon - i_w + i_t)}{d\alpha_t/d\delta_e} + \frac{C_{m_{nac}} + C_{m_{fus}} + C_{m_{nac}}}{dC_m/d\delta_e} \right] \quad (9:72)$$

where $\delta_{e_{max}}$ is the maximum up deflection of elevator

Ground Effects

When the airplane is close to the ground, the problem of attaining equilibrium at $C_{L_{max}}$ is aggravated by the ground effects.

The ground effects reduce the downwash at the tail and increases the slope of the lift curves of both the wing and tail. However the greatest effect is the reduction of downwash of the tail, which effectively increases the angle of attack at the tail surfaces, which requires an increased up deflection of the elevator to keep the airplane in equilibrium. A thorough method of calculating downwash with ground effects is given in NACA T.R. 738 "Ground Effect on Downwash Angle and Wake Location," by Katzoff and H. Sweberg.

A very approximate method of lumping all these effects into one correction is just to assume that the downwash with ground effects is equal to .5 ϵ in flight.

It is then possible to obtain X_{cg} forward from Equation 9:72 as all the data is known to determine the other factors. Assuming that the C_m of the fuselage and the nacelles is zero at $C_L = 0$ then C_m for maximum C_L can be obtained by multiplying dC_m/dC_L

by maximum C_L . Extreme care must be used in selecting units and assigning the correct signs.

9-11 Design Parameter

Due to the requirements that the airplane be stable with and without power for stick fixed position, the most aft center of gravity location was determined. The most forward center of gravity location was determined by the specification that the tail surface be powerful enough aerodynamically, to keep the airplane in equilibrium at $C_{L_{max}}$ near the ground. It will be noted from Equation 9:72 that the elevator power term $dC_m/d\delta_e$ is a significant factor in the forward center of gravity location. The power term, $dC_m/d\delta_e$, Equation 9:69 is presented again.

$$dC_m/d\delta_e = \frac{dC_L}{d\alpha_t} \frac{S_t}{S_w} \frac{l_t}{MAC} \eta_t \frac{d\alpha_t}{d\delta_e} \quad (9:73)$$

From Equation 9:61 it will be noted that in determining the aft location of the center of gravity, the last term, denoted by,

$$\frac{a_t}{a_w} \frac{S_t}{S_w} \frac{l_t}{MAC} \eta_t \left(1 - \frac{d\epsilon}{d\alpha}\right) \quad (9:74)$$

is the deciding factor.

From experience it could be found that certain values of $dC_m/d\delta_e$ and of Equation 9:74 resulted in a desired center of gravity travel. It should be noted that the term $S_t l_t / S_w MAC$ is common to both $dC_m/d\delta_e$ and Equation 9:74. Now if all the other factors in these equations were combined with the experimental values that resulted in the desired center of gravity travel, and called some constant K_t , then,

$$S_t = \frac{K_t S_w (MAC)}{l_t} \quad (9:75)$$

In Chapter IV the size of the horizontal tail was determined from

$$S_{HT} = C_{HT} \frac{(S_w) (MAC)}{l_t} \quad (9:76)$$

It will be noted that 9:75 and 9:76 are the same if K_t is called

C_{HT} , the tail volume coefficient. Therefore C_{HT} used in obtaining the horizontal tail area required, is a function of the optimum $\frac{dC_L}{d\alpha_t}$ and $d\alpha_t/d\delta_e$ of the tail, $(dC_L/d\alpha)_w$, $d\epsilon/d\alpha$, η_t and the

center of gravity travel required for a conventional transport airplane. It is therefore very important in the design that the center of gravity travel of the airplane be kept to a minimum. The tail volume coefficient decreases with reduction in center of gravity travel, thereby requiring a smaller horizontal tail, and resulting in a more efficient airplane.

9-12 Longitudinal Stability - Stick Free

General

The preceding study of longitudinal stability was for the stick fixed condition. It will be shown that the aft center of gravity location will be more critical for the stick free condition.

Assuming that there is no friction in the elevator hinges, the elevator will float up or down depending upon the pressure distribution over the airfoil. If the elevator floats up with an increase in airplane lift coefficient, a down force on the tail with its corresponding stalling moment results, thereby decreasing the airplane stability. If the elevator floats down, with an increase in lift coefficient, an up force with its corresponding pitching moment results, thereby increasing the stability.

The floating characteristic is a function of the hinge moments about the elevator hinge line and therefore of the aerodynamic balance of the elevator. Figure 9:29 shows a typical pressure distribution over the tail surface for two positive angles of attack.

If the hinge line were at the nose of the elevator it would tend to float up with increase in angle of attack. This floating tendency, $C_{h\alpha}$, is a function of the change in hinge moment coefficient with change in angle of attack of the tail surface. However, as

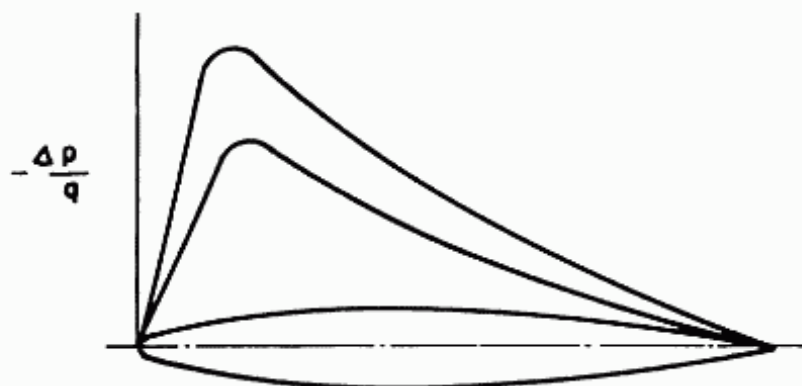


Fig. 9:29. Typical pressure distribution on horizontal tail.

the elevator floats up there is a new pressure distribution which tends to counteract this floating tendency. This counteracting effect, the restoring tendency, is a function of the change in hinge moment coefficient with change in deflection of the elevator, called $C_{h\delta}$. The angle at which the two tendencies offset each other, that is, the point at which the elevator stops rotating is called the "floating angle."

$$C_{h\alpha} = \frac{d C_h}{d\alpha} = \text{floating tendency} \quad (9:77)$$

$$C_{h\delta} = \frac{d C_h}{d\delta_e} = \text{restoring tendency} \quad (9:78)$$

C_{h_0} = hinge moment coefficient at $\alpha = 0^\circ$

$$C_{h_{\text{total}}} = (C_{h\alpha}) \alpha + (C_{h\delta}) \delta_e + C_{h_0} \quad (9:79)$$

The floating angle, δ_e , is the elevator deflection when $C_{h_{\text{total}}} = 0$.

Therefore,

$$\delta_e = - \frac{C_{h\alpha}}{C_{h\delta}} \alpha - \frac{C_{h_0}}{C_{h\delta}} \quad (9:80)$$

For symmetrical airfoils, $C_{h_0} = 0$. Therefore

$$\delta_e = - \frac{C_{h\alpha}}{C_{h\delta}} \alpha \quad (9:81)$$

Later it will be shown that it is important to keep the floating tendency to a minimum. One method of accomplishing this is to set the hinge back. This is called aerodynamic balancing.

If the hinge was at the nose of the elevator, at 0° elevator deflection and some positive angle of attack, the moment about it would tend to rotate the surface upwards. There would be a resultant restoring tendency but the floating angle would still be up. As the hinge line is moved aft the floating tendency is reduced until at some point the moment is zero and the surface would not rotate. If the hinge line is moved aft of this point, the moment about the hinge line is reversed and the surface rotates in the opposite direction. This condition is called overbalancing.

Neutral Point - Stick Free

Assume that an airplane is in equilibrium at some C_L with the controls free, that is the δ_e required for equilibrium is equal to the floating δ_e . If a gust hits the airplane so that the α is changed the floating angle will change as seen from equ. 9:81. At this new α any of three conditions will exist

- 1) airplane will continue to fly at this new α
- 2) airplane will tend to return to its original equilibrium α
- 3) airplane will tend to diverge further from its original equilibrium α

The actual condition that will result is a function of the relation of the floating angle of the elevator in this new α to the δ_e required for equilibrium at this new α .

If the floating δ_e is equal to the δ_e required for equilibrium at this new α the airplane would stay at this new attitude since equilibrium would exist. This is equivalent to condition 1 and is called static longitudinal neutral stability, stick free.

If the absolute value of the floating δ_e is less than the absolute value of the δ_e required for equilibrium at this new α then there would be a smaller moment existing than required to maintain this new α and the airplane would tend to return to the original equilibrium α . This is equivalent to condition 2 and is called static longitudinal stability, stick free.

If the absolute value of the floating δ_e is more than the absolute value of the δ_e required for equilibrium at this new α , then there would be a larger moment existing than required to maintain this new α , and the airplane would tend to diverge further from the original equilibrium α . This is equivalent to Condition 3 and is called static longitudinal instability, stick free.

Actually the original definition of longitudinal stability that the dC_m/dC_L must be negative holds for both stick free and stick fixed stability. If the neutral point stick free is denoted by N_0^1 , then

$$N_0^1 = N_0 - \frac{a_t}{a_w} \frac{S_t}{S_w} \frac{l_t}{MAC} \eta_t \left(1 - \frac{d\epsilon}{d\alpha} \right) \frac{C_{h\alpha}}{C_{h\delta}} \quad (9:82)$$

This equation for stick free neutral point is derived by following the method presented for the stick fixed condition. When the expression for dC_m/dC_L stick free is determined, it is set equal to zero and solved for X_{cg} . This results in Equation 9:82.

Equation 9:82 shows that the difference in stick fixed neutral

point and stick free neutral point is a certain term times $C_{h\alpha}/C_{h\delta}$. This term as seen from Equation 9:43 is the $dC_{m_{cg}}/dC_L$ of the tail, stick fixed. As stated previously it is desirable to keep $C_{h\alpha}$ to a low value. If this is done, the last term in Equation 9:82 is small and N_0^1 is close to N_0 . It should be noted that $C_{h\delta}$ also has a desired range. If $C_{h\delta}$ is high the stick forces required to maneuver the airplane is high. However if it is too low, a little stick force exerted by the pilot would result in a violent maneuver.

The neutral point stick free could be calculated if $C_{h\alpha}$ and $C_{h\delta}$ were known. However these terms are functions of hinge setting, chord of the elevator/chord of the tail, airfoil section, nose shape of control surface, gap at control surface nose and aspect ratio of total surface. NACA WRL-663 "Wind Tunnel Data in the Aerodynamic Characteristics of Airplane Control Surfaces" by R. I. Sears presents the values of the desired coefficients as a function of a large number of variables. The value of $N_0 - N_0^1$ is usually between .02 and .05 of the mean aerodynamic chord.

Figure 9:30 shows the relationship of the floating angles that result in stick free stability and instability, to the angle required for equilibrium. Figure 9:30a is for a negative angle required for equilibrium while Figure 9:30b is for a positive angle required for equilibrium.

9-13 Effect of Thrust on Center of Gravity Limits

In the preceding sections it has been established that the condition that limits the aft center of gravity location is that the

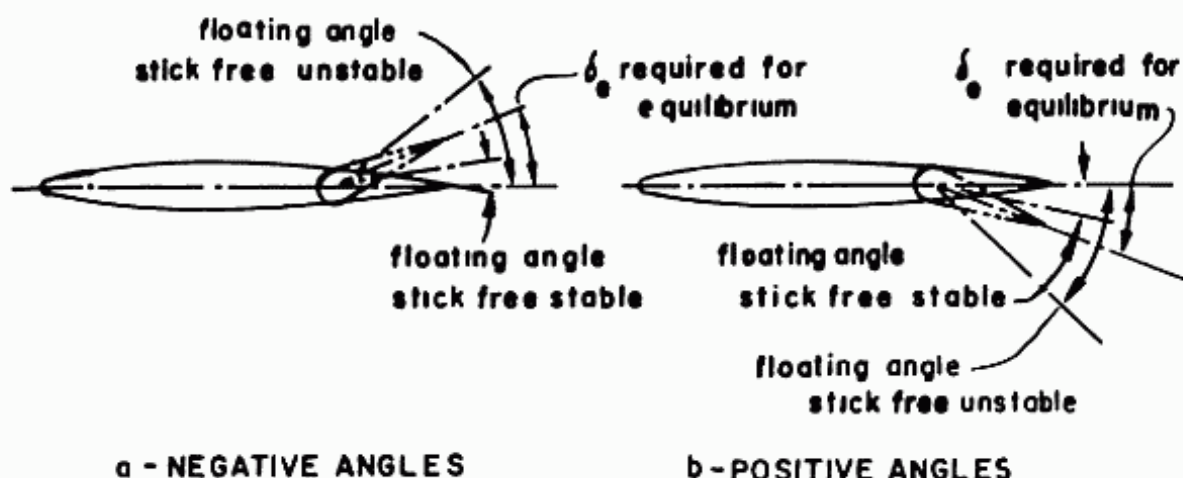


Fig. 9:30. The effect of the relation of floating angle to the equilibrium angle on stick free stability.

airplane must be stable, that is, dC_m/dC_L cannot be greater than 0, for all center of gravity positions. The critical condition is with the engines producing thrust.

It has also been established that the condition that limits the forward center of gravity location is that it should be possible to maintain equilibrium, that is, $C_m = 0$, for all center of gravity positions and at any C_L . The critical condition is without thrust. This effect of thrust on the critical conditions requires a more thorough presentation.

Forward Center of Gravity

The condition that sets the forward limit of the center of gravity is that equilibrium must be maintained at $C_{L_{max}}$ for any center of gravity position, with or without thrust, that is,

$$C_{m_{cg}} = 0 = C_L (x_{cg} - x_{ac}) + C_{m_{ac}} + C_{m_{fus}} - \left(\frac{dC_L}{d\alpha} \right)_t \alpha_t \frac{S_t}{S_w} \frac{l_t}{MAC} \eta_t \quad (9:83)$$

Figure 9:31 shows the variation of C_m with C_L for a particular airplane for different elevator deflections, with and without thrust. It was previously established in Section on Power Effects that for most airplane designs the effect of thrust is destabilizing. In addition, it was shown from Equations 9:62 and 9:64 that $C_{m_{cg}}$ due thrust equals zero when C_L equals zero, if there is no induced flow effect.

Refer to Figure 9:31. At x_{cg} equals .15 and elevator deflection equals zero, at $C_{L_{max}}$ C_m equals -.20 with no thrust, and equals -.15 with thrust. If the elevator is moved up to its maximum deflection, (up deflection is considered negative) and x_{cg} is still at .15, C_m equals -.05 with no thrust, but equals zero with thrust. This change in $C_{m_{cg}}$ is due to the change in effective α_t , (Equation 9:83) caused by elevator deflection. If the center of gravity moves forward, that is x_{cg} becomes less than .15, C_m for the thrust condition again becomes negative as can be seen from Equation 9:83. Since the elevator is already at its maximum deflection, equilibrium cannot be reached. Therefore $x_{cg} = .15$ is the furthest forward that the center of gravity can go and still maintain equilibrium with thrust at maximum C_L .

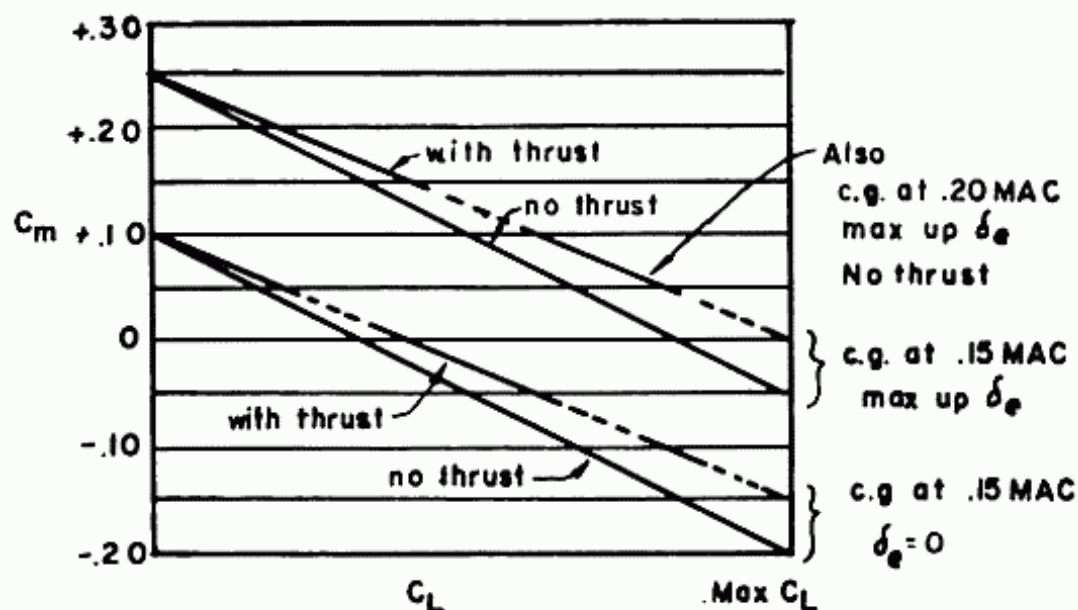


Fig. 9:31.

For the condition with no thrust, elevator at maximum up deflection, $x_{cg} = .15$ and airplane at maximum C_L , C_m is equal to $-.05$. Therefore at this condition, equilibrium is not attained. For a given design, the only way equilibrium can be attained at C_{Lmax} and no thrust, is to move the center of gravity aft until $C_{m_{cg}}$ does equal zero. For a $C_{Lmax} = 1.0$, x_{cg} will then equal 0.20 . That is, equilibrium cannot be maintained forward of x_{cg} equal to 0.20 with no thrust. Therefore the condition with no thrust is critical for forward center of gravity location.

Aft Center of Gravity

The condition that sets the aft limit of the center of gravity is that the airplane be stable for any center of gravity position, with or without thrust, that is

$$\frac{dC_m}{dC_L} = 0 = x_{cg} - x_{ac} + \left(\frac{dC_m}{dC_L} \right)_{fus nac} - \frac{a_t}{a_w} \frac{S_t}{S_w} \frac{l_t}{MAC} \eta_t \left(1 - \frac{d\epsilon}{d\alpha} \right) + \left(\frac{dC_m}{dC_L} \right)_{due thrust} \quad (9:84)$$

Figure 9:32 shows the variation of C_m with C_L for the same airplane as in Figure 9:31.

Refer to Figure 9:32. With x_{cg} equal to $.15$, the values of C_m vs. C_L are the same as in Figure 9:31. For no thrust dC_m/dC_L equals $-.20$. For the thrust condition, dC_m/dC_L equals $-.17$.

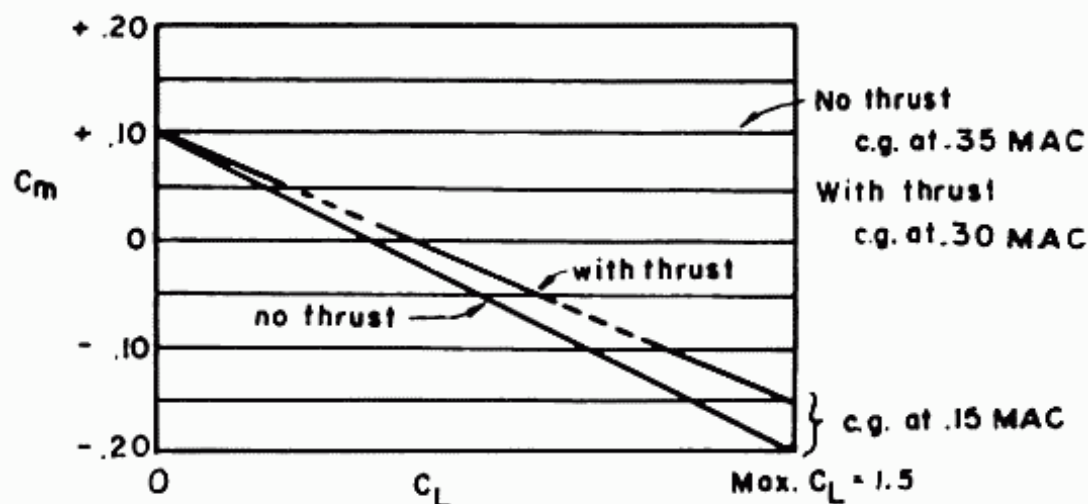


Fig. 9:32

As can be determined from Equation 9:84, dC_m/dC_L becomes larger positively as x_{cg} becomes larger. When x_{cg} reaches .32, dC_m/dC_L equals zero for the thrust condition. However, for the no thrust condition, x_{cg} can increase to .35 before dC_m/dC_L becomes zero. For the thrust condition if x_{cg} increases beyond .32, dC_m/dC_L becomes positive, that is the airplane becomes unstable. For the no thrust condition, the x_{cg} must increase beyond .35 before the airplane becomes unstable. Therefore the thrust condition is critical for the aft center of gravity location. Equation 9:84 shows that elevator deflection does not affect dC_m/dC_L . A change in elevator deflection merely moves the C_m vs. C_L curve up or down as seen in Figure 9:31.

9-14 Optimum Position of Center of Gravity

As has been shown, it is desirable for efficiency in horizontal tail design to keep the center of gravity travel of the airplane to a minimum. It will now be explained why it is desirable to locate the center of this line of travel approximately at the aerodynamic center of the wing. That is, if the center of gravity travel must be 20% of the mean aerodynamic chord, the forward point should be at approximately .15 MAC and the aft point at approximately .35 MAC, assuming the aerodynamic center is at .25 MAC. This is true for a conventional wing-tail relation, that is, the horizontal tail is aft of the wing. A canard type airplane presents some interesting aspects of stability and control and will be discussed in the next section. It is necessary to refer to the longitudinal stability equation once more.

$$\frac{dC_m}{dC_L} = x_{cg} - x_{ac} + \left(\frac{dC_m}{dC_L} \right)_{\text{fus}} - \frac{a_t}{a_w} \frac{l_t}{\text{MAC}} \frac{S_t}{S_w} \eta_t \left(1 - \frac{d\epsilon}{d\alpha} \right)$$

nac

If the center of gravity was always forward of the aerodynamic center, its travel would have to be between approximately .04 and .24 MAC. In this case the airplane would probably be stable at all times without a horizontal tail. However a horizontal tail would still be required for control. Since a surface behind the c.g. is always stabilizing, a very stable airplane would result, particularly when the center of gravity is at .04 MAC. A very large horizontal tail would then be required to control the airplane at maximum C_L and center of gravity at this forward position. If the center of gravity was always aft of the aerodynamic center, that is, between .26 and .46 MAC, the airplane without tail would be exceedingly unstable at its most aft position. An excessively large horizontal tail would then be required for stability at this aft position of center of gravity. This condition would be aggravated a little more by the reduced tail arm.

If a compromise is affected, that is, have the center of gravity travel centered at the aerodynamic center, the tail does not have to be as large for control at the most forward center of gravity or for stability at the most aft center of gravity.

9-15 Canard Type Airplane

This type of airplane is interesting because it presents an interesting point in stability and control, and because it has distinct advantages for airplanes that are critical for landing distance. The effect on landing distance was discussed in Section 2:3. A canard type airplane is one that has its horizontal tail in front of the wing.

To attain a stable canard airplane, the center of gravity of the airplane must always be in front of the aerodynamic center of the wing. A surface in front of the center of gravity, as a canard surface, is destabilizing. This is so, because an increase in airplane C_L caused by an increase in angle of attack, increases the lift on the forward surface thereby producing a stalling moment. That is, the dC_m/dC_L due to the canard surface is positive. Since the canard surface is destabilizing, the airplane without the canard must always be stable enough to overbalance the canard surface. Therefore the wing aerodynamic center must always be aft of the center of gravity.

With the surface in front of the center of gravity the surface

must produce a force in the up direction to control the airplane at high C_L , as in landing. This up force reduces the load on the wing and therefore the landing speed and distance.

There are other advantages of a canard surface for a jet transport, particularly with a bicycle gear. They are:

- 1) With the wing further aft on the fuselage, the jet exhaust noise is less likely to disturb the passenger compartment.
- 2) With a bicycle gear, the distance from the surface to the rear tire is greatly increased. This long arm would increase the power of the surface in rotating the airplane about the rear tire, in both landing and take-off.
- 3) The horizontal control surface is out of the wing wake and jet exhaust.
- 4) The upload on the control surface aids maneuverability.

However there are definite disadvantages. They are:

- 1) The shorter tail arms of both the horizontal and vertical tails mean larger areas.
- 2) Some problems of control, and efficiency of the surface.
- 3) Stall problems

On an airplane with the conventional tail the wing is made to stall first. This is done so that (a) control is maintained up to the stall, and (b) with the wing stalled the airplane is still stable due to the stabilizing tail.

On a canard airplane if the wing stalls first the airplane is unstable due to the unstable canard surface, and pitches up further tending to stall the canard. If the canard surface stalls first then control is lost.

It is felt that because of the advantages offered by a canard for a jet transport that might be critical for landing distance, the canard type airplane should be re-investigated.

PROBLEMS

- 1) Calculate the most aft center of gravity with stick fixed and power on.
- 2) Calculate the most forward center of gravity with ground effects.

REFERENCES

- 9:1 C. D. Perkins and R. E. Hage, "Airplane Performance, Stability and control", publisher John Wiley and Sons.

- 9:2 Walter D. Wolhart and David F. Thomas, Jr., "Static Longitudinal and Lateral Stability Characteristics at Low Speed of Unswept-Midwing Models Having Wings with an Aspect Ratio of 2, 4, or 6, NACA TN 3649, May 1956.
- 9:3 Walter D. Wolhart and David F. Thomas, Jr., "Static Longitudinal and Lateral Stability Characteristics at Low Speed of 60° Sweptback-Midwing Models Having Wings with an Aspect Ratio of 2, 4, or 6, NACA TN 4397, September 1958.
- 9:4 Marvin Schuldenfrei, Paul Comisarow, and Kenneth W. Goodwon, "Stability and Control Characteristics of a Complete Airplane Model Having a Wing with Quarter-Chord Line Swept Back 40°, Aspect Ratio 2.50, and Taper Ratio 0.42, NACA TN 2482, December 1951.
- 9:5 Walter C. Williams, Hubert M. Drake, and Jack Fischel, "Comparison of Flight and Wind-Tunnel Measurements of High-Speed-Airplane Stability and Control Characteristics, NACA TN 3859, August 1956.
- 9:6 Noel K. Delany, "Exploratory Investigation of the Low-speed Static Stability of a Configuration Employing Three Identical Triangular Wing Panels and a Body of Equal Length", NACA RM A55C28, April 29, 1955.
- 9:7 Noel K. Delany, "Additional Measurements of the Low-speed Static Stability of a Configuration Employing Three Triangular Wing Panels and a Body of Equal Length", NACA RM A55FO2a, July 25, 1955.
- 9:8 Alex Goodman and Byron M. Jaquet, "Low-speed Pitching Derivatives of Low-aspect Ratio Wings of Triangular and Modified Triangular Plan Forms", NACA RM L50CO2, April 17, 1950.
- 9:10 Peter C. Boisseau, "Low-subsonic Static Stability and Damping Derivatives at Angles of Attack From 0° to 90° for a Model with a Low Aspect Ratio Unswept Wing and Two Different Fuselage Forebodies" NASA Memo 1-22-59L, March 1959.
- 9:11 Murray Tobak and William R. Wehrend, "Stability Derivatives of Cones at Supersonic Speeds", NACA TN 3788, September 1956.
- 9:12 B. Etkin "Dynamics of Flight-Stability and Control" John Wiley and Sons, 1959.

Chapter X

DIRECTIONAL AND LATERAL STABILITY AND CONTROL, AND MANEUVERING FLIGHT

10-1 Introduction

Chapter IX presented, in some detail, the problem of longitudinal stability. For an understanding of airplane design it is felt that a study of lateral and directional stability and control and maneuvering flight is also desirable. A comprehensive presentation of these topics can be obtained from texts on stability and control. Since most actual design of the control surfaces are based on previous experience and wind tunnel tests, only a brief outline of the theory is included here.

10-2 Directional Stability and Control

The study in the preceding chapter involved only stability and control in the longitudinal plane, that is, about the Y axis. It is now necessary for the design of the vertical tail, to consider motion about the Z axis. In the longitudinal study the angle which varied the coefficient of lift is called the angle of attack. In studying motion about the Z axis the equivalent angle is called the angle of slip. However reference to another angle, called the angle of yaw, is required. Some explanation of the difference in these is necessary.

The angle of yaw is the angular displacement of the center line of the airplane to some assumed azimuth direction. The angle of slip is the angle that the airplane center line makes with the flight path or the free stream velocity. In flight, if an airplane is turning so that the center line of the airplane at the center of gravity is tangent to the flight path, the angle of slip is zero but the angle of yaw depends on the reference line chosen for it. In wind tunnel work it can be seen that angle of yaw and angle of slip will be the same magnitude since the flight path, that is, direction of freestream velocity and the reference line, the center of the tunnel, are the same. However the term yaw is usually used in wind tunnel work.

The definition of static directional stability is similar to that of static longitudinal stability. The airplane is statically stable if the airplane tends to return to equilibrium when it is displaced from that position, and $dC_N/d\beta$ is equivalent to dC_m/dC_L in longitudinal stability, where C_N is the yawing moment coefficient and β is the angle of

10:2 SUPERSONIC AND SUBSONIC AIRPLANE DESIGN

sideslip. This $dC_n/d\beta$ can be developed in the same manner as dC_m/dC_L was in the longitudinal case, by obtaining the contribution of the component parts. The derivation will not be followed but only some qualitative effects mentioned.

Whereas the wing effect was the major factor to be balanced by the tail in the longitudinal static stability, it is of small consequence in directional static stability, although the stability does increase with sweepback.

The interference effects between the fuselage and wing are negligible for the low wing configuration, and slightly stabilizing for the midwing and high wing airplanes. The fuselage and nacelles are the major factors in directional stability.

Besides determining directional stability, the vertical tail must be powerful enough to overcome yawing moments that are developed by certain flight conditions. The critical one for a transport airplane is often the condition of one engine inoperative. The unbalanced moment developed by one engine inoperative is $(T)(l_y)$ as shown in Figure 10:1.

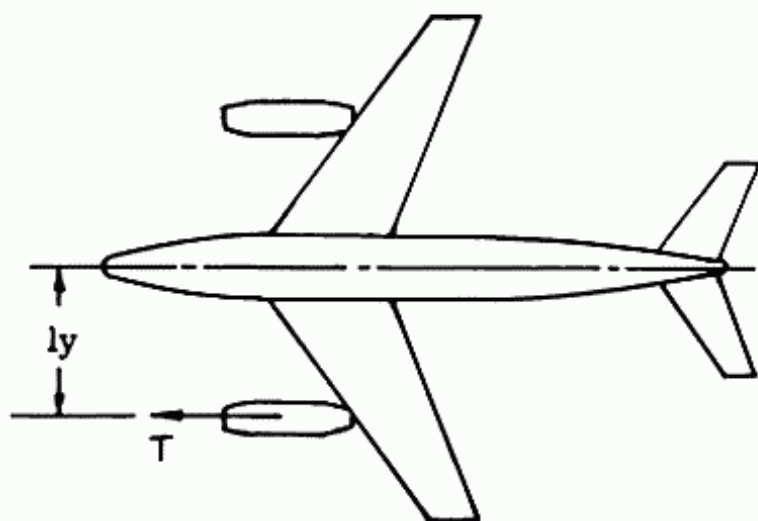


Fig. 10:1. Airplane with one engine inoperative.

This moment can be calculated for all velocities and altitudes that the airplane is expected to fly at, and the coefficient C_y can be determined.

$$C_{n_{th}} = \frac{T l_y}{q S_w b} \quad (10:1)$$

The C_n for the rudder with full deflection may be calculated just as C_m for the elevator was:

$$N_{VT} = L_v \times l_v \quad (10:2)$$

where

N is the yawing moment about the center of gravity

L_v is the side force on the vertical tail

l_v is the distance from the center of gravity to the aerodynamic center of the vertical tail

$$C_n = \frac{C_{L_v} S_v q_v l_v}{q S_w b} = C_{L_v} \frac{S_v l_v}{S_w b} \eta_t = a_v \alpha_v \frac{S_v l_v}{S_w b} \eta_t \quad (10:3)$$

$$\text{where } a_v = \left(\frac{dC_{L_v}}{d\alpha_v} \right)_v$$

then

$$\frac{dC_n}{d\delta_r} = a_v \frac{d\alpha_v}{d\delta_r} \frac{S_v l_v}{S_w b} \eta_t \quad (10:4)$$

where

a_v and $d\alpha_v/d\delta_r$ can be determined exactly as a_t and $d\alpha_t/d\delta_e$ were, as outlined in Section on Stick Fixed Longitudinal Stability.

The maximum deflection for most rudders is 30° , as its effectiveness drops off rapidly beyond this. Therefore C_{nV} may be obtained by multiplying $dC_n/d\delta_r$ by δ_r maximum.

If C_{n_r} and $C_{n_{th}}$ are plotted vs. speed, the point at which the curves cross, determines the lowest speed at which the airplane can maintain zero slip with one engine inoperative. See Figure 10:2.

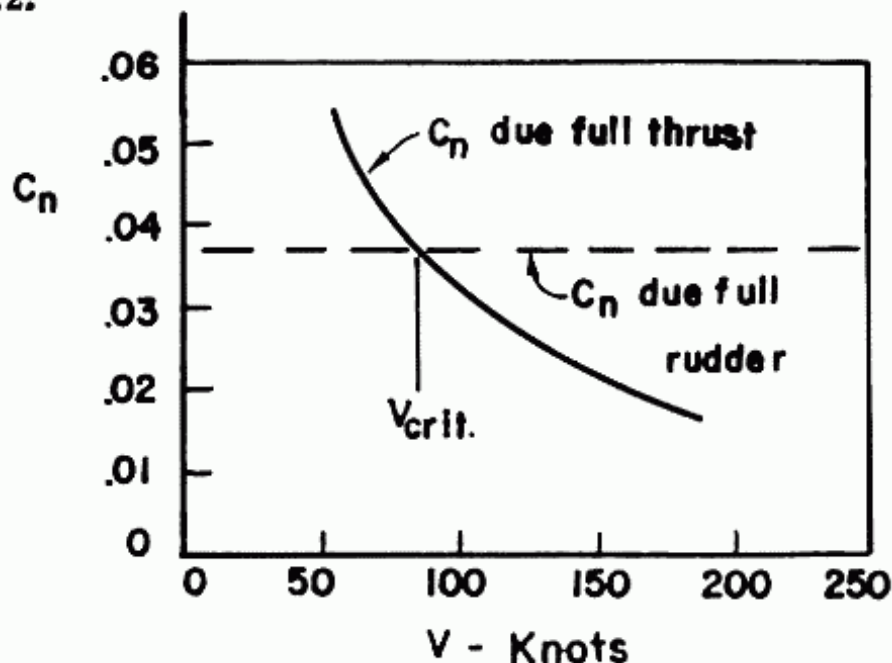


Fig. 10:2. Critical speed for vertical tail.

10:4 SUPERSONIC AND SUBSONIC AIRPLANE DESIGN

If the stalling speed is below the critical speed, zero sideslip cannot be maintained and the rudder power must be increased.

10:3 Lateral Stability and Control

General

Lateral stability and control is the study of airplane motion about the longitudinal axis. This motion is called rolling, the moments causing it are rolling moments and the coefficient of rolling moment is denoted by C_l .

Rolling is created by two separate conditions. One is by manipulation of some control to modify the lift distribution over the wings so that the lift on one wing is greater than the other. The other condition is the existence of a certain geometry of the wing that combined with an angle of slip will change the spanwise lift distribution to cause a rolling moment. This is called dihedral effect. The dihedral angle is the angle between the plane of the wing chords, and the plane perpendicular to the vertical plane of symmetry of the airplane and passing through the root chord. Many other factors aside from the dihedral angle influence the dihedral effect. They are the wing tip effect, the vertical location of the wing on the fuselage, flap deflection, and wing sweep.

If an airplane is displaced from its equilibrium position, either about its Y or Z axis, and it tends to return to this equilibrium position, it is said to be longitudinally or directionally stable. There is no equivalent condition of stability about the X axis. No airplane is laterally stable for roll alone. The criteria for lateral stability is the dihedral effect. If the total dihedral effect results in a rolling moment due to sideslip in the same direction as would result from a positive dihedral angle, it is said to have stable dihedral effect. Figure 10:3 shows typical curves of C_l versus β , the angle of slip, for an airplane with stable and

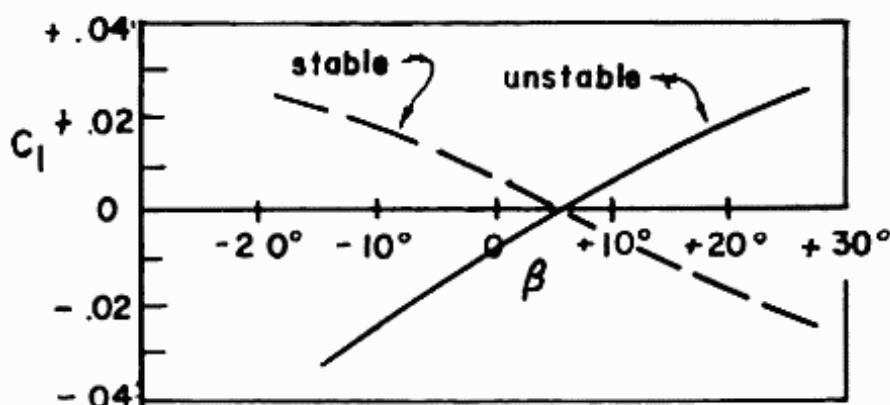


Fig. 10:3. C_l vs. β for an airplane with stable and unstable dihedral effect.

unstable dihedral effect. A rolling moment is considered negative when it causes the left wing to go down.

A brief explanation why positive dihedral is considered a stable rolling effect and actually tends to return the airplane to its equilibrium position, is presented.

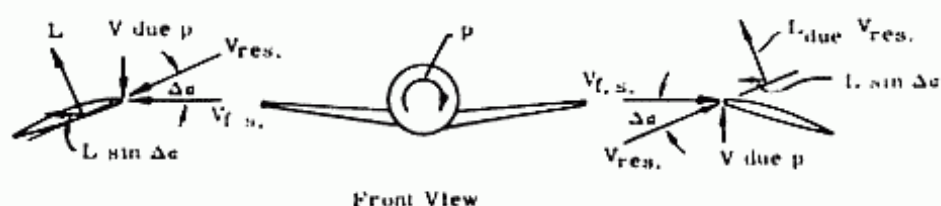


Fig. 10:4. Drag forces due to rolling velocity.

It can be seen from fig. 10:4 that the left forces of an airplane with an induced rolling velocity p , produces forces fore and aft parallel to the freestream that result in a yawing moment. This yawing moment in turn causes a sideslip angle as seen in fig. 10:5.

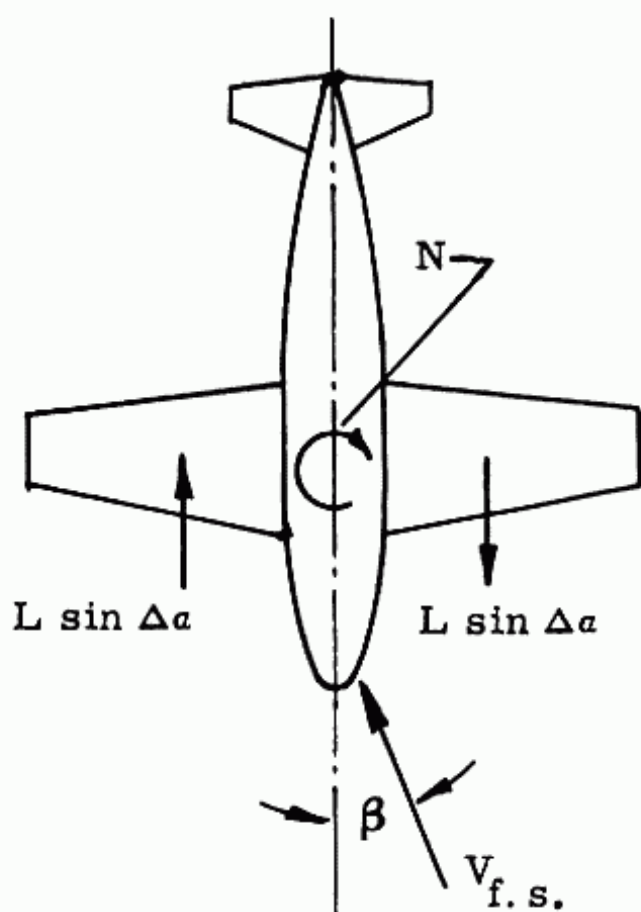


Fig. 10:5. Yawing moment due rolling velocity.

This resulting sideslip angle, β , on an airplane with positive dihedral will result in a rolling velocity p , opposite in direction to the original imposed p and therefore is considered a stabilizing effect. In addition if the airplane is already rolled to an angle ϕ as seen in Fig. 10:6, the side force will produce a sideslip which in combination with positive dihedral effect will produce a rolling moment that will tend to right the airplane.

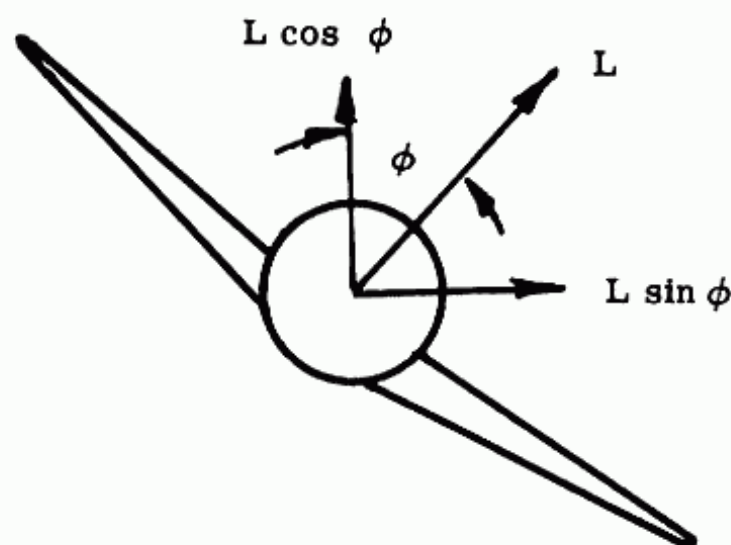


Fig. 10.6. Forces on airplane in bank.

If an angle of sideslip is imposed on an airplane in straight and level flight, the resulting roll due to dihedral effect will cause a yawing moment that will tend to oppose the original imposed β .

All the above phenomena show that positive dihedral effect is a stabilizing influence in either roll or sideslip. However, it is not static stability since it involves an element of time and motion before the stabilizing moment is set up.

Dihedral Effect

The dihedral angle has the greatest influence on the dihedral effect of the airplane. It is considered positive if the wing tip is above the wing chord for zero sweepback. The dihedral angle causes rolling in sideslip due to the fact that the forward wing will have a higher angle of attack than the rear wing. This change in rolling moment due to sideslip is called dihedral effect.

Of all the other effects the most significant is wing sweepback. It should be remembered that lift forces are a function of the velocity perpendicular to the wing quarter chord. From fig. 10:7 it is seen that the velocity perpendicular to the quarter chord

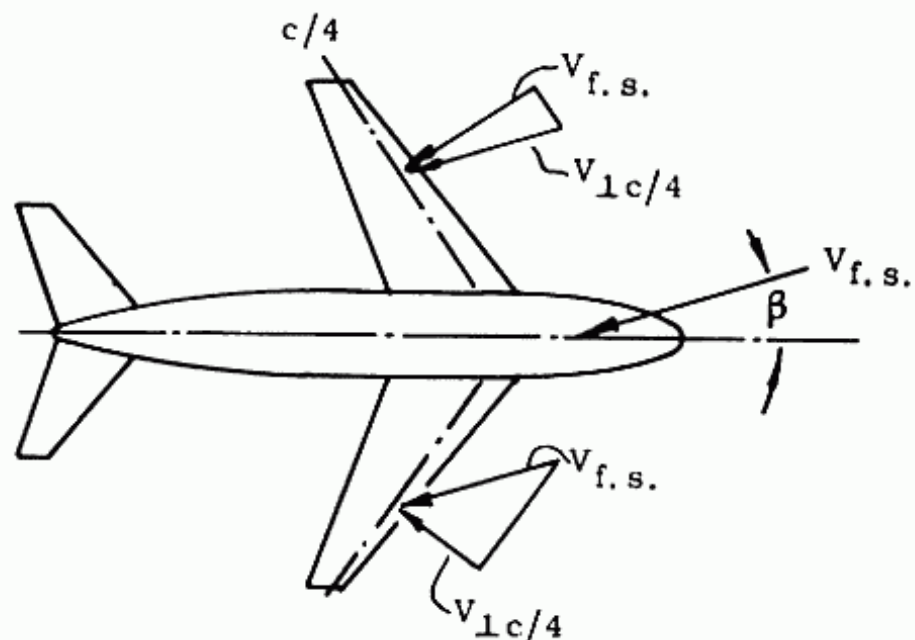


Fig. 10.7. Effect of sweepback on dihedral effect.

is greater for the forward wing in a sideslip. This forward wing will therefore have a greater lift than the trailing wing and the airplane will roll in the same direction as if it had a positive dihedral angle. This is particularly true at high angles of attack, where a high coefficient of lift of a sweptback wing increases the dihedral effect considerably. Therefore the dihedral effects of a high speed jet airplane with sweepback would be very large at low speeds and it is for this reason that they generally have very little dihedral angle, or even a negative one. This effect is exaggerated if the airplane has a high wing configuration since the interference between a high wing and the fuselage causes a positive dihedral effect. The low wing has a negative effect and a midwing no effect at all.

The side load on the vertical tail contributes to the dihedral effect. This $dC_l/d\beta$ can be considerable, with its value depending on the distance from the tail a.c. to the airplane roll axis as well as the magnitude of the side load.

The requirements for dihedral effect have never been accurately established, and therefore is left to the discretion of the designer. It is usually felt by the pilot that some stable dihedral effect is desirable. However it is possible to attain so much dihedral effect that it will be undesirable in connection with directional control and fast rolling maneuvers. If it is required to sideslip due to a one or two engine out condition, a large stable dihedral effect would cause a large rolling moment, that

would have to be overcome. The Air Force has used a criterion that the dihedral effect $dC_l/d\beta$ be one half the value of the directional stability, $dC_n/d\beta$.

Aileron Control

Because of the fact that a rolling moment is caused by dihedral effect, and the desirability of banking the airplane in a turn, some control over rolling is required. This is usually accomplished by the use of flaps at the outboard, trailing edges of the wing. These are called the ailerons. The aileron is rotated up on one wing tip and down on the other, thereby creating a difference in lift between the wings and causing a rolling moment.

As the rolling velocity increases due to aileron deflection, a damping moment is set up that tends to stop the rolling motion. When this increment of damping moment reaches in magnitude the increment in rolling moment that is causing the roll, a steady rolling velocity is maintained. Since the damping moments are quite large, effective ailerons are required on airplanes designed for high rolling maneuverability.

The criteria usually specified for lateral control is the parameter $pb/2V$, where p is the rate of roll in radians per second, b , the wing span in feet and V , the true speed in feet per second. For geometrically similar airplanes and lateral control arrangements, this parameter is the same. The minimum values for full aileron deflection as set by the military are:

Cargo and bombers	=	.07
Fighters	=	.09

This criterion usually determines the size of the ailerons. Another condition that might be critical for aileron size is an unsymmetrical load on the wings due to a gust. The aileron must be powerful enough to control the airplane at low speeds under this condition.

Aileron Reversal Speed - Spoilers

Although ailerons are employed as a device to control the rolling moment of the airplane, pitching moments are induced on each wing due to its location at the trailing edge of the wing. These moments cause the wing to twist in such a manner that the rolling moment due to the aileron deflection is decreased. Since these moments are proportional to the velocity squared, at high enough speeds they might counteract the rolling moments due to the ailerons, and result in the loss of lateral control. This speed, called the aileron reversal speed, can be increased by

making the wing stiffer in torsion. It should be noted that the advent of high speed flight has made the problem more critical in two ways. First, for the same design of the wing and aileron, that is the same aileron reversal speed, it is more likely that the airplane will reach this speed. Secondly, because of compressibility effects the wings must be made thinner for efficient high speed flight. The thinner wing results in a more flexible structure in torsion and therefore a lower aileron reversal speed. It is necessary that this aileron reversal speed be greater than any speed that the airplane might be required to fly.

Because of the possibility of encountering the aileron reversal speed problem, a spoiler type of aileron has been studied for high speed airplanes. This spoiler was given its name due to the fact that it reduces, or spoils, the lift on one side of airplane while leaving the lift of the other side unaffected. It is a flap mounted on the top side of wing as shown in Figure 10:8.

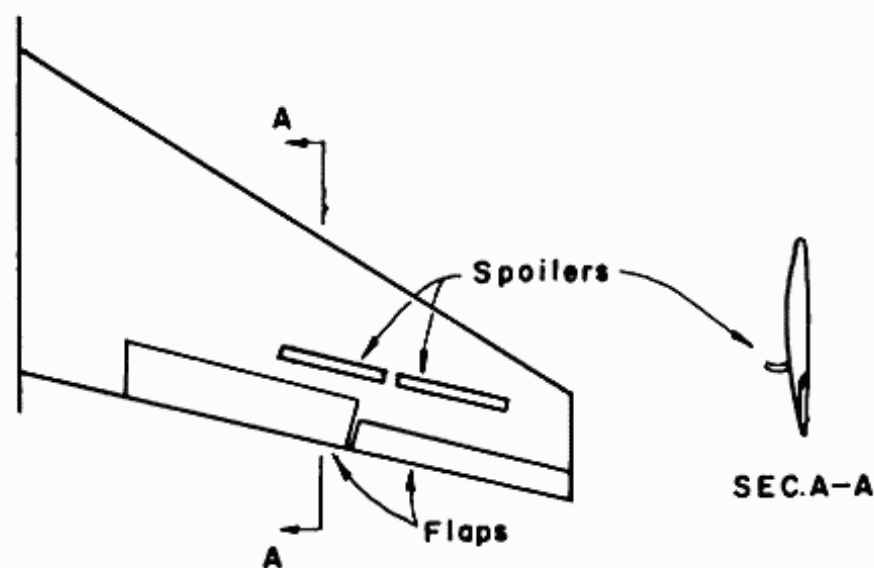


Fig. 10:8. Spoilers.

Although it is more effective as it moves forward, the lag in its action is also increased.

The primary reason for using a spoiler is that it reduces the pitching moment that accompanies the roll, and therefore just about eliminates the possibility of the 'aileron' reversal speed being critical. Another important advantage is that it allows the use of full span flaps. The greatest disadvantages of the spoiler are (1), since it only affects the lift on one side of the airplane, it is not as effective as the conventional aileron, and (2) it decreases the total lift on the airplane and therefore causes the airplane to sink, unless corrected by up elevator.

10:10 SUPERSONIC AND SUBSONIC AIRPLANE DESIGN

10:4 Maneuvering Flight

In all the previous discussions the airplane has been considered as being in an unaccelerated flight condition, load factor = 1. However all airplanes must be maneuvered, that is, be in accelerated flight where the lift is greater than the weight. Probably the two most important maneuvers are the pull-up and banked turn. If an airplane is in level flight, lift is equal to weight and $C_L V^2$ is equal to a constant. If the pilot suddenly pulls on the stick so that C_L increases before V can be reduced, the lift is greater than the weight and the flight path will be curved upward. This is called a pull-up, shown in Figure 10:9.

In turning it is desirable to bank the airplane. Figure 10:10 shows a banked airplane in front view.

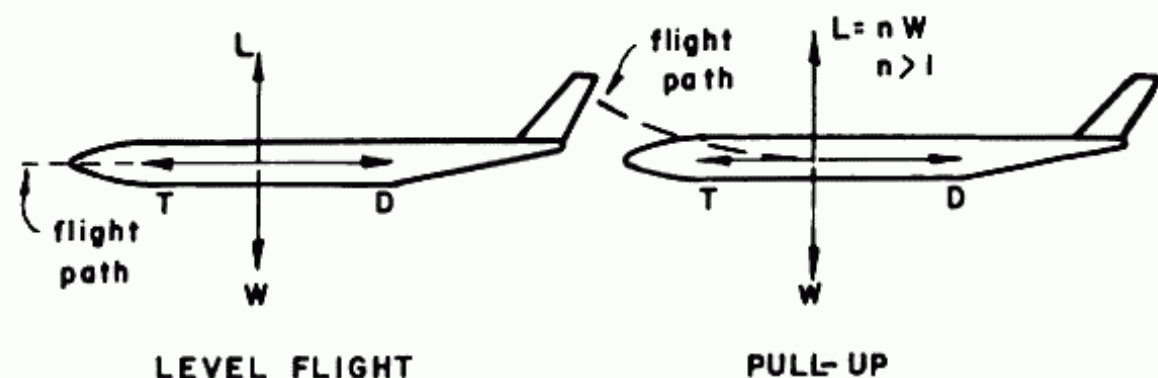


Fig. 10:9. Airplane in a pull-up.

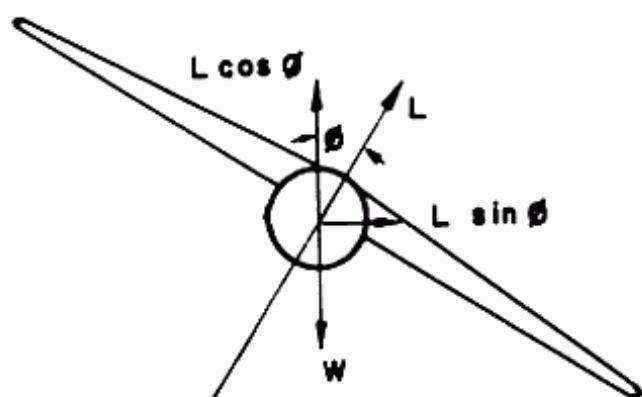


Fig. 10:10. Airplane in a banked turn.

The side component of lift, $L \sin \phi$, is the force that causes the airplane to turn. This side force would cause the airplane to sideslip. To prevent sideslipping, the rudder is deflected setting up a moment of such a magnitude that the airplane rotates to the angle required for zero sideslip. This relationship between yawing and rolling is called coordinating the turn. The vertical com-

ponent, $L \cos \phi$, determines whether the airplane will climb, sink or stay at the same altitude while turning. It is noted that to keep level flight, that is $L \cos \phi = W$, the lift L must be greater than the weight and therefore have a load factor greater than one. In fact the load factor in turning is equal to $\frac{1}{\cos \phi}$, where ϕ is the angle of bank.

It is apparent that in a pull-up the airplane is rotated about the Y axis. That the airplane also rotates about its Y axis in a banked turn is not so evident. If the airplane is banked with the elevator in the same position, that is the angle of attack of the wing is unchanged, $L \cos \phi$ is less than W (Figure 10:10) and the airplane will sink. To increase L so that $L \cos \phi$ is equal to W , without increasing speed, the elevator must be deflected so that the angle of attack is increased. This rapid increase in angle of attack is actually rotation of the airplane.

It is therefore evident that the ability of the airplane to maneuver is a function of the ability of the pilot to rotate the airplane about the Y axis, and to increase its angle of attack with the speed virtually unchanged. This angular rotation of the airplane produces damping effects tending to stop this rotation, and in effect increase the longitudinal stability of the airplane. To overcome these added stability moments as the lift coefficient increases, greater stick force and more elevator movement are required. These stick forces and elevator motions are a function of the center of gravity location of the airplane, just as the stability characteristics in unaccelerated flight were. It is possible to develop the formula for the change in stick force required for a change in desired load factor, dF_S/d_n . Although the effects of dF_S/d_n are quite important on fighter and interceptor airplanes, particularly large ones, they are relatively unimportant for transport airplanes.

PROBLEMS

- 1) Determine $pb/2V$ for the airplane designed.
- 2) Determine whether the vertical tail is powerful enough to control the airplane at $1.20 V_{SO}$ with the critical engine inoperative. Show by use of C_n vs. V diagram.

Chapter XI

SUPERSONIC EFFECTS ON STABILITY AND CONTROL

11-1 Introduction

Chapters IX and X have presented an abbreviated analysis of subsonic stability and control for design purposes. This chapter will discuss some of the more important effects that supersonic flow, and the necessary aircraft design changes that have resulted, have had on stability and control. Therefore only the changes of parameters, or of methods required, from the subsonic analysis will be discussed. It should be noted that extensive use has been made of Ref. 11:1.

11-2 Longitudinal Stability and Control

These changes can be divided into two categories, the effect on static stability, and on dynamic stability.

I. Static

There are two prime effects in static stability and control, one due to movement of the a.c., and the other primarily due to change in geometry of supersonic airplanes.

A. An important change is due to the difference in the a.c. of surfaces in subsonic and in supersonic flow. For two dimensional wings the a.c. subsonically is approximately .25 chord while supersonically it is approximately .50 chord. A conventional airplane, that is stable in landing and take-off, i.e. in subsonic flight with a.c. at .25 MAC, will become much more stable in supersonic flight.

This can easily be seen from the expression for the contribution of the wing to static stability, as shown:

$$\frac{dC_m}{dC_L} = X_{c.g.} - X_{a.c.} \quad (11:1)$$

A shift in X_{ac} from .25 to .50 will cause dC_m/DC_L to become .25 larger negatively which is a significant increase in static longitudinal stability.

This change in a.c. position also changes the control problem since the moment coefficient about the c.g. can be written as

$$C_m = C_L (X_{c.g.} - X_{a.c.})$$

Evidently this variation in $x_{a.c.}$ of the wing at supersonic speed from the $x_{a.c.}$ subsonically will affect C_m and therefore the moments and forces involved. For conventional airplanes large control forces are usually required for trim, because of this shift in a.c. at supersonic speeds. A low trimmed lift-drag ratio therefore results. Ref. 11:5 shows that this effect may be relieved somewhat by introducing a constant positive C_m by using a cambered body, without increasing C_D .

B. The change in the downwash on the tail is another important factor caused by supersonic flight. This downwash is affected not only by supersonic flow but also by the lower aspect ratios required for efficient supersonic design. This low aspect ratio of the wing will cause a large increase in downwash for the same C_L thereby decreasing the effectiveness of the tail in contributing to static stability.

$$\left(\frac{dC_{m,c.g.}}{dC_L} \right)_{\text{tail}} = -\frac{a_t}{a_w} \frac{S_t}{S_w} \frac{\ell_t}{MAC} \eta_t \left(1 - \frac{d\epsilon}{d\alpha} \right) \quad (11:2)$$

It can be seen that a value of $d\epsilon/d\alpha$ greater than 1.0 results in a positive value of dC_m/dC_L , which indicates an unstable surface.

Ref. 11:2 presents some data on $d\epsilon/d\alpha$ for supersonic wings but more comprehensive data must be obtained from wind tunnel tests. Ref. 11:3 studies the effect of variation in the vertical position of the horizontal tail on static longitudinal stability and control and in fig. 10 presents the change in downwash angle with change in α for four different horizontal tail positions at $M = 2.01$, as shown in figure 11:1. From this data $d\epsilon/d\alpha$ may be calculated for various configurations.

C. Changes in geometry required for efficiency in supersonic flight often cause a pitch-up problem at high subsonic M . The factors and their effects are listed below:

1. High values of sweepback causes the tip to stall first at high C_L 's with the result that the c.p. moves forward thereby causing pitch-up.
2. High values of ϵ due to low wing A.R. reduces upload on tail, also contributing to pitch-up.
3. Long slender fuselages may cause large downwash at the tail due to fuselage vortices, thereby having similar effect as low wing A.R.

II. Dynamic

A. The effect of supersonic flow on longitudinal dynamic stability is negligible for the phugoid mode, but considerable on the

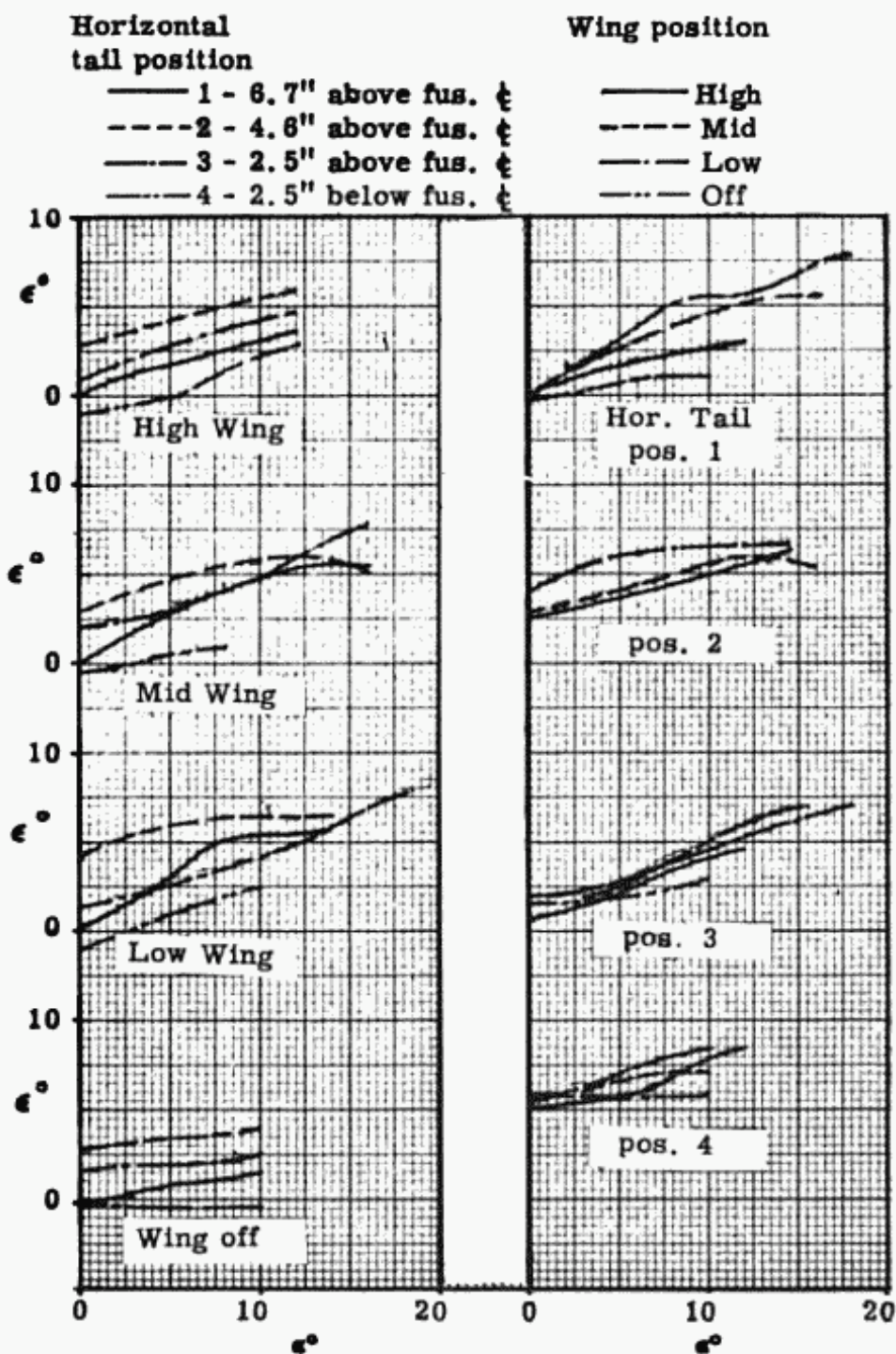


Fig. 11:1. Effect of tail position on variation of effective downwash angle with α . Distance from wing .25 MAC to tail .25 MAC = approx. 15 in. Wing M.A.C. = 6.9 in.

short period oscillation. For a first order approximation

$$\frac{t_{1/2}}{T} = K \sqrt{\frac{-dC_m/dC_L}{\sigma C_{L\alpha}}} \tag{11:3}$$

11:4 SUPERSONIC AND SUBSONIC AIRPLANE DESIGN

where T = period

$t_{1/2}$ = time to damp to 1/2 initial amplitude

K = is a constant dependent on the mean density, I_y , and on aerodynamic damping.

This relationship $t_{1/2}/T$ is actually dependent on the relative values of a and b obtained from $\lambda = a \pm ib$ and used in equs. 9:28 and 9:29.

It has been found by experience that this ratio of $t_{1/2}/T$ is important to the pilot as to handling qualities for ranges of T from approximately 1.0 to 10.0 seconds. For safety purposes it is felt that the value of this ratio should not be much greater than 1.0. The factors that tend to increase this ratio to much higher values for supersonic airplanes than for subsonic are:

1. K has approximately doubled due to the increases in mean density and in moment of inertia in pitch, and due to the reduction in $dC_L/d\delta$
2. As mentioned previously, $-dC_m/dC_L$ increases in supersonic flight due to the rearward shift in the a.c. in supersonic flight, while still requiring that dC_m/dC_L be negative in subsonic flight. The maximum $-dC_m/dC_L$ for the supersonic airplane might be four times the maximum value for a subsonic airplane.
3. The value of $dC_L/d\alpha$ might be cut in half in supersonic flight due to low values of A.R. and to the direct effects of M greater than 1.0.
4. Due to the higher cruising speed of supersonic airplanes, σ becomes much lower. For example, σ at 35,000 ft. = .3096, while at 60,000 ft. it is only .0941, or the ratio equals approximately 0.3.

It has been calculated that a supersonic fighter has a value of $t_{1/2}/T$ about ten times that of a World War II fighter such as the Spitfire, each at its top speed and operational ceiling.

B. Another problem that results from supersonic flight is the sluggishness in the change of lift in response to a change in control, or actually in response to change in α . This can actually be shown by the fundamental equation of lift rewritten to present the effect of certain parameters, i.e.;

$$\Delta L = 1/2 \rho \frac{W}{W/S} V^2 \frac{dC_L}{d\alpha} \Delta\alpha \quad (11:4)$$

Therefore the following changes in values associated with

supersonic flight all tend to reduce ΔL for a constant weight and fixed $\Delta\alpha$.

1. increased altitude, therefore reduced ρ
2. probable increased W/S
- and 3. decreased $dC_L/d\alpha$ due to low A.R.

However, offsetting these values that reduce ΔL is the effect of the increase in V which increases ΔL by V^2 . This effect is slightly reduced by the additional decrease in $dC_L/d\alpha$ resulting from M greater than unity.

The seriousness of this effect, called mushing, depends on the relative values of all the factors mentioned. In subsonic flight it was felt only near the stall where $dC_L/d\alpha$ was very low.

11-3 Lateral Stability and Control

I. Directional

In subsonic aircraft the required directional stability and control ability is due to asymmetric power considerations, and possibly by maximum β permissible in maneuver from structural strength viewpoint. The requirement of recovery from spin might also be a determining factor.

Present indications on supersonic aircraft are that the required degree of directional stability will be based either on supersonic lateral dynamic stability considerations, particularly the Dutch roll oscillation previously discussed, or on considerations of avoiding inertia coupling between the lateral and longitudinal degrees of freedom during roll. Suffice to say now that large values of subsonic directional stability will be required for supersonic aircraft to provide satisfactory dynamic characteristics at M greater than 1.0 and at high altitudes.

The directional stability is primarily made up of the small difference between the stability characteristics of the vertical tail and the instability of the fuselage. The instability of the fuselage on supersonic airplanes (particularly single engine jet fighters as compared to propeller driven single engine fighters) is increased due to the fact that there is a larger portion of the fuselage forward of the c.g. especially those with canard surfaces. This is not necessarily true of all supersonic airplanes. However, the fin effectiveness may be reduced with speed due to the elastic deformations of the thin sections, and the lower $dC_L/d\alpha$ of the low A.R. surface and at the high M . Since the destabilizing effect of the fuselage is practically independent of M and the fin does lose effectiveness with M above 1.0, the directional stability becomes critical at high M , as shown in Figure 11:2.

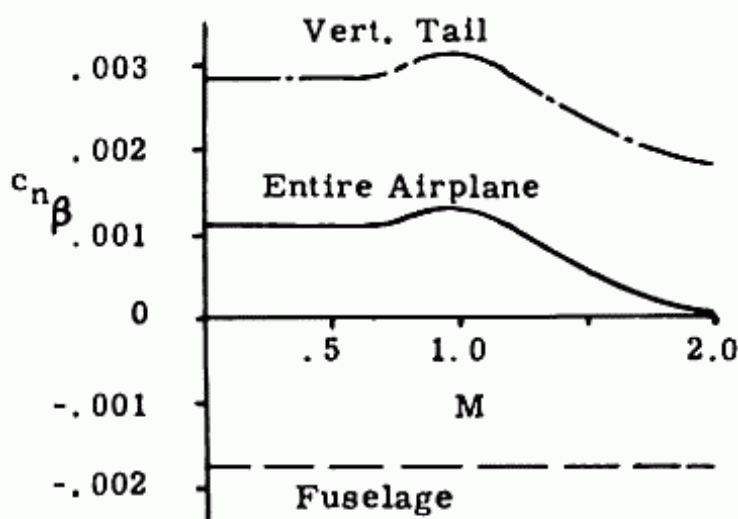


Fig. 11:2. Typical variation of directional stability with M .

The problem of directional stability is accentuated at high angles of attack, both subsonically and supersonically. It probably is aggravated supersonically by the effects of the low A.R. highly tapered wings, the long slender fuselage in front of the vertical tail, and wing-fuselage interference effects. Since directional control is more of a problem supersonically than subsonically even at low α 's, it is more severe at high α 's. For this reason practically all supersonic airplanes have ventral fins, i.e., fins below the fuselage, that will maintain their effectiveness at high α 's, and at the same time be less affected by aeroelasticity because of the smaller deflection for the same vertical tail area. Because of the problems connected with supersonic directional stability, and, too a lesser degree control, supersonic airplanes have larger vertical tail areas than their subsonic counterpart, and probably all movable fins.

Ref. 11:5 shows the effect of vertical wing position and vertical tail design on $C_{n\beta}$ for supersonic Mach numbers up to 2.6. As expected it shows the efficiency of the ventral fin, and the desirability of keeping the tail out of wing wake. Fig. 11:3 shows the effect of M on $C_{n\beta}$ of the vertical tail. Fig. 11:4 shows the effect of vertical position of the wing on $C_{n\beta}$ of the vertical tail at $M = 2$.

II. Aileron Control:

This problem of effective aileron control, which can produce aileron reversal due to aeroelasticity effects, is the same as in subsonic flight except that it is aggravated by the low A.R.'s associated with supersonic aircraft. This low A.R. makes the

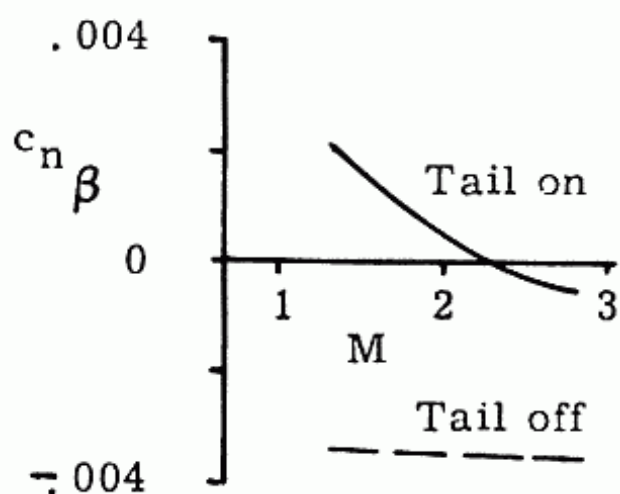


Fig. 11:3. Effect of M on directional stability at $\alpha = 0$.

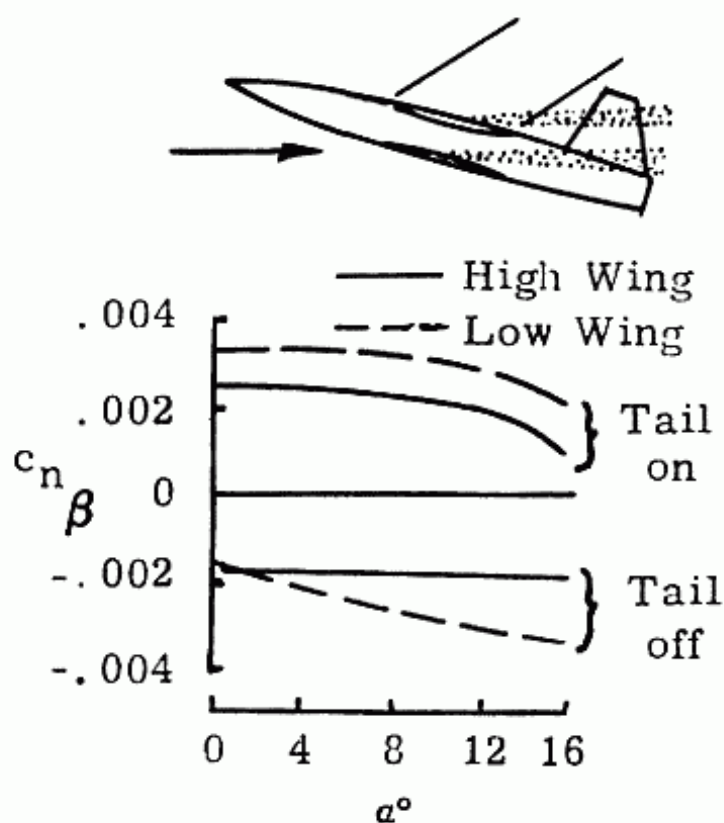


Fig. 11:4. Effect of Wing-Body on Directional Stab.; $M = 2$.

aileron less effective due to smaller arm, but tends to make the wing more rigid in torsion (which is partially offset by the required lower thickness ratios) and reduces the aerodynamic damping. Wing tip ailerons and spoilers have been used effectively. It would appear that leading edge ailerons would be most effective in supersonic flight.

There is also an unusual effect on aileron reversal that has been observed in some supersonic aircraft, that is strictly aerodynamic and not an aeroelastic one. For a certain combination of $C_{n\beta}/I_{zz}$ and $C_{l\beta}/I_{xx}$ the airplane's roll response to aileron deflection will be conventional. As in all rolling maneuvers caused by aileron deflection, an adverse yawing moment is produced that tends to yaw the airplane out of the turn. The resulting sideslip causes a rolling moment in the same direction that would result from a stable dihedral effect. This rolling moment opposes the rolling moment which the aileron is trying to produce, but is not large enough to overbalance it and normal rolling due to aileron deflection results. However, if the airplane was so designed that $dC_n/d\beta$ was lower (less directional stability) while still maintaining a high $dC_l/d\beta$ (high stable dihedral effect) the sideslip due to adverse yaw produces a high enough rolling moment to override the rolling moment due aileron deflection. The resulting motion is one in which normal roll due to aileron deflection is followed by a roll in the opposite direction as soon as sufficient sideslip develops. This is not a very serious effect since the pilot can correct the sideslip by rudder deflection if he is warned of the phenomena beforehand.

III. Lateral Dynamic Stability

The main motions in lateral or antisymmetrical motion are a roll subsidence mode, a spiral divergence and the Dutch Roll.

The roll subsidence mode is dependent on the ratio of the aerodynamic damping to the moment of inertia in roll, and at low altitudes is damped out very rapidly. However, at high altitudes, which is associated with supersonic flight, the damping is low and the time to damp will be longer.

A. Spiral Divergence

The spiral divergence mode is not a serious problem for supersonic aircraft. It depends on the relative values of $dC_n/d\beta$ (the direction stability criteria), $dC_l/d\beta$ (the dihedral effect), $dC_n/d\dot{\beta}$ (damping in yaw), and $dC_l/d\dot{\beta}$ (rolling caused by yawing velocity). A discussion of $dC_n/d\beta$ and $dC_l/d\beta$ has been presented previously. The $dC_n/d\dot{\beta}$ is due to the change in effective

angle of attack of the vertical tail due to the angular velocity, while $dC_L/d\beta$ is due to the greater effective velocity of the outer wing as compared to the inside wing, with the resultant greater lift on the outer wing.

Although the values of directional stability criteria and dihedral effects of subsonic airplanes may result in spiral instability at high values of C_L when $dC_L/d\beta$ is large, it does not present a problem of control to the pilot since the divergence is very low. Supersonic aircraft with straight wings will have similar characteristics as the subsonic airplane unless $dC_N/d\beta$ becomes low at high values of α and then the airplane may be spirally convergent at all values of C_L . Supersonic aircraft with highly swept wings, as a result of the large added dihedral effect of this sweep at high α , often requires negative dihedral angle. It therefore tends to be spirally unstable at low C_L , and stable at high C_L , because of the changing dihedral effects of sweepback.

B. Dutch Roll

Dutch roll, besides being affected by all the parameters already discussed, is influenced by dC_N/dp (the change in yawing moment coefficient with change in rolling velocity) and $dC_N/d\beta$, (the change in side force with change in sideslip angle. The value of dC_N/dp is made up of one part that results from the inclination of the lift vectors due to the variation in α from the up-going and down going wing, and the other part that results from side force on a vertical tail above the roll axis caused by a rolling velocity. The dC_N/dp resulting from inclination of vectors is proportional to the mean α and is smaller for supersonic low aspect ratio wings than for subsonic high aspect ratio wings because of its lower $dC_L/d\alpha$. Since the dC_N/dp due to vertical position of the vertical tail is independent of α and acts opposite to the inclination of the vectors effect, the net dC_N/dp may change sign as α is increased. Therefore since the lateral stability derivatives vary considerably with α and M it is necessary to investigate the Dutch roll for each configuration under various flight conditions, and general conclusions are difficult to present. Nevertheless, some generalizations can be made.

Very important in all of these considerations is the fact that supersonic flight is usually at high altitude and therefore the stability derivatives which depend on force and moment coefficients are quite low. Combined with this is the fact that at high altitude inertia effects are practically unaffected and therefore become comparatively more important. Therefore the periods of oscillations will generally be greater and the aerodynamic damping

lower. Since the lateral parameters vary with α , it is necessary to investigate Dutch roll for conditions of high C_L and of low C_L .

Fig. 11:5, showing the spiral divergence and Dutch Roll stability boundaries for a particular airplane at two values of C_L , presents interesting data. Note that $-C_{l\beta}$ and $+C_{n\beta}$ are the signs for positive dihedral effect and positive directional stability.

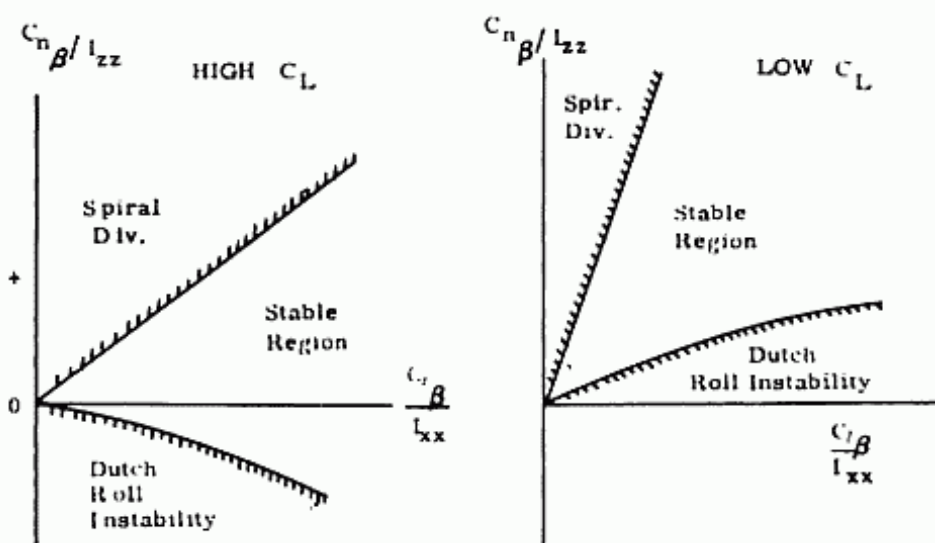


Fig. 11:5. Typical Lateral Stability Boundaries.

An airplane with a very low value of directional stability will tend to have Dutch Roll instability at any value of positive dihedral effect for low C_L . As I_{xx} gets lower (as those of supersonic aircraft tend to do, that is $-C_{l\beta}/I_{xx}$ becomes larger) a larger value of $C_{n\beta}/I_{zz}$ is required for Dutch Roll stability. However, the trend of $C_{n\beta}$ is to become lower for supersonic aircraft (with I_{zz} changing relatively little), thereby making it difficult to obtain Dutch Roll stability except by increased vertical tail area or possibly by some artificial means.

A similar relationship between $C_{n\beta}/I_{zz}$ and $C_{l\beta}/I_{xx}$ exists for obtaining spiral stability at high C_L . There is no practical interest in the characteristics of airplanes with negative values of $dC_n/d\beta$ since this denotes directional instability, and all airplanes require directional stability.

The problems are more severe for highly swept wing aircraft since the dihedral effect increases with increase in α , and at the same time $dC_n/d\beta$ is lower as explained previously.

Another important point of interest is that although large values of $dC_n/d\beta$ (directional stability) are normally desirable, the correspondingly large value of dihedral effect required for spiral stability can become undesirable because of sensitivity in roll to rudder deflections. In addition there are objectionable effects in fast rolling maneuvers, in obtaining accurate coordination of rudder and aileron, and lastly in flight with asymmetric power. It is therefore often more desirable to accept a small degree of spiral instability with the lower value of $dC_l/d\beta$.

IV. Roll Instability

A. Physical Aspects of Cross Coupling - Inertial and Aerodynamic

Cross coupling effects between roll and either pitch or yaw do exist in subsonic flight, particularly near stall where $dC_L/d\alpha$ is low. However in supersonic flight where $dC_L/d\alpha$ is usually low because of low aspect ratio and high M , and where altitude is high, this cross-coupling problem is more severe. In investigating the problem we will consider first the condition when the airplane is rolling about the free stream axis, and second when rolling about the airplane principal longitudinal axis.

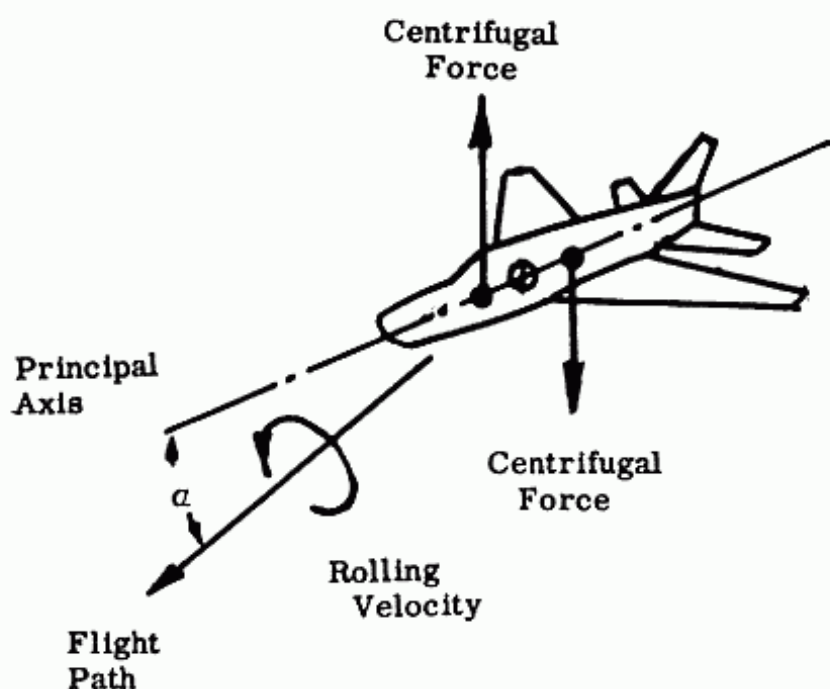


Fig. 11:6. Inertial Coupling Forces Acting on an Airplane Rolling about its Flight Path.

If the airplane is rolling about the flight path as shown in Fig. 11:6, and the airplane is considered divided into two masses, one

11:12 SUPERSONIC AND SUBSONIC AIRPLANE DESIGN

fore of the airplane c.g. and the other aft, then forces F will be set up at the c.g.'s of these fore and aft masses. The centrifugal forces, F , are destabilizing, i.e. increase α when airplane is at a positive α , and decrease α when at a negative α , and tend to rotate the airplane to an α perpendicular to the flight path. The pitching moment caused by these centrifugal forces are proportional to the product of p , the rolling velocity, and α , and is resisted by the inherent longitudinal stability of the aircraft. If the critical rolling velocity (i.e. the rolling velocity at which the inertia moment is equal to the restoring moment) is exceeded, the airplane will perform a whirling divergence, that is, align itself normal to the flight path.

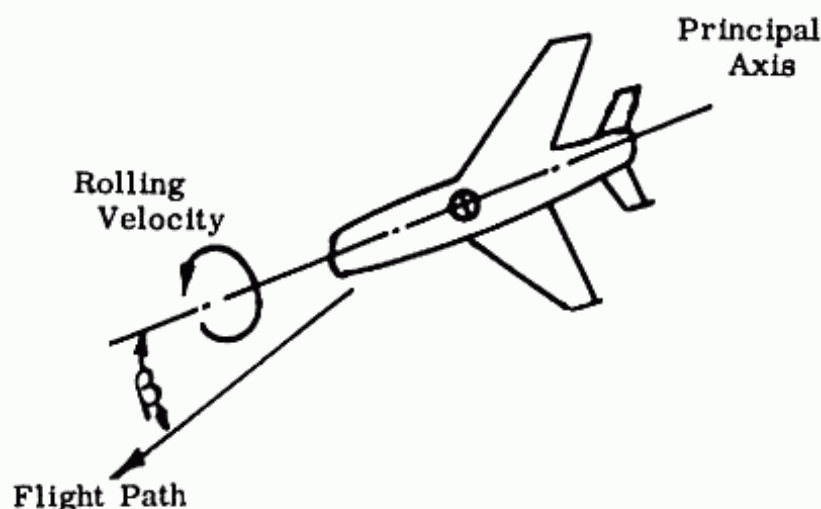


Fig. 11:7. Reversal of α & β on an Airplane Rolled 90° about its Principal Axis.

If the airplane is rolling about the airplane principal longitudinal axis as shown in fig. 11:7 there is no inertia coupling. However as the airplane rotates, α becomes β and then α again, in fact at 90° and 270° roll α becomes entirely β . Due to the longitudinal and directional stability of the airplane these changes in α and β set up pitching and yawing moments which try to return the aircraft to zero sideslip and the equilibrium α . These new moments rotate the airplane so that the rolling is no longer about the principal axis, but some axis between this principal axis and the freestream velocity, thereby again introducing some inertia coupling effects.

As shown above an airplane will usually roll about some axis near the principal axis, and the aerodynamic stability effects of the airplane will be greater than the destabilizing inertia affects.

However, for some airplanes the rolling may become critical for those conditions where the inertia forces are large compared to the aerodynamic restoring forces. The aerodynamic forces are low when the air density is low, i.e. at high altitude, and when directional and longitudinal stability are low, i.e. in supersonic flight and $dC_L/d\alpha$ is small. The inertia forces are high when α is high (the higher the altitude the higher is α for the same speed and wing loading) and when p is high. Therefore this condition is not critical for transports where maximum p is low, but for fighters and the like, in which large values of maximum p are important.

Another factor that is important in the rolling stability is dihedral effect. This is so because rolling velocity, p , causes an inclination of the relative velocities on the inside and outside wings, which results in a yawing moment. Since dihedral effect is the rolling moment caused by sideslip, a rolling velocity due to this dihedral effect opposite to the original impressed p results in the initial motion. This further complicates the problem.

B. Analysis

The preceding physical picture presented may be analyzed (see ref. 11:1) so that serious instability in rolling flight can be avoided. If damping is neglected and it is assumed that the aircraft performs small oscillations about the pitch axis, then the pitch and yaw frequencies of the non-rolling aircraft are:

$$\omega_{\alpha} = \frac{1}{2\pi} \sqrt{\frac{(-dC_m/dC_L)(dC_L/d\alpha) q S c}{I_{yy}}} \quad (11:5)$$

$$\omega_{\beta} = \frac{1}{2\pi} \sqrt{\frac{(dC_n/d\beta) q S b}{I_{zz}}} \quad (11:6)$$

where ω_{α} = undamped pitch frequency in cycles/sec

ω_{β} = undamped yaw frequency in cycles/sec.

It should be noted that the higher the static stability the higher the frequency, and as would be expected, the higher the inertias the lower are the frequencies. And in addition if the rolling velocity is low and the static stability moments are high, then these moments will be able to nearly maintain the original values of α and β and the aircraft will rotate about an axis close to the flight-path. Conversely if the rolling velocity is high and the static moments are low, these static moments will not have time to correct

the cyclic variations in α and β and the aircraft will rotate closely about the principal longitudinal axis of the aircraft.

The time required to correct changes in α and β is a function of the natural undamped frequencies of the non-rolling airplane shown in equs. 11:5 and 11:6. It should be noted that when one of the frequencies, in either pitch or roll, of the non-rolling aircraft is equal to the rolling frequency the aircraft becomes neutrally stable in that mode. This can be explained on the basis that the centrifugal forces of the rolling airplane which tend to swing the fuselage out of line with the flight path is exactly offset by the restoring forces acting on the non-rolling aircraft during its oscillations. This means that the static stability is reduced to zero by the moments set up by inertia forces due to the rolling velocity.

It can also be shown that when one frequency of the non-rolling aircraft is less than the steady rolling frequency and the other is greater, then the aircraft becomes statically unstable in one mode and performs a straight divergence. In this case the moments set up by the inertia forces due to rolling velocity exceed the moments set up by the static stability (i.e. instability exists) and divergence results.

One important factor has been omitted in this discussion as no mention has been made of the effect of the mass distributed along the wings. The centrifugal forces acting on these masses when the aircraft rotates about the flight path will set up restoring inertia moments in yaw, with no moments in pitch. The critical roll frequency at which effective static stability becomes zero is increased by $I_{zz} (I_{yy} - I_{xx})$.

The conditions necessary to avoid serious instability in rolling flight are:

a) Both ω_α and ω_β ($I_{zz}/I_{yy} - I_{xx}$) should be as high as possible and preferably higher than ω_p , (where $\omega_p = p/2\pi$), i.e.,

$$\frac{\omega_\alpha}{\omega_p} > 1$$

$$\text{and } \frac{\omega_{\beta_0}}{\omega_p} > 1 \quad (11:7)$$

where

$$\omega_{\beta_0} = \omega_\beta \sqrt{I_{zz}/(I_{yy} - I_{xx})} \quad (11:8)$$

b) If ω_p must exceed ω_α or ω_{β_0} then ω_α and ω_{β_0} should be as close as possible, so the possible region of instability is a minimum; i.e.

$$\omega_\alpha \approx \omega_{\beta_0} \quad (11:9)$$

or

$$\frac{-dC_m}{dC_L} = \frac{dC_n}{d\beta} \frac{1}{1 - I_{xx}/I_{yy}} \left(\frac{b/c}{dC_L/d\alpha} \right) \quad (11:10)$$

c) Design Trends

It is useful to write equations 11:7 as

$$\frac{\omega_\alpha}{\omega_p} = \left(\frac{pb}{2v} \right) \left(\frac{k'}{b/2} \right) \sqrt{\frac{(-dC_m/dC_L)(dC_L/d\alpha)\sigma c}{W/S}} > 1$$

$$\frac{\omega_{\beta_0}}{\omega_p} = \left(\frac{pb}{2v} \right) \left(\frac{k'}{b/2} \right) \sqrt{\frac{(dC_n/d\beta)\sigma b}{(W/S)(1 - I_{xx}/I_{yy})}} > 1$$

where k' is the radius of gyration in pitch

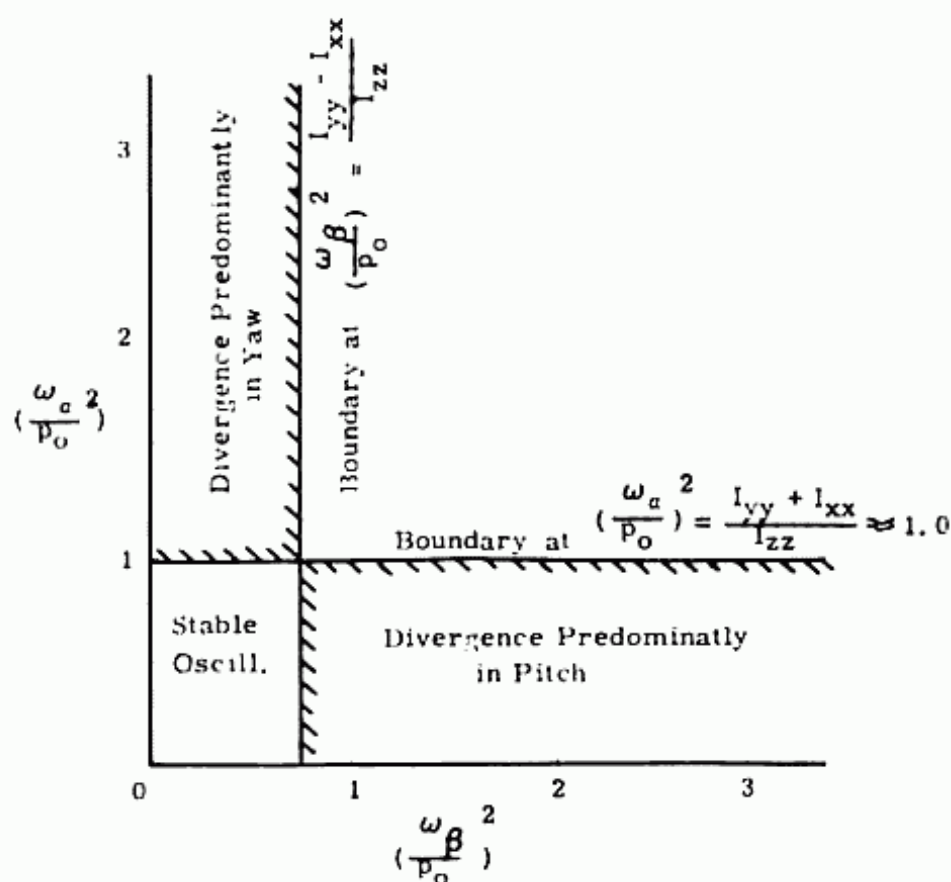
There are four principal characteristics of supersonic aircraft which tend to make ω_α/ω_p and $\omega_{\beta_0}/\omega_p$ each less than 1.0.

- 1) increased k'/b due to long slender fully loaded fuselages, and very much lower values of b due to higher values of W/S and lower aspect ratios.
- 2) increased W/S
- 3) increased values of $(1 - I_{xx}/I_{yy})$; = .25 for the Spitfire and .90 for the F104
- 4) decreased σ due to higher operational altitudes.

It is difficult at this point to correct this trend toward roll instability for high values of p , and particularly at high α . The most obvious answer is to increase the degree of static longitudinal stability and static directional stability. However the $-dC_m/dC_L$ of supersonic flight is already quite high due to the aft a.c. movement from sub to supersonic flight, and the $dC_n/d\beta$ decreases with increasing M . For fast rolling airplanes the best solution might be some form of auto stabilization.

Another look at this problem is taken by W. J. G. Pinsker (ref. 11:4) which is best presented by figures 11:8, 11:9 and 11:10.

Fig. 11:8 shows the stability boundaries as a function of $(\omega_\alpha/p_0)^2$ versus $(\omega_{\beta_0}/p_0)^2$, assuming no damping in pitch and yaw.



ω_α = Frequency of Uncoupled Pitching Oscill.

ω_β = Frequency of Uncoupled Lateral Oscill.

p_0 = Steady Rate of Roll in Rad./sec

Fig. 11:8. Stability Boundaries of a Rolling Aircraft assuming zero damping in pitch and yaw.

Fig. 11:9 reproduces Fig. 11:8 with the stability characteristics of three airplane with different values of $\omega_\alpha/\omega_\beta$. Fig. 11:10 shows the effects of damping in pitch and yaw. This effect makes it easier to design an airplane that will be stable for all rolling velocities at least for a small range of M . This condition can only be true for a limited range of Mach numbers since the stability derivatives change with M .

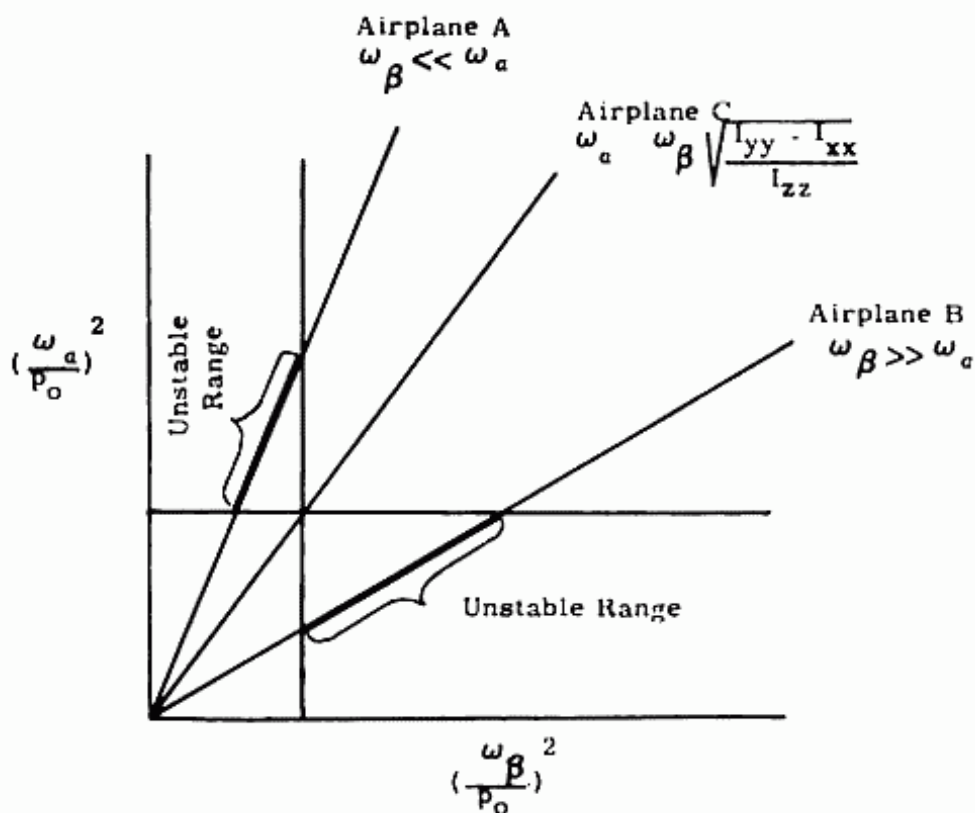


Fig. 11:9. Effect of Inertia Cross Coupling on Stability of a Rolling Airplane.

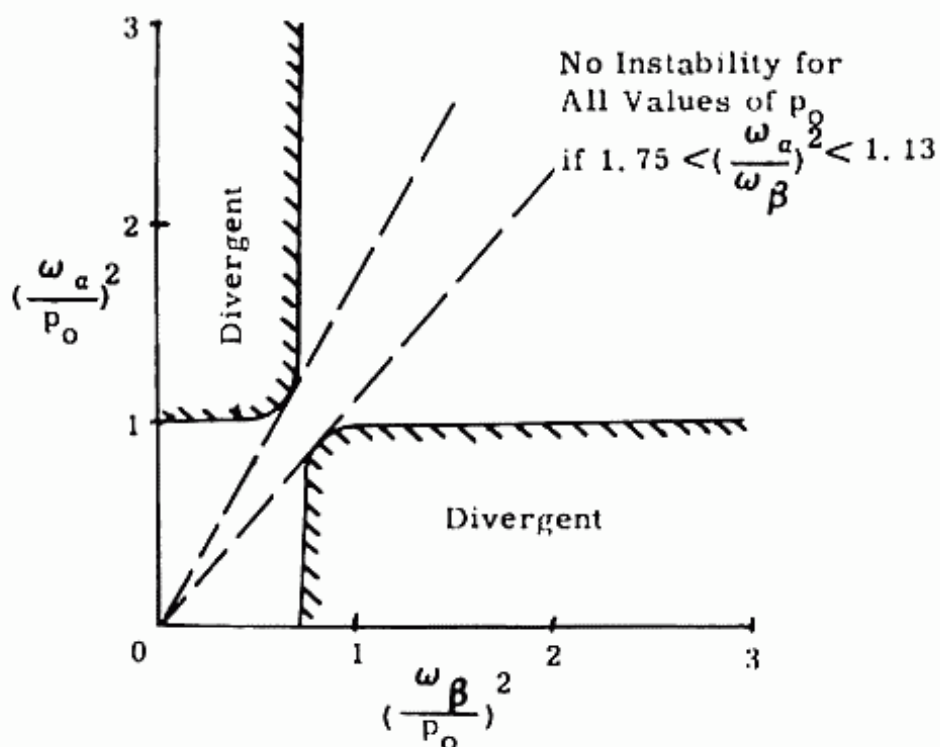


Fig. 11:10. Effect of Damping in Pitch and Yaw on the Divergent Boundaries.

11:18 SUPERSONIC AND SUBSONIC AIRPLANE DESIGN

REFERENCES

- 11:1 O. E. Michaelsen "Stability and Control Problems Associated with Supersonic Aircraft", Nat'l Research Council of Canada, Div. of Mech. Engr., Jan. 1957.
- 11:2 E. A. Bonney "Engineering Supersonic Aerodynamics" by McGraw Hill
- 11:3 M. L. Spearman and Driver, RML55L06 "Investigation of Aerodynamic Characteristics in Pitch and Sideslip of a 45° Swept-back Wing Airplane Model with Various Vertical Locations of Wing and Horizontal Tail-Static Longitudinal Stability and Control, $M = 2.01$ " February 1956, declassified February 1959.
- 11:4 W. J. G. Pinsker, AGARD Report No. 107 "Critical Flight Conditions and Loads Resulting from Inertia Cross-Coupling and Aerodynamic Stability Deficiencies", May 1957.
- 11:5 M. L. Spearman and A. Henderson, Jr., RML55L15a "Some Effects of Aircraft Configuration on Static Longitudinal and Directional Stability Characteristics of Supersonic M below 3. Feb. 1956, declassified Feb. 1959.

PART III

LOADS

Chapter XII

LOADS

12-1 Introduction

Structural design of the airplane may be divided into two parts. The first, loads on the airplane, takes into account both aerodynamic and structural considerations and is a compromise between safety and statistics. The second, the design of the airplane components to safely withstand the airloads, is primarily structural and is covered in texts on "Stress Analysis". Although the primary function of the structural engineer is to design the structure to be strong enough to safely withstand the loads, a very important aspect of his work is to design it for minimum weight.

12-2 General

The loads that the airplane must withstand will be considered in this text. For commercial transports they are specified by the Civil Aeronautics Regulations. In setting up these regulations the conditions that must be met are based upon past experience. Although they must provide a maximum of safety to the passengers, it would be completely impractical to design for every possible condition. If an attempt was made to include in the design every combination of circumstances, the airplanes would be so cumbersome and uneconomical that there would be no place for them in competition with other modes of travel.

A few simple cases are presented. The regulations require that the load factor used in designing the landing gear be based upon a certain height of free drop. This height is the maximum that could be normally expected. No matter how high this figure is set, it is possible that a pilot might let it drop further. In determining the gust load factor to be used in designing the wing, a specific gust velocity is set for each of 3 different speeds. This gust velocity is the maximum that the airplane would be expected to meet under a vast majority of cases. It is not the maximum that has ever occurred at any place, as it is felt that this maximum occurs so rarely that it is not likely to ever be encountered under the conditions specified. The loads required by the Civil Air Regulations will be presented briefly. They are divided into two categories - airloads and ground loads.

There are three important aspects of airloads: total loads,

12:2 SUPERSONIC AND SUBSONIC AIRPLANE DESIGN

chordwise distribution, and spanwise distribution. These topics will be discussed in greater detail later, but it is important to note now that the distributions are quite significant as many parts of an airplane are critical at total loads below the maximum because of a particular chordwise or spanwise distribution.

12-3 Load Factors

Before progressing with specific loads on the airplane it is necessary to first present some general data on load factors.

Load Factors, General

An airplane in level constant speed flight is in equilibrium since the lift is equal to the weight, the drag is equal to the thrust, and the moment about the airplane center of gravity is equal to zero. In Figures 12:1a and 12:1b only vertical loads are shown as only load factors in the vertical direction are being considered here.

Since the prime considerations are with constant speed conditions and loads in the vertical direction, thrust and drag loads will hereafter be neglected. If due to an external gust, or a movement of the control surface by the pilot, the lift of the airplane is increased from L to nL , equilibrium no longer exists and an acceleration in the direction of the nL force will result. It is convenient to apply inertia forces to the airplane in accelerated motion, so that it can be treated as a static equilibrium condition.

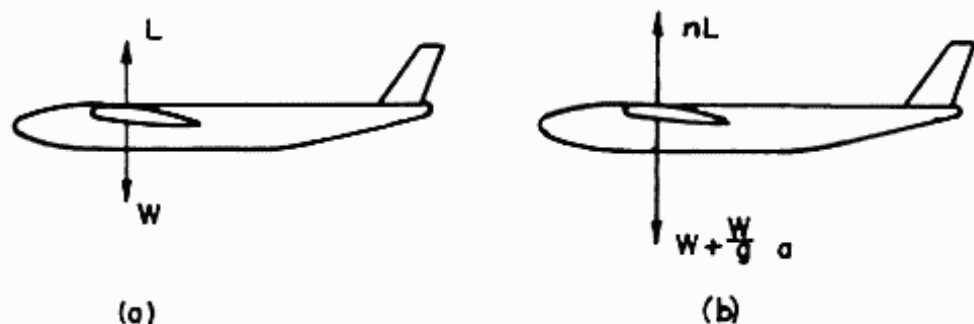


Fig. 12:1. Vertical forces on airplane in accelerated and unaccelerated flight.

This can be accomplished by applying d'Alembert's principle which states that every state of motion may be considered, at any instant, as a state of equilibrium, provided appropriate inertia forces are introduced. Therefore, using Newton's first law

$$F = ma \quad (12:1)$$

$$nL - W = \frac{Wa}{g} \quad (\text{See Figure 12:1b}) \quad (12:2)$$

where g = acceleration of gravity

Since $L = W$

$$n = 1 + \frac{a}{g} = 1 + \Delta n \quad (12:3)$$

The term n is the limit load factor, and a/g , called the load factor increment, is denoted by Δn . The limit load factor is the maximum load factor that is encountered in any actual condition in flight or landing. The design load factor is the limit load factor times a factor of safety equal to 1.5. For special cases such as fittings and castings, there may be additional factors of safety. In all load specifications the load factor referred to is the limit load factor.

Load factors greater than one are developed due to a maneuver of the airplane, or due to an external gust. The maneuver and gust V - n diagrams (sometimes called V - g diagrams) are shown in figures 12:2 and 12:3. As quoted in the CAM 4b, "The strength requirements shall be met at all combinations of air speed and load factor on and within the boundaries of the V - n diagrams of figures 12:2 and 12:3 which represent the maneuvering and gust envelopes. These envelopes shall also be used in determining the airplane structural operating limitations."

Load Factors, Maneuver

The following is quoted from CAM 4b:

"(a) Maneuvering load factors. (See fig. 12:2). The airplane shall be assumed to be subjected to symmetrical maneuvers resulting in the limit load factors prescribed in subparagraphs (1) and (2) of this paragraph, except where limited by maximum (static) lift coefficients. Pitching velocities appropriate to the corresponding pull-up and steady turn maneuvers shall be taken into account. Lower values of maneuvering load factor shall be acceptable only if it is shown that the airplane embodies features of design which make it impossible to exceed such values in flight.

(1) The positive maneuvering load factor n for any flight speed up to V_D shall be selected by the applicant, except that it shall not be less than 2.5.

(2) The negative maneuvering load factor shall have a minimum value of -1.0 at all speeds up to V_C , and it shall vary linearly with speed from the value at V_C to zero at V_D ."

It should be noted that CAM 4b, as all other Civil Air

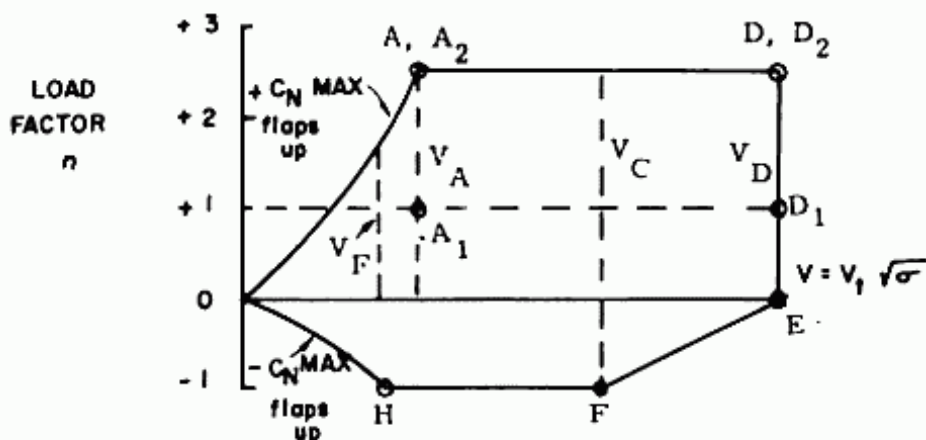


Fig. 12:2. Maneuvering load factor envelope.

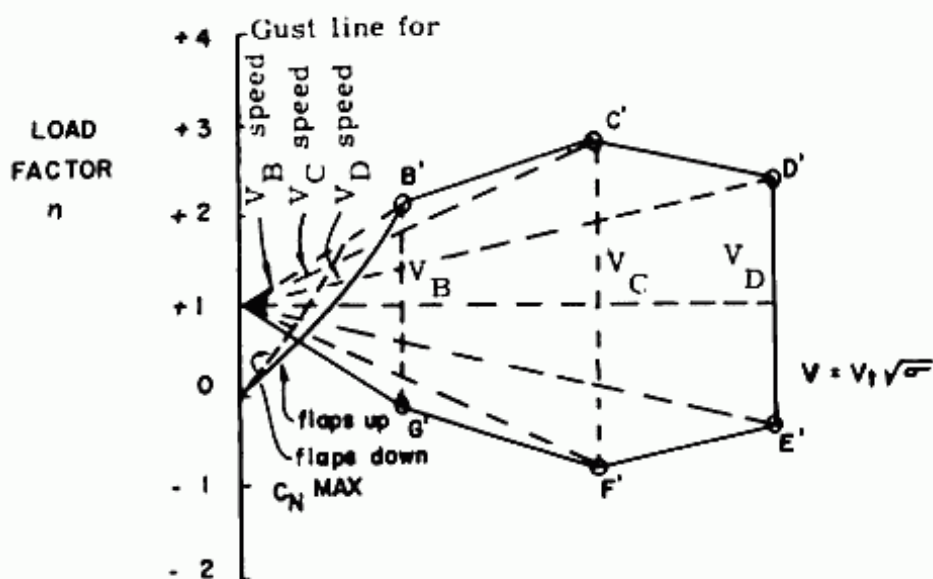


Fig. 12:3. Gust load factor envelope.

Regulations at this time, do not consider supersonic flight. However, all that can be done now is to assume that these same regulations hold, unless it can be shown that for the sake of safety and efficiency that they should be modified.

Gust Load Factor - Straight Wing

The following is quoted from CAM 4b: 211b

*Gust Load Factors: The airplane shall be assumed to be subjected to symmetrical vertical gusts while in level flight. The resulting limit load factors shall correspond with the conditions prescribed in subparagraphs (1) through (5) of this paragraph. The shape of the gust shall be assumed to be:

$$U = \frac{U_{de}}{2} \left(1 - \cos \frac{2\pi s}{25 C} \right) \quad (12:4)$$

where:

s = distance penetrated into gust (ft.);

C = mean geometric chord of wing (ft.); = S/b

U_{de} = derived gust velocity referred to in subparagraphs (1) through (3) of this paragraph (fps).

(1) Positive (up) and negative (down) rough air gusts of 66 fps at the speed V_B shall be considered at altitudes between sea level and 20,000 feet. At altitudes above 20,000 feet, it shall be acceptable to reduce the gust velocity linearly from 66 fps at 20,000 feet to 38 fps at 50,000 feet.

(2) Positive and negative gusts of 50 fps at the speed V_C shall be considered at altitudes between sea level and 20,000 feet. At altitudes above 20,000 feet, it shall be acceptable to reduce the gust velocity linearly from 50 fps at 20,000 feet to 25 fps at 50,000 feet.

(3) Positive and negative gusts of 25 fps at the speed V_D shall be considered at altitudes between sea level and 20,000 feet. At altitudes above 20,000 feet, it shall be acceptable to reduce the gust velocity linearly from 25 fps at 20,000 feet to 12.5 fps at 50,000 feet.

(4) Gust load factors shall be assumed to vary linearly between the specified conditions B' through G', as shown on the gust envelope of Figure 12:3.

(5) In the absence of a more rational analysis, the gust load factors shall be computed in accordance with the following formula:

$$n = 1 + \frac{K_g U_{de} V a}{498 (W/S)} \quad (12:5)$$

where:

$$K_g = \frac{.88 \mu_g}{5.3 \tau \mu_g} = \text{gust alleviation factor:} \quad (12:6)$$

$$\mu_g = \frac{2(W/S)}{\rho C a g} = \text{airplane mass ratio} \quad (12:7)$$

U_{de} = derived gust velocities referred to in subparagraphs (1) through (3) of this paragraph (fps);

ρ = density of air (slugs/cu.ft.);

W/S = wing loading (psf);

12:6 SUPERSONIC AND SUBSONIC AIRPLANE DESIGN

C = mean geometric chord (ft.);

g = acceleration due to gravity (ft./sec.²);

V = airplane equivalent speed (knots);

a = slope of the airplane normal force coefficient curve, C_{NA} , per radian, if the gust loads are applied to the wings and horizontal tail surfaces simultaneously by a rational method. It shall be acceptable to use the wing lift curve slope C_L per radian when the gust load is applied to the wings only and the horizontal tail gust loads are treated as a separate condition."

The term U_{de} is called the derived velocities as it was derived from the gust load factors recorded in many aircraft flights. (ref. 12-5) The velocity was calculated to result in these recorded load factors assuming the gust intensity profile was of the shape

$$U = \frac{U_{de}}{2} \left(1 - \cos \frac{2\pi s}{25C} \right) \quad (12:8)$$

as seen in fig. 12:4. For most design purposes the load factor

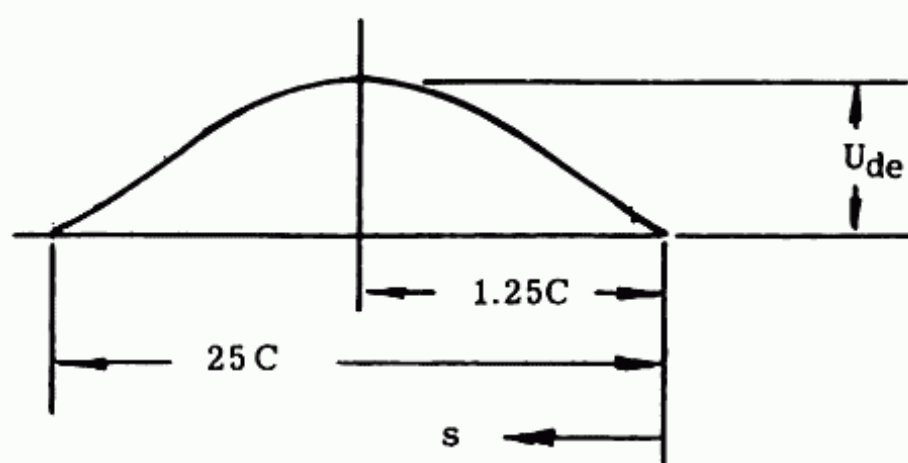


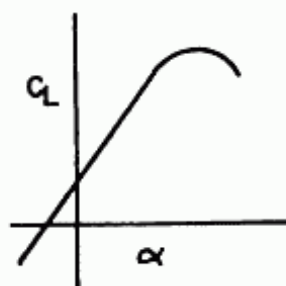
Fig. 12:4. Gust velocity intensity profile.

increment Δn , may be determined by the formula suggested in CAM 4b, i.e.

$$\Delta n = \frac{K_g U_{de} V a}{498 (W/S)} \quad (12:9)$$

This formula may be simply explained by the following:

Figure 12:5 shows a typical C_L vs angle of attack curve. An airplane flying at C_{L_1} at α_1 is struck by a gust so that it is

Fig. 12:5. Typical C_L vs. α curve.

changed to C_{L_2} at α_2 , (as shown in figure 12:6). Then, for small angles, the angle in radians equals the tangent of the angle.

$$\Delta \alpha = \tan \Delta \alpha = \frac{K_g U_{de}}{V} \quad (\text{from fig. 12:6b}) \quad (12:10)$$

$$\Delta C_L = a \Delta \alpha = \frac{aK_g U_{de}}{V} \quad (\text{from fig. 12:6a})$$

$$L = 1/2 \rho_0 S V_e^2 C_L \quad (12:11)$$

$$nL = 1/2 \rho_0 S V_e^2 (C_L + \Delta C_L) \quad (12:12)$$

Dividing Equation 12:12 by Equation 12:11,

$$n = \frac{C_L + \Delta C_L}{C_L} \quad (12:13)$$

$$1 + \Delta n = 1 + \frac{\Delta C_L}{C_L} \quad (12:14)$$

$$\begin{aligned} \Delta n &= \frac{\Delta C_L}{C_L} = \frac{K_g U_{de} a/V_e}{2W/\rho_0 V_e^2 S} \\ &= \frac{K_g U_{de} V_e a}{498 (W/S)} ; V \text{ in knots} \end{aligned} \quad (12:15)$$

The gust load factor is very important in high speed jet transports as it very often is higher than the maneuver load factor. This is especially true of airplanes with low landing field specifications since the corresponding low wing loading required results in a high gust load factor. It is interesting to note that the highest possible wing loading to meet the landing field requirement is best both aerodynamically and structurally.

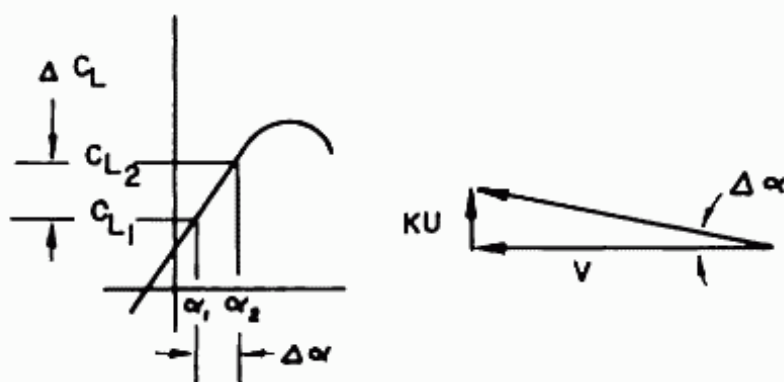


Fig. 12:6. Effect of gust on C_L .

Some additional regulations as to the gust velocity to be used at altitudes above 50,000 ft. will be required for the supersonic transports that will cruise above this altitude. The value of U_{de} will, of course, depend on the disturbances that occur at these high altitudes and these values will determine whether or not gust load factor will be critical for these conditions.

Examination of equ. 12:9 indicates that there is a very strong possibility that gust condition will be critical. This is so primarily due to the great increase in V . Other factors which influence Δn are: The decrease in a at supersonic speeds due to the very low values of A.R. used, the probable increase in K_g and the probable increase in W/S . See figure 12:7 for the values of K_g as a function of W/S for various values of σCa .

Gust Load Factor - Sweptback Wing

One factor that tends to reduce the gust load factor on sweptback wings is the wing flexibility. A wing in flight tends to bend along its elastic axis. It has been stated that the forces on the wing are a function of the velocity perpendicular to the quarter chord and that it is unaffected by the spanwise flow. This spanwise flow is the flow that is parallel to the elastic axis. However, in a flexible swept wing this spanwise flow introduces a velocity V_1 , perpendicular to the plane of the wing chords which modifies the angle of attack of the section by $\Delta\alpha_e$. Figure 12:8 shows this variation. The plan form shows the free stream velocity broken into components perpendicular to the quarter chord, and parallel to the elastic axis. The front view shows the spanwise flow, V_{span} , broken into two components: V_0 , tangent to the deflected elastic axis, and V_1 perpendicular to V_0 . The side view shows the V perpendicular to the quarter chord in plan view; V_1 perpendicular to the chord in side view, and the resultant V of these mutually perpendicular velocities. This resultant velocity

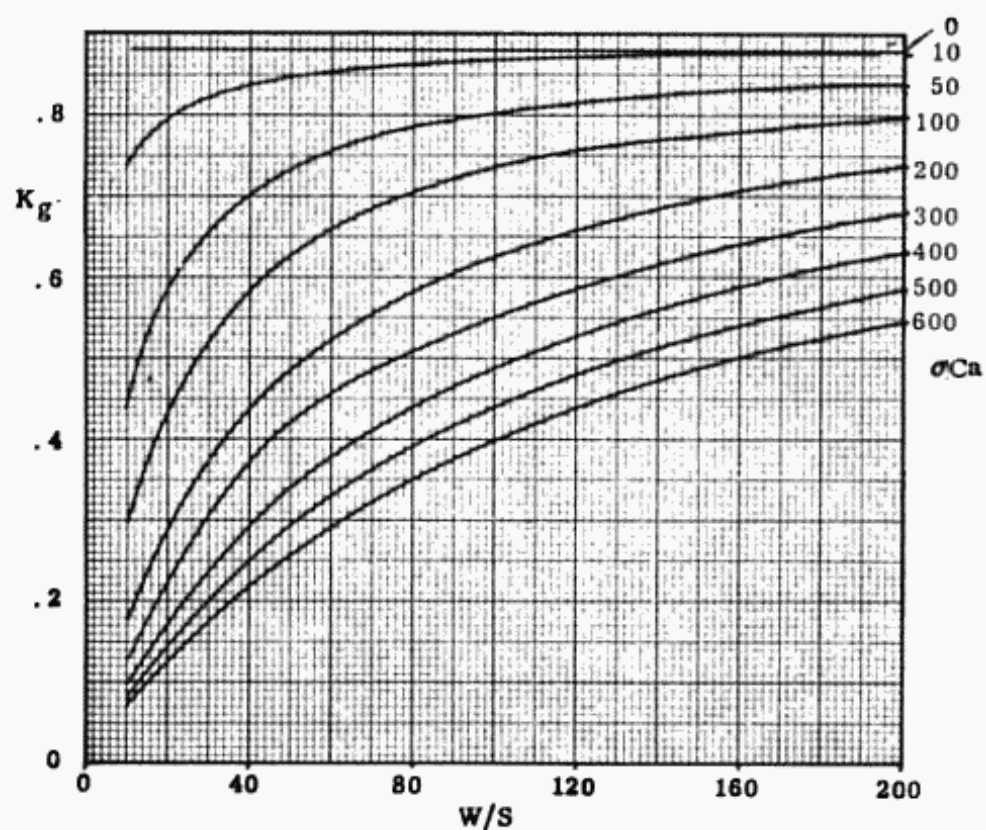


Fig. 12:7. K_g vs. W/S .

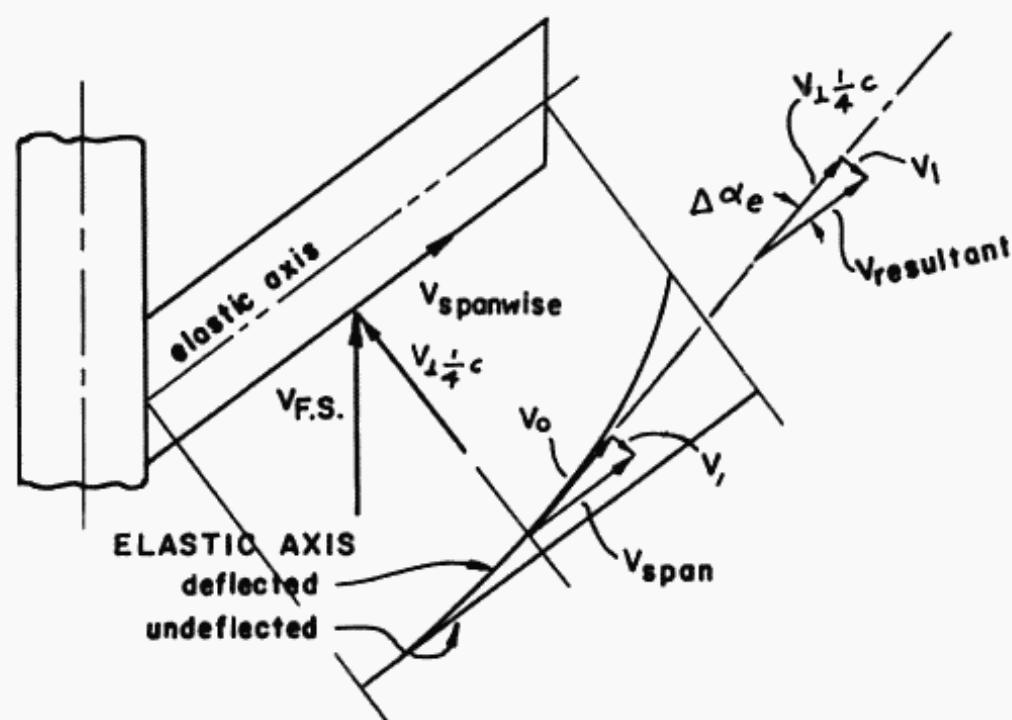


Fig. 12:8. Effect of flexibility of sweptback wing on spanwise load distribution.

12:10 SUPERSONIC AND SUBSONIC AIRPLANE DESIGN

on the deflected wing is at an angle of attack lower than the angle of attack of the undeflected wing, while its value is insignificantly larger.

This reduction in angle of attack decreases the C_L and therefore the effect of the gust load factor. This reduction in gust load factor can be determined after the wing is designed but requires a lengthy and rigorous calculation. However, for preliminary design purposes a reduction in load factor of approximately 15% is recommended for wings with 35° sweepback, and aspect ratio of between 6 and 8. For supersonic aircraft with very low aspect ratio delta wings, the reduction due to flexibility will probably be less.

12-4 Airloads - Wing and Tail, General

The $V-n$ maneuver and gust envelopes, figs. 12:2 and 12:3 designate the flight load factors that shall be assumed to act normal to the longitudinal axes of the airplane, shall be equal in magnitude, and shall be opposite in direction to the airplane inertia load factor at the center of gravity. It should be noted that if the flight path and the longitudinal axis of the airplane do coincide, as they often do in transport airplanes, then the flight load factors can be applied directly to the lift of the airplane as well as to the force normal to the longitudinal axis.

Gust Loads, Wing and Tail

The gust $V-n$ diagram (fig. 12:3) should be constructed using equation 12:5 to determine the Δn 's required. A rational method of obtaining the gust loads on the wing and on the tail is to apply the gust n to the level flight load on the wing and to the balancing level flight load on the tail.

The above $V-n$ diagram is for the wing. The gust load factors cannot be calculated for the tail until the balancing load on the tail is determined, thereby obtaining the W/S of the tail.

Maneuver Loads, Wing and Tail

Assuming that the longitudinal axis is parallel to the flight path, or that the angle between them is small enough that the cosine can be assumed equal to one, it can then be said that the total lift on the airplane is equal to nW , where n is obtained from fig. 12:2 the maneuver envelope,

$$nW = L_w + L_t$$

$$L_w = \text{Lift on wing}$$

$$L_t = \text{Lift on tail}$$

Therefore the load on the wing is dependent on the tail load, and since the tail load can be calculated from the specifications of CAM 4b, it will be obtained first.

12-5 Airloads - Horizontal Tail, Maneuver - General

A. CAM Requirements

The following is taken from CAM 4b, para. 4b.213

*Symmetrical flight conditions

(a) Procedure of analysis.

In the analysis of symmetrical flight conditions at least those specified in paragraphs (b), (c), and (d) of this section shall be considered. The following procedure of analysis shall be applicable:

(1) A sufficient number of points on the maneuvering and gust envelopes shall be investigated to insure that the maximum load for each part of the airplane structure is obtained. It shall be acceptable to use a conservative combined envelope for this purpose.

(2) All significant forces acting on the airplane shall be placed in equilibrium in a rational or a conservative manner. The linear inertia forces shall be considered in equilibrium with wing and horizontal tail surface loads, while the angular (pitching) inertia forces shall be considered in equilibrium with wing and fuselage aerodynamic moments and horizontal tail surface loads.

(3) Where sudden displacement of a control is specified, the assumed rate of displacement need not exceed that which actually could be applied by the pilot.

(4) In determining elevator angles and chordwise load distribution in the maneuvering conditions of paragraphs (b) and (c) of this section in turns and pull-ups, account shall be taken of the effect of corresponding pitching velocities.

(b) Maneuvering balanced conditions.

The maneuvering condition A through I on the maneuvering envelope (fig. 12:2) shall be investigated, assuming the airplane to be in equilibrium with zero pitching accelerations.

(c) Maneuvering pitching conditions.

The following conditions on figure 12:2 involving pitching acceleration shall be investigated:

(1) A_1 , Unchecked pull-up at speed V_A . The airplane shall be assumed to be flying in steady level flight (point A_1 on fig. 12:2) and the pitching control suddenly moved to obtain extreme positive pitching (nose up), except as limited by pilot

12:12 SUPERSONIC AND SUBSONIC AIRPLANE DESIGN

effort. (The tail loads are only calculated up to the time that the maximum maneuver load factor is attained.)

(2) A_2 , Checked maneuver at speed V_A . (As defined in CAM 4b a checked pitching maneuver is one in which the pitching control is suddenly displaced in one direction and then suddenly moved in the opposite direction, the deflections and timing being such as to avoid exceeding the limit maneuvering load factor.)

(i) The airplane shall be assumed to be maneuvered to the positive maneuvering load factor by a checked maneuver from an initial condition of steady level flight (point A_1 on fig. 12-2). The initial positive pitching portion of this maneuver may be considered to be covered by subparagraph (1) of this paragraph.

(ii) A negative pitching acceleration (nose down) of at least the following value shall be assumed to be attained concurrently with the airplane maneuvering load factor (point A_2 on fig. 12-2), unless it is shown that a lesser value could be exceeded:

$$-\frac{30}{V_A} n (n - 1.5) \text{ (radians/sec.}^2\text{)}$$

where n is equal to the value of the positive maneuvering load factor as defined by point A_2 on figure 12-2.

(3) D_1 and D_2 checked maneuver at V_D . The airplane shall be assumed to be subjected to a checked maneuver from steady level flight (point D_1 on fig. 12-2) to the positive maneuvering load factor (point D_2 on fig. 12-2) as follows:

(i) A positive pitching acceleration (nose up), equal to at least the following value, shall be assumed to be attained concurrently with the airplane load factor of unity, unless it is shown that lesser values could not be exceeded:

$$\frac{45}{V_D} n (n - 1.5) \text{ (radians/sec.}^2\text{)}$$

where n is equal to the value of the positive maneuvering load factor as defined by point D_2 on figure 12-2.

(ii) A negative pitching acceleration (nose down) equal to at least the following value shall be assumed to be attained concurrently with the airplane positive maneuvering load factor (point D_2 on fig. 12-2), unless it is shown that lesser values could not be exceeded:

$$-\frac{30}{V_D} n (n - 1.5) \text{ (radians/sec.}^2\text{)}$$

where n is equal to the value of the positive maneuvering load factor as defined by point D_2 on figure 12-2."

12-6 Maneuvering Balanced Condition

1) General

The total load on the tail is equal to the sum of F_{H_α} (the tail load due to angle of attack) and F_{H_δ} (the tail load due to elevator deflection). In addition to solving for the magnitude of these loads it is also necessary to determine their centers of pressure.

The aerodynamic forces considered are the lift and moment of the wing-fuselage combination acting at the tail-off aerodynamic center, the tail load due to α and the tail load due to δ_e , each acting at its respective c.p. (The drag forces are assumed not to contribute to the moment). These aerodynamic forces are balanced by the weight and inertia forces. The airplane is assumed to be flying in a circular arc with the radius required to produce the normal n , and the resulting angular velocity is assumed to produce a damping tail load.

F_{H_α} and F_{H_δ} are developed as functions of q , n , W , x (the c.g. position in inches aft of the leading edge of the M.A.C.) and $C_{N_{A-T}}$ (the force coefficient normal to the fuselage reference line due to airplane minus tail).

As noted above

$$F_H = F_{H_\alpha} + F_{H_\delta} \quad (12:16)$$

Load due to angle of attack, F_{H_α}

F_{H_α} is composed of 2 parts, one due to damping and the other due to the moment of the airplane less tail.

2) Damping tail load; F_{H_θ}

The damping tail load, F_{H_θ} , is the result of the pitching velocity of the airplane, and is some function of $\dot{\theta}$. Since $\Delta\alpha_H$ is some function of $\dot{\theta}$,

$$F_{H_\theta} = \frac{dF}{d\alpha} \Delta\alpha_H \quad (12:17)$$

12:14 SUPERSONIC AND SUBSONIC AIRPLANE DESIGN

It therefore follows that it is necessary to determine how $\Delta \alpha_H$ varies with the pitching velocity, $\dot{\theta}$.

The pitching velocity of the airplane needed to produce the required load factor n may be explained as follows:

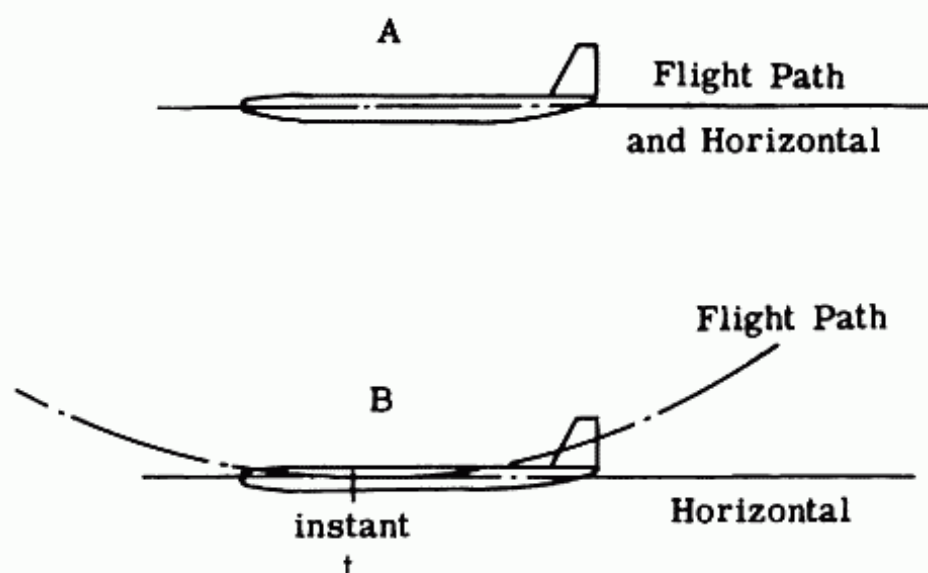


Fig. 12:9. Airplane flight paths.

Airplane A is in level flight, not rotating, and has a certain tail load required to maintain equilibrium.

Airplane B is on a curved flight path, and therefore at instant t has some angular pitching velocity, and a damping load in addition to the tail load of airplane A. It should be noted that again this can be set up in the form of

$$n = 1 + \Delta n$$

by letting $m = \frac{W}{g}$ and realizing that $\frac{V^2}{R}$ is the centrifugal acceleration. To place the system in equilibrium, it is necessary that the vertical forces = 0 at any instant: Therefore

$$nW = W + m \frac{V^2}{R} \quad (12:18)$$

$$nW - W = \frac{W}{g} \left(\frac{V^2}{R} \right)$$

$$(n - 1)g = \frac{V^2}{R} \quad (12:19)$$

At this point it is necessary to define the relationship between some angles that are used in this analysis.

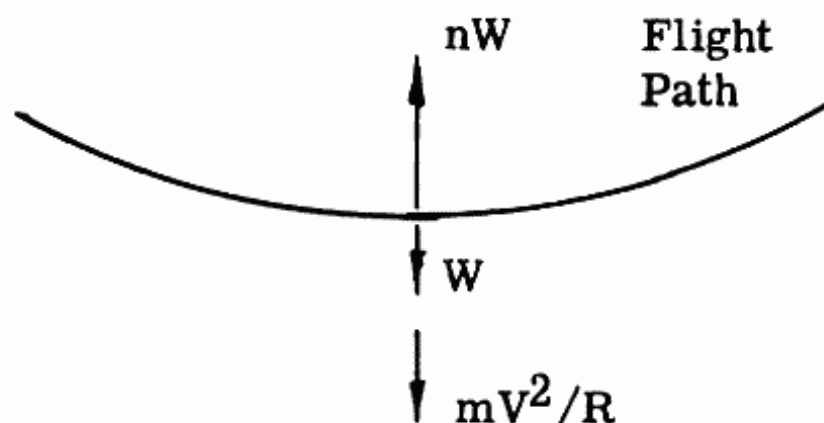


Fig. 12:10. Vertical forces on an airplane in a curved flight path.

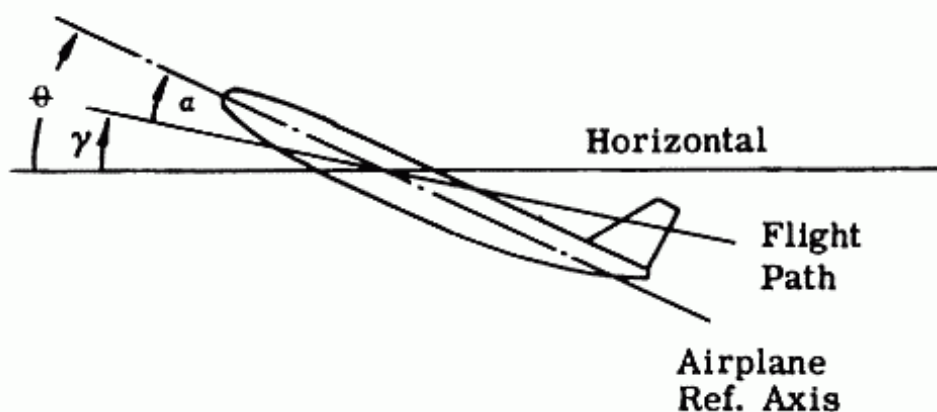


Fig. 12:11. Angles about the YY axis.

Fig. 12:11 defines the angles θ , γ and α , also showing their positive direction.

$$\begin{aligned} \text{Note } \theta &= \gamma + \alpha \\ \text{and } \therefore \gamma &= \theta - \alpha \end{aligned} \quad (12:20)$$

For a circular flight path as shown in fig. 12:9

$$V = \dot{\gamma} R$$

However since

$$\dot{\gamma} = \dot{\theta} - \dot{\alpha} \quad (12:20a)$$

and $\dot{\alpha} = 0$ for this maneuvering balanced condition,

$$\dot{\gamma} = \dot{\theta}$$

12:16 SUPERSONIC AND SUBSONIC AIRPLANE DESIGN

Therefore $V = \dot{\theta} R$ and $R = V/\dot{\theta}$
 Substituting into Eq. 12:19

$$(n - 1)g = \frac{V^2}{V/\dot{\theta}} = V \dot{\theta} \quad (12:21)$$

and therefore

$$\dot{\theta} = \frac{(n - 1)g}{V} \quad (12:22)$$

From the fig. 12:12 of an airplane with an angular velocity, $\dot{\theta}$,

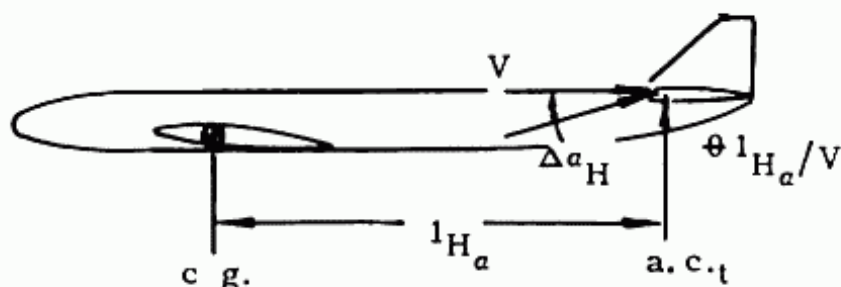


Fig. 12:12. Change in α_H due damping.

It can be seen that

$$\tan \Delta \alpha_H = \dot{\theta} l_{H_\alpha}/V = \frac{(n - 1) g l_{H_\alpha}}{V^2} \quad (12:23)$$

and, since for small angles the angle is equal to the tangent of the angle,

$$\Delta \alpha_H = \frac{(n - 1) g l_{H_\alpha}}{V^2} \quad (12:24)$$

Since the damping tail load, $F_{H\dot{\theta}}$ is caused by $\dot{\theta}$, and $\dot{\theta}$ results in $\Delta \alpha_H$

$$F_{H\dot{\theta}} = \frac{dF}{d\alpha} \Delta \alpha_H = \frac{dC_F}{d\alpha} (1/2 \rho S_H V^2) \frac{(n - 1) g l_{H_\alpha}}{V^2} \quad (12:25)$$

Note: above equation only holds for linear portion of C_L vs α curve, and therefore does not apply to the stall condition.

letting

$$\frac{dC_F}{d\alpha} = \alpha_H$$

$$F_{H\theta}^* = \alpha_H (n - 1) g l_{H\alpha} \frac{\rho}{2} S_H \quad (12:26)$$

It should be noted at this point that there should also be a load on the wing due to this θ , in fact

$$F_{W\theta}^* = a_w (n - 1) g l'_w \frac{\rho}{2} S_w$$

where l'_w is the distance from the c.g. to the wing a.c. and is positive when the a.c. is aft of the c.g.

However this may usually be neglected since l'_w is normally very small, in the order of .1 MAC while $l_{H\alpha}$ for the tail is in the order of 3.0 MAC. Nevertheless if desired, this form can easily be included in the analysis applied at the wing a.c.

3) Tail load due moment, $F_{H_{mom}}$

$$F_{H_{mom}} = \frac{C_{m_{c.g.}} c q S}{l_{H\alpha}} \quad (12:27)$$

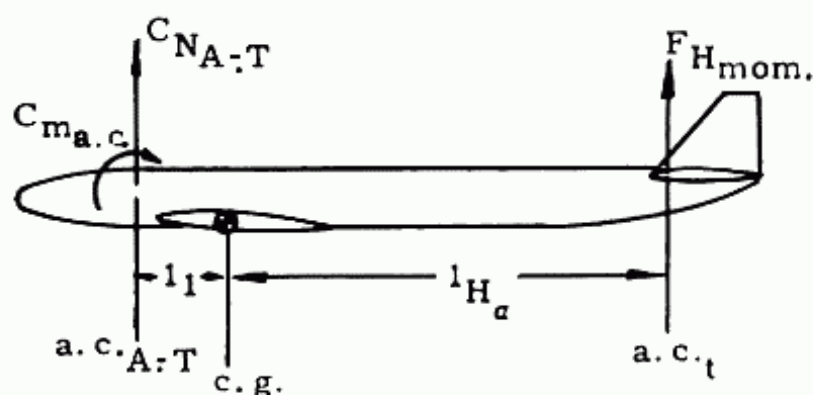


Fig. 12:13. Tail load due A.T. loads.

$$C_{m_{c.g.}} = C_{m_{a.c. A-T}} + C_{N_{A-T}} (x_{c.g.} - x_{a.c.}) \quad (12:27a)$$

$C_{m_{a.c. A-T}}$ = moment coef. about tail off a.c.

$C_{N_{A-T}}$ = normal force coef. of airplane minus tail

$a.c. A-T$ = tail off aerodynamic center, that is the point at which the normal force of the airplane minus tail acts, due to α .

$x_{c.g.}$ = distance from l.e. of MAC to the c.g. divided by the MAC

$x_{a.c.}$ = distance from l.e. of MAC to the a.c. divided by the MAC

For accurate results wind tunnel tests are required to obtain $C_{N_{A-T}}$, its c.p. and its $C_{m_{a.c.}}$. For subsonic flight, an estimate may be made by considering that the fuselage and nacelle effects are negligible. This would result in making a.c._{A-T} the a.c. of the wing, the A-T $C_{m_{a.c.}}$ the same as $C_{m_{a.c.}}$ of the wing, and $C_{N_{A-T}}$ equal the C_N of the wing. For supersonic flight, the effects of the nose cone and tail cone should be included even for preliminary estimates.

4) Total load due α ; F_{H_α}

$$F_{H_\alpha} = F_{H_\theta} + F_{H_{mom}} \quad (12:28)$$

$$= a_H (n - 1) g l_{H_\alpha} \frac{\rho}{2} S_H + \frac{C_{m_{c.g.}} c q S}{l_t} \quad (12:29)$$

5) Equilibrium Equations

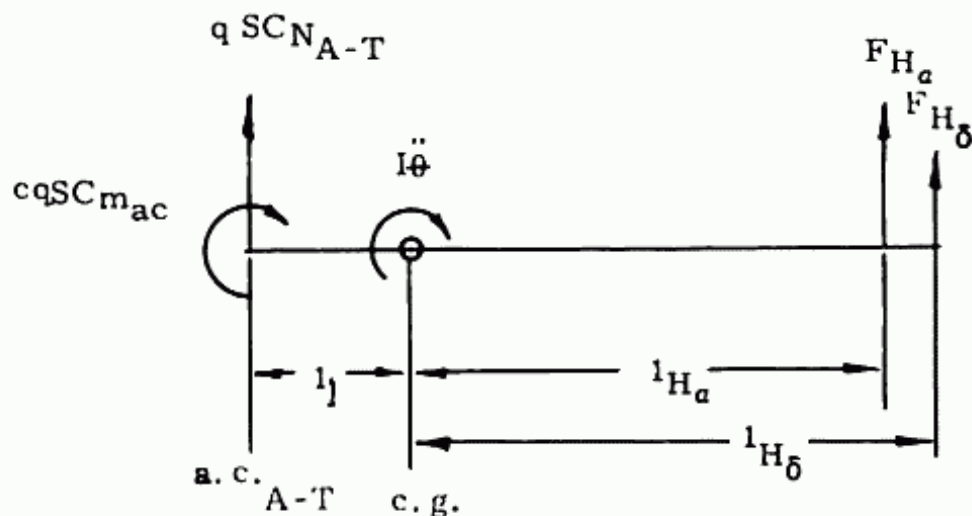


Fig. 12:14. Forces and moments on airplane.

Summation of forces = 0 can be written from considering figure 12:14, i.e.

$$\Sigma F = 0; nW = C_{N_{A-T}} q S + F_{H_\alpha} + F_{H_\delta} \quad (12:30)$$

It might appear at first observation that between eqs. 12:29 and 12:30 $F_{H\alpha}$ and $F_{H\delta}$ might both be obtained for a given n . However this is not so as q is not known because $q = \text{wing } L / SC_L$, and wing L is not known since $W = L_w + L_t$, and L_t (equal to $F_{H\alpha}$ and $F_{H\delta}$) is not yet known. It is therefore necessary to write summation of moments equal to zero and have another equation involving q .

$$\Sigma M_{c.g.} = 0; \quad (12:31)$$

$$I \ddot{\theta} - F_{H\alpha} l_{H\alpha} - F_{H\delta} l_{H\delta} + C_{m_{a.c.}} c q S + C_{N_{A-T}} q S l_1 = 0$$

All distances are positive as shown

Up airloads are positive

Stalling moments are positive

6) Determination of Tail Loads

a) V and n known.

If the velocity and load factor are given as specified in the V - n diagram, and W is known, it is noted from equ. 12:30 that $C_{N_{A-T}}$ is still unknown since F_H is an unknown. Therefore F_H can be obtained from equ. 12:32 which is the result of eliminating $C_{N_{A-T}}$ from eqs. 12-17, 12:29, 12:30 and 12:31.

It should be noted that for this balancing condition $\ddot{\theta}$ in equ. 12:31 is equal to zero as it is specified in CAM 4b.213b that the airplane is assumed to be in equilibrium with zero pitching acceleration.

$$F_H = \frac{nWl_1 + C_{m_{ac}} qSc + a_H(n-1) qL^2 H_\alpha \frac{\rho}{2} S_H \left(1 - \frac{l_{H\alpha}}{l_{H\delta}}\right)}{l_1 + l_{H\alpha}} \quad (12:32)$$

If $C_{N_{A-T}}$, $C_{m_{A-T}}$ and airplane less tail aerodynamic center are not available from wind tunnel test, then an approximation can be made that

$$\begin{aligned} C_N \text{ wing alone} &= C_{N_{A-T}} \\ C_{m_{ac}} \text{ wing alone} &= C_{m_{a.c.}} \text{ airplane less tail} \\ &\text{and wing ac} = \text{A-T a.c.} \end{aligned}$$

After F_H has been determined from equ. 12:32, $C_{N_{A-T}}$ can then be obtained from using eqs. 12:30 and 12:17, that is:

$$C_{N_{A-T}} = \frac{nW - F_H}{qS} \quad (12:33)$$

Then from 12:29 (obtaining $C_{m_{cg}}$ from 12:27a and 12:33)

$$F_{H_\alpha} = a_H (n-1) g l_{H_\alpha} \frac{\rho}{2} S_H + \frac{C_{m_{c.g.}} c q S}{l_{H_\alpha}} \quad (12:34)$$

and finally

$$F_{H_\delta} = F_H - F_{H_\alpha} \quad (12:34a)$$

b) At $C_{N_{max}}$

Fig. 12:20 shows the maneuvering V-n diagram with V_A as the velocity at which $n = 2.5$ with $C_{N_{max}}$ acting on wing. To calculate this velocity it is necessary to know the tail load at this value of n and $C_{N_{max}}$ since

$$nW = L_w + L_t$$

and L_t is unknown. Therefore at this time not only is the tail load calculated but also the correct value of V_A .

Although $C_{N_{max}}$ airplane less tail can be obtained from wind tunnel tests, q is unknown as just explained. Therefore, F_H can be obtained from equ. 12:35 which was obtained from eliminating q from eqs. 12:17, 12:29, 12:30 and 12:31.

$$F_H = \frac{nW \left(l_1 + \frac{C_{mac}}{C_{N_{A-T}}} \right) + a_H (n-1) g l_{H_\alpha}^2 \frac{\rho}{2} S_H \left(1 - \frac{l_{H_\alpha}}{l_{H_\delta}} \right)}{l_1 + l_{H_\alpha} + \frac{c_{mac}}{C_{N_{A-T}}} c} \quad (12:35)$$

With F_H obtained from 12:35, q can be determined from equ. 12:30, i.e.

$$q = \frac{nW - F_H}{C_{N_{A-T}} S} \quad (12:36)$$

From q the value of V_A can then be obtained.

c) General

It should be noted that the formulas for F_H , eqs. 12:32 and 12:35, merely give the total balancing static tail load for the load factor specified, and the combination of q and C_N investigated. Since this is a static load it would appear that it could be obtained by a simpler method. The slight complication presented arises from the fact that in subsonic flight there are two positions on a chord that the lift acts, at .25 chord due to change in α , and at the .50 chord due to change in camber. The load acting at the .25 chord of the tail is presented in equ. 12:39 and is due to the load factor (or θ) and the $C_{m_{c.g.}}$ due to the airplane less tail. Therefore the rest of the load acting on the tail to result in equilibrium must be acting at the .50 chord, either due to camber or elevator deflection.

As will be seen from calculation, or from observation, the total tail load must act up for a c.g. position between the airplane-minus-tail a.c. and the tail a.c. However the F_{H_δ} will be down, while F_{H_α} will be up. The values of F_{H_δ} and F_{H_α} and their point of application are most important in designing the tail structure, although it is only the total F_H that affects the wing load.

For an airplane with symmetrical wing and tail sections, and an all-movable tail, there is only one chordwise location of the airloads, that is the aerodynamic center. In this case F_H can simply be obtained by taking moments about the airplane-minus-tail a.c., without being concerned with either F_{H_δ} or F_{H_α} or F_{H_δ} . -2

7) Graphical Presentation of Maneuver Balancing Tail Loads.

For the stall condition, the tail load and V_A can be determined at any weight, load factor and c.g. location desired.

Figure 12:15 shows the variation of maneuver balancing tail load, with variation in gross weight and c.g. location, at V_A and a load factor of 2.5. Note that this l.f. of 2.5 corresponds to a certain radius of flight path, or equivalent θ . A similar graph can be drawn for each speed and load factor considered.

12-7 Maneuvering Pitching Conditions

1) General

The determination of the maneuver balanced tail load was based upon the assumption that there was no pitching acceleration, only pitching velocity. In the maneuvering pitching conditions, the airplane is no longer assumed to have $\dot{\theta} = 0$, but is

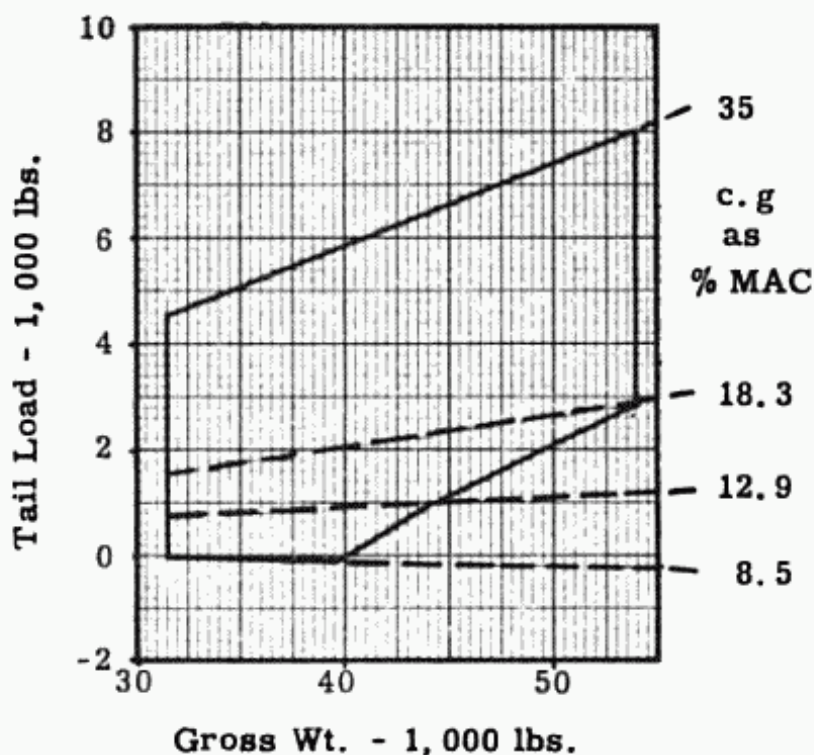


Fig. 12:15. Tail loads.

analyzed as a dynamic condition with effects of damping, downwash, change in downwash due α , and angular pitching acceleration, $\dot{\theta}$.

As noted in the CAM 4b.213c, in analyzing these maneuvers the airplane is assumed to be in steady level flight when the pitching control is moved. Therefore to obtain the maneuvering pitching tail load, the balancing load in steady level flight should be first obtained and then the additional load due to the movement of the pitching control should be added.

These additional loads are a function of time and therefore of $\dot{\alpha}$ and $\dot{\theta}$, as well as the previous functions found in the balancing tail load.

These maneuvers can now be analyzed assuming that the elevator is suddenly moved to its maximum deflection to reach the extreme positive pitching moment. The four equations set up to calculate the forces on the tail are: the tail load due to $\Delta\alpha$, $F_{H\alpha}$; the tail load due to δ , $F_{H\delta}$; and the two equilibrium equations, $\Sigma F = 0$, and $\Sigma M = 0$, including the effects of normal and angular accelerations.

2) Derivation of equations

- a) $F_{H\alpha}$, the change in load due to $\Delta\alpha$

$$F_{H\alpha} = q_t S_H C_F = \eta_t q S_H a_H \alpha_H \quad (12:37)$$

where $\eta_t = q_t/q$

q = free stream dynamic pressure

Since in this pitching condition, the load on the tail calculated is to be added to the balancing condition at $n = 1$, it is really a change in the load, $\Delta F_{H\alpha}$, and is dependent on the change in the α of attack, $\Delta\alpha$, from the α in the balancing condition. Therefore,

$$\Delta F_{H\alpha} = \eta_t q S_H a_H \Delta\alpha_H \quad (12:37a)$$

and

$$\Delta\alpha_H = \underbrace{\left(1 - \frac{d\epsilon}{d\alpha_w}\right) \Delta\alpha_w}_{\substack{\Delta\alpha_H \text{ due } \Delta\epsilon \\ \text{due } \Delta\alpha \\ \text{with } \dot{\alpha} = 0}} + \underbrace{\dot{\theta} l_{H\alpha}/V_t}_{\substack{\Delta\alpha_H \text{ due} \\ \text{to angular} \\ \text{velocity, } \theta}} + \underbrace{\frac{d\epsilon}{d\alpha} \frac{2l_2}{V+V_t} \dot{\alpha}}_{\substack{\Delta\alpha_H \text{ due time} \\ \text{lag in } \epsilon \text{ due } \dot{\alpha} \\ \text{(see explanation} \\ \text{following)}}} \quad (12:38)$$

$\Delta\alpha$ due time lag in ϵ due $\dot{\alpha}$

$$= d\epsilon = \frac{d\epsilon}{dt} t \quad \text{where } t = \text{time required for air to flow from wing a.c. to tail a.c.}$$

$$\frac{d\epsilon}{dt} = \frac{d\epsilon}{d\alpha} \frac{d\alpha}{dt} = \frac{d\epsilon}{d\alpha} \dot{\alpha} \quad (12:39)$$

$$\therefore \Delta\alpha = \frac{d\epsilon}{d\alpha} \frac{2l_2}{(V+V_t)} \dot{\alpha} \quad (12:41)$$

where l_2 is the distance from the a.c. of the wing to the a.c. of the horizontal tail

$$\therefore \Delta F_{H\alpha} = \eta_t q S_H a_H \left[\left(1 - \frac{d\epsilon}{d\alpha}\right) \Delta\alpha + \frac{\dot{\theta} l_{H\alpha}}{V_t} + \frac{d\epsilon}{d\alpha} \frac{2l_2}{V+V_t} \dot{\alpha} \right] \quad (12:42)$$

b) $\Delta F_{H\delta}$, the change in tail load due to $\Delta\delta_e$

$$\begin{aligned} \Delta F_{H\delta} &= a_H \Delta \alpha q_t S_H \\ \Delta \alpha &= \left(\frac{d\alpha}{d\delta} \right) \Delta \delta_e \\ \Delta F_{H\delta} &= a_H \left(\frac{d\alpha}{d\delta} \right) \Delta \delta_e q_t S_H \end{aligned} \quad (12:43)$$

See Fig. 9:27 for $d\alpha/d\delta$

c) Equilibrium equation, $\Sigma \Delta F = 0$

Referring to fig. 12:14 and realizing that this condition involves changes in loads;

$$\Delta nW = \frac{dC_{N_{A-T}}}{d\alpha} \Delta \alpha q S + \Delta F_{H\alpha} + \Delta F_H \quad (12:44)$$

It is now necessary to evaluate Δn in terms of the angular velocities of the airplane since the δ_e causes a pitching velocity. For an airplane in a curved flight path

$$\Delta nW = \frac{mV^2}{R} \quad (12:45)$$

$$V = \dot{\gamma} R \quad \text{where } \gamma \text{ is the angle between the (12:46) flight path and the horizontal}$$

$$\text{and } R = V/\dot{\gamma}$$

therefore,

$$\Delta nW = mV \dot{\gamma} \quad (12:47)$$

$$\text{As noted in equ. 12:20a, } \dot{\gamma} = \dot{\theta} - \dot{\alpha}$$

$$\text{and therefore } \Delta nW = mV(\dot{\theta} - \dot{\alpha}) \quad (12:48)$$

and $\dot{\alpha} \neq 0$ for this maneuvering pitching condition

From 12:44 and 12:48

$$mV(\dot{\theta} - \dot{\alpha}) = \frac{dC_{N_{A-T}}}{d\alpha} q S \Delta \alpha + F_{H\alpha} + \Delta F_{H\delta} \quad (12:49)$$

d) Equilibrium equ., $\Sigma \Delta M = 0$

$$I \ddot{\theta} = \left(\frac{dC_{m_{c.g.}}}{d\alpha} \right)_{A-T} \Delta \alpha c q S - \Delta F_{H\alpha} l_{H\alpha} - \Delta F_{H\delta} l_{H\delta} \quad (12:50)$$

where

$$C_{m_{c.g.}} = C_{m_{ac}}_{A-T} c q S + C_{N_{A-T}} q S l_1$$

3) Determination of $\dot{\alpha}$

If all the physical characteristics of the airplane and the aerodynamic data obtained from wind tunnel tests are substituted in equation 12:42, 12:43, 12:49 and 12:50, equations in the form of eqs. 12-51 to 54 may be obtained.

Note: $\frac{d\delta_e}{dt}$ is obtained by dividing the max. δ_e by the time required by the pilot to deflect the elevator to this angle; may assume this total time is .3 sec. To obtain δ_e at any time, t

$$\delta_e = \frac{d\delta_t}{dt} t$$

From equ. 12:42

$$\Delta F_{H\alpha} = C_1 \alpha + \dot{C}_2 \dot{\alpha} + C_3 \dot{\theta} \quad (12:51)$$

From equ. 12:43

$$\Delta F_{H\delta} = C_4 \delta_e = C_5 t \quad (12:52)$$

Substituting $\Delta F_{H\delta}$ (from 12:52) and $\Delta F_{H\alpha}$ (from 12:51) into equ. 12:49 and transposing

$$\ddot{\theta} = C_6 \alpha + C_7 \dot{\alpha} + C_8 t + C_9 \quad (12:53)$$

Substituting $\Delta F_{H\delta}$ and $\Delta F_{H\alpha}$ into equ. 12:50 and transposing

$$\ddot{\theta} = C_{10} \alpha + C_{11} \dot{\alpha} + C_{12} \dot{\theta} + C_{13} t \quad (12:54)$$

To solve for α and $\dot{\alpha}$ it is now necessary to eliminate $\ddot{\theta}$ and $\dot{\theta}$ from equ. 12:54. This can be done by substituting $\dot{\theta}$ from 12:53 into 12:54, and then differentiating 12:53 in respect to time and obtain $\ddot{\theta}$, which can then be substituted for $\ddot{\theta}$ in 12:54. Collecting terms an equation in the following form results:

$$\ddot{\alpha} + C_{14} \dot{\alpha} + C_{15} \alpha = C_{16} t + C_{17} \quad (12:55)$$

This equation can be solved by assuming that the form of the solution for α is

$$\alpha = e^{\omega t} (c' \cos \eta t + c'' \sin \eta t) \quad (12:56)$$

For an actual commercial airplane in service the equations for α and $\dot{\alpha}$ become (see appendix 12:A)

$$\alpha = e^{-.95t} (.362 \cos 2.35 t - .404 \sin 2.35 t) + 1.3t = .362 \quad (12:57)$$

12:26 SUPERSONIC AND SUBSONIC AIRPLANE DESIGN

$$\dot{\alpha} = e^{-.95t} (-.467 \sin 2.35t - 1.30 \cos 2.35 t) + 1.3 \quad (12:58)$$

4) Evaluation of Tail Loads

a) General

These values of α and $\dot{\alpha}$ obtained from eqs. 12:57 and 12:58 may be substituted in equ. 12:53 so that θ also becomes a function of time. By substituting the values of α , $\dot{\alpha}$ and $\dot{\theta}$ in equ. 12:51, $\Delta F_{H\alpha}$ may be determined. $\Delta F_{H\delta}$ can be obtained from equ. 12:52.

The final values of $F_{H\alpha}$ and $F_{H\delta}$ are determined by adding the $\Delta F_{H\alpha}$'s and $\Delta F_{H\delta}$'s, at each t investigated, to the balancing tail load at $t = 0$, that is at $n = 1.0$. The corresponding values of Δn may be calculated from eq. 12:48.

b) Unchecked pull up at speed V_a

Again quoting CAM 4b

"The airplane shall be assumed to be flying in steady level flight (point A_1 on fig. 12:2) and the pitching control suddenly moved to obtain extreme positive pitching (nose up) except as limited by pilot effort."

Since the n reaches a maximum value of 2.5 at V_a , Δn need not exceed 1.5. The value of Δn obtained is a function of the rotational speed that the pilot can induce on the elevator. Although the pilot may, and usually can, exert enough effort to exceed this $\Delta n = 1.5$, it is only necessary to determine the tail loads up to this value of Δn , and design the tail for these loads. This unchecked maneuver at maximum gross weight and most forward c.g. location usually gives the highest down load on the tail. In carrying out the calculations it should be noted that elevator effectiveness ($C_{m\frac{MAC}{4}}$ produced by the elevator deflection) plotted

against elevator deflection is not a straight line, but drops off close to max. throw. See fig. 12:16. A reasonable value for the time required to deflect the elevator to its maximum position is about .3 secs. The added tail loads, $\Delta F_{H\alpha}$ and $\Delta F_{H\delta}$ and the change in load factor, Δn , are obtained simply by filling out the following table:

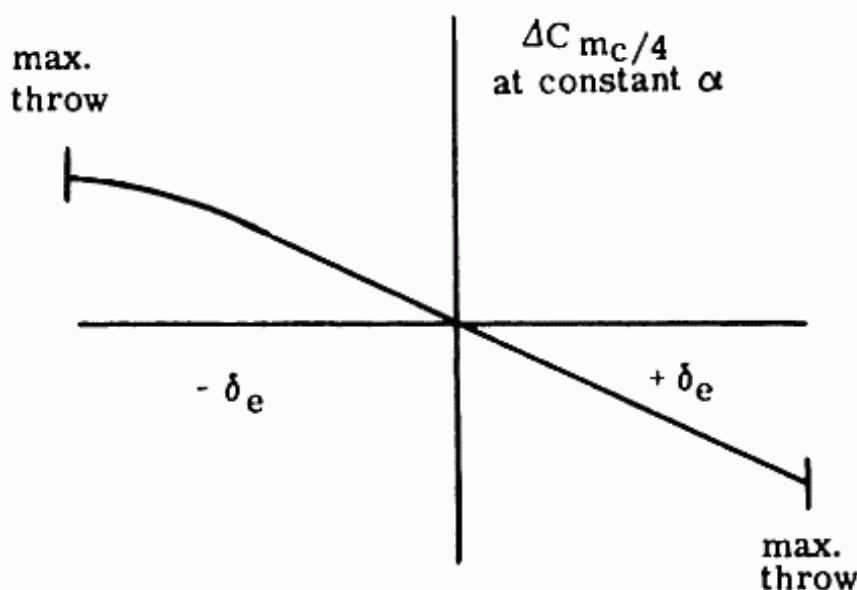
Fig. 12:16. $C_{mC/4}$ vs. δ_e .

Table XII - 1

t	α	$\dot{\alpha}$	$\dot{\theta}$	Δn	$\Delta F_{H\alpha}$	$\Delta F_{H\delta}$
.0						
.1						
.2						
.3						

Note α obtained from equ. 12:55 in similar form as equ. 12:57

$\dot{\alpha}$ " " differentiating α above

$\dot{\theta}$ " " 12:53

Δn " " 12:48

$\Delta F_{H\alpha}$ " " 12:51

ΔF_H " " 12:52

Note: only calculate up to $\Delta n = 1.5$.

c) Checked maneuver at V_a

Quoting from CAM 4b.213(2)

"The airplane shall be maneuvered to the positive maneuvering load factor by a checked maneuver from an initial condition of steady level flight (point A_1 on fig. 12:2). The initial positive pitching portion of this maneuver may be considered to be covered by subparagraph (1) of this paragraph.

A negative pitching acceleration (nose down) of at least the following value shall be assumed to be attained concurrently with

the airplane maneuvering load factor (point A_2 on fig. 12-2, unless it is shown that a lesser value could not be exceeded:

$$-\frac{30}{V_A} n (n - 1.5) \text{ (radians/sec.}^2\text{)}$$

where n is equal to the value of the positive maneuvering load factor as defined by point A_2 on figure 12-2^a.

A checked maneuver is one in which the control is moved to its maximum deflection and then immediately returned to its original position. Figure 12:17 shows the δ_e vs. time for an elevator assuming that the maximum δ_e is reached in .3, and the same time is required to return it to its original equilibrium position at $n = 1$, δ_{e_0} .

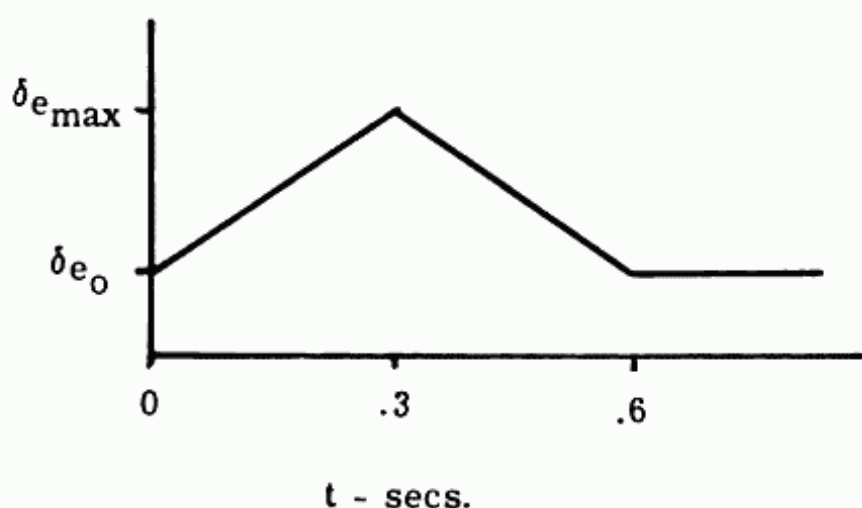


Fig. 12:17. δ_e vs. time.

The equations for α , $\dot{\alpha}$, $\dot{\theta}$, $F_{H\delta}$ and $F_{H\alpha}$ are the same as those used in the unchecked condition. In fact for the same speed and gross weight, the values would be identical for the same $d\delta_e/dt$, up to the maximum deflection. The method of obtaining the values of α , $\dot{\alpha}$, $\dot{\theta}$, $F_{H\alpha}$, and $F_{H\delta}$ at different values of t that is easiest to see physically, is to consider each change in $d\delta_e/dt$ as a separate interval, thus:

- 1) Find the required characteristics for the interval from $t = 0$ to $t = .3$ (the time at which maximum deflection is reached). Since an up deflection of the elevator is minus,

$$\frac{d\delta_e}{dt} = - \left(\frac{\delta_{e_{\max}} - \delta_{e_0}}{.3} \right)$$

- 2) For the period from $t = .3$ to $t = .6$ (the time at which the elevator returns to its original equilibrium position) add the change in values obtained from the equations with

$$\frac{d\delta_e}{dt} = + \frac{\delta_{e_{\max}} - \delta_{e_0}}{.3}$$

to the values calculated for $t = .3$

- 3) For the period beyond $t = .6$ calculate the change in the values required with $d\delta_e/dt = 0$ and add to the values obtained at $t = 0.6$

A method that requires much less time is based on the principle of superposition i.e., (using Δn as an example)

$$\Delta n_t = \Delta n_{1t} - 2 \Delta n_{1t-.3} + \Delta n_{1t-.6} \quad (12:59)$$

where Δn_t is the Δn for the checked maneuver at any time t , and Δn_{1t} is the Δn that would result if the $d\delta_e/dt$ was kept constant at the value from $t = 0$ to $t = .3$ (see fig. 12:18)

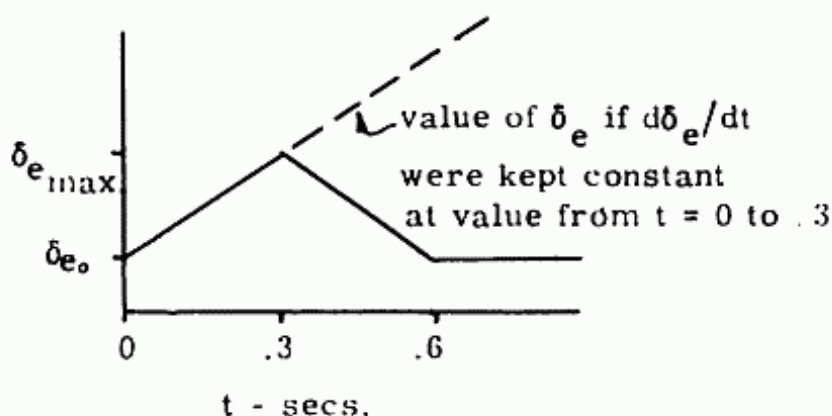


Fig. 12:18. Extension of δ_e vs. time.

Note that the $-2 \Delta n_{1t-.3}$ accounts for the fact that the change in $d\delta_e/dt$ at $t = .3$ is actually minus two times the value of $d\delta_e/dt$ between $t = 0$ and $t = .3$, and the $+ \Delta n_{1t-.6}$ accounts for the fact that the change in $d\delta_e/dt$ at $t = .6$ is actually equal to $d\delta_e/dt$ in the interval $t = 0$ and $t = .3$.

The tail loads and load factors for this checked maneuver can then be obtained by the use of Table I extended for values of t far beyond $\Delta n = 1.5$. By applying equ. 12:59 for Δn , and similar equations for ΔF_{H_α} and ΔF_{H_δ} , all the desired values may be obtained, up to the specified Δn . Note that if the Δn specified is exceeded, with the assumed $d\delta_e/dt$ and maximum δ_e , before the

12:30 SUPERSONIC AND SUBSONIC AIRPLANE DESIGN

checked maneuver is completed, it is necessary to change either the assumed value of $d\delta_e/dt$ or the maximum δ_e , or both, so that the specified Δn is not exceeded. The tail loads are then obtained for these modified assumed values.

Fig. 12:19 shows the results obtained for a particular transport where it was assumed that the control was reversed after .3 seconds although the maximum deflection was not reached.

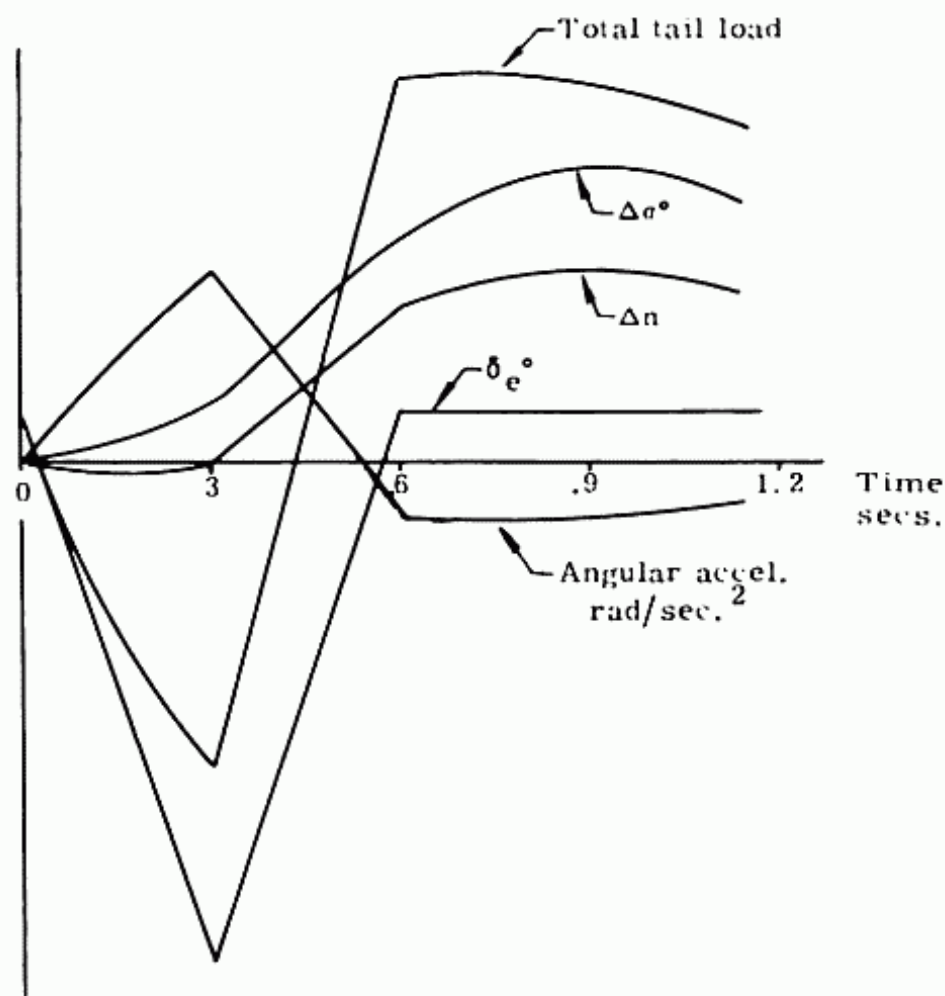


Fig. 12:19. Actual response of an airplane to δ_e .

It should be noted that CAM 4b specified that a negative pitching acceleration of at least the following value shall be attained with the maneuvering load factor (point A_2 on fig. 12:2) unless it is shown that a lesser value cannot be exceeded.

$$-\frac{30}{V_A} n (n - 1.5) \text{ (rad/sec.}^2\text{)}$$

This checked maneuver at V_A with maximum weight and aft c.g. location usually results in the highest upload on the tail.

d) Checked maneuver at V_D

The tail loads must be obtained for the checked maneuver at V_D as specified in CAM 4b. The procedure is exactly the same as that followed for the maneuvers at V_A .

5) Effects of Flexibility

The tail load analysis presented is based upon an assumption of a non-flexible structure. The actual effect of flexibility is primarily its influence on the location of the airplane minus tail a.c., and on the tail effectiveness.

Fig. 12:20 presents the variation of wing-fus. a.c. due to flexibility for a 35° swept wing bomber as determined from free flight data. This variation in a.c. would have a large effect on the tail load required for equilibrium, since it would produce a pronounced effect on $M_{c.g.}$.

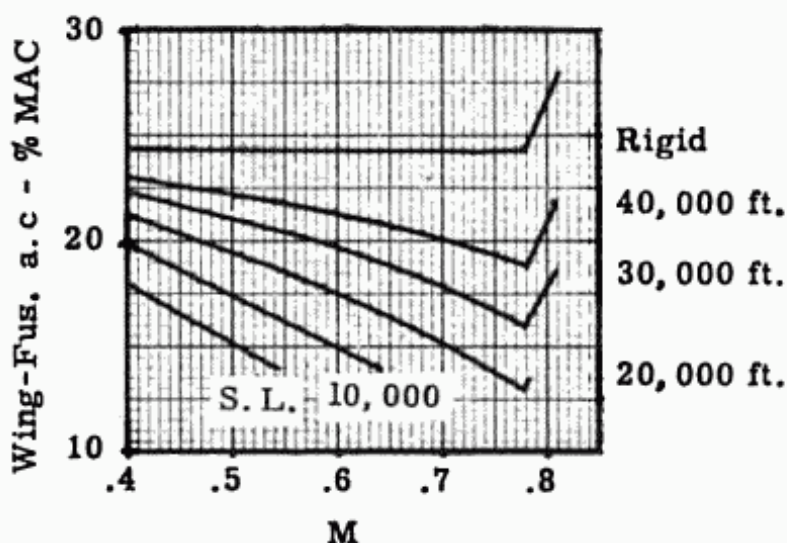


Fig. 12:20. Wing-fus. a.c. for flexible wing. (Ref. 12-2)

The effect of reduced effectiveness of the tail due to flexibility is realized in the value of the $dC_{m_{c.g.}}/d\delta_e$ term in equ. 12:43.

For a rigid structure

$$C_{m_{c.g.}} \text{ due to } \delta_e = \frac{dC_L}{d\alpha} \frac{d\alpha}{d\delta_e} \delta_e \frac{l_t}{MAC}$$

where $d\alpha/d\delta_e$ is purely a aerodynamic term independent of flexibility. However for a flexible structure an upward deflection of

the elevator produces a download on the tail which bends the fuselage down, thereby causing an increase in α_t . This increase in α_t causes an upload on the tail which of course reduces the value of the desired down load. Therefore the effectiveness of the tail is primarily affected by the bending rigidity of the fuselage, and can be accounted for by calculating either a change in $d\alpha/d\delta_e$ or a change in $(dC_L/d\alpha)_t$, due to flexibility.

6) Effects of Supersonic Flow

Although this method of determining tail loads was originally devised for subsonic flow, the principles and methods will be the same for supersonic flow. The value of various parameters will change in supersonic flow due to the characteristics of the supersonic flow and also due to the change in aircraft physical characteristics dictated by efficiency in this new Mach number regime. As was mentioned under subsonic flow, if the airfoils are symmetrical and the control surface is all movable (which is usually the case for supersonic airplanes) then the balancing control surface load can be obtained simply by taking moments about the airplane-minus-tail aerodynamic center.

7) Effect of Canard Design

The method presented was outlined based upon a conventional tail design, i.e. the horizontal control surface at the aft end of the fuselage. The change to a canard control surface introduces some new problems. There are some simple changes required in the signs of some of the terms in the equation due to the fact that positive tail loads now cause positive moments about the airplane c.g. whereas the conventional surface positive tail loads caused negative moments about the c.g.

The expression for F_{H_α} in equ. 12:42 becomes much simpler, that is there is no downwash acting on the surface, thereby eliminating the $d\epsilon/d\alpha$ terms, resulting in

$$\Delta F_{H_\alpha} = -q S_H a_H (\Delta \alpha + \frac{\dot{\theta}}{V_T} l_{H_\alpha})$$

The prime complication arises from the downwash effect of the canard on the wing. On the conventional control surface, the airplane minus tail characteristics could be obtained and then the tail loads and moments made to balance these, since the tail had negligible effect on the wing and body. However, this is no longer true with a canard since the downwash from this surface significantly affects the wing-body loads. It is therefore necessary to

add an additional load at the wing a.c. Thus,

$$\Delta L_{W\epsilon} = \frac{dC_N}{d\alpha} \left[\left(\frac{d\epsilon}{d\alpha} \Delta \alpha + \frac{d\epsilon}{d\alpha} \frac{l_w}{V} \dot{\alpha} \right) \right]$$

where

$\Delta L_{W\epsilon}$ = lift on wing due to downwash from canard

l_w = distance from canard a.c. to wing a.c.

$\frac{d\epsilon}{d\alpha}$ = the change in downwash angle on wing from canard with change in angle of attack of canard.

A most significant problem is the determination of $d\epsilon/d\alpha$ for the canard in both subsonic and supersonic flow; that is the effect of planform of the canard, of canard span to wing span, and at supersonic speeds the effect of M . If no data is available wind tunnel tests of the model being investigated must be run.

In the canard design where the subsonic a.c. of the wing must be far enough aft of the c.g. location to offset the instability of the canard, the wing supersonic a.c. might be considerably aft of the c.g. It might therefore be necessary to consider the effect of $\dot{\theta}$ on the wing lift, i.e. add

$$F_{W\dot{\theta}} = a_W (n - 1) g l_w \frac{\rho}{2} S_W$$

to the wing lift at the a.c. For a supersonic canard airplane, the loss in wing lift due to downwash from the canard will probably be in the order of 10 to 20%. This, of course, will require a larger α to give the same lift. Also, the increase in the downwash from the canard with an increase in canard deflection, will introduce a down load on the wing, which will add to the canard effectiveness in producing a moment about the airplane c.g.

It should be noted that for canard missiles where the canard surface area may be a larger proportion of the wing area than on a passenger airplane, all the aforementioned downwash effects will be much larger.

12-8 Spanwise Load Distribution

There are many methods of determining the spanwise lift distribution on a wing. The complexity of the method depends upon the desired level of accuracy required, and the type of wing planform being considered. An extensive discussion of the subject is presented in references 12:3 and :4. These present methods (and references) for calculation of the distribution including sweep-back, compressible and elastic effects.

Only a very simple approximation for preliminary work will be presented here, Schrenck's method.

If the plan form of a rigid wing is elliptical, and there is no aerodynamic wing twist or change in airfoil section along the span, the spanwise airload distribution is elliptical. This is due to the fact that for elliptical plan form the downwash is constant throughout the span. As the plan form changes from the elliptical, the downwash is no longer constant along the span and the distribution changes. However it still tends to conform somewhat to the same pattern. Figure 12:21 shows the spanwise lift coefficient and the total lift distribution for the elliptical and conventionally tapered plan forms. It was noticed that if the distribution is drawn half way between an assumed elliptical distribution and the plan form of the wing, a fairly accurate spanwise airload distribution is obtained. Figure 12:22 shows the method used on a typical plan form.

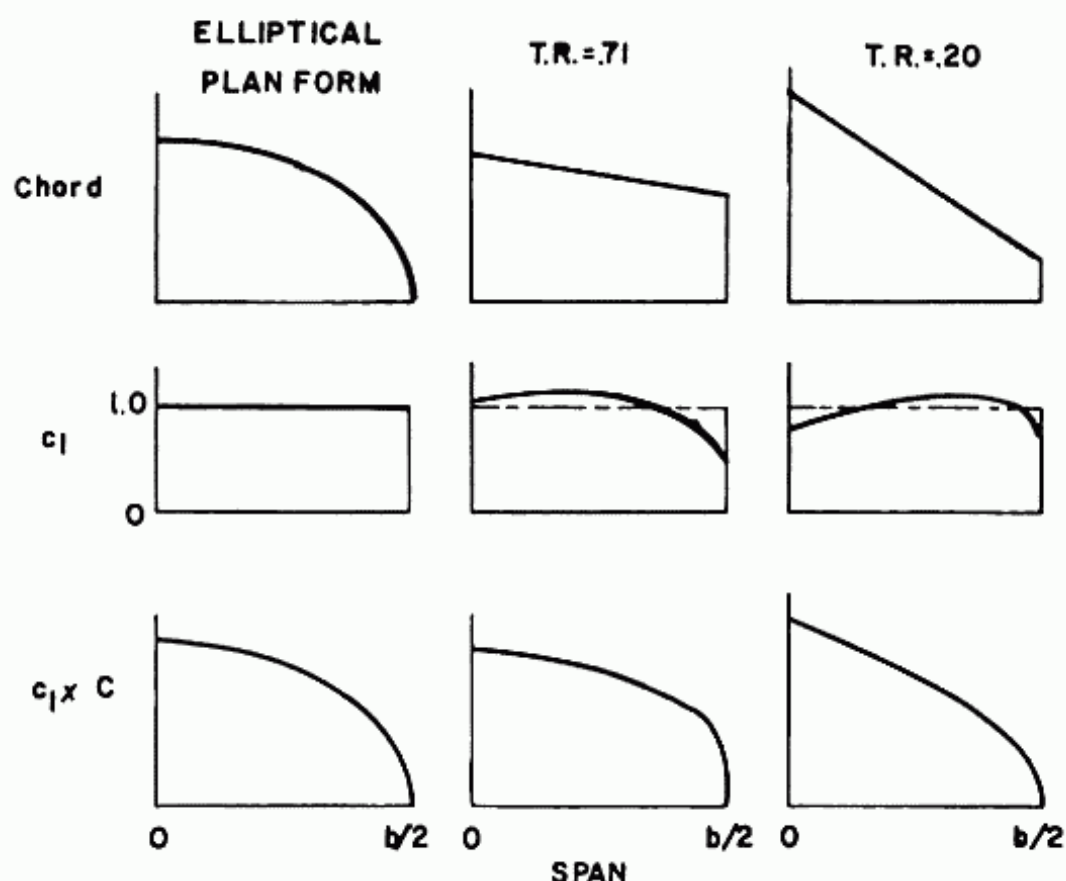


Fig. 12:21. Spanwise load distribution for various plan forms.

This is Schrenk's method and can be modified to account for twist, plan form, and varying airfoils spanwise. The added factor involved is that at zero lift for the total wing, the local

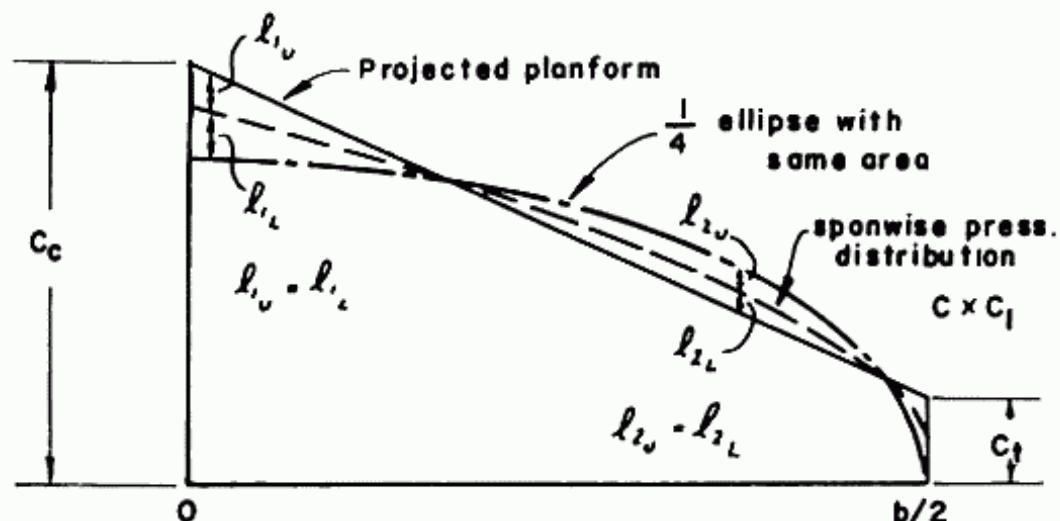


Fig. 12:22. Schrenk's method of spanwise load distribution.

spanwise lift coefficients are not zero. They vary, with some being positive and some negative, so that the total lift is zero. The lift coefficients denoted as c_{1b} , do not vary with angle of attack. The part of the lift coefficient that does vary with angle of attack is denoted by c_{1a} . The total c_1 at any section is c_{1a} plus c_{1b} .

Spanwise Load Distribution - Flexible Sweptback Wing

The above presentation of the spanwise load distribution does not include either the effect of introducing sweepback or of considering wing flexibility. Figure 12:23 presents the spanwise lift distributions for rigid wings with zero and 35° sweepback. As shown, the load on a rigid wing moves outboard with increase in sweepback. This is due to the increased upwash on the staggered lifting sections on the outboard portions of the wing.

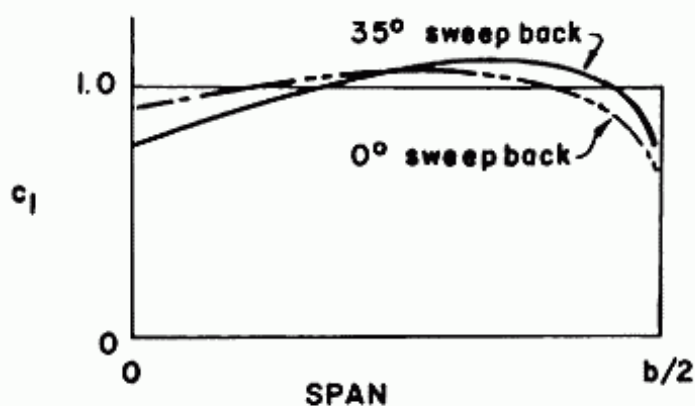


Fig. 12:23. Spanwise load distribution; sweptback and unswept wings.

The flexibility effects are somewhat more complex. If the chordwise centers of pressure on an unswept wing are along the elastic axis, as determined by our standard methods, the wing has no torsion, and therefore the spanwise loading distribution is independent of deflection.

On a sweptback wing this is not true. Assuming that the centers of pressure are at the elastic axis of the swept wing (if it is possible to determine a significant elastic axis) and no torsion did exist, a downflow is still induced by the bending deflection, as explained in the "Gust Load Factor-Flexible Wing" section. This down flow decreases effective angle of attack outboard and tends to reduce the loads towards the tip.

In both the sweptback and unswept wings spanwise load distribution is affected by torsional deflection. Subsonically the c.p. and the a.c. are most always forward of the shear center and therefore the torsional deflection increases the α outboard, throwing the load outboard. The more flexible wings, whether due to increased sweepback or smaller thickness ratios, will be affected more than the more rigid wings. In the supersonic airplanes, where the a.c. is at approximately .50 MAC, the a.c. is usually very close to the shear center, or possibly behind it, and the effect of torsional deflection on the spanwise load distribution is much less pronounced.

It should be noted that the deflections that tend to throw the load inboard are a function of the bending rigidity, and the deflections that usually tend to throw the loads outboard, if the a.c. is forward of the shear center, are a function of torsional rigidity. If care is taken in design, the torsional flexibility effect can be minimized and the net effect of flexibility on spanwise load distribution can throw the loads inboard, tending to cancel the effects of upwash on the sweptback wing.

For a first rough approximation the net effect of sweepback and flexibility on spanwise load distribution can be assumed negligible. The accuracy of this approximation depends upon the relative rigidities of the wing in bending and torsion, the values of sweepback and aspect ratio, and the relative positions of the center of pressure and the elastic axis. It will therefore vary from one design to another. Accurate results require a rigorous solution, as presented in references 12:3 and 4.

12-9 Critical Conditions

A. Symmetrical Flight

Paragraph 4b.211 of C.A.M. states:

"Flight Envelopes: The strength requirements shall be met

at all combinations of air speed and load factor on and within the boundaries of the V - n diagrams of figures 12:2 and 12:3 which represent the maneuvering and gust envelopes."

However paragraph 4b.213a states:

"Procedure of analysis. In the analysis of symmetrical flight conditions at least those specified in paragraphs (b), (c), and (d) of this section shall be considered."

The paragraphs b, c, d referred to the above specified maneuvering balanced conditions, which includes all points on the V - n diagram from A thru I, the checked and unchecked maneuvering pitching conditions at V_A and V_D , and all the points on the gust V - n envelope from B' thru J'.

It is therefore necessary to check all these conditions to find the critical conditions for each part of the wing.

B. Unsymmetrical flight

Rolling Condition; C.A.M. 4b.214 states:

"The airplane shall be designed for rolling loads resulting from the conditions specified in paragraphs (a) and (b) of this section. Unbalanced aerodynamic moments about the center of gravity shall be reacted in a rational or a conservative manner considering the principal masses furnishing the reacting inertia forces.

(a) Maneuvering. The following conditions, aileron deflection, and speeds, except as the deflections may be limited by pilot effort (see 4b.220 (a)), shall be considered in combination with an airplane load factor of zero and of two-thirds of the positive maneuvering factor used in the design of the airplane. In determining the required aileron deflections, the torsional flexibility of the wing shall be taken into account in accordance with 4b.200 (d).

(1) Conditions corresponding with steady rolling velocity shall be investigated. In addition, conditions corresponding with maximum angular acceleration shall be investigated for airplanes having engines or other weight concentrations outboard of the fuselage. For the angular acceleration conditions, it shall be acceptable to assume zero rolling velocity in the absence of a rational time history investigation of the maneuver.

(2) At speed V_A a sudden deflection of the aileron to the stop shall be assumed.

(3) At speed V_C the aileron deflection shall be that required to produce a rate of roll not less than that obtained in condition (2) of this paragraph.

(4) At speed V_D the aileron deflection shall be that required to produce a rate of roll not less than one-third of that in condition (2) of this paragraph.

(b) Unsymmetrical gusts. The condition of unsymmetrical gusts shall be considered by modifying the symmetrical flight conditions B' or C' of fig. 12:2, whichever produces the greater load. It shall be assumed that 100 percent of the wing air load acts on one side of the airplane, and 80 percent acts on the other side."

Part (a) Maneuvering. An analysis similar to the maneuvering pitching conditions must be made with the necessary $d\delta_a/dt$ replacing the $d\delta_e/dt$ and meeting the further requirements specified.

Part (b) "Unsymmetrical gusts" specified an unsymmetrical load condition which demonstrates how a load below the maximum can be critical for certain parts of the wing. It specified that condition B' or C' of the gust V-n envelope, whichever is critical, be modified so that 100% of the airload acts on one side of the airplane and only 80% on the other.

It can easily be shown that this condition is critical for the wing-fuselage connection, particularly for narrow fuselages and large wing spans where the moment due to the unsymmetrical 20% load produces high shears at these points.

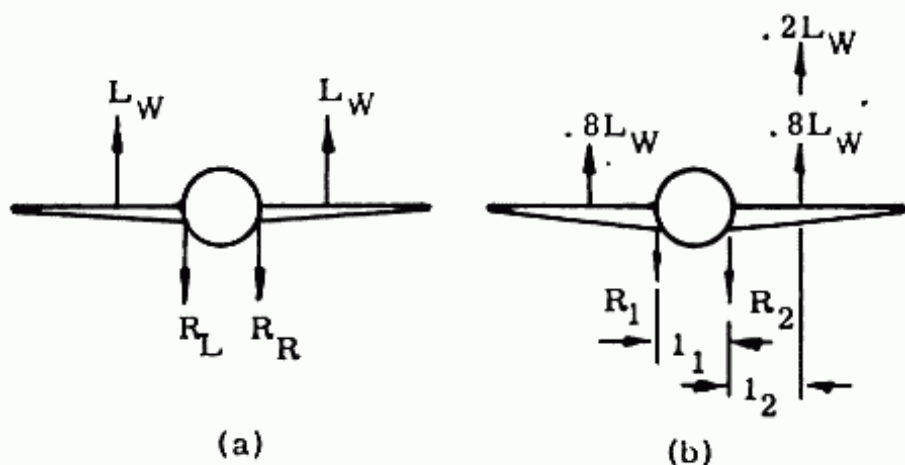


Fig. 12:24. Unsymmetrical wing loading.

From fig. 12:24 for maximum load on each side, $R_1 = R_2 = L_W$. However from fig. 12:22b, with $.8L_W$ acting on one side and L_W (or $.8L_W + .2L_W$) acting on the other side.

$$R_2 = .8L_W + \frac{(.2L_W)(l_1 + l_2)}{l_1}$$

or

$$R_2 = .8L_W + .2L_W \left(1 + \frac{l_2}{l_1}\right)$$

It can therefore be seen that under these conditions R_2 will always be greater than L_w and can become much larger for high values of l_2/l_1 , i.e. large wing spans and narrow fuselages.

C. Reduced Loads

C.A.M. 4b-210c states:

"Design Fuel Loads. The disposable load combinations shall include fuel loads in the range from zero fuel to the maximum fuel load selected by the applicant. It shall be permissible for the applicant to select a structural reserve fuel condition not exceeding 45 minutes of fuel under operating conditions defined in 4b.437 (c). If a structural reserve fuel condition is selected, it shall be used as the minimum fuel weight condition for showing compliance with the flight load requirements as prescribed in this subpart, in which case, the provisions of subparagraphs (1) through (3) of this paragraph shall apply.

(1) The structure shall be designed for a condition of zero fuel at limit loads corresponding with:

(i) A maneuver load factor of + 2.25, and

(ii) Gust intensities equal to 85 percent of the values prescribed in 4b.211 (b).

(2) Fatigue evaluation of the structure shall take into account any increase in operating stresses resulting from the design condition of subparagraph (1) of this paragraph (See ¶ 4b.270).

(3) The flutter, deformation, and vibration requirements shall also be met with zero fuel (see ¶ 4b.308)."

(a) Maneuver load factor:

Although the C.A.R. states that $n = 2.25$ for the minimum fuel weight condition, as opposed to a value of 2.50 for the design fuel weight condition, there is no specification for the weights in between. The following discussion to determine under which conditions the reduced weight might be critical assumes for simplicity that n does not vary with weight. It can be adapted to account for variations in n .

D. Reduced Weight

(a) Maneuver Load Factor

The bending moments, shears and torsions along the wing span are equal to the sum of the effects due to airloads and the dead weights of the wing and its contents. The airload is equal to the airplane weight times the load factor; the dead weight is equal to the weight of the wing and its contents times the load factor. Fig. 12:25 shows a diagram of a wing with the application of the airloads, dead weight minus fuel, and fuel weight, with their corresponding arms from their center of pressures to the side of the fuselage.

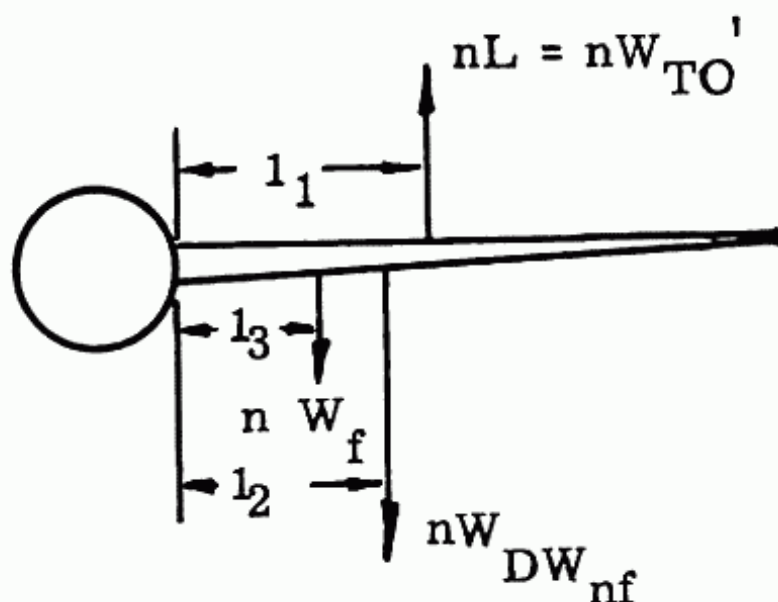


Fig. 12:25. Loads on wing.

$$\text{T.O. Gr. Wt. B.M.} = nW_{TO}' l_1 = nW_{DW_{nf}} l_2 - nW_f l_3 \quad (12:62)$$

$$\text{T.O. Gr. Wt. less fuel B.M.} = n(W_{TO}' - W_f) l_1 - nW_{DW_{nf}} l_2 \quad (12:63)$$

$$= nW_{TO}' l_1 - nW_f l_1 - nW_{DW_{nf}} l_2 \quad (12:64)$$

$$\Delta \text{B.M.} = \text{T.O. Gr Wt. less fuel B.M.} - \text{T.O. Gr. Wt. B.M.} \quad (12:65)$$

$$= -nW_f l_1 - (-nW_f l_3) \quad (12:66)$$

$$\text{where} \quad = nW_f(l_3 - l_1)$$

B.M. = bending moment at side of the fuselage

n = maneuver load factor

$W_{DW_{nf}}$ = total dead weight of 1/2 wing, no fuel

W_{TO}' = take-off weight/2

W_f = weight of fuel in 1/2 wing

l_1, l_2, l_3 = arms to the side of the fuselage

For a wing that originally had a positive bending moment at the side of the fuselage, the use of a reduced weight for design has three possibilities.

- (1) If $l_2 = l_1$, then there would be no change in the bending moment at the side of the fuselage.
- (2) If l_2 is greater than l_1 , the bending moment at the side of the fuselage increases.
- (3) If l_2 is less than l_1 , the bending moment at the side of the fuselage decreases.

Note that these conclusions are true only for the assumption that n is the same value at take-off gross weight and at reduced load. Actually n varies from 2.5 to 2.25 and the relation between l_2 and l_1 for zero change in bending moment will be slightly different. For bending moments at points on the span other than the side of the fuselage, similar studies may be made. The side of the fuselage was used in this derivation as it is the section at which the highest bending moments and greatest weight occur.

As fuel is used, the air loads on the sections outboard of the area where fuel is carried decrease, while the dead weights remain constant. Therefore if the net bending moment at maximum weight is in the direction of the airload bending moment, it will be critical for the maximum weight. However if the net bending moment at maximum weight is in the direction of the dead weight bending moment, it will be critical for the minimum weight.

(b) Gust load factor

The reduced weight condition is more complex if the gust load factor is critical. For the maneuver condition, the load factor remained constant and only the weight was variable. In the gust condition, the gust load factor increment varies inversely as weight. However the actual airload varies as a complex function of the weight.

$$n = 1 + \frac{K_g U_{de} V a}{498 W/S} \quad (12:67)$$

$$\begin{aligned} \text{Total airload} &= nW = \left(1 + \frac{K_g U_{de} V a}{498 W/S}\right)W & (12:68) \\ &= W + \frac{K_g U_{de} V a S}{498} \end{aligned}$$

It can be seen that the second term of Equ. 12:69 is independent of W . Therefore although a decrease in weight increases the gust load factor, the total airload decreases. If an airplane had a total gust load factor at take-off weight equal to 3.0, and it was reduced to one half the take-off weight, taking into account that

U_{de} is reduced by 15% for the reduced weight condition, the new gust factor would equal 4.4, an increase of 44%. At the same time the actual airload decreases 26.7%.

For the condition where the fuel is in the fuselage, not in the wing, the bending moment is definitely critical at the side of the fuselage for maximum weight. As the weight decreases, Equ. 12:69 shows that the airload decreases and therefore the airload bending moment decreases. The dead weight bending moment increases since the dead weight in the wing remains the same while the load factor increases. If the net bending moment was originally in the direction of the airload bending moment, the net bending moment will be less at the lower weight since the airload bending moment decreases while the relieving dead weight moment increases.

For the maneuver condition at constant n , the bending moment at the side of the fuselage did not change at lower weights if the center of gravity of the fuel was at the center of pressure of the airloads. If the fuel was outboard, it was critical with fuel. For the gust condition no such general statement can be made. The center of gravity location at which no change in bending moment at the side of fuselage occurs, depends upon the original gust load factor and the change in weight, in addition of the position of center of gravity. For each airplane a separate study must be made.

12-10 Effect of High Lift Devices

C.A.M. 4b.212 states:

"When flaps or similar high lift devices intended for use at the relatively low air speeds of approach, landing, and take-off are installed, the airplane shall be assumed to be subjected to symmetrical maneuvers and gusts with the flaps in landing position at the design flap speed, V_F , resulting in limit load factors within the range determined by the following conditions:

(a) Maneuvering to a positive limit load factor of 2.0.

(b) Positive and negative 15 f.p.s. derived gusts acting normal to the flight path in level flight.

(c) In designing flaps and supporting structure on tractor type airplanes, slipstream effects shall be taken in to account as specified in ¶ 4b.221. For other than tractor type airplanes, a headon gust equivalent to the intensity prescribed in ¶ 4b.211 (b) (3) with no alleviations acting along the flight path shall be considered.

(d) When automatic flap operation is provided, the airplane shall be designed for the speeds and the corresponding flap positions which the mechanism permits."

It should be noted that V_F is the design flap speed specified in C.A.M. 4b.210 b-1 as "The minimum value of the design flap speed shall be equal to $1.4 V_{S_1}$ or $1.8V_{S_0}$, whichever is the greater, where V_{S_1} is the stalling speed with flaps retracted at the design landing weight, and V_{S_0} is the stalling speed with flaps in the landing position at the design landing weight."

The specification limiting the maneuver load factor to a value of 2.0 with the flaps in landing position at V_F (where V_F must be at least $1.8 V_{S_0}$) actually is limiting the angle of attack in this condition.

$$L = nW = 1/2 \rho S V_F^2 C_L$$

with C_L the value of max C_L with flaps deflected

For the specification of $n = 2.0$, and $V_F = 1.8V_{S_0}$

$$L = 2W = 1/2 \rho S (1.8V_{S_0})^2 C'_L \quad (12:70)$$

with C'_L the value of C_L with flaps deflected, but

at such an α so that equ. 12:70 is satisfied

Since

$$L = W = 1/2 \rho S V_{S_0}^2 C_{L_{\max}} \text{ with flaps}$$

$$C'_L = \frac{C_{L_{\max}} \text{ with flaps}}{(1.8)^2 / 2} = \frac{C_{L_{\max}} \text{ with flaps}}{1.62} \quad (12:71)$$

Therefore α is limited to such an angle that C'_L with flaps is equal to $C_{L_{\max}} \text{ with flaps} / 1.62$.

12-11 Vertical Tail Loads

C.A.M. 4b.215 Yawing Conditions states:

"The airplane shall be designed for loads resulting from the conditions specified in paragraphs (a) and (b) of this section. Unbalanced aerodynamic moments about the center of gravity shall be reacted in a rational or a conservative manner considering the principal masses furnishing the reacting inertia forces.

(a) Maneuvering. At all speeds from V_{MC} to V_A the following maneuvers shall be considered. In computing the tail loads it shall be acceptable to assume the yawing velocity to be zero.

(1) With the airplane in unaccelerated flight at zero yaw, it shall be assumed that the rudder control is suddenly displaced

to the maximum deflection as limited by the control stops or by a 300 lb. rudder pedal force, whichever is critical.

(2) With the rudder deflected as specified in subparagraph (1) of this paragraph it shall be assumed that the airplane yaws to the resulting sideslip angle.

(3) With the airplane yawed to the static sideslip angle corresponding with the rudder deflection specified in subparagraph (1) of this paragraph, it shall be assumed that the rudder is returned to neutral.

(b) Lateral gusts. The airplane shall be assumed to encounter derived gusts normal to the plane of symmetry while in unaccelerated flight. The derived gusts and airplane speeds corresponding with conditions B' thru J' on Fig. 12:3 as determined by C.A.M. 4b.211 (b) and 4b.212 (a) (2) or 4b.212 (b) (2) shall be investigated. The shape of the gust shall be as specified in 4b.211 (b). In the absence of a rational investigation of the airplane's response to a gust, it shall be acceptable to compute the gust loading on the vertical tail surfaces by the following formula:

$$L_t = \frac{K_{gt} U_{de} V a_t S_t}{498} \quad (12:72)$$

where:

L_t = vertical tail load (lbs.);

$K_{gt} = \frac{.88\mu_{gt}}{5.3 + \mu_{gt}}$ = gust alleviation factor;

$\mu_{gt} = \frac{2W}{\rho C_t g a_t S_t} \left(\frac{K}{l_t} \right)^2$ = lateral mass ratio;

U_{de} = derived gust velocity (fps)-same values as specified for in CAM 4b.211b

ρ = air density (slugs/cu.ft.);

W = airplane weight (lbs.);

S_t = area of vertical tail (ft.²);

C_t = mean geometric chord of vertical surface (ft.);

a_t = lift curve slope of vertical tail (per radian);

K = radius of gyration in yaw (ft.);

l_t = distance from airplane c.g. to lift center of vertical surface (ft.);

g = acceleration due to gravity (ft./sec.²);

V = airplane equivalent speed (knots)."

Maneuvering Tail Load

The maneuvering vertical tail load must be calculated for specifications (1), (2) and (3), so that the critical condition may be obtained.

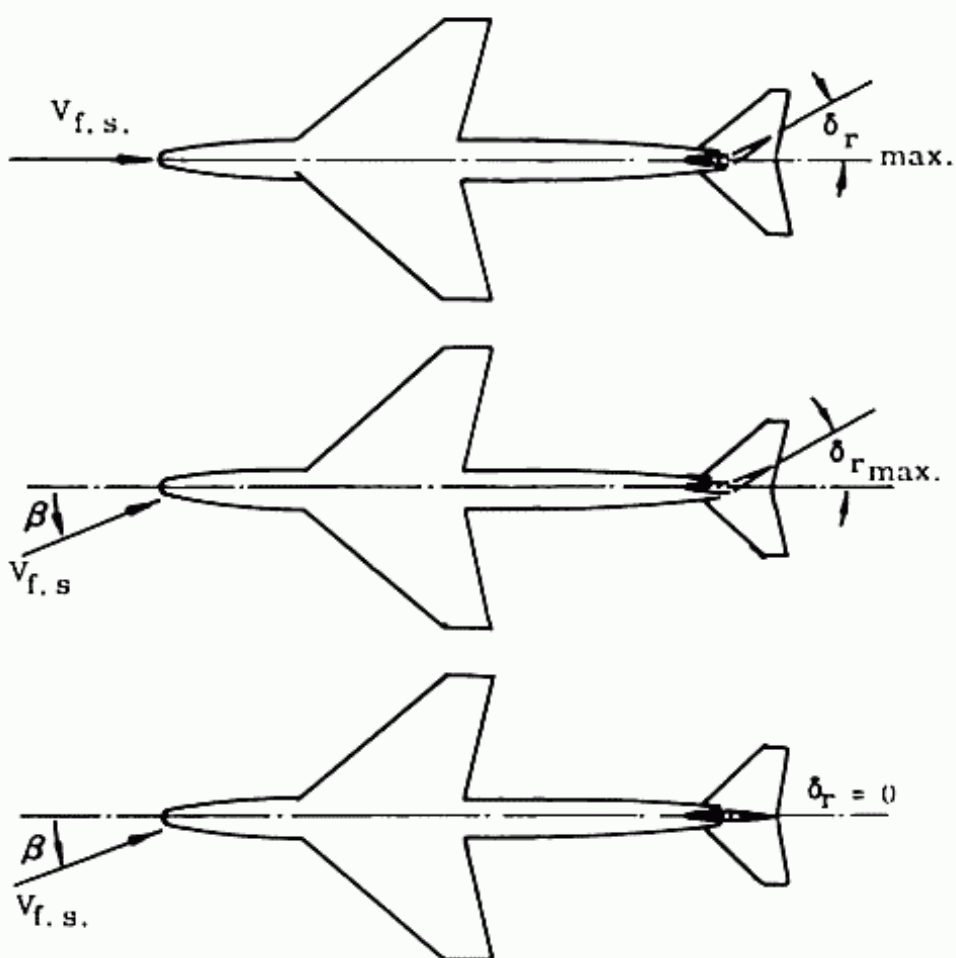


Fig. 12:26. Vertical tail loads.

Fig. 12:26 shows the conditions (1), (2) and (3) specified for vertical tail maneuver loads, with yawing velocity equal to zero.

In condition (1) all that is required is to calculate the vertical tail load with δ_r maximum and $\beta = 0$. For condition (2) it is required to calculate β so that $\Sigma M_{cg} = 0$, i.e. that the moment due to the fuselage is equal and opposite to the moment produced

by the vertical tail with δ_r at the same maximum deflection. The tail load is then calculated at this attitude. Condition (3) simply has $\delta_r = 0$ with the sideslip equal to the β calculated in condition (2). Then the vertical tail load is calculated, i.e. at $\delta_r = 0$ and β at value calculated for (2). As has been stated previously these loads have been set up for the subsonic conditions. For supersonic flight some change will have to be made in the rudder deflection since the loads become unrealistically high at supersonic speed with maximum deflection.

Gust Load

The gust tail load must be calculated for all the points on the gust envelope to determine the critical condition. However from the formula for L_t it can be seen that it is proportional to $U_{de} V$ with all the other factors being constant for any given weight.

12-12 Engine Loads

C.A.M. 4b:216 a, b and c states:

*Supplementary flight conditions:

(a) Engine torque effects:

Engine mounts and their supporting structures shall be designed for engine torque effects combined with basic flight conditions as described in subparagraphs (1) and (2) of this paragraph. The limit torque shall be obtained by multiplying the mean torque by a factor of 1.33 in the case of engines having 5 or more cylinders. For 4, 3, and 2-cylinder engines, the factors shall be 2, 3, and 4, respectively.

(1) The limit torque corresponding with take-off power and propeller speed shall act simultaneously with 75 percent of the limit loads from flight condition A (see fig. 12:2).

(2) The limit torque corresponding with maximum continuous power and propeller speed shall act simultaneously with the limit loads from flight condition A (see fig. 12:2).

(b) Side load on engine mount.

The limit load factor in a lateral direction for this condition shall be equal to the maximum obtained in the yawing conditions, but shall not be less than either 1.33 or one-third the limit load factor for flight condition A (see fig. 12:2). Engine mounts and their supporting structure shall be designed for this condition which may be assumed independent of other flight conditions."

It should be noted that the specifications for the combination of torque and normal loads do not apply to jet engines since there is no torque developed that must be transmitted to the engine mount. The side limit load factor may be assumed to equal 1.33

unless the analysis of the yawing condition shows that this value is exceeded.

12-13 Pressurized Cabin Loads

C.A.M. 4b 2:16 c states:

"When pressurized compartments are provided for the occupants of the airplane, the following requirements shall be met. (see 4b.373.)

(1) The airplane structure shall have sufficient strength to withstand the flight loads combined with pressure differential loads from zero up to the maximum relief valve setting. Account shall be taken of the external pressure distribution in flight. Stress concentration and fatigue effects shall be accounted for in the design of pressure cabins (see 4b.270).

(2) If landings are to be permitted with the cabin pressurized, landing loads shall be combined with pressure differential loads from zero up to the maximum to be permitted during landing.

(3) The airplane structure shall have sufficient strength to withstand the pressure differential loads corresponding with the maximum relief valve setting multiplied by a factor of 1.33. It shall be acceptable to omit all other loads in this case.

(4) Where a pressurized cabin is separated into two or more compartments by bulkheads or floor, the primary structure shall be designed for the effects of sudden release of pressure in any compartment having external doors or windows. This condition shall be investigated for the effects resulting from the failure of the largest opening in a compartment. Where intercompartment venting is provided, it shall be acceptable to take into account the effects of such venting."

Since the development of the difficulties in the Comet Jet Transports, these specifications take on added significance. The combination of stress concentrations and fatigue as caused by both airloads and internal pressure acting simultaneously must be very carefully investigated, and can only be determined reliably by testing.

12-14 Control System Loads

C.A.M. 4b. 224 states:

"Primary flight control systems.

Elevator, aileron, and rudder control systems and their supporting structures shall be designed for loads corresponding with 125 percent of the computed hinge moments of the movable control surface in the conditions prescribed in 4b.220, subject to the following provisions.

(a) The system limit loads, except the loads resulting from ground

gusts (4b.226), need not exceed those which can be produced by the pilot or pilots and by automatic devices operating the controls. Acceptable maximum and minimum pilot loads for elevator, aileron, and rudder controls are shown in fig. 4b-5. These pilot loads shall be assumed to act at the appropriate control grips or pads in a manner simulating flight conditions and to be reacted at the attachment of the control system to the control surface horn.

(b) The loads shall in any case be sufficient to provide a rugged system for service use, including considerations of jamming, ground gusts, taxiing tail to wind, control inertia, and friction.

4b.225 Dual primary flight control systems.

(a) When dual controls are provided, the system shall be designed for the pilots operating in opposition, using individual pilot loads equal to 75 percent of those obtained in accordance with 4b.224, except that the individual pilot loads shall not be less than the minimum loads specified in figure 4b-5.

(b) The control system shall be designed for the pilots acting in conjunction, using individual pilot loads equal to 75 percent of those obtained in accordance with 4b.224.

Control	Maximum Load	Minimum Load
Aileron:		
Stick	100 lbs.	40 lbs.
Wheel*	80 D in.lbs.**	40 D in.lbs.
Elevator:		
Stick	250 lbs.	100 lbs.
Wheel	300 lbs.	100 lbs.
Rudder	300 lbs.	130 lbs.

*The critical portions of the aileron cont. sys. shall be designed for a single tangential force having a limit value equal to 1.25 times the couple force determined from these criteria.

**D - wheel diameter.

Fig. 4b-5 Pilot cont. force limits (primary controls)*

All control systems are designed for limit loads 25 per cent greater than those corresponding to the limit loads specified for the control surfaces to which they are attached. The standard factor of safety of 1.5 is also used on the limit loads to change to design loads. This additional 1.25 factor is used to account for various features such as

(a) Difference between actual and assumed control load surface distribution.

- (b) Desire of extra rigidity in control system to reduce deflection.
- (c) Reduction in strength due to wear, play in joints, etc.

The forces on the control system are either from the airload on the surface, or the load applied at the stick by the pilot, whichever is critical for the system. It is obvious that a maximum load should be specified. The minimum load is specified to account for a condition where the airload on the surface results in a load in the system less than this minimum specified. The control systems must also be investigated for ground gust conditions as specified in 4b:226. In addition 4b.227 specifies the loading conditions for the secondary controls, i.e. wheel brakes, spoilers and tabs.

12-15 Ailerons, Flaps, Tabs and Fins.

The loads on these surfaces shall be obtained from the following specifications of C.A.M. 4b

4b.214 ailerons

4b.220 fins, and general information for all surfaces

4b.221 flaps

4b.222 tabs

12-16 Ground Load Specifications

The following ground load specifications are quoted from C.A.M. 4b

*4b.230 General.

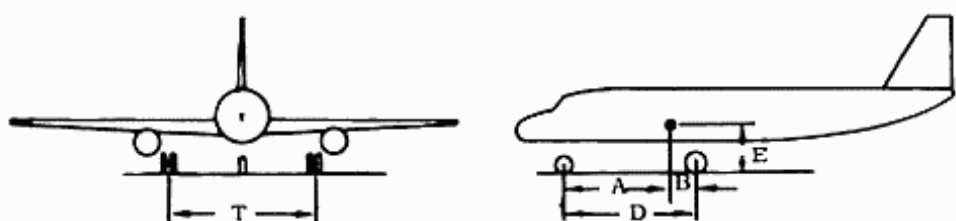
The limit loads obtained in the conditions specified in 4b.231 through 4b.236 shall be considered as external forces applied to the airplane structure and shall be placed in equilibrium by linear and angular inertia forces in a rational or conservative manner. In applying the specified conditions the provisions of paragraph (a) of this section shall be complied with. In addition, for the landing conditions of 4b.231 through 4b.234 the airplane shall be assumed to be subjected to forces and descent velocities prescribed in paragraph (b) of this section. *The basic landing gear dimensional data are given in figure 4b-7) See fig. 12:27.

(a) Center of gravity positions.

The critical center of gravity positions within the certification limits shall be selected so that the maximum design loads in each of the landing gear elements are obtained in the landing and the ground handling conditions.

(b) Load factors, descent velocities, and design weights for landing conditions.

- (1) In the landing conditions the limit vertical inertia load



Nose Wheel

Fig. 12:27. Basic landing gear dimensions.

factors at the center of gravity of the airplane shall be chosen by the applicant, except that they shall not be less than the values which would be obtained in the attitude and subject to the drag loads associated with the particular landing condition, and with the following limit descent velocities and weights:

- (i) 10 f.p.s. at the design landing weight, and
- (ii) 6 f.p.s. at the design take-off weight.

(2) It shall be acceptable to assume a wing lift not exceeding the airplane weight to exist throughout the landing impact and to act through the center of gravity of the airplane.

(3) The provisions of subparagraphs (1) and (2) of the paragraph shall be predicated on conventional arrangements of main and nose gears, or main and tail gears, and on normal operating techniques. It shall be acceptable to modify the prescribed descent velocities if it is shown that the airplane embodies features of design which make it impossible to develop these velocities. (See 4b.332 (a) for requirements on energy absorption tests which determine the minimum limit inertia load factors corresponding with the required limit descent velocities.)

4b.231 Level landing conditions.

(a) In the level attitude the airplane shall be assumed to contact the ground at forward velocity components parallel to the ground ranging from V_{L_1} to $1.25 V_{L_2}$ and shall be assumed to be subjected to the load factors prescribed in 4b.230 (b) (1) where V_{L_1} is equal to V_{S_0} (TAS) at the appropriate landing weight and in standard sea level conditions and where V_{L_2} is equal to V_{S_0} (TAS) at the appropriate landing weight and altitudes in a hot day temperature of 41° F above standard.

(1) Condition of maximum wheel spin-up load.

Drag components simulating the forces required to accelerate the wheel rolling assembly up to the specified ground speed shall be combined with the vertical ground reactions existing at the

instant of peak drag loads. A coefficient of friction between the tires and ground need not be assumed to be greater than 0.8. It shall be acceptable to apply this condition only to the landing gear, directly affected attaching structure, and large mass items; i.e., external fuel tanks, nacelles, etc.

(2) Condition of maximum wheel vertical load.

An aft acting drag component not less than 25 percent of the maximum vertical ground reaction shall be combined with the maximum ground reaction of 4b.230 (b).

(3) Condition of maximum spring-back load.

Forward-acting horizontal loads resulting from a rapid reduction of the spin-up drag loads shall be combined with the vertical ground reactions at the instant of the peak forward load. It shall be acceptable to apply this condition only to the landing gear, directly affected attaching structure, and large mass items; i.e., external fuel tanks, nacelles, etc.

(b) Level landing; tail-wheel type.

The airplane horizontal reference line shall be assumed to be horizontal. The conditions specified in paragraph (a) of this section shall be investigated. (fig. 4b-8.) See Fig. 12:28.

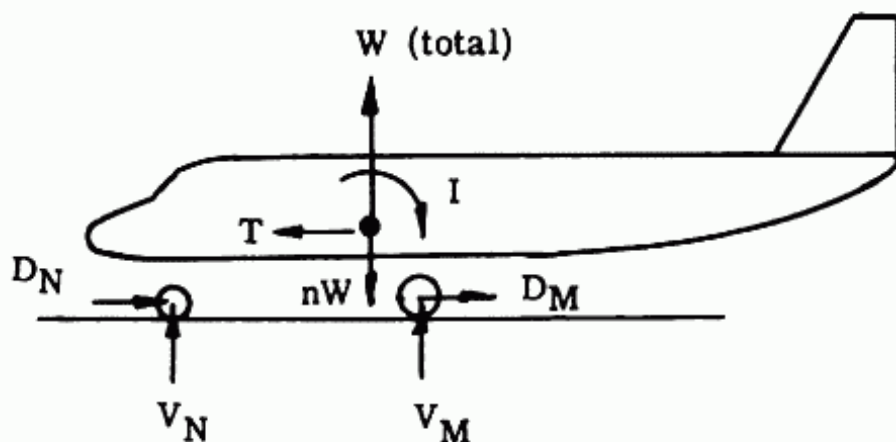


Fig. 12:28. Level landing.

(c) Level landing; nose-wheel type.

The following airplane attitudes shall be considered: (See fig. 4b-8).

(1) Main wheels shall be assumed to contact the ground with the nose wheel just clear of the ground. The conditions specified in paragraph (a) of this section shall be investigated.

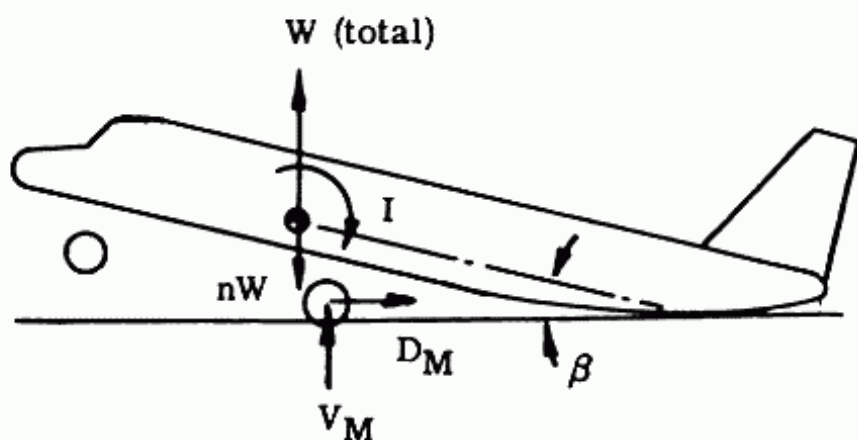
(2) Nose and main wheels shall be assumed to contact the ground simultaneously. Conditions in this attitude need not be

investigated if this attitude cannot reasonably be attained at the specified descent and forward velocities. The conditions specified in paragraph (a) of this section shall be investigated, except that in conditions (a) (1) and (a) (3) it shall be acceptable to investigate the nose and main gear separately neglecting the pitching moments due to wheel spin-up and spring-back loads, while in condition (a) (2) the pitching moment shall be assumed to be resisted by the nose gear.

4b.232 Tail-down landing conditions.

In the conditions of paragraphs (a) and (b) of this section the airplane shall be assumed to contact the ground at forward velocity components parallel to the ground, ranging from V_{L_1} to V_{L_2} where V_{L_1} and V_{L_2} are as indicated in 4b.231 (a). The load factors prescribed in 4b.230 (b) (1) shall apply. The combination of vertical and drag components specified in 4b.231 (a) (1) and 4b.231 (a) (3) shall be considered acting at the main wheel axle centerline.

(a) Tail-wheel type.



β = Angle for main gear and tail contacting ground except need not exceed stall angle.

Fig. 12:29. Tail down landing.

The main and tail wheels shall be assumed to contact the ground simultaneously. (fig. 4b-9). See Fig. 12:29. Two conditions of ground reaction on the tail wheel shall be assumed to act in the following directions:

(1) Vertical

(2) Up and aft through the axle at 45° to the ground line

(b) Nose-wheel type.

The airplane shall be assumed to be at an attitude corresponding with either the stalling angle or the maximum angle permitting clearance with the ground by all parts of the airplane other than the main wheels, whichever is the lesser. (See fig. 4b-9.)

4b.232 One-wheel landing condition

The main landing gear on one side of the airplane center line shall be assumed to contact the ground in the level attitude. (fig. 4b-10.) See fig. 12:30. The ground reactions on this side shall be the same as those obtained in 4b.231 (a) (2). The unbalanced external loads shall be reacted by inertia of the airplane in a rational or conservative manner.

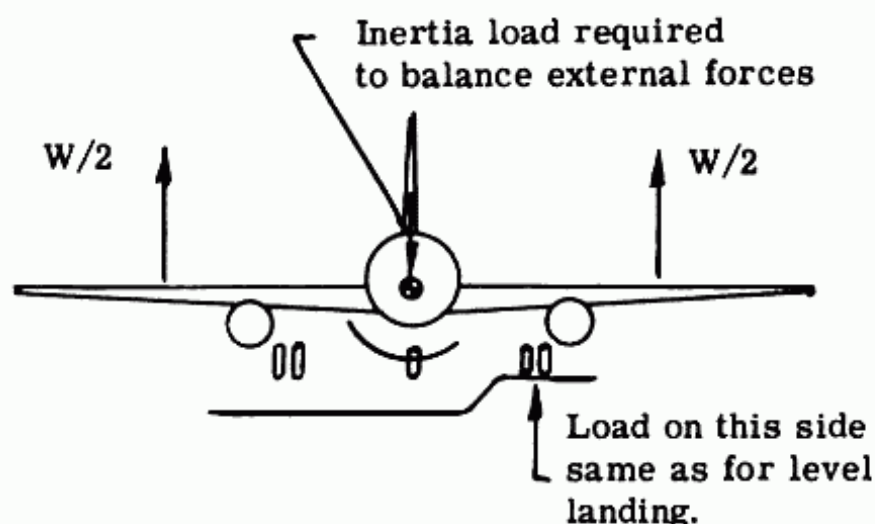


Fig. 12:30. One wheel landing.

4b.234 Lateral drift landing condition

(a) The airplane shall be assumed to be in the level attitude with only the main wheels contacting the ground (see fig. 12:31)

(b) Side loads of 0.8 of the vertical reaction (on one side) acting inward and 0.6 of the vertical reaction (on the other side) acting outward shall be combined with one-half of the maximum vertical ground reactions obtained in the level landing conditions. These loads shall be assumed to be applied at the ground contact point and to be resisted by the inertia of the airplane. It shall be acceptable to assume the drag loads to be zero.

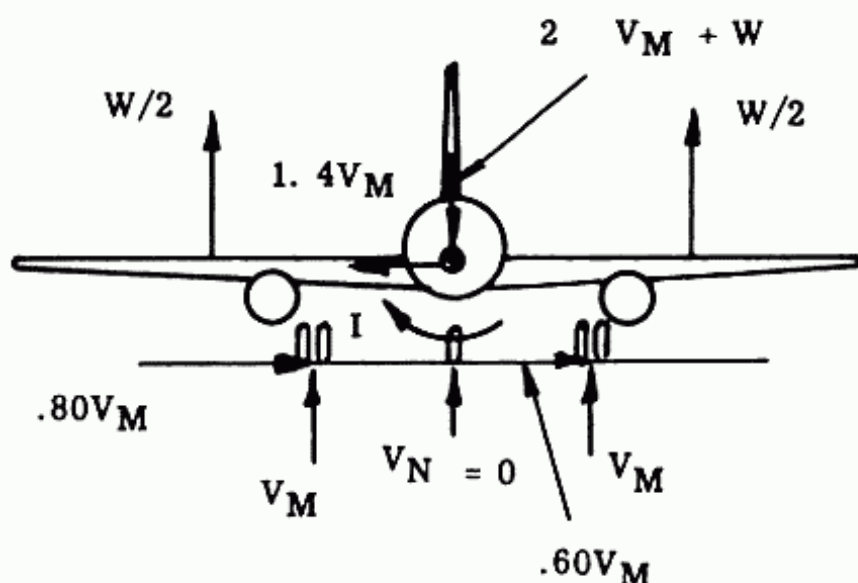


Fig. 12:31. Lateral drift landing.

4b.234a Rebound landing condition.

The landing gear and its supporting structure shall be investigated for the loads occurring during rebound of the airplane from the landing surface. With the landing gear fully extended and not in contact with the ground, a load factor of 20.0 shall act on the unsprung weights of the landing gear. This load factor shall act in the direction of motion of the unsprung weights as they reach their limiting positions in extending with relation to the sprung portions of the landing gear.

12-17 Ground Load Determination

I. General

The specifications state that "the limit vertical inertia load factors at the c.g. of the airplane shall be chosen by the applicant except that they should not be less than would be obtained with the following limit descent velocities and weights.

- (1) 10 f.p.s. at design landing wt.
- (2) 6 f.p.s. at design take-off wt.

In the absence of such data satisfactory preliminary estimate for transport airplane is 2.90 limit load factor.

II. Static Conditions

The landing conditions specified except for the spin-up and spring back loads can be considered a static condition, and may be analyzed by assuming that $\sum F = 0$ and $\sum M = 0$. Since these are normally simple mechanical problems set up by the C.A.M.

requirements it is assumed that no explanation is required here. In addition to the landing conditions presented here, which are taken from CAM 4b, the ground loads must be determined for "Ground Handling Conditions", CAM4b.235 and "Unsymmetrical Loads on Multiple Wheel Units, CAM 4b.236.

III. Dynamic Conditions:

Conditions of maximum wheel spin-up load and maximum spring-back load are specified for the Level Landing Condition.

Spin-Up and Spring Back Loads:

When the airplane tires strike the ground upon landing they are usually not rotating, and the wheels do not roll but slide. Due to the sliding coefficient of friction, drag loads will be set up until the wheels reach the rotational speed required so that the airplane tires will roll. The drag load, being a friction load, is a function of the vertical load. Since the vertical load varies with time due to the shock absorber action, the time for the vertical load to build up to a maximum is therefore a function of the shock absorber design. When the vertical load reaches its maximum, the wheel is already rotating due to the drag load that has been acting. Until the wheel is rotating only, there is a combination of sliding and rolling motion. The maximum drag load is therefore a complex function of the landing weight of the airplane, the shock absorber action, the radius and moment of inertia of the tire, landing gear structure flexibility, and the landing speed of the airplane.

Dynamic springback loads are a result of the deflection of the gear due to the spin uploads. Subsequent to the instant of maximum spin up load and corresponding rearward deflection, the wheel rotational speed is considered to have reached the airplane's rolling speed and the magnitude of the sliding friction on the ground rapidly reduces to zero. The strain energy stored in the rearward deformation of the gear is considered to result in a springing forward of the axle and its associated masses so that, at the instant of reaching the maximum forward deformation, a dynamic springback load may be considered to consist of the inertia of the effective mass at the axle acting forward normal to the oleo. At this instant the vertical ground reaction is considered to have reached its maximum value.

If applicable test data enabling an accurate determination of these loads is not available, a method of determination that will be considered acceptable is presented in ANC-2, Ground Loads. The following is taken from this bulletin:

Maximum Spin-Up.

Assuming that the vertical load on the wheel develops

12:56 SUPERSONIC AND SUBSONIC AIRPLANE DESIGN

sinusoidally with time and that an average coefficient of sliding friction equal to 0.55 exists during the spin-up period, the basic maximum spin-up loads may be considered as:

$$\left. \begin{aligned} F_{V_{SU}} &= F_{V_{MAX}} \sin \left(\frac{\pi}{2t_v} t_{su} \right) \\ F_{D_{SU}} &= 0.55 F_{V_{MAX}} \sin \left(\frac{\pi}{2t_v} t_{su} \right) \end{aligned} \right\} \text{for } t_{su} < t_v \quad (12:73)$$

or

$$\left. \begin{aligned} F_{V_{SU}} &= F_{V_{MAX}} \\ F_{D_{SU}} &= 0.55 F_{V_{MAX}} \end{aligned} \right\} \text{for } t_{su} > t_v \quad (12:74)$$

The basic loads ($F_{V_{SU}}$, $F_{D_{SU}}$) should be resolved parallel to, and normal to the oleo axis. After modifying the component normal to the oleo axis to account for dynamic magnification, the resultant design loads will then be determined as comprising the following components (see fig. 12:32):

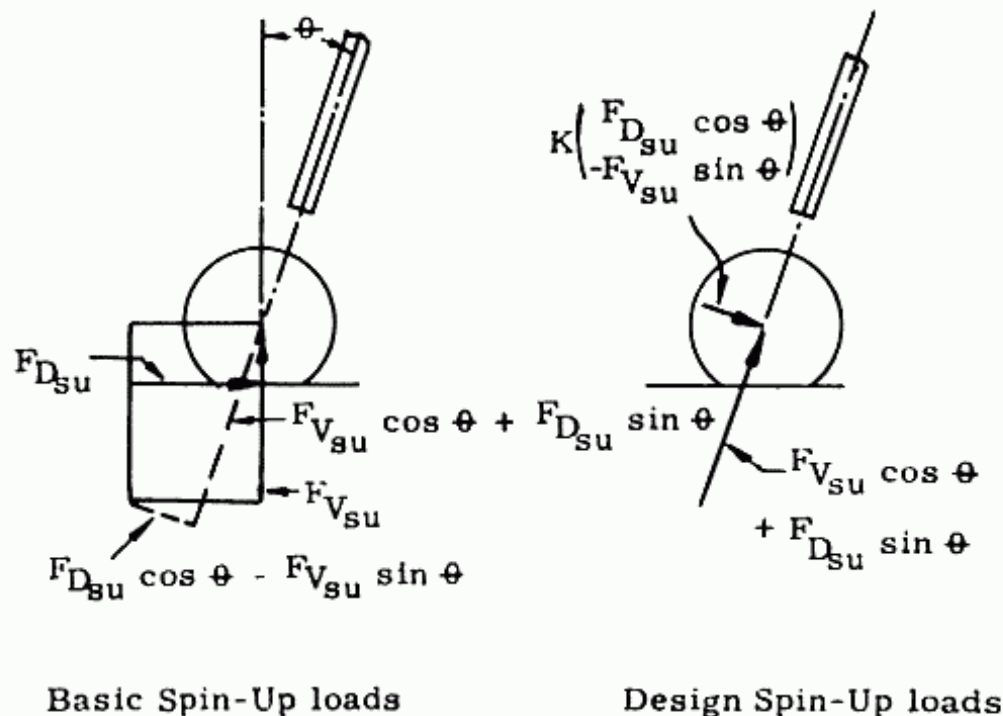


Fig. 12:32. Spin-Up reactions.

Normal to oleo (aft)

$$= K_{SU} (F_{D_{SU}} \cos \theta - F_{V_{SU}} \sin \theta)$$

Parallel to oleo

$$= F_{V_{SU}} \cos \theta + F_{D_{SU}} \sin \theta$$

(See fig. 12:33 for the determination of the dynamic response factor, K_{SU}).

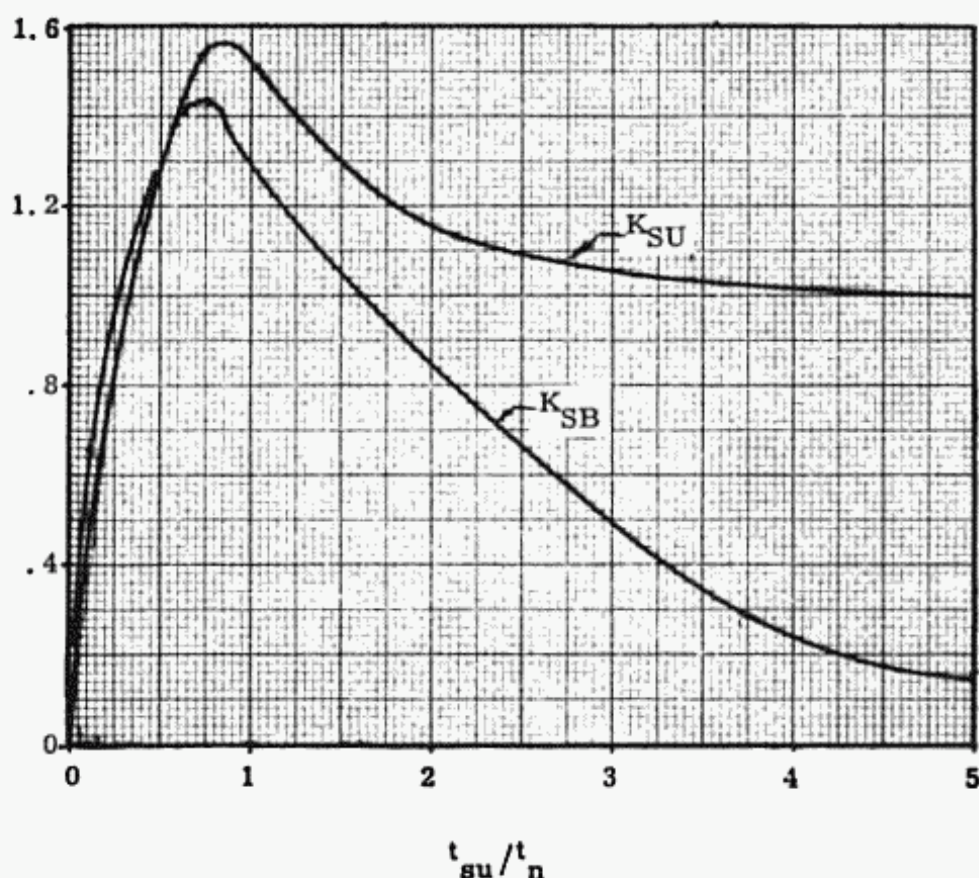


Fig. 12:33. K_{SU} and K_{SB} .

In lieu of applicable test data, the values of t_v and t_{SU} may be obtained from the following formulas:

$$t_v = \frac{V_v - (V_v^2 - 29.8 d_v n_g)^{1/2}}{14.9 n_g}$$

$$t_{SU} = \frac{2t_v}{\pi} \cos^{-1} \left(1 - \frac{V_L I_w \pi}{1.1 t_v r^2 F_{V_{MAX}}} \right) \text{ for } t_{SU} < t_v$$

(12:75)

or

$$t_{SU} = \frac{V_L I_w}{.55 r^2 F_{V_{MAX}}} + .363 t_v \text{ for } t_{SU} > t_v$$

Dynamic Spring-Back.

Taking into account dynamic magnifications resulting from the rapid reduction in spin-up load and the elasticity of the structure, the resulting design load will be determined as comprising the following components.

Normal to oleo (fwd)

$$= K_{SB} (F_{Dsv} \cos \theta + F_{Vsu} \sin \theta) + F_{Vsu} \left(0.9 \frac{F_{VMAX}}{F_{Vsu}} \right) \sin \theta$$

Along oleo

$$= F_{VMAX} \cos \theta$$

(See fig. 12:33 for the determination of the dynamic response factor, K_{SB}).

Dynamic Response.

Dynamic Response Factors. The dynamic response factors, K_{SU} and K_{SB} shall be calculated by the use of figure 12:33. However, to eliminate the necessity for calculating the parameter t_n , required to determine the dynamic response factors, K_{SU} may be taken equal to 1.4 and K_{SB} may be taken equal to 1.25.

Landing Gear Natural Period.

The landing gear natural period, t_n , is best determined from vibration tests of the gear as actually installed in the airplane. It may be computed from landing gears having oleo struts whose longitudinal center lines are within 20° of the vertical with the airplane thrust line horizontal, by the following formula^o

$$t_n = 0.32 \sqrt{x}$$

where x is the structural deflection (inches) of the axle, with the oleo fully extended, caused by an aft load which is normal to the oleo and equal to the total weight of the wheel assembly and the part of the strut extending from the center line of the wheel to a distance equal to the tire radius. The reactions for this force shall be assumed to be applied at the airplane fuselage.

Special Dynamic Analysis.

Special dynamic analysis should be made for landing gears having oleo struts whose longitudinal center lines are at an angle greater than 20° with the vertical, with the airplane thrust line horizontal, since for these cases the method used to compute figure 12:33 may not be applicable.

Symbols

The following symbols are used throughout this bulletin:

d_v	Total deflection (feet) at time t_v taken equal to $x_t + 0.5 x_0$, where x_t = tire deflection and x_0 = total oleo stroke.
F_{DSU}	Maximum spin-up drag load, parallel to ground line, before correction for dynamic magnification, lbs.
F_V	Vertical load, lbs.
$F_{V_{MAX}}$	Maximum vertical load, lbs.
$F_{V_{SU}}$	Vertical load at time t_{su}
I_w	Polar mass moment of inertia of rotating wheel assembly, slug ft. ²
K_{SB}	Dynamic response (magnification) factor for spring-back load.
K_{SU}	Dynamic response (magnification) factor for spin-up load.
n_g	Ground reaction factor; the ratio of the vertical component of the total ground reaction on any gear to the vertical component of the static reaction on that gear.
r	tire rolling radius, ft.
t_n	Natural period of landing gear in fore and aft vibration, secs.
t_{su}	Time required for wheel circumferential velocity to reach ground velocity, secs.
t_v	Time required to develop maximum vertical reaction after initial instant of contact, secs.
V_L	Landing speed for condition under investigation, ft/sec.
V_v	Airplane vertical velocity (sinking speed), ft/sec.
θ	Angle between oleo center line and the vertical, deg. (Positive for oleo inclined forward from wing or fuselage.)

Ref. 12:1 which investigates the maximum spin-up coefficients of friction obtained during tests of a landing gear also presents the time histories of ground loads (drag and vertical) and coefficients of friction for various forward and vertical velocities.

12:60 SUPERSONIC AND SUBSONIC AIRPLANE DESIGN

- Ref. 12:1 S. A. Batterson, NACA Memo 12-20-58L "Investigation of the Maximum Spin-up Coefficients of Friction Obtained During Tests of a Landing Gear Having a Static Load Rating of 20,000 Pounds. Jan. '59.
- 12:2 Wm. S. Aiken - An Analysis of Horizontal Tail Loads in Pitching Maneuvers on a Flexible Swept Wing Bomber." N.A.C.A. TN 4191
- 12:3 Bisplinghoff, Ashley and Haltman, "Aeroelasticity," published by Addison Wesley
- 12:4 Y. C. Fung "The Theory of Aeroelasticity" published by John Wiley and Sons.
- 12:5 K. G. Pratt and W. Walker "Revised Gust Load Formula and a Reevaluation of V-g Data, taken on Civil Transport Airplanes from 1933 to 1950." N.A.C.A. TR. 1206

APPENDIX

SAMPLE CALCULATIONS

1 General

Chapters I, II, IV and VI presented a method and the required charts for designing a jet transport. An illustrative example is now shown. The specifications are as follows:

1. All out range = 2,000 n.m.
2. Cruising speed = 480 knots
3. Number of passengers = 40
4. Field length = 6,000 feet

The all out range is the climb range plus the cruise range plus the maneuver range. It will be noted that there is no allowance for range in descent, or fuel used in warm-up or ground run. This standard procedure is used for the purpose of simplification and has proven to be satisfactory. The Civil Air Regulations for reserve are set as a function of holding time and range. For jet transports it was felt that a straight range allowance of 700 miles would be more practical and would meet the service requirements. The C.A.R. also requires that some allowance be made for maneuvering, .17 hours for a four engine airplane. Therefore the all out range of 2,000 n.m. permits only 1,220 miles for scheduled airline distance with no allowance for headwind. If there is a required headwind on a particular flight the scheduled airline distance must be further reduced.

The cruising speed of 480 knots is the desired speed during the entire flight except for climb. The climb speed should be the one that results in the highest rate of climb at take-off power except that (1) take-off power should not be used for more than 30 minutes continuously and (2) the rate of depressuration of the cabin should not exceed the equivalent of climbing 500 feet per minute in free air. Since the cabin is to maintain 8,000 ft. pressure at altitude, an equivalent depressurization of 500 ft/min. would require that climbing time should not be less than 16 minutes.

The number of passengers should equal forty. In addition to providing seats for the passengers, space must be allowed for 40 pounds of baggage per passenger, bringing the total weight allowance to 200 pounds per passenger. The weight of cargo to be carried was set at twenty percent of the weight of passenger

and baggage; that is, cargo weight is also 40 pounds per passenger. For a 40 passenger airplane, the total weight of passenger and cargo is then 9,600 pounds.

The field length specification of 6,000 feet is to conform to the Civil Air Regulation requirements for both take-off and landing. Allowance is also made for the hot day conditions effect on both jet engine thrust and lift for take-off.

In addition to these prime specifications, it should be realized that certain design criteria based upon experience must be assumed to make this procedure possible. Most of these have been presented in Chapter II. Wherever it is deemed necessary these assumptions will be discussed along with the calculations.

2 Results

A series of airplanes, which started their cruise at 35,000 ft. and continued at constant W/δ s, were designed to meet the specifications. Airplanes I, II, III and IV assumed combinations of airfoil thickness ratio and wing sweepback that resulted in the same M_{crD_0} . They were calculated at aspect ratio 10, where there is no effect of aspect ratio of M_{crD} . Fig. 2:37 presents the direct operating cost versus sweepback for these airplanes, showing that 35° is the optimum.

Airplanes V, VI and VII were then designed with varying aspect ratios at the optimum sweepback. It should be noted from Fig. 2:8 that ΔM_{crD} varies with aspect ratio and that at 35° sweepback this ΔM_{crD} is the greatest. Since 35° sweepback is the optimum at aspect ratio = 10 where there is no aspect ratio effect on M_{crD} , the airplane will definitely be optimum at any aspect ratio where there is an effect on M_{crD} . Fig. 2:38 presents the direct operate cost versus aspect ratio for the optimum sweepback 35° . The optimum aspect ratio is approximately 7. The sample calculations as shown in section 3 is for the airplane with 35° sweepback and aspect ratio = 8.

3 Sample calculations for airplane 1.

A. Wing Loading, sweepback and thickness ratio.

To design the wing for sweepback and thickness ratio, the maximum design speed must be known. The maximum design speeds of the jet transports in this example will be assumed to be the speed corresponding to $M_{cruise} + \Delta M_{due\ to\ \Delta C_D = .001}$. The ΔM corresponding to $\Delta C_D = .001$, the compressibility drag coefficient, is obtained from Fig. 2:23. This maximum M will be the M_{crD} of the wing and is expressed in Equ. 1.

$$M_{crD_0} + \Delta M_{crD} \text{ due } C_L + \Delta M_{crD} \text{ due AR} = M_{\text{high speed}} \quad \text{Equ. 1}$$

therefore

$$M_{crD_0} = M_{\text{high speed}} - \Delta M_{crD} \text{ due } C_L - \Delta M_{crD} \text{ due AR}$$

where

$$M_{crD_0} = M_{crD} \text{ at } C_L = 0, \text{ and AR effect} = 0$$

If cruise is at 35,000 feet or above and aspect ratio = 8,

$$\text{From Fig. 2:23; } \Delta M_{\text{due } \Delta C_D} = .001 = 0.04$$

$$M_{crD} = M_{\text{high speed}} = \frac{480}{575} + .04 = .876$$

$$\text{From Fig. 2:8; } \Delta M_{crD} \text{ due A.R} = .002$$

$$\text{Therefore, } (M_{crD} \text{ at } C_L, \text{ and AR effect} = 0) = .876 - .002 - M_{crD} \text{ due } C_L$$

If C_L were known, ΔM_{crD} due C_L could be chosen from Fig. 2:7 and M_{crD_0} calculated. From Fig. 2:9 and M_{crD_0} , wing sweep-back and thickness ratio would be determined.

As stated previously, there are two cruise altitudes that should be investigated. One is 35,000 feet at beginning of cruise and then proceeding at a constant $W/\delta S$ which condition is equivalent to a continuous climb. The other is the altitude for maximum range. This sample calculation will consider the 35,000 foot condition. Since the airplane is to cruise at a constant $W/\delta S$, C_L could be obtained from Equ. 3 if $W/\delta S$ at beginning of cruise were known.

$$W/\delta S = 1481 M^2 C_L \quad \text{Equ.3}$$

The wing loading, W/S , could be determined from Fig. 2:12 using the requirement that the field length equal 6,000 feet, if maximum C_L were known. However $C_{L_{\text{max}}}$ cannot be obtained from Figs. 2:11a and b unless wing thickness ratio and sweep-back are known.

At this point either maximum C_L or cruising C_L could be assumed and then checked. Since it is felt that estimation of cruising C_L is more direct, let us assume cruising $C_L = 0.30$.

From Fig. 2:7

$$\Delta M_{crD} \text{ due } C_L = -.025$$

Therefore from Equ. 2

$$M_{crD_0} = .876 - .002 - (-.025) = .899$$

From Fig. 2:9, and sweepback = 35°

$$\text{equivalent streamwise } t/c = .0795$$

It is now necessary to determine W/S , and then check the value of .3 assumed for cruising C_L . From Fig. 2:12, the landing W/S can be obtained if σC_L and the deceleration are known. Knowing the thickness ratio and sweepback, maximum C_L can be determined from Fig. 2:11. First it is necessary to obtain t/c perpendicular to the $1/4$ chord from Fig. 2:18. For 35° sweepback

$$\frac{t/c \perp 1/4 c}{t/c \text{ stream}} = 1.163$$

therefore

$$t/c \perp 1/4 c = (1.163) t/c \text{ stream} = (1.163)(.0795) = .0925$$

From Fig. 2:11 with $t/c \perp 1/4 c = .0925$, $\Lambda = 35^\circ$, and using a value of $S_f/S_w = .16$,

$$\begin{aligned} C_{L_{\max}} \text{ with flaps undeflected} &= 1.070 \\ \Delta C_{L_{\max}} \text{ with } S_f/S_w = .16 &= .625 \\ C_{L_{\max}} \text{ with flaps} &= 1.695 \end{aligned}$$

For sea level condition, $\sigma = 1.0$, and therefore $\sigma C_L = 1.695$.

With this value of σC_L , and average deceleration of 6 ft/sec.^2 , and the specified C.A.R. field length = 6,000 ft., from Fig. 2:12 landing $W/S = 40.0$. If the landing weight is equal to take-off weight minus one-half of the total fuel, then take-off W/S can be calculated from

$$\text{Take-off } W/S = \frac{(W/S) \text{ landing}}{1.0 - .5 \frac{(\text{total weight of fuel})}{\text{take-off weight}}}$$

At this point an estimate of fuel weight/take-off weight must be made. For an airplane with 2,000 n.m. all-out range, forty

passengers, a cruising speed of 480 knots and a field length of 6,000 ft., the first estimate from Fig. 2:13

$$\frac{W_f}{W_{TO}} = .275$$

then

$$\text{Take-off } W/S = \frac{40.0}{1 - (.5)(.275)} = 46.4 \text{ lbs/sq.ft.}$$

It is now possible to check the value of cruising C_L assumed. First it is necessary to obtain W/S at 35,000 feet. From empirical data it has been found that the reduction in W/S from take-off to 35,000 feet is approximately 3.5%. Therefore W/S at 35,000 feet = $(46.4)(.965) = 44.7$

Then from

$$C_L = \frac{W/\delta S}{1481M^2}$$

$$C_L = \frac{44.7/.2351}{1481 (.835)^2} = .184$$

Since the calculated cruising C_L of .184 is not equal to the assumed value of .30, another cruising C_L must be tried. Assume cruise $C_L = .20$ (or less since ΔM_{cr} due $C_L = 0$ below $C_L = .20$)

$$\Delta M_{crD} \text{ due } C_L = 0$$

$$M_{crD_0} = .876 - .002 - 0 = .874$$

$$\text{equiv. stream. } t/c = .093$$

$$t/c \perp 1/4 c = (1.163)(.093) = .1082$$

$$C_{L_{max}} \text{ with flaps undeflected} = 1.140$$

$$\Delta C_{L_{max}} \text{ with } S_f/S_w = .16 = \underline{.625}$$

$$C_{L_{max}} \text{ with flaps} = 1.765$$

$$\text{Landing } W/S = 41.5$$

$$\text{Take-off } W/S = 48.1$$

$$W/S \text{ at } 35,000 \text{ ft.} = 46.4$$

$$C_L = \frac{46.4 / .2351}{1481 (.835)^2} = .191$$

Now that the calculated C_L , .191, is equal to the assumed C_L of .20 or less, the sweepback and thickness ratio calculated are satisfactory.

Results	Take-off W/S	= 48.1
	1/4 c sweepback	= 35°
	streamwise t/c	= .093
	maximum C_L	= 1.765

B. Thrust Loading

Fig. 2:14 is used to determine the W/T required for take-off. The curve as plotted is for all engines operating and sea level, standard day, take-off thrust. To account for one engine becoming inoperative during take-off, multiply the required field length by 0.83. From take-off field = (.83)(6000) = 4980 and Fig. 2:14 $K = 245$

$$K = (W/S)(W/T)(1/C_{L_{TO}})(1/\sigma) = 245$$

$$W/T = \frac{(245)(0.926)(1.325)}{(48.1)}$$

$$W/T \text{ (standard day engine thrust)} = 6.25$$

Note: $C_{L_{TO}} = .75 C_{L_{max}}$

$$\sigma = .926 \text{ for a hot day of } 100^{\circ}\text{F}$$

However at this temperature, there is approximately a 10% loss in jet thrust. Therefore to account for hot day requirements, standard W/T must be multiplied by 0.90.

Therefore,

$$W/T = (.9)(6.25) = 5.62$$

C. Weight Estimation

From section 2-5, for structural aspect ratio = 13 and thickness ratio perpendicular to 1/4 chord = .116, (equ. 2:32)

$$W_{\text{struct}} = (.16 W_{\text{TO}} + \frac{9.8}{(100/\frac{W}{S})}.63 \frac{W_{\text{TO}}}{W/S}) (K_{t/c})(K_{A.R.})(K_{\lambda})$$

To correct weight of structure for difference in structural aspect ratio and thickness ratio perpendicular to 1/4 chord,

$$\text{from } A.R_{\text{struct.}} = A.R_{\text{aero.}}/(\cos \Lambda)^2$$

Λ = angle of sweepback along the 1/4 chord

$$A.R_{\text{struct.}} = 8/ (.819)^2 = 11.93$$

and from Fig. 2:18

$$t/c \perp 1/4 c = (1.163)(.093) = .1082$$

Then from Fig. 2:19, $K_{A.R.}$ is equal to .986; from Fig. 2:20,

$K_{t/c} = 1.021$, and from Fig. 2:19a $K_{\lambda} = 1.0$.

Therefore

$$\begin{aligned} W_{\text{struct.}} &= (.16 W_{\text{TO}} + \frac{9.8}{(100/\frac{W}{S})}.63 \frac{W_{\text{TO}}}{W/S}) (1.021)(.986)(1.0) \\ &= .1615 W_{\text{TO}} + \frac{9.9}{(100/\frac{W}{S})}.63 \frac{W_{\text{TO}}}{W/S} \end{aligned}$$

Therefore from Equ. 2:38,

$$W_{\text{TO}} = .1615 W_{\text{TO}} + \frac{9.9}{(100/\frac{W}{S})}.63 \frac{W_{\text{TO}}}{W/S} + 1.95 (10^{-3}) N_e T_e^{1.55}$$

$$+ W_{\text{fuel} + \text{system}} + 400 N_p + W_{\text{crow}} + .045 W_{\text{TO}}$$

$$W/S = 48.1$$

$$\text{Since } W/T = 5.62 = W_{\text{TO}}/T; T = W_{\text{TO}}/5.62$$

$$T_e = \frac{W_{\text{TO}}}{(5.62)(4)} = \frac{W_{\text{TO}}}{22.48}$$

$$W_f/W_{\text{TO}} = .275$$

$$W_{f + \text{system}} = (1.0175)(.275) W_{\text{TO}} = .280 W_{\text{TO}}$$

Then

$$\begin{aligned} W_{\text{TO}} = & .1615 W_{\text{TO}} + \frac{9.9 W_{\text{TO}}}{(100/48.1)^{.63}(48.1)} \\ & + 1.95(10^{-3})(4)\left(\frac{W_{\text{TO}}}{22.48}\right)^{1.55} + .28 W_{\text{TO}} + 400(40) \\ & + (230)(4) + .045 W_{\text{TO}} \end{aligned}$$

Simplifying

$$.3835 W_{\text{TO}} - .63(10^{-4}) W_{\text{TO}}^{1.55} - 16,920 = 0 \quad \text{Equ.3b}$$

The best way of solving for W_{TO} is by trial and error

Finally with $W_{\text{TO}} = 47,000$

$$(.3835)(47,000) - 63(10^{-4})(47,000)^{1.55} - 16,920 = 0 \quad \text{Equ.4}$$

Therefore $W_{\text{TO}} = 47,000$

D. Parasite Drag

From section 2-6, C_{D_p} , the parasite drag coefficient, is defined as f/s , where f is the summation of the wetted area of the components times their corresponding coefficients, C_f . And Equ. 2:44 states

$$f = 1.10 + .128 N_p + .0070 S + .0021 N_e T_e^{.7}$$

$$S = \frac{W_{\text{TO}}}{W/S} = \frac{47,000}{48.1} = 987 \text{ sq. ft.}$$

$$T_e = \frac{W_{TO}}{4 W/T} = \frac{47,000}{(4)} = 2,090 \text{ lbs}$$

$$f = 1.10 + (.128)(40) + (.0070)(987) + (.0021)(4)(1,090)^.7 = 14.82$$

E. Climb

$$R/C = \frac{(T_a - T_{req}) 101 V}{W}$$

The rate of climb will be calculated at a few velocities and the results studied to determine the maximum. To reduce the amount of calculations a few velocities near $1.3 V_{L/D_{max}}$ will be tried.

$$V_{L/D_{max}} = \frac{12.90}{\sqrt{f_e}} \sqrt{\frac{W}{\sigma b}}$$

From Section 3, W/S_{TO} equals 48.1 and W/S at 35,000 equals 46.4. Therefore the average $W/S = 47.3$ and the average $W = 46,600$.

$$\text{From } A.R. = \frac{b^2}{s}, \quad b = \sqrt{(A.R.)(S)}$$

$$b = \sqrt{(8)(987)} = 88.8$$

Assuming that the average σ is the density ratio at (20/35) times altitude at top of climb, then from Fig. 2:26, σ at 20,000 feet = .5325. The airplane efficiency factor, e , is assumed equal to 0.80.

$$V_{L/D_{max}} = \frac{12.90}{[(14.82)(.8)]^{1/4}} \left[\frac{46,600}{(.5325)(88.8)} \right]^{1/2} = 218 \text{ knots}$$

$$\text{and } 1.3 V_{L/D_{max}} = 284 \text{ knots}$$

Using Equ. 2:83

$$T_{req} = \frac{\sigma f V^2}{296} + \frac{94.1}{\sigma e} \left(\frac{W}{b} \right)^2 \frac{1}{V^2}$$

SAMPLE CALCULATIONS

$$\begin{aligned}
 &= \frac{(.5325)(14.82)V^2}{296} + \frac{94.1}{(.5325)(.8)} \left(\frac{46,600}{88.8} \right)^2 \frac{1}{V^2} \\
 &= .0266 V^2 + \frac{61.0 (10)^6}{V^2} \qquad \text{Equ. 4a}
 \end{aligned}$$

Table 1

V	T _{req}	T _a	T _a - T _{req}	R/C
255	2,610	4,910	2,300	1,275
260	2,640	4,910	2,270	1,280
270	2,720	4,910	2,190	1,282
280	2,810	4,910	2,100	1,276
300	3,030	4,910	1,880	1,225

T_{req} is calculated from Equ. 4a

From Fig. 2:27 the take-off thrust available at 20,000 feet for the J-1 engine may be determined. To obtain the available thrust per airplane, the thrust from the J-1 must be multiplied by $\frac{4T_e}{4,000}$, or $\frac{(4)(2,090)}{4,000} = 2.09$

$$T_a = (2.09)(2,350) = 4,910$$

It is seen that the maximum rate of climb is equal to 1,282 feet per minute at 270 knots.

$$\text{time to climb} = \frac{\text{altitude}}{R/C} = \frac{35,000}{(1,282)} = 27.3 \text{ minutes}$$

therefore range in climb = (Velocity)(time)

$$= \frac{(270)(27.3)}{60} = 123 \text{ n.m.}$$

From Fig. 2:28, the miles per pound of fuel may be determined. Miles per pound of fuel is inversely proportional to the specific fuel consumption. Since the specific fuel consumption of the J.T. 1 engine is assumed to be equal to that of the J-1 engine, the miles per pound of four J.T. 1's equal the miles per pound of the J-1 engine times $\frac{4,000}{(T_e)(4)} = \frac{4,000}{(2,090)(4)} = .479$

From Fig. 2:28 n.m./lb of fuel of J-1 engine = (.128)

Therefore n.m./lb fuel of four J.T.1's = (.128)(.479) = .0614

Fuel consumed in climb = $\frac{123}{.0614} = 2,000$ pounds

$\frac{W_f \text{ in climb}}{\text{T.O. wt.}} = \frac{2,000}{47,000} = .0425$

It should be noted that this was assumed to be .035.

F. Range

From Equ. 2:59

$$\text{Range} = [(n.m./lb)_0 + (n.m./lb)_1] W_f/2$$

From previous calculation cruise $C_L = .191$

$$C_D = C_{D_i} + C_{D_p} + C_{D_{\text{comp}}}$$

$$C_{D_i} = \frac{C_L^2}{\pi A R_e} = \frac{(.191)^2}{\pi(8)(.8)} = .00182$$

$$C_{D_p} = f/S = \frac{(14.82)}{(987)} = .01500$$

$$C_{D_{\text{comp}}} = .001 \text{ (assumed, see p. 2:8)}$$

$$C_D = .00182 + .01500 + .0010 = .0178$$

$$L/D = \frac{.191}{.0178} = 10.75$$

$$D/\delta = \frac{(W/\delta S) S}{L/D} = \frac{(46.4/.2351)(987)}{10.75} = 18,100$$

$$(T/\delta) = \frac{(D/\delta)}{4} = \frac{18,106}{4} = 4,525$$

Scaling up $(T/\delta)_{\text{req JT-1}}$ to $(T/\delta)_{\text{J-1}}$

$$(T/\delta)_{J-1}^{\text{req}} = \frac{4,000}{2,090} \times (4,525) = 8,750$$

From Fig. 2:22, it is seen that the normal (T/δ) available = 6,260. Since the $(T/\delta)_{\text{req}}$ is greater than the $(T/\delta)_{\text{avail}}$, the engine on the J.T.-1 with $W/T = 5.62$ is not large enough. It is now evident that a W/T lower than that required for take-off is necessary for the specified cruise condition. The calculations must now be revised for a W/T that will result in a thrust required equal to between 80 and 100% of thrust available.

G. Thrust Loading for Cruise Conditions

It is now necessary to assume a new W/T to meet cruising conditions, calculate a new weight estimate and continue with the design. Assuming $W/T = 3.60$.

Take-off Weight

$$.3835 W_{\text{TO}} - 1.95 (10^{-3})(4) \left[\frac{W_{\text{TO}}}{(4)(3.6)} \right]^{1.55} - 16,920 = 0$$

$$.3835 W_{\text{TO}} - .126 (10^{-3}) W_{\text{TO}}^{1.55} - 16,920 = 0 \quad \text{Equ. 4b}$$

$$W_{\text{TO}} = 51,000 \text{ lbs.}$$

Parasite Drag

$$f = 1.10 + .128 N_p + .0070 S + .0021 N_e T_e^{.7}$$

$$S = \frac{51,000}{48.1} = 1,060 \text{ sq. ft.}$$

$$T_e = \frac{51,000}{3.6 \times 4} = 3,540$$

$$f = 1.10 + (.128)(40) + (.0070)(1,060) + (.0021)(4)(3,540)^{.7} \\ = 16.18$$

Climb

$$T_{\text{req}} = \frac{\sigma f V^2}{296} - \frac{94.1}{e} \left(\frac{W}{b} \right)^2 \frac{1}{V^2}$$

$$b = [(8)(1,060)]^{1/2} = 92.0 \text{ ft}$$

$$W_{\text{ave}} = \frac{51,000}{1.0175} = 50,000 \text{ lbs}$$

$$T_{\text{req}} = \frac{(.5325)(16.18)}{296} V^2 + \frac{94.1}{(.5325)(.8)} \left(\frac{50,000}{92.0} \right)^2 \frac{1}{V^2}$$

$$= .0291 V^2 + \frac{64.4 (10)^6}{V^2}$$

Table 2

V	T_{req}	T_a	$T_a - T_{\text{req}}$	R/C
260	2,920	8,320	5,400	2,840
280	3,100	8,320	5,220	2,940
300	3,330	8,320	4,990	3,020
310	3,470	8,320	4,850	3,050
320	3,610	8,320	4,710	3,040

$$\max R/C = 3,050 \text{ ft/min}$$

$$V_{\max} R/C = 310 \text{ knots}$$

$$\text{Time to climb} = \frac{35,000}{3,050} = 11.5 \text{ min.}$$

$$\text{Range in climb} = (310) \frac{(11.50)}{60} = 60 \text{ n.m.}$$

$$\text{n.m./lb for J-1 engine} = .168$$

$$\text{n.m./lb for J.T.-1 engines} = .168 \left[\frac{4,000}{(4)(3,540)} \right] = .0475$$

$$\text{Fuel consumed in climb} = \frac{60}{.0475} = 1,265 \text{ lbs.}$$

Range

$$W_0 = 51,000 - 1,265 = 49,735$$

SAMPLE CALCULATIONS

$$W_1 = (1 - .275)(51,000) = 37,000$$

$$W/\delta S = \frac{49,735}{(.2351)(1,060)} = 225$$

$$C_L = \frac{225}{(1481)(.835)^2} = .218$$

$$C_{Di} = \frac{(.218)^2}{(\pi)(8)(.8)} = .00237$$

$$C_{Dp} = \frac{16.18}{1,060} = .01525$$

$$C_{Dcomp} = .0010$$

$$C_D = .00237 + .01525 + .0010 = .01862$$

$$L/D = \frac{.218}{.01862} = 11.70$$

$$(T/\delta)_{eng} = \frac{(225)(1.060)}{4(11.7)} = 5,100 \text{ lbs.}$$

Scaling up $(T/\delta)_{req}$ for J.T.-1 to (T/δ) for J-1

$$(T/\delta) \text{ for J-1} = \frac{4,000}{3,540} (5,100) = 5,760$$

From Fig. 2:22 normal $(T/\delta)_{available} = 6,260$

$$\frac{T_{req}}{T_{av}} = \frac{5,760}{6,260} = .92$$

which is satisfactory

From Fig. 2:22, with $V = 480$ knots and $T/\delta = 5,760$

$$\text{n.m. } \delta/lb = .094 \text{ per engine, J-1}$$

$$= .0266 \text{ per airplane, J.T.-1's}$$

At beginning of cruise, altitude is 35,000 feet, $\delta = .2351$, and
 $W/\delta S = 225$

At end of cruise with $W/\delta S = 225$, $W = 37,000$ and $S = 1,060$

$$\delta = \frac{37,000}{(225)(1,060)} = .155$$

$$\begin{aligned} R &= [(n.m./lb)_1 + (n.m./lb)_2] \frac{\text{cruise } W_f}{2} \\ &= \left[\frac{.0266}{.2351} + \frac{.0266}{.155} \right] \frac{(49,735 - 37,000)}{2} \\ &= 1,815 \text{ n.m. in cruise} \end{aligned}$$

$$\begin{aligned} \text{Total } R &= R_{\text{cruise}} + R_{\text{climb}} \\ &= 1,815 + 60 = 1,875 \text{ n.m.} \end{aligned}$$

This range of 1,875 n.m. is 125 n.m. less than the requirement of 2,000 n.m.

To get the desired result, W_f/W_{TO} should be increased from .275 to about .295.

To do this, first take-off W/S must be changed minutely since,

$$\text{take-off } W/S = \frac{\text{landing } W/S}{1 - .5 (W_f/W_{TO})}$$

and W_f/W_{TO} has changed from .275 to .295, while landing W/S remains constant.

The more significant change is to use $W_f = .295 W_{TO}$ in the weight equation.

With the new weight, the method must be gone thru once more.

H. Direct Operating Cost

See Section 2:10

Will use the airplane with 1,875 n.m. range.

Cost of fuel

Although the all out range is equal to 1,875 n.m., the D.O.C. costs are based upon the scheduled airline distance, 1,095 n.m. It is then necessary to obtain the weight of fuel

required for this range plus maneuver which is equivalent to 80 n.m.

Range in climb = 60 n.m.

Cruise range required for fuel cost = 1,095 + 80 - 60 = 1,115 n.m.

$$R = 2.3 (L/D) (V/c) \log_{10} \frac{W_0}{W_1}; c = \frac{V}{(\text{mi } \delta / \text{lb}) (T/\delta)} = \frac{480}{(.094)(5.760)} = .885$$

$$1,115 = 2.3 (11.70) (480/.885) \log_{10} \frac{49,735}{W_1}$$

$$W_1 = 41,400 \text{ lbs.}$$

Weight of fuel used = 51,000 - 41,400 = 9,600 lbs.

From Sec. 2:10

$$C_{\text{fuel}} = \frac{2.23 W_f}{R P} + \frac{175 N_e}{V_B P}$$

$$= \frac{(2.23)(9,600)}{(1,115)(4.8)} + \frac{(175)(4)}{(435)(4.8)} = 4.30 \text{ ¢/ton n.m.}$$

note: P is pay load in tons; See next page for V_B .

40 passengers x 200	= 8,000
cargo	= 1,600
total	= 9,600 lbs.

Cost of Crew

$$\text{Crew} = \frac{2,614 + (3.41 G. W/1,000)}{V_B P} + \frac{.051}{P}$$

$$V_B = \frac{\text{Range}}{\text{time to (climb, cruise and maneuver)}}$$

$$= \frac{1,115}{(11.5/60) + \left(\frac{1,115 - 60}{480}\right) + .17} = 435 \text{ knots}$$

$$C_{\text{crew}} = \frac{2,614 + (3.41)(51,000)/1,000}{(435)(4.8)} + \frac{.051}{4.8} = 1.34 \text{ ¢/ton n.m.}$$

Cost of Insurance

$$C_{\text{insurance}} = \frac{.0668 W_e}{V_B P} + \frac{.10}{P}$$

$$W_e = \text{weight empty} = W_{\text{TO}} - (W_f + W_{\text{payload}} + W_{\text{crew}})$$

$$W_{\text{TO}} = 51,000 \text{ lbs.}$$

$$W_f = 14,000 \text{ lbs.}$$

$$W_{\text{payload}} = 9,600 \text{ lbs.}$$

$$W_{\text{crew}} = 920 - 90 = 830; \text{ 90 lbs. is for seats}$$

$$W_e = 51,000 - (14,000 + 9,600 + 830) = 26,570$$

$$C_{\text{ins}} = \frac{(.0668)(26,570)}{(435)(4.8)} + \frac{.10}{4.8} = 87 \text{ ¢/ton n.m.}$$

Cost of Airframe

$$C_{\text{airframe}} = \frac{627 + .261 W_a}{V_B P}$$

$$W_a = W_e - W_{\text{engs.}}$$

$$W_{\text{engs.}} = 1.95 (10^{-3}) N_e T_e^{1.55}$$

$$= (1.95) (10^{-3}) (4) (3,540)^{1.55} = 2,500$$

$$W_a = 26,570 - 2,500 = 24,070 \text{ lbs.}$$

$$C_{\text{airframe}} = \frac{627 + .261 (24,070)}{(435)(4.8)} = 3.31$$

Cost of engines

$$C_{\text{engine}} = \frac{.915 W_{\text{eng}} N_e + 375}{V_B P}$$

$$= \frac{(.915)(2,500)}{(435)(4.8)} = 1.09$$

D.O.C.

$$= C_f + C_{crew} + C_{ins} + C_{airframe} + C_{engine}$$

$$= 4.30 + 1.34 + .87 + 3.31 + 1.09$$

$$= 10.91 \text{ ¢/ton n.m.}$$

J. The following is a summary of the more important characteristics of the airplane designed to meet the specifications stated in Section 5:1

1. Take-off weight	= 51,000 lbs.
2. Total fuel weight	= 14,000 lbs.
3. Fuel weight/take-off weight	= .275
4. Fuel to climb	= 1,265 lbs.
5. Fuel to climb/take-off weight	= .025
6. Wing loading - take-off	= 48.1
7. Wing area	= 1,060 sq. ft.
8. Wing A.R.	= 8
9. Wing sweepback at 1/4 c	= 35°
10. Wing thickness ratio, equivalent	= .093
11. $C_{L_{max}}$	= 1.765
12. $C_{L_{cruise}}$	= .191
13. Thrust loading required for take-off	= 5.62
14. Thrust loading required for cruise	= 3.60 critical
15. Thrust per eng., T.O., S.L., Static	= 3,540 lbs.
16. T_{req}/T_{avail} in cruise	= .92
17. Range - total	= 1,875 miles
18. Climb range	= 60 miles
19. Altitude at beginning of cruise	= 35,000 ft.
20. Altitude before reserve	= 40,500 ft.
21. Cruise speed	= 480 knots
22. $W/\delta S$ at cruise	= 225
23. (mi δ /lb) at cruise per airplane	= .0266
24. Block speed	= 435 knots
25. Landing Field	= 6,000 ft.
26. Take-off field	= 3,000 ft.
27. D.O.C.	= 10.91 ¢/ton n.m.

All the above except (20), altitude before reserve, and (26), take-off field, have been presented in the sample calculations.

Take-off field has been calculated from Fig. 2:14 using $W/T = 3.96$ corrected for a hot day, and the critical one engine inoperative condition. Altitude before reserve has been obtained from calculating the weight at that point and therefore the δ for the constant $W/\delta S$.

4. Climb Requirements

The airplane must still be checked to see whether it meets the climb requirements as specified by the Civil Air Regulations. If it does not, the W/T must again be lowered, and the entire calculations repeated. However for the four engine high speed jet transports the cruise thrust is usually more critical than that required for climb.

5. Airplane at optimum altitude

The same principles and charts as were used on the 35,000 foot airplane are applied to the airplane at optimum altitude. However there are a few variations, which lead to somewhat lengthier calculations.

For the 35,000 feet airplane the cruise C_L can be determined early in the calculations and the correct effect of it on M_{CRD} used. However on the optimum airplane the cruise C_L is not known until much later on in the work. It is therefore necessary to assume a cruise C_L when calculating M_{CRD_0} .

The method is then the same as presented except that the optimum $W/\delta S$ is calculated as described in section 2:11. From the optimum $W/\delta S$ the actual cruise C_L is determined. If it does not check the cruise C_L assumed to obtain M_{CRD_0} then new estimates of cruise C_L must be made until the estimated value does equal the calculated one. The climb calculations cannot be performed until the optimum $W/\delta S$ is known.

6. Navaer Method

The performance calculations can also be done by the Navaer method. It can be used to check what has been done, and in addition to obtain other data as explained in section 6:2.

7. Parasite Drag

After the airplane has been drawn by following method in Chapter III, the new and more accurate "f" may be calculated from section 6:3.

8. Take-off Distance

With the data now established and the method of section 6:4 a more accurate take-off distance may be calculated. However since the take-off distance is now less than the landing distance, this characteristic is not critical.

INDEX

- Activity factor, 8:6
- Aerodynamic center, 4:5
- Aerodynamic heating, 5:12
- Aeronca 15A, weights, 8:31, 8:38
 - tail volume coefficients, 8:38
- Aileron, control, 10:8, 11:6
 - reversal speed, 10:8
 - size, 4:6, 5:4
- Airfoil
 - designation, 4:15
 - selection and characteristics, 4:13, 5:5
- Airline schedules, 7:6
- Airloads
 - wing, 12:10, 12:38
 - horizontal tail, 12:10, 12:11
 - vertical tail, 12:43
 - high lift devices, 12:42
- Airplane efficiency factor, 7:12
- Airplane layout, 4:1, 5:1
- Allison Turbo-prop, 8:17
- Altitude
 - cruise at 35,000 ft, 2:46
 - discussion of factors, 2:45
 - effect on D.O.C., 7:8
 - optimum, 2:71
- Angle of attack, effect on "e," 7:13
- Angle
 - of yaw, 10:1
 - of sideslip, 10:1
- Area rule
 - general, 3:28
 - transonic, 3:29
 - supersonic, 3:31
- Aspect ratio
 - aerodynamic, 2:29
 - effect on C_{Di} , and a , 4:4
 - effect on "e," 7:14
 - effect on M_{CRD} , 2:7, 2:8
 - effect on wing weight, 2:29, 2:30
 - optimum, 2:12
 - structural, 2:29
 - in supersonic design, 3:2
- Avro Jet Liner, 2:17, 2:20, 4:39, 8:12, 8:13, 8:14
- Banked turn, 10:10
- Boeing
 - Stratocruiser, 2:17, 2:20, 4:39, 8:12, 8:13, 8:14
- B 52, 1:6
 - 707, 2:17, 2:20, 4:39
 - 707 inboard profile, 4:34
 - Turbo jet engine, 8:33
 - Turbo-prop engine, 8:34
- Breguet's range formula, 2:37, 2:40
- Buseman bi-plane, 3:33
- C_f , 2:36, 2:38, 2:39
- Canard, 2:21, 5:1, 5:2, 9:53, 12:32
- Caravelle-3 View, 4:35, 4:39
- Center of gravity, 4:1, 4:41, 5:12
 - movement, 4:28, 4:41
 - limits by stability, 9:49, 9:23
 - forward limit, 9:50
 - aft limit, 9:51
- Cessna airplanes, weights, 8:31
 - tail volume coefficients, 8:38
- Checked maneuver, 12:27
- Chute, landing, 2:14
- Climb, 2:48, 3:43
 - fuel in, 2:56
 - range in, 2:54
 - requirement, 2:64, 3:44
 - time to, 2:54
 - thrust at angle with line of flight, 2:52
 - unaccelarated, 2:50, 2:49
 - with acceleration, 2:51
- Climb out, 2:27
- Comet, DeHavilland, 4:39, 8:12, 8:13
- Compressibility, 2:2
- Controlability
 - specifications, 9:1
 - in landing, 9:40
 - directional, 10:1
 - lateral, 10:4
- Control Surfaces, 5:10
 - choice supersonic, 5:2
- Convair
 - 240, 2:17, 2:20, 4:39, 8:12, 8:13, 8:14
 - 600, 2:20, 4:39
 - F 106, 3 view, 8:35
 - B 58, 3 view, 8:37
- Costs
 - direct operating, 2:67
 - indirect operating, 2:67
 - total operating, 2:67
- Creep, 5:16, 5:17, 5:22

450 SUPERSONIC AND SUBSONIC AIRPLANE DESIGN

- Crew weight, 2:34
- Critical Mach number, 2:3, 2:7
- Cross coupling, 11:11, 11:17
- Deceleration, on ground, 2:14
 - effect on D.O.C., 7:5
- DeHavilland Comet, 2:17, 2:20, 4:39
- Delta wing, 3:8
- Density ratio vs. altitude, 2:55
- Dihedral
 - angle, 4:11, 5:4
 - effect, 4:12, 10:6
 - effect on dyn. lat. stability, 9:20
- Direct operating cost, 2:67
 - vs. M. supersonic, 7:17
 - crew, insurance, airframe, 2:68, 2:69
 - engines, 2:70
 - fuel, 2:68
 - vs. A.R., 2:72
 - vs. sweepback, 2:71
- Directional Stability and Control, 8:2
- Douglas DC-3-4-6, 2:17, 2:20
 - DC-8, 2:17, 2:20, 4:39
- Downwash, 8:12, 8:13, 8:14
 - $d\epsilon/d\alpha$, 9:33
- Drag
 - base, 3:23, 3:27
 - Critical Mach number, 2:3, 2:5, 2:7, 2:9, 2:12
 - divergence Mach No., 2:3
 - due flap deflection, 2:65
 - due normal force, supersonic, 3:22, 3:26
 - friction, supersonic, 3:17, 3:34
 - wave, supersonic, 3:17, 3:18, 3:19, 3:21, 3:35
 - for propeller airplanes, 8:13, 8:15
 - induced, ground effect, 2:66
 - of landing gear, 2:66
 - parasite, 2:36
 - trim, effect on "e," 5:13
- Drag coefficient, 2:3
 - definition, 2:35
 - due compressibility, 2:37, 2:44
 - ground effect, 2:66
 - induced, 2:42, 7:12
 - minimum, 4:14
 - vs. M, 2:3
- Dutch roll, 11:9
- e, airplane efficiency factor, 7:12
- Elastic axis, 2:29
- Elevator power, 9:42
- Engine choice, 7:11
- Engine performance
 - P & W JT-12-Supersonic, 8:24, 8:25
 - P & W JT-4A-Supersonic, 8:26, 8:27, 8:28
 - P & W JT-6B, 8:23
 - P & W Wasp Major, 8:16
 - Allison 500, 501, 8:17
 - Boeing 502, 8:33
 - Continental 185 H.P., 8:32
- Equivalent shaft horsepower, 8:5
- Equilibrium, definition, 9:2
- Ercoupe, weights, 8:31
 - tail volume coefficients, 8:38
- External fuel tanks, 2:61, 2:63
- f, equivalent parasite drag area, 2:36, 6:4, 7:11
 - for propeller airplanes, 8:13
 - vs. wetted area, 8:15
- Factor of safety
 - field length, 2:13
- Fairchild F-27, Layout, 4:33
- Field length, 2:2
 - effect of one engine out, 2:26
 - effect on weight, D.O.C., and optimum A.R., 7:2
 - take-off distance, 2:24, 6:6
 - vs. wing loading, 2:19
- Fighter design, 8:4
 - weights, 8:22
- Flap, 2:14, 2:15, 5:4
 - area, effect on CL_{max} , 2:16
 - area, transport airplane, 2:17
 - types and characteristics, 4:8
- Flexibility
 - effect on a.c., 12:31
 - effect on stability, 9:20
 - effect on tail load, 12:31
 - effect on span. load dist., 12:35
- Floating tendency, 9:41
- Fuel
 - function of T_r/T_a , 2:47
 - consumption, jet engine, mi δ /lb, 2:43
 - dumping system, 2:19
 - storage, external, 2:59
 - storage, internal, 2:58, 2:60
 - effect of high temp., 5:31
 - weight estimation, 2:20, 2:21
 - weight in climb, 2:56
 - weight, in landing, 2:20

- Fuel (contd.)
 - weight, transports, 2:20
- Fuselage, 4:27, 5:9
 - twin lobe, 4:26, 4:27
- Ground effect
 - on C_{D1} , 2:66
 - on slope of lift curve, 4:10
 - on stability, 9:44
- Ground run
 - landing, 2:14, 7:10
 - take-off, 2:24, 2:26
- Ground turning loads, 4:21
- Gross weight
 - vs. M-supersonic, 7:17
- Headroom, 4:29
- Inboard profiles
 - 40 pass. airplane, 4:30
 - 60 pass. airplane, 4:32
 - Boeing 707-320, 4:34
 - Fairchild F-27 transport, 4:33
- Incidence angle, 4:7, 5:4
- Insulation, 5:22
 - Min-K properties, 5:23
- Interceptor design, 8:29
 - weights, 8:22
- Interference effects, 3:32
- J-1 jet engine, typical subsonic
 - mi./lb., sea level to 30,000 ft., 2:57
 - performance, 35,000 ft. & above, 2:43
 - thrust, s.l. to 30,000 ft., 2:56
- J-2 jet engine, typical supersonic
 - Thrust vs. M, 3:16, 3:45
 - n.m./lb. vs. M, 3:16, 3:45
- Judgment in design, 1:1, 1:3
- Kinematic viscosity vs. altitude, 2:55
- Landing field
 - formula for, 2:15
 - specified by C.A.R., 2:13
- Landing gear, 4:15, 5:3
 - bicycle, 4:7, 4:16
 - choice of, 4:18
 - drag of, 2:66
 - general, 4:15
 - layout, 4:19
 - outrigger, 4:16, 4:21
- Landing gear (contd.)
 - tall wheel, 4:15
 - tires, 4:18, 4:19
 - tricycle, 4:16, 4:17
- L/D, 2:18
 - vs. C_L , & A.R., supersonic, 3:7, 3:8
 - vs. altitude, A.R., W/S, 3:10, 3:11, 3:12
- Lift coefficient, 2:3, 2:22
 - design, 4:14
 - effect on $MCRD$, 2:6, 2:5, 2:8
 - formula for, 2:23
 - maximum, 2:15, 2:16, 2:17, 4:13
 - take-off, 2:25
- Lift curve slope
 - aspect ratio effect on, 9:28
 - vs. sweepback, supersonic, 3:5
 - ground effect on, 4:10
 - Mach number effect on, 9:32
 - sweepback effect on, 9:29
- Load factors, 12:2
 - maneuver, 12:3
 - limit, 12:3
 - increment, 12:3, 12:6
 - gust, 12:4, 12:8
 - gust envelope, 12:4
 - maneuver envelope, 12:4
 - alleviation factor, 12:5
- Loads
 - airloads, 12:1
 - spanwise distribution, 12:33
 - unsymmetrical, wing, 12:38
 - pressurized cabin, 12:47
 - control system, 12:47
 - ground loads, 12:49
 - spin-up, 12:55
 - spring back, 12:58
- Lockheed
 - Jet star, 3 View, 8:39
 - Constellation, 2:17, 2:20, 4:39, 8:12, 8:13, 8:14
- $MCRD_0$, definition, 2:9
 - vs. t/c and sweepback, 2:10
 - equation for, 2:12, 2:13
- Mach critical drag
 - definition, 2:3
 - effect of AR, 2:8, 2:9
 - effect of C_L ; 2:7, 2:9
 - effect of t/c, 2:5, 2:9
 - effect of sweepback, 2:5, 2:9
 - in airfoil selection, 4:14

- Mach critical lift**
 definition, 2:3
 in airfoil selection, 4:14
- Mach number**
 critical, 2:3, 2:5, 4:14
 definition of, 2:3
 equation for, 2:22
 high speed, 2:9
- Maneuvering flight** 10:10
- Maneuvering pitching condition**, 12:11, 12:21,
- Maneuvering balanced condition**, 12:11, 12:13
- Martin 340**, 2:17, 4:39, 8:12, 8:13, 8:14
 404, 2:20
- McDonnell**
 F 4H-1, three view, 8:36
- Mean aerodynamic chord**, 4:4
- Method of design**, 2:1
- Missiles**, 8:38
- Moment coefficient about a.c.**, 4:12
- Motions of airplane**, 9:15
 longitudinal, 9:15, 9:16
 lateral, 9:15, 9:17
- Nacelle**
 arrangement, 4:24, 5:10
 location, 4:36
 size, 4:38
- Navaer Method of Performance**, 6:1
- Navion**, weights, 8:31, 8:38
 tail volume coefficients, 8:38
- Neutral point**, stick fixed, 9:36
 stick free, 9:48
- Noise in cabin**, 4:36, 4:37
- Optimum airplane**, 2:66, 2:70, 3:44
- Optimum altitude**, 2:71, 3:46
 Navaer method, 6:4
- Passenger loading**, 7:6
- Payload**, 2:33
 effect on D.O.C., 7:5
 Piper PA-20 weights, 8:38
- Phugoid Mode**, 9:15, 9:18
- Period of oscillation**, 9:13
- Pressure ratio vs. altitude**, 2:56
- Private airplane design**, 8:30
 engines, 8:32, 8:33, 8:34
 tail volume coefficients, 8:38
 weights, 8:31, 8:38
- Propeller efficiency**
 calculation, 8:1, 8:5
- Propeller efficiency (Contd.)**
 compressibility effects, 8:8
 definition, 8:4
 in range, formula, 2:37
 vs. $J(C_p)^{1/3}$, 8:7
 vs. M , 8:2, 8:4
- Propellers**
 activity factor, 8:6
 plan forms, 8:3
 reversible pitch, 2:15
 slipstream effect on drag, 8:13
 supersonic, 8:2, 8:4
 thickness, 8:3
 weights, 8:4
- Range**, 2:37
 at constant altitude, 6:9
 by Navaer method, 6:1
 Breguet's formula, 2:37, 3:41
 cruise, 2:37, 3:41
 effect on D.O.C., 7:6
 total, 2:57
 vs. $W/\delta S$, 2:73
- Rate of climb**, 2:48
- Reciprocating engines**, 8:9
 Continental 185, 8:32
 P. and W. Wasp Major, 8:16
- Refused take-off**, 2:27
- Restoring tendency**, 9:47
- Reynold's Number**
 effect on max. C_L , 2:17, 4:2
 effect on C_f , 2:38, 2:39
- Routh's discriminant**, 9:11
- Schrenck's method**, 12:34
- Seats**, rearward facing, 4:31
- Shock detachment angle**, 3:18
- Slats**, 4:7
- Spoilers**, 10:8
- Spanwise load distribution**,
 effect on "e," 7:12
- Spar location**, 4:6, 5:3
- Specific fuel consumption**, 2:36
- Speed**
 block, 2:69
 effect on D.O.C., wt, and optimum A.R., 7:1
 take-off, 6:8
 cruise, 2:9
 never exceed, 2:9
 normal operating, 2:9
- Speed of sound ratio vs. altitude**, 2:56
- Stability**, 9:3
 specifications, 9:1

- Stability (contd)
 definition, 9:2
 derivation, 9:14
 directional, 10:1
 diagrams, 9:18
 Dutch roll, 11:9
 effects of supersonic, 11:1
 effects of flexibility, 9:2
 lateral dynamic, 9:19, 10:4, 11:5
 longitudinal dynamic, 9:4, 9:18, 11:2
 longitudinal static, 9:22, 9:24, 9:46, 11:1
 period, 9:13
 quartic, 9:10
 spiral divergence, 9:15, 11:8
 static, 9:21
 static directional 9:20
 stick fixed, 9:4, 9:24
 stick free, 9:13
- Stall, characteristics of airfoils, 4:14
- Stratocruiser, Boeing, 4:39, 6:14, 8:12, 8:13
- Supersonic boom, 3:1, 3:2
- Supersonic propeller, 8:2, 8:4
- Sweepback, 2:2, 2:5
 determination, 2:9
 effect on fuselage, 2:30
 effect on wing weight, 2:29
 for optimum airplane, 2:71
 tapered, 2:6
- Tail load, in landing, 2:21
- Tail surfaces, design, 4:38
- Tail volume coefficients, 4:38
- Take-off distance, 2:24, 6:6
- Taper ratio
 effect on CD_i and a , 4:3, 4:4
 effect on fuel capacity, 2:61
 effect on tip stall, 4:3
 effect on weight, 2:29, 2:32, 4:1
 in supersonic design, 3:2
- Temperature
 ratio vs. altitude, 2:56
 recovery, 5:18
 stagnation, 5:18
 wall, 5:18
- Thermal stresses, 5:13, 5:20
- Thickness ratio, 2:2, 2:5
 determination, 2:9
 effect on CL_{max} , 2:16
 effect on wing weight, 2:29, 2:33
 for optimum airplane, 2:70
- Thickness ratio (Contd)
 perpendicular to $1/4 c$, 2:31
 spanwise variation, 2:11
- Three View Drawings
 Convair F 106, 8:35
 Convair B 58, 8:37
 Lockheed Jet star, 8:39
 McDonnell F4H-1, 8:36
- Thrust
 hot day, 2:25
 required/available, 2:47
 required in climb, 2:53
 required, Navaer method, 6:2
 reversers, 2:14, 2:15
- Thrust loading, 2:1, 2:23
 for cruise conditions, 2:46
 for max. mi/lb, 2:73
 for propeller airplanes, 8:9
 for take-off, 2:23
 vs. take-off distance, 2:24
 supersonic, 3:14
- Turbo-prop engines, 8:9
 Allison 500, 501, 8:17
 Boeing, 502, 8:33
 Performance of typical, 8:18, 8:19
- Unchecked maneuver, 12:26
- Useful load, 8:14
- V-g diagrams, 12:4
- Wave drag coefficients
 vs. sweepback, supersonic, 3:6
- Weight
 engine effect on wing, 4:36
 estimation-supersonic, 3:15
 estimation for transports, 2:27, 8:10
 fixed equipment, 2:34
 fuel, 2:33
 military aircraft, 8:22
 payload, 2:33, 4:42
 power plant, 2:30
 ratio, supersonic, vs. M, 7:16
 structural, 2:28, 4:41, 5:12
 take-off, 2:34
 transport components, 8:10
- Weight, take-off, 2:1
 design gross, transports, 2:9
 estimation of, 2:27
- Wetted area, 6:5
- Wind axes, 9:5
- Wing
 area, transport planes, 2:17
 plan form, 4:1, 5:3

Wing (Contd)

sweepback, 2:1, 2:2, 2:8
taper ratio, 4:1
thickness ratio, 2:1, 2:2, 2:8
vertical location of—on fuselage,
4:23, 4:26, 5:8

Wing loading, 2:1, 2:12
effect on altitude performance
for propeller airplanes, 8:9
landing—vs. field length, 2:19
supersonic airplane, 3:13

